ONE DIMENSIONAL COMPRESSION BEHAVIOUR OF UNSATURATED GRANULAR SOILS AT LOW STRESS LEVELS

BY

ANDREW KEITH GOODWIN

A THESIS SUBMITTED TO THE UNIVERSITY OF SHEFFIELD
IN PARTIAL FULFILMENT FOR THE
DEGREE OF DOCTOR OF PHILOSOPHY

DEPARTMENT OF CIVIL AND STRUCTURAL ENGINEERING

UNIVERSITY OF SHEFFIELD

SEPTEMBER 1991

BRITISH LIBRARY

IMAGING SERVICES NORTH

Boston Spa, Wetherby
West Yorkshire, LS23 7BQ
www.bl.uk

CONTAINS PULLOUTS

SUMMARY

Poor performance of trench reinstatements affects the quality and safety of highways. As materials in shallow trenches are unsaturated and under low stresses, the factors affecting their behaviour are not understood clearly. This thesis reports on an experimental investigation into the one dimensional compression behaviour of typical coarse granular trenchfill materials.

Literature from the fields of rockfills and unsaturated soils are reviewed, and some experimental difficulties faced when working with such materials are noted. The limestone test material is classified using standard specification tests for aggregates.

Four series of tests were performed to investigate the behaviour of three gradings over a range of water contents. Monotonic, constant strain and repeated load conditions were used, and investigations made into the influence of inundation on strain development, the influence of water content on K_o and shear strength for a given density, and the influence of compactive effort.

A new consolidation cell was developed to perform two of the test series. This cell allowed the measurement and control of suctions within the test specimens, and allowed inundation under controlled conditions. Air diffusion effects were allowed for in the design.

The experimental work shows measurable suctions exist within coarse granular soils. Compressibility and repeated load behaviour are both shown to be a function of water content and dry density for a given compactive effort, and soil suction is shown to be an important influence. Collapse settlements on inundation were recorded and were shown to be directly influenced by soil suction. Shear behaviour was shown to be affected by the suctions also, but the K_o tests were inconclusive.

A qualitative model to explain the influence of suction in coarse materials is presented, and the current test results compared with those of previous workers. The practical implications of the research are discussed.

The research reported in this thesis was conducted within the Department of Civil and Structural Engineering of the University of Sheffield under the supervision of Dr W F Anderson and Dr I C Pyrah, and in conjunction with the British Gas Engineering Research Station. Liaison staff at the Research Station were Dr R Owen, Mr D Boyes and Mr G Leach. The author wishes to express his sincere gratitude to them all for their time and efforts, but in particular wishes to thank Dr Anderson and Dr Pyrah for their guidance, suggestions and patience both during the experimental work and the prolonged period over which the thesis was written. Thanks also go to Professor T Hanna, the Head of the Department of Civil and Structural Engineering, for the use of the departmental facilities throughout the work.

The design and development of the apparatus was helped greatly by the enthusiasm and competence shown by all technical staff at the University, but the greatest endeavours were provided by Mr P L Osborne and Mr M Foster. Their input does not go unrecognised, and neither does the cooperation received from Mrs S Rowe and her staff when the soils laboratory at the British Gas Engineering Research Station was extensively used for several months.

Additional thanks go to all those who provided useful discussions throughout the period of the research, and to my postgraduate colleagues with whom some useful discussions were had in the local hostelries. Those discussions and the balance in life they provided does not go unremembered!

I am grateful to the Science and Engineering Research Council and British Gas plc for funding the research, and I thank also Scott Wilson Kirkpatrick for their financial input to the production of this thesis. In particular the secretaries who typed the text and the technicians who prepared the figures deserve special mention - your efforts were much appreciated. Thanks go also to British Gas for their permission to utilise photographs of the work performed within their premises.

Finally, I wish to thank my parents and Penny for all the encouragement and support they showed throughout this work. Without them this thesis may never have been completed.

ACKNOWLEDGEMENTS

The research reported in this thesis was conducted within the Department of Civil and Structural Engineering of the University of Sheffield under the supervision of Dr W F Anderson and Dr I C Pyrah, and in conjunction with the British Gas Engineering Research Station. Liaison staff at the Research Station were Dr R Owen, Mr D Boyes and Mr G Leach. The author wishes to express his sincere gratitude to them all for their time and efforts, but in particular wishes to thank Dr Anderson and Dr Pyrah for their guidance, suggestions and patience both during the experimental work and the prolonged period over which the thesis was written. Thanks also go to Professor T Hanna, the Head of Department of Civil and Structural Engineering, for the use of the departmental facilities throughout the work.

The design and development of the apparatus was helped greatly by the enthusiasm and competence shown by all technical staff at the University, but the greatest endeavours were provided by Mr P L Osborne and Mr M Foster. Their input does not go unrecognised, and neither does the cooperation received from Mrs S Rowe and her staff when the soils laboratory at the British Gas Engineering Research Station was extensively used for several months.

Additional thanks go to all those who provided useful discussions throughout the period of the research, and to my postgraduate colleagues with whom some useful discussions were had in the local hostelries. Those discussions and the balance in life they provided does not go unremembered!

I am grateful to the Science and Engineering Research Council and British Gas plc for funding the research, and I thank also Scott Wilson Kirkpatrick for their financial input to the production of this thesis. In particular the secretaries who typed the text and the technicians who prepared the figures deserve special mention - your efforts were much appreciated. Thanks go also to British Gas for their permission to utilise photographs of the work performed within their premises.

Finally, I wish to thank my parents and Penny for all the encouragement and support they showed throughout this work. Without them this thesis may never have been completed.

TABLE OF CONTENTS (Continued)

TABLE OF CONTENTS (Continued)

TABLE OF CONTENTS (Continued)

TABLE OF CONTENTS (Continued) PAGE

LIST OF TABLES

LIST OF TABLES (Continued)

LIST OF FIGURES

LIST OF FIGURES (Continued)

LIST OF PLATES

β_m, β_w - compressibility of air water mixture and pure water

δ - deflection

$\delta_{i,j}$ - Kronecker delta

$\varepsilon_p, \varepsilon_u$ - strain at peak (minimum) stress of repeated load cycle

θ - half angle subtended at centre of a particle by water in a lenticular state

ϕ', ϕ_b - angle of internal friction, due to effective stresses and suction stresses

σ - total stress

σ_1, σ_3 - total normal (radial) stress on triaxial specimen, at failure if subscript f attached

σ' - effective stress

$\bar{\sigma}_{i,j}$ - equivalent intergranular stress tensor

$\bar{\sigma}'_{i,j}$ - effective deviatoric stress tensor

ρ, ρ_d - bulk (dry) density of soil

ρ_w - density of pure water

γ_w - unit weight of pure water

- total shear stress, at failure if subscript f attached

χ - chi, effective stress parameter for coupled variable effective stress equation for unsaturated soils

- Poissons ratio

a - area of wavy plane through particle contacts above a single particle

a_a - area of air-solid contact for a single particle on a wavy plane

a_s - area of solid-solid contact for a single particle on a wavy plane

a_w - area of water-solid contact for a single particle on a wavy plane

a,b,c - principal dimensions of particles

b,d,l - breadth, depth and span of rectangular ceramic test specimens

e - void ratio

h - vertical separation of top and bottom platens

m - inverse of Poisson ratio

r,t - radius (thickness) of circular ceramic test specimens

r - radius of spherical particles

u_A, u_W = pore air (water) pressure

w = force per unit area on circular ceramic test specimen

w_A, w_F = absorbed (free) water content of soil

x = perimeter length of contractile skin contact on a single particle

A = degree of angularity of a particle, or air void ratio

At = ratio of the area of the air-water meniscus contact on a single particle to the area a

A_W = $\sum (a_w/a)$ on wavy plane

AAV = aggregate absorption value, in percent

B = pore water pressure parameter

C_m, C_t = compression indices for consolidation of unsaturated soils

E = Youngs modulus

F = failure load of ceramic

G_s = specific gravity of soil particle material

M_s = Mass of dry particles in soil

M_w = Mass of water in soil

M_p = Mass of dry particles plus mass of absorbed water

M_{wa} = Mass of water absorbed into particles

M_{wf} = Mass of water free to move in the inter-particle voids

M_R = modulus of rupture

P = total mean normal stress

Sr = Degree of saturation

T = surface tension force per unit length of contractile skin

V = Total volume

V_A = Volume of air

V_s, V_p = Volume of dry solid particles, and volume of dry particle plus absorbed water

V_v = Volume of voids

V_{WA}, V_{WF} = Volume of absorbed water and volume of free water in the interparticle voids

A - degree of angularity of a particle, or air void ratio

A_t - ratio of the area of the air-water meniscus contact on a single particle to the area a

A_w - $\sum (a_w/a)$ on wavy plane

AAV - aggregate absorption value, in percent

B - pore water pressure parameter

C_m, C_t - compression indices for consolidation of unsaturated soils

E - Youngs modules

F - failure load of ceramic

G_s - specific gravity of soil particle material

M_s - Mass of dry particles in soil

M_w - Mass of water in soil

M_p - Mass of dry particles plus mass of absorbed water

M_{wa} - Mass of water absorbed into particles

M_{wf} - Mass of water free to move in the inter-particle voids

M_R - modulus of rupture

P - total mean normal stress

S_r - Degree of saturation

T - surface tension force per unit length of contractile skin

V - Total volume

V_A - Volume of air

V_s, V_p - Volume of dry solid particles, and volume of dry particle plus absorbed water

V_v - Volume of voids

V_{WA}, V_{WF} - Volume of absorbed water and volume of free water in the interparticle voids

CHAPTER 1

INTRODUCTION

Following the onset of urban development in the late nineteenth century, extensive networks of gas mains were installed underground. Today, development and maintenance of these and other services require frequent excavations to be made in the highways of the UK to the detriment of highway quality and safety. In an effort to deal with the problem, the utilities voluntarily established in 1974 a Model Agreement for trench reinstatements which incorporated a method specification. However, this non-statutory code proved ineffective on a national basis and Horne (1985) recommended to government in his committee's report on the 1950 Public Utilities Street Works Act that a national specification for reinstatements be established in terms of materials, workmanship and performance. Work towards this goal is in progress, but the proposed performance specification is being hampered by the lack of a fundamental understanding of the behaviour of trenchfill materials, which are typically unsaturated, at low stress levels and, when imported fill is used, of a coarse granular nature.

Previous research relevant to understanding the behaviour of granular reinstatements may be broadly sub-divided into the two areas of unsaturated soils and rockfills. Work on unsaturated soils has shown that soil suctions induced by non-saturation decrease as the coarseness of the soil increases. Consequently, most efforts in this relatively young field of research have concentrated on silts and clays within which high suctions may be expected and their influence may be more clearly seen. Little work has been reported on sands and coarser materials.

Rockfill research covers a wide area, from true rockfills used in embankments and dams, to compaction of coarse mine and quarry wastes. However, throughout this field it appears that most workers have concentrated on the dry and saturated conditions, and have considered only moderate to high stress levels. At such stresses small suctions induced by non-saturation have been ignored.

The behaviour of reinstatements thus falls between two active areas of work, and research is required to fill the void in current knowledge. Both theoretical and experimental developments are required, but this first part of an ongoing programme of research into the problem has concentrated on the acquisition of high quality experimental data that may be used in future theoretical work. The objectives of the research were:

i) to review current knowledge relevant to the behaviour of trenchfill

ii) to develop experimental apparatus suitable for high quality testing of unsaturated coarse granular soils at low stress levels (<100 kPa)

iii) to obtain reliable data on the behaviour of typical trenchfill materials under monotonic and repeated loads, in varying degrees of compaction, and at a range of water contents

iv) to assess the factors affecting the observed behaviour of the trenchfill materials, make comparisons with previous work and make recommendations for future work.

The research is principally concerned with trenchfill, but may be applied to other problems such as ground movements associated with pipe bursting at shallow levels, and pipe jacking through embankments.

The thesis starts with a review of the relevant theoretical and experimental literature in Chapter 2. Descriptions of the test materials, experimental apparatus, calibration checks on apparatus and test programme follow in chapters 3 to 6, with particular attention being given to the design and calibration of a new one dimensional consolidation cell. The results of the research are presented in chapter 7, with discussion of the results and comparisons with previous work in chapter 8. The final chapter contains the conclusions and recommendations for future work.

CHAPTER TWO

LITERATURE REVIEW

The behaviour of trench reinstatements, which are typically unsaturated, coarse grained and under low in situ stresses, represents an area of research which has received little attention in the past. The unsaturated state of the materials gives rise to surface tension forces and suction stresses within the mass which become significant even in coarse grained soils at low stresses. Consequently the first part of this review considers the physics of unsaturated media and the influence of non-saturation on soils. The second section focuses on the importance of the particulate nature of the media, and reviews past work on the behaviour of coarse materials. Such work has concentrated almost entirely on the behaviour at moderate to high stress levels as are present in rockfill dams.

Following consideration of these two main area of previous research, the experimental difficulties faced when testing coarse unsaturated soils are briefly reviewed.

2.1 Physics of Unsaturated Soils

2.1.1 Phase States Within a Soil

Several categories of unsaturated soil may be defined on the basis of the continuity of the air and water phases, as shown in Figure 2.1. As these different conceptual states may exist simultaneously within a given soil due to spatial variations of the degree of saturation, the understanding of the behaviour of unsaturated soils represents a complex undertaking.

Unsaturated soil is often considered as a three phase medium, that is solid particle, water and air, but the air-water meniscus (or contractile skin) shown in Figure 2.1 could be identified as a fourth phase as it possesses physical properties distinct from the other phases

(Fredlund and Morgenstern, 1977). In particular, the contractile skin is able to sustain a tensile force and should therefore be considered independently for stress analysis purposes. However, volumetrically this phase is neglible and may be considered part of the water phase (Fredlund, 1979), which may otherwise be present in a soil in three idealised states:

i) water adsorbed by electro-chemical forces associated with the dipolar nature of water and mineralogy of the soil, and which properties are modified by the electro-chemical forces (and which could thus be classed either as fifth phase or as part of the soil "particle");

ii) water absorbed within the interstices of the particles, and held there by surface tension and/or adsorption; and

iii) "free" water present in the pores between particles and which is either free to move under a gravitational potential or is retained at a particular point by virtue of surface tension effects. As shown in Figure 2.1, such water may be discrete and/or continuous, dependent upon the degree of saturation.

Water is likely to be present also as gaseous water vapour, within the air phase, which itself may be present as either small bubbles within the adsorbed film of water around clay particles, or as absorbed air within the particle interstices, or as "free" air between the particles. Air within adsorbed water is thought to be under very high pressure (Aitchison, 1956) and thus to have a low compressibility with respect to external pressures. The free and absorbed air in contrast may be in either a discrete or continuous form, and will both obey the normal hydrodynamic laws.

The free and absorbed water and air sub-divisions are largely only conceptual as in these states the air and water are free to move in and out of the particle interstices under gravitational, hydrodynamic or thermodynamic influence (Raudkivi and U'u, 1976). However, under the

isothermal conditions considered in this review such movement is considered negligible. It is considered also that adsorbed water does not play a significant role in coarse grained materials like limestone.

2.1.2 Stresses in an Unsaturated Soil

It is necessary to consider total stresses and pore water pressure as in saturated media, and also to consider the pore air pressures and surface tension forces where these act at an interparticle contact, in order to model realistically the various possible states of an unsaturated soil.

The difference in pore air and pore water pressures ($u_A - u_W$) is termed the soil suction, and is comprised of matrix (or capillary) and osmotic components (eg Bolt and Miller, 1958; Olson and Langfelder, 1965). The former is that pressure difference ($u_A > u_W$) resulting from the formation of the contractile skin or an applied pressure differential, and the latter results from variations in spatial ionic concentration. Appropriate techniques for measuring each component individually are available, as reviewed by Krahn and Fredlund (1972), but it is the matrix suction and its variations which appear to affect soil behaviour (Alonso et al, 1987). Only matrix suctions are considered in this review hence forward.

Moisture content variations directly affect the matrix suction. Numerous workers have demonstrated the hysteresis of the suction-water content curve shown diagrammatically in Figure 2.2, and Croney and Coleman (1948) have presented data showing the influence of particle size and clay content on the measured suctions (see Figure 2.3). This work implies that as the coarseness of a soil increases so the maximum suction that may exist in that soil decreases, and this may have encouraged generations of subsequent workers to concentrate on measuring suctions with clays and silts. Figure 2.3 also implies though that large suctions may be present even in coarse grained soils, and these may directly affect its behaviour. Previous researchers have apparently ignored this potential stress or considered it to be negligible in view

of the large gravitational forces involved in coarse soils, and thus quantitative data on suctions in such soils is limited. However, Jones and Hurt (1978) measured matrix suction of up to pF3.9 (778 kPa) during tests on a limestone aggregate at about 2% moisture content, confirming the implication of Figure 2.3.

Other factors affecting suction include relative humidity and temperature (Croney and Coleman, 1960), and experimental data on these factors appears to suggest that these factors have only a small influence generally. It is considered that although these effects are unlikely to be entirely insignificant in a typical trench reinstatment, they are probably of secondary importance under the isothermal conditions considered herein.

The moisture content also directly affects the magnitude of the tensile forces, and hence intergranular stresses, generated where the contractile skin contacts two or more particles. Haines (1925) and Fisher (1926) showed that for water present in a lenticular state (see Figure 2.4) in an ideal soil comprised of spherical particles of radius r, the intergranular force generated between two particles could be expressed as shown in equation 2.1:

$$F = \frac{2 \pi r T}{(1 + \tan \Theta/2)} \qquad \text{..... equation 2.1}$$

where T = surface tension force per unit length of contractile skin

2Θ = angle subtended at the centre of the particle by lenticular water.

In a real soil, the wide range of possible values of "r" renders equation 2.1 of academic interest only. However, for ideal open and close packings, the effective area of any one contact equals $4r^2$ and $\sqrt{2}r^2$, respectively (Aitchison and Donald, 1956), and thus a conceptual view of the change in the magnitude of the intergranular stress in a granular soil due to the combined effects of particle size and water

content (implicitly incorporated through the value of θ) may be derived. Aitchison and Donald calculated this intergranular stress to equal 3.8T/r in a close packing arrangement with the pore water having just drained to the lenticular state and calculated a stress of 12.9T/r immediately before drainage (ie the water is at its limiting moisture tension). They presented data for sand showing the variation of intergranular stress with water content to be of the order 5 to 15 kPa. At low applied stresses this will be a significant factor.

2.1.3 Stress Analysis

Aitchison and Donald expressly considered the most complicated states of Figure 2.1, namely those involving continuous air voids. The analysis of soil containing small occluded air bubbles has long been appreciated to represent an extension of the saturated state to include a compressible pore fluid (eg Hilf, 1956; Koning, 1963; Barden et al, 1965) and numerous workers have considered the mathematical description of the compressibility of such an air water mixture (eg Schuurman, 1966; Fredlund, 1976; Dussealt, 1979; Verruijt, 1982). More recently, soil mechanics problems offshore have lead to research into soils containing large gas bubbles (eg Wheeler, 1988). However, both these cases represent states unlikely to form within a coarse granular trench reinstatement and are not considered further in this review.

The modelling of soils containing continuous air was initially attempted in terms of modified single effective stress equations (eg Croney et al, 1958; Bishop, 1960; Jennings, 1960) by coupling two stress state variables $(\sigma - u_A)$ and $(u_A - u_w)$ in a single equation such as that shown in equation 2.2. This form of equation implicitly incorporates the surface tensions into the term $(u_A - u_w)$.

$$\sigma' = (\sigma - u_A) + X\,(u_A - u_w) \qquad \text{.... equation 2.2}$$

Experimental work on shear behaviour of unsaturated silts and clays (eg Skempton, 1960; Bishop and Donald, 1961; Bishop and Blight, 1963)

initially seemed to confirm the correctness of this simple equation, but the parameter X was soon accepted as being a function (Blight 1965) dependent upon numerous factors including those noted by Aitchison (1965). Further, the function was shown to be discontinuous in nature when applied to collapsing soils (eg Jennings and Burland, 1962; Burland 1965). The phenomenon of collapsing soils showed that the principle of effective stress is not valid in unsaturated soils, as the reduction in suction which may induce collapse represents a decrease in effective stress and would therefore be expected to induce an increase in volume, not a decrease.

As further research demonstrated the fallacy of applying a single effective stress equation to a complex behavioural pattern induced by the soil fabric(s), Bishop and Blight (1963) suggested plotting test results in a three dimensional stress space (see Figure 2.5). This idea of uncoupling the stress state variables has been adopted widely since the mid 1960's to the present day for volume change (eg Burland, 1964; Matyas and Radhakrishna, 1968; Barden et al 1968; Fredlund and Morgenstern, 1976) and shear strength (eg Bishop and Blight, 1963; Fredlund et al, 1978).

In 1968, Matyas and Radhakrishna abandoned the effective stress concept and proposed analysing soil behaviour in terms of stress tensors as shown in equation 2.3:

$$\bar{\sigma}_{ij} = [(P-u_A) + A_w\,(u_A-u_w) + \int T dx]\,\delta_{ij} + \sigma'_{ij} \qquad \text{.... equation 2.3}$$

where $\bar{\sigma}_{ij}$ - equivalent stress transmitted by the solid contacts

P - total mean normal stress $(\sigma_{11} + \sigma_{22} + \sigma_{33})/3$

u_A, u_w - pore air and pore water pressures, respectively

T - surface tension force per unit length of contractile skin

- perimeter of contractile skin

A_w - $\sum a_w/a$ [See Figure 2.6]

δ_{ij} - Kronecker delta

δ'_{ij} - deviatoric stress tensor

Theoretical models to determine the term $\int T dx$ in an idealised soil have been attempted but its value is unobtainable in a real soil as previously realised by Aitchison and Donald (1956). Hence Matyas and Radhakrishna assumed this term is equivalent to At $(u_A - u_w)$ as previously suggested by M.I.T. (1963). However, and as recognised by them, this simplification ignores the fact that "while $(u_A - u_w)$ acts uniformly over the wetted surface of the solid particles, surface tension forces are concentrated at small areas of solid contact. Thus a change in the air water meniscus would not only produce a corresponding change in intergranular stress but could also cause a redistribution in the interparticle stresses". Where the surface tension forces play a significant role in the behaviour of the soil, it may thus be expected that the resultant model proposed by Matyas and Radhakrishna (1968) in terms of the two stress state variables $(\sigma - u_A)$ and $(u_A - u_w)$ could lead to erroneous results.

The same two stress state variables had been previously suggested by Coleman (1962), and were later demonstrated by Fredlund (1973) and Fredlund and Morgenstern (1977) as being suitable for the analysis of soils using the results from a series of oedometer and triaxial volumetric null tests. These variables have been widely adopted in recent research (eg Lloret and Alonso, 1980; Alonso et al, 1987; Toll, 1990; Wheeler, 1991) and represent the state of the art.

2.1.4 Volume Change Behaviour

Following the suggestion by Bishop and Blight (1963), Blight (1965) and Matyas and Radhakrishna (1968) demonstrated that a unique surface in e-$(\sigma - u_A)$ - $(u_A - u_w)$ stress space (see Figure 2.5) was defined by the results of isotropic compression tests on an expansive clay and loess-type soil (Blight) and a mixture of flint powder (80%) and Kaolin (20%) (Matyas and Radhakrishna) provided that:

i) the void ratio was always decreasing, and
ii) the degree of saturation was increasing.

If these conditions were not met then the stress path fell below the state surface due to soil structure hysteresis. Subsequently, Alonso et al (1990) showed from a literature review of experimental work mainly on clays that the volumetric response of such soils is highly dependent on the stress path (eg Maswoswe, 1985). In a clay soil susceptible to swelling, it is apparent that the state surface defines either swelling or collapse behaviour as suction is reduced to zero, dependent upon the mean stress level. Blight (1965) defined the "swelling pressure" as that stress level at which zero volume change occurs as the soil is wetted. Burland (1965) and Barden and Sides (1970) explained this phenomenon in terms of clay "packets" in a flocculated structure. Below the swelling pressure, the swelling of the packets is larger than the volume reduction induced by inter-packet slippage as the suction decreases, and vice versa above the swelling pressure.

In granular soils, the absence of a swelling tendency should result in a volume reduction at all ambient stress levels as the suction decreases. If before a stress increase a large number of the particles are in or near limiting equilibrium, either due to the existing total stress regime or the soil suctions, large collapse settlements may occur in response to the stress change.

A second state surface was also found by Matyas and Radhakrishna (1968), relating the degree of saturation to $(\sigma - u_a)$ and $(u_a - u_w)$, as shown in Figure 2.7. Similar conditions relating its uniqueness applied, as has been confirmed subsequently. In addition it should be noted that the uniqueness of both the state surfaces assumes also that data from soils of similar soil fabric are plotted only. Hence, materials compacted to different dry densities may not be analysed in this way, as noted by Campbell (1973).

A one dimensional mathematical model to describe the generally accepted form of the volume change relationships shown in Figures 2.5 and 2.7 was

first suggested by Fredlund and Hasan (1979) using logarithmic scales for the stresses:

$$e = e_o - C_t \log (\sigma - u_a) - C_m \log (u_a - u_w) \quad \text{... equation 2.4}$$

where C_t, C_m are constant compression indices. The model is based on Terzaghis theory for saturated soils and assumes constant coefficients of permeability for the air and water phases (as defined by Darcy's law).

Although subsequently extended to cover the two dimensional case (Fredlund, 1982), the fundamental flaw in the theory is that it is not valid for all stress ranges as it fails to fully model the variable curvature of the state surface. Lloret and Alonso (1980, 1985) subsequently modified equation 2.4 to overcome the latter problem and enabled the whole warped surface to be approximately modelled.

Recent theoretical studies have largely concentrated on the development of a general constitutive model for unsaturated soils linking volume change and shear strength although some specific consolidation theories are still being proposed (eg Tekinsoy and Haktanir, 1990). Before considering these models, it will be useful to review the models of shear behaviour first. This behaviour was first modelled independent of volume change by Fredlund et al (1978) in terms of a modified Mohr - Coulomb type failure criterion (see Figure 2.8). However, subsequent work showed that a simple linear failure plane in $(\sigma - u_a), (u_a - u_w)$ stress space did not model realistically the observed behaviour of all soils (Escario and Saiz, 1986; Fredlund et al 1987; Escario and Juca, 1989). Nevertheless, Toll (1990) proposed what is essentially an extension of the work by Fredlund et al (1978) in terms of a modified critical state model employing 3 independent variables. This model was based on triaxial tests on a lateritic gravel with 9% clay content. Subsequently, Wheeler (1991) proposed a reduced version of Toll's work using 2 independent variables. However, neither of these models is suitable for the prediction of volumetric behaviour and are applicable in their current form to shear tests only.

Turning once more to a general model for both volume change and shear strength, the critical state model has also been used as a basis (Alonso et al, 1987; Karube, 1988). The most successful model to date appears to be the elasto-plastic model suggested by Alonso et al, (1990). Quantitative predictions made using this model gave reasonable agreement with experimental results published by a variety of authors. However, the model is specifically aimed at predicting the behaviour of expansive clays. No theoretical treatments have been proposed yet dealing specifically with the volume change behaviour of unsaturated granular soils.

2.2 Compression Behaviour of Coarse Granular Soils

Early researchers in the field of granular soils typically concentrated on testing either dry or saturated materials at moderate to high stress levels (eg Jones, 1954; Kjaernsli and Sande, 1963; El - Sohby, 1964; Pellegrino, 1965; Pigeon, 1969). This led to a general appreciation of the factors affecting the compressibility of coarse grained materials, of which the following are noted:

i) compressibility decreases rapidly with increasing relative density

ii) compressibility decreases as the soil grading broadens

iii) grain size is important only for narrow graded materials, compressibility increasing up to a limiting size beyond which an approximately constant value is obtained.

iv) soils comprised of angular particles are more compressible than soils with rounded particles, for a given relative density.

v) compressibility generally decreases with increasing particle strength, and a significant correlation between particle strength and strain at any stress level apparently exists

vi) creep deformations may be expressed as a logarithmic function of time, at least approximately

vii) inundation (or sluicing) may induce collapse settlements

More recent work has concentrated at the higher stress levels also (eg Penman and Charles, 1975; Nataatmadja and Parkin, 1988; Brady and Kirk, 1990) but this current study is concerned primarily with the behaviour of unsaturated materials at low stresses. Recent research directly relevant in part to the current work has been recently reported by Brady and Kirk (1990). The results of relatively simple incremental loading tests on a limestone aggregate at low to high stresses were presented, and this data is discussed further in section 8.5. Other work that has been reported at lower stresses has been particularly related to the behaviour of road materials under repeated loads. Pappin (1979) investigated the resilient behaviour of a well graded crushed limestone at low to moderate stresses, and also included a limited number of tests on partially saturated soil. McVay and Taesiri (1985) also investigated the cyclic behaviour of pavement base materials, and Thom and Brown (1988) investigated the effect of grading and density on the mechanical properties of a crushed dolomite. The general applicability of the influences noted to be relevant at higher stresses has not been questioned as a result of this work, and thus it may be expected that granular reinstatement behaviour will follow these general rules also.

The influence of non-saturation on the settlement of granular soils has largely been neglected also. None of the workers noted above expressly considered the influence of soil suctions induced by non-saturation on the behaviour. Similarly field records of the settlement of rockfill dams (eg Clements, 1984) and backfills (eg Leigh and Rainbow, 1979; Brandon et al, 1990) have often been reported but suction determinations have not been made in order to quantitatively link the variation of this parameter, either due to sluicing, rainfall or groundwater recharge, to settlements, although settlements are generally accepted as resulting from these moisture changes (eg Charles et al, 1984).

More recently Houston et al (1988) and El-Ehwany and Houston (1990) reported results of a monitoring programme for a full-scale footing on a collapsible soil subjected to water infiltration from above. This programme included field suction measurements, and laboratory studies of moisture infiltration rates were reported also. Their work clearly demonstrated the influence of the reduction in soil suction from pF5.26 (17850 kPa) to pF4.4 (2460 kPa) due to the passage of a sharp wetting front down the soil profile on the settlement records (see Figure 2.9). The existence of the sharp wetting front was inferred from the suction profile following 2 distinct water infiltration events, and confirmed earlier work by Bond and Collis-George (1981) and others regarding this feature.

In the absence of suction measurements, and possibly the belief that suctions could affect the behaviour of coarse materials, settlements due to inundation have variously been attributed to reduction of interparticle friction due to wetting (Pigeon, 1969), the washing of fines into the voids between particles (Roberts, 1958), and reduction in particle strength leading to crushing at the interparticle contacts (Terzaghi, 1960). However, published opinion and data are divided with respect to each of these explanations.

Pigeon (1969) reported reduced interparticle friction for a mudstone and a granite due to wetting, whereas Terzaghi (1960) found no such effect in his work. It is suggested that slightly reduced frictional properties may result provided additional water is able to get between particle contacts, but the net effect of such ingress of water is likely to be small in terms of settlements. In the case of an absorbent material, such additional water could accrue even without interparticle movement as the material wets up from a particularly dry state, but beyond some critical water content, expressed possibly as a percentage of the saturated water content of the aggregate, negligible effects could be expected as sufficient water would already be present at the contact for the coefficient of friction to be at a minimum already. In a low absorbency aggregate, particle movement would be required for water to get between otherwise dry contacts and thus for any effect on the frictional properties to be manifested.

With respect to the washing of fines inducing settlements, previous workers (eg Pigeon, 1969) have found it difficult to conceptualise the process by which the movements would occur. It is considered that decreased stability due to the destruction of surface tension forces between fines near a contact between several larger particles may be involved, but in the absence of this mechanism the action of sluicing away non-structural fines cannot affect the behaviour. Turning to the structural fines which form part of the compaction induced soil skeleton, such fines would surely not be washed away unless high water velocities were involved or the fines reduced in strength and/or stiffness following wetting, and either crushing of elastic compression occurred. Hence settlements resulting from this source are likely to be very small.

Thus only the crushing of particles following water softening is a likely alternative mechanism to suction stresses. Kjaernsli and Sandes (1963) found that the unconfined compressive strength of all the materials they tested decreased when the rock was saturated. Similar results have been reported by others, although some workers failed to find this effect in all materials tested (eg Sowers et al, 1965). If the decrease in strength is reflected also in a reduced stiffness, movements could result from crushing and elastic compression.

The magnitude of crushing may be quantified by measuring the particle breakdown of a soil under load. Various methods have been proposed using the change in particle size distributions (eg Inman, 1952; Marsal, 1965, Pigeon, 1969), and Marsal (1967) proposed a simple relationship between his breakdown index, the average normal contact force between particles, and the strength of the particles. However, this relationship presupposed that the contact forces could be calculated reliably, and that the normal contact force was the major influence on crushing. Methods to calculate the former have been attempted over the years (eg Marsal, 1963; Schlosser and Walter, 1986) with varying degrees of success, and conceptually it is difficult to justify the latter assumption. In fact, Brauns and Leussink (1967) showed that for regular packings of spheres shear stresses are the major influence on crushing. No other relationships have since been

proposed to the knowledge of the author, and it is now generally accepted that crushing is taken to be quantified by the change in the grading curve.

As a final note, Pigeon (1969) reported work by Howkins that showed compression due to wetting of a mudstone was related to the degree of saturation, and that beyond a critical value of 7% water content the strains were equal to those for saturated specimens. This effect could be related to either suction effects or degradation and loss of strength in the mudstone, but unfortunately no strength tests were carried out.

2.3 Experimental Difficulties of Testing Unsaturated Coarse Granular Soils

2.3.1 Unsaturated Soils

In order to accurately measure the volume change behaviour of all the volumetrically significant phases in an unsaturated soil, it is necessary to measure changes of all but one of the total volume and air phase and water phase volumes, if it is assumed that at low stresses the change in volume of the soil particles is negligible. Due to the effects of temperature and pressure on the air phase, it is this volume which is frequently calculated rather than measured (Fredlund, 1973). In addition, it is necessary to account for all possible losses of air and water volume, and to measure and/or control the pore air and pore water pressures independently. Standard techniques for saturated soils may generally be used, with the exception of pore water pressure and air volume measurements for specimens with continuous air voids.

The direct measurement of negative pore water pressures that result if the continuous air voids in a specimen are open to the atmosphere has long been appreciated (Bishop, 1960) as impractical, and impossible at water pressures less than one atmosphere below atmospheric due to cavitation of the water. Hilf (1956) was the first to use the axis-translation technique, whereby a known air pressure greater than atmospheric is applied to the specimen such that the pore water pressures become greater

than atmospheric, ie positive gauge pressure. The veracity of this technique was demonstrated by Olson and Langfelder (1965) and modelled theoretically by Bocking and Fredlund (1980), and it has subsequently become standard practice for testing unsaturated soils.

Despite the positive pore water pressure established in the soil, it is still necessary to separate the air and water pressures. This is conventionally done (eg Gibbs and Coffey, 1969; Barden et al, 1969; Fredlund, 1973, Maswoswe, 1985) using high air entry value ceramics, which rely on fine pores saturated with water to transmit the pore water pressures to a transducer behind the ceramic. Air pressure is prevented from reaching the transducer by virtue of surface tension effects, provided the water column is maintained continuous. However, air may still diffuse through the ceramic and gradually accumulate near the transducer, leading to erroneous pressure measurements. As a result, various techniques to flush the diffused air away and measure its volume have been improvised (eg Bishop and Donald, 1961; Fredlund, 1975). It is generally recognised that some such device is an essential for accurate measurements, but not all early workers appreciated this (eg Matyas and Radhakrishna, 1968; Aitchison and Woodburn 1969). All experimental data from tests of more than about 1 day duration which do not allow for diffused air should be treated with caution.

As an alternative to high air entry ceramics, or in addition, some workers have made use of the filter paper approach (eg El-Ehwany and Houston, 1990). For standard filter papers, the percentage increase in weight of the paper by water absorbtion is directly related to the soil suction. Such an approach has often been used in triaxial equipment.

If high air entry ceramics are used though, Fredlund and Morgenstern (1973) noted that low permeability to water of the ceramics will cause time lag, and thus proposed a model to predict this lag. Figure 2.10 shows a typical reponse curve obtained by Fredlund (1973) during his doctoral research. Theoretical studies of the compliance in the pressure measurement system were made also by Fredlund, but require the knowledge of a compliance factor to predict the response.

The major problems related to testing coarse granular soils are specimen size and membrane penetration. Head (1982) quotes a height to diameter ratio of between 1/3 and 1/4 as being the optimum range for consolidation tests, in order to minimise the effects of side friction whilst ensuring the height is sufficiently large for accurate strain measurements. Pigeon (1969) similarly suggests on the basis of side friction measurements and calculations a ratio of 1/2 or less for consolidation tests.

As the ratio decreases, so the frictional component of a total stress increase will decrease proportionately, but at the risk of invalidating the test data due to the ratio of height to maximum particle size. Penman (1971) suggested minimum ratios of specimen dimension (ie height) to maximum particle size of 4 and 6 for well and narrowly graded specimens respectively. This ratio appears to be generally accepted based upon published details of experimental apparatus and specimens tested therein. Kjaernsli and Sandes (1963) used particles up to 125 mm nominal diameter in a floating ring oedometer approximately 500 mm high and 1000 mm diameter, and a similar apparatus has been built at the Building Research Establishment (Penman and Charles, 1975). Marsal (1973) tested 76 mm particles in 500 mm diameter by 500 mm high specimens, and this minimum was observed also by Boyce (1976) and Egretti and Singh (1988).

Membrane penetration into a triaxial specimen of coarse granular soil is a phenomenon that has long been recognised (Newland and Allely, 1959). It can lead to pore pressure changes in saturated media, and in unsaturated media depending upon the degree of saturation, and can cause erroneous phase volume changes to be measured. Numerous workers have proposed correction formulae, based upon work with mainly sand and silt sized particles (Frydman et al, 1973; Romana and Raju, 1982; Vaid and Negussey, 1984) and others have suggested mitigating procedures such as the use of liquid rubber coatings to the specimens (Kiekbusch and Schupenner, 1977) or thicker membranes (Frydman et al, 1973).

2.3.2 Coarse Granular Soils

The major problems related to testing coarse granular soils are specimen size and membrane penetration. Head (1982) quotes a height to diameter ratio of between 1/3 and 1/4 as being the optimum range for consolidation tests, in order to minimise the effects of side friction whilst ensuring the height is sufficiently large for accurate strain measurements. Pigeon (1969) similarly suggests on the basis of side friction measurements and calculations a ratio of 1/2 or less for consolidation tests.

As the ratio decreases, so the frictional component of a total stress increase will decrease proportionately, but at the risk of invalidating the test data due to the ratio of height to maximum particle size. Penman (1971) suggested minimum ratios of specimen dimension (ie height) to maximum particle size of 4 and 6 for well and narrowly graded specimens respectively. This ratio appears to be generally accepted based upon published details of experimental apparatus and specimens tested therein. Kjaernsli and Sandes (1963) used particles up to 125 mm nominal diameter in a floating ring oedometer approximately 500 mm high and 1000 mm diameter, and a similar apparatus has been built at the Building Research Establishment (Penman and Charles, 1975). Marsal (1973) tested 76 mm particles in 500 mm diameter by 500 mm high specimens, and this minimum was observed also by Boyce (1976) and Egretti and Singh (1988).

Membrane penetration into a triaxial specimen of coarse granular soil is a phenomenon that has long been recognised (Newland and Allely, 1959). It can lead to pore pressure changes in saturated media, and in unsaturated media depending upon the degree of saturation, and can cause erroneous phase volume changes to be measured. Numerous workers have proposed correction formulae, based upon work with mainly sand and silt sized particles (Frydman et al, 1973; Romana and Raju, 1982; Vaid and Negussey, 1984) and others have suggested mitigating procedures such as the use of liquid rubber coatings to the specimens (Kiekbusch and Schupenner, 1977) or thicker membranes (Frydman et al, 1973).

In a saturated coarse granular soil, the effects may be expected to be far greater than in sands, as shown in Figure 2.11. Consideration of the effects on unsaturated coarse granular materials appears to be lacking in the literature, though Evans (1987) reported on the effect on undrained cyclic triaxial tests on dry gravel. If a high degree of saturation exists, the problems will be similar to those for saturated media, but the induced pore pressure changes would in turn lead to compression of the occluded air. If the air is continuous and drained, pore water pressure changes may be expected to be minimal, as penetration will be at the expense of changes in the air volume. This artificial replacement of the air should be treated as part of the air volume, and hence a correction should be applied. If the air is continuous and undrained, both pore water and pore air pressures will be affected due to changes in the air volume.

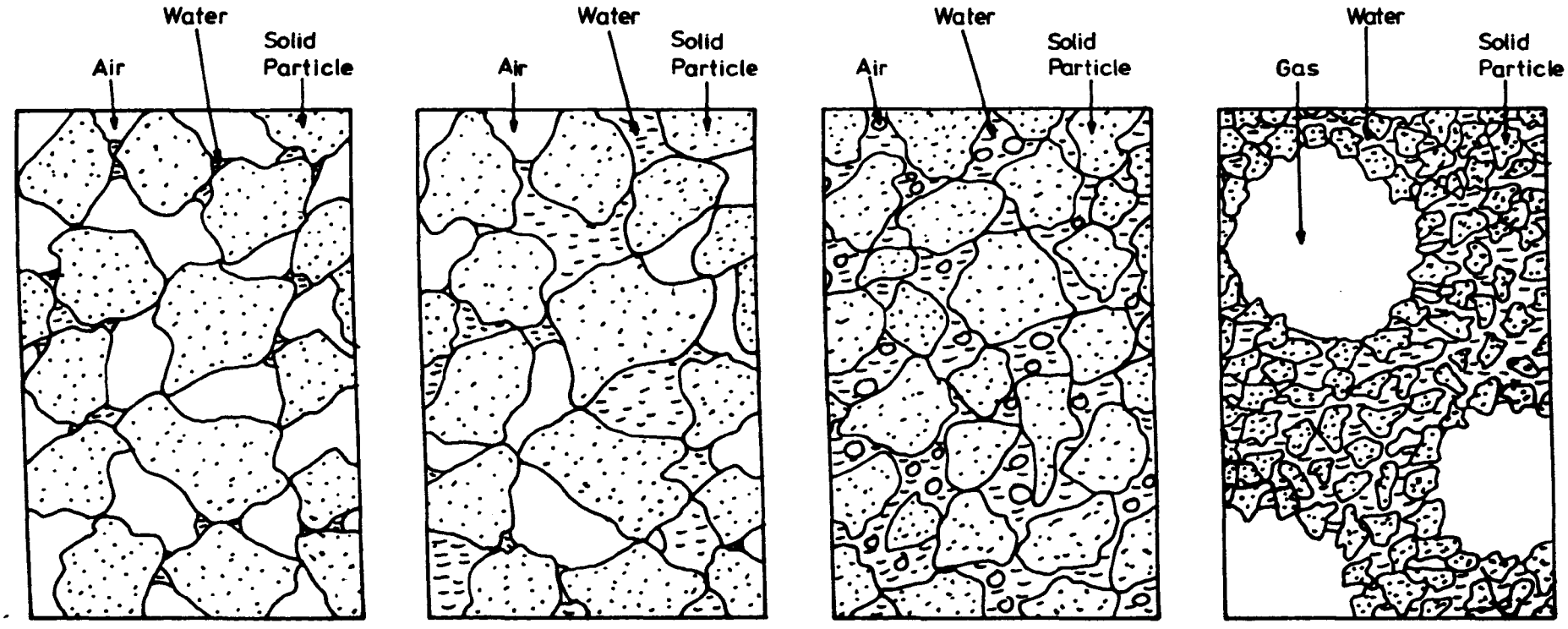

Figure 2.1 Categories Of Unsaturated Soil

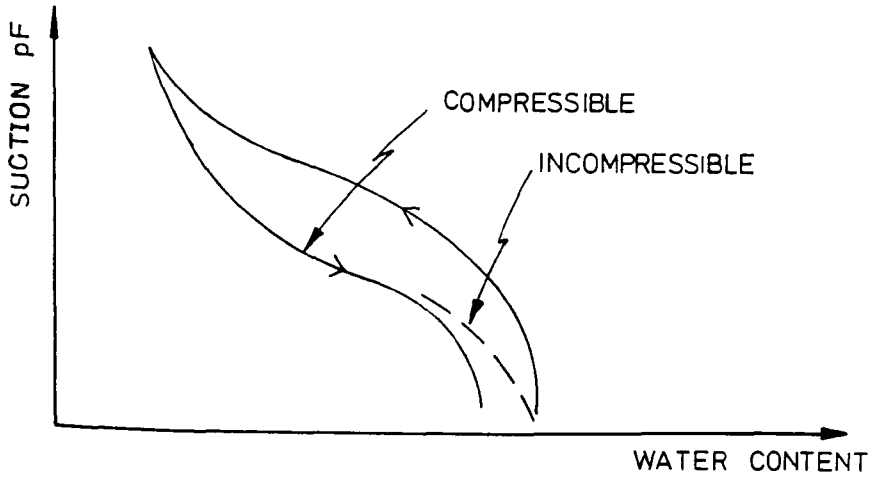

Figure 2·2 Hysteresis of Suction - Water Content Curve

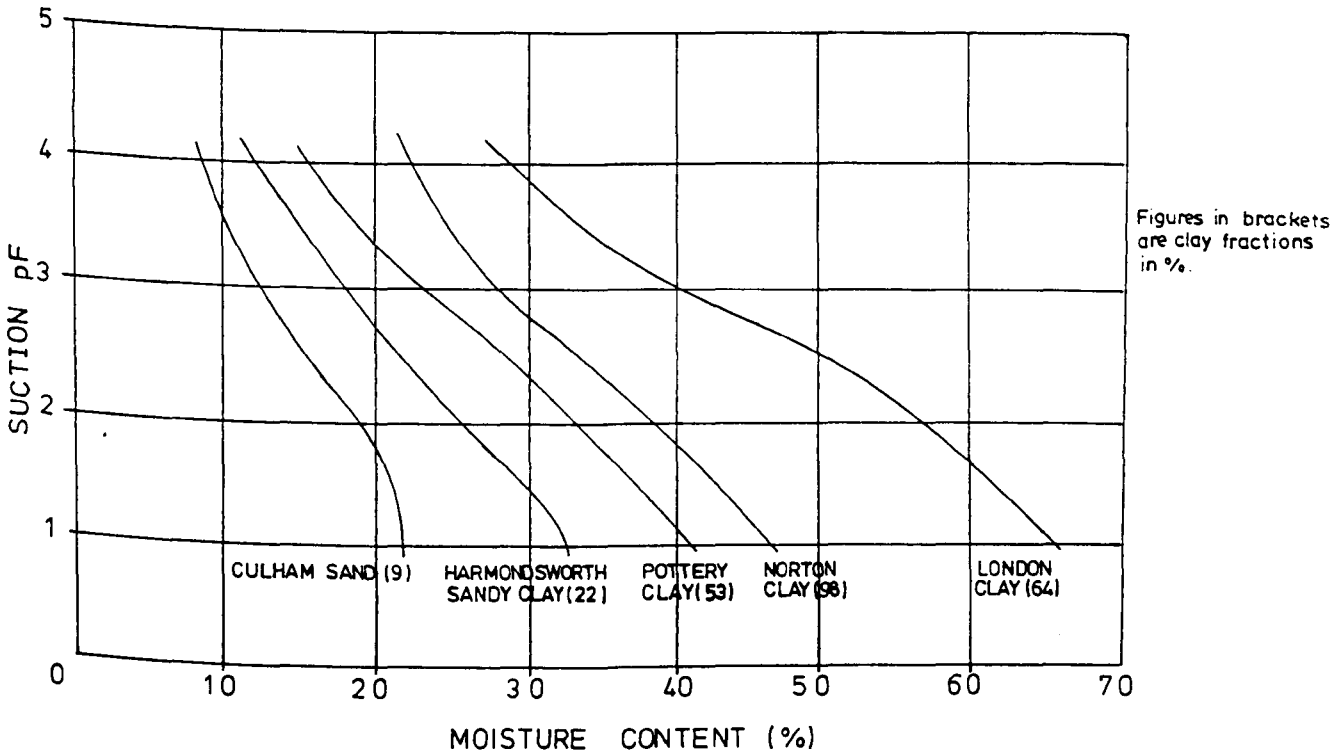

Figure 2·3 - Effect of Clay Fraction on Suction (after Croney and Coleman 1948)

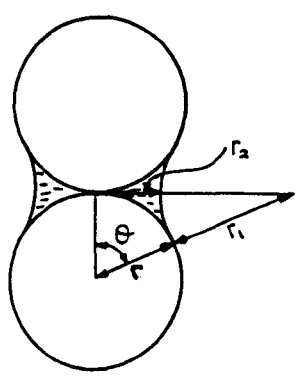

Figure 2·4 Lenticular Phase Of Pore Water

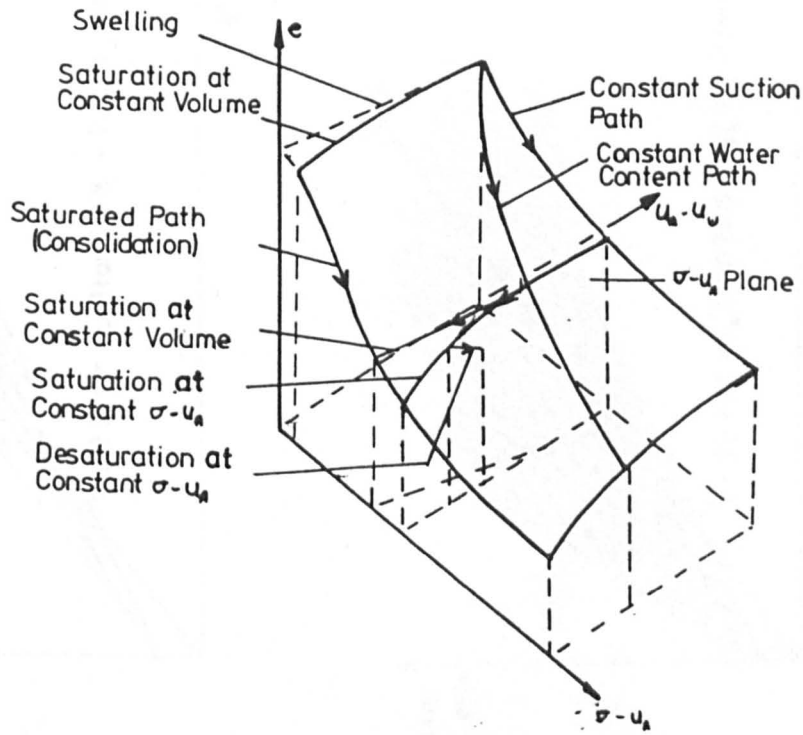

Figure 2.5 – State Surface for Volume Change Behaviour
(after Matyas and Radhakrishna,1968)

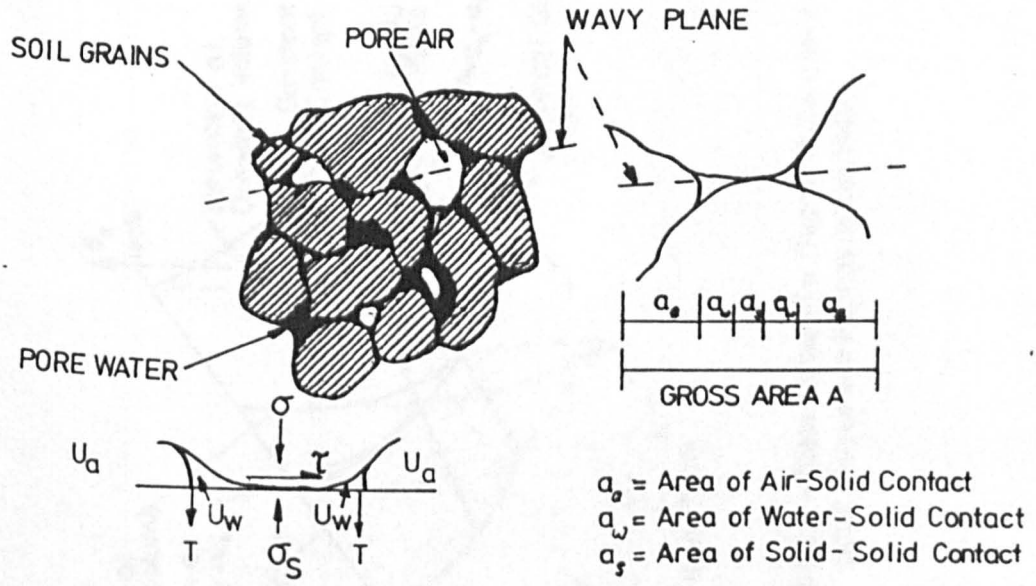

Figure 2.6 – Model of Unsaturated Soil
(after Matyas and Radhakrishna.1968)

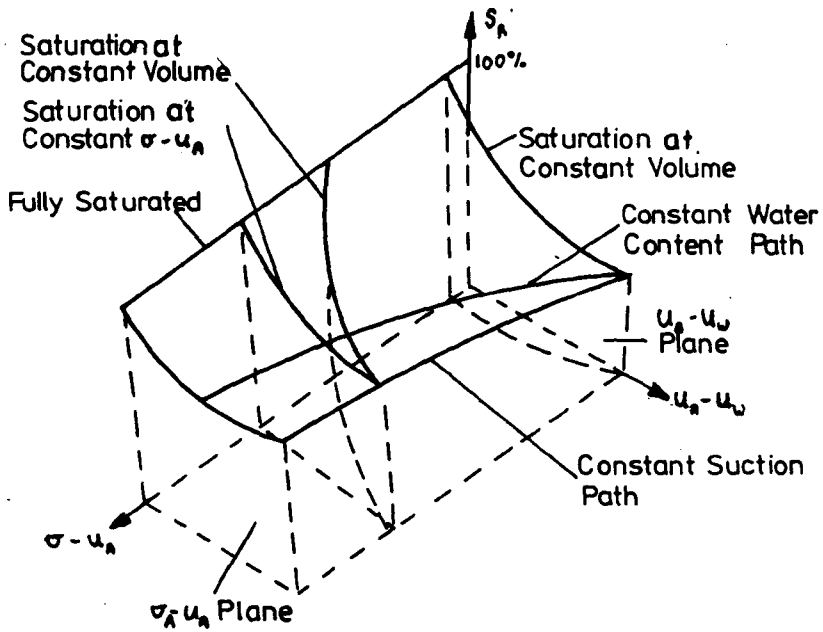

Figure 2.7 – State Surface for Degree of Saturation
(after Matyas and Radhakrishna,1968)

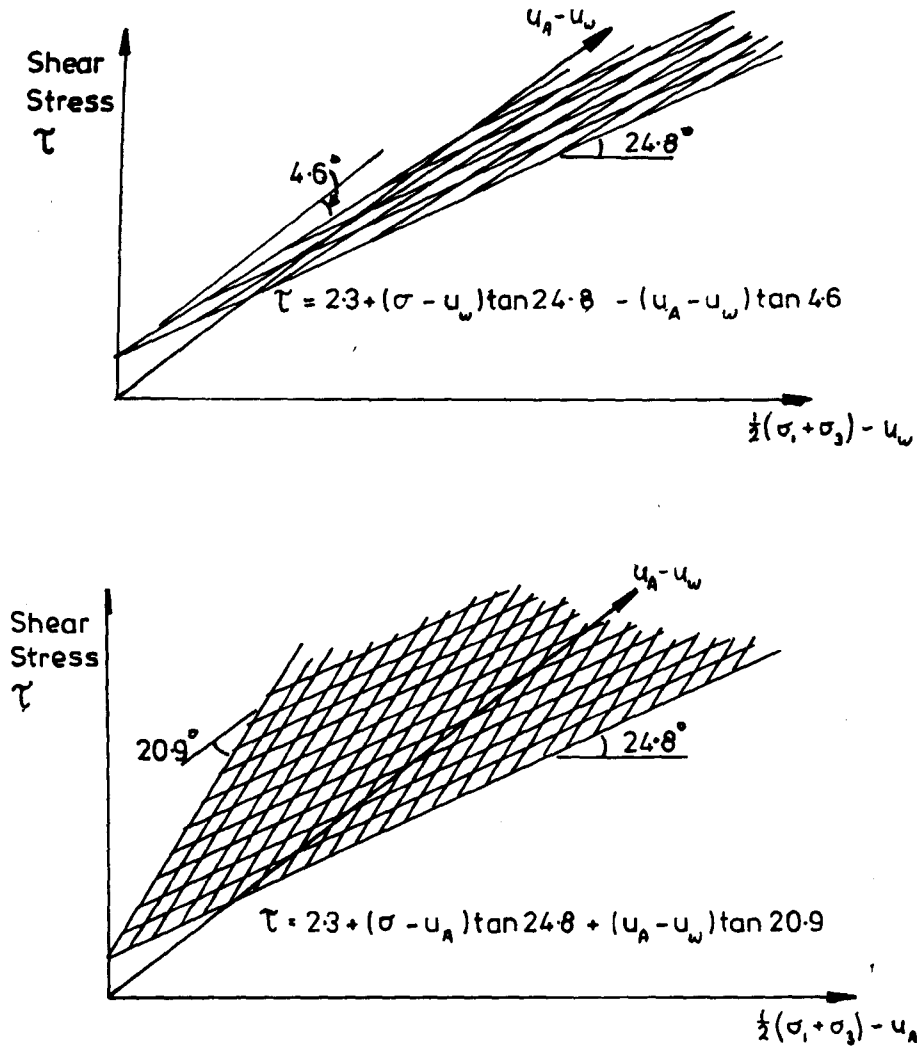

Figure 2.8 – Failure Criteria for Unsaturated Soils
(after Fredlund et al,1978)

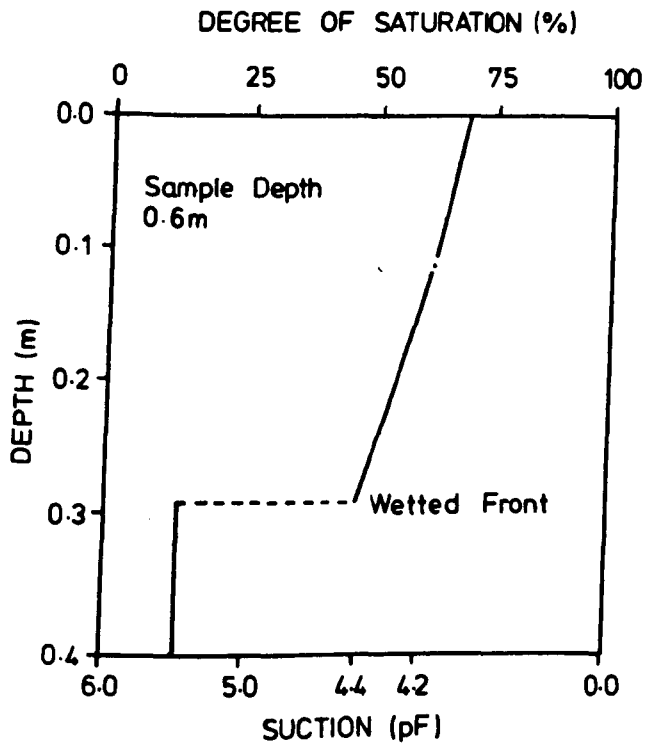

Figure 2·9 - Effect Of Wetting On The Suction Profile In A Soil (After El-Ehwany And Houston, 1990)

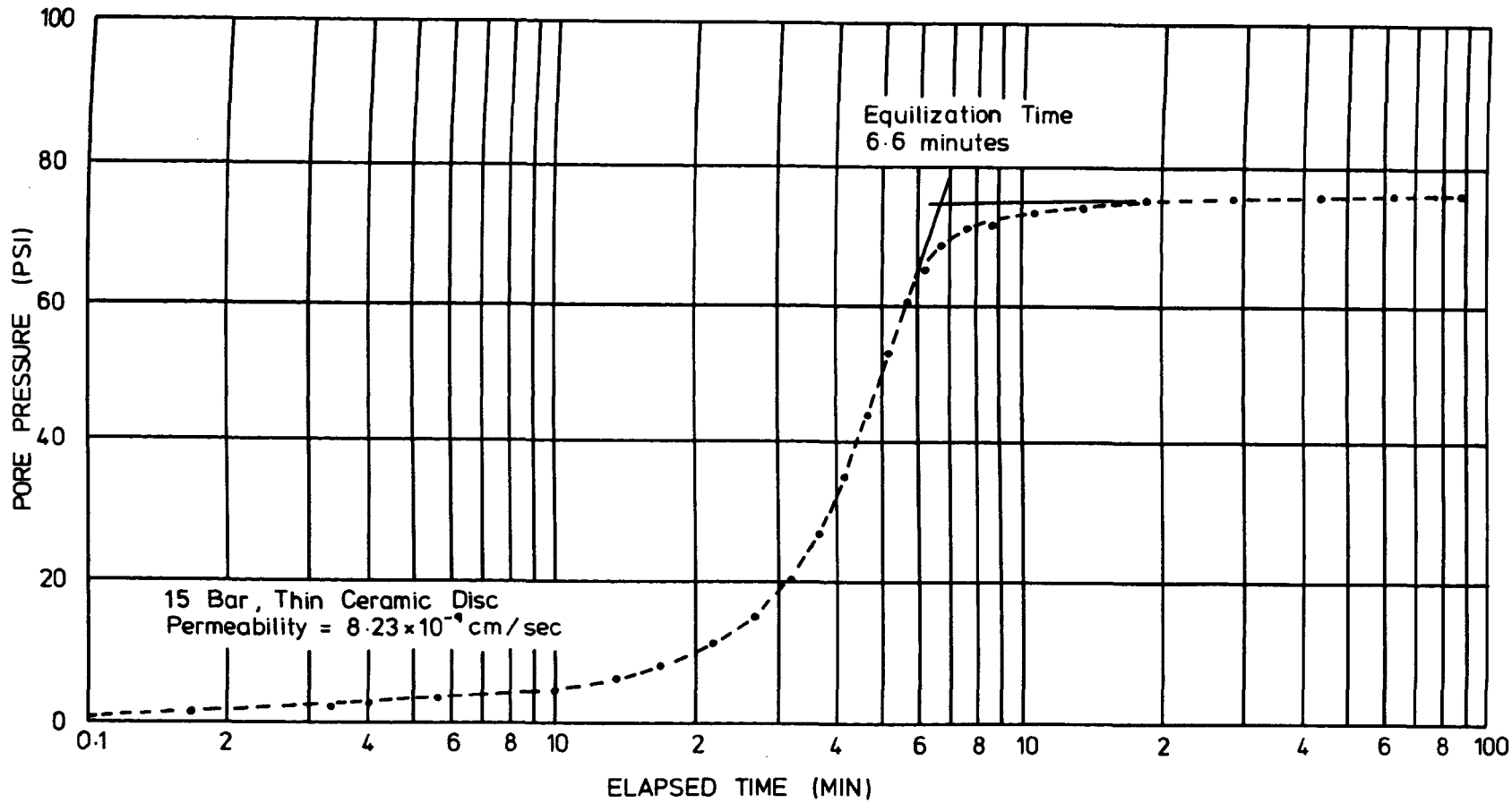

Figure 2·10 Typical Pore Water Pressure Response Curve For High Air Entry Value Ceramic (after Fredlund, 1973)

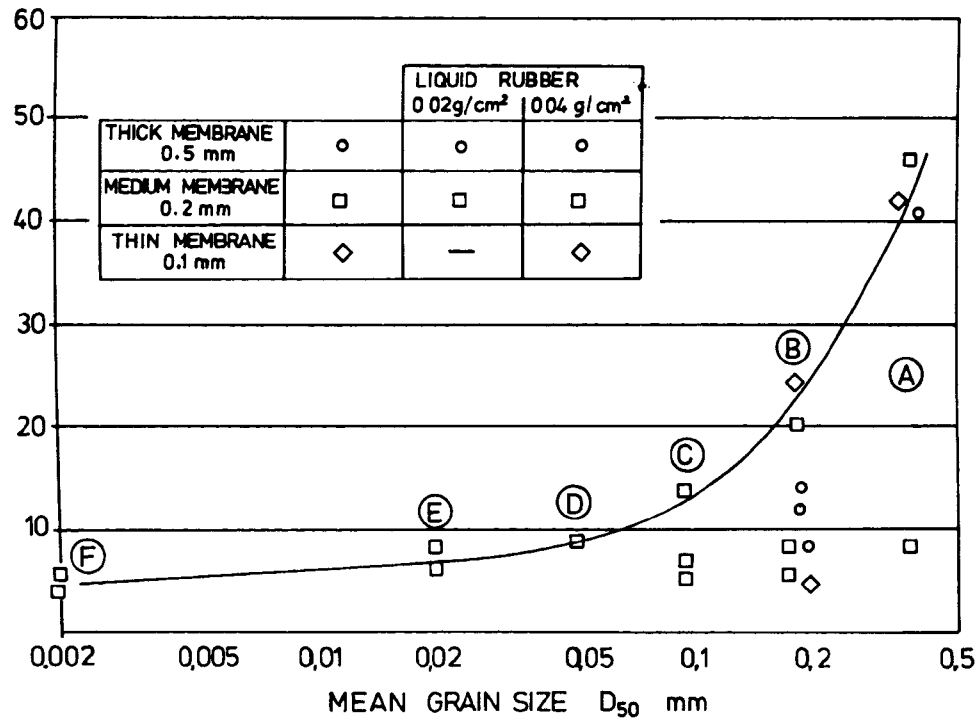

Figure 2·11 - Effect of Particle Size on Membrane Penetration.

(after Kiekbusch and Schuppener, 1977)

CHAPTER 3

TEST MATERIALS

The importance of a full and accurate description of a soil has long been recognised as a pre-requisite to the confident interpretation of test data. There are numerous discussions in the literature on the quantitative description of a grading by single or multiple parameters (eg Selley, 1976), on measures of particle strength (eg Pigeon, 1969; BS812: 1975), and on measures of particle shape (eg Marsal, 1963), but less information is available on the relative merits of the various parameters suggested in relation to the behaviour of soil under load. The classification tests performed on the test materials used in the experimental programme have been chosen from those available in the literature with an engineering usage in mind. New indices have deliberately not been introduced though some modifications have been made.

3.1 Origin and Description of Test Material

The test material was a limestone aggregate supplied by North Tyne Roadstone Limited from the Mootlaw Quarry, near Matfen, Northumberland. The material belongs to the Upper Limestone Series of the Upper Carboniferous Period, is known locally as Blue Mountain Limestone, and may be described as blue-grey in colour, fine grained, with occasional veins of calcite.

The aggregate was supplied pre-bagged in four industrially sieved nominal size ranges of less than 5 mm, 5 mm to 10 mm, 10 mm to 20 mm, and 20 mm to 40 mm (see Plate 3.1). The 'as supplied' particle size distributions of the aggregates were determined using wet sieving (Test 7A of BS1377; 1975) and are shown in Figure 3.1. A petrographic analysis on a representative sample of the aggregate using X-Ray Fluorescence gave the chemical composition listed in Table 3.1, which is typical of Carboniferous Limestone.

3.2 Test Gradings

3.2.1 Specification Compliance

Unbound materials used in trenches (see Figure 3.2) usually comply with the Department of Transport (DTp) Specification for Highway Works, 1986, or its earlier version, the Specification for Road and Bridge Works 1975. In order to test gradings representative of field practices, the clauses listed in Table 3.2 were adopted as guidelines for choosing the gradings to be used in the research project. The gradings were chosen also to investigate the effect of maximum particle size, and to yield data that could be compared with published test results on fine and very coarse materials.

Calculations using the wet sieve grading curves of the supplied aggregate were made to determine the mix ratios required to prepare suitable materials. The final proportions used, the calculated nominal gradings and the DTp grading envelopes are shown in Figures 3.3a to 3.3c.

3.2.2 Preparation of Test Gradings

The gradings were batched in a 180 kg capacity concrete mixing drum in total batch masses varying from 50 kg to 150 kg. The aggregate was added to the drum in an air dry condition in the required proportions and mixed for a period of 10 minutes per 100 kg. Following this the material was tipped onto a clean dry concrete floor and quartered until specimens suitable for the intended tests were produced. These were double bagged and stored ready for testing. Details of the batching procedure are presented in Appendix A.

A preliminary test series verified that consistent results were produced using this method provided that at least two source bags of any size fraction were used for each batch. As a standard laboratory precaution, two wet sieve analyses were made on representative specimens from every subsequent batch to check for deviations from the expected grading.

Figure 3.4 shows that the level of repeatability obtained was good, but comparison of the grading curves with the expected nominal gradings calculated previously from the 'as supplied' gradings showed that significant breakdown was occurring during batching (see Figure 3.5). Similar differences had been observed during the preliminary work. The cause of the discrepancy was investigated by preparing carefully by hand, as opposed to using the concrete mixer, five specimens and comparing the results of wet sieve analyses on these with the calculated nominal gradings. Negligible differences were found, confirming that breakdown was occurring as a result of using the automatic batcher.

Despite the breakdown, no changes were made to the established procedure as the DTp specification was still being complied with, and the automated mixing procedure was similar to that used by North Tyne Roadstone for production of commercially used materials. The final gradings actually tested are presented in Figure 3.5c.

3.3 Particle Classification Tests

3.3.1 Specific Gravity

Specific gravity determinations were made using test 6A and 6B of BS1377: 1975, and during aggregate absorption value tests (see section 3.3.2). An average of 2.71 was consistently recorded during the 16 tests on the coarse (>5 mm) fraction of the medium and coarse test gradings, whereas 8 tests on the fine grading (minus particles greater than 2 mm) all gave a value of 2.75. A further 24 tests on material less than 5 mm using a pycnometer gave results varying between 2.6 and 2.8, with an average of 2.67, but this scatter was later attributed to equipment problems and the results should be treated with caution.

It is considered that the recorded higher specific gravity for the fines represents a real difference in material properties between the coarse and fine fractions, as produced by quarrying. Nataatmadja and Parkin (1988) also found a higher specific gravity for the fine fraction of base course

materials. Possible causes are the presence of calcite veins in the coarse particles, or a tendency for fines produced by blasting to exclude the larger particle interstices, or both. The average value of 2.71 obtained over several months, and valid for the majority fraction of all gradings, has been adopted in all calculations.

3.3.2 Aggregate Absorption Value Tests

A total of 8 samples per grading were tested in accordance with methods 5.4 and 5.5 of BS812: Part 2: 1975. Each sample was sieved to produce two specimens, one containing particles between 5 mm and 63 microns, and the other containing particles greater than 5 mm. All were tested using the appropriate method and the results are presented in Table 3.3. The data was used to calculate the absorption value for each test grading using the relative fractions of the fine and coarse size ranges in the gradings and assuming that the material passing through the 63 microns sieve had an absorption equal to that for the material less than 5 mm. The calculations yielded the following results which show the importance of particle size on absorption characteristics:

Coarse grading, absorption value = 0.8%
Medium grading, absorption value = 1.2%
Fine grading, absorption value = 1.4%

These absorption values have been used in the analysis of the main test series to calculate soil parameters, such as water content and degree of saturation, by assuming the absorbed water forms part of the "solids" component. Table 3.4 summarises the definitions of the classical soil parameters based on this premise.

3.3.3 Grain Shape

The structural arrangement and behaviour of granular materials is influenced by the grain shape. Numerous quantitative and qualitative parameters have been reported in the sedimentary petrology literature to

describe particles in terms of their overall form (eg Aschenbrenner, 1956) and the roundness of their asperities (eg Wadell, 1932), but engineers have preferred to use a qualitative assessment of a single parameter, the "angularity" of a particle (Head, 1980). Angularity is largely a measure of roundness although it takes account of the amount of curvature between asperities as well and, as such, is a partial measure of overall form. A quantitative measure of angularity was put forward by Lees (1963).

A quantitative approach has been adopted during this work. The average overall partical shape of the test material has been assessed by measuring the principal dimensions (a, b, c where $a > b > c$) of a representative number of particles, and plotting the dimensional ratios b/a and c/b against each other as shown in Figure 3.6. Based upon this diagram, a general descriptive term for the particle shape using the ratio limits suggested by Lees (1964) has been attributed to the particle. In addition, the Degree of Angularity proposed by Lees (1963) has been adopted as a quantitative measure of particle shape as it is believed this method is correct in its recognition of the importance of the roundness of the asperities and the relationship between the asperities.

A total of 124 particles from five size ranges, varying from 5 mm to 50 mm in nominal diameter, were examined. The particles were placed individually on a three sided orthogonal perspex container, and the images of the three principal planes cast onto a wall in turn using an overhead projector. To eliminate scale effects, all particle images were made similar in size by moving the projector relative to the wall. The tracings of these images, and the calculated magnification ratio, were later used to determine the principal dimensions and the degree of angularity of the particles.

The results of the current work are summarised in Tables 3.5 and 3.6. The estimation chart used is reproduced from Lees (1963) as Figure 3.7, and the dimensional ratios for each of the size ranges are summarised in Figure 3.8.

Examination of the results shows that the majority of the particles, regardless of size, are intermediate between "flaky" and "equidimensional", with the overall average lying on the arbitrary boundary between these shapes. The standard deviation of the shape distribution for each size range is similar, confirming that the size of particle has little effect on its shape within the limits of this work.

The degree of angularity of all the particles is generally 2100 ± 200, although the angularity of the finest particles appears to be slightly higher with a value of 2500. In conventional terminology, the particles may be described as "angular" to "sub-angular". An approximate correlation suggested to relate this usually qualitative description to the quantitative degree of angularity is presented in Figure 3.9.

3.3.4 Strength Tests

The compressibility of a particulate mass will be influenced by the strength of its individual components and their susceptability to crushing as noted in section 2.2. In dry or saturated soil, the products of particle degradation are unlikely to affect the soil mass other than to effect a reduction in pore space and hence permeability. In unsaturated soils, the collection of finer particles in the voids between the main load carrying particles may cause some local re-distribution of free water and its associated surface tension forces. This may induce further local instabilities and small time dependent creep settlement. It is therefore considered important to obtain an assessment of particle strength.

The traditional method for measuring rock strength is the unconfined compression test which requires carefully trimmed specimens and is time consuming. As a result only a small number of specimens are usually tested. Further, weak specimens may fracture during preparation and will not be tested, tending to lead to overestimated strengths. Other methods of assessing rock strength are available, such as point load tests or irregular lump tests. However the applicability of the strength of the intact rock to the behaviour of its aggregate form has been shown to be

inconsistent (Dhir et al, 1971), and direct measures of the performance of the aggregate are preferred. BS812: 1975 details three such tests, namely Aggregate Crushing Value (ACV), Aggregate Impact Value (AIV), and 10% Fines Value. The ACV and AIV measure the resistance to pulverisation of a uniform aggregate under static and dynamic loading conditions respectively. The 10% Fines test is a variation on the ACV test.

The ACV and AIV tests have been used to classify the aggregate in the present work, and values of 22 and 18 were obtained respectively. Similar numerical values were expected, as the AIV was intended to be auxiliary to the ACV by design. Further discussion of these and other strength tests is contained in a report edited by Collis and Fox (1985).

3.4 Behavioural Characteristics of Gradings

3.4.1 Limiting Density Tests

The behaviour of granular soil depends amongst other things upon the initial density and packing arrangement of the mass. However, for a given soil, its density will take some account of its packing arrangement particularly if related to the limiting densities for that soil. This indication has been accepted as sufficient for present purposes, even though it is appreciated that, for spheres at least, more than one packing arrangement will give the same density (Graton and Frazer, 1935).

The limiting densities of a given soil are material properties, but standard methods for their determination were not available until publication after the research was completed of BS1377:1990. The methods of test that had been adopted in the absence of a British Standard were based on those proposed by Kolbuzewski (1948) and Head (1980) for materials ranging from clean sands to gravelly soils. BS1377:1990 appears also to be based upon these references, and the methods used in this research were largely in accordance with the new standard.

3.4.1.1 Minimum Density

Four specimens of each grading were tested, yielding consistent minimum densities of 1.56 Mg/m^3 and 1.63 Mg/m^3 for the fine and medium gradings respectively, or maximum void ratios of 0.74 and 0.66 respectively. For the coarse grading, small variations in the minimum density were recorded, the average value being 1.61 Mg/m^3, or a maximum void ratio of 0.68.

3.4.1.2 Maximum Density

The maximum densities obtained were 2.30 Mg/m^3, 2.33 Mg/m^3 and 2.39 Mg/m^3 for the fine, medium and coarse gradings, respectively, or in terms of minimum void ratio, 0.18, 0.16 and 0.13, respectively.

The particle breakdown of each grading during the tests was investigated also. The results of wet-sieve analyses on two specimens of each grading are compared with their pre-compacted gradings in Figure 3.10 a, b, c.

3.4.2 Compaction Characteristics

The results of the compaction stages of all main series tests in which the compactive effort was not a variable (see Chapter 4 and Appendix A), plus extra compaction tests at the same compactive effort, are presented in Figure 3.11 for the coarse grading. It is apparent from this figure that the optimum free water content is 6.4%, with an associated maximum dry density of 2.275 Mg/m^3. This condition is equivalent to a void ratio of 0.20, or a relative density of 88%. In Figure 3.12, comparison of these characteristics has been made with the results of compaction data on a similar test material (grading curve given in Figure 3.13) provided by British Gas Engineering Research Station using BS1377:1975 Tests 12, 13 and 14. This figure suggests that the compactive effort applied in the majority of tests reported in this thesis probably lies between that applied by BS1377:1975 Tests 12 and 13. However, this comparison between compaction results is not strictly accurate as the materials involved were undoubtedly dissimilar in some respects, as indicated by a comparison

between the maximum dry density achieved during the compaction of the non-standard material to BS1377:1975 Test 14, and the maximum limiting density reported in section 3.4.1.2.

Insufficient data has been collected to define the optimum water content and maximum dry density achieved using the standard compactive effort for the fine and medium gradings. The compaction data obtained during the main series tests are presented in Figure 3.14 along with the dry density-free water content relationship for the coarse grading. This figure clearly shows that, as the coarseness of the soil increases, the dry density achieved for the given compactive effort increases for a given free water content. Comparison of the relative densities achieved for each grading at the optimum compaction conditions are not possible, but at a free water content of 3.0%, the relative densities achieved were 32%, 39% and 68%, for the fine, medium and coarse gradings respectively.

Table 3.1 Results of Petrographic Analysis on Quarried Limestone Aggregate

Chemical Compound	Percentage of Total, by Mass
$CaCO_3$	79.97
$MgCO_3$	11.50
SiO_2	2.80
$CaSO_4$	2.28
Fe_2O_3	2.03
Al_2O_3	1.00
K_2O	0.12
MnO	0.06
P_2O_5	0.05
TiO_2	0.03
Na_2O	<0.10
TOTAL	99.84 exc Na_2O

Table 3.2 Compliance of Test Gradings with Relevant Department of Transport Specifications*

Nominal Test Grading	Specification Clauses	Description of Material Covered by Clause
Coarse	803 (Table 8/2) 805 (Table 8/4)	Granular Sub-Base Material, Type 1 Wet-Mix Macadam
Medium	804 (Table 8/3)	Granular Sub-Base Material, Type 2
Fine	503 (Table 5/6)	Material for Bedding, Laying and Surrounding of Pipes

* Department of Transport Specification for Highway Works, 1986

Table 3.3 Results of Aggregate Absorption Value Tests

Grading	Number of Specimens Tested	AAV (%)	Specific Gravity		
			Oven-Dry Basis	Saturated Surface Dry Basis	Apparent
Fine	8	1.4±0.2	2.57±0.05	2.61±0.07	2.67±0.15
Medium					
>5 mm	8	0.7±0.1	2.65±0.01	2.67±0.01	2.70±0.01
<5 mm	8	1.4±0.1	2.57±0.05	2.61±0.05	2.67±0.06
Coarse					
>5 mm	8	0.6±0.1	2.67±0.01	2.69±0.01	2.72±0.01
<5 mm	8	1.1±0.2	2.58±0.10	2.62±0.10	2.69±0.07

± Limits quoted are absolute range of values measured, not standard deviations

Table 3.4 Definition of Soil Parameters Allowing for Water Absorption

Parameter	Symbol	Equation
Mass of absorbed water	M_{WA}	$w_A M_s$
Mass of free water	M_{WF}	$M_W - w_A M_s$
Mass of particles	M_p	$M_s + w_A M_s$
Volume of absorbed water	V_{WA}	$\rho_w w_A M_s$
Volume of free water	V_{WF}	$\rho_w (M_W - w_A M_s)$
Volume of particles	V_p	$(M_s/\rho_w G_s) + \rho_w w_A M_s$
Volume of voids	V_u	$V - (M_s/\rho_w G_s) - \rho_w w_A M_s$
Volume of air	V_A	$V - (M_s/\rho_w G_s) - V_W$
Voids ratio	e	V_v/V_p
Degree of saturation	Sr	V_{WF}/V_v
Air void ratio	A	V_A/V
Dry density	ρ_d	M_p/V
Bulk density	ρ	$(M_s + M_W)/V$

* where measured quantities are:

w_A = aggregate absorption value
M_s = dry mass of specimen
M_W = total mass of water in specimen
G_s = specific gravity
V = volume of specimen (including membrane penetration into triaxial specimens)

and ρ_w = density of water

Table 3.5 Summary of Particle Shape Analyses: Overall Form of Particles

Particle Size Range	Number of Particles	Average Dimensions ± Standard Deviation			Average Dimensional Ratios ± Standard Deviation		Average dimension $\frac{(a+b+c)}{3}$
		a	b	c	b/a	c/b	
37.5-50	4	60±5	46±3	36±7	0.770±0.029	0.784±0.179	47.3
28-37.5	30	49±10	37±5	22±5	0.768±0.141	0.619±0.182	36.0
20-28	30	40±8	27±4	17±3	0.696±0.124	0.639±0.171	28.0
10-14	30	18±4	13±2	9±2	0.779±0.114	0.665±0.186	13.3
5-6.3	30	9±2	6±1	4±1	0.745±0.160	0.622±0.219	6.3
Weighted Average Dimensional Ratio of all Particles					0.748	0.641	

Table 3.6 Summary of Particle Shape Analyses: Degree of Angularity of Particles

Particle Size Range	Number of Particles	Average Degree of Angularity ± Standard Deviation			
		Aab	Aac	Abc	A
28-37.5	30	643±142	693±149	723±163	2058±351
20-28	30	596±112	696±142	660±127	1952±260
10-14	30	611±169	791±213	682±158	2084±395
5-6.3	30	735±182	845±168	732±214	2312±424
Weighted Average of all Particles		646	756	699	2102

NOTE: INSUFFICIENT PARTICLES IN THE SIZE RANGE 37.5 mm TO 50 mm WERE AVAILABLE TO ALLOW AN ACCURATE ESTIMATE OF THE DEGREE OF ANGULARITY TO BE MADE

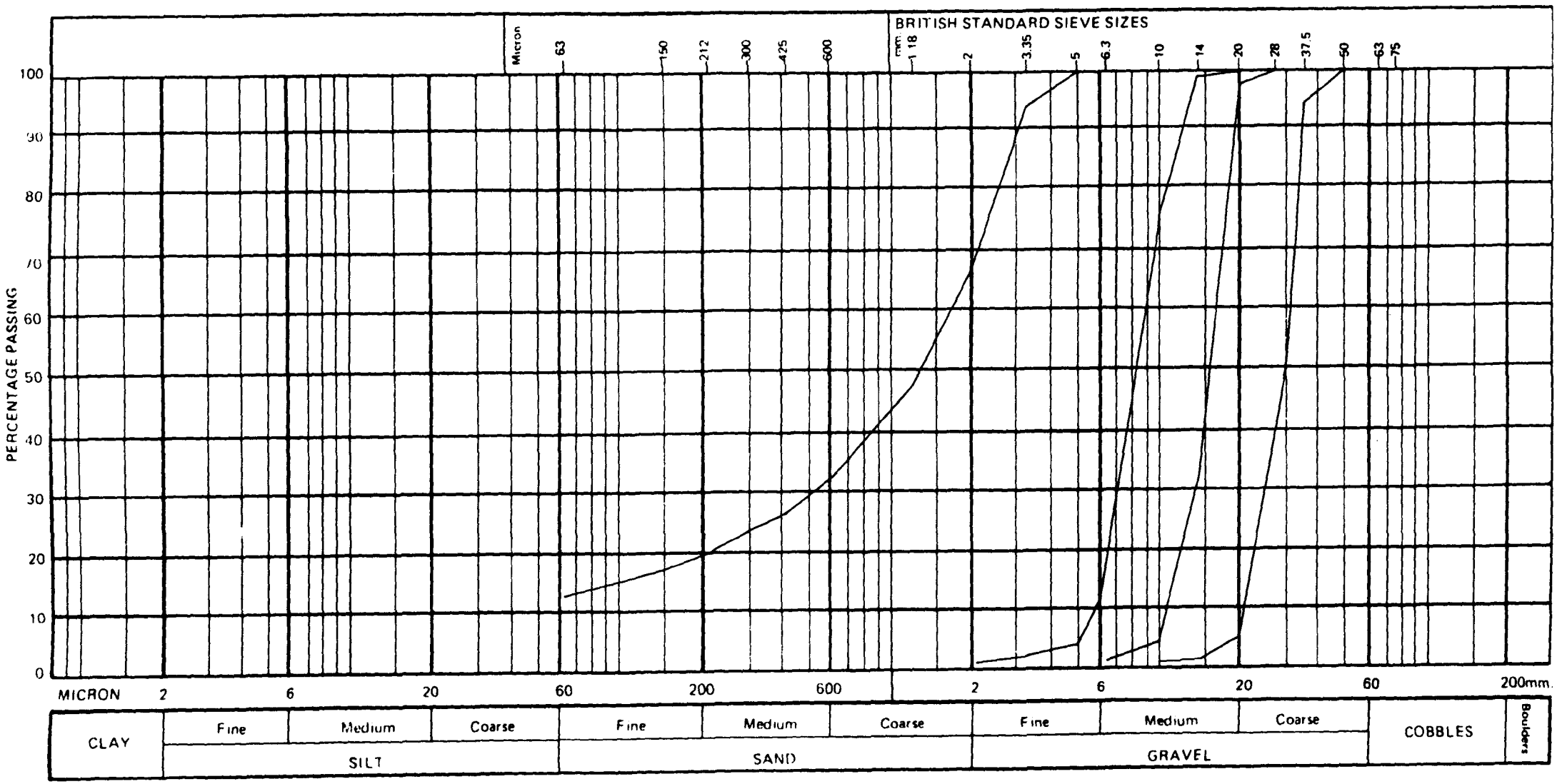

Figure 3·1–Grading Curves for Supplied Limestone Aggregate

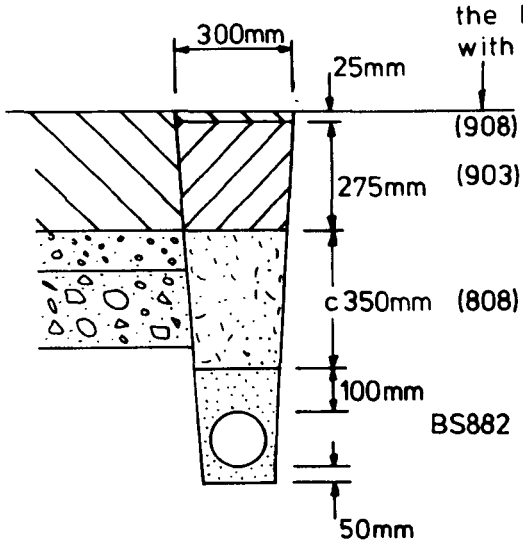

Figures in brackets refer to the clause number in the DTp specification for road and bridgeworks (1976) with which the material complies.

(908) Dense bitumen macadam wearing course, 10mm size
(903) Dense bitumen macadam base course, 20mm size
(808) Wet mix macadam
BS882 Zone 1 natural sand

TYPE 1

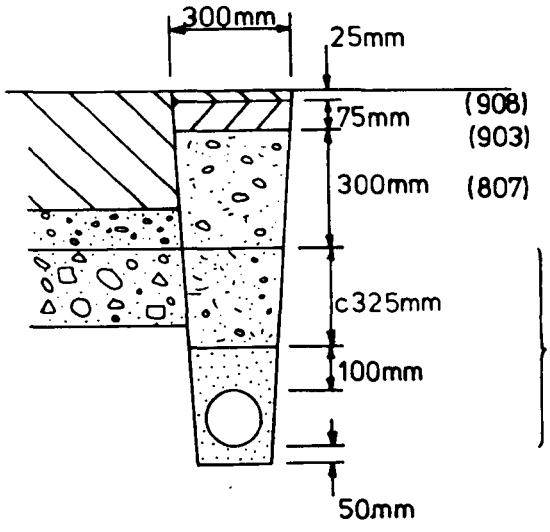

(908) Dense bitumen macadam wearing course, 10mm size
(903) Dense bitumen macadam base course, 20mm size
(807) Dry lean concrete (18:1 aggregate cement, 6% moisture content)
5mm crushed dolomite

TYPE 2

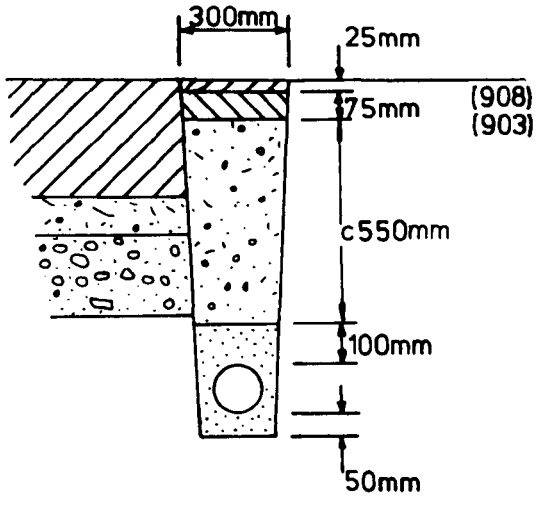

(908) (903) Dense bitumen macadam wearing course, 10mm size; Dense bitumen macadam base course, 20mm size
5mm crushed dolomite (Stabilised with 4% cement, at 11% moisture content)
5mm crushed dolomite

TYPE 3

Figure 3·2-Three Typical Unbound Trench Reinstatements after Owen (1985)

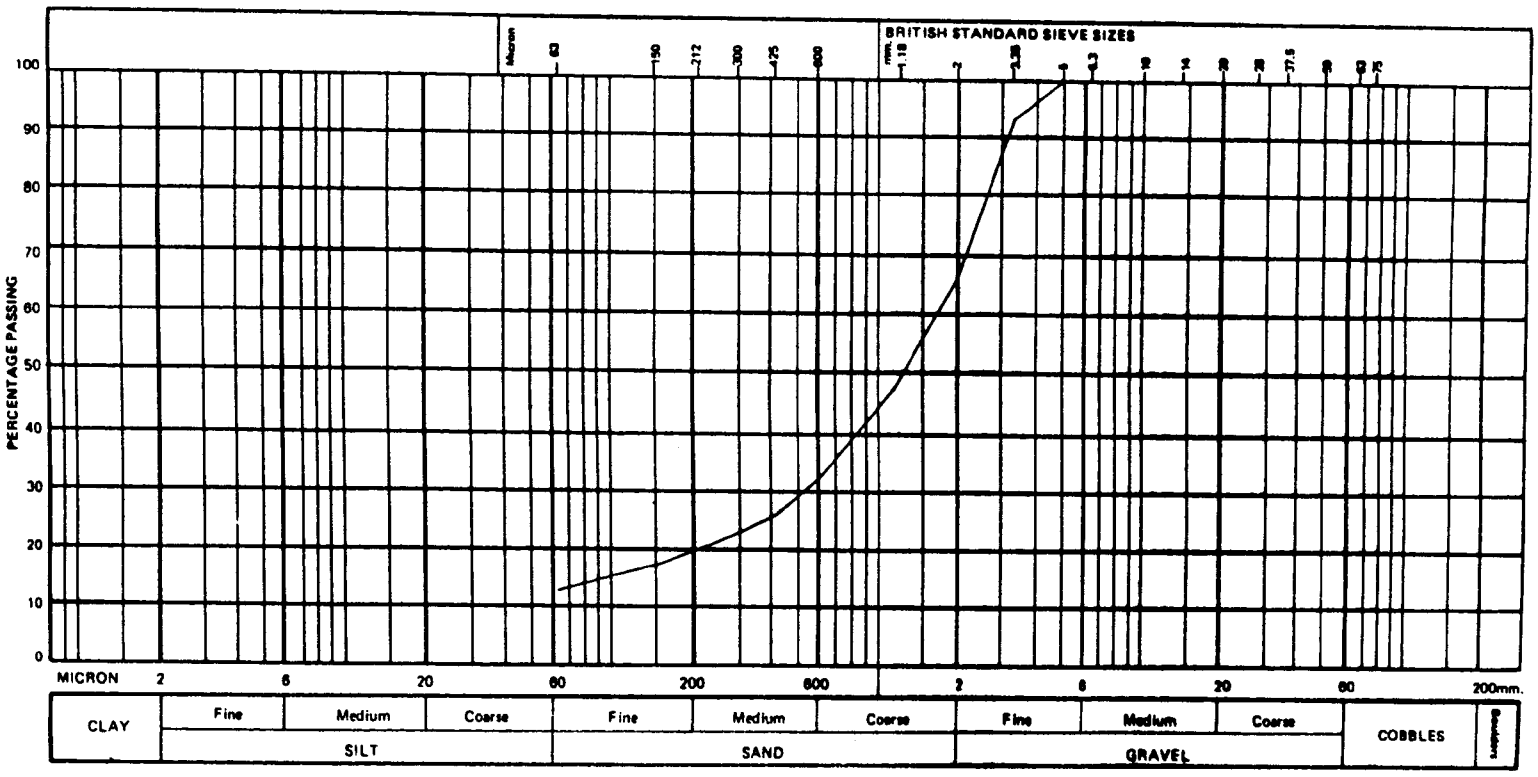

(a) Fine Grading

Preparation: Fine aggregate as supplied by North Tyne Roadstone Limited
DTp specification compliance: Clause 503, Material for bedding, laying and surrounding pipes

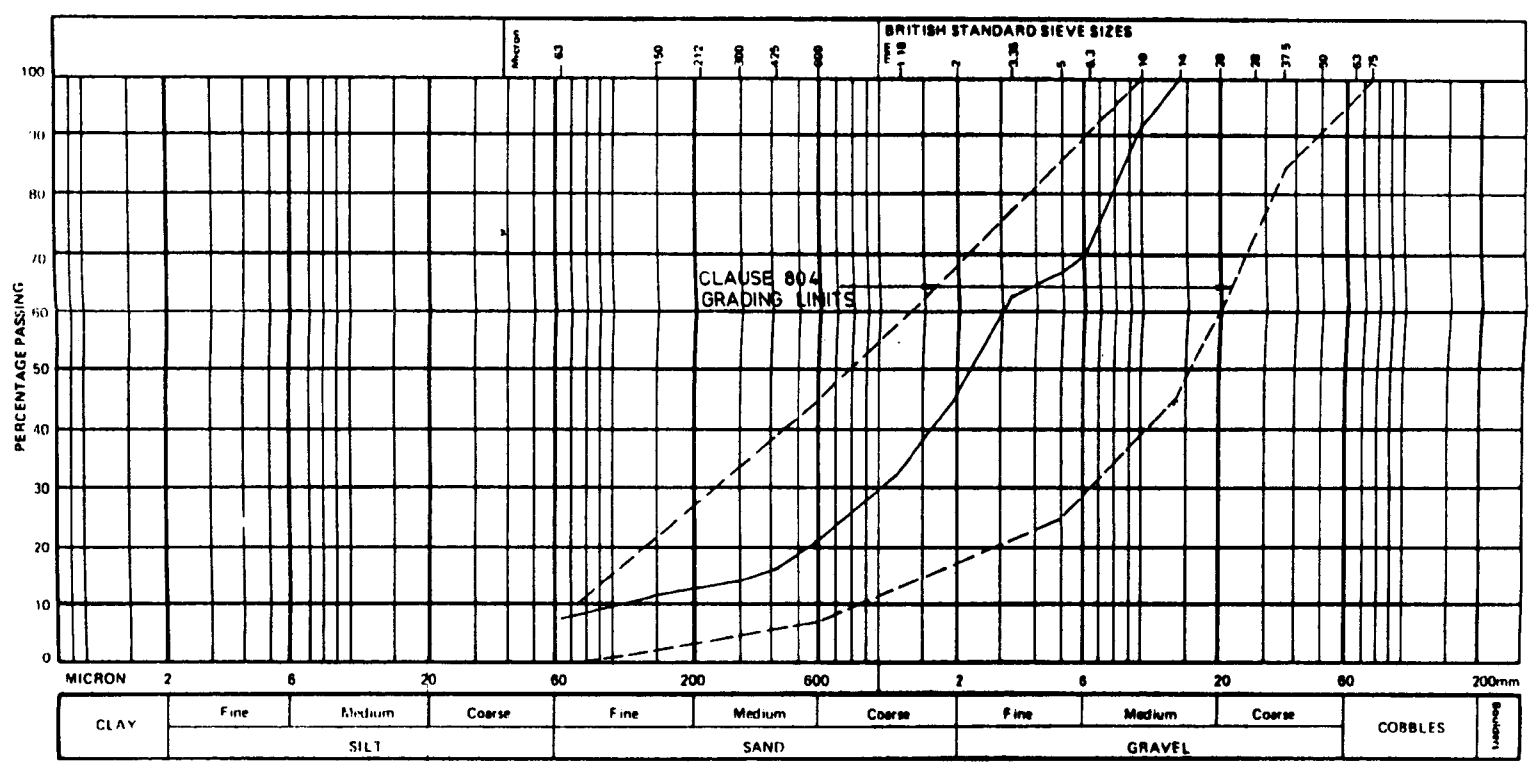

(b) Medium Grading

Preparation: Ratio of as supplied aggregates = 2:1 for fine: medium size ranges
DTp specification compliance: Clause 804 Granular sub-base material Type 2

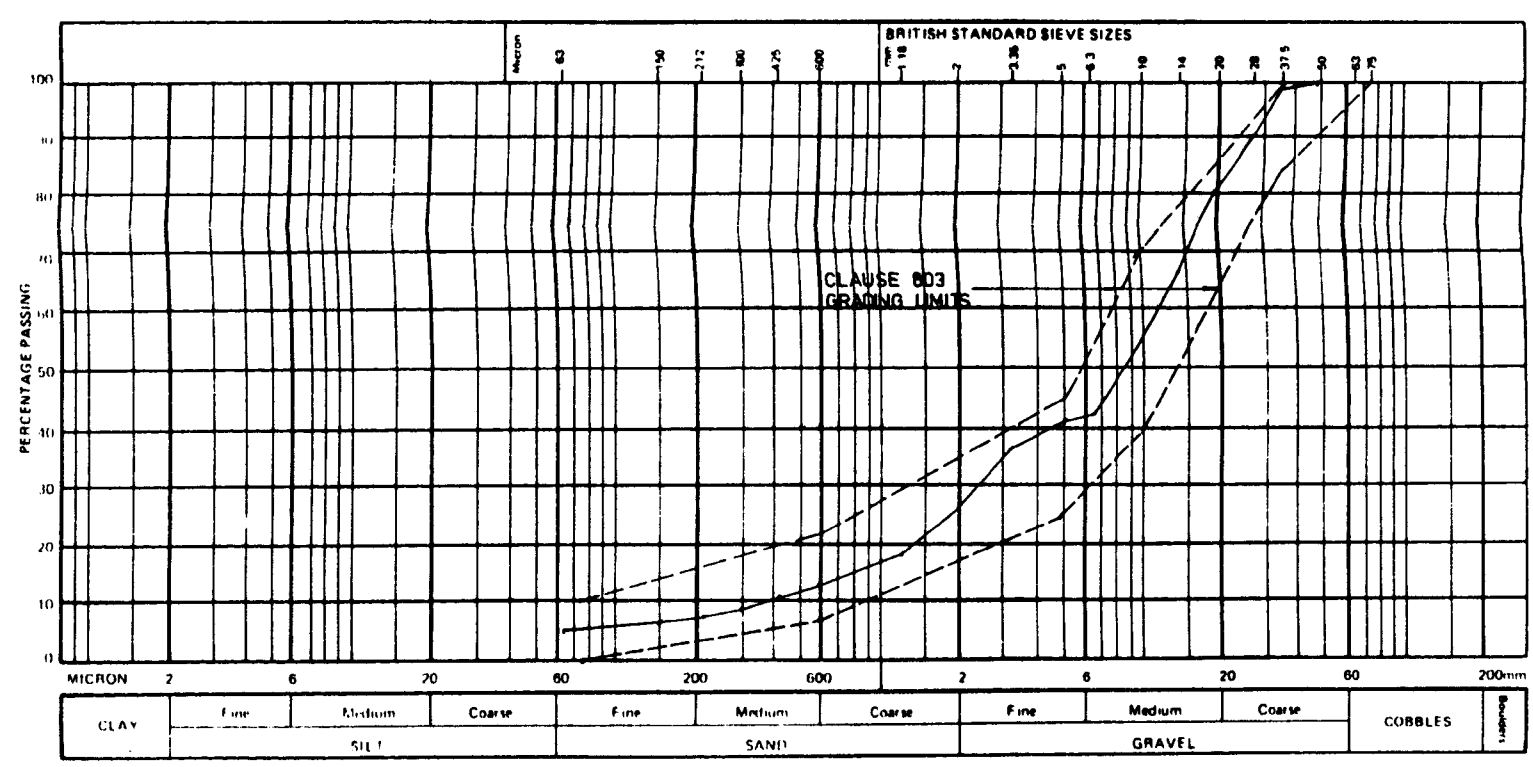

(c) Coarse Grading

Preparation: Ratio of as supplied aggregates = 2:1:1:1 for fine: medium: coarse: very coarse size ranges
DTp specification compliance: Clause 803, Granular sub-base material Type 1

Figure 3·3 – Calculated Nominal Grading Curve and Specification Compliance

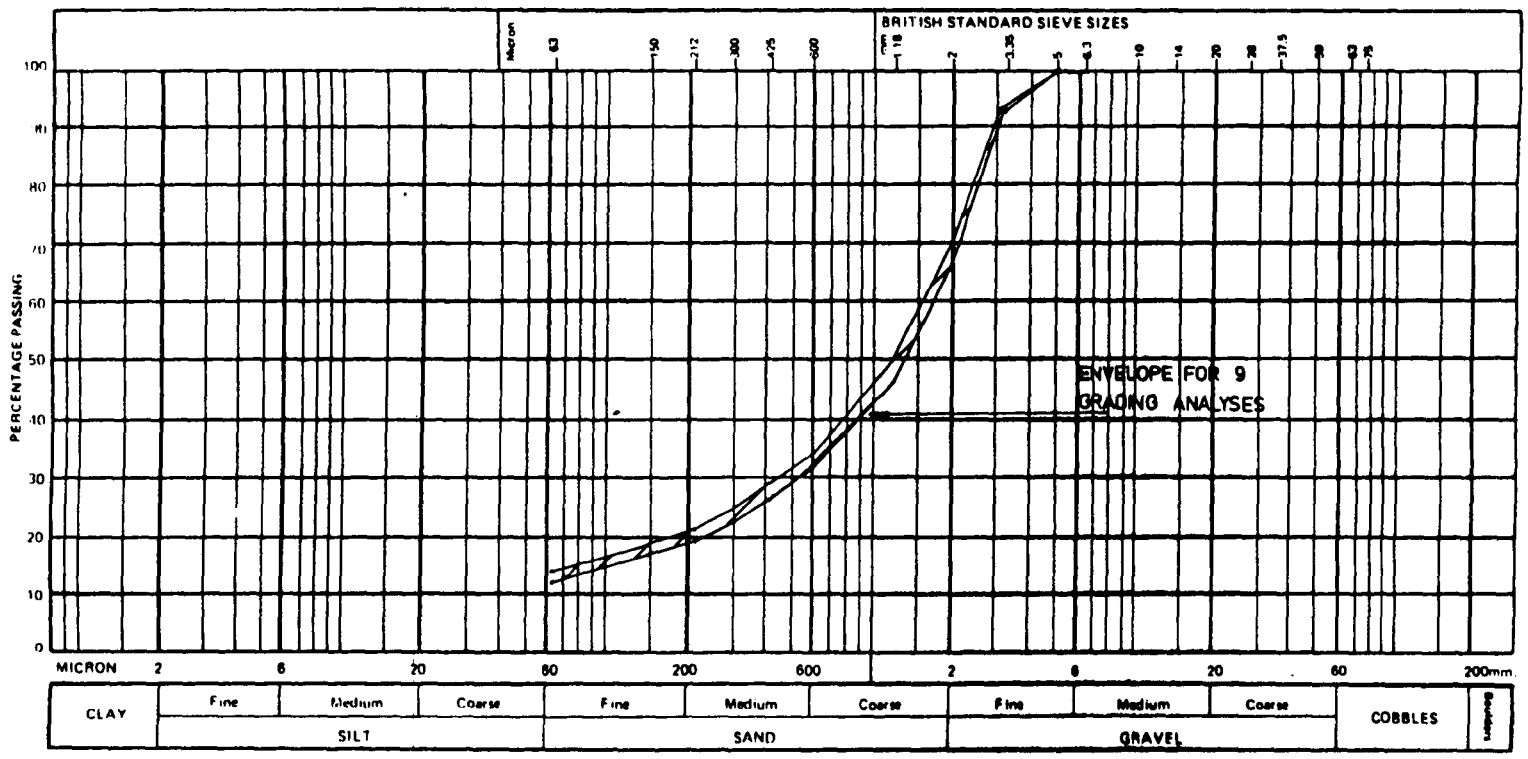

(a) Fine Grading

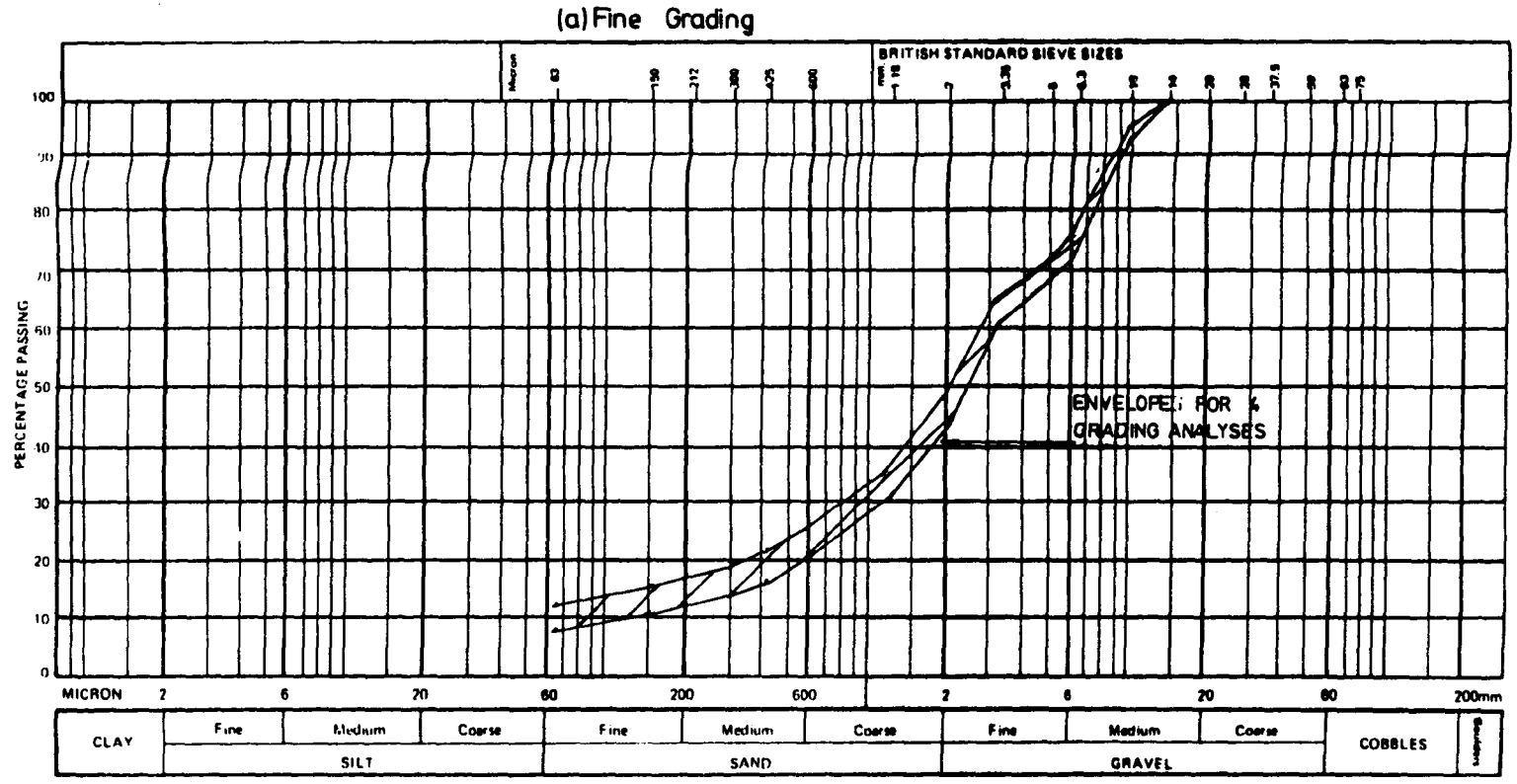

(b) Medium Grading

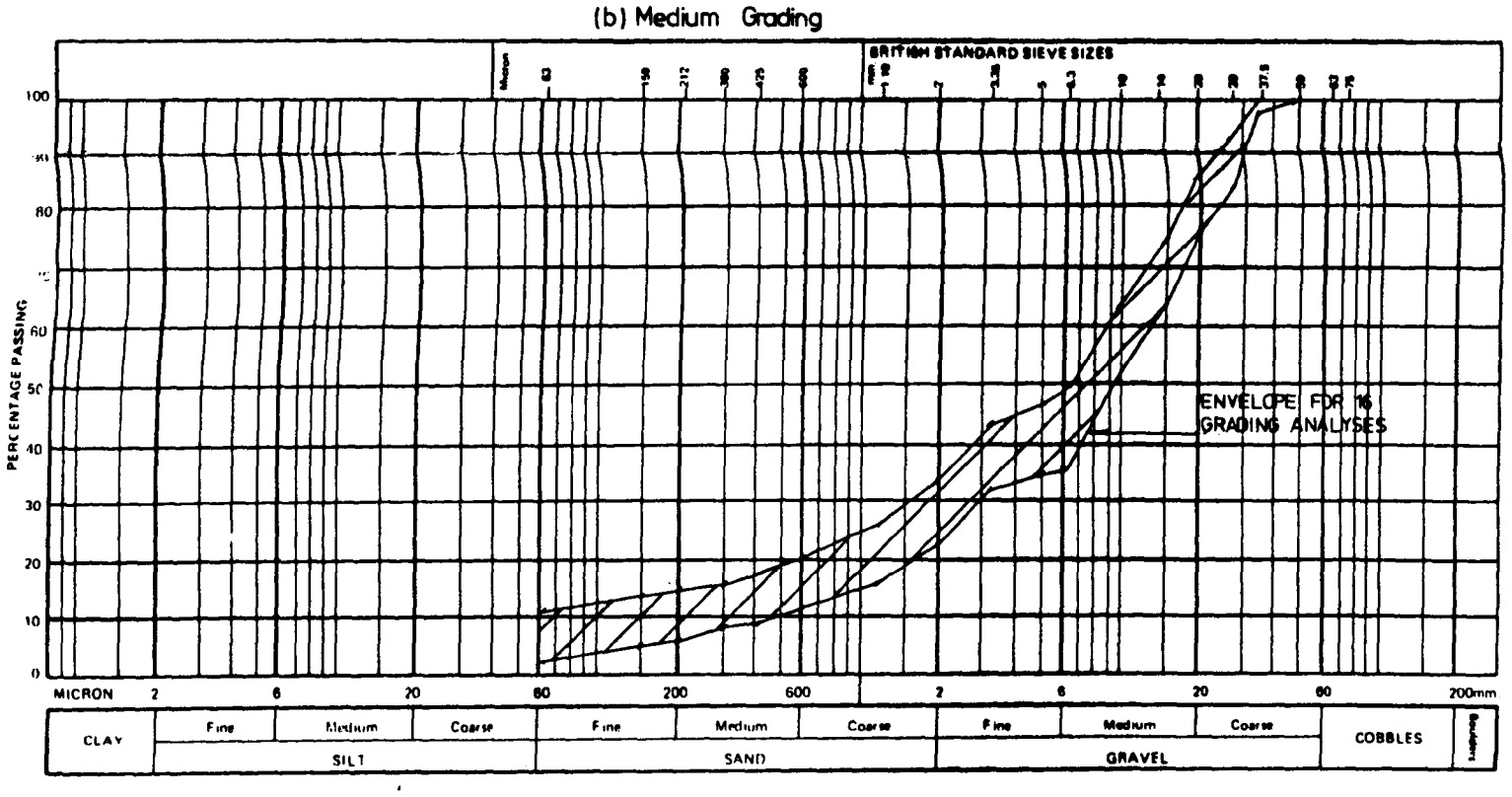

(c) Coarse Grading

Figure 3·4 - Maximum/Minimum Grading Envelopes for Batched Test Gradings

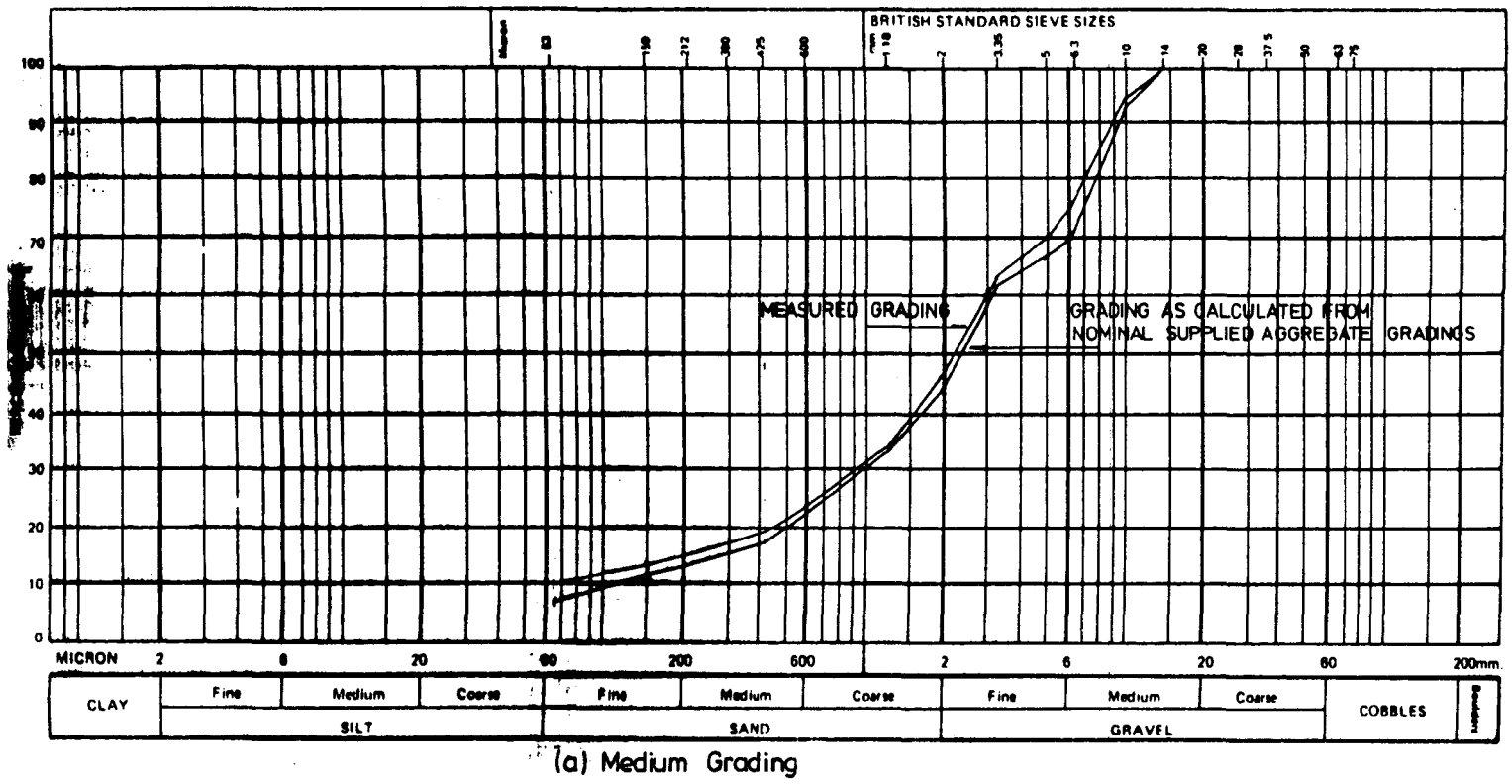

(a) Medium Grading

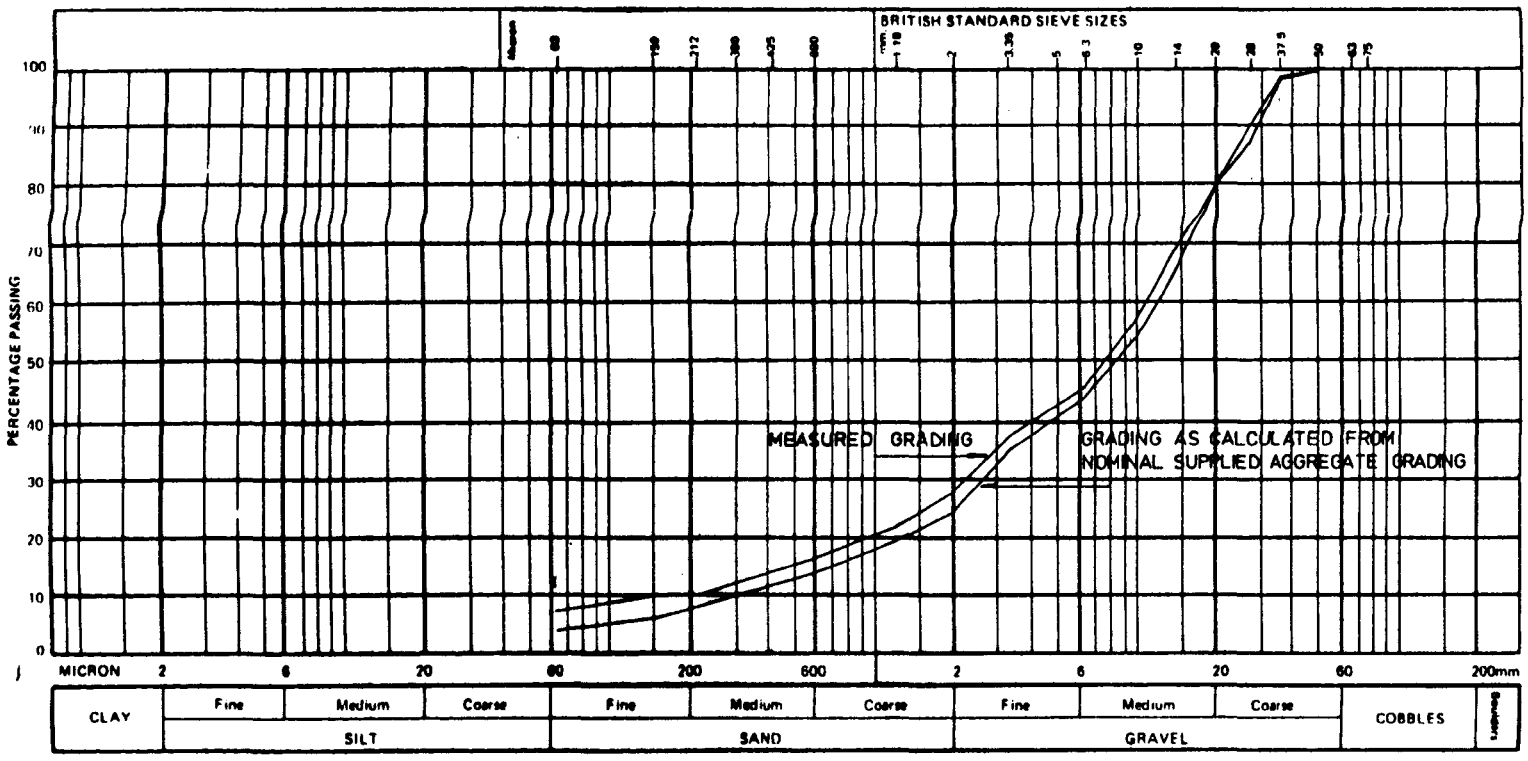

(b) Coarse Grading

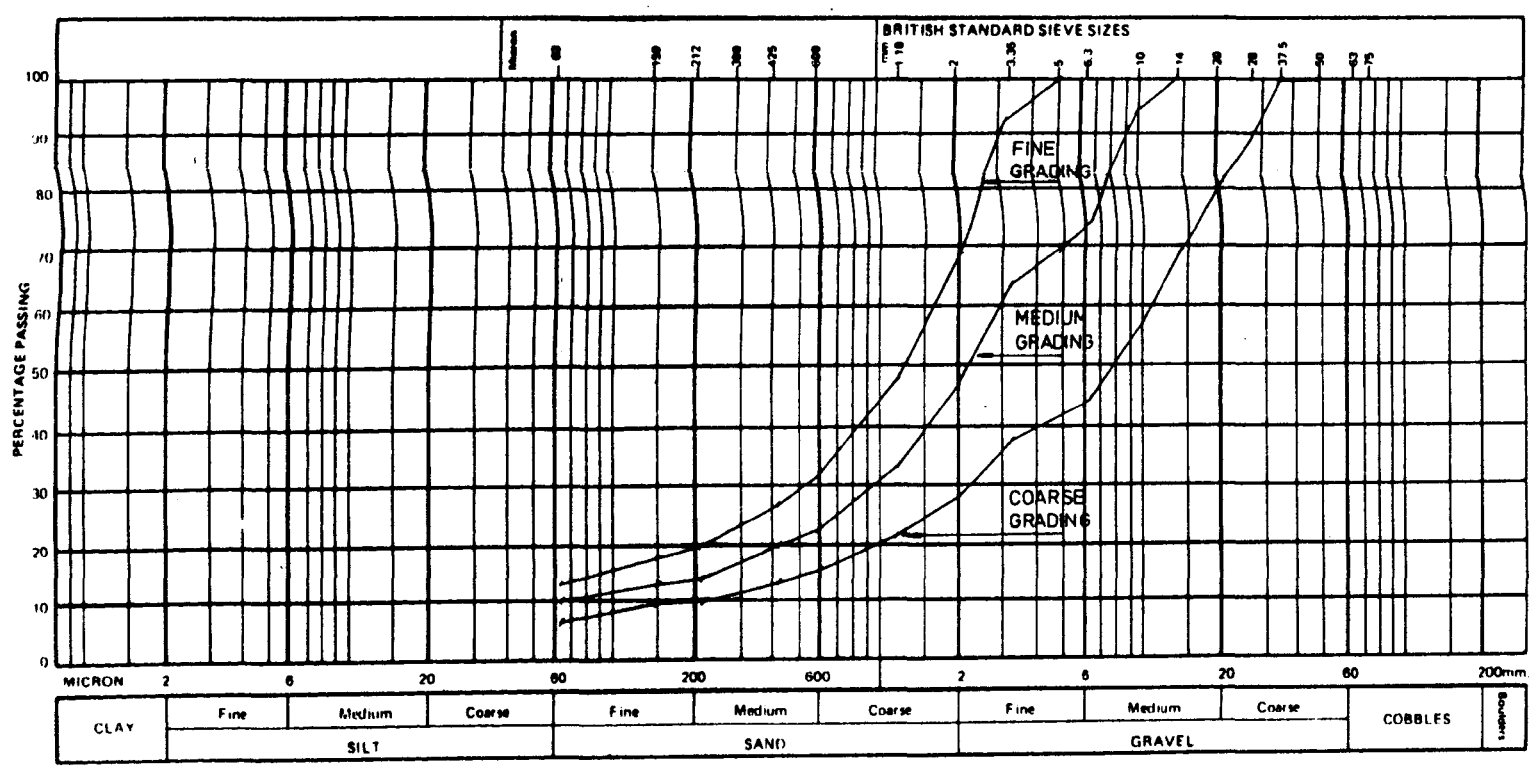

(c) Summary of Average Gradings Actually Tested

FIGURE 3·5 – Particle Breakdown During Batching

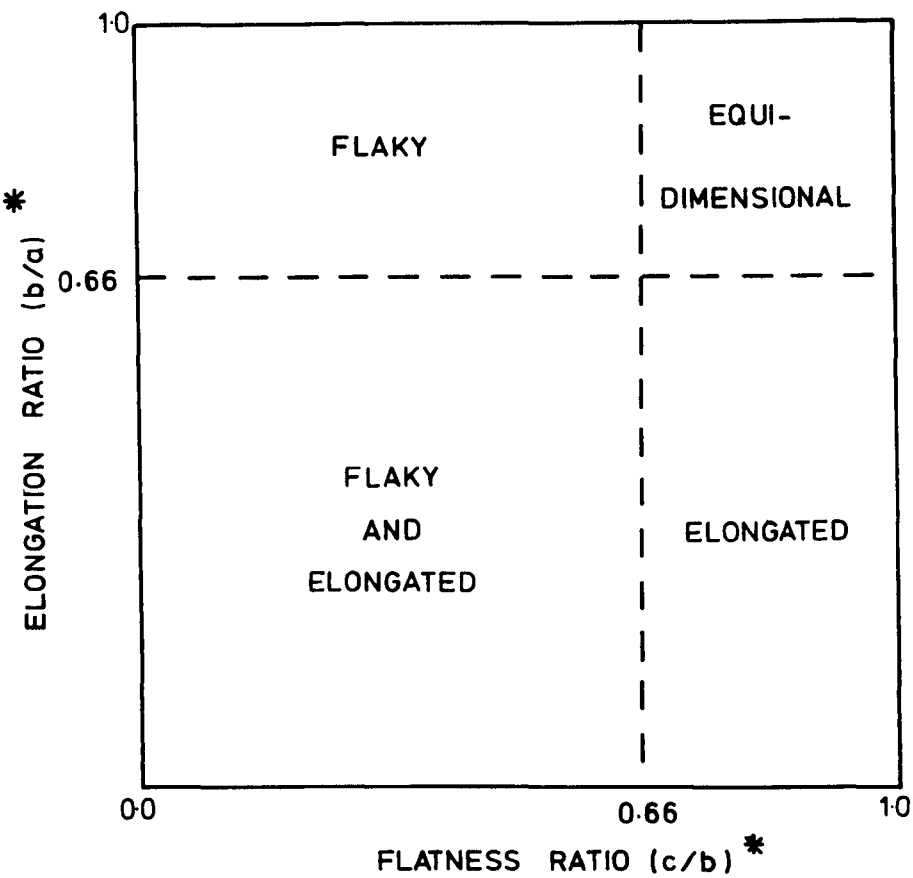

* Where the dimensions $a \geq b \geq c$ represent the principal dimensions of the smallest rectangular box that will just encompass the particle under consideration.

Figure 3·6–Method For The Graphical Representation Of General Particle Shape
(after Lees, 1964)

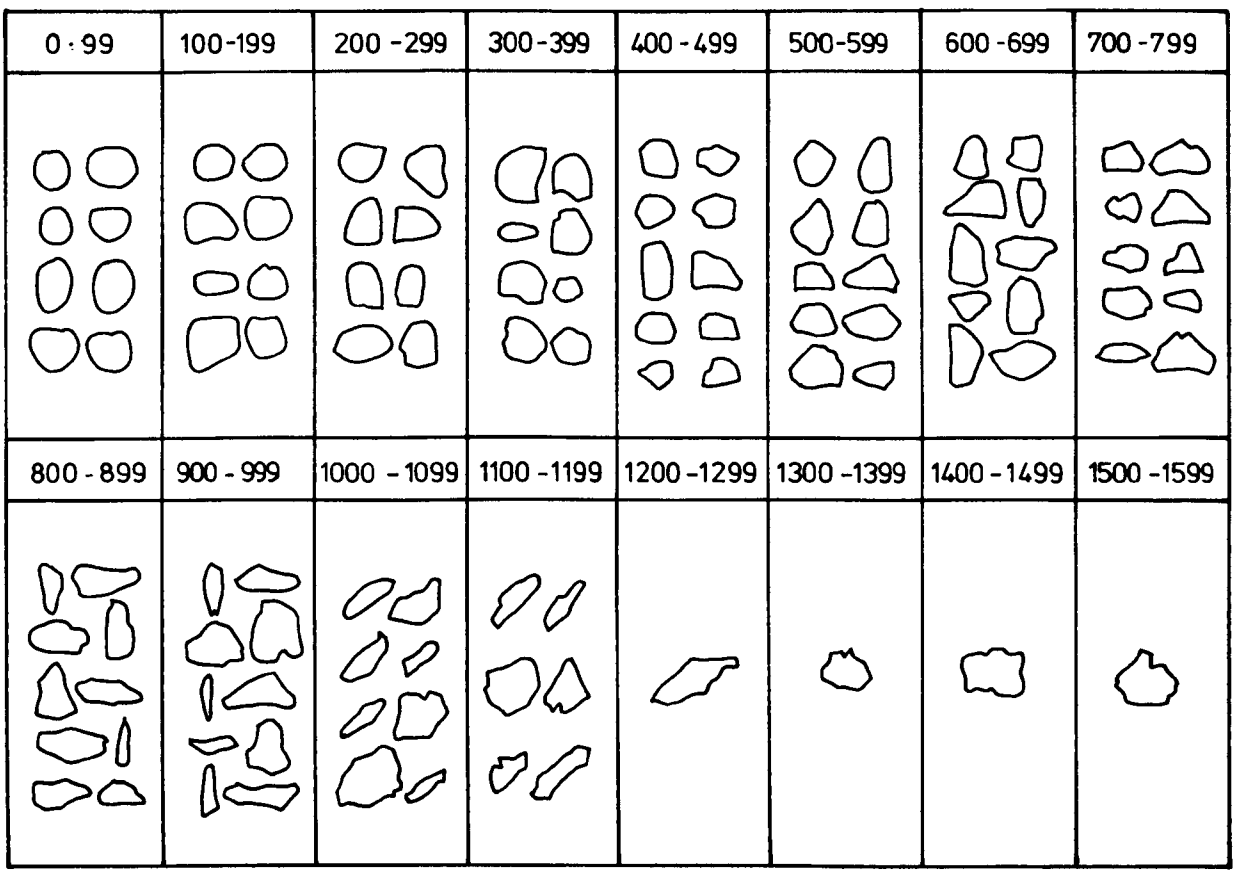

Figure 3·7 - Chart For The Visual Estimation of The Degree of Angularity (after Lees, 1963)

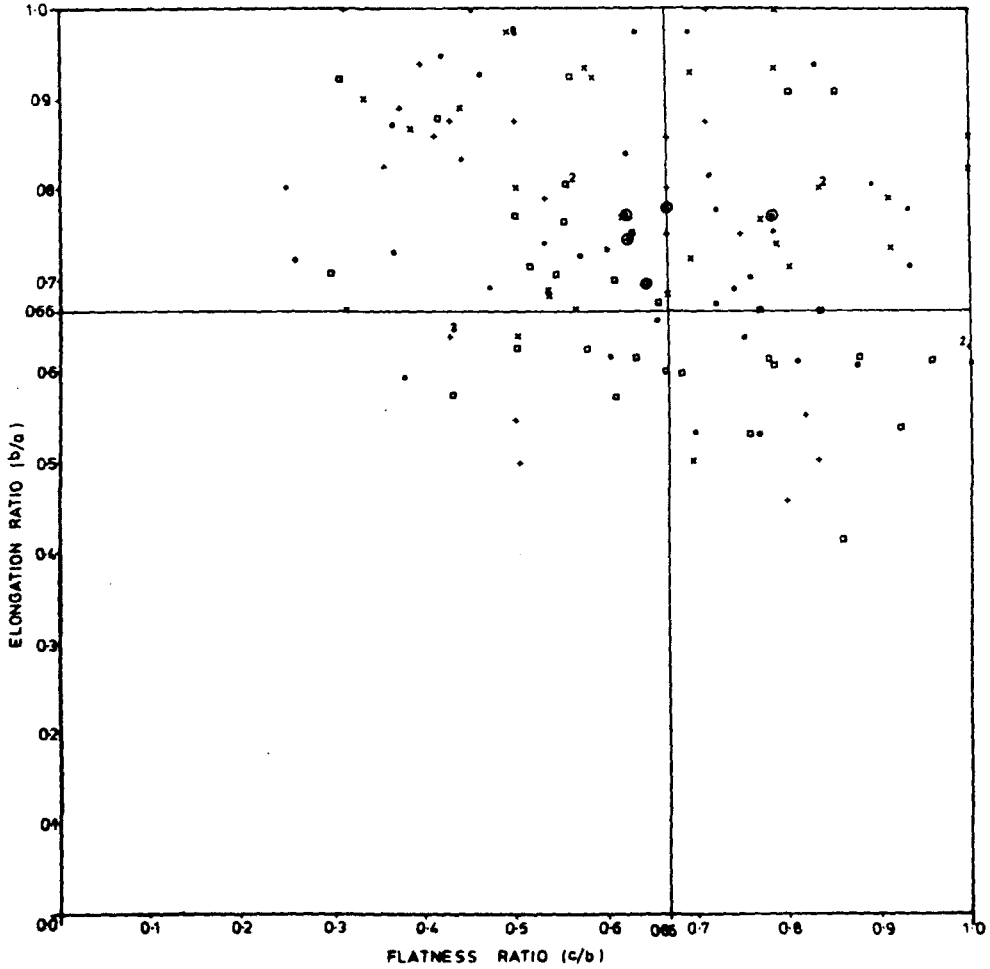

(a) Individual Test Results

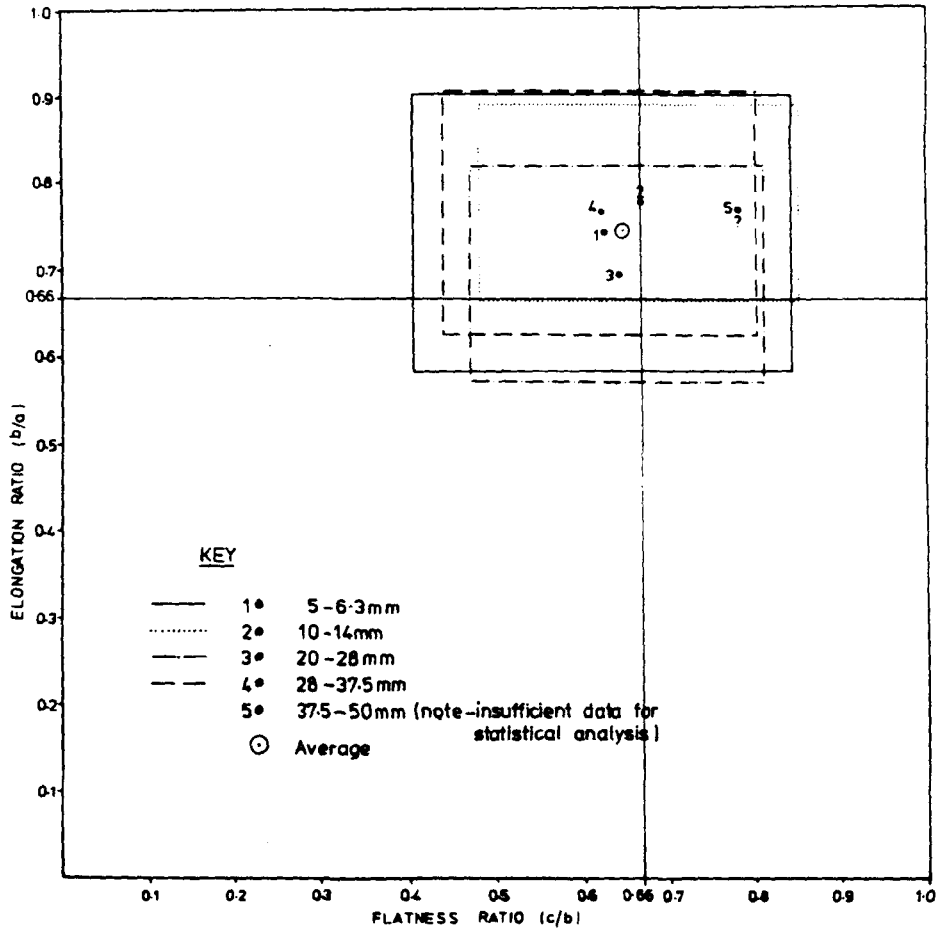

(b) Mean and Standard Deviation of Results

KEY
- 5-6·3 mm
- 10-14·5mm
- 20-28 mm
- 28-37·5mm
- 37·5-50mm

Figure 3·8-Results of Particle Shape Analysis

Degree of Angularity	Equivalent Descriptive Angularity Term	Typical Particle Shapes
3000 or greater	Extremely Angular	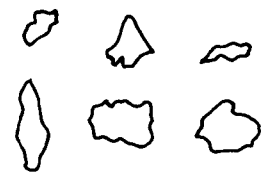
2000 - 2999	Angular	
1250 - 1999	Sub-Angular	
600 - 1249	Sub-Rounded	
Less than 600	Rounded	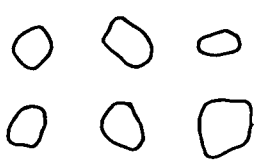

Figure 3.9 - Suggested Relationship Between The Quantitative Degree of Angularity and Conventional Qualitative Visual Assessment of Angularity

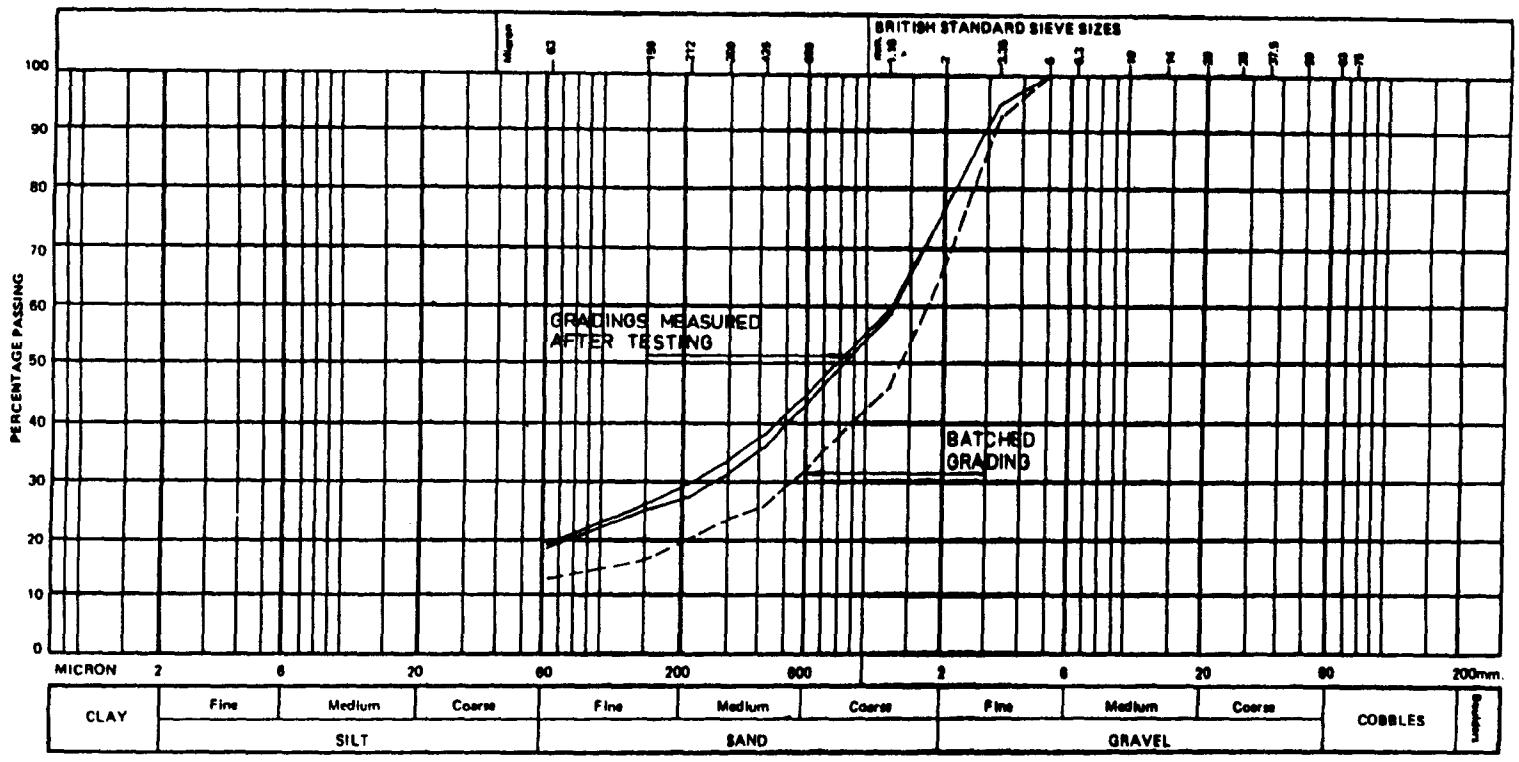

(a) Fine Grading

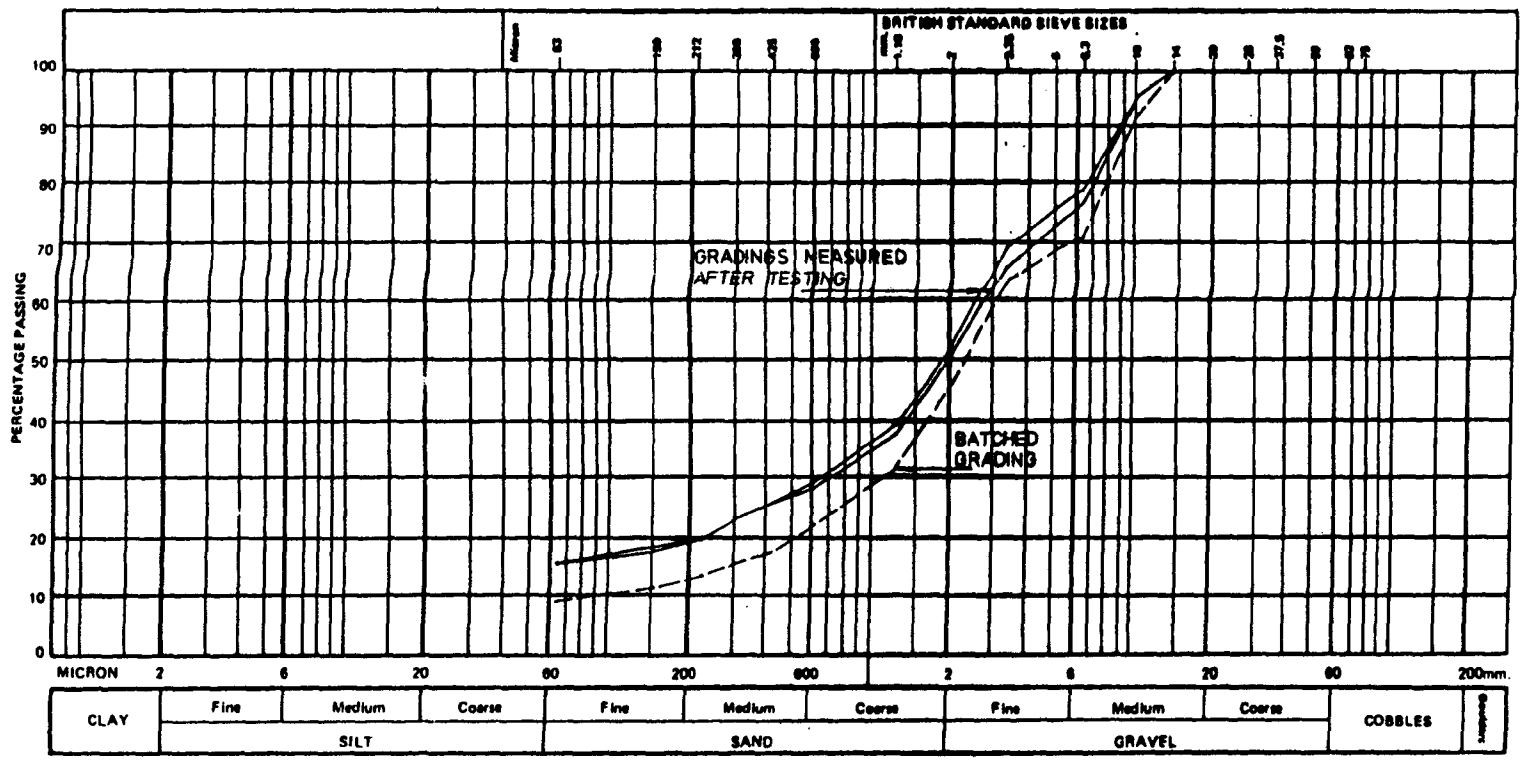

(b) Medium Grading

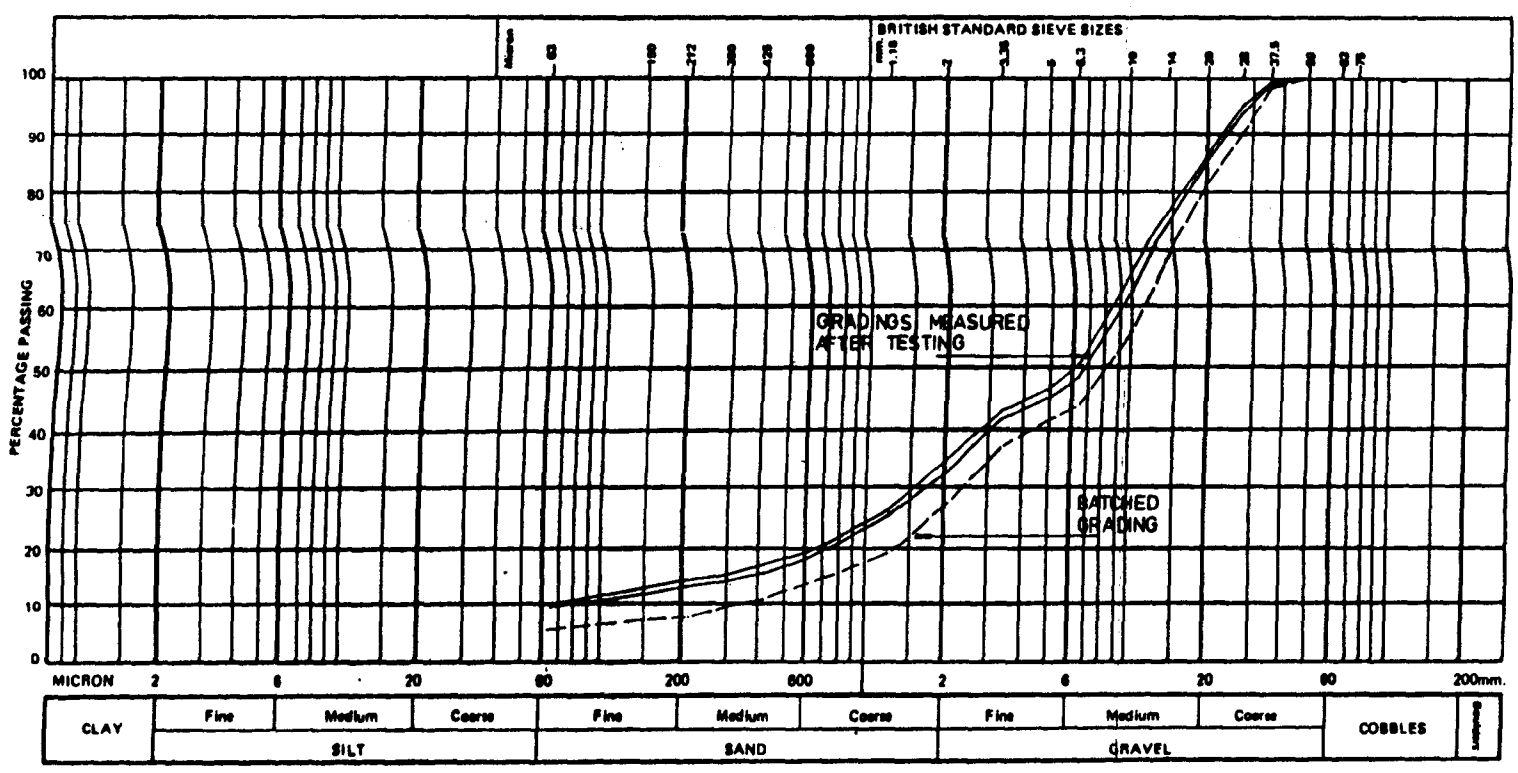

(c) Coarse Grading

Figure 3·10 - Degree of Breakdown During Maximum Density Tests

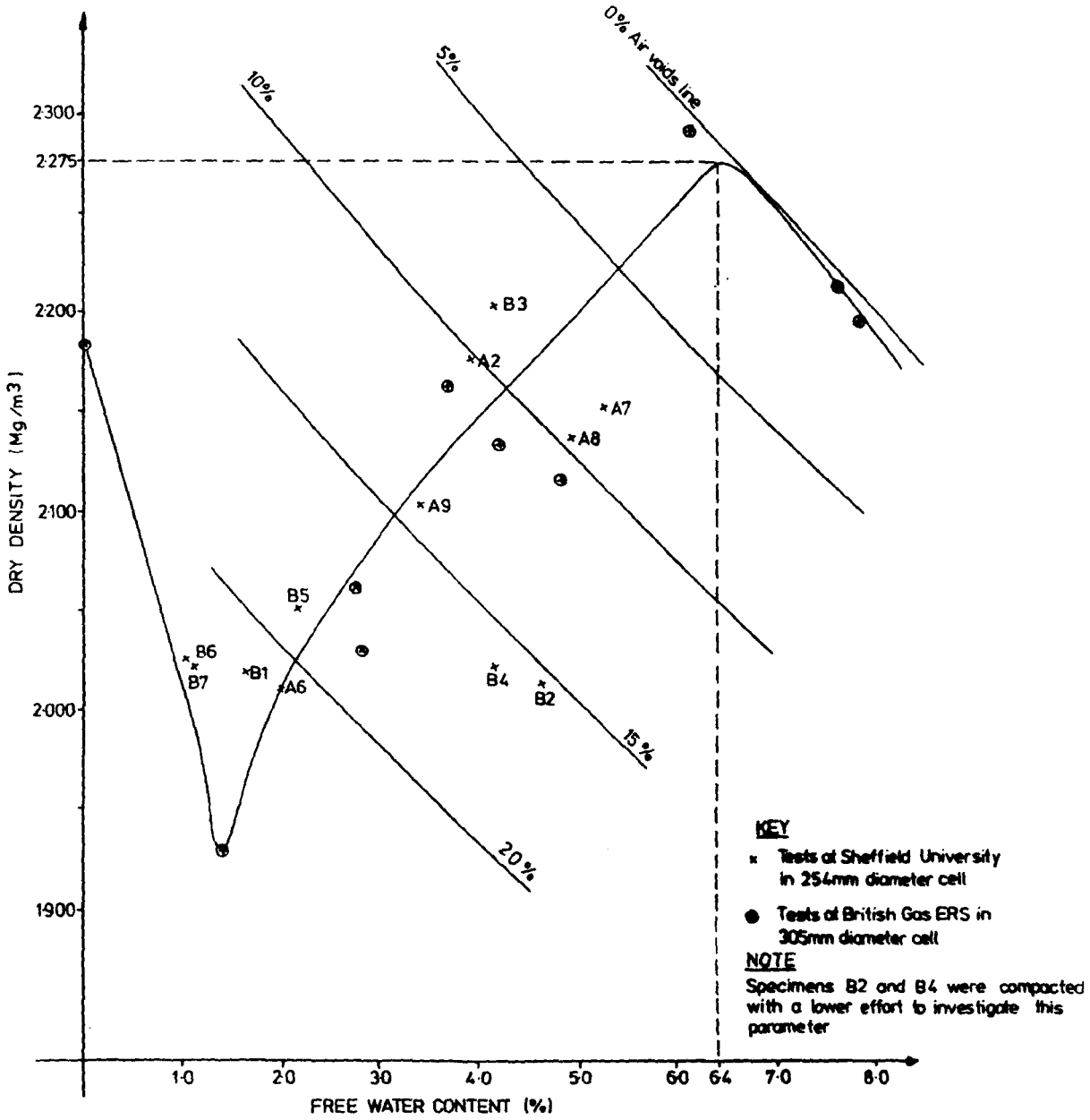

Figure 3·11 - Dry Density - Free Water Content Relationship For Coarse Grading At Standard Test Programme Compactive Effect

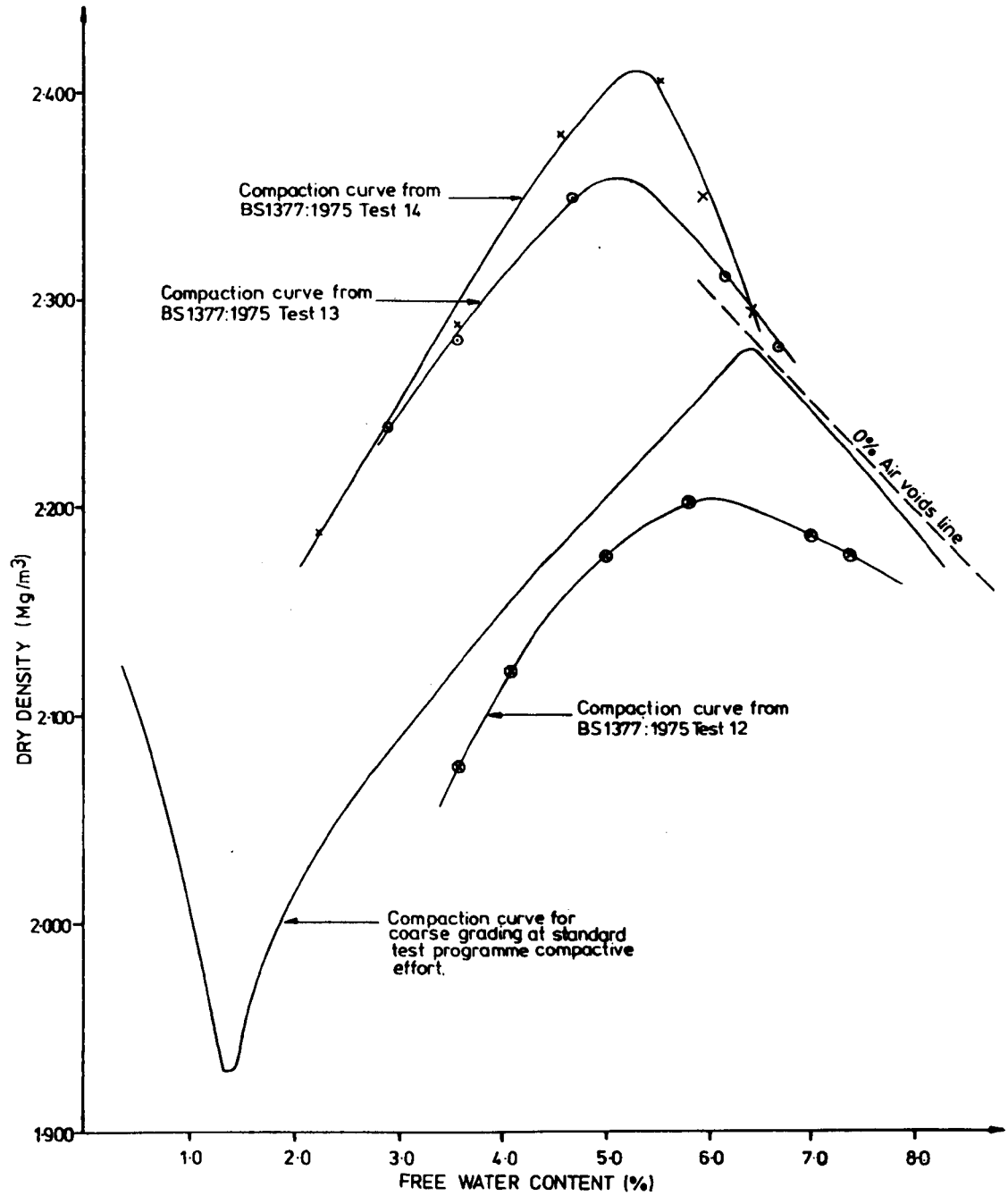

Figure 312–Comparison of the Compaction of the Coarse Grading at Standard Test Programme Compactive Effort with BS 1377 : 1975 Tests 12 13 and 14 on a Similar Material.

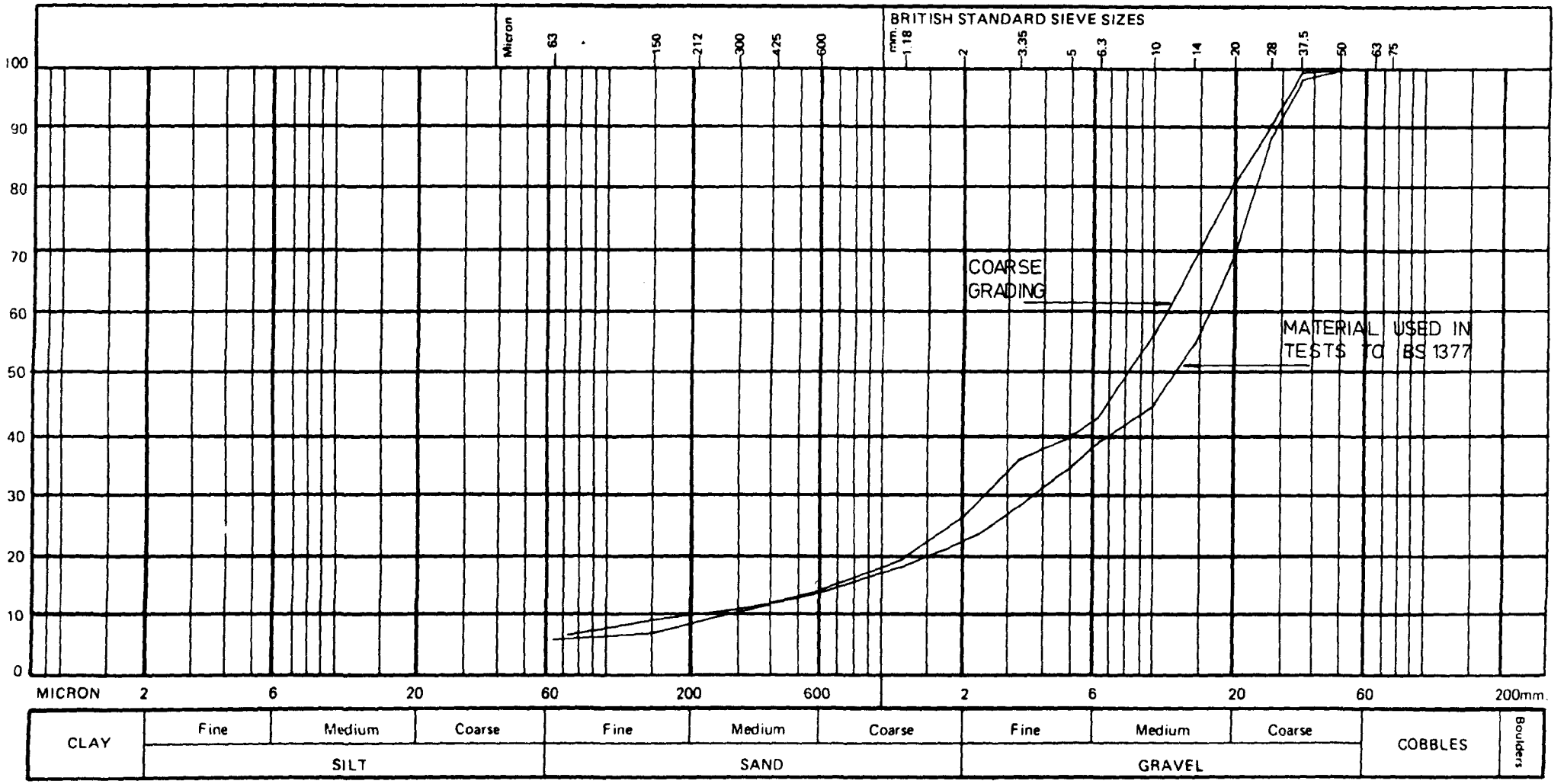

Figure 3·13 – Comparison of Grading Curve for Material Tested Using BS1377: 1975 Tests 12, 13 and 14 with Main Test Programme Coarse Grading

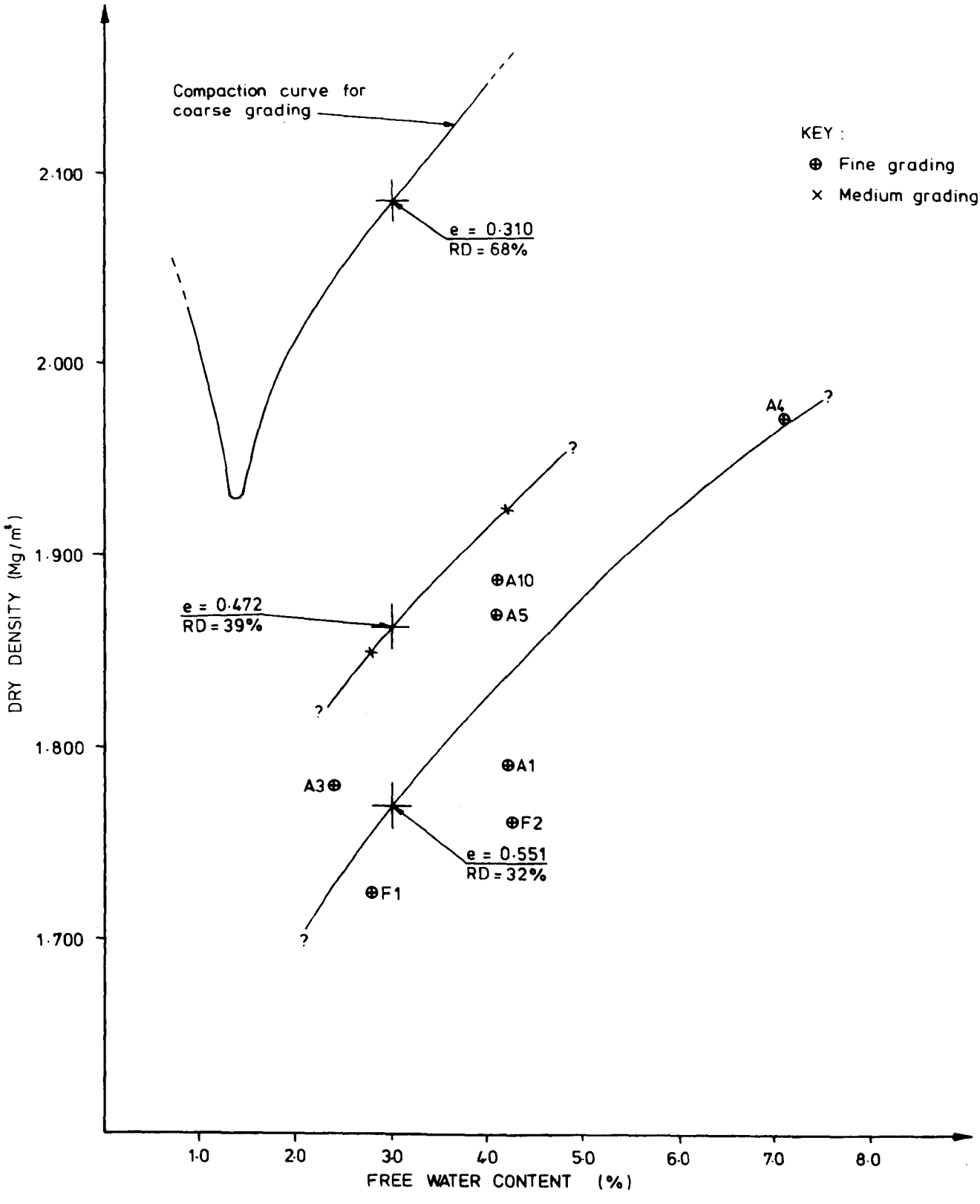

Figure 314 – Dry Density-Free Water Content Relationship for Fine and Medium Gradings at Standard Test Programme Compactive Effort

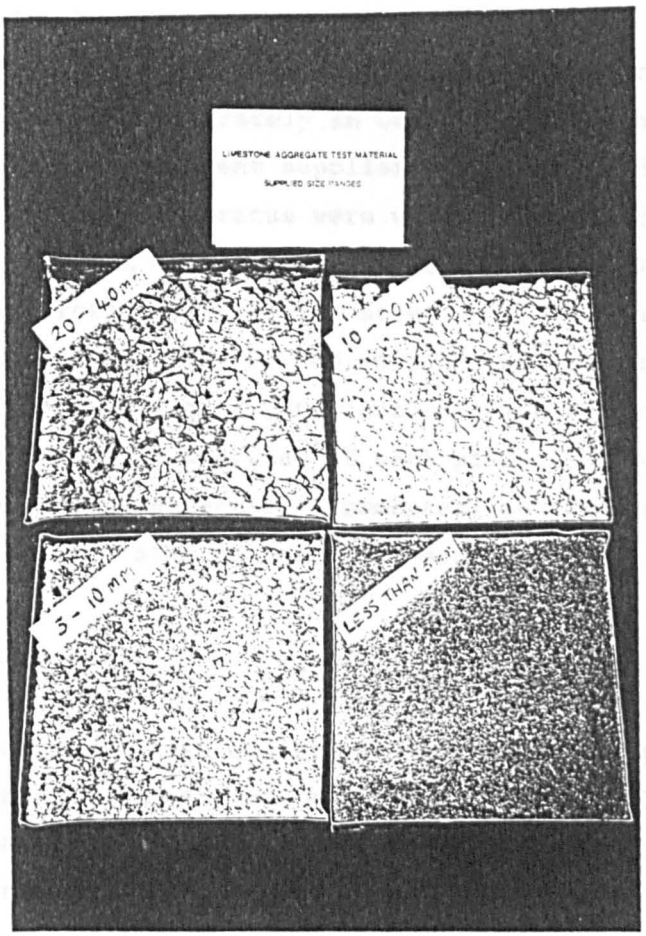

Plate 3.1 Limestone aggregate supplied by North Tyne Roadstone Limited

CHAPTER 4

DESCRIPTION AND DEVELOPMENT OF EXPERIMENTAL APPARATUS

This chapter presents details of the experimental apparatus and ancillary equipment used in the main test series. Details of the calibration and operational checks made on the apparatus to ensure their correct functioning are presented separately in Chapter 5, and the names and addresses of the specialist equipment suppliers are presented in Appendix B. Three major pieces of apparatus were used, namely a 254 mm internal diameter one dimensional consolidation cell specifically developed for testing unsaturated soils at low stresses, a conventional triaxial cell modified to allow testing of 200 mm diameter unsaturated specimens, and a 305 mm internal diameter strain controlled compression cell. In the following sections an overview of each piece of apparatus is presented initially, with a more detailed commentary on the important aspects of each part of the apparatus in later sub-sections.

4.1 Consolidation Cell

A consolidation cell suitable for high quality testing of the proposed materials at the low stresses envisaged was not commercially available at the start of the project. The requirements of a suitable cell were that it allow repeatable testing of specimens containing coarse particles, that it allow the control and/or measurement of the pressure and volume of the air and water phases within the specimen, and that it allow accurate measurement of the applied vertical stress.

The general assembly of the new cell that was developed to meet these requirements is shown in Figure 4.1 a and the associated plumbing system in Figure 4.1 b . Two identical cells were manufactured and used simultaneously during the test programme. Each cell essentially consisted of a fixed base platen and a top platen through which vertical stress was applied to a specimen radially confined by a 254 mm internal diameter bronze alloy cylinder. Pore water pressure was measured at

both platens using high air entry value ceramics. Specimens up to 120 mm high with a maximum particle size of 40 mm could be accommodated, and incremental net stresses to 165 kPa could be applied through the top platen.

The top platen (see Figure 4.2) consisted of an upper and lower body primarily connected at three points only using three 2.5 kN load cells manufactured as detailed in Appendix C. The upper body used three circumferential 'O' rings to achieve a seal between the specimen and pressurised water above that was used to apply vertical stress to the soil. Direct measurement of the loads transmitted to the lower body using the load cells allowed frictional losses in the applied vertical stress due to the seals to be negated. This allowed accurate calculation of the stress applied to the specimen. The lower body was prevented from contacting the cell body and developing additional friction losses by virtue of its slightly smaller diameter, and also by the height of the upper body combining with its 'O' ring seals to minimise platen tilt during a test.

Air pressure was regulated within the specimen at a constant raised value via a line passing through the top platen, ensuring that the otherwise negative pore water pressures in the specimen were positive (see section 2.3.1). The pore water pressures were separated from the air pressure at both platens using large diameter saturated high air entry value ceramics. The ceramics were supported on spiral drainage basins and were connected to a pore water pressure transducer via a central drainage line. An additional inlet at the outer edge of the spiral basin was used periodically to flush away air that had accumulated within the basin as a result of slow diffusion of air through the ceramics.

Total specimen volume change was calculated from the cross sectional area of the cell and the changes in specimen height as measured with an LVDT resting on a central piston rod connected to the top platen. As already noted, the length of the top platen and the action of its seals

minimised tilt and therefore allowed accurate observation of total changes in volume.

Water volume changes could be measured using Imperial College type volume change units if water drained conditions were required. The constant back pressure applied to the volume change units effectively controlled the applied pore water pressure at the top and/or bottom of the specimen in this mode. Alternatively, pore water pressures could be measured using conventional pore water pressure transducers in a water undrained mode.

The air phase in the specimens was permanently drained to the atmosphere via a pressure regulator, and no attempt was made to measure directly air phase volume changes. However, as noted in section 2.3.1, air is able to diffuse slowly through the high air entry value ceramics, leading to incorrect measurement of pore water pressure or water volume change. Consequently, the volumes of diffused air removed during periodic flushing of the platens were measured using new diffused air volume indicators.

Details of the cell, its ancillary equipment, and the data acquisition software used with the cell are presented below, together with details of the temperature controlled laboratory within which the cell was always used.

4.1.1 Cell, Plumbing and Instrumentation

4.1.1.1 Cell Dimensions

The cell was basically composed of two conventional 254 mm internal diameter Rowe Cell bodies, each 127 mm high, which were rigidly bolted together concentrically with eight bolts. To reduce any diametrical eccentricities at the joints of the bodies, the internal faces were smoothed locally with silicon carbide paper after assembly and never dismantled again during the work. An approximately 4 mm thick rubber

gasket was sealed onto one end face of the cell using Araldite adhesive, and holes punched for the bolts. At the other end, a small chamfer was machined on the internal face of the cell to ease top platen insertion.

The dimensions of the fully assembled top platen reduced the maximum specimen height to about 120 mm, although actual heights ranged from 89.0 mm to 119.1 mm. As discussed in the literature review, a minimum specimen dimension to maximum particle size ratio of four at least is usually considered sufficient to ensure repeatable test results are obtained for well graded specimens. This implies a maximum particle size of about 20 mm in the new cells. However, it was judged at the start of the research that the coarse grading could be used in the cell despite a maximum particle size of 37.5 mm, as only 11% by mass of material would exceed 28mm and 20% by mass would exceed 20 mm (see Figure 3.5c). Justification of this judgement is contained in section 8.4.1.

4.1.1.2 Base Platen

The three part base platen shown in Figure 4.3 consisted of a five high air entry value ceramics in an aluminium locking ring which rested on an anodised aluminium spiral grooved drainage basin which connected the central drainage outlet and the flushing inlet. This in turn was supported on a conventional Rowe Cell base with a pore water pressure transducer housing block on its drainage outlet port. These components were of the same diameter as the cell base and, when in use, were clamped between the base and the main cylindrical body using eight bolts. Greased 'O' ring seals on the underside of the drainage basin body around the drainage and flushing holes prevented water loss between parts A and B, and a further 'O' ring between the ceramic locking ring and the outer rim of the drainage basin ensured a seal between these bodies. The pressure of the soil on the ceramic ensured efficient operation of the flushing mechanism (see Section 5.2).

The ceramic had a 45° bevelled edge and was permanently sealed into its locking ring using Silastic RTV732 plastic sealant. When sealed in place, the ceramic was machined flush with its locking ring using a

grinding belt to ensure that a sufficiently flat surface would be exposed to the accurately machined upper surface of the drainage basin. This was considered essential as even a small capacity for flexing of the ceramic across the full diameter of the cell could have lead to cracking of the brittle ceramic and a significant reduction of its air entry value. A series of tests aimed at quantifying the flexual behaviour of the high air entry value ceramic and the effects on its air entry value is reported in Appendix E. The 4 mm width of the spiral groove was adopted on the basis of this work.

4.1.1.3 Top Platen

Details of the top platen are shown in Figure 4.2. The lower body was essentially the same as the base platen, except that its 250 mm diameter allowed it to move freely within the main cell body. Further, four small air lines were bored through the metal to connect the specimen to the void between the upper and lower bodies. This space was pressurised with air during a test, and the bores allowed this raised pressure to be transmitted to the specimen. The bores were capped with small diameter porous plastic plugs to prevent any water that was temporarily displaced up the sides of the top platen during a test from flowing into the air void between the two main bodies of the platen and affecting the load cells.

Stress transfer between the bodies of the top platen was possible through three routes:

(i) the coiled flexible plastic pipes between the drainage basin and the drainage and flushing lines in the upper body

(ii) the maximum 3 mm wide bead of RTV732 Silastic around the circumference of the bodies

(iii) the three load cells which were mated, bolted and sealed into the recesses in both bodies.

Of these three possible stress paths, it was considered that the use of coiled flexible pipe connections for the flushing and drainage lines ensured negligible unmeasured stress transmission through this inter body contact. Also, simple experimental work showed that the Youngs Modulus of cured Silastic is about 0.2 N/mm^2, and thus unrecorded stress transmission through the circumferential bead at the small strains required for full stress transmission to occur through the load cells could be shown to be negligible. Consequentially, it was confidently assumed that all significant stress transfer between the bodies would be measured by the load cells.

The 2.5 kN capacity load cells designed and developed specifically for the research and details of their manufacture are given in Appendix C. The design strain of the cells at their maximum working load of 2.5 kN was 800 microstrain, which allowed for a 250% overload before the linear elastic region of the material would be exceeded. This design strain ensured also that the cells were stressed within their most linear region, and minimised creep potential in the cell body. Aluminium to the specification 2014 T6 was used as the cell body material as it shows especially linear behaviour. The electrical circuitry employed 6mm gauge length epoxy backed strain gauges, type Kyowa FLA-6-350-23, in a full Wheatstone bridge for self temperature compensation, and a low 5v energising voltage was used to minimise gauge creep. A high gauge resistance and a long gauge length were employed to improve current and heat dissipation characteristics, and an epoxy rather than a polyamide backing was adopted as it exhibits a lower creep potential.

The upper body of the top platen served primarily as an efficient seal and tilt reducing mechanism as explained in section 4.1. The central drainage piston was rigidly screwed into the body, and the air and flushing lines connected to it from the cell top using coiled flexible pipe. Provision was made in the design for use of up to five 'O' ring seals but only the three shown in Figure 4.2 proved necessary in practice. Verification of the sealing efficiency is covered in Section 5.2, but it is noted that the sizes of the 'O' rings adopted for use

were determined from a series of trials aimed at ensuring a seal whilst minimising side friction. The pressurised water used to apply the specimen vertical stresses was regulated by air pressure from either a 0-100 psi (690 kPa) or 0-30 psi (207 kPa) air pressure regulator acting on a air-deaired water bladder cell. The regulators were Nullmatic Pressure Regulators, models 40-100 or 40-30HF, respectively.

Once the cell was assembled and the specimen compacted the top platen was pushed into the consolidation cell using a hydraulic press until the platen was flush with the upper flange. After full assembly of the cell the platen would be forced slowly down into contact with the specimen using the water pressure in the upper cell chamber.

4.1.1.4 Measurement of phase volume changes

In an unsaturated soil, measurement of two of either total specimen volume change, or volume change of either of the fluid phases, allows calculation of all volume changes affecting the soil if the solid phase has a constant volume. In this work it was decided to measure total specimen volume change and water phase volume change, and to calculate the air volume changes.

Total volume change of a specimen in the consolidation cell was calculated from the average specimen compression during a test and the known constant cross sectional area of the specimen. Measurement of axial compression to 0.01mm using Sangamo 50 mm stroke LVDT's (Type LSC HS550) allowed calculation of total volume changes to 0.5 cm^3, as the cell diameter was measured to be 254.0 $\pm$ 0.5 mm.

Water volume changes were measured to 0.1 cm^3 using Imperial College type volume change units connected to the cell using rigid walled plastic piping. Water back pressure to the volume change units was applied by 0-30 psi (207 kPa) air pressure regulators acting on an air-deaired water bladder cell, and observed on a 0-1 bar (100 kPa) or 0-5 bar (500 kPa) Budenburg Bourdon gauge.

Based on the foregoing, air volume changes were calculated to an accuracy of 1.0 cm^3. However, diffusion of the gas mixture that forms air through the saturated ceramics in response to partial pressure differences across the ceramics would result in apparent changes in water being recorded by the Imperial College type units, and would lead to erroneous interpretation of test data. To overcome this potential problem, the platens were designed to allow flushing away of accumulated air periodically. A flushing pressure about 10 kPa higher than the current pore water pressure would be applied to the drainage basin through the flushing inlet, and the drainage line to the volume change unit opened. Air and water would then be displaced through the plumbing to the volume change units in response to the pressure gradient applied. However during the operation a bypass line would be opened to connect a "diffused air volume indicator" between the cell and volume change units (see Figure 4.1b).

The air volume indicator consisted of an inner sealed 0.01 cm^3 graduated glass burette with a partial column of water with an inlet pipe above the outlet pipe, as shown. When the flushed fluids entered the unit at the slow rate of flow governed by the applied pressure gradient, the air bubbles separated from the water and rose to be trapped in the burette. In contrast, the water flowed without resistance through the lower outlet pipe to the volume change units. The flushing pressure applied was connected also to the outer chamber of the air volume indicator to ensure the integrity of the burette during use. The sometimes large changes in water volume used to ensure flushing were accommodated using reversal valves to govern flow direction into the volume change units. From the readings of the burette before and after flushing, at the known pressure applied to the volume change units, the volume of air displaced was calculated.

4.1.1.5 Measurement and Control of Pore Water Pressures

Specimen air pressure was regulated at a constant value of typically 50 kPa using a 0-100 psi (690 kPa) air pressure regulator, and measured using a 0-5 bar (500 kPa) Bourdon gauge. The resultant raised pore water

pressures in the specimen were measured using pressure transducers in the conventional manner. Cell A utilised 0-350 kPa range transducers (Bell and Howell model 4-366-0002-01 Mohm), and cell B utilised 0-140 kPa range tranducers (Druck model PDCR10), the variation being chosen originally to reflect the different gradings to be used in each cell and their respective anticipated maximum suctions. However, measured suctions proved to be considerably smaller than expected and lower range transducers could have been employed for all tests.

4.1.2 Ancillary Equipment

4.1.2.1 Compaction Apparatus

The brittle nature of the high air entry value ceramics and the requirement to apply a high compactive effort to the specimens during preparation required that ancillary compaction apparatus be developed to allow compaction on to a rigid unbreakable surface before assembly of the test cell with minimal disturbance to the specimen. The equipment developed is shown in Figure 4.5 and consisted of a 19.05 mm (0.75") thick steel compaction base mounted upon four adjustable legs with a semi-circular recess at one end and a hydraulic assembly jack at the other. During compaction with a Kango hammer (Type 900, 60Hz, 900W) the brass body of the consolidation cell was bolted with its greased rubber gasket in contact with the greased compaction base using seven bolts. Afterwards, the hydraulic ram was used to slide the specimen in the now unbolted cell body slowly and smoothly across the base onto the base platen of the test cell, which had been placed into and restrained in the semi-circular recess using the guide bars shown in Figure 4.5. A slight height difference between the ceramic and the base surface of the compaction plate was set to minimise abrasion of the ceramic and reorientation of compacted particles during sliding, whilst water loss was prevented by the gasket between the plate and the base, and plasticine plugs in the bolt holes in the base platen over which the specimen had to slide.

A second piece of compaction apparatus was designed and built to ensure that the compaction plate attached to the Kango hammer was guided near vertically during use. Figure 4.6 shows the compaction plate and the guide developed. The guide consisted of a 75 mm long steel collar welded onto a 12 mm thick plate with a hole bored through it for the hexagonal compaction base shaft to pass through. The hexagonal bar was restrained on three faces at two separate heights using three sets of adjustable and lockable screws orientated at 120° in plan. The screws were adjusted and locked onto the hexagonal bar such that tilt of the bar was prevented and the bar was able to fall between the screws under its own weight. The whole assembly was bolted onto the consolidation cell during use.

4.1.2.2 Jack for Removal of Top Platen

The 'O' ring seals around the circumference of the upper body of the top platen prevented it from being inserted and removed manually from the main cell body. Rather, insertion was facilitated using a hydraulic press followed by water pressure above the platen after full assembly of the cell to bring the platen into contact with the specimen.

Removal was facilitated by the screw jack arrangement shown in Figure 4.7. The jack was bolted to the top platen at three anchorage points after removal of all pipe connections to the top platen. It was bolted also to the consolidation cell body on its upper flange at four points, with spacers between the cross bar supporting the jack and cell flange to allow the top platen to be wound clear of the cell. The jack was operated manually.

4.1.3 Data Acquisition System

4.1.3.1 Hardware

The data acquisition system was set up as shown in Figure 4.8, using a BBC B Computer (24 k memory) with dual disk drive, an Acorn IEEE interface, an MC Computer's analogue input unit (model 13683) and a 16

channel DIN plug connection box. In addition a parallel printer or a Hewlett Packard A3/A4 plotter could be attached to the BBC for hard copies of the data acquired.

Preliminary data analysis was completed using the BBC, but final interpretation and manipulation of the data for more complex analysis was made on an IBM compatible VIGLEN 48 megabyte hard disk personal computer. Transfer of data between the BBC and the VIGLEN was aided by the public domain software "KERMIT".

4.1.3.2 Software

The data acquisition software "LOG3" was written by the author for use with the BBC and up to 16 data input channels. The programme allowed for:

(i) simultaneous independent monitoring of two cells if required, with the capacity to open and close data files for each cell independently

(ii) allocation and in-test variation of independent linear scanning rates for each cell

(iii) input of conversion factors and offsets for the data on each channel for real time data output in engineering units to the screen and disk (and printer if required)

(iv) in-test display of test details and calibration information

(v) in-test display, averaging and interpretation of output from the load cells to allow accurate control of the applied vertical stress.

An additional option for semi-automatic compensation of water volume change measurements for flow reversal to the volume change units proved not to be required in practice. Further details of the software and data processing options are presented in Appendix C. Software for the BBC was written also by the author to allow output of test data in tabulated and graphical formats.

4.1.4 Constant Temperature Apparatus

A thermostat controlled fan driven heater was used in conjunction with a variable speed roof mounted air circulation fan to maintain a temperature of 20°C± 1°C in the approximately 36 m^2 by 4 m high square laboratory. The thermostat was located near the windows at about the level of the experimental apparatus, with the heater several metres above. The roof fan was found to be necessary to assist the heater to achieve good air circulation and a negligible temperature gradient with height or location in the laboratory. Room temperature, atmospheric pressure and humidity adjacent to the test equipment were continually recorded using an Isuzu thermo-hygro-barograph (model 3-1135) which could be used in either 24 hour or 7 day chart mode. In addition, temperature variations were observed at two other locations in the laboratory using maximum/minimum thermometers. The thermometers confirmed that temperature gradients within the room were negligible.

4.2 Triaxial Cell

Two triaxial cells of similar design (see Figure 4.9) and suitable for testing specimens of 200 mm diameter and 400 mm height were used for part of the experimental work. The cells and their ancillary equipment were essentially conventional in nature but modified slightly to allow the testing of both unsaturated and saturated soils. The cells were made and commissioned by staff at the British Gas Engineering Research Station, then calibrated by the author with the co-operation of British Gas before the work reported in this thesis was performed. Details are given below. The cells were not used in a constant temperature laboratory but corrections were made for temperature effects.

4.2.1 Load Application and Measurement

Axial straining of specimens was applied during tests at a constant pre-set rate using a Wykeham Farrance strain control compression machine. Axial stresses developed within the specimen were measured internally using a 10 kN Wykeham Farrance submersible load cell (model WF17109) in one version of the triaxial cell, and measured externally using a 20 kN Sensotec load cell (mode 41) in the other.

4.2.2 Platen Details

The base platen comprised a 1 bar air entry value ceramic sealed with Araldite into a locking ring similar to that shown in Figure 4.3 d which was then mounted upon a grooved drainage chamber. The platen was connected to a back pressure and volume change measurement system which allowed either passive measurement of pore water pressure, if water undrained conditions were enforced, or active control of the pore water pressure if water drainage was allowed.

The upper platen was grooved similar to the base drainage chamber. When unsaturated specimens were to be tested, the platen was placed in direct contact with the soil and a regulated air pressure greater than atmospheric pressure applied to the specimen through it in order to maintain positive pore water pressures throughout (the axis translation technique). When saturated specimens were to be tested, a porous plastic disc was placed between the platen and the soil, and pore water pressure at the top of the specimen was measured passively.

4.2.3 Measurement of Volume Changes and Pressures

Axial strains were measured externally. An RDP 100 mm stroke LVDT (Type D5/2000A) accurate to about 0.2 mm was fixed to the rigid compression machine cross beam with its armature resting on the triaxial cell, and the vertical movement of the cell relative to the cross beam was measured. Strains were computed assuming the total compression or extension of the specimen corresponded to that measured by the LVDT.

Volume change units doubling as air-water interfaces were used to measure water volume change and total cell chamber volume change. The 1000 cm^3 interfaces were developed and built at British Gas Engineering Research Station to a design similar to the Imperial College type volume change units used at the University. Displacement of the piston was measured using either a Penny and Giles Rectilinear Potentiometer (type HLP 190SA1/100 mm/4 kohm) or RDP 100 mm stroke LVDT (type D5/2000A). The units were nominally accurate to about 2 cm^3 at a constant temperature. Air volume changes were not measured.

From a knowledge of the nominal cell chamber volume change, and the effects of piston ram movements and changes in the applied cell pressures on the nominal cell volume, the average total volume change and the average degree of radial strain of the specimen were calculated. Diffused air that had accumulated beneath the base ceramic was flushed out without measurement after consolidation of the specimen, and any diffusion that occurred during the relatively short duration main stages of the tests was shown to be negligible. Total specimen volume changes were nominally measured to about 0.1 cm^3.

The system employed up to 3 no 100 psi (690 kPa) capacity Sensotec pressure transducers (TJE series, 2 gauge) to record the cell chamber pressure, specimen air pressure, and back pressure to the base volume change unit. The pressures were measured also on Bourdon gauges to coarse check the output from the transducers.

4.2.4 Data Acquisition System

All data acquisition was made using a Digital Equipment Corporation DEC PDP 11/44 mini computer, connected via a serial link to a Mowlem Microsystems ADU 700 Datalogger which allowed 0 to 10 volt analogue input from up to 64 channels. All transducers were used in conjunction with either Protech or RDP transducer signal amplifiers, which employed individual removable amplification cards stored in a rack unit. Each card was calibrated for use with only one specific transducer such that

full scale amplified output from the transducer amplified output was approximately 10 volts and maximum use of the input range of the data logger could be made. The system is summarised in Figure 4.10, which shows also that coarse checks on the recorded output were possible using digital voltmeters connected to the amplifier output. This check system was used during all tests, with output on the voltmeters noted periodically by hand for subsequent correlation with the computer recorded data.

The software for simultaneous data acquisition from several independent concurrent tests was developed in house at British Gas Engineering Research Station. It allowed nominated channels associated with any given test to be scanned and their current output displayed on screen in engineering units based upon the transducer zero values and calibration factors stored in the computer. Data was periodically recorded on disk on either a root time or linear time basis in millivolts, but was usually presented in engineering units.

4.3 Compression Cells

A large number of one dimensional compression tests were made at the Research Station in the relatively simple piece of apparatus shown in Figure 4.11. It consisted of a 305 mm diameter metal cell into which a specimen of maximum height 200 mm was compacted, and a conventional strain controlled Wykeham Farrance compression machine with a rigid plane metal top platen attached to the reaction bar of the machine via either a 20 kN or 111 kN capacity model 41 Sensotec load cell. In use, the compression cell was mounted on the compression machine and load cycles applied to the specimen at a constant strain rate. The applied strain was recorded using an RDP 100 mm stoke LVDT in a similar manner to that described in section 4.2.3, and data acquisition was made using the system noted in section 4.2.4.

Compaction was applied to the specimens as noted in Appendix A using either a Kango hammer or a tamping rod. The Kango hammer was the same used as that described above in section 4.1.2.1, but with a 300 mm diameter compaction plate and a modified version of the compaction guide suitable for the larger cell diameter. The tamping rod consisted of a 2 m wooden pole with a 100 mm diameter cylindrical 2 kg mass at the end.

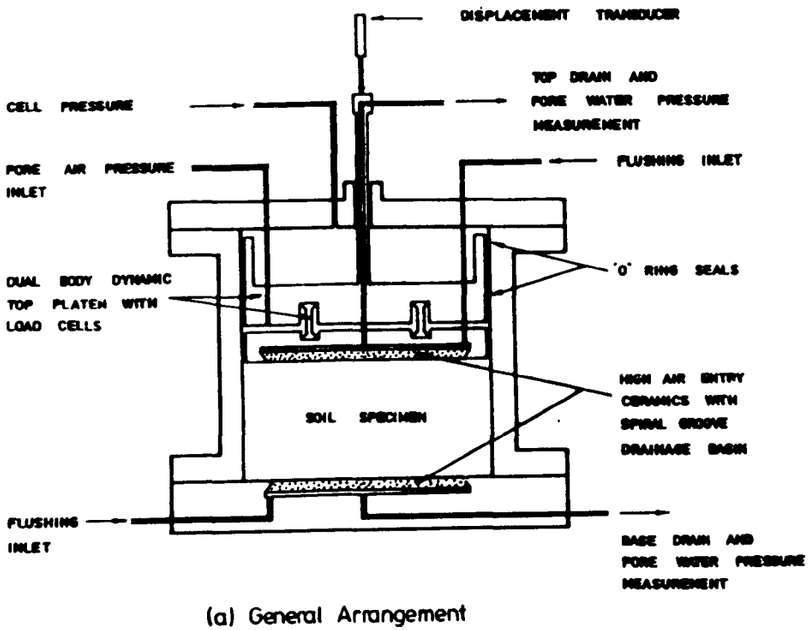

(a) General Arrangement

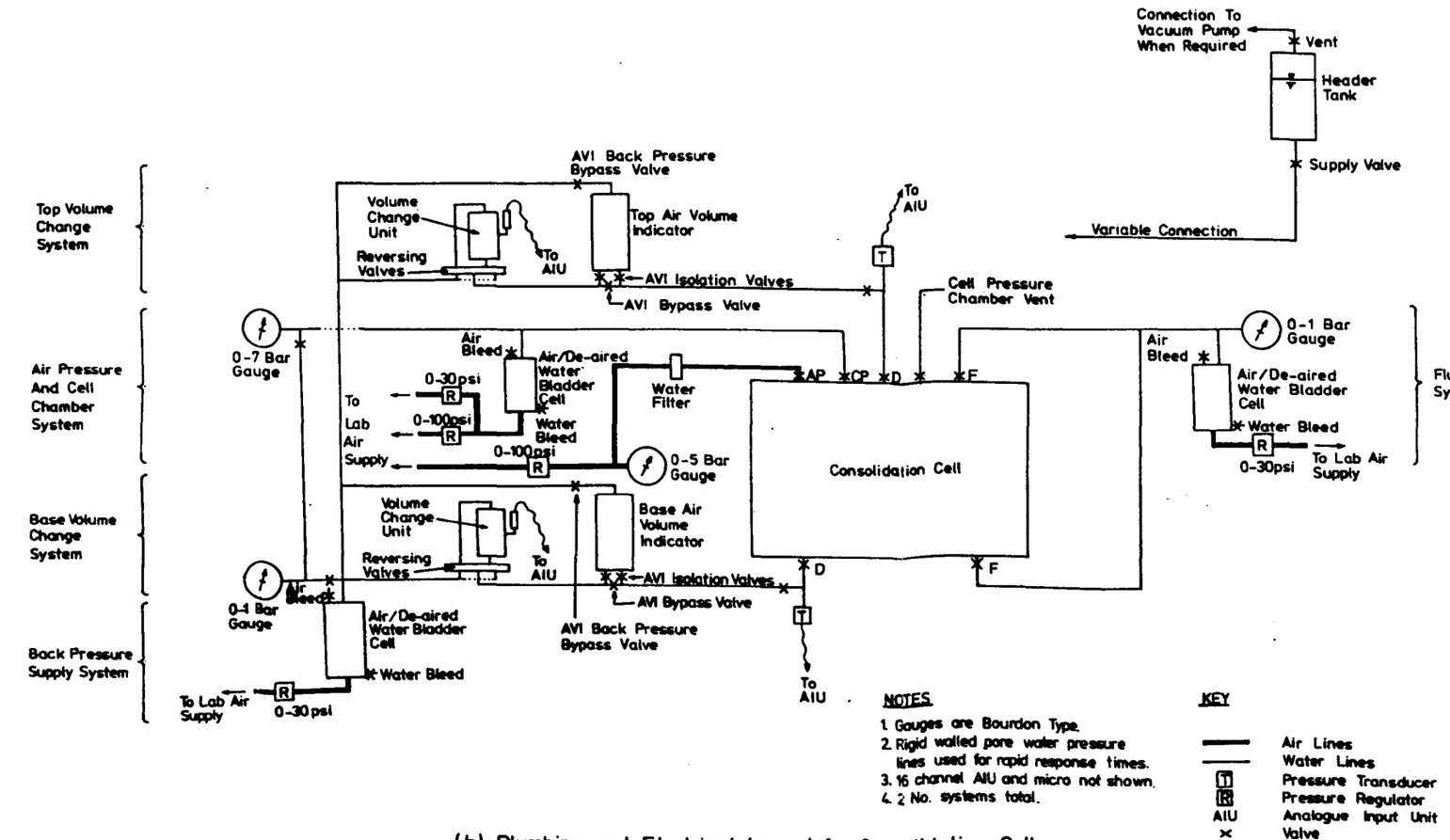

(b) Plumbing and Electrical Layout for Consolidation Cell

Figure 4.1 - New Consolidation Cell and Ancillary Instrumentation

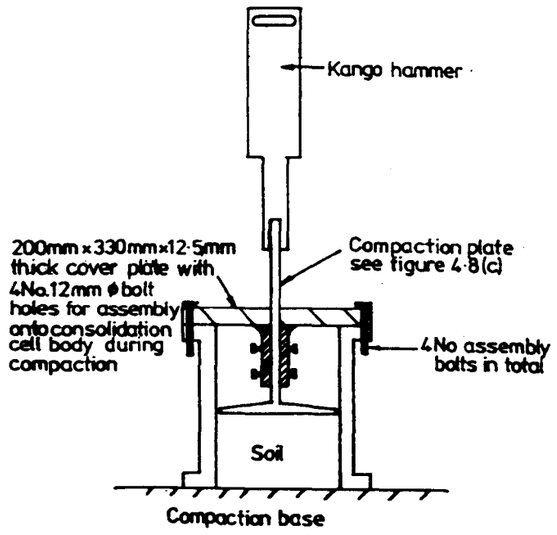

(a) General Assembly

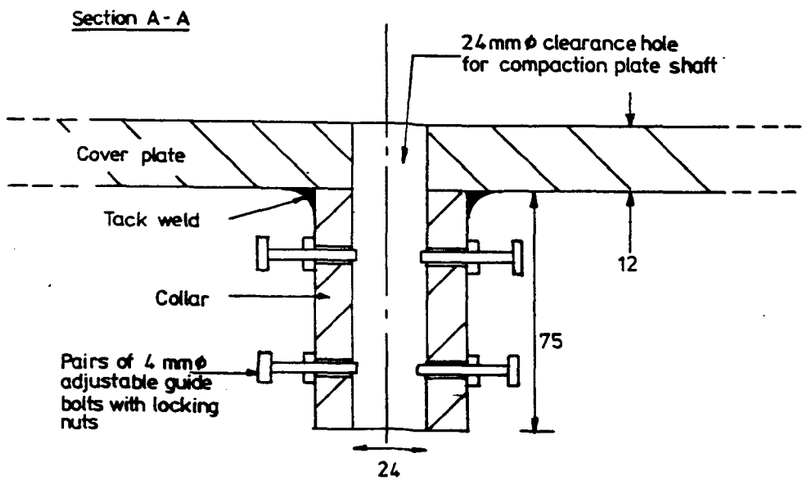

(b) Details of Guide For Compaction Plate

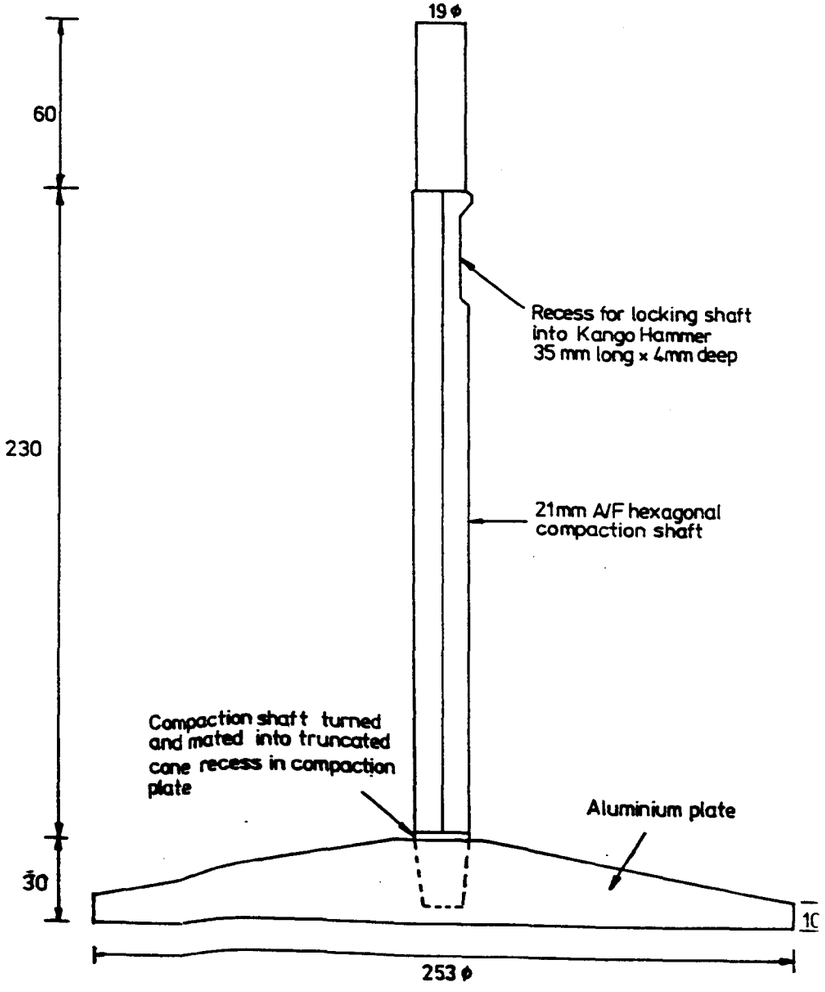

(c) Compaction Plate

Figure 4·6 - Compaction Guide and Plate Used During Test Series A and B

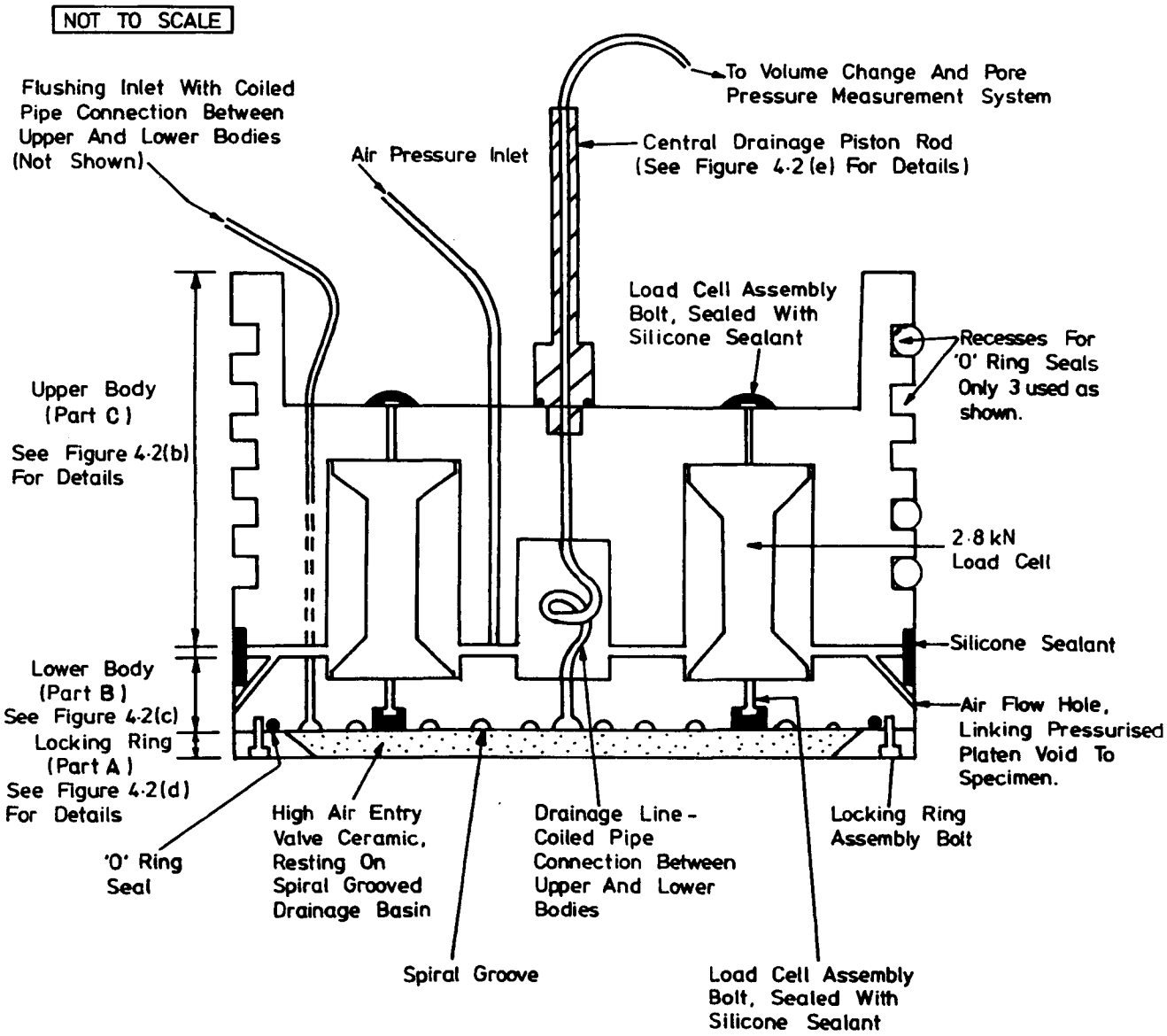

(a) General Assembly

Figure 4·2 - Top Platen For Consolidation Cell

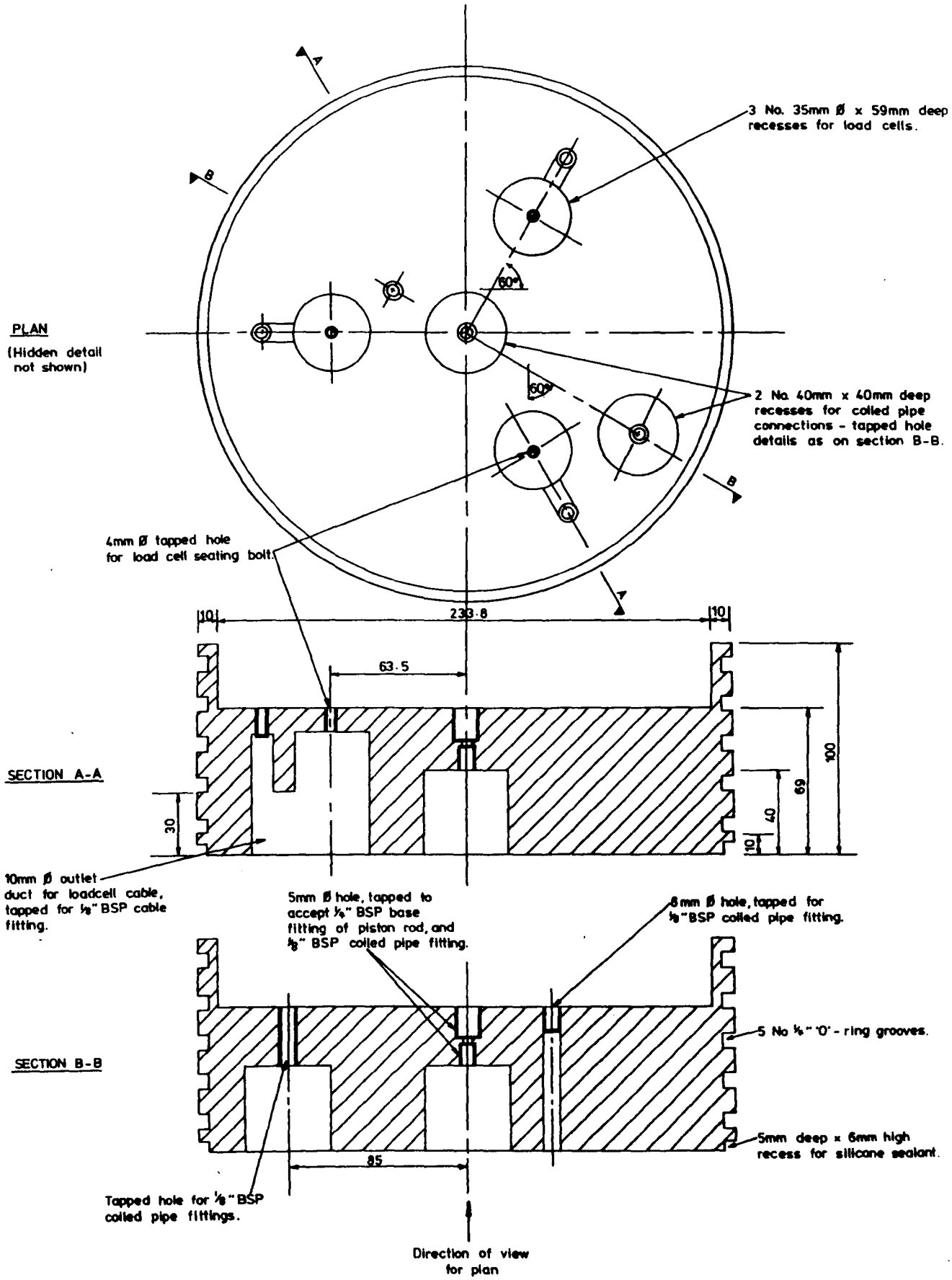

(b) Details Of Upper Body

Figure 4·2 - Top Platen For Consolidation Cell

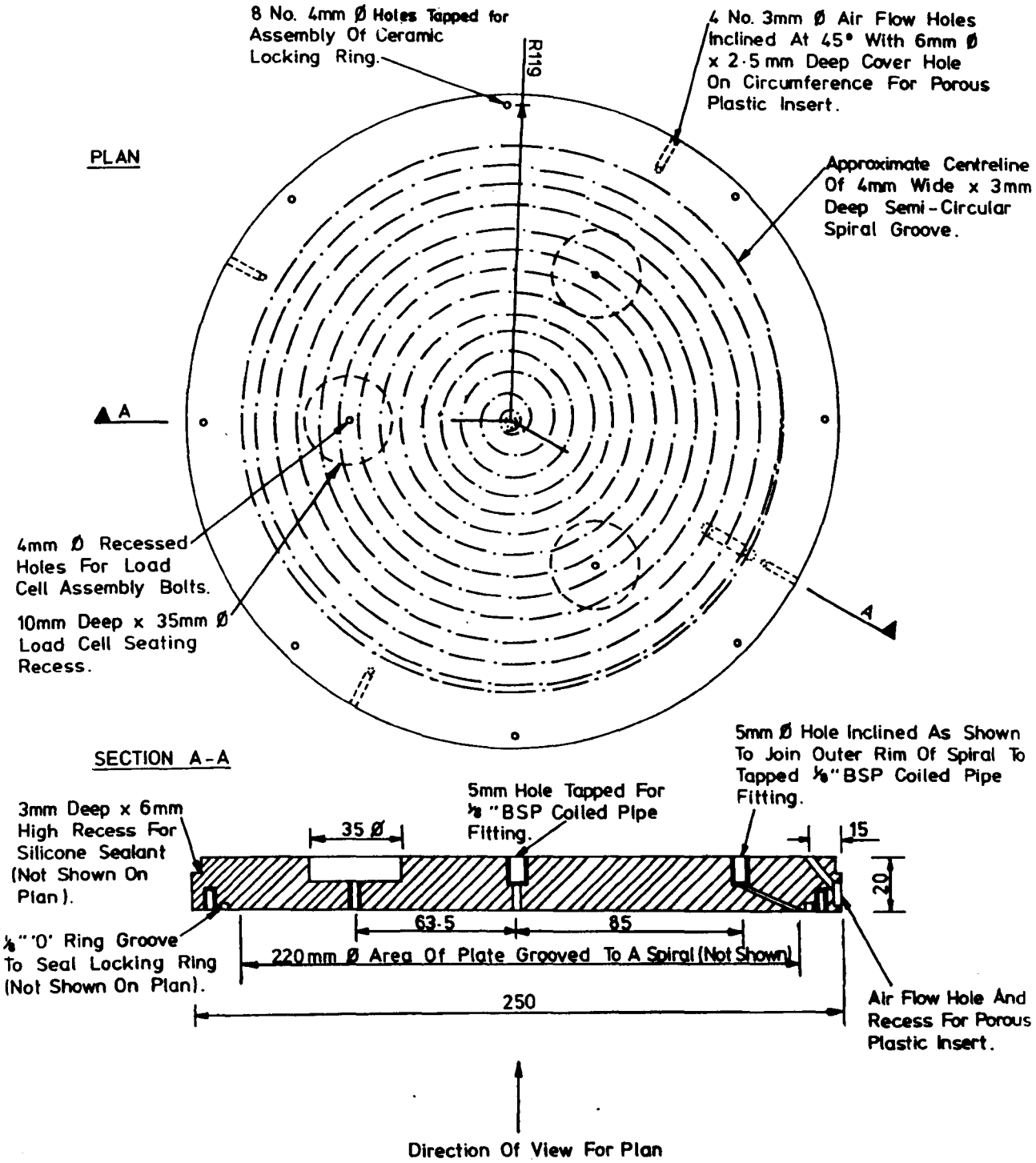

(c) Details Of Lower Body

Figure 4·2 Top Platen For Consolidation Cell

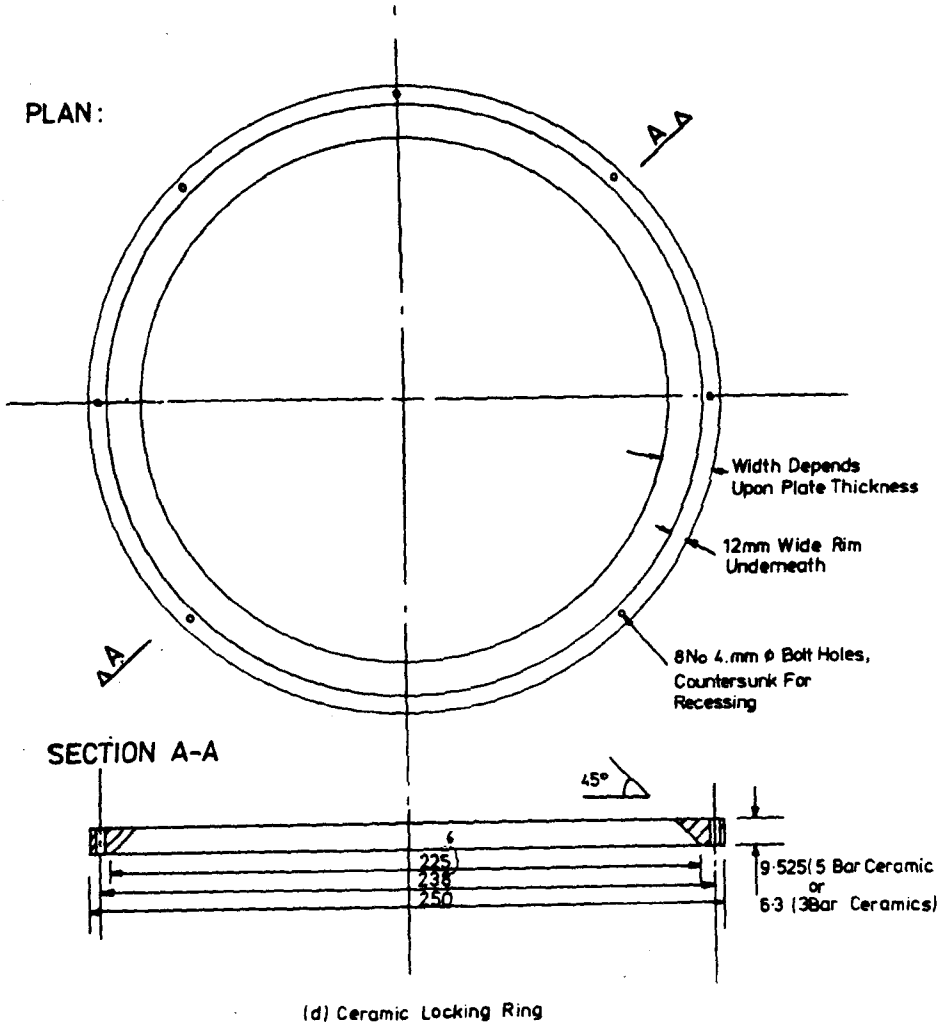

(d) Ceramic Locking Ring

Figure 4·2 - Top Platen For Consolidation Cell

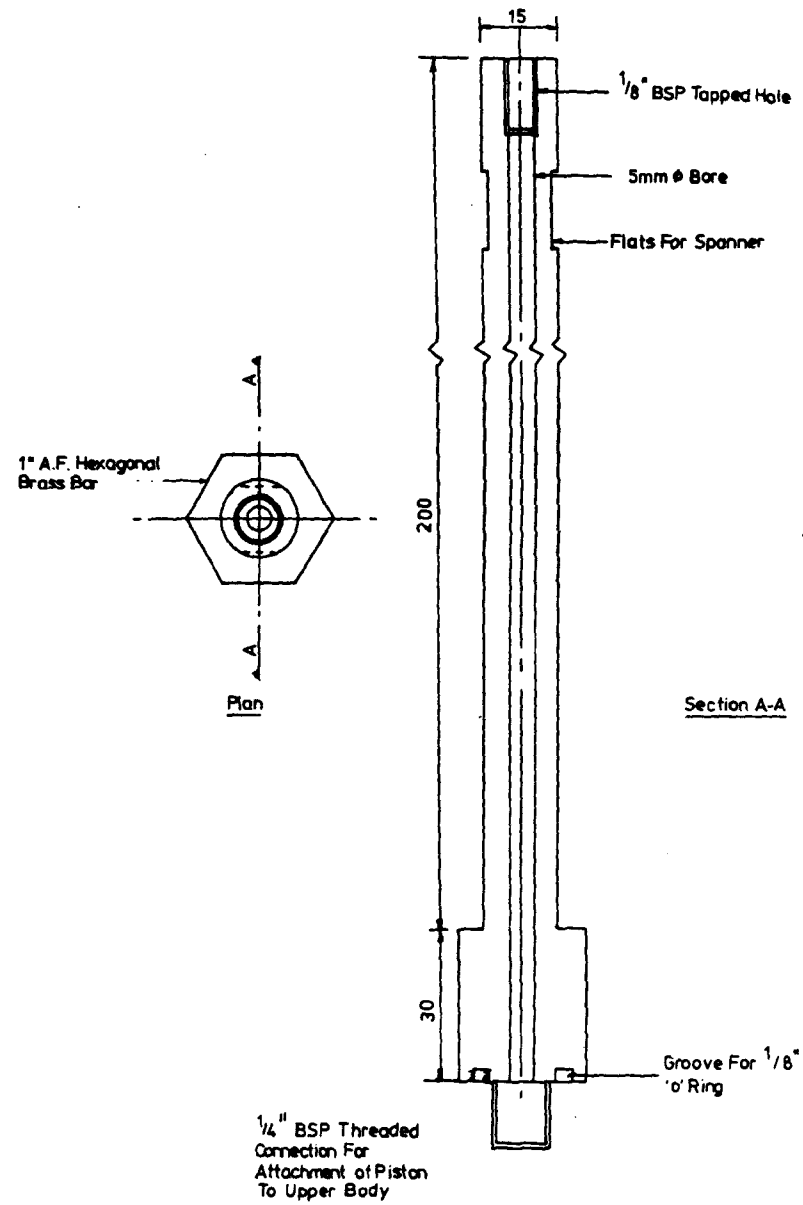

(e) Central Drainage Piston Rod

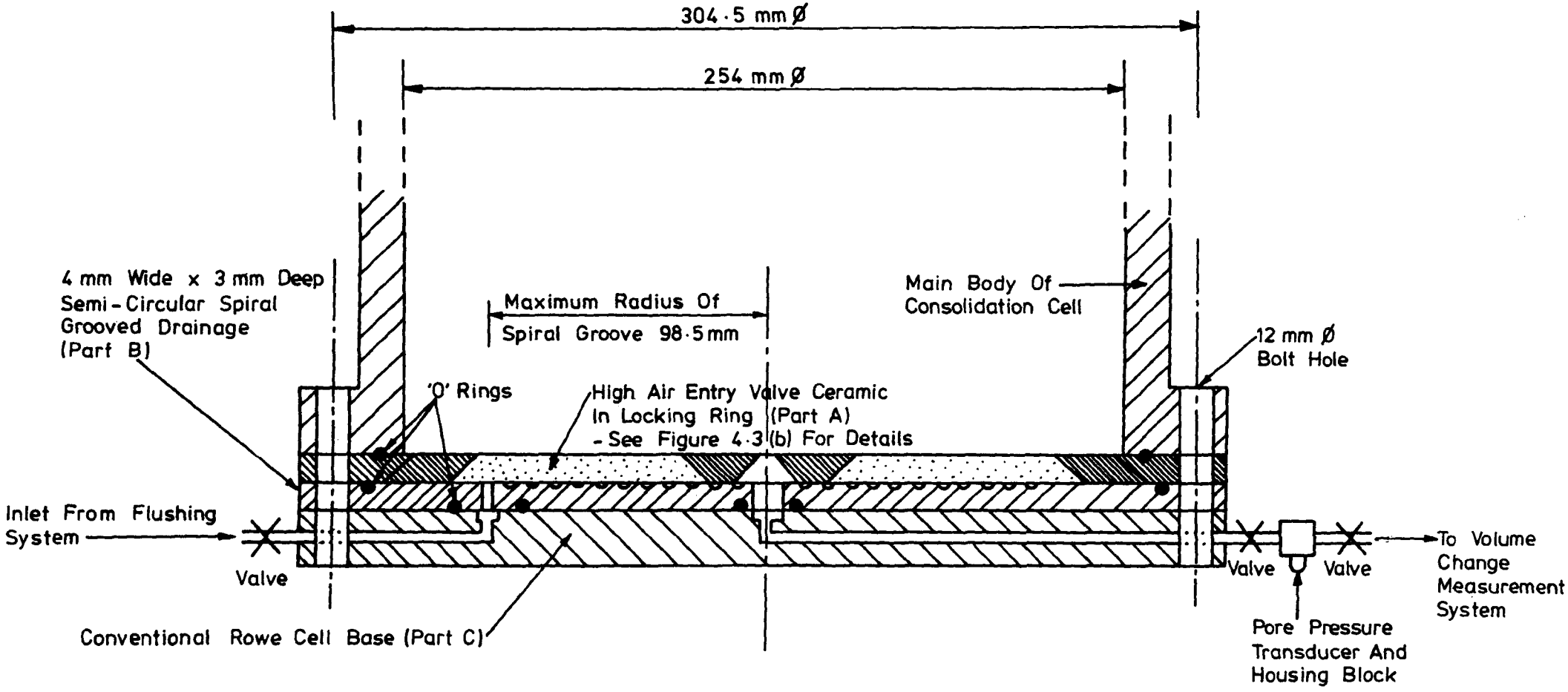

(a) General Assembly

Figure 4·3 Base Platen For Consolidation Cell

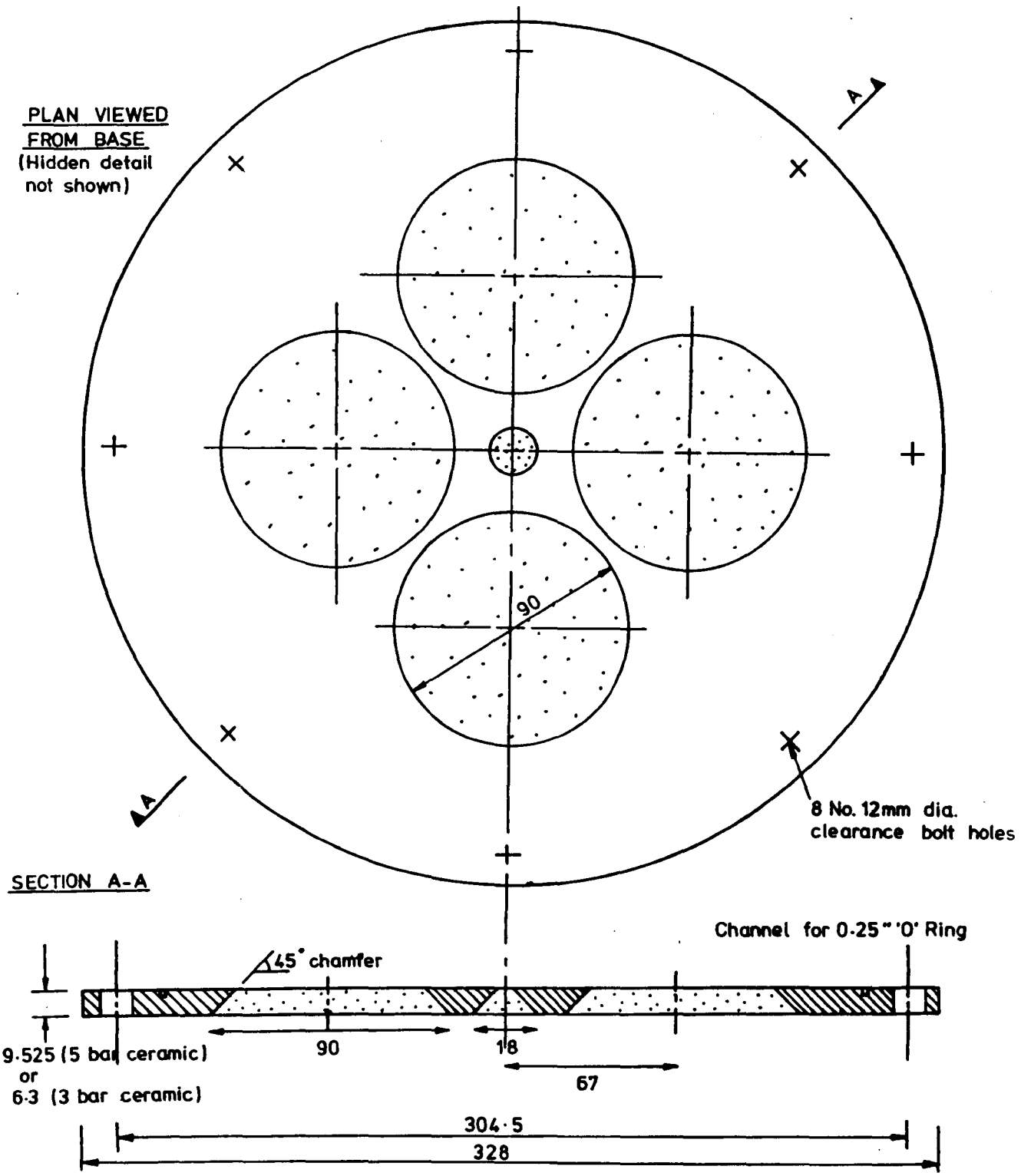

(b) Ceramic Locking Ring

Figure 4·3 - Base Platen for Consolidation Cell

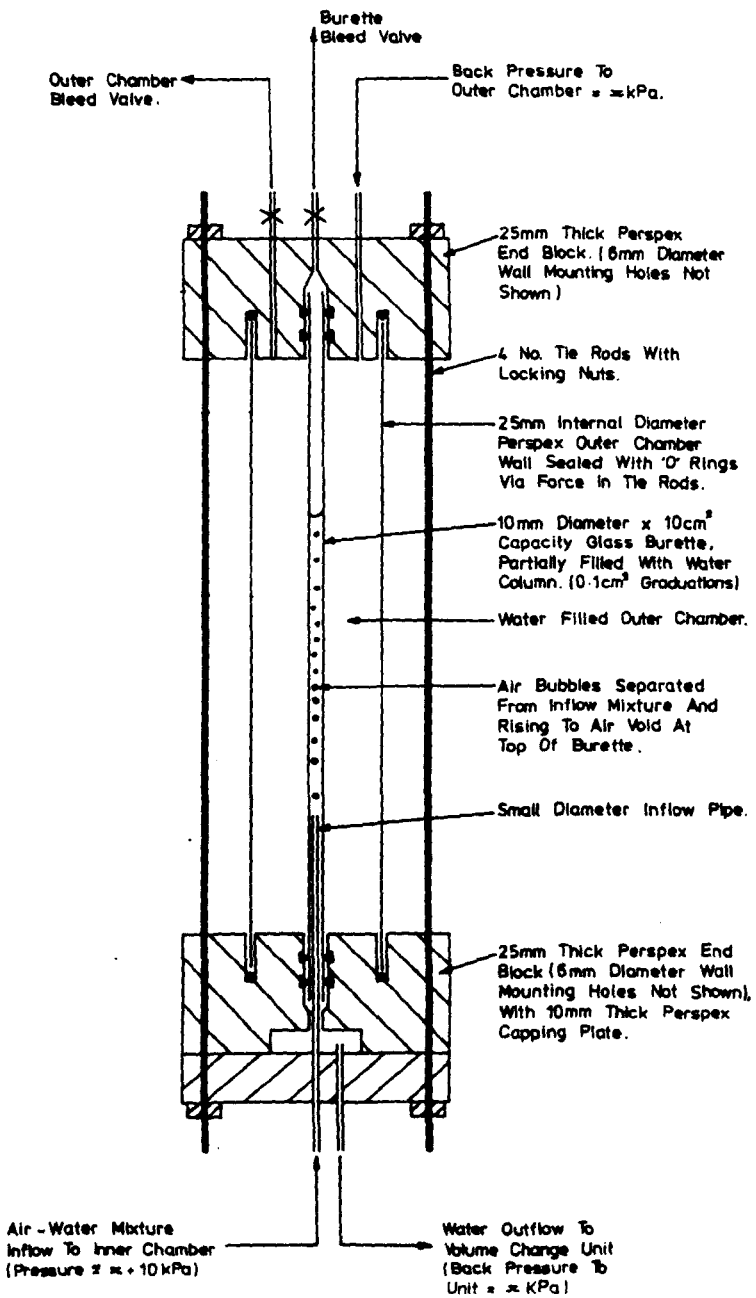

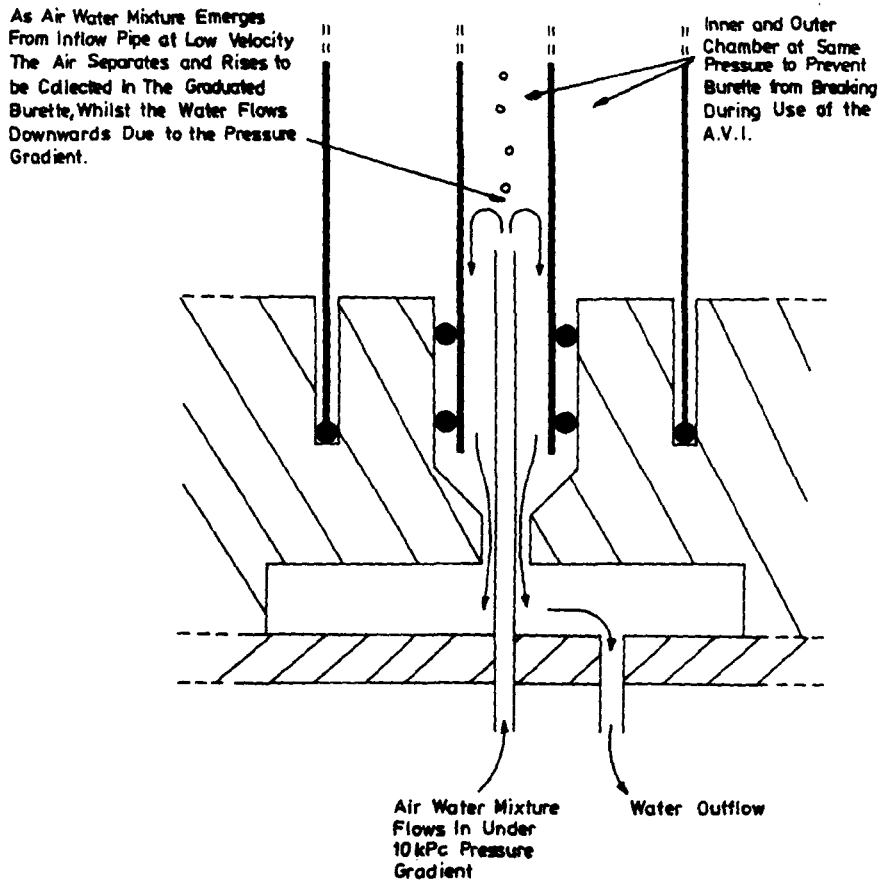

(a) Left: Cross Section
(b) Above: General Principles of Operation

Figure 4.4 - Diffused Air Volume Indicator

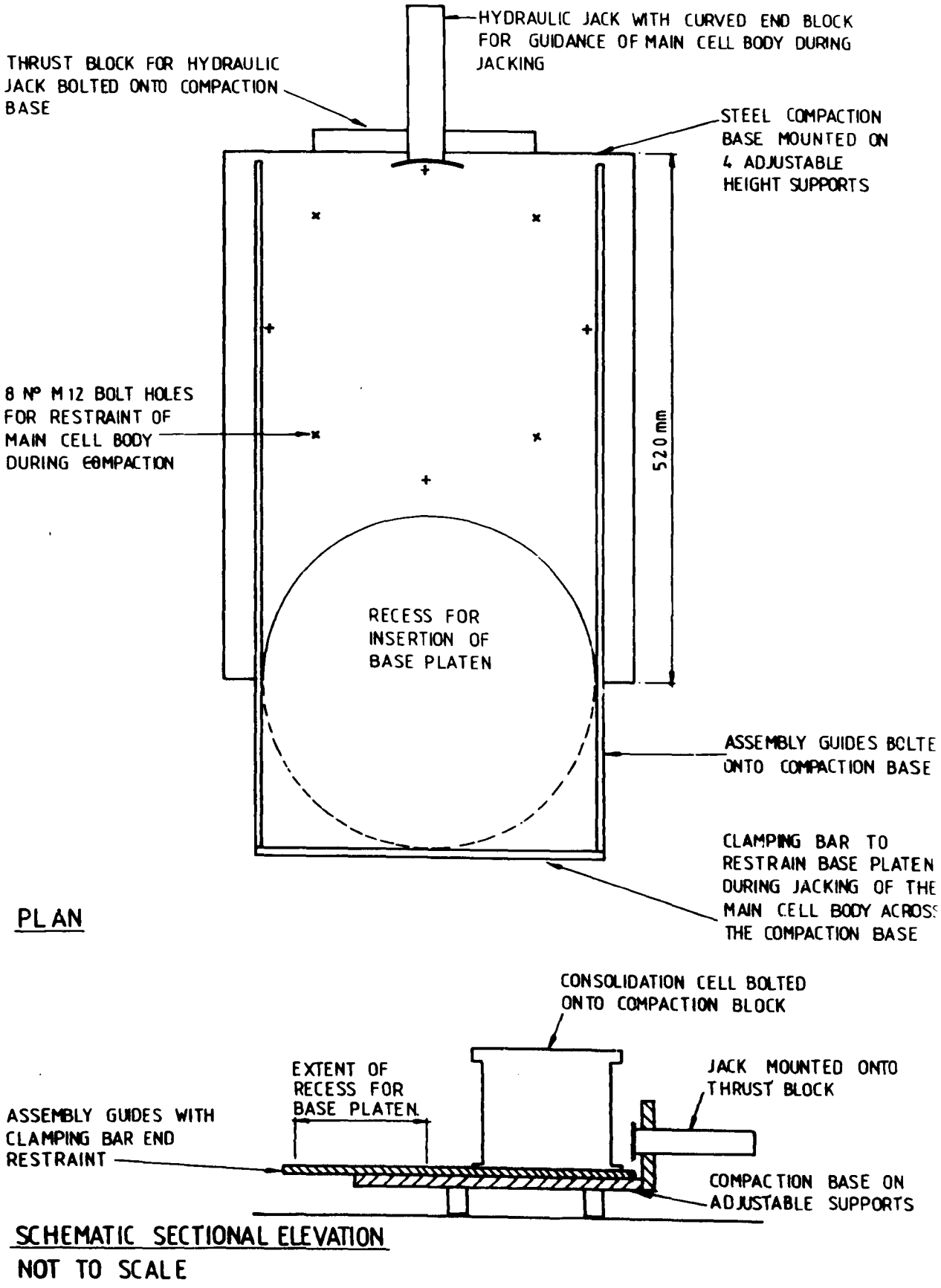

Figure 4·5–Compaction Base Used During Test Series A and B

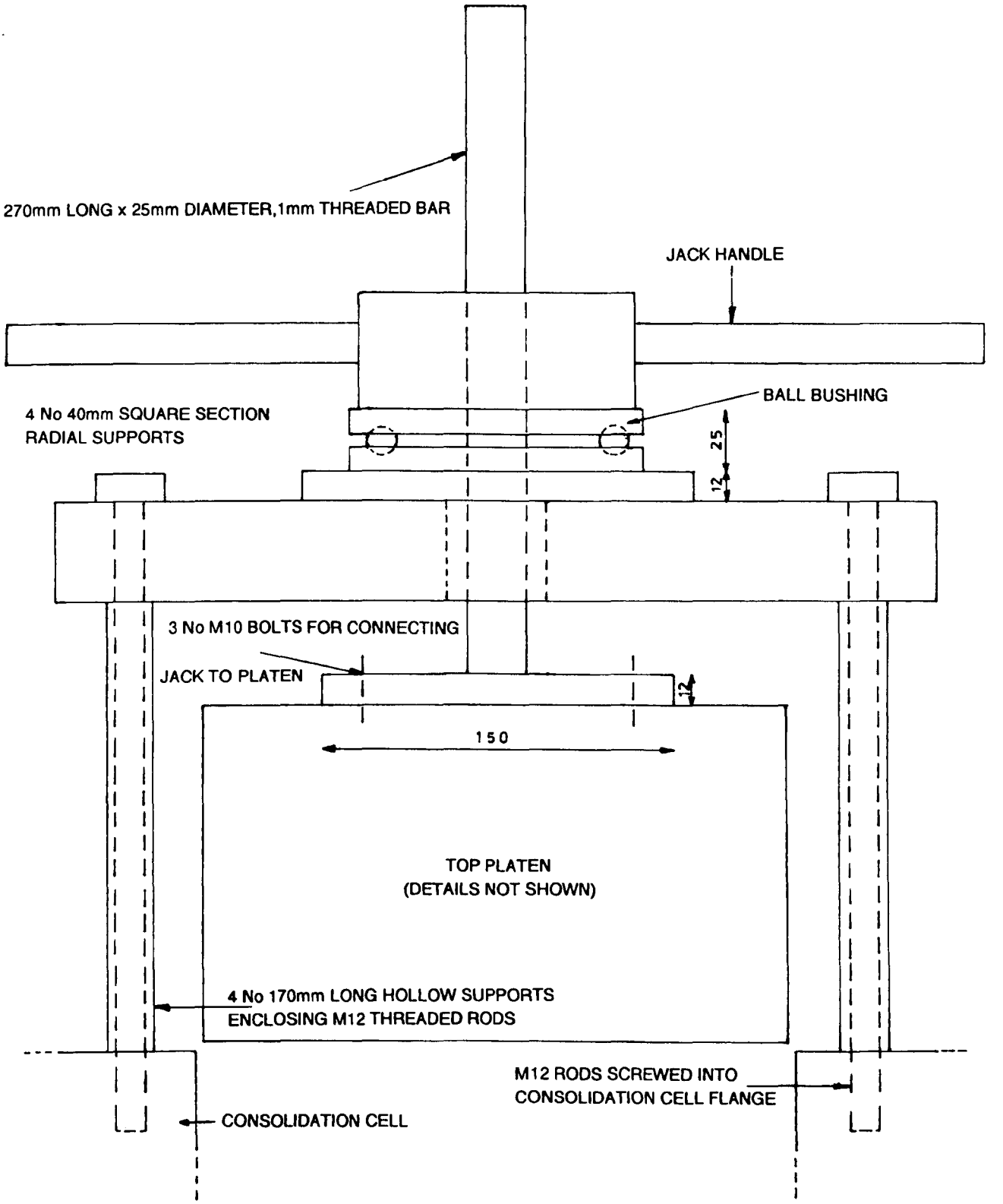

Figure 4.7 – Screw Jack for Removal of Top Platen from Consolidation Cell

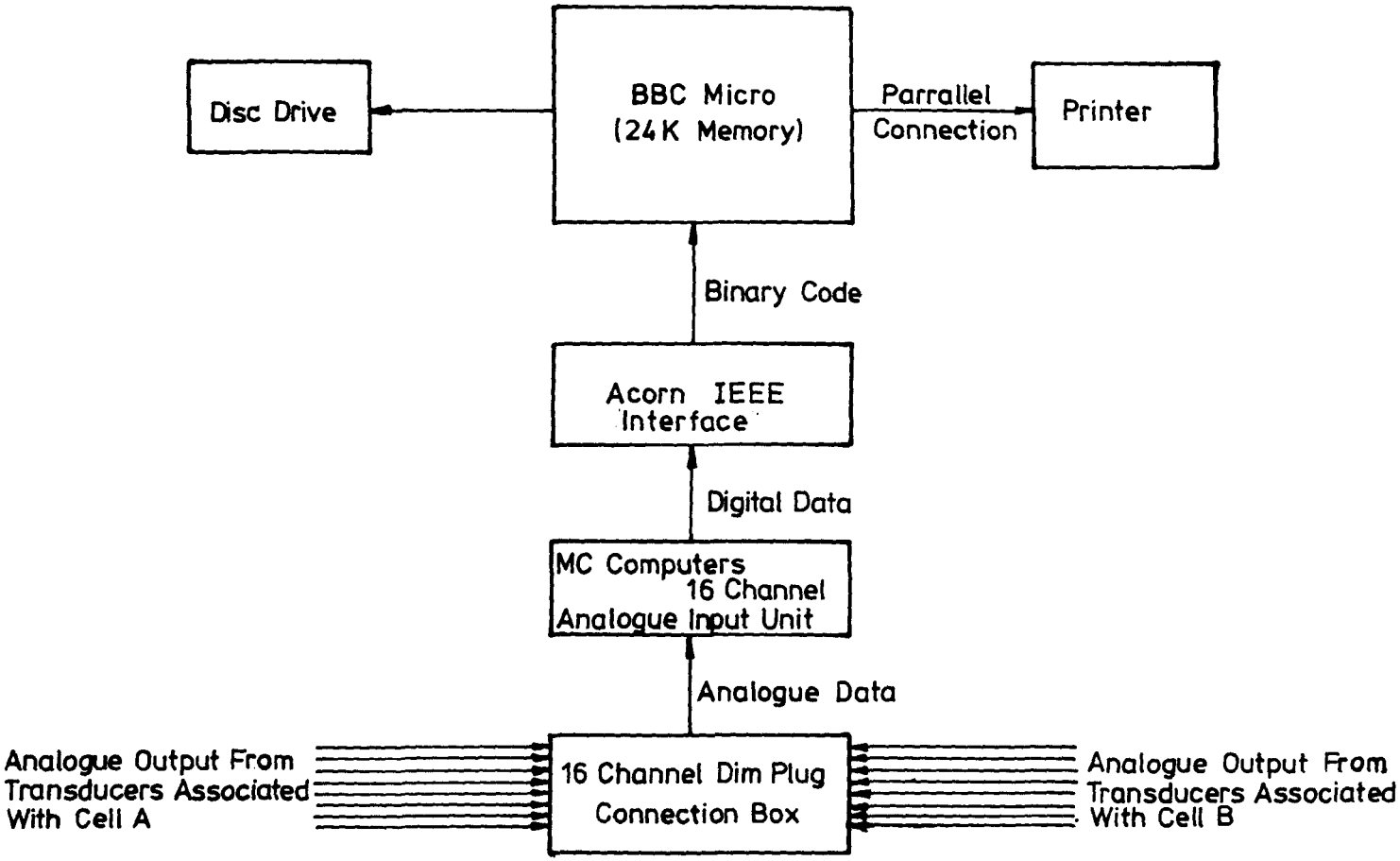

Figure 4.8- Data Acquisition System For
Test Series A and B

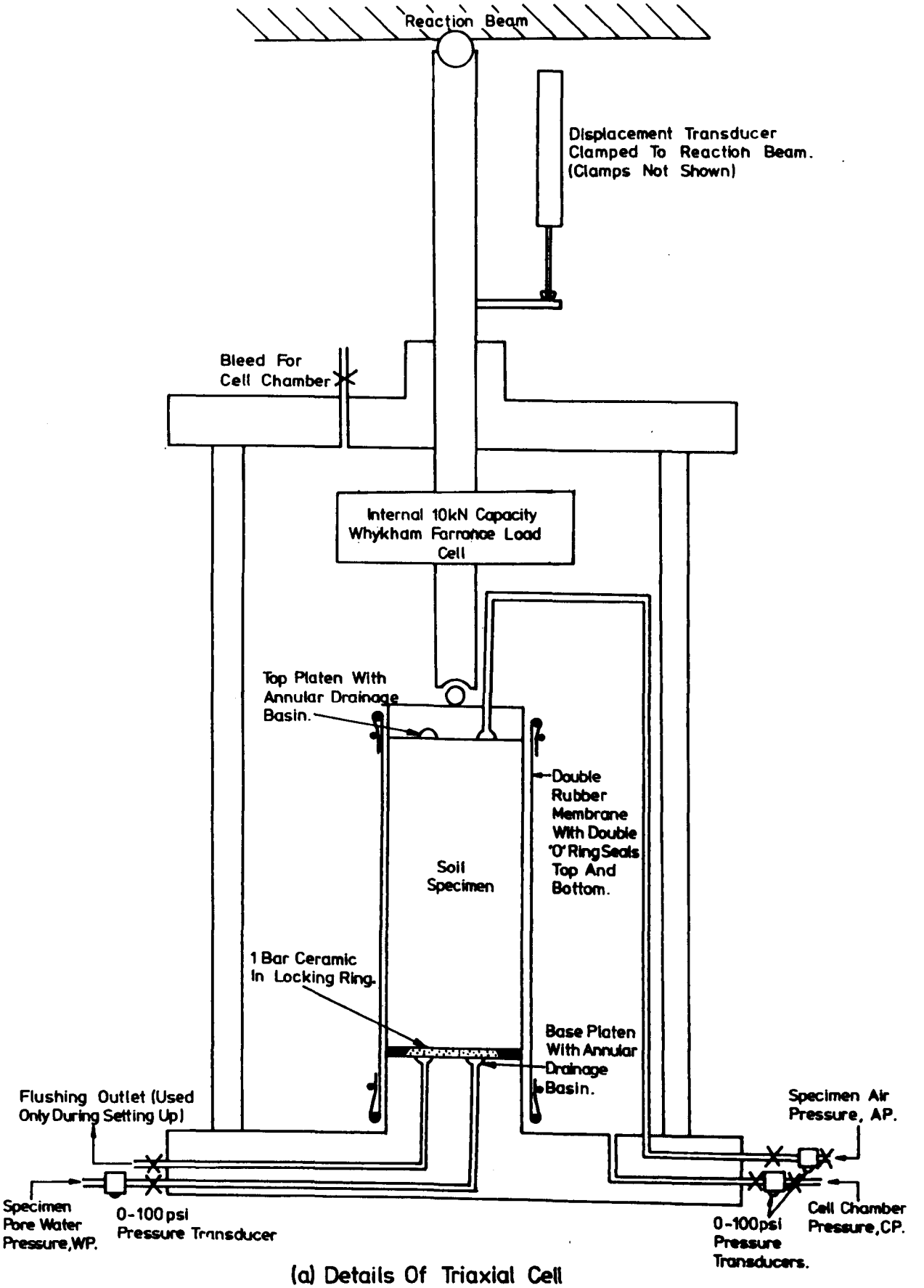

(a) Details Of Triaxial Cell

Figure 4.9 Modified Triaxial Cell And Instrumentation Used For Test Series C

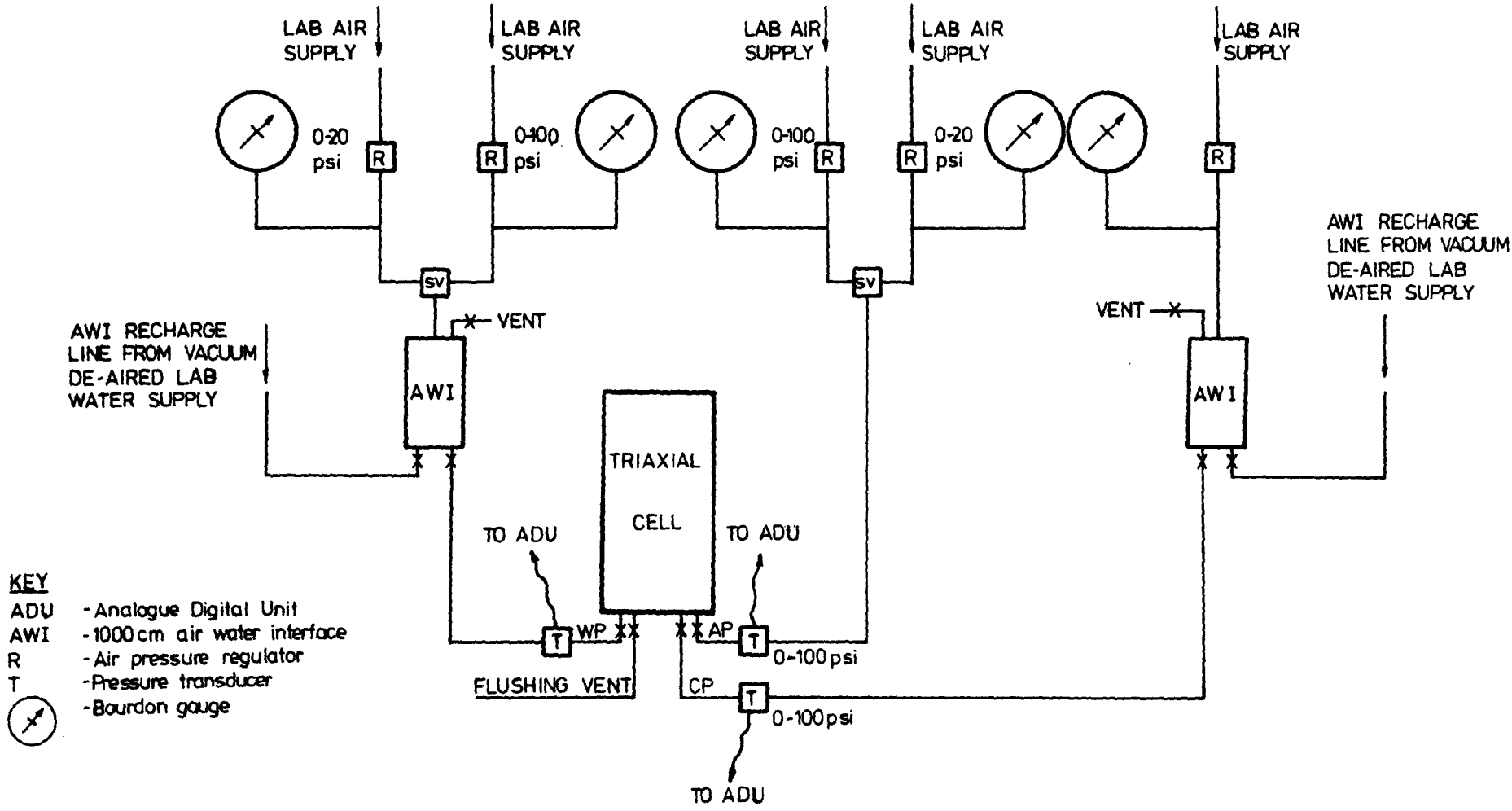

(b) Plumbing Details

Figure 4.9 - Modified Triaxial Cell and Instrumentation Used For Test Series C.

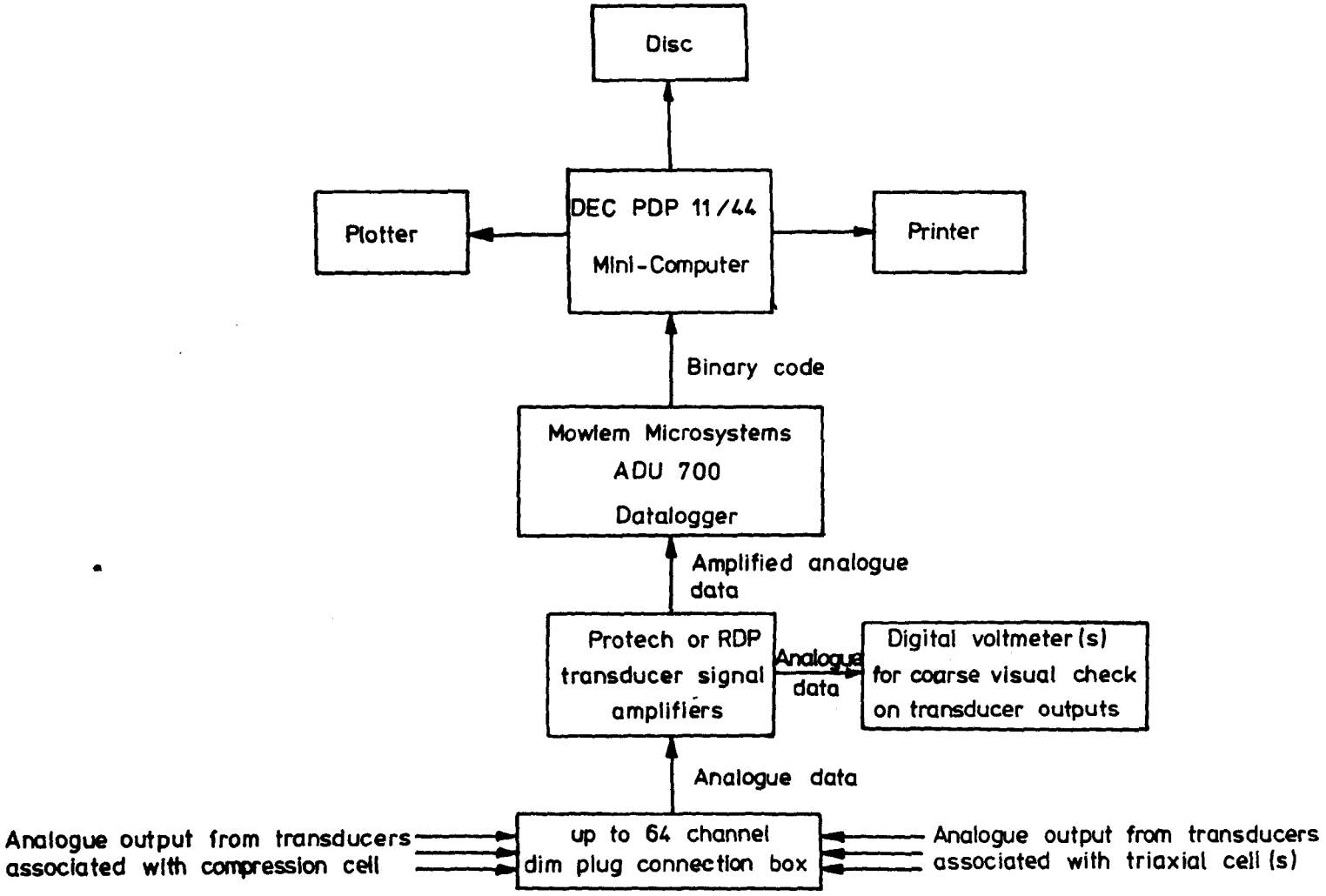

Figure 4.10 Data Acquisition System For Test Series C and D

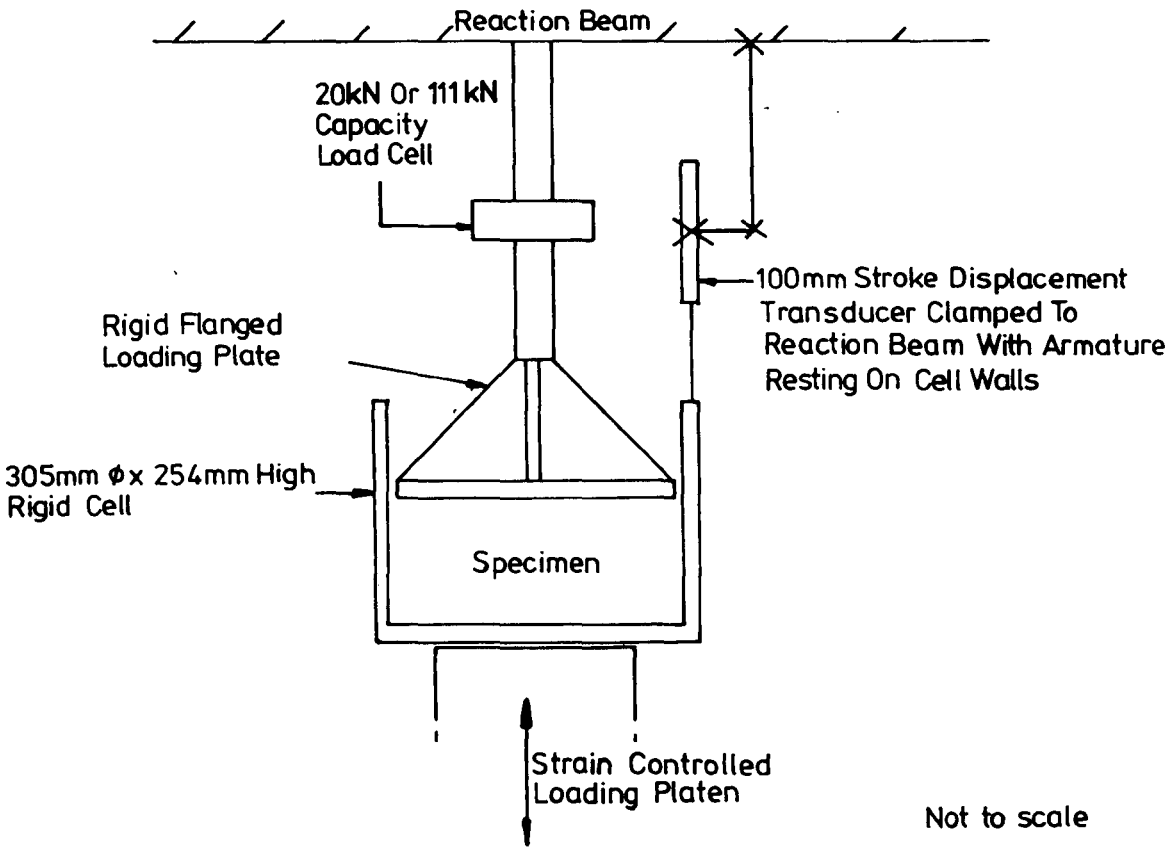

Figure 4.11- Compression Cell For Test Series D

CHAPTER 5

CALIBRATION OF INSTRUMENTATION AND OPERATIONAL CHECKS ON APPARATUS

This chapter presents the methods used for and results from the calibrations and operational checks on the experimental apparatus. Emphasis is given to non-standard calibrations, and calibrations on the new consolidation cell. All calibrations were made using a voltage supply of 5 volts at the University, or 10 volts at the British Gas Engineering Research Station. Least square linear regression analyses were applied to all calibrations to determine the best straight line fit and confidence limits for the data.

5.1 Calibration of Instrumentation

5.1.1 Temperature

5.1.1.1 University Apparatus

As noted in section 4.1.4, a nominally constant temperature laboratory was used for test series A and B. Temperatures recorded on the Isuzu drum chart were compared with two independent mercury thermometers and a second 7 day drum recorder over a period of several weeks, and no discrepancies were revealed. Humidity and atmospheric pressure measurements were not verified. Prior to adoption of the drum recorder, attempts were made to utilise the temperature sensor capabilities of the Analogue Input Unit (AIU) but the low accuracy of the instrument precluded its use. A typical chart from the recorder is presented in Figure 5.1, which shows that temperatures were maintained usually within 1°C of 20°C, and humidity varied between 50% and 60%. Atmospheric pressure varied according to the weather conditions.

5.1.1.2 Research Station Apparatus

Temperature in the soils laboratory of the Research Station was not controlled at the time of the experimental work reported in this thesis. Temperature was recorded twice daily at two positions in the laboratory on the mercury thermometers and the temperature of water in the de-aired water supply tank could be recorded also. As shown in Figure 5.2, large temperature fluctuations occurred as heaters warmed the laboratory during the day, but ceased operating at night. Variations in air temperature of up to 5°C were recorded, but corresponding water temperature changes were limited by the containing vessel to about 2°C.

5.1.2 Volume Change Units

5.1.2.1 University Apparatus

The 100 cm^3 capacity Imperial College volume change units (VCU's) used with the new consolidation cell were de-aired prior to calibration in the following manner:

a) The header tank containing de-aired water was connected through the top and bottom of the units as shown in Figure 5.3.

b) With valves A and C open, and valves B and D closed, valve H was opened and water flowed into chamber 1. The VCU was gently agitated to aid flushing of air out of the vent, then valves A and C closed when no further air was being flushed out.

c) The VCU was inverted and valves B and D opened. The VCU was gently agitated again until chamber 2 was apparently de-aired. Valves B and D were closed and the unit inverted again.

d) Steps 2 and 3 were repeated twice more each, then all valves closed.

Once de-aired, the VCU was connected as shown in Figure 5.4 to two Geotechnical Digital Systems digital pressure controllers (Model INTEL 8085), which were microprocessor based hydraulic servo mechanisms. These units, which were previously de-aired in accordance with the manufacturer's instructions, were capable of measuring volume changes to an accuracy of 0.5 mm^3 and pressure to 0.25 kPa. Connection of the GDS units and VCU was made underwater to ensure that no air was allowed to enter the system, and the connection made such that a nearly full GDS unit was connected to a nearly empty VCU chamber.

Calibration was executed semi-automatically using a specially written computer programme "VOLCAL" (see Appendix D) together with the BBC computer and AIU used for the main series test, an Electroplan interface, one GDS unit actively computer controlled, and one GDS unit in a passive mode. In the passive state, a GDS unit had its operational pressure set by the four digit wheels and its stored volume varied in response to external changes, in this case volume changes caused by the active unit. The active unit had its stored volume controlled by the computer, but its pressure was governed by the passive GDS unit.

The programme worked by instructing the active GDS unit to change its volume by a specified amount, and allowing it a variable time period (dependent upon the volume increment specified) to achieve this change and for the equilibrium back pressure to be set up in this system as a whole. After equilibrium was reached, the programme recorded the output from the displacement transducer that formed part of the VCU. The target total volume change to be applied to a VCU chamber was cycled within a specified range (usually 100 cm^3) for a specified number of cycles (usually 3), for specified increments (usually 5 cm^3), and the displacement transducer/volume data stored on floppy disk in a form suitable for direct input into the least squares fit programme. Output from the programme gave the best straight line fit and confidence limits for the data determined for the active VCU chamber. The results of the calibrations are presented in Table 5.1 for a back pressure of 100 kPa.

Investigations into the influence of back pressure on the calibrations showed that if the back pressure varied in the range 50 kPa to 200 kPa, negligible change in the calibration factor or confidence limits resulted provided the VCUs were rigorously de-aired.

Investigations into the stability of the VCU output when isolated from the rest of the plumbing were made also, and these showed that transducer stability was not a problem.

5.1.2.2 Research Station Apparatus

Calibration of the 1000 cm^3 volume change units, known as air-water interfaces (AWI) at the Research Station, was made by the staff at the Station using a graduated burette as the control. Water was pushed into the water chamber of the unit in known increments and output from the displacement transducer recorded by the computer each time. A single half cycle was used to calibrate the units, and the results of the calibrations are presented in Table 5.3.

Additional checks on the units were made by the writer in order to:

(a) determine the performance of the displacement transducers when their armatures were fixed, and

(b) determine the performance of the whole unit when real volume changes were prevented by isolating the units from the rest of the plumbing.

The investigations into the performance of the displacement transducers alone utilised AWI5, and showed that its sensitivity to typical temperature fluctuations in the laboratory was negligible. A drift equivalent to an apparent change in volume of 1.3 cm^3, equating to about 0.1% of full scale, was observed over the five day test period but subsequent checks on the manufacturer's data showed that this lay within the confidence limits for the transducer and was therefore not significant.

Performance of an isolated AWI was checked also using unit AWI5. The output from the AWI was recorded over a 1 month period and compared with measurements of ambient laboratory air and water temperatures (see Figure 5.5). This work revealed that a slow leak existed during the test, but that after correction of the AWI data for this linear drift, a clear correlation between temperature and output existed. An apparent change in volume of 10 cm^3 resulted from every 1°C rise in temperature. However, only a small portion of this potential error would be expected to be manifested during a real test as the air volume change component would be eliminated by regulation of the air pressure, and only expansion of the water in the system and the materials of the AWI should contribute to the problem. Allowing for the larger water volume involved during a test, it is estimated that temperature effects during use were less than 5 cm^3 per degree C.

5.1.3 Load Cells

5.1.3.1 University Apparatus

Before calibration, the load cells were pre-loaded to twice their maximum 2.5 kN working load for 15 load - unload cycles using a compression machine and load ring. The load cells were then left under power for at least 24 hours before detailed calibration with an oil filled 50 kN capacity Budenburg dead weight tester (Model 500 used in conjunction with Model 380L) certified to be accurate to 0.04% of the applied load. Calibration entailed applying five cycles of 2.8 kN preload to the cell, followed by the main calibration run of five further cycles of load in 0.2 kN increments up to a maximum of 2.5 kN. A least squares analysis of the data was carried out and the calibration data and confidence limits obtained are presented in Table 5.4 in terms of "equivalent pressure" per millivolt change in load cell output. The "equivalent pressure" to a force of 1 kN measured on a load cell is that pressure which would result if 1 kN were applied over a third of the cross sectional area of the new consolidation cell (total area = 0.1520 m^2), ie 19.7 kPa.

Following initial calibration, output from all cells at zero load was monitored for at least 72 hours in order to assess zero drift and the effects of atmospheric pressure and humidity variations. The results of this work showed that zero drift, atmospheric pressure variations, and temperature variations did not present a problem but that the load cells were sensitive to small changes in relative humidity. A typical variation is shown in Figure 5.6.

When in use though, the load cells would be effectively sealed into the consolidation cell by the regulated air pressure, and the relative humidity maintained at a sensibly constant value during any test once equilibrium between the soil water content and atmospheric conditions was achieved. The observed influence of relative humidity was therefore considered to be irrelevant after the initial setting up stage of a test.

5.1.3.2 Research Station Apparatus

The commercial load cells used in the Research Station were calibrated using an oil-filled Budenburg dead weight tester by British Gas staff. A preload cycle to the load cell capacity was followed by a single load - unload calibration cycle to the maximum load in ten increments. The results of the calibrations are given in Table 5.5. Comparison of the calculated confidence limits with the published accuracy showed that the load cells were generally under performing. This may be due to poor standards of calibration, or the age of the load cells. The effects of temperature on the performance of the load cells was not investigated due to the relatively short period (less than 12 hours) over which readings were taken.

5.1.4 Pressure Transducers

All transducers measured gauge pressure and were calibrated using a Budenburg dead weight tester connected to a pressure chamber. Transducers were subjected to at least one cycle of preloading to

capacity followed by 3 load - unload cycles to capacity in ten increments at the University, or one loading cycle to capacity in five increments at the Research Station. Results of the calibrations are presented in Table 5.6.

5.1.5 Displacement Transducers

5.1.5.1 University Apparatus

Displacement transducers were calibrated at the University by clamping the transducers in a specially made calibration block (see Plate 5.1) with the sprung captive armature of the transducer resting on the flat movable surface, or, in the case of the submersible transducer, the free arm was clamped to the movable surface such that any movement of the arm in to the transducer body was along its central axis. Displacement of the armature was effected by rotating the low geared bushing, and the relative displacement of the arm from a pre-set zero position was measured with a Mitutoyo digital vernier accurate to 0.001 mm.

Calibrations used three extension-compression cycles, each half cycle comprising at least 20 increments of displacement. Initial calibration employed the full range of the instrument to identify the most linear region of the transducer, before a more detailed calibration was completed over this shorter range using the increased resolution afforded by the AIU for such a smaller range. Results of the calibrations are presented in Table 5.7.

5.1.5.2 Research Station Apparatus

Slip gauges were used to apply known displacements to the armatures of the transducers at the Research Station, with the transducer body clamped in a vertical position and output recorded by the computer. The results of only one of the calibrations made by British Gas staff was available for checking, but it is understood that the calibrations for this and all other transducers consisted of increasing the displacement

from zero (full extension of the armature) to full compression in ten increments, but with no further cycling. The data available for the 100 mm stroke RDP LVDT (serial No D14) gave a 95% confidence limit of 0.2 mm for the linear regression, and a calibration factor of 9.958 mm per millivolt. This equates to a measured accuracy of 0.2% of full scale, which compares well with the accuracy quoted by the manufacturer of 0.1% over the middle of the range or 0.4% over the full scale. Performance of the other transducers was assumed to follow that noted by the manufacturer.

5.1.6 Bourdon Gauges

All Bourdon Gauges at the University and Research Station were checked and reset if necessary in accordance with the manufacturer's instructions using a Bourdon dead weight tester with an air-water interface between the tester and the gauge to ensure that only water entered the gauges. When reset, the pressure read on the gauge was the same as that applied to within 0.5 kPa. Linear regression analyses of the data were not made as, except in the case of the 1 bar University gauges 12380388 and 12380389, the gauges were used only for visual control and checking of the applied pressure. The exceptions were used to control the air pressure in the new consolidation cell and for this purpose reference to the calibration runs allowed the applied air pressure to be measured to within 0.2 kPa.

5.2 Operational Checks on Apparatus

5.2.1 Operation of Air Volume Indicators and Flushing System

Following construction of the air volume indicators and spiral grooved platen used in the consolidation cell and their connection to the plumbing system, the following checks were made on their performance:

(a) Medium term leakage checks were made on the air volume indicators by observing the variations of air volume indicator readings with time at initial water pressures of atmospheric pressure and

100 kPa gauge. The inner glass burette used for measurement was isolated from the external plumbing during these tests.

(b) Efficiency of air transport in the spiral flushing grooves was checked by G-clamping at three locations a 25 mm thick perspex block onto the platen, and applying variable flushing pressures to dislodge any visible air.

(c) Efficiency of air bubble transport through the plumbing to the air volume indicator was checked at variable back pressures.

The check on the performance of the isolated air volume indicators showed that both at atmospheric and 100 kPa back pressure, very small (less than 0.2 cm^3 at 100 kPa or less than 0.3 cm^3 at atmospheric pressure) or zero changes in meniscus level were observed over a period of about 10 days, as shown in Figure 5.7. The initial rise in meniscus levels when the back pressure was at 100 kPa is attributed to solution of air in the burette into the water, masking a very slow leak, an effect that would be expected to be absent or reduced at atmospheric pressure.

As further tightening of the air volume indicators to eliminate any leaks risked damage to the glass burettes, the observed level of leakage was accepted provided that before and after flushing the air volume indicator reading was noted, and that the units were isolated from the plumbing drainage system during a drained test.

The air transport efficiency checks showed that unless the perspex (or the ceramic) was placed onto a previously saturated spiral groove and base platen, air would be permanently trapped between the perspex (or ceramic) and the metal even up to a flushing pressure of 200 kPa. If the platen was saturated initially, it was found that air bubbles entering the spiral from the flushing inlet would flow only partly through it before adhering to the metal platen by surface tension. Once this had occurred, the air could not be dislodged unless flushing

pressures exceeded 50 kPa. This problem was overcome by using a very dilute solution of Teepol (a detergent) as the flushing medium, rather than water alone. Addition of 5 cm^3 of Teepol per air-water bladder cell was sufficient to ensure that all bubbles were dislodged at a flushing pressure of 10 kPa.

Having solved the problem of air-bubble transport through the spiral , it was noted also that air flowed easily through the plumbing to the air volume indicators provided the flushing pressure exceeded 5 kPa. However it was found that volumes of Teepol in excess of 20 cm^3 per bladder cell combined with high flushing pressures (ie greater than 20 kPa) caused frothing in the plumbing lines. High flushing pressures resulted also in relatively high bubble speeds through the plumbing such that a current set up in the inner burette of the air volume indicators was sufficient to prevent most air bubbles entering this burette from rising upwards to register as an air volume. Instead, bubbles were entrained into the current and flowed straight through the inner burette to the volume change units unhindered by the need to travel downwards.

Based on the foregoing, a flushing pressure of 10 kPa together with a very dilute Teepol flushing medium was adopted for the tests to ensure efficient operation of the flushing system. It was noted also that at least 100 cm^3 of flow was required to ensure all bubbles in the flushing spiral reached the air volume indicator.

5.2.2 Response Tests on Ceramics

The low permeability of the high air entry value ceramics and the compressibility of the fluid between the ceramic and the pore water pressure transducer result in a minimum response time being required for the system to record a change in suction conditions within a specimen (see section 2.3.1). For confident interpretation of the pore pressure data from the main series tests, it was necessary to ensure that the ceramics were as completely de-aired as possible before use and to ensure that air entry by diffusion and evaporation of water in the

ceramic during tests did not reduce the response time to below an acceptable level.

De-airing was completed by assembling the consolidation (or triaxial) cell with the ceramics sealed in their test positions, and the cell and platen filled with de-aired water (see Figure 5.8). A cell pressure of 600 kPa was applied for 24 hours before the drainage and flushing lines from behind the ceramic(s) were opened and water flushed through from the cell chamber for at least 5 minutes. After closing the lines, the 600 kPa cell pressure was reapplied and the sequence repeated at least twice more. After flushing for five minutes on the third cycle, the cell pressure was reduced to 50 kPa (or some other nominal value) and the drainage lines closed. Equalisation of pore pressures above and below the cell was checked using the pore pressure transducer behind the ceramic and comparing it with the applied cell pressure. After equalisation the cell chamber was isolated, a cell pressure of 100 kPa (or some other nominal value) applied to the line up to the cell, then immediately after a data logging cycle the cell chamber line was opened and the response of the pore pressure transducer behind the ceramic monitored.

Typical response curves for three and five bar ceramics in the consolidation cell and a one bar ceramic in the triaxial cell, are shown in Figure 5.9 after three days de-airing. These are typical for both pressure increments and decrements. All observed response curves on de-aired ceramics in the consolidation cell showed that the top platen ceramic always had a much faster response time than a base ceramic of the same air entry value, such that often 99% of response would be within 10 seconds for the three and five bar ceramics used in this apparatus. In contrast, 95% response time for a base ceramic of three or five bar air entry value would typically be less than 2 minutes or less than five minutes, respectively.

The lack of a clear response curve suggested that an unknown leakage path consistently existed in the top platen, but investigations into the behaviour of the ceramics after two main series tests showed that a

response curve similar to that of the base was exhibited by the top ceramics if the degree of de-airing was relatively low (see Figure 5.10). After only one cycle of de-airing though, the top ceramic exhibited its usual response pattern, implying that the top platen ceramic design is more efficient at responding to pressure changes. Comparison of the platen designs confirmed that more "dead" ceramic exists in the base design, supporting the explanation given above. The hypothesis is further supported by the relatively slow response of the one bar high flow ceramics used in the triaxial cell, which is believed to be related to the small drainage basin beneath the ceramic.

Based on the above, ceramics were accepted as sufficiently de-aired for use after a minimum of three days de-airing, although checks on their response were always made after this time to ensure no poorly de-aired ceramics were used. Ceramics were usually used for two tests (equivalent to about one months's test use) before de-airing again.

The effect of the period of de-airing and applied pressure increment were investigated also for a five bar ceramic, and typical plots are shown in Figure 5.11. Comparison of Figures 5.11 a and 5.11 b shows that the response time does decrease with an increase in de-airing period, but that the increase in efficiency is gained at a progressively slower rate as the time increases. The curves show also that a decrease in the pressure increment applied results in higher response times, as predicted by Fredlund (1973) and others. The shape and equalisation times of the response tests agree also with those predicted by Fredlund.

5.2.3 Permeability and Air Entry Tests on Ceramics

Permeability and air entry tests were made to check that micro-cracking of the ceramics had not occurred during transit from the USA, or during machining or installation of the ceramics in their locking rings.

Permeability tests were made on ceramics immediately following completion of de-airing by connecting the drainage line(s) to a VCU and

applying a known pressure gradient, usually 100 kPa, across the ceramic. The coefficient of permeability derived from the tests using Darcy's law usually agreed reasonably well with the typical coefficients given by the manufacturer, although some ceramics exhibited a coefficient approximately 50% of that expected. Typical coefficients of permeability for a one bar high flow ceramic, a three bar ceramic and a five bar ceramic, are 0.86×10^{-9} m/sec, 1.73×10^{-9} m/sec and 1.21×10^{-9} m/sec respectively.

Air entry tests were made on all new ceramics using the same apparatus arrangement as that shown in Figure 5.8, except that the cell chamber fluid was air rather than de-aired water. A differential pressure of up to 250 kPa (the maximum suction expected to be measured within the test specimens) was applied across the de-aired ceramics and the rate of flow of air measured as an apparent water volume change by the volume change units. The tests lasted approximately 24 hours, and the observed rates of flow were compared with those predicted by diffusion theory and found to be in reasonable agreement. Hence it was concluded that the air entry value of the ceramics was sufficient for use in the tests, although the absolute entry value of the ceramics was not determined.

Table 5.1 Calibration Constants and Confidence Limits for Imperial College Volume Change Units at a Back Pressure of 100 kPa

Unit	Chamber	Calibration Factor (cm^3/mV)	Confidence Limits (cm^3) 95%	99%
VCU25	Top	3.5804	0.10	0.13
	Bottom	3.5656	0.13	0.17
VCU28	Top	3.1220	0.13	0.18
	Bottom	3.1064	0.17	0.22
VCU55*	Top	4.1534	0.23	0.31
	Bottom	4.1432	0.22	0.29
VCU145	Top	3.0961	0.12	0.16
	Bottom	3.0838	0.10	0.13

*VCU55 exhibited non-linearity over the first $20cm^3$ at each end of piston travel. Quoted data is for the range $20cm^3$ to $80cm^3$ of capacity.

Table 5.2 Influence of Back Pressure on Calibration Data for I.C. Volume Change Unit 28

VCU28	Calibration Factors (cm3/mV)			95% Confidence Limits (cm3)		
Back Pressure	50kPa	100kPa	200kPa	50kPa	100kPa	200kPa
Top Chamber	3.1321	3.1220	3.1221	0.23	0.13	0.22
Bottom Chamber	3.1134	3.1064	3.1051	0.25	0.17	0.19

(a) Calibration Data

Chamber	Volume Changes (cm^3) Calculated using Calibration Factor for Output Change of 30mV		
	Pressure = 50kPa	Pressure = 100kPa	Pressure = 200kPa
Top	93.96	93.66	93.66
Bottom	93.40	93.19	93.15

(b) Effect of Back Pressure on Calculated Volumes

Table 5.3 Calibration Factors and Confidence Limits for British Gas Air Water Interfaces

Unit	Calibration Factor (cm^3/mV)	Confidence Limits (cm^3) 95%	99%
AW3	95.42	1.7	2.3
AW4	98.52	1.2	1.6
AW5	105.93	1.6	2.1
AW6	104.17	1.8	2.3

Table 5.4 Calibration Constants and Confidence Limits for 2.5kN Load Cells

Load Cell	Calibration Factor (kPa/mV)	Confidence Limits (kPa) 95%	99%
LCA	-25.4032	0.10	0.14
LCB	24.5719	0.11	0.14
LCC	24.7259	0.09	0.11
LCD	25.3720 or 25.0079*	0.06 0.11*	0.07 0.15*
LCE	25.2584	0.07	0.09
LCF	26.3176 or 26.0914*	0.04 0.08*	0.06 0.11*

*Load cells D and F were damaged during Test A8. Following re-wiring and re-calibration the new calibration data were marginally different, as shown.

Table 5.5 Calibration Constants and Confidence Limits for Commercial Load Cells

Load Cell Serial Number	Model	Range (kN)	Calibration (kN/mV)	Confidence Limits (kN) 95%	99%
LC6	Whykham Farrance Model WF 17109	10	1.1846	0.038	0.050
LC14	Sensotec Model 41	20	0.5023	0.030	0.039
LC16	Sensotec Model 41	111	0.9980	0.135	0.178

Table 5.6 Calibration Constants and Confidence Limits for Commercial Pressure Transducers

Transducer Serial No	Model	Range (kPa)	Calibration Factor (kPa)	Confidence Limits (kPa) 95%	99%	Offset (mV)	Standard deviation of offset (mV)
University Calibrated transducers							
34522	Druck PDCR10	0-140	2.74478	0.030	0.040	1.6788	0.0011
34527	Druck PDCR10	0-140	2.73535	0.050	0.065	1.7734	0.0019
L83586	Bell and Howell 4-366-0002-01Mohm	0-350	15.93910	1.03	1.36	1.0108	0.0066
L83588	Bell and Howell 4-366-0002-01Mohm	0-350	16.75137	0.60	0.79	0.3395	0.0037
Research Station Calibrated Transducers							
P8	Sensotec TJE Series	0-690	1.000	*	*	5.000	-
P10	Sensotec TJE Series	0-690	1.000	1.0	1.3	-1.800	0.542
P18	Sensotec TJE Series	0-690	1.005	0.6	0.8	-0.300	0.332
P19	Sensotec TJE Series	0-690	1.000	*	*	-2.000	-
P21	Sensotec TJE Series	0-690	1.003	0.6	0.8	-0.500	0.332
P22	Sensotec TJE Series	0-690	1.000	*	*	2.000	-

* The calibrated confidence limits were 0.0 kPa as all recorded data lay on a perfectly straight line. The manufacturers published nominal accuracy (95% confidence) of 0.5 kPa was adopted in view of the limited number of calibration points.

Table 5.7 Calibration Constants and Confidence Limits for Commercial Displacement Transducers used at the Unversity

Transducer Serial Number	Manufacturer	Range (mm)	Calibration Constant (mm/mV)	Confidence Limits (mm) 95%	99%
L3890	Novatech	0-50	2.8150	0.046	0.061
	LSC HS550	0-10*	2.8237	0.009	0.012
L3900	Novatech	0-50	2.79806	0.048	0.063
	LSC HS550	0-10*	2.79041	0.014	0.019
Submersible	Sangamo	0-10+			
		8-9*	1.589E-3	0.003	0.004

* Range of maximum accuracy

\+ Distinct non-linearity of displacement - output relationship observed from zero (armature fully out) to 5 mm, thus linear regression analysis not valid.

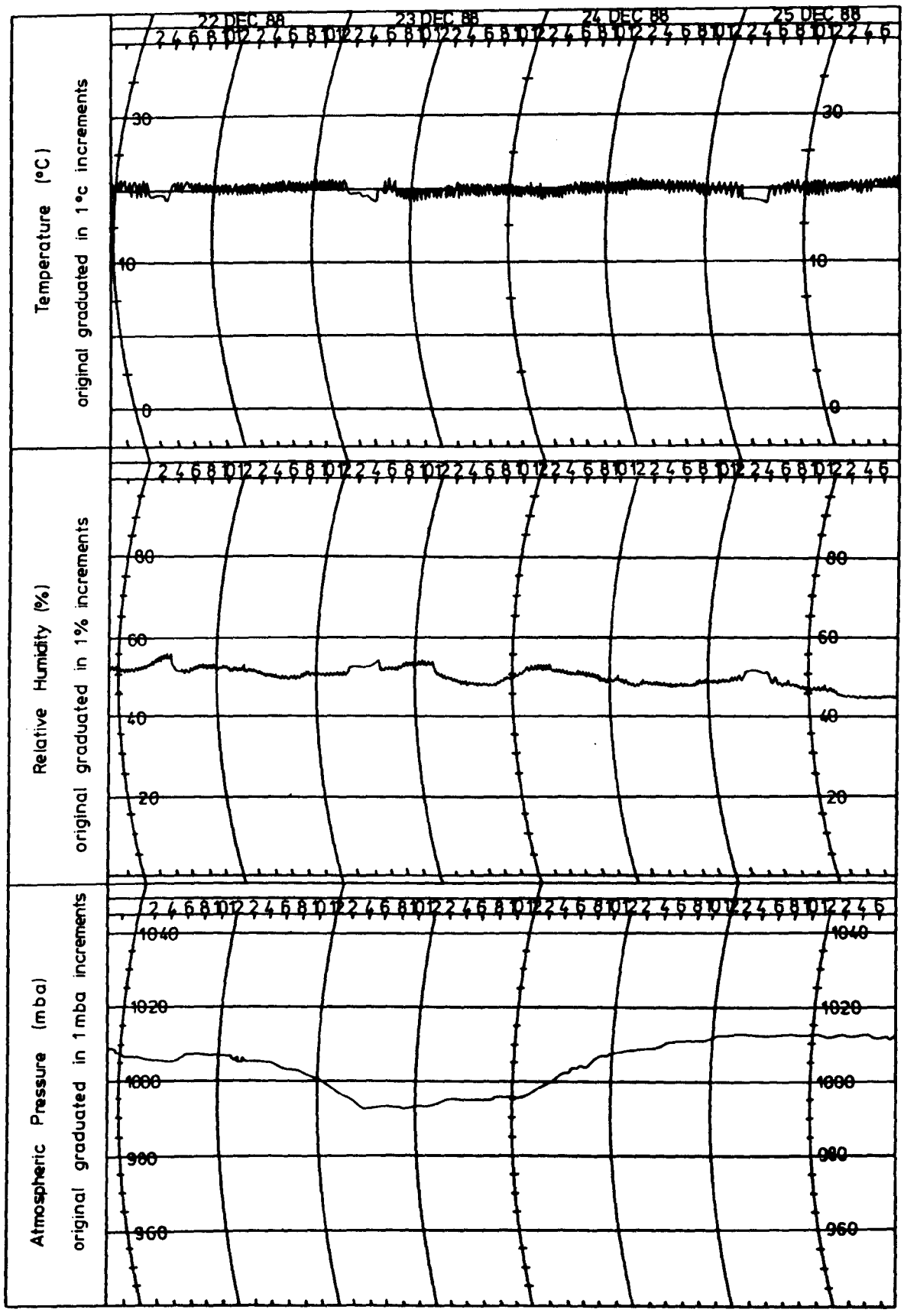

Figure 5·1 - Typical Plot of Atmospheric Variations in Constant Temperature Laboratory
(based on original Isuzu paper chart)

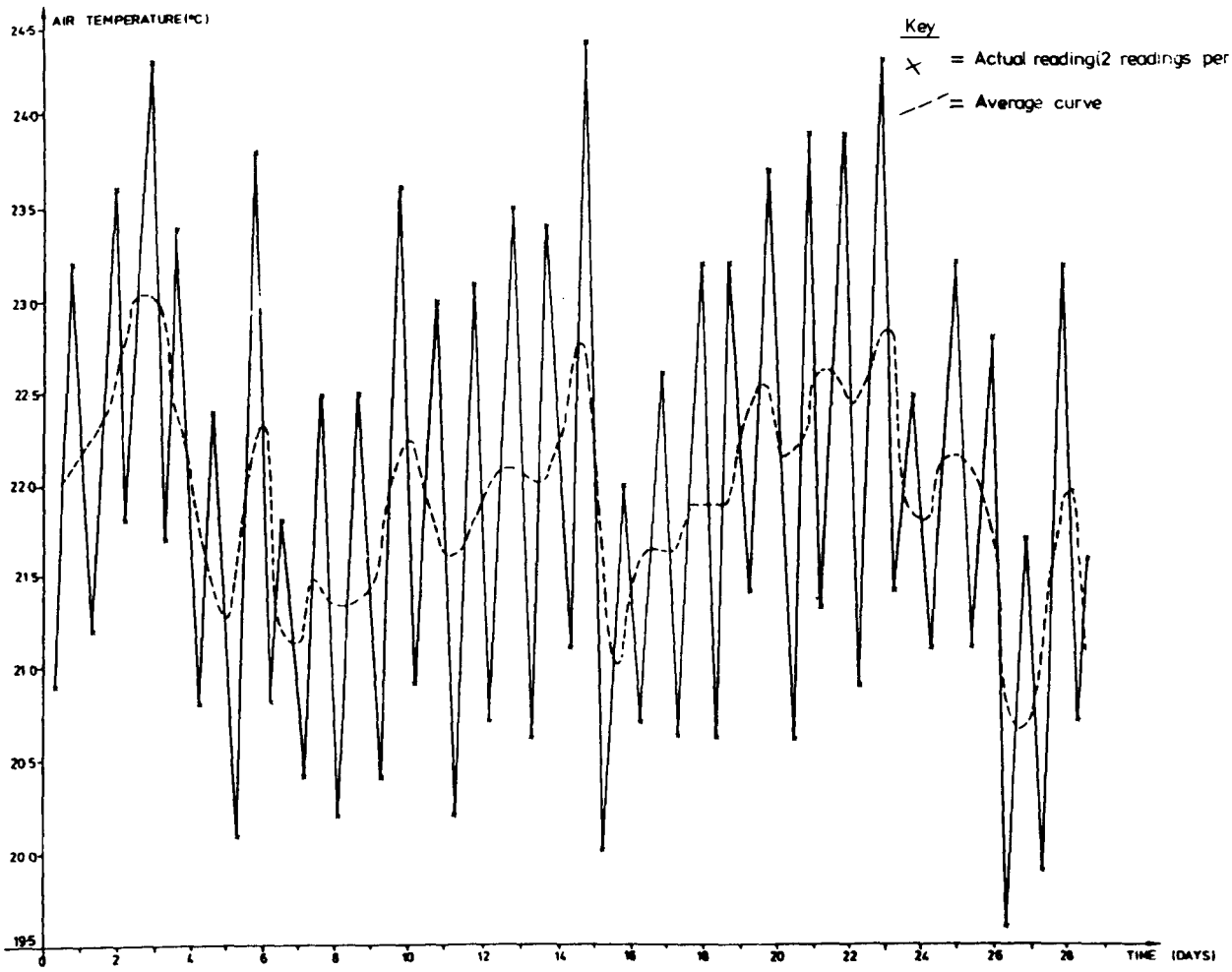

(a) Ambient Laboratory Air Temperature

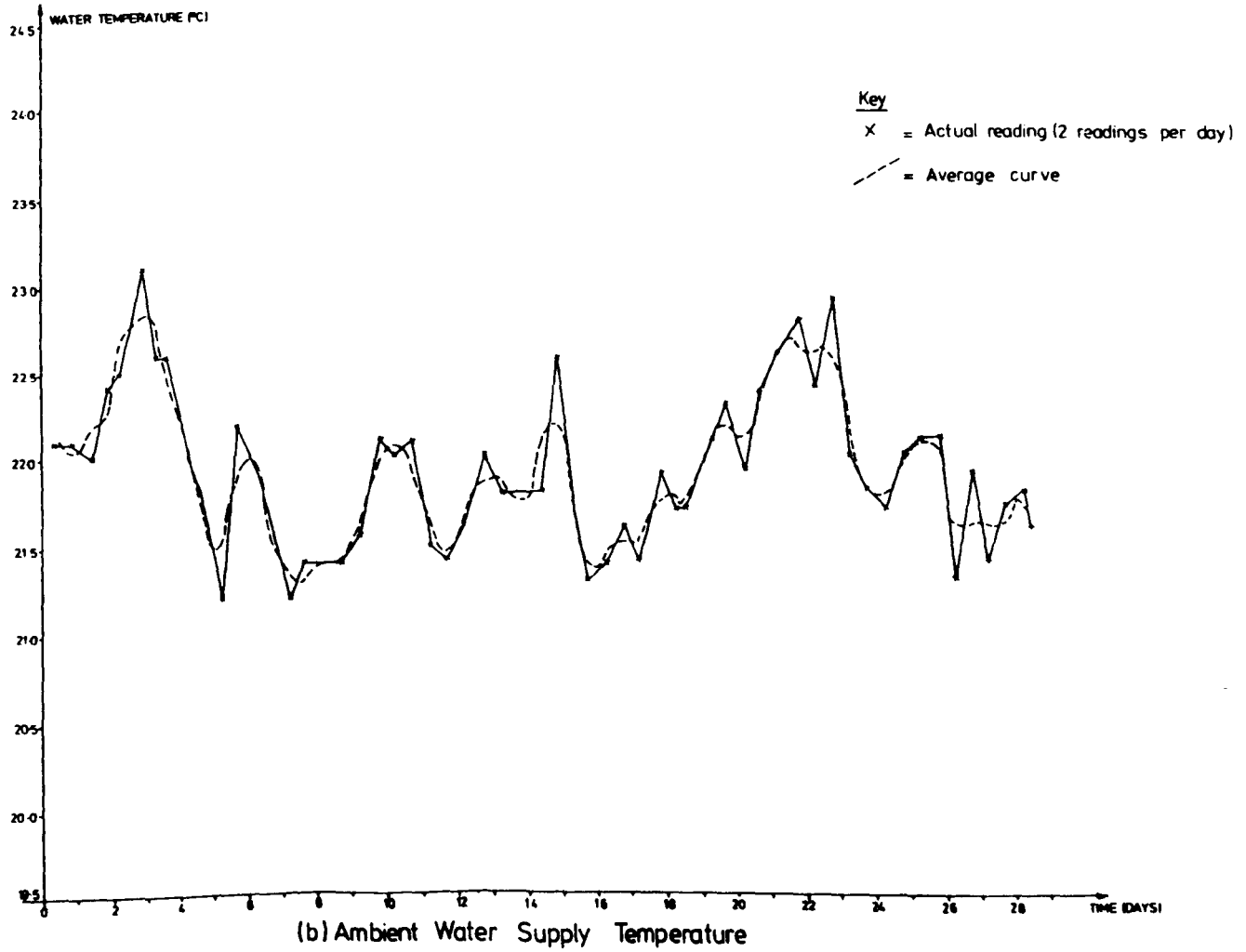

(b) Ambient Water Supply Temperature

Figure 5·2 - Record of Air and Water Supply Temperatures at the British Gas Research Station over a 29 Day Period

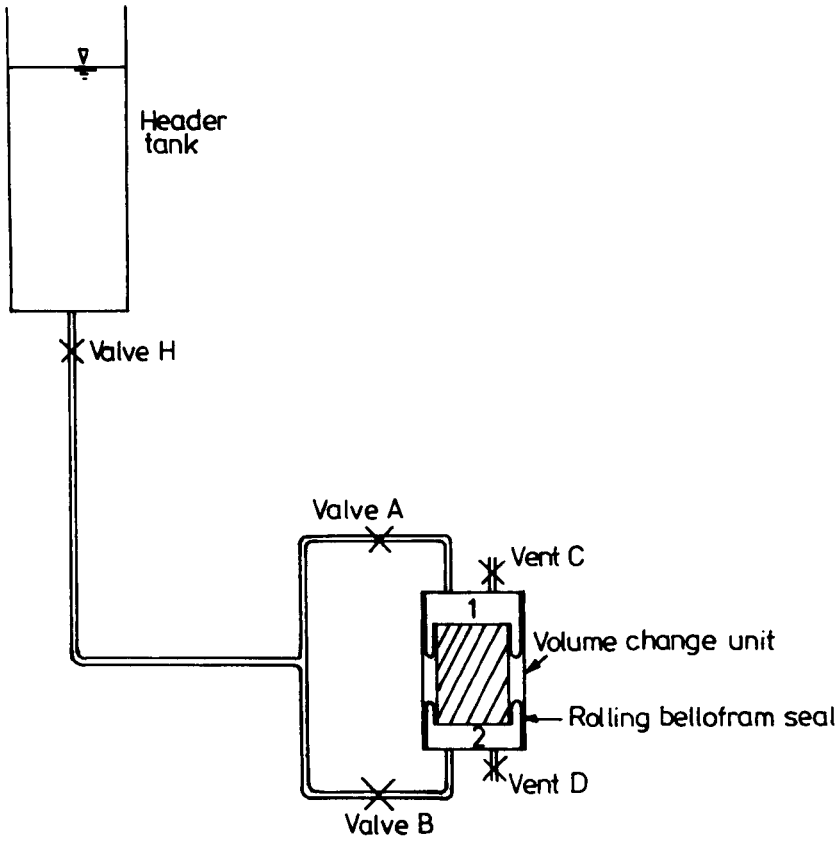

Figure 5·3-Apparatus For De-Airing Of Volume Change Unit

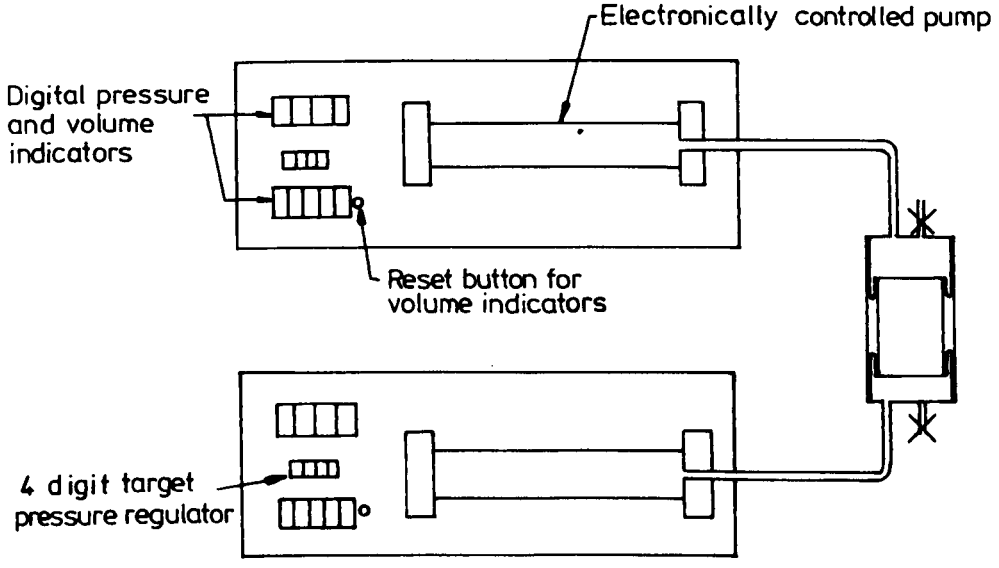

Figure 5·4-Apparatus For Calibration Of Volume Change Unit

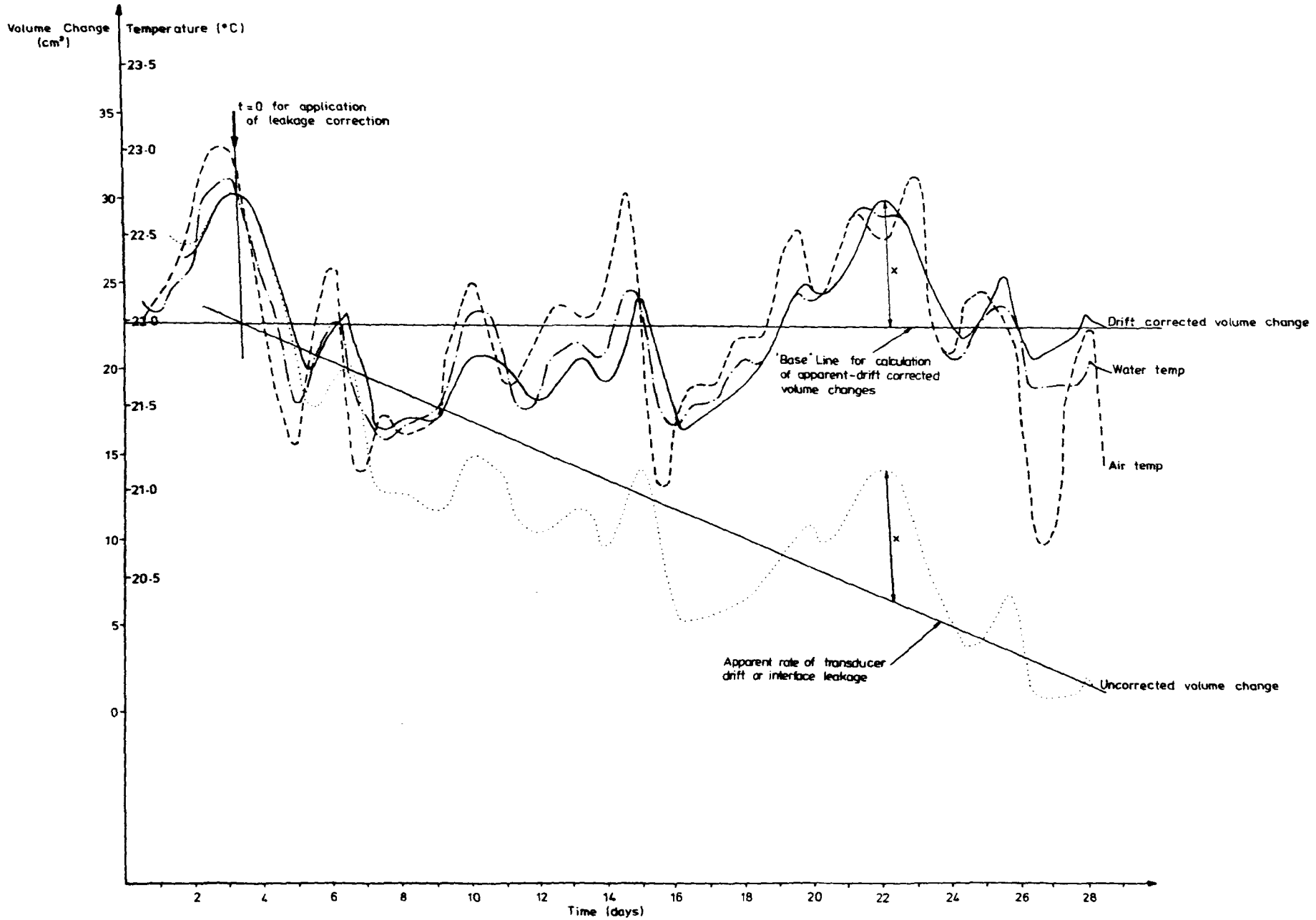

Figure 5·5 – Correlation Between Temperature Changes and Apparent Water Volume Change for British Gas Air Water Interfaces

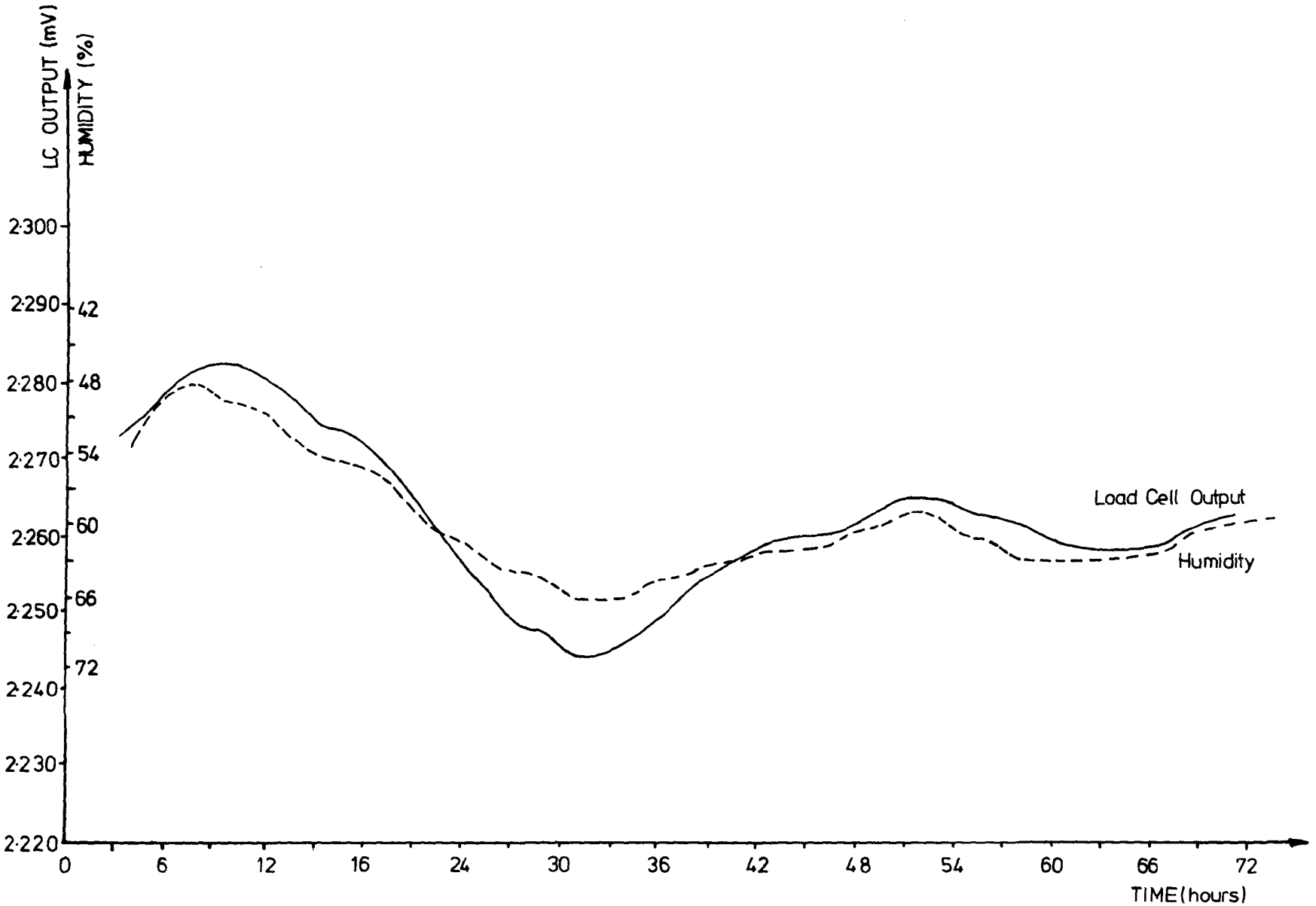

Figure 5·6-Effect of Atmospheric Humidity on Load Cell A

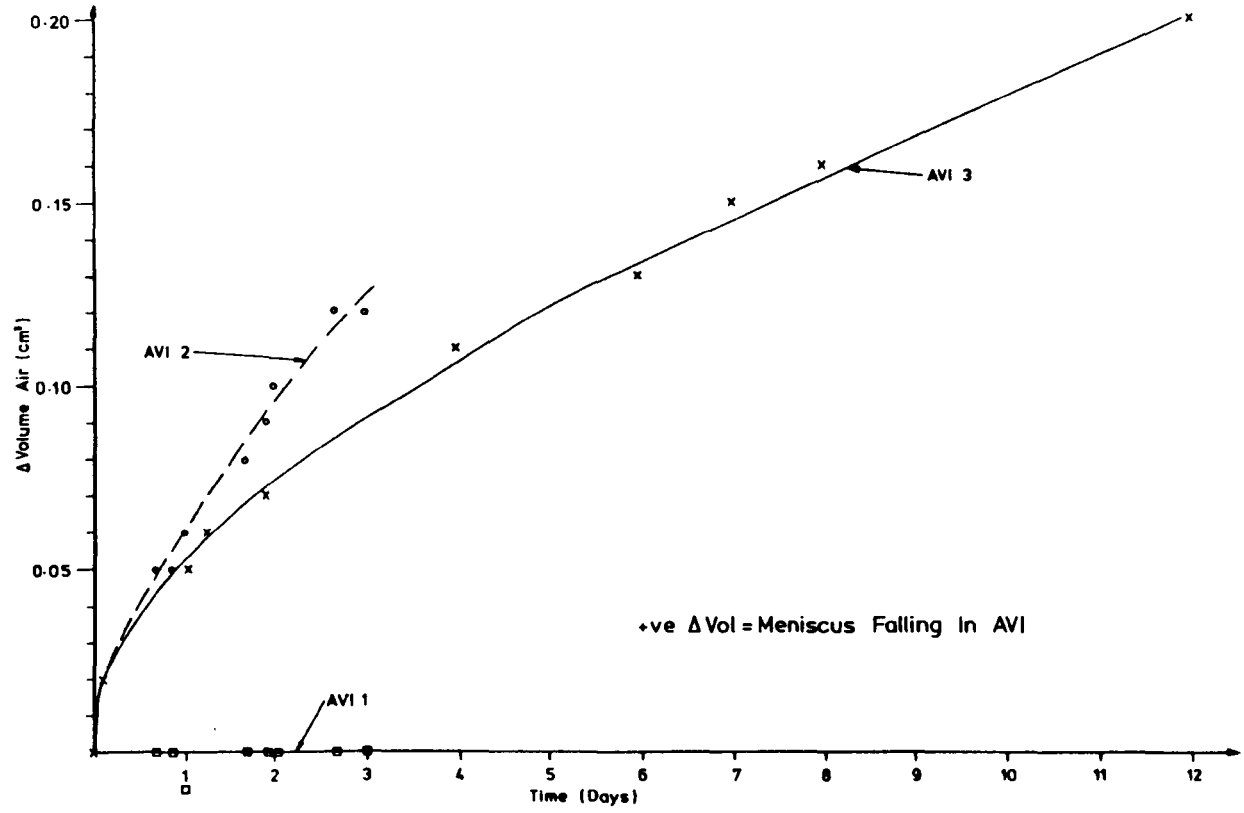

(a) Change in Levels of Air Volume Indicators with Atmospheric Back Pressure

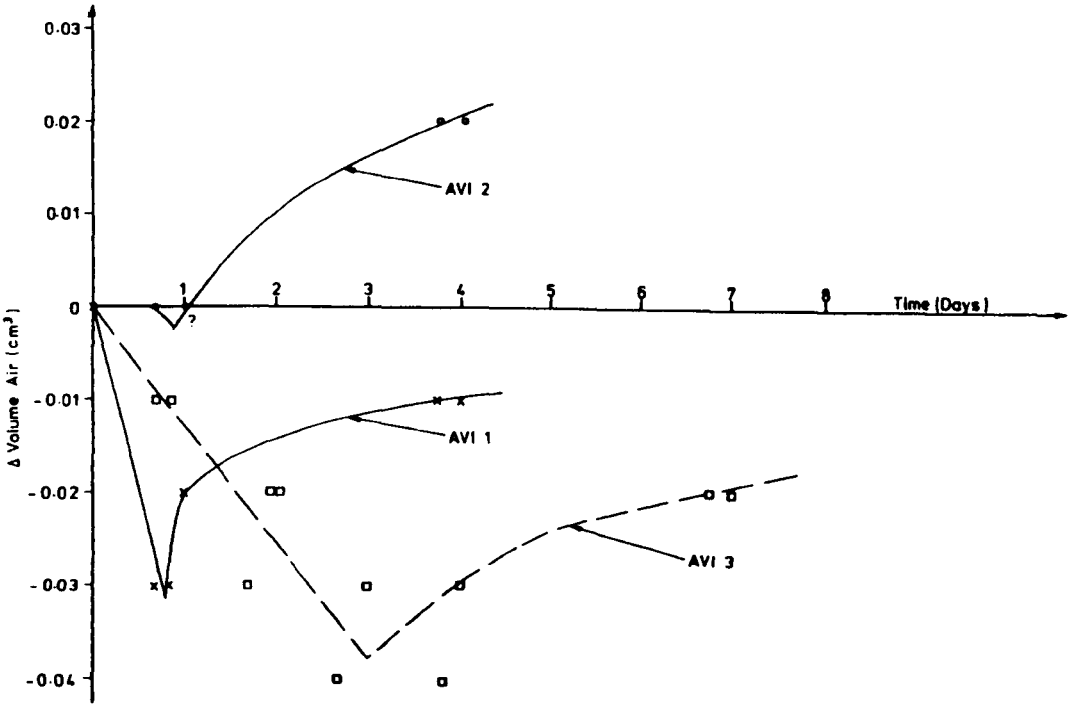

(b) Change in Levels of Air Volume Indicators with Back Pressure of 100kPa

Figure 5·7 - Medium Term Observations of Isolated Air Volume Indicator Water Level

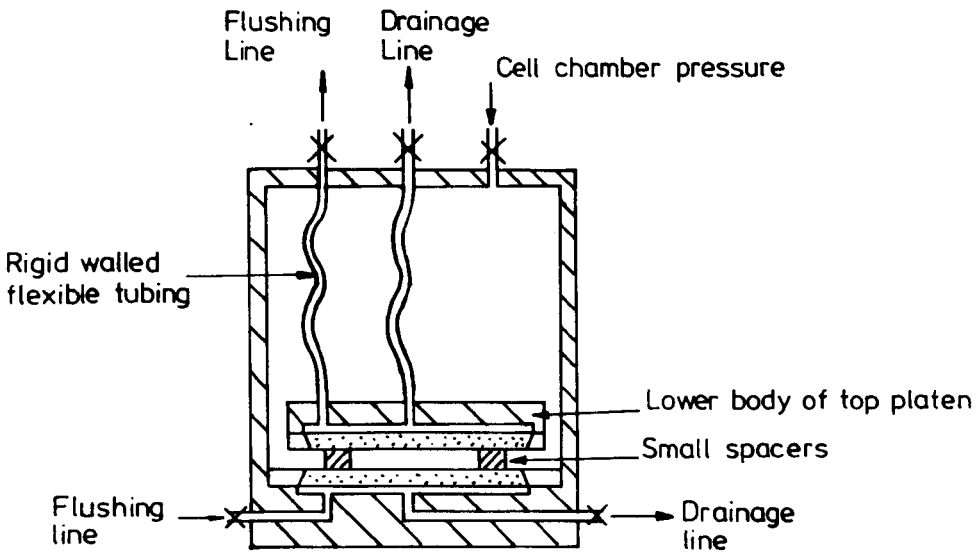

(a) Consolidation Cell

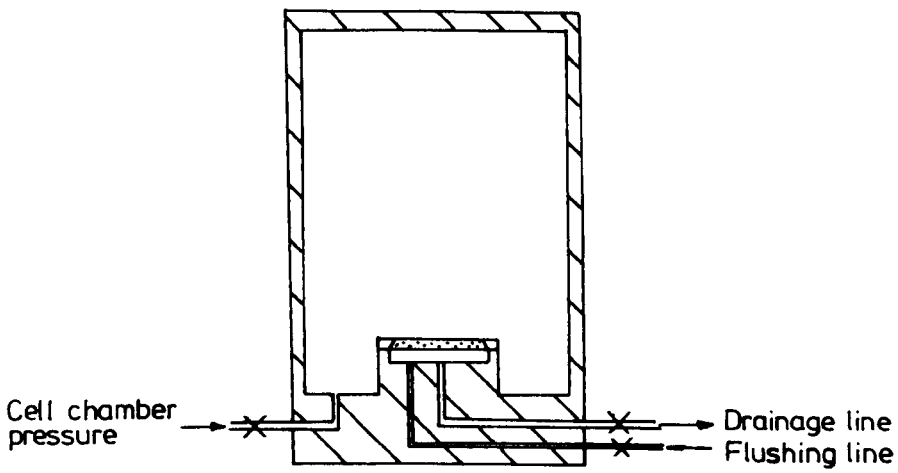

(b) Triaxial Cell

Figure 5·8 -Schematic Arrangement Of Apparatus For Response And Permeability Tests On High Air Entry Ceramics

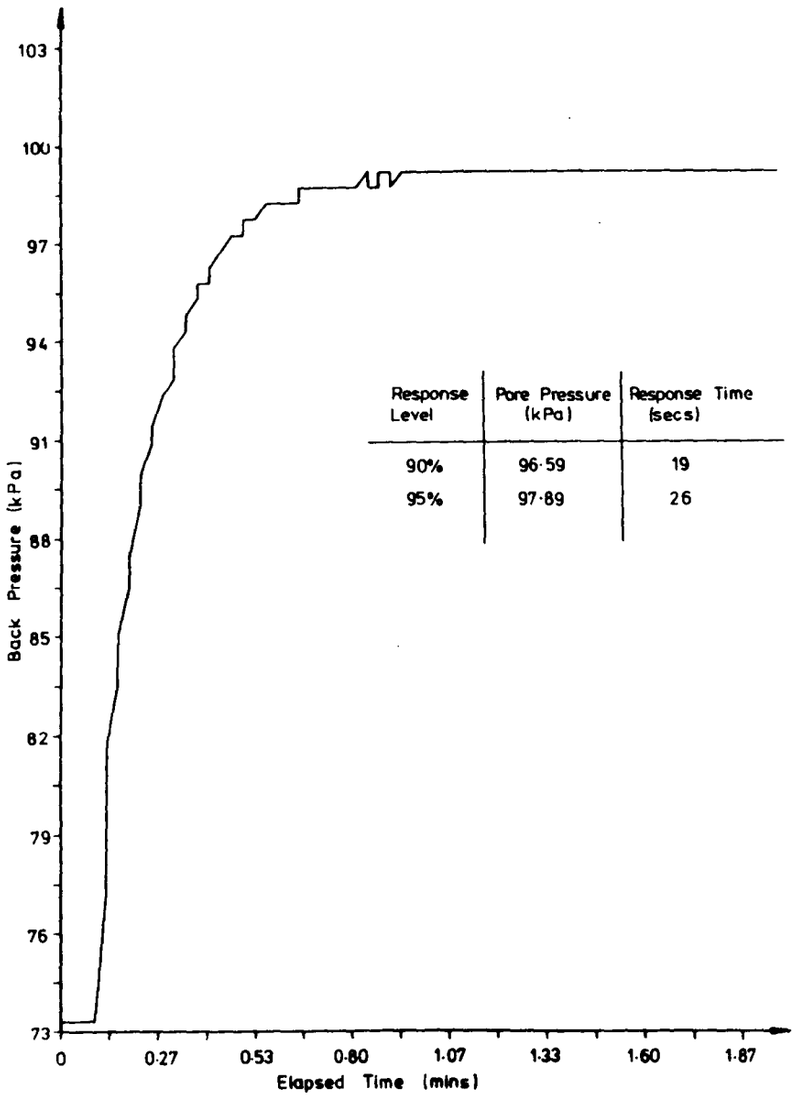

Response Level	Pore Pressure (kPa)	Response Time (secs)
90%	96·59	19
95%	97·89	26

(a) 1 Bar Ceramic in Triaxial Cell

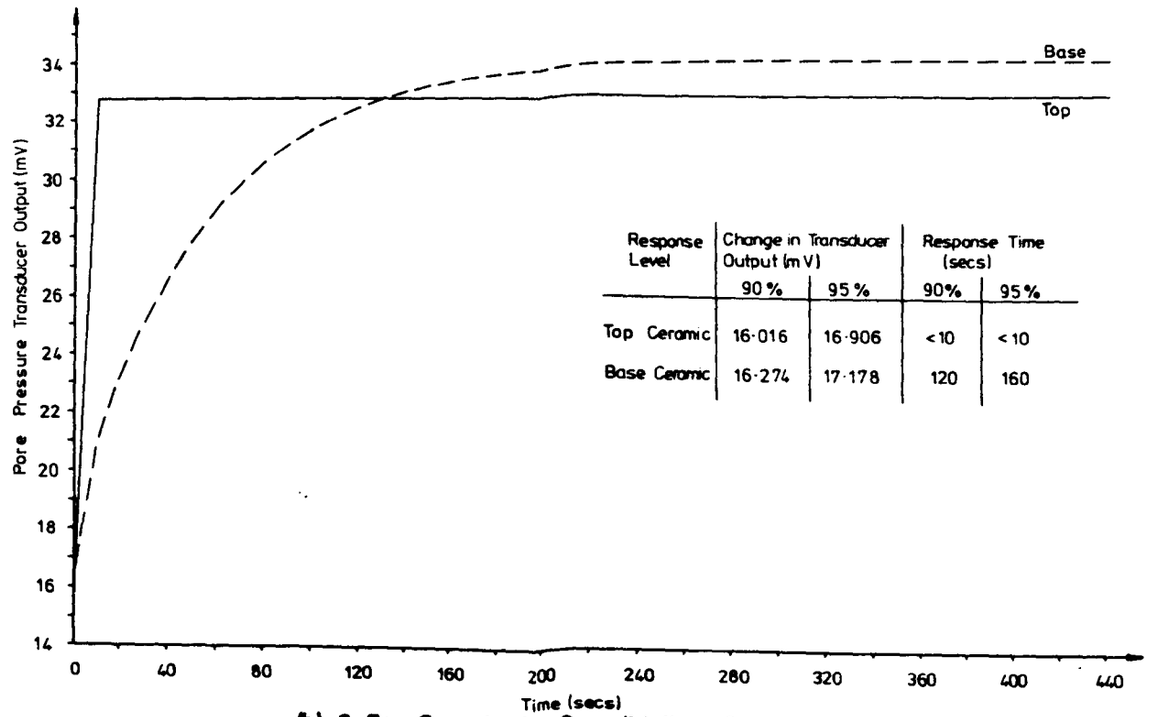

Response Level	Change in Transducer Output (mV)		Response Time (secs)	
	90%	95%	90%	95%
Top Ceramic	16·016	16·906	<10	<10
Base Ceramic	16·274	17·178	120	160

(b) 3 Bar Ceramic in Consolidation Cell

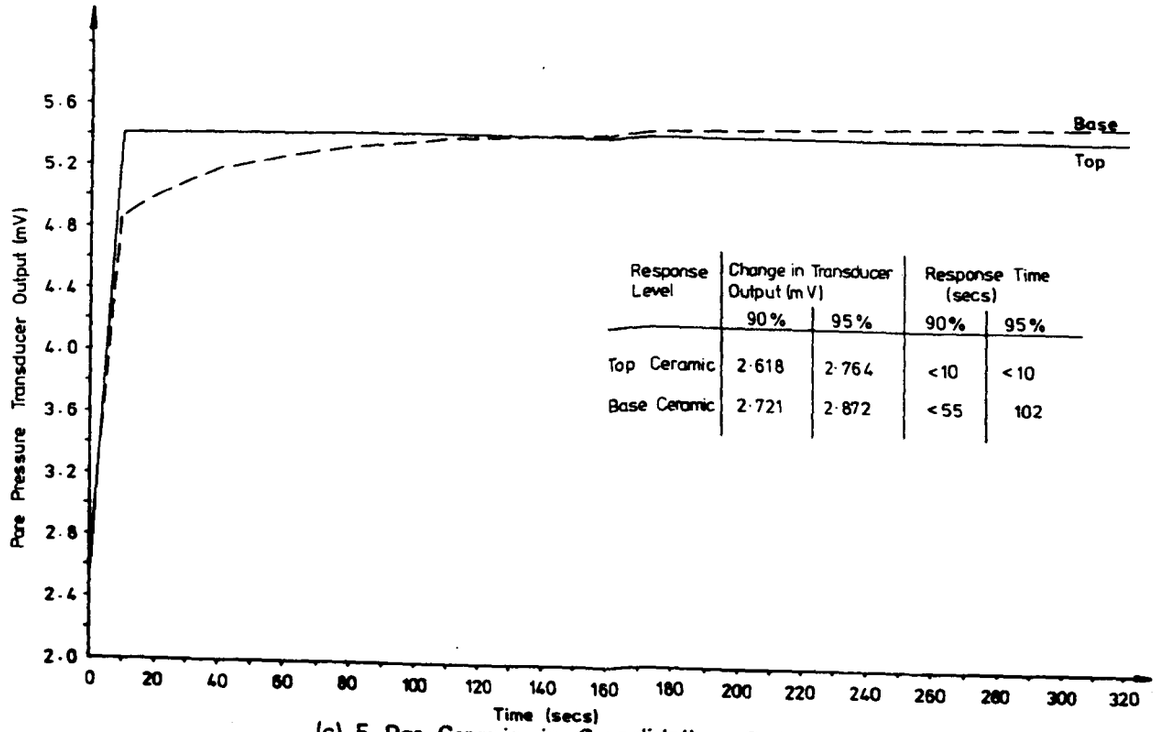

Response Level	Change in Transducer Output (mV)		Response Time (secs)	
	90%	95%	90%	95%
Top Ceramic	2·618	2·764	<10	<10
Base Ceramic	2·721	2·872	<55	102

(c) 5 Bar Ceramic in Consolidation Cell

Figure 5.9 - Typical Response Curves For High Air Entry Ceramic (After 3 Days De-airing: Pressure Increment 50 - 100 kPa)

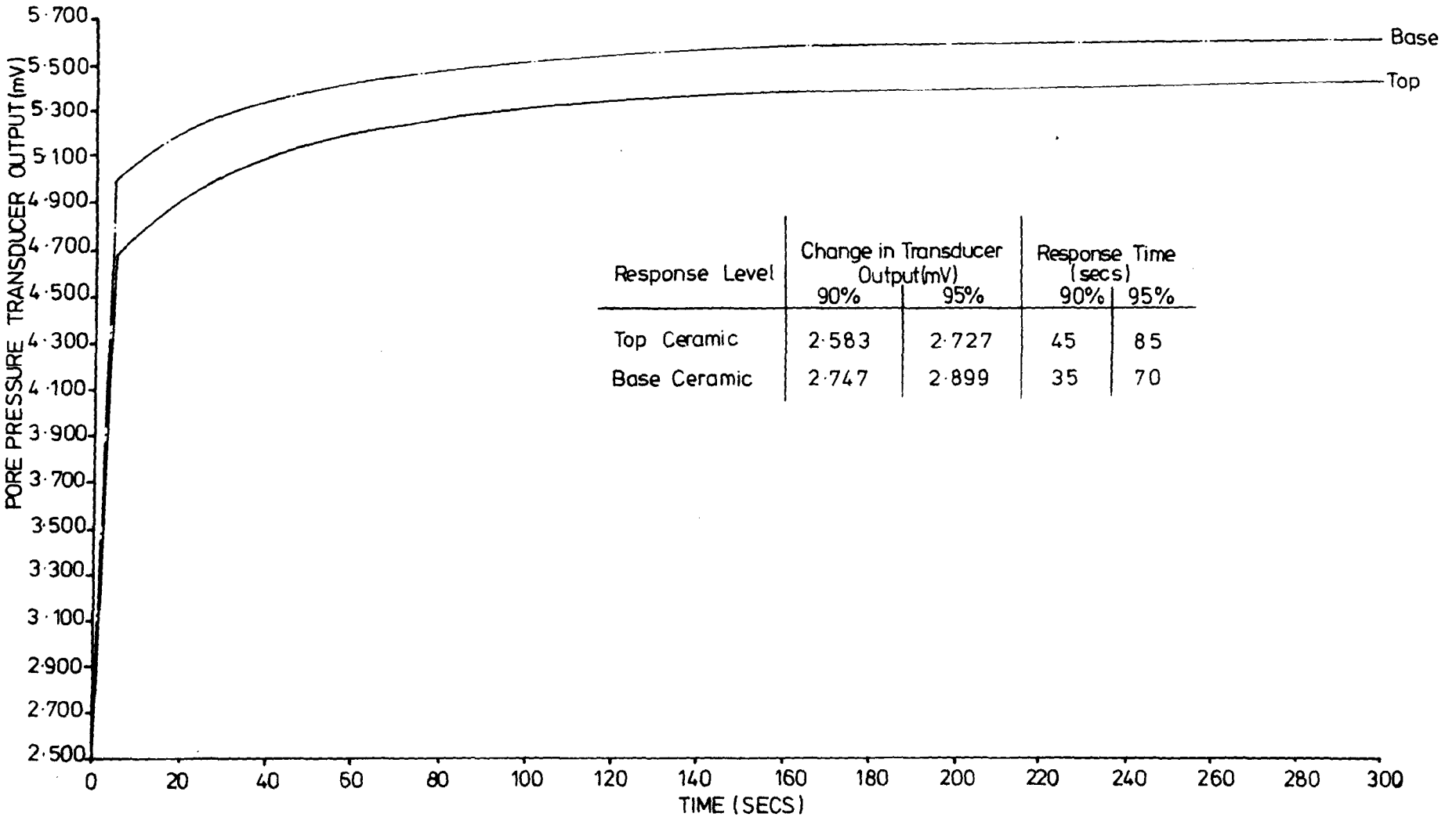

Response Level	Change in Transducer Output(mV)		Response Time (secs)	
	90%	95%	90%	95%
Top Ceramic	2·583	2·727	45	85
Base Ceramic	2·747	2·899	35	70

Figure 5·10 – Typical Response Curve For 3 Bar Ceramic After Use In 2 Main Series Tests

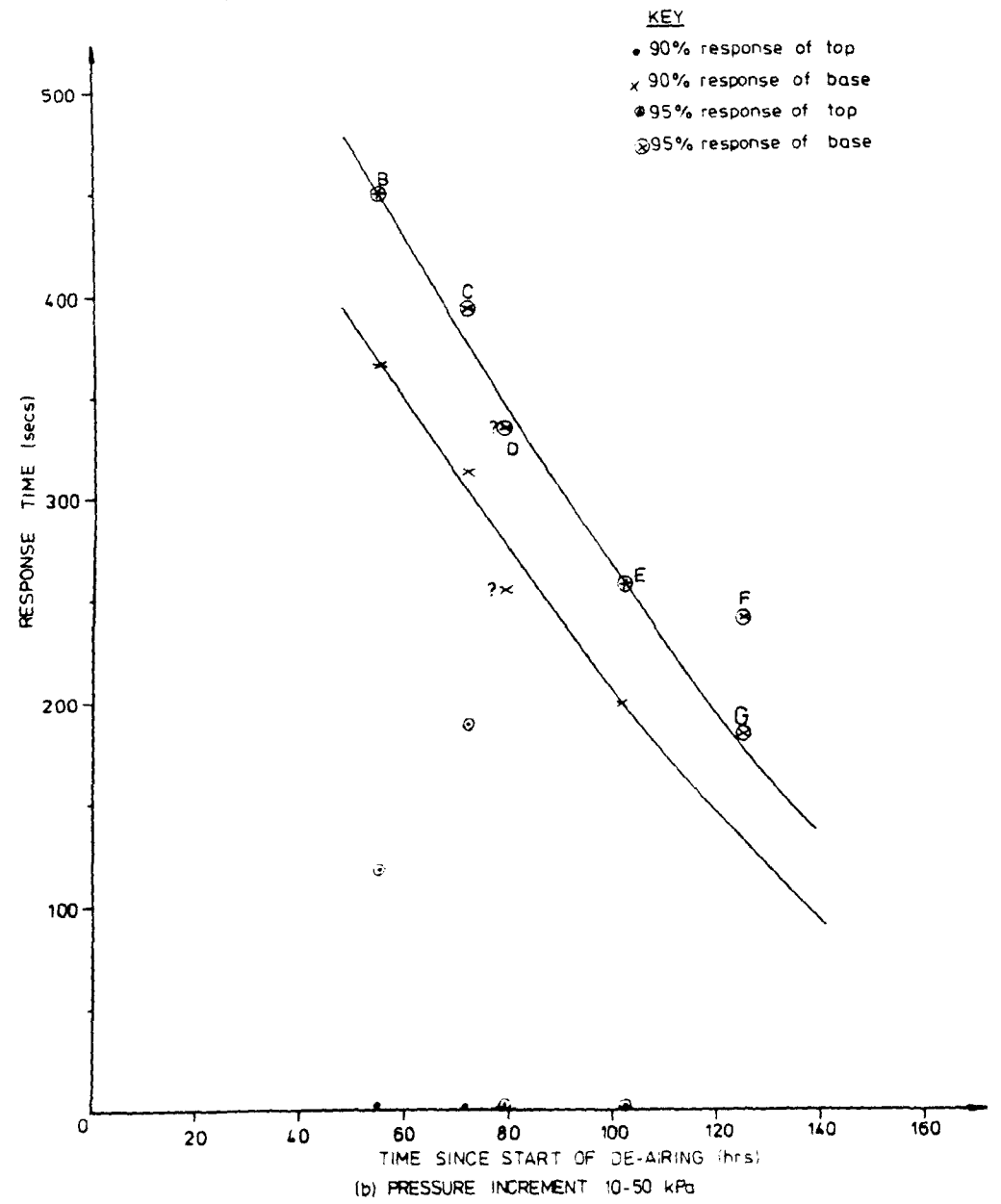

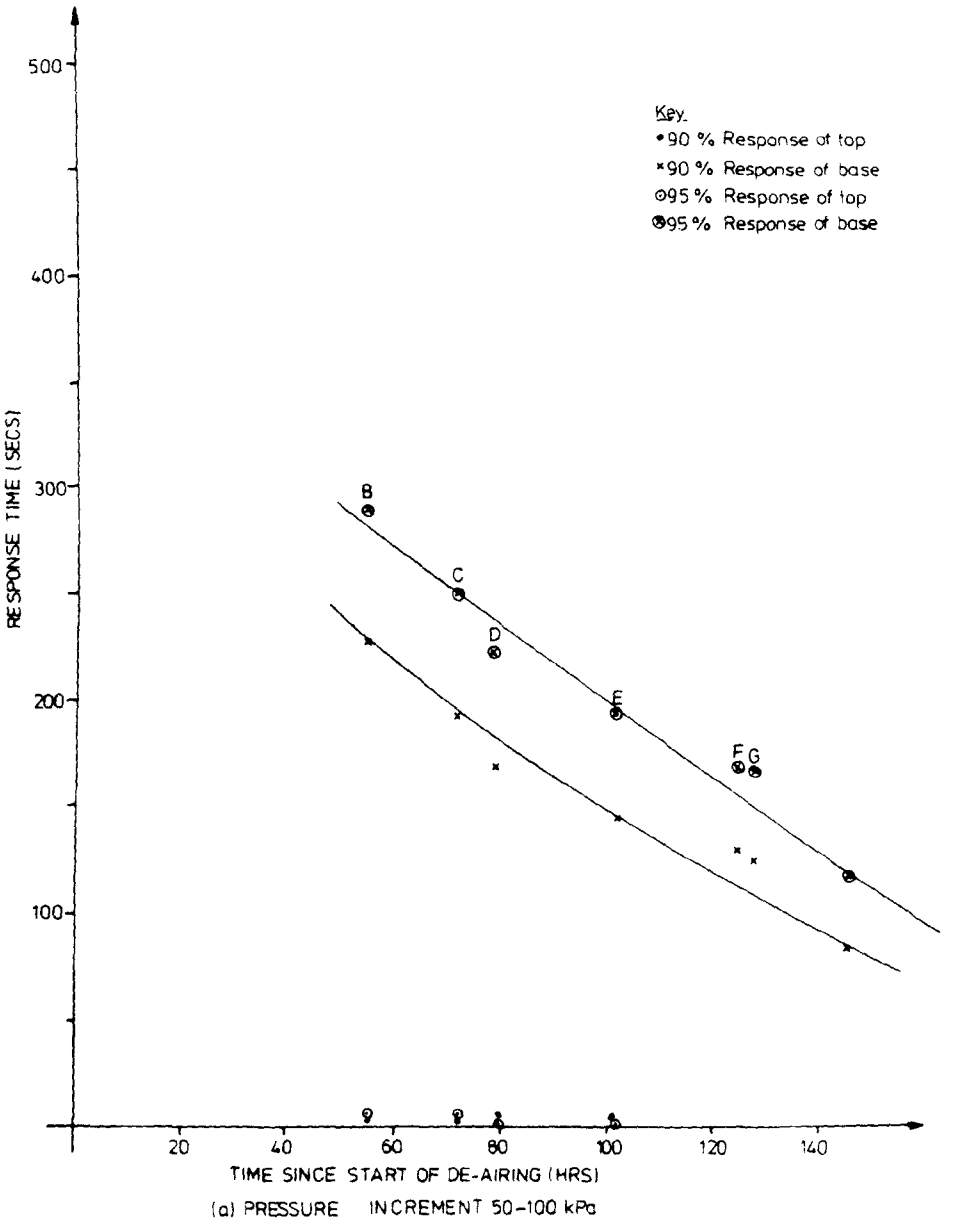

Figure 5·11 - Dependence of Response Time on Period of De-airing
5 Bar Ceramic

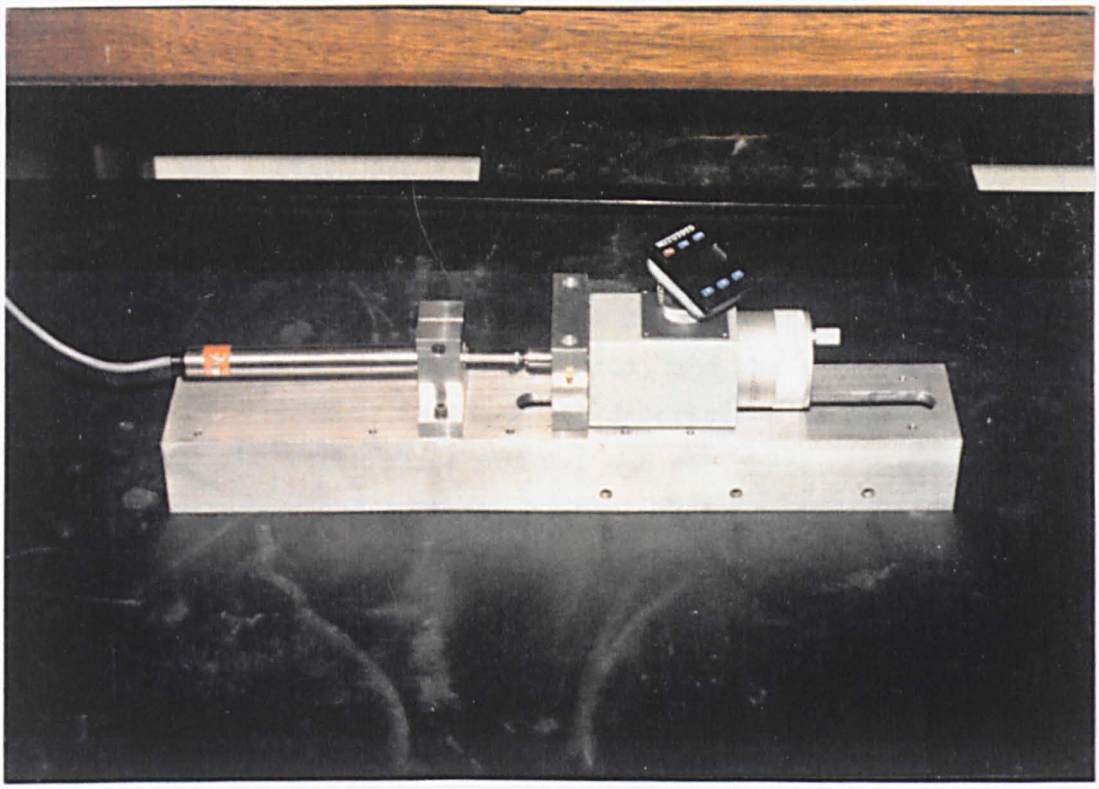

Plate 5.1 Apparatus for calibrating displacement transducers

CHAPTER 6

TEST PROGRAMME AND EXPERIMENTAL PROCEDURES

6.1 Summary of Test Programme

Four main series of tests were performed to investigate the one dimensional compression properties of the three granular soils prepared with gradings as detailed in Section 3.2. Series A and B were performed at the University in the new consolidation cell, and Series C and D were performed at the British Gas Engineering Research Station in the large diameter triaxial cell and the compression rig, respectively. Details of the apparatus are given in Chapter 4, and the nature of the series are summarised in Table 6.1. All tests had a constant air pressure in the test specimens (ie air drained), and the reference to drained or undrained conditions in the brief description of test type in Table 6.1 relates to the water phase and not the air phase. The test procedures used are summarised in this chapter and further details are available in Appendix A.

6.2 Test Series A

The aim of Series A was to establish the compression behaviour of the fine and coarse gradings under monotonic incremental loading compression and to measure the changes in water content and soil suction of the specimens due to the applied stress changes. This behaviour could be compared with the behaviour observed in Series D under constant strain rate compression and repeated loading conditions. A summary of the tests reported in this thesis, and the parameters varied for each test, are given in Table 6.2.

All specimens were batched in the concrete mixing drum as described in Section 3.2.2 and prepared to a known water content by adding the required mass of water and carefully mixing the soil and water together. The material was then covered with a plastic sheet to reduce evaporation and left for the water content to equalise for two hours. At the end of

this period, the material was mixed once more, weighed, and placed into the consolidation cell to form a layer approximately 130 mm thick. Two water content samples were taken at one-third and two-thirds uncompacted height to check for proper mixing of the material. The cell had been previously bolted onto the compaction base and its internal height measured. The legs of the compaction base had been adjusted such that level of the compaction surface and the upper surface of the base platen were nearly flush, as noted in Appendix A.

After placement of the soil, the remaining mass in the mixing tray was weighed and dried to provide a third check water content sample. The specimen was compacted using a Kango hammer and compaction plate, which was constrained to move vertically by a compaction guide. The standard compactive effort applied was a force of 350 N to 400 N on the vibrating Kango Hammer for a period of ten seconds, although this effort was varied in some tests to investigate the effect of compactive effort.

Following compaction, the depth to the specimen was measured from the cell flange and the specimen height calculated. The consolidation cell body was then unbolted from the compaction base, slid slowly and smoothly across the base onto the base platen and ceramic, and bolted to the base platen. At this stage, a damp cloth was placed across the top of the cell to reduce evaporation whilst the top platen was retrieved from the constant temperature laboratory. This platen would have been fully assembled and the load cells connected to the power supply at least 24 hours previously.

After retrieval, the top platen was placed on top of the cell using the bevelled edge as a seating guide and inserted into the cell using a hydraulic press. The whole cell was then transported to the constant temperature laboratory for bolting on of the cell top and connection to the plumbing and data acquisition systems detailed in Chapter 4.

When the cell was completely assembled and the logging software installed, cell pressure was applied above the top platen to push it down slowly into contact with the soil, such that the initial contact

pressure (measured by the load cells) was less than 5 kPa. The specimen air pressure and applied cell pressure were then increased alternately in small steps in order to raise the air pressure to 100 kPa whilst maintaining a maximum vertical stress on the specimen ($\sigma - u_A$) of about 5 kPa. At this stage, the displacement transducer was re-set to its most accurate range for measurement of subsequent strains and the specimen left under its initial contact stress for pore water pressure equalisation to be achieved. This stage typically lasted one to three days, and allowed the initial suction conditions of the specimen to be measured. At the end of this period, a back pressure equal to the equilibrium water pressure at the base was applied to the base volume change unit and the base drain opened. The remainder of the test was water drained at the base, and air drained, with the base suction kept at the equilibrium value.

After equalisation, the tests were continued by increasing the cell pressure such that an average vertical stress of 10 kPa was applied to the specimen within approximately 5 minutes. This stress was maintained until a new equilibrium in terms of soil suctions and axial strains had been established, typically after one or two days. Further increments and decrements would be similarly applied, using the nominal loading sequence of 10 kPa to 25 kPa, 25 kPa to 50 kPa, 50 kPa to 75 kPa, 75 kPa to 100 kPa, and nominal unloading sequence of 100 kPa to 50 kPa, 50 kPa to 25 kPa, 25 kPa to 5 kPa, and 5kPa to zero.

Periodically during the tests, the volume of any diffused air that had accumulated in the top and base platens was measured by flushing the air through the plumbing to the diffused air volume indicators.

Following completion of the tests, the top platen was removed using the special jack, and the water content - depth profile of the specimen determined. Some specimens were used also for post-test grading analyses to quantify the degree of particle breakdown that had occurred.

6.3 Test Series B

Test Series B aimed to provide data supplementary to that obtained in Series A on the compression behaviour of the coarse grading under water undrained loading conditions up to a nominated stress level, and thereafter to yield data on the behaviour of the specimens during inundation under a constant vertical stress. As such, the procedure for Series B was identical to that for Series A until equilibrium was reached under the vertical stress to be maintained during inundation, except that the test was water undrained (ie the base drain was not opened and a back pressure to control the suction was not applied). This stress at which inundation took place was usually 75 kPa but ranged between 59 kPa and 126 kPa. A summary of the tests performed in Series B is presented in Table 6.3.

The inundation stage commenced with the application of a back pressure of 50 kPa to the top volume change unit and "drainage" line as far as the consolidation cell. After initiation of the data acquisition software, the top "drain" was opened and water would start to inundate the specimen at a slow rate. Gradually the inundation pressure was increased to about 150 kPa, such that the inundation rate into the specimen was between 1.0 cm^3 per minute and 1.5 cm^3 per minute. However, as the inundation pressure increased there was a tendency for the top ceramic to bow away from the top platen, and the risk of ceramic cracking increased. Consequently, in some cases when the ceramic appeared to be less permeable than usual, a lower flow rate had to be accepted. A rate of 0.5 cm^3 per minute was used in one test.

The bowing action of the ceramic also tended to increase the vertical stress on the specimen, as the friction seal around the top platen and the applied cell pressure prevented the platen from receding from the specimen as the inundation pressure increased. As a result, it proved necessary to apply the inundation pressure in stages, with a reduction in the applied cell pressure after each stage in order to maintain a constant stress on the specimen to within 1 kPa.

Inundation was continued up to saturation, which took between 8 and 15 hours, during which time the specimen response was measured. When saturation was achieved, the inundation pressure line was closed and the applied cell pressure raised incrementally to compensate for the gradual decrease in the top pore water pressure and ceramic bowing. This was necessary to ensure that the vertical stress applied to the specimen was still maintained constant. Following equalisation of the top pore water pressure the specimen was left to equalise for a further 12 hours at least, after which the specimen was unloaded and the test dismantled as in Series A. However, in tests B6 and B7 this procedure was varied and a second load-unload cycle to 125 kPa was applied after initial unloading.

6.4 Test Series C

This series aimed to measure the effect of water content, and hence soil suction, on the K_0 of the coarse grading at a constant initial compacted dry density, and to subsequently acquire data on the shear properties of this material. The work was carried out at the Research Station in the modified triaxial cells.

Four specimens were tested, as summarised in Table 6.4. Each specimen was batched as previously described in Section 3.2.2, and compacted dry in four layers, approximately 100 mm thick, into a three-piece split former which had been assembled around the base pedestal of the triaxial cell with a double rubber membrane in place. Compaction was applied through 35 light blows of a wooden tamping rod on each layer.

For all except the dry specimen, inundation to near-saturation with a measured volume of water followed compaction, after which the top platen was inserted, the rubber membranes sealed to it, and a 15 kPa suction applied to the top of the specimen with a manometer and vacuum pump to drain some of the water out. This volume was measured and the suction locked into the material by closing the valve at the base of the triaxial cell. The specimen former was then dismantled and a free-standing specimen left. At this stage, the seals achieved and the intactness of the membranes following compaction were simultaneously

checked by observing movement of air and water in the suction line between its inlet to the triaxial cell base and its connection to the top of the specimen. Any movement in the pipe would have implied a poor seal and a non-testable specimen, but this never occurred. The average specimen dimensions were measured after verification of the seals.

Next, the triaxial cell was assembled around the specimen, the cell chamber filled with water, and a nominal cell pressure of 30 kPa (or 80 kPa for the dry specimen) applied. With the specimen now supported laterally, a nominal air pressure of 20 kPa (or 70 kPa for the dry specimen) was applied to the unsaturated and dry specimens, and the cell pressure increased in 10 kPa increments until a cell pressure of 80 kPa and an air pressure of 70 kPa was achieved. This ensured a maximum applied stress (σ- u_A) of 10 kPa at this stage, compared to the 15 kPa during specimen formation. For the saturated specimen, a back pressure of 20 kPa to the base platen followed application of a cell pressure of 30 kPa. The cell pressure was then increased in steps according to the formula below (50 kPa maximum) and the pore water pressure response measured each time to determine the pore pressure parameter B. After each application of the cell pressure and equalisation of the base pore water pressure, the base pore water pressure was increased to within 10 kPa of the cell pressure before the next cell pressure increment was applied. This process was repeated until B was greater than 0.95, when the cell pressure was 380.9 kPa and the back pressure was 367.8 kPa.

$$\Delta\sigma_3 = \frac{30 + u - \sigma_3}{1-B}$$

were $\Delta\sigma_3$ = change in cell pressure, u = current pore water pressure, and all pressures are in kPa.

With the specimen set-up, the data acquisition software was started and consolidation commenced with the pore pressures and cell pressure set to the values shown in Table 6.4. Consolidation was continued until volumetric strain had sensibly ceased, equivalent to less than 24 hours

for the dry and saturated specimens, and 4 weeks for the unsaturated specimens. Near the end of consolidation of the unsaturated specimens, the applied pressures were all increased by a nominal 100 kPa in steps in order to ascertain the influence, if any, of the mean stress level on the volumetric stain behaviour.

K_0 compression under water drained conditions followed completion of consolidation. A constant strain rate of 0.1 mm per minute was applied and the cell pressure varied in response to the observed change in specimen volume, as inferred from changes in triaxial cell volume. Cell volume corrections were applied for:

(i) Increasing membrane penetration with increased cell pressure, at about 0.5 cm^3 per kPa (for further details of the calculation of this value, see Chapter 7),

(ii) cell chamber deflection due to increase in the cell pressure,

(iii) volume of water displaced as the loading ram entered the triaxial cell chamber.

At a deviator stress of 100 kPa, the loading platen was stopped and the water drainage lines closed. The deviator stress was reduced to zero by lowering the platen at a constant cell pressure, and then the cell pressure was reduced to its pre K_o stage value in small steps. Observation of the apparent change in cell volume during this stage (after correction for the cell pressure effects) provided a method for determining the approximate relationship between change in membrane penetration and change in cell pressure, assuming volumetric strain of the specimen was negligible during this unloading. This allowed back analysis of the K_o stage using the inferred membrane penetration volume relationship for the particular specimen. The value of 0.5 cm^3 per kPa was based upon initial work and found to be reasonably accurate for all specimens tested in Series C.

Shearing to failure at a constant cell pressure and at a strain rate of 0.1 mm per minute followed the "membrane penetration" stage. Failure was defined as a peak in the deviator stress - axial strain curve. The specimen was water drained during this stage, and during unloading after shearing.

The specimen was dismantled in four layers at the end of the test and the water content - depth profile of the specimen determined. Throughout each test, manual readings of the digital voltmeters from each transducer were taken to back up and verify the computer readings.

6.5 Test Series D

The aim of Series D was to establish the one dimensional compression behaviour of all three test gradings under strain controlled undrained conditions. The effects of water content, strain rate and repeated loading were investigated. All specimens were batched and prepared to a nominal water content as described previously for Series A and B, then compacted into the compression cell in a single 200 mm thick layer using either a high or low compactive effort. Two samples were taken during preparation of each specimen to verify the compaction water content.

A high compactive effort required the application for 35 seconds of a 350 N to 400 N force to the soil using the same vibrating Kango hammer employed in series A and B. This compactive effort had been shown by compaction trials to be equivalent to that used in Series A and B. The Kango hammer was maintained vertical during compaction by a compaction guide. A light compactive effort required the application of 35 evenly distributed blows with a compaction rod to two successive soil layers, each 100 mm thick before compaction.

Following compaction, the depth to the specimen was measured from the cell flange and the initial specimen parameters determined. The specimen was transferred to the triaxial machine, and the top platen and load cell slowly lowered into light contact with the soil. The

displacement transducer was then clamped to the loading frame with its armature nearly full extended and its free end resting on the cell flange.

After initiation of the data acquisition software, testing commenced with between 3 and 5 cycles of applied total vertical stress, nominally between 10 kPa and 125 kPa and at a constant strain rate of 0.5 mm per minute. This was followed by a further 3 to 5 cycles between 10 kPa and 250 kPa at the same strain rate. The final stage of the test involved cycling the applied stress between 10 kPa and 250 kPa at a strain rate of 2 mm per minute for 3 to 5 cycles. Data acquisition intervals were changed for each stage of the test to ensure that more than sufficient data was obtained regardless of the stage duration.

The test was completed by removing the specimen in three approximately equal layers and the water content of each determined to establish the water content-depth profile of the specimen. Some specimens were also used for an investigation into particle breakdown during testing.

Table 6.1 Summary of Test Series

Series	Brief Description of Test Type	Number of Tests per Grading			Variables Investigated	Specimen Size	
		Coarse	Medium	Fine		Height (mm)	Diameter (mm)
A	Incremental loading compression under drained conditions	5	0	5	Water content	Approx 100 to 110	254.0
B	Incremental loading compression under undrained conditions followed by inundation at constant vertical stress	7	0	0	Water content Stress level during inundation	Approx 100 to 110	254.0
C	Drained constant strain rate K_o compression followed by shearing to failure	4	0	0	Water content	Approx 400	Approx 200
D	Undrained constant strain rate compression with repeated loading	11	2	2	Water content Compactive effort Strain Rate Repeated Loading	Approx 150 to 180	305.0

Table 6.2 Summary of Tests in Series A

Test Ref No	Grading Tested	Initial Height (mm)	Initial Free Water Content (%)	Initial Dry Density (Mg/m^3)	Initial Voids Ratio	Initial Free Degree of Saturation (%)	Initial Air Voids Ratio (%)	Comments
A1	Fine	89.0	4.2	1.79	0.48	23.0	24.9	-
A2	Coarse	90.5	3.9	2.18	0.28	37.6	13.5	-
A3	Fine	109.5	2.4	1.78	0.49	12.9	28.6	-
A4	Fine	96.1	7.1	1.97	0.34	54.0	11.7	-
A5	Fine	100.4	4.1	1.87	0.42	25.8	21.8	Repeatability for A1
A6	Coarse	111.6	2.0	2.01	0.33	16.1	20.8	-
A7	Coarse	117.8	5.2	2.15	0.24	56.9	8.4	-
A8	Coarse	113.8	4.9	2.14	0.25	51.9	9.7	Repeatability for A7
A9	Coarse	115.3	3.4	2.10	0.27	33.3	14.2	-
A10	Fine	102.1	4.1	1.88	0.41	26.1	21.5	-

Table 6.3 Summary of Tests in Series B

Test Ref No	Initial Height (mm)	Initial Free Water Content (%)	Initial Dry Density (Mg/m^3)	Initial Voids Ratio	Initial Free Degree of Saturation (%)	Initial Air Voids Ratio (%)	Inundation Stress (kPa)	Comments
B1	119.1	1.6	2.02	0.33	13.1	21.3	76.4	-
B2	110.1	4.6	2.01	0.33	37.6	15.4	76.0	Lower compactive effort used
B3	110.6	4.1	2.20	0.21	51.9	8.5	126.0	-
B4	112.6	4.1	2.02	0.32	34.1	16.1	74.5	Lower compactive effort applied, and repeatability for B2
B5	111.7	2.3	2.05	0.30	20.2	18.5	59.0	-
B6	116.7	1.1	2.03	0.34	8.4	23.7	74.0	Additional load cycle after inundation
B7	116.1	1.1	2.02	0.32	9.3	22.1	76.3	Repeatability for B7

Table 6.4 Summary of Tests in Series C

Test Reference Number	Initial Free Water Content* (%)	Initial Dry Density* (Mg/m^3)	Pressures During Consolidation			Comments
			Cell	Air	Water	
C1	10.5	2.02	400	-	368	Saturated
C2	0.0	2.03	102	68	-	Dry
C3	3.5	2.01	100 199	70 170	55 156	Applied suction = 15 kPa
C4	4.2	2.09	100 200	71 170	66 166	Applied suction = 4 kPa

* Value at start of K_o stage.

Table 6.5 Summary of Tests in Series D

Test Ref No	Grading Tested	Initial Height (mm)	Initial Free Water Content (%)	Initial Dry Density (Mg/m^3)	Initial Voids Ratio	Initial Free Degree of Saturation (%)	Initial Air Voids Ratio (%)	Compaction Level	Comments
D1	Coarse	161.5	2.8	2.05	0.31	24.0	17.8	Heavy	-
D2	Coarse	168.0	7.6	2.23	0.20	100.0	0.0	Heavy	-
D3	Coarse	179.0	0.0	2.18	0.21	0.0	17.5	Heavy	-
D4	Coarse	165.8	4.2	2.15	0.24	45.6	10.7	Heavy	-
D5	Coarse	161.5	2.8	2.08	0.29	26.0	16.5	Heavy	Repeatability for D1
D6	Coarse	161.1	0.0	1.96	0.38	0.0	27.6	Light	-
D6A	Coarse	179.8	0.0	1.88	0.44	0.0	30.5	Light	Computer failure during test Repeat for D6
D7	Coarse	169.8	2.7	1.79	0.50	14.4	28.4	Light	-
D8	Coarse	164.0	2.9	1.78	0.50	15.3	28.4	Light	Repeatability for D7
D9	Coarse	165.2	5.4	2.08	0.28	50.6	10.9	Light	-
D10	Coarse	171.8	4.1	1.99	0.34	31.8	17.4	Light	-
D11	Medium	151.2	2.8	1.85	0.44	16.8	25.3	Heavy	-
D12	Medium	147.6	4.2	1.92	0.38	29.0	19.6	Heavy	-
D13	Fine	146.3	3.0	1.73	0.53	14.7	29.7	Heavy	-
D14	Fine	140.0	4.3	1.76	0.50	22.4	25.9	Heavy	-

CHAPTER 7

RESULTS OF TESTS

The results of all tests are reported in this chapter, together with some initial interpretation of the data. Discussion of the results, comparisons between the test series and the implications of the findings are presented in Chapter 8.

7.1 Compressibility Tests with Suction Measurements

The results of test series A, and those for series B up to commencement of the inundation stage, are considered under this heading. The term "compressibility" has been used in preference to "consolidation" even though, by the nature of the air drained incremental load-unload tests, pore water pressures induced by the loading changes were given time to dissipate. Unlike conventional consolidation tests on saturated materials, the pore water pressure in the series B tests was not confined to return to a back pressure but was free to attain a new equilibrium with the induced soil fabric changes. Hence the measured pore water pressure was not an excess pore pressure in the conventional sense.

7.1.1 Specimen Response to a Single Total Stress Change

A typical response of the load cells to a stress increment is shown in Figure 7.1, together with the average total stress applied. The application of this increment resulted in the strain time curve shown in Figure 7.2, and the incremental strain against incremental stress curve shown in Figure 7.3. The form of these figures is typical for all tests, whether loading or unloading, and shows that the intended constant total vertical stress increments/decrements were quickly applied. The immediate and time dependent strain components may be inferred from Figure 7.3.

The top and base pore water pressure response curves are plotted against time in Figure 7.4, and show an initial surge due to system compliance when a back pressure is not applied to the ceramic (ie the top ceramic in Figure 7.4). The compliance influence may be seen more clearly in Figure 7.5, which shows the suction stress path in response to total stress changes. Figure 7.4 shows also simultaneous fluctuations in pressure of up to 0.5 kPa from the mean pressure in response to fluctuations in the regulated air pressure in the specimen. Small volume changes were sometimes recorded at the base during the water drained series A tests, but as will be discussed in Chapter 8, these were negligible.

7.1.2 Results of Suction Measurements

The equilibrium suctions at a total stress of 10 kPa for the coarse and fine gradings are presented in Figure 7.6 against average free water content. The measured suctions increase as the water content decreases, but a large degree of scatter is associated with the results for the coarse grading. An improved relationship for the coarse grading may be seen in Figure 7.7, which plots the suction at 25 kPa total stress against free water content. The surprisingly similar order of magnitude of suctions for both gradings is discussed further in section 8.3.

The warped form of the state surface for volume change shown in Figure 2.5 implies suctions should decrease as the total stress increases. The results for both gradings confirm this expectation, as typified by Figure 7.8. The influence of the free water content on the size of the load-unload hysteresis loop is shown for the fine grading in Figure 7.9. A similarly clear trend for the coarse grading was not discernible due to the scatter in equilibrium suction values noted previously.

The variable vertical separations of the top and bottom suction - water content curves in Figure 7.5 suggests a non-linear water content - depth profile within the specimens. The results of the water content profile measurements at the end of each test in series A are tabulated in Table

7.1 and plotted in Figure 7.10. The profiles are related to the total water content in Figure 7.11. These figures confirm the implication of Figure 7.5, and suggest also that, except for test A4 which has a high average total water content, the soil water had not redistributed to form a saturated layer at the base of the specimen.

7.1.3 Effect of Compaction Water Content and Dry Density on Compressibility

The strain-stress curves for the coarse and fine gradings are shown separately in Figures 7.12 and 7.13, respectively. Inspection of these curves shows that compressibility is a function of the compaction water content and dry density for a given compactive effort, and this is shown more clearly in Figures 7.14 and 7.15 which plot the strain at any given stress level against the free water content of the soil for loading only. Both graphs consider behaviour dry of optimum over a range in which the dry density continually increases with increasing water content.

7.2 Inundation Tests

The results for the inundation stage of the Series B tests are presented in this section. Figure 7.16 shows the typical forms of the load cell and average total stress, strain and top pore water pressure curves with time recorded during each inundation stage. The apparent decrease in strain as inundation commences (shown by the increase in the top pore water pressure in Figure 7.16c) is a function of ceramic flexure following application of the inundation water pressure exceeding the induced collapse strains at the constant total vertical stress. Correction of the strain-time curve for flexure by assuming a linear relationship between apparent strain and applied inundation pressure was made using the apparent strain at constant vertical stress as the inundation pressure was reduced following saturation as the benchmark. Figure 7.17 shows the corrected curve, and Figure 7.18 shows the influence of the inundation stage on the strain-stress curves (excluding

unloading stages) for the tests. As may be seen from Figure 7.17, a large proportion of the collapse strains were manifested in the first minutes after the start of inundation.

The pore water pressure response at the base of the specimens during inundation is typified by figure 7.19, which shows that no change was recorded for the first 1 to 2 hours of inundation. After this time, there is a rapid reduction in suction to near zero followed by an approximately linear decrease in suction during the remainder of the infiltration stage. The finite period of time between start of inundation and a recorded influence at the base of the specimen reflects the rate of descent of the first wetting front through the specimen, and the linear increase in pressure thereafter represents the gradual increase in the height of the near saturated layer at the base of the specimen. The equilibrium pore water pressure of typically 1.0 kPa to 1.2 kPa at the end represents the typically 100 mm to 120 mm high saturated head of water within the specimen.

7.3 K_o and Shear Tests

7.3.1 Membrane Effects

The results of the four tests in series C on the coarse grading are presented in the following sub-sections. However, interpretation of the results required preliminary assessments be made of the effects of the membrane on behaviour, as noted below.

The strength correction applied to the deviator stress measurements for the double membrane were determined experimentally by British Gas personnel to be 0.2226 kPa multiplied by the axial strain, the determination being made using a dummy specimen of known properties.

Correction for membrane penetration was more difficult, and had implications for the calculated specimen phase volumes, volumetric strains, and the deviator stresses as noted over:

True total volume change of specimen = Cell volume change less correction for cell pressure less correction for ram penetration

True air phase volume change = True total volume change of specimen less measured water phase volume change

True specimen cross sectional area = $\frac{\text{original area}}{\text{(1-axial strain)}}$. (1-true volumetric strain)

True deviator stress = $\frac{\text{change in deviator load}}{\text{true specimen area}}$, less membrane strength correction

Consideration was initially given to developing a method for preventing penetration at all, but it was decided this was not merited for such a short series of tests. Instead, a simple and approximate method was devised to calculate the correction for each specimen individually from cell volume measurements. The method relied upon the assumption that, following the Ko stage of the test, and reduction of the deviator stress to zero, the true volumetric strain of the specimen during σ_3 unloading in a water undrained state would be negligible. The near vertical unload stress-strain curves for the radially confined tests in series A and B suggested such an assumption would not be greatly in error. If the assumption is correct, any recorded cell volume change due to the reduction in σ_3 above (corrected for expansion/contraction of the cell walls due to σ_3) should represent the total change in membrane penetration as the drained and pressure regulated air phase pushes the membrane out. A linear relation between change in cell pressure and penetration was then assumed. It was also assumed that membrane penetration was the same during unloading and the preceding loading stages.

The major drawback of this method was that it had to follow the K_o stage, which itself relied upon a reliable estimate of the membrane penetration factor to maintain K_o conditions. Consequently a trial test was performed and a factor of 0.5 cm^3/kPa obtained. The actual tests subsequently yielded values of 0.89, 0.32, 0.39 and 0.45 cm^3/kPa for tests C1 to C4 respectively, which resulted in true K_o conditions only being reliably maintained in test C4.

7.3.2 Consolidation Curves

The pressures on the four specimens during the isotropic consolidation are summarised in Table 6.4. A conventional consolidation curve was obtained for each specimen, as typified by Figure 7.20, but the times for consolidation were noticeably different. The saturated and dry specimens (C1 and C2) took about 16 hours and 27 hours respectively, whereas the unsaturated specimens (C3 and C4) which were consolidated from near saturation at a constant applied suction each took about 28 days. The changes in specimen water content, void ratio and dry density, plus the total and free water volumetric strains during consolidation are presented in Table 7.2. The effect of raising the ambient consolidation pressures by a constant value was investigated near the end of consolidation for each specimen and found to have negligible effects.

7.3.3 K_o Determinations

As a result of testing difficulties and significant discrepancies between the assumed and subsequently measured membrane penetration correction factors, K_o conditions were not sufficiently maintained for a reliable K_o value to be measured from tests C1, C2 and C3. The results for specimen C4 are shown in Figure 7.21, and a K_o value of 0.41 was obtained by taking K_o to equal $\Delta (\sigma_3 - u_A)/\Delta (\sigma_1 - u_A)$ for this unsaturated case. A tentative value of 0.39 was obtained from the latter stages of test C1 when K_o conditions were achieved, but initial anisotropic stress changes render this value suspect.

7.3.4 Shear Stages

The complex stress paths followed by the specimens up to the start of the shear stages are summarised in Tables 7.3 to 7.6, together with their impact on the main specimen parameters. These stress paths will have led to initially overconsolidated specimens and are likely to have significantly affected the early stages of the shear tests in particular.

The results of the shear stages are presented in Table 7.7 in the light of the above comments. All specimens failed (ie peak shear stress) through dilatant plastic deformations, and only exhibited shear plane deformation movements near the ends of the tests. A typical plot of the stress-strain curves obtained and the measured volumetric strains are presented in Figures 7.22 and 7.23, respectively. All specimens failed at axial strains of about 5%, but as will be discussed in Chapter 8 volumetric strains differed significantly between specimens.

7.4 Strain Controlled Compression Tests

The results of the 15 tests in series D are presented in this section. Tables 7.8 and 7.9 summarise the virgin compression line and repeated load data for each test, respectively, and Figure 7.24 shows a typical stress-strain curve for all stages of a test. Similar forms of curves were obtained for all tests regardless of grading or compactive effort.

Figures 7.25 and 7.26 present the virgin compression lines only for the usual and low compactive efforts, and Figure 7.27 presents the curves for the fine and medium grading tests. Inspection of the curves for the coarse grading show that in common with the series A and B tests compressibility is a function of the dry density and water content. These effects are more clearly seen in Figure 7.28, which plots the strain at a given stress level against the total water content. The more heavily compacted specimens gave a relatively flat curve with a slight peak over the water content range of 0% to about 5.5%, but the

compressibility then rapidly increases as optimum water content is approached and passed. The lightly compacted specimens show a similar trend but the range of water contents tested was insufficient to show the increase in compressibility as the optimum water content is approached. The interactions of the dry density and water content may not be determined from the two tests on the fine and medium gradings.

The effects of repeated loading on strain accumulation are typified by Figure 7.29, which plots the strain at the maximum and minimum stresses of each load cycle against cycle number. All the curves showed a discontinuity when the peak stress was increased from 125 kPa to 250 kPa after the first 4 or 5 cycles, there being also a time gap between this cycle and the next due to the low (0.5 mm/minute) strain rate. After the eighth to tenth cycle the strain rate was increased to 2 mm/minute. Each of the four groups of tests (coarse grading with heavy and light compaction, and fine and medium gradings) exhibited a different typical response as shown by the figure, but all showed that strain rate had no influence on the behaviour.

The effects of water content and dry density on the repeated load behaviour have been drawn out by Figures 7.30 and 7.31, which plot the difference in strain after one and four cycles against the free water content (a) and dry density (b) for the heavily and lightly compacted coarse graded specimens, respectively.

The water content - depth profile measurements at the end of each test are summarised in Table 7.10. Except for the wettest specimen, insufficient time (<4 hours usually) had elapsed for significant moisture redistribution to occur within the specimens.

Table 7.1 Water Content Distribution Profiles After Series A Tests

Test Number	Measured Total Water Content (%)			Average Total Water Content (%)
	Top	Middle	Bottom	
Coarse Grading				
A2	Not Measured			4.7
A6	2.4	2.7	3.2	2.8
A7	5.6	6.0	6.4	6.0
A8	5.1	5.3	6.7	5.7
A9	4.0	4.1	4.4	4.2
Fine Grading				
A1	Not Measured			5.6
A3	3.6	3.8	4.0	3.8
A4	7.4	8.4	9.7	8.9
A5	5.2	5.4	6.0	5.5
A10	5.3	5.4	5.8	5.5

Table 7.2 Change in Specimen Parameters During Consolidation Stages of Series B Tests

Test Number	Free Water Content (%) Initial	Final	Void Ratio Initial	Final	Final Free Degree of Saturation (%)	Dry Density (Mg/m^3) Initial	Final	Volumetric Strain (%) Free Water	Total
C1	10.7*	10.5	0.31	0.28	100.0	1.97	2.02	2.6	0.72
C2	0.0	0.0	0.35	0.34	0.0	2.00	2.03	N/A	0.88
C3	7.9	3.5	0.31	0.31	31.0	2.01	2.01	60.5	0.31
C4	9.0	4.2	0.26	0.24	45.6	2.06	2.09	46.8	1.21

* 9.1% before saturation stage

Table 7.3 - Stress Path History and Variation of Soil Parameters for Test C1

Parameter / Stage	σ_1 (kPa)	σ_3 (kPa)	u_A (kPa)	u_w (kPa)	e	Free water content (%)	Free degree of saturation (%)	Dry density (Mg/m3)
After isotropic consolidation	398	400	-	368	0.28	10.5	100.0	2.02
After air and water drained K_o stage	626	515	-	369	0.25	9.2	100.0	2.02
After anisotropic water undrained reduction of $(\sigma_1 - \sigma_3)$ at constant σ_3	517	515	-	369	0.25	9.2	100.0	2.02
After anisotropic water undrained reduction of σ_3	401	401	-	368	0.26	9.6	100.0	2.02

Table 7.4 - Stress Path History and Variation of Soil Parameters for Test C2

Parameter / Stage	σ_1 (kPa)	σ_3 (kPa)	u_a (kPa)	u_w (kPa)	e	Free water content (%)	Free degree of saturation (%)	Dry density (Mg/m3)
After isotropic consolidation	202	202	167	-	0.34	0.0	0.0	2.03
After air and water drained K_o stage	451*	451	167	-	0.31	0.0	0.0	2.06
After anisotropic water undrained reduction of (σ_1 - σ_3) at constant σ_3	451	451	167	-	0.31	0.0	0.0	2.06
After anisotropic water undrained reduction of σ_3	202	202	167	-	0.32	0.0	0.0	2.06

* 1st test attempted - loading ram failed to contact during K_o stage but apparent contact as increasing cell pressure caused increased stress on external load cell

Table 7.5 - Stress Path History and Variation of Soil Parameters for Test C3

Parameter / Stage	σ_1 (kPa)	σ_3 (kPa)	u_a (kPa)	u_w (kPa)	e	Free water content (%)	Free degree of saturation (%)	Dry density (Mg/m3)
After isotropic consolidation	-	199	170	156	0.31	3.5	31.0	2.01
After air and water drained K_o stage	451	360	170	156	0.30	3.5	31.5	2.01
After anisotropic water undrained reduction of (σ_1 - σ_3) at constant σ_3	360	360	170	156	0.30	3.5	31.3	2.01
After anisotropic water undrained reduction of σ_3	202	202	170	157	0.31	3.5	30.7	2.01

Table 7.6 - Stress Path History and Variation of Soil Parameters for Test C4

Parameter / Stage	σ_1 (kPa)	σ_3 (kPa)	u_A (kPa)	u_W (kPa)	e	Free water content (%)	Free degree of saturation (%)	Dry density (Mg/m3)
After isotropic consolidation	-	200	170	166	0.24	4.2	45.6	2.09
After air and water drained K_o stage	427	312	170	166	0.23	4.2	48.7	2.11
After anisotropic water undrained reduction of (σ_1 - σ_3) at constant σ_3	312	312	170	166	0.23	4.2	48.6	2.11
After anisotropic water undrained reduction of σ_3	201	201	130	167	0.23	4.2	47.6	2.11

Table 7.7 Results of Shear Tests

Test No	Pore Pressures During Test (kPa) u_A	u_w	$(u_A - u_w)$	Failure Stresses+ (kPa) σ_{1f}	σ_{3f}	Shear Stress at Failure (kPa) $\frac{1}{2}(\sigma_{1f} - \sigma_{3f})$	Mean Stress at Failure (kPa) $\frac{1}{2}(\sigma_{1f} + \sigma_{3f} - 2u_A)$	Volumetric Failure Strains (%) Axial	Total	Free Water	Soil Parameters at Failure (at start) Free Water Content (%)	Free Degree of Saturation (%)	Voids Ratio	Dry Density (Mg/m^3)
C1	-	368	-	602	401	101	134*	5.30	-0.91	-0.91	10.1 (9.6)	100.0 (100.0)	0.27 (0.26)	2.00 (2.02)
C2	167	-	-	710	202	254	289	4.30	-1.28	-	0.0 (0.0)	0.0 (0.0)	0.33 (0.32)	2.03 (2.06)
C3	170	157	13	701	202	250	282	5.15	-2.25	+3.671	3.4 (3.5)	25.5 (30.7)	0.36 (0.31)	1.96 (2.01)
C4	170	167	3	420	201	110	141	5.05	-2.20	-0.47	4.2 (4.2)	39.9 (47.6)	0.28 (0.23)	2.03 (2.11)

\+ Failure defined as peak value of shear stress
* $\frac{1}{2}(\sigma_{1f} + \sigma_{3f} - 2u_w)$ for saturated soil

Table 7.8 Virgin Compression Line Data for Test Series D

Test No	Strains (%) and Various Stresses (kPa) on VCL							
	5	10	25	50	100	150	200	250
D1	0.00	0.24	0.31	0.37	0.40	0.42	0.45	0.47
D2	0.00	0.15	0.44	0.77	1.14	1.41	1.64	1.85
D3	0.00	0.05	0.13	0.23	0.35	0.44	0.50	0.57
D4	0.00	0.09	0.16	0.20	0.24	0.27	0.31	0.36
D5	0.00	0.23	0.28	0.32	0.35	0.38	0.41	0.44
D6A	0.00	0.33	0.93	1.47	2.10	2.52	2.85	3.14
D7	0.00	0.38	0.84	1.34	2.46	3.11	3.62	4.11
D8	0.00	0.40	1.31	2.24	3.40	4.18	4.77	5.34
D9	0.00	0.17	0.42	0.68	1.03	1.27	1.47	1.66
D10	0.00	0.20	0.53	0.86	1.30	1.62	1.85	2.08
D11	0.00	0.40	0.69	0.82	0.96	1.03	1.06	1.11
D12	0.00	0.09	0.18	0.22	0.29	0.34	0.36	0.40
D13	0.00	0.10	0.23	0.34	0.50	0.62	0.71	0.79
D14	0.00	0.05	0.14	0.23	0.34	0.43	0.53	0.61

Table 7.9 Repeated Load Data Summary for Test Series D

(a) Coarse Grading, "Standard" Compaction

Test No	Strain Rate (mm/min)	Cycle 1		Cycle 2		Cycle 3		Cycle 4		Cycle 5	
		E_p	E_u	E_p	E_u	E_p	E_u	E_p	E_u	E_p	E_u
D1	0.5	0.61	0.51	0.61	0.54	0.61	0.54	0.61	0.54	-	-
	0.5	0.69	0.58	0.79	0.58	0.72	0.58	-	-	-	-
	2.0	0.76	0.58	0.76	0.58	0.72	0.58	0.72	0.63	0.76	0.58
D2	0.5	1.48	1.42	1.53	1.42	1.59	1.42	1.62	1.53	1.65	1.53
	0.5	2.05	1.91	2.14	1.99	2.23	2.02	-	-	-	-
	2.0	2.20	2.02	2.23	2.05	2.26	2.08	2.29	2.08	-	-
D3	0.5	0.41	0.22	0.41	0.20	0.41	0.22	0.41	0.22	-	-
	0.5	0.58	0.27	0.63	0.33	0.65	0.33	0.63	0.36	-	-
	2.0	0.77	0.48	0.77	0.48	0.79	0.48	0.77	0.48	0.77	0.48
D4	0.5	0.55	0.38	0.55	0.38	0.55	0.38	0.55	0.38	0.55	0.41
	0.5	0.67	0.44	0.67	0.44	0.67	0.44	0.70	0.47	-	-
	2.0	0.70	0.47	0.70	0.47	0.70	0.47	0.70	0.49	0.70	0.49
D5	0.5	0.72	0.60	0.72	0.60	0.72	0.63	0.72	0.63	0.72	0.63
	0.5	0.80	0.63	0.81	0.66	0.81	0.66	0.84	0.66	-	-
	2.0	0.84	0.69	0.87	0.69	0.84	0.66	0.84	0.69	0.87	0.69

(b) Coarse Grading, Light Compaction

Test No	Strain Rate (mm/min)	Cycle 1		Cycle 2		Cycle 3		Cycle 4		Cycle 5	
		Ep	Eu	Ep	Eu	Ep	Eu	Ep	Eu	Ep	Eu
	0.5	3.32	3.16	3.35	3.19	3.37	3.19	3.40	3.19	3.43	3.24
D6A	0.5	4.21	3.97	4.29	4.02	4.32	4.08	4.37	4.13	4.40	4.15
	2.0	4.40	4.15	4.45	4.18	4.48	4.18	4.48	4.24	4.51	4.26
	0.5	2.43	2.34	2.49	2.40	2.51	2.43	2.57	2.49	2.57	2.49
D7	0.5	4.23	4.05	4.34	4.14	4.40	4.23	4.45	4.28	4.51	4.31
	2.0	4.57	4.37	4.62	4.42	4.65	4.45	4.68	4.48	4.68	4.51
	0.5	3.79	3.66	3.82	3.73	3.87	3.76	3.93	3.82	3.93	3.82
D8	0.5	5.85	5.65	5.95	5.77	6.06	5.85	6.09	5.91	-	-
	2.0	6.18	5.98	6.21	6.00	6.27	6.06	6.30	6.09	6.33	6.15
	0.5	1.30	1.12	1.35	1.17	1.44	1.23	1.44	1.30	1.50	1.32
D9	0.5	2.00	1.73	2.09	1.79	2.14	1.85	2.17	OOS	-	-
	2.0	2.20	1.94	2.23	1.94	2.26	2.00	2.32	2.00	2.35	2.03
	0.5	1.80	1.47	1.83	1.53	1.89	1.61	1.92	1.64	1.92	1.66
D10	0.5	2.65	2.17	2.74	2.32	2.82	2.40	OOS	(2.46)	-	-
	2.0	2.99	2.49	3.02	2.46	3.05	2.57	3.08	2.60	3.10	2.60

(c) Fine Grading:

Test No	Strain Rate (mm/min)	Cycle 1		Cycle 2		Cycle 3		Cycle 4		Cycle 5	
		Ep	Eu	Ep	Eu	Ep	Eu	Ep	Eu	Ep	Eu
	0.5	0.83	0.66	0.87	0.66	0.87	0.70	0.87	0.66	0.87	0.66
D13	0.5	1.07	0.73	1.10	0.77	1.13	0.80	1.13	0.80	1.13	0.83
	2.0	1.16	0.90	1.16	0.87	1.16	0.87	1.20	0.83	1.16	0.87
	0.5	0.52	0.38	0.52	0.38	0.52	0.38	0.52	0.38	0.52	0.38
D14	0.5	0.76	0.52	0.79	0.55	0.83	0.55	0.86	0.59	0.86	0.59
	2.0	0.86	0.58	0.86	0.62	0.90	0.62	0.90	0.62	0.94	0.66

(d) Medium Grading:

Test No	Strain Rate (mm/min)	Cycle 1		Cycle 2		Cycle 3		Cycle 4		Cycle 5	
		E_p	E_u	E_p	E_u	E_p	E_u	E_p	E_u	E_p	E_u
	0.5	1.70	1.61	1.70	1.61	1.70	1.64	1.30	1.64	1.70	1.64
D11	0.5	1.87	1.77	1.87	1.77	1.89	1.77	1.89	1.77	1.89	1.77
	2.0	1.87	1.77	1.87	1.77	1.87	1.77	1.87	1.77	1.87	1.77
	0.5	0.49	0.36	0.49	0.36	0.49	0.36	0.49	0.36	0.49	0.36
D12	0.5	0.59	0.43	0.62	0.43	0.66	0.43	0.66	0.46	0.66	0.46
	2.0	0.66	0.46	0.66	0.46	0.69	0.46	0.69	0.46	0.69	0.46

Note: E_p - strain at peak stress in cycle, being either 125 kPa or 250 to 275 kPa

E_u - strain at minimum stress level in cycle, 10 kPa

OOS - Out Of Scans

Table 7.10 Water Content Distribution Profiles After Series D Tests

Test No	Total Water Content - Depth Profile		
	Top	Middle	Base
D1	3.2	4.0	3.6
D2	9.2	6.8	7.2
D3	0.0	0.0	0.0
D4	4.6	5.3	5.2
D5	3.3	3.6	3.8
D6A	0.0	0.0	0.0
D7	3.5	3.4	3.5
D8	3.3	3.8	4.1
D9	5.0	5.4	8.3
D10	4.0	4.7	5.9
D11	3.8	4.0	4.0
D12	5.2	5.2	5.7
D13	4.4	4.4	4.3
D14	5.7	5.8	5.7

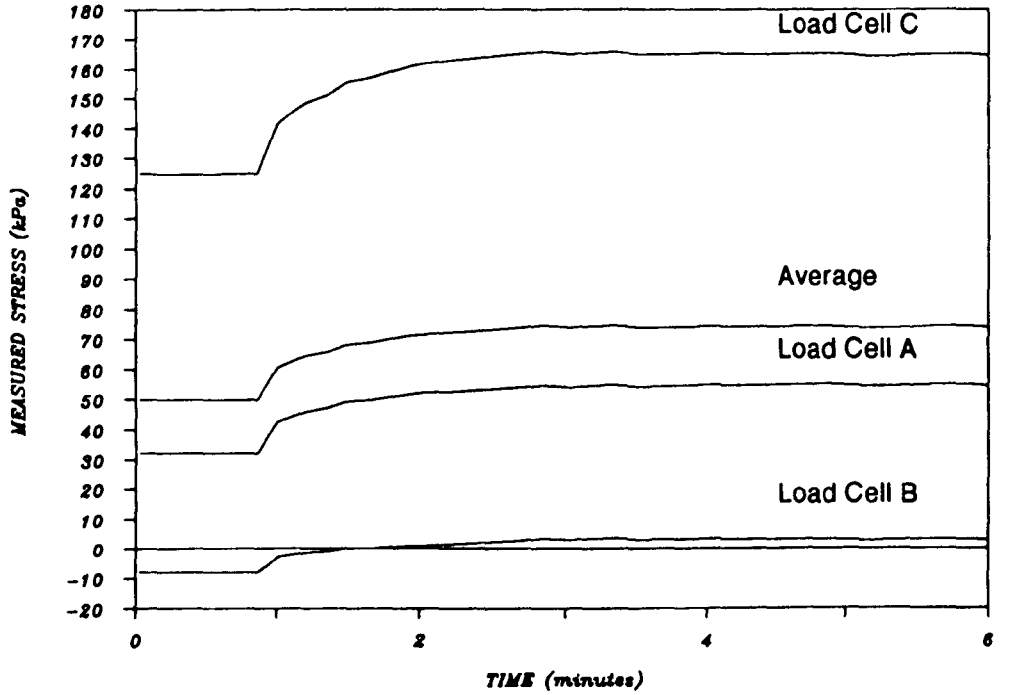

(a) First 6 Minutes of Loading Stage

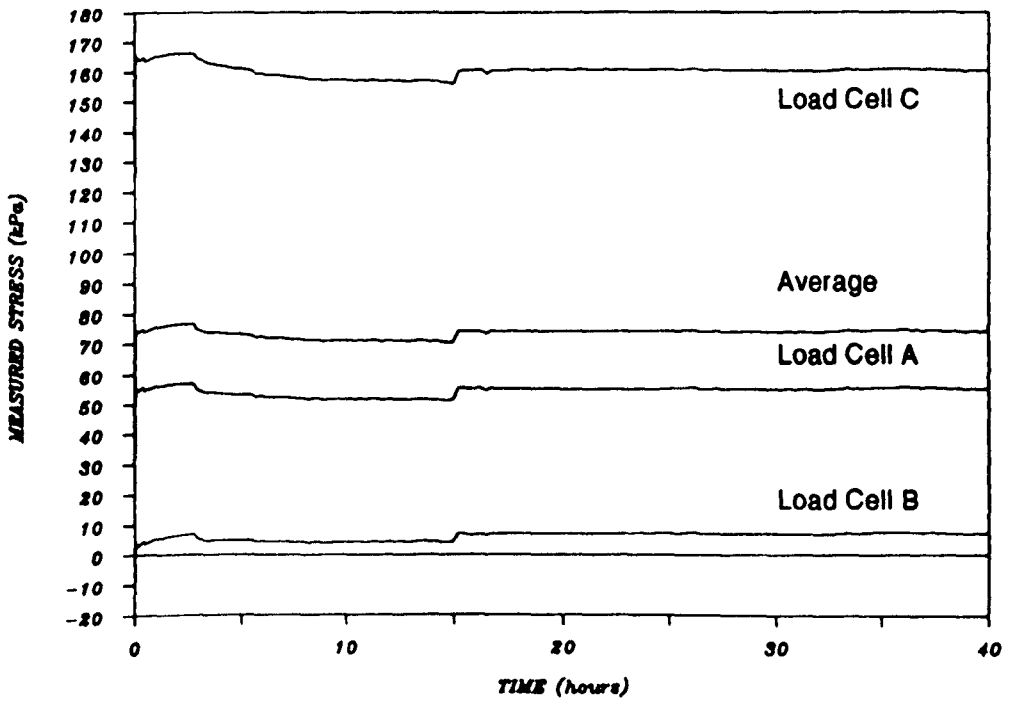

(b) Entire Duration of Loading Stage

Figure 7.1 - Typical Load Cell Output Variation During a Loading Stage
(Load Stage 3 of Test A10)

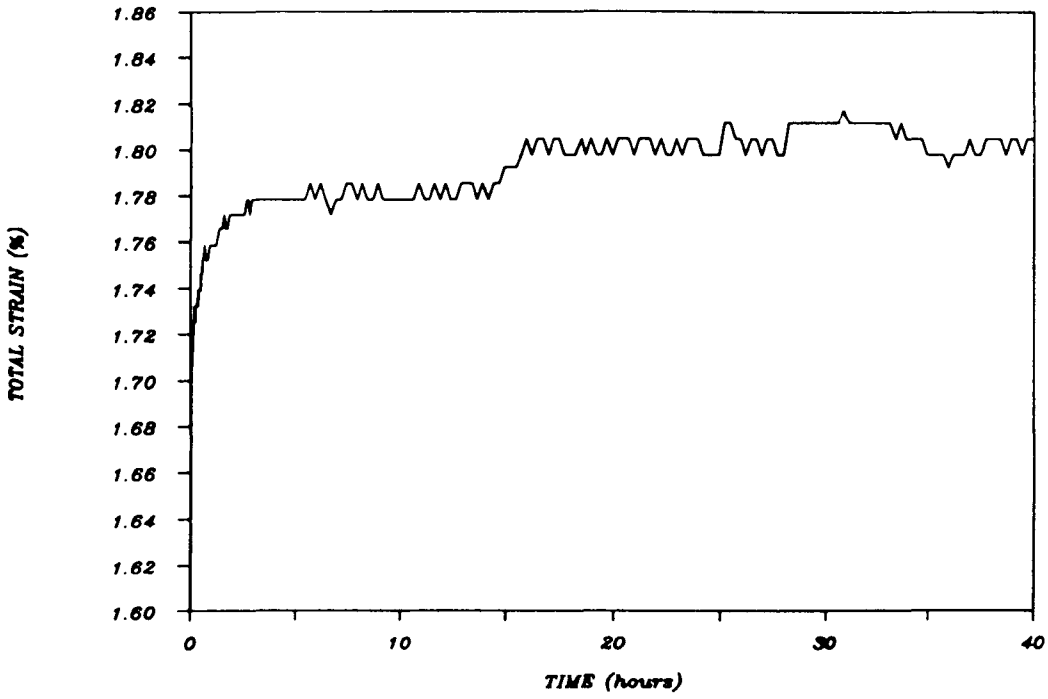

Figure 7.2 – Typical Strain Development During a Loading Stage
(Load Stage 3 of Test A10)

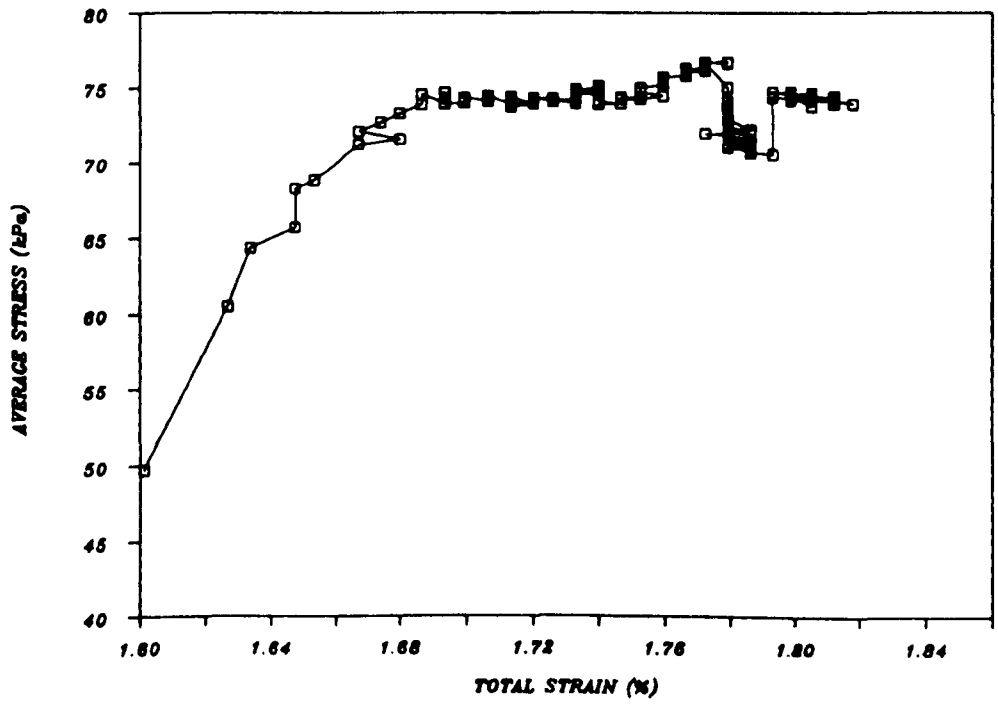

Figure 7.3 – Typical Stress–Strain Curve For Single Loading Stage
(Load Stage 3 of Test A10)

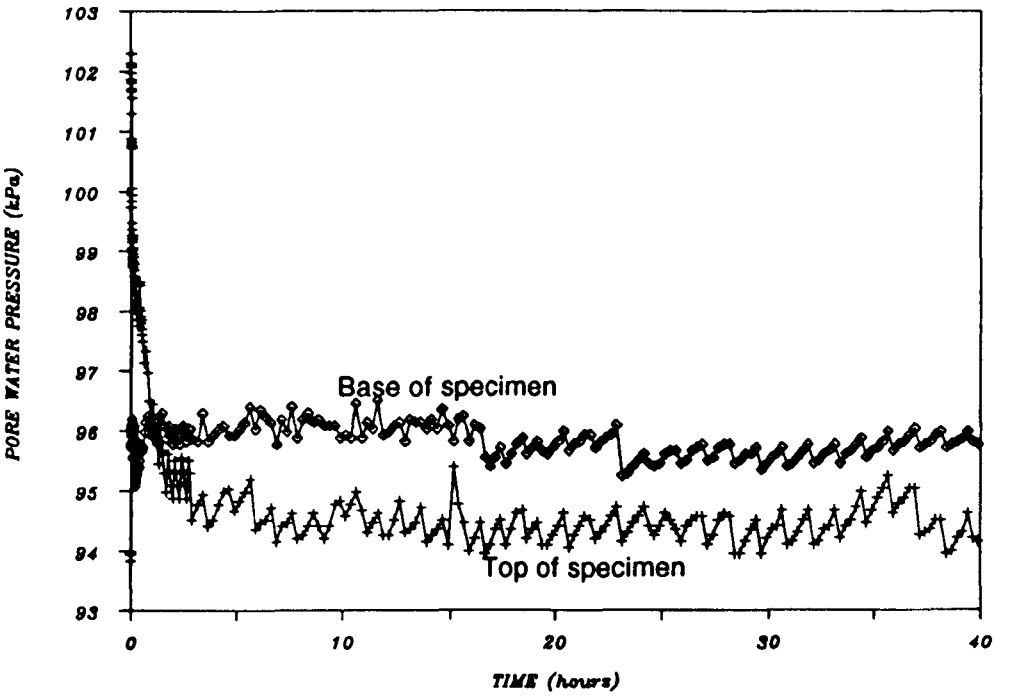

Figure 7.4 - Typical Pore Pressure Variation During a Loading Stage
(Load Stage 3 of Test A10)

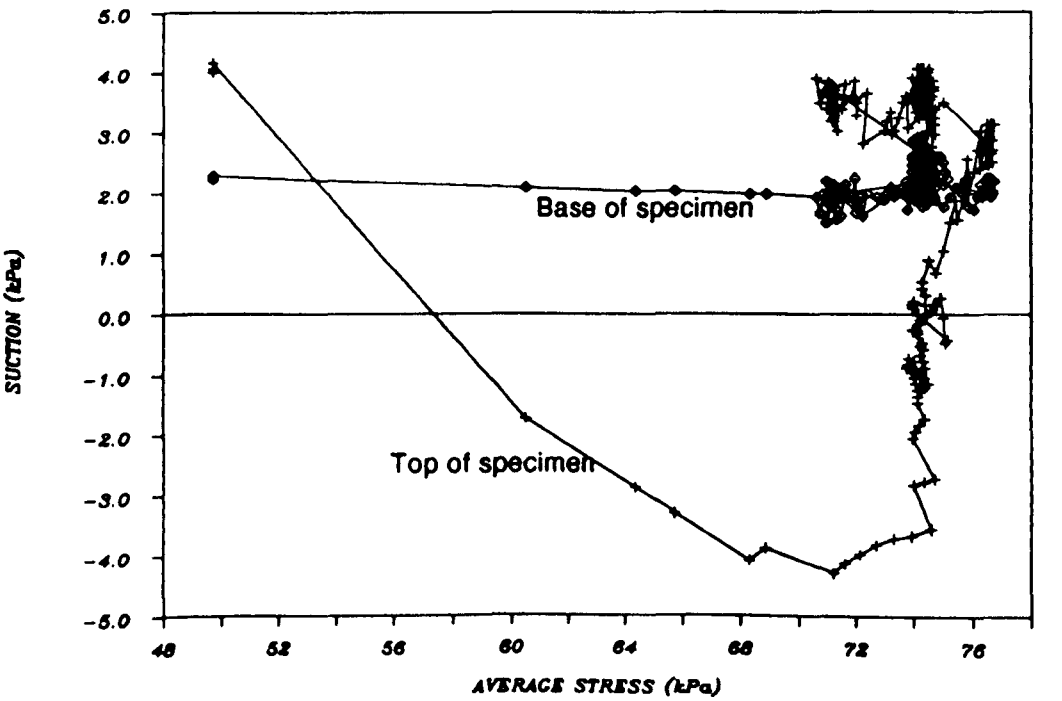

Figure 7.5 - Typical Suction-Stress Curve For Single Loading Stage
(Load Stage 3 of Test A10)

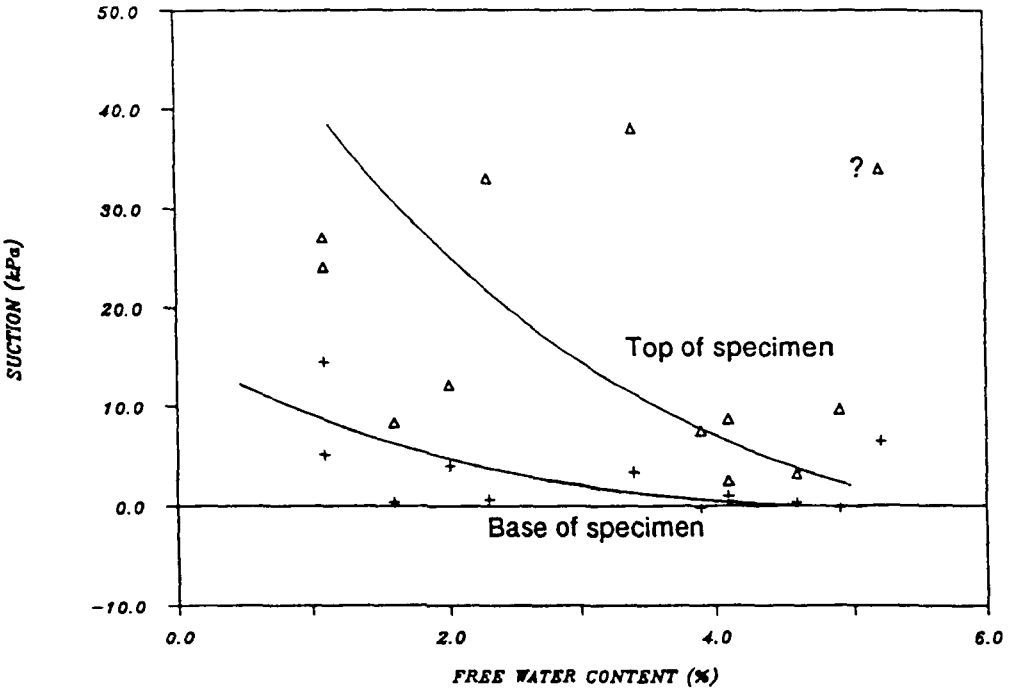

(a) Coarse Grading

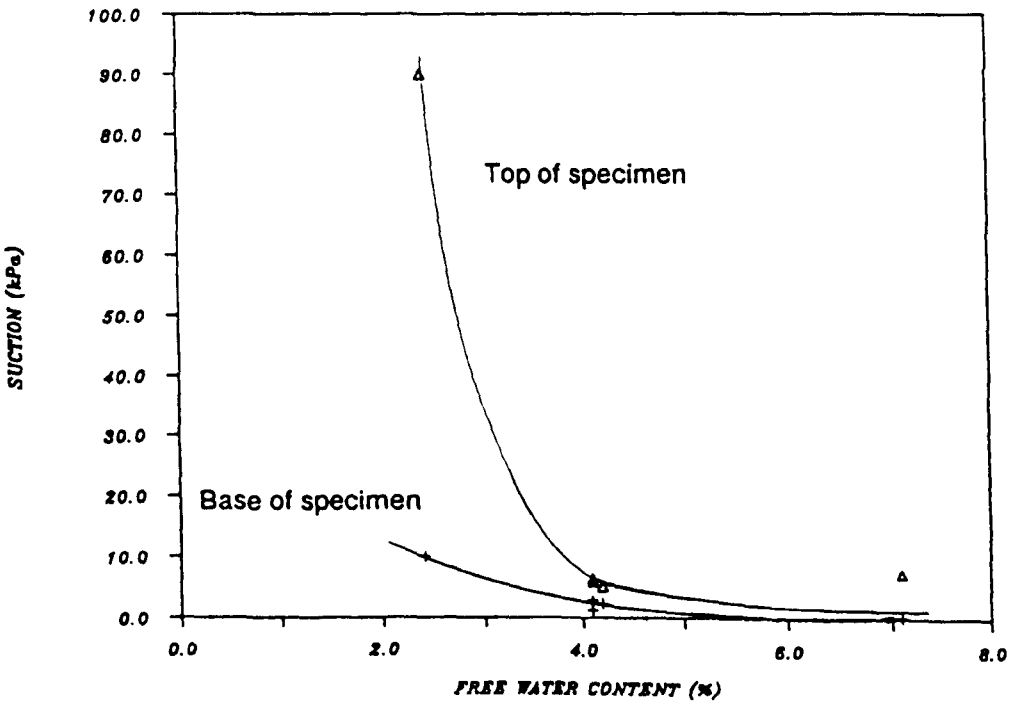

(b) Fine Grading

Figure 7.6 - Suction-Water Content Relationships for Coarse and Fine Gradings at Vertical Stress of 10kPa

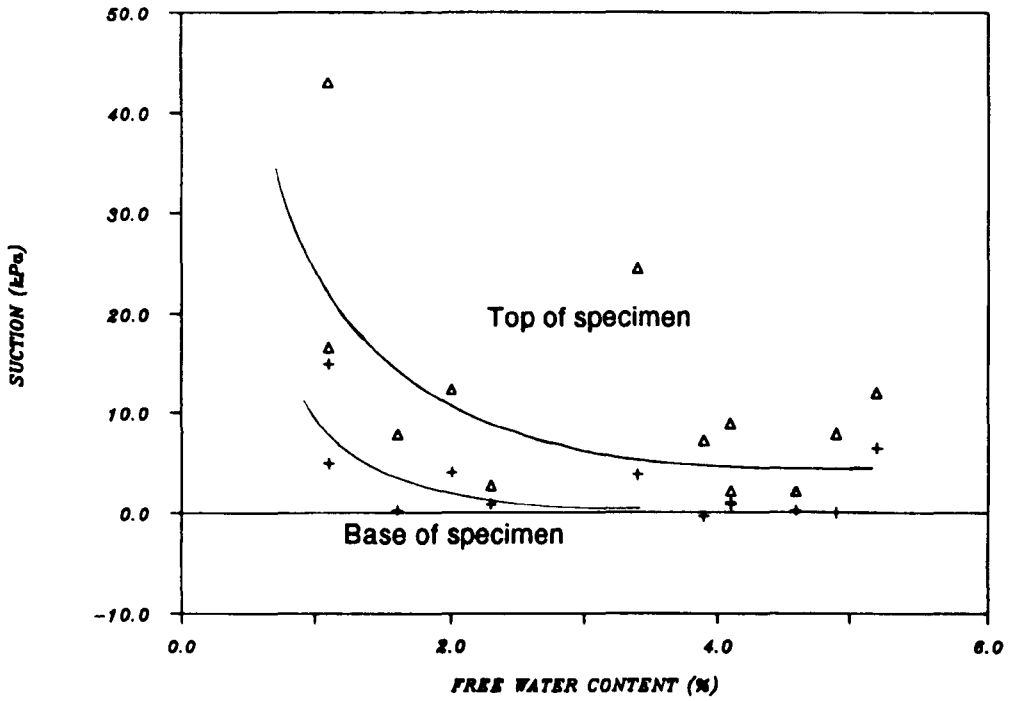

Figure 7.7 - Suction-Water Content Relationship for Coarse Grading at Vertical Stress of 25kPa

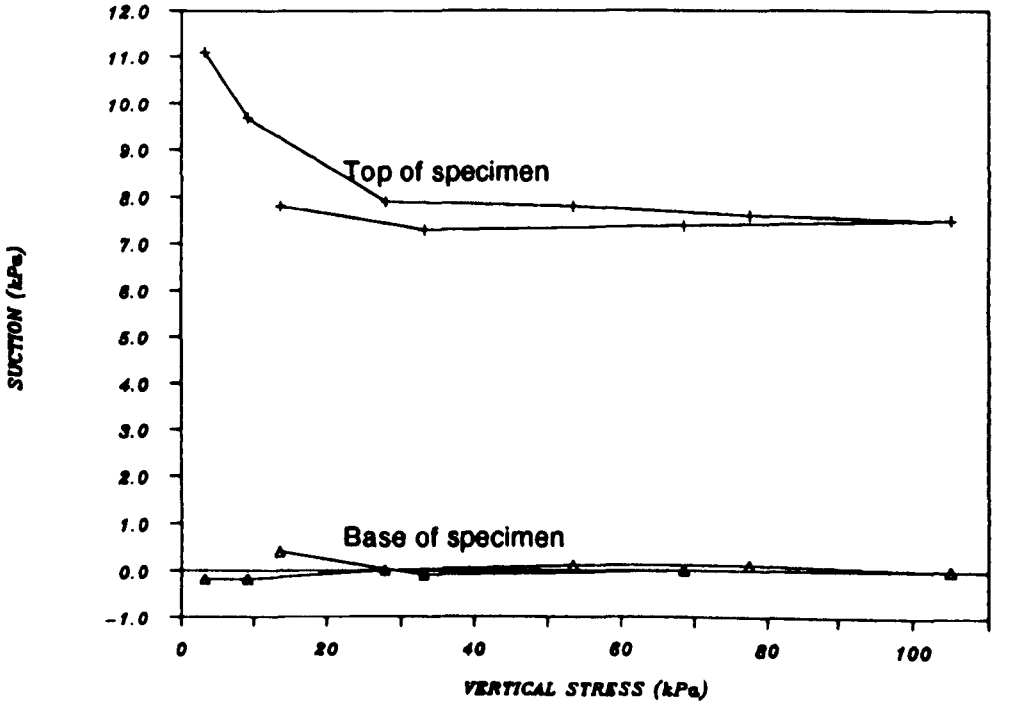

Figure 7.8 - Suction-Vertical Stress Relationship for Test A8 (Coarse Grading)

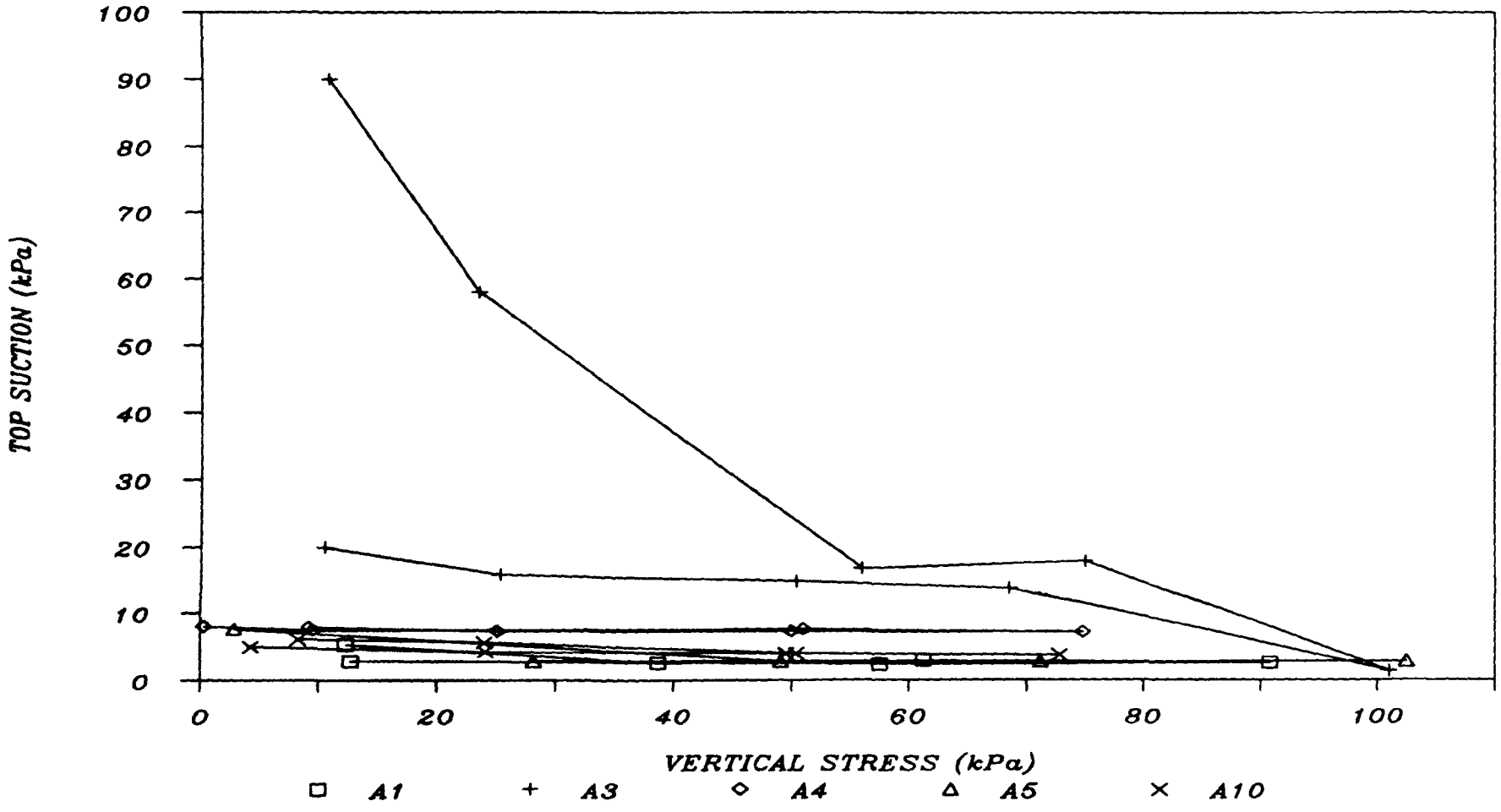

Figure 7.9 – Variation of Top Suction with Vertical Stress for Fine Grading

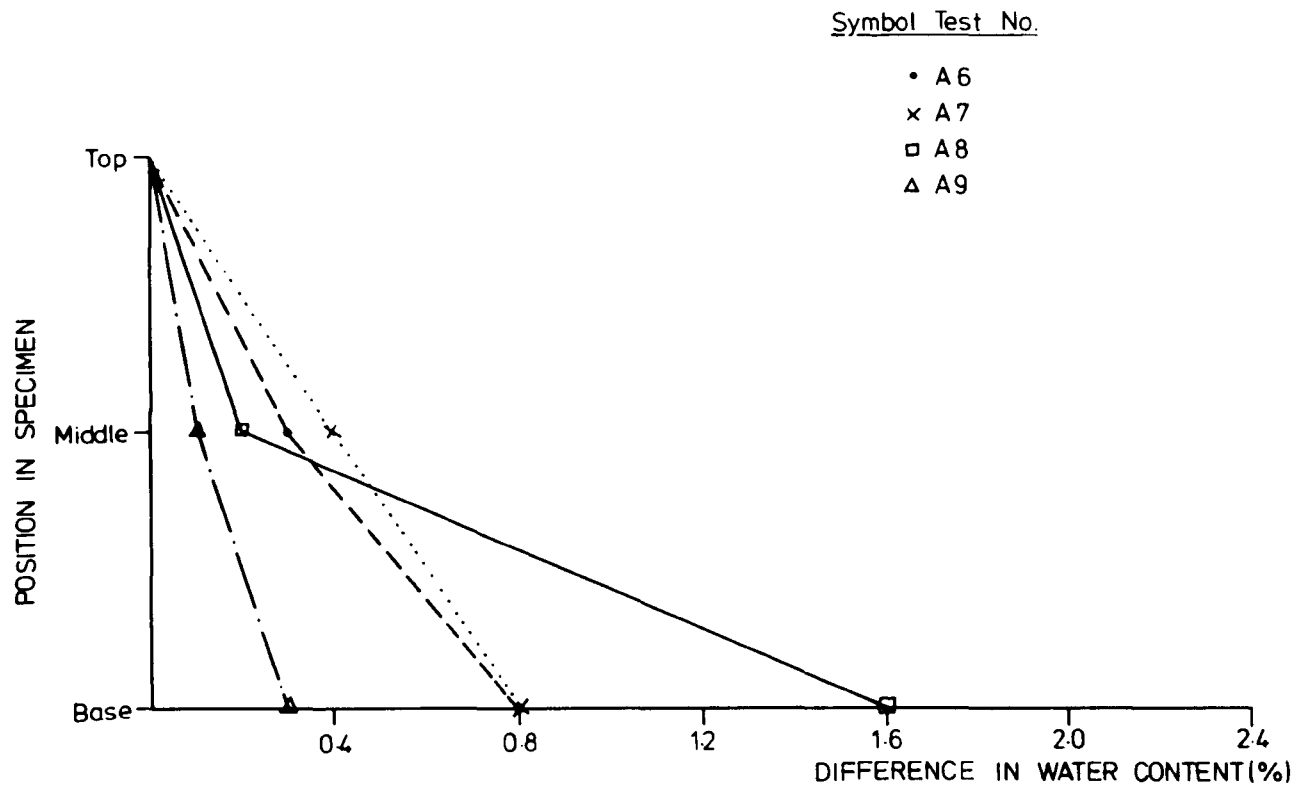

(a) Coarse Grading

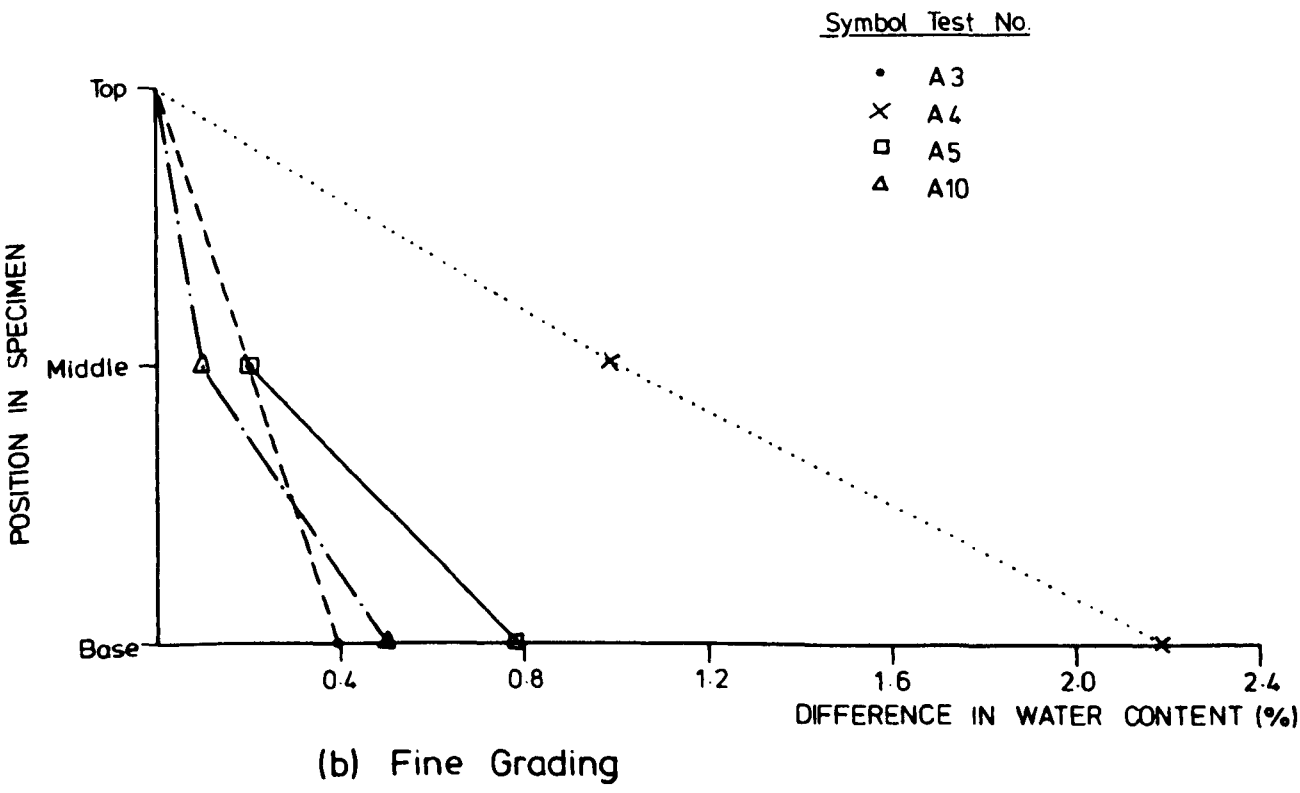

(b) Fine Grading

Figure 7·10 - Measured Water Content-Depth Profiles after Series A Tests

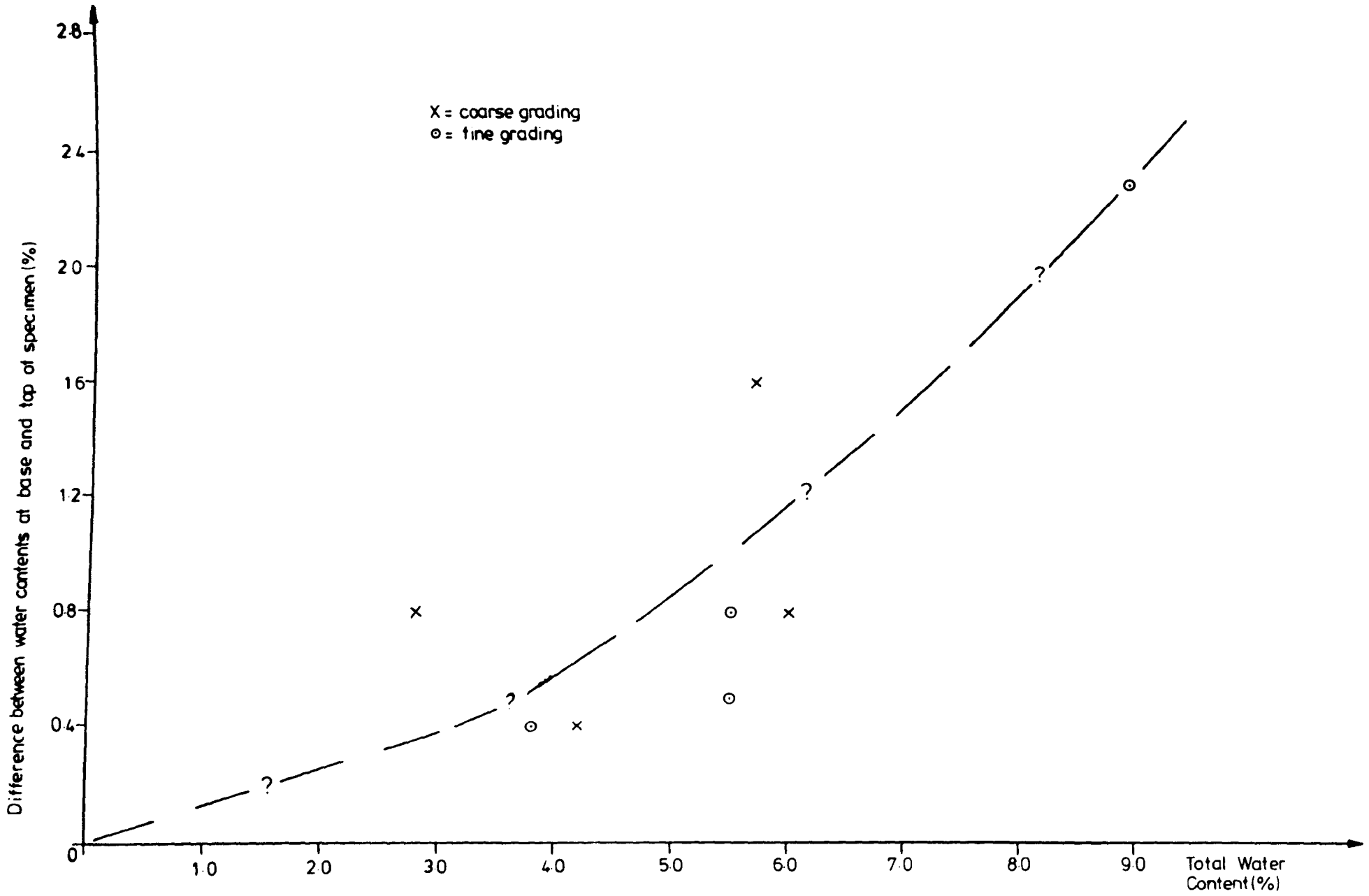

Figure 7·11 – Effect of Total Water Content on Vertical Water Content Profile

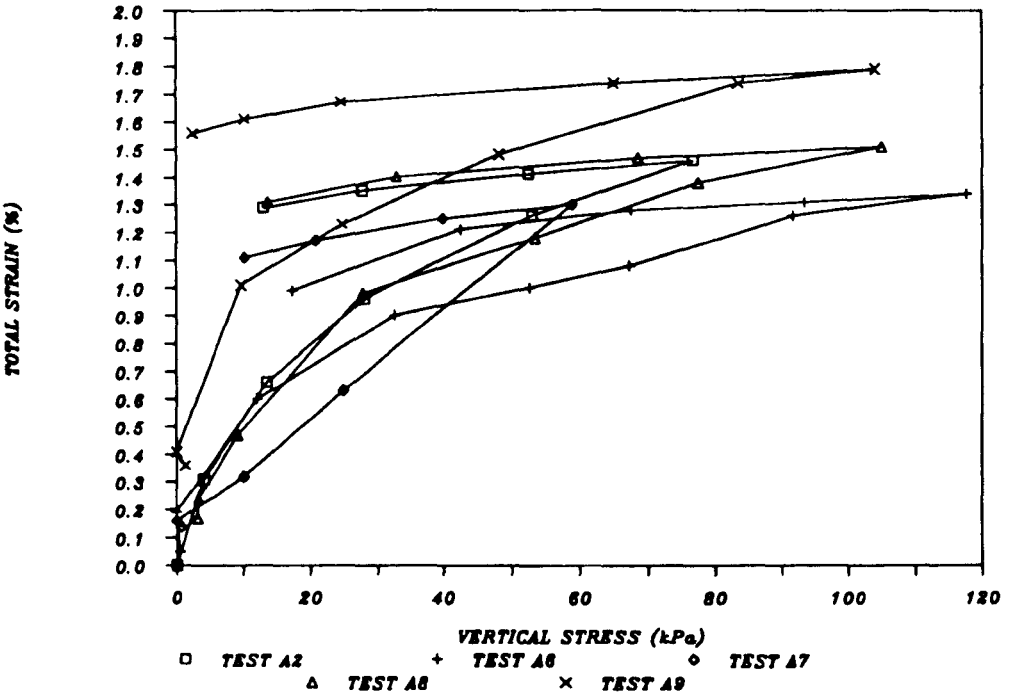

(a) Series A Tests

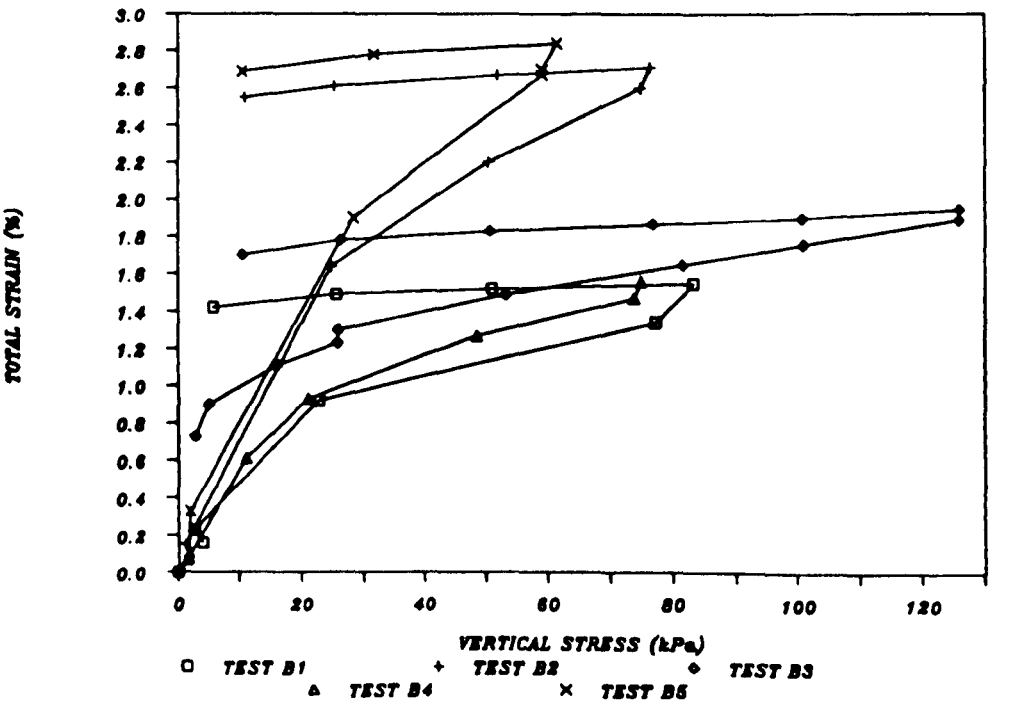

(b) Series B Tests (to B5 inc.)

Figure 7.12 - Strain-Stress Curves for Coarse Grading from Series A and B Tests
(continued overleaf)

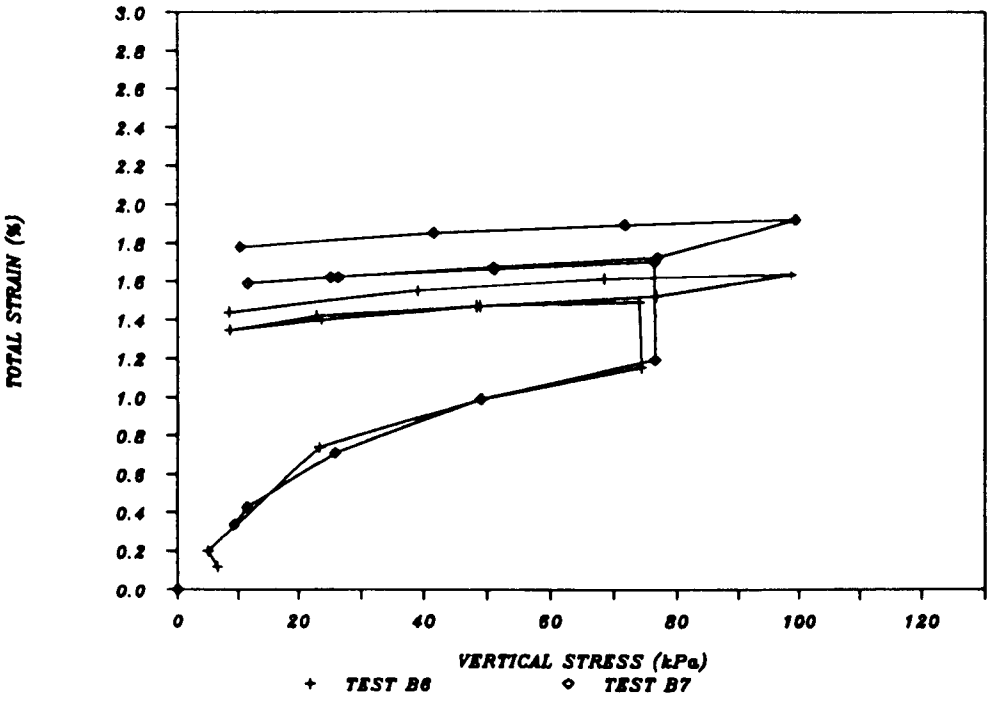

(c) Series B Tests (B6 and B7)

Figure 7.12 - Strain-Stress Curves for Coarse Grading from Series A and B Tests (continued)

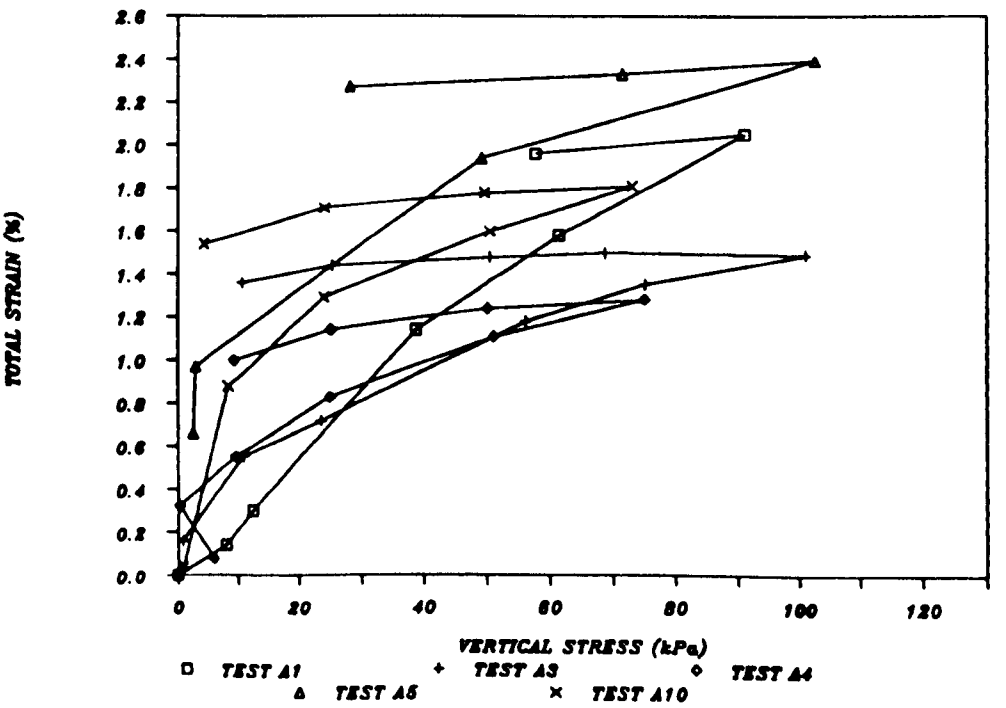

Figure 7.13 - Strain-Stress Curves for Fine Grading from Series A Tests

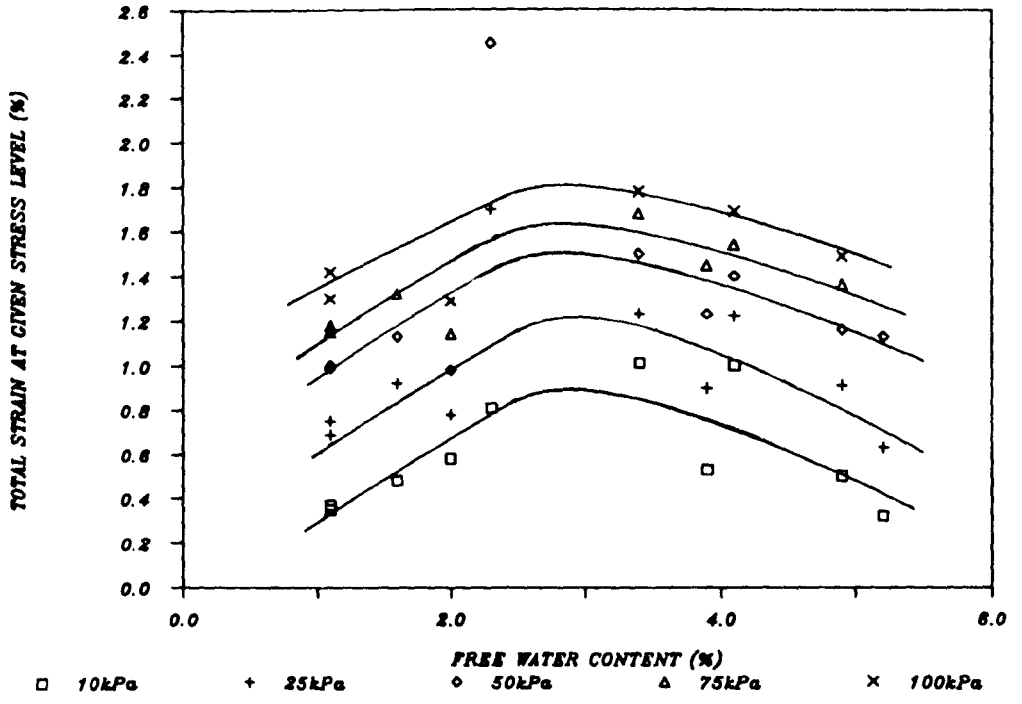

Figure 7.14 – Effect of Free Water Content on Compressibility of Coarse Grading from Test Series A and B at Usual Compactive Effort

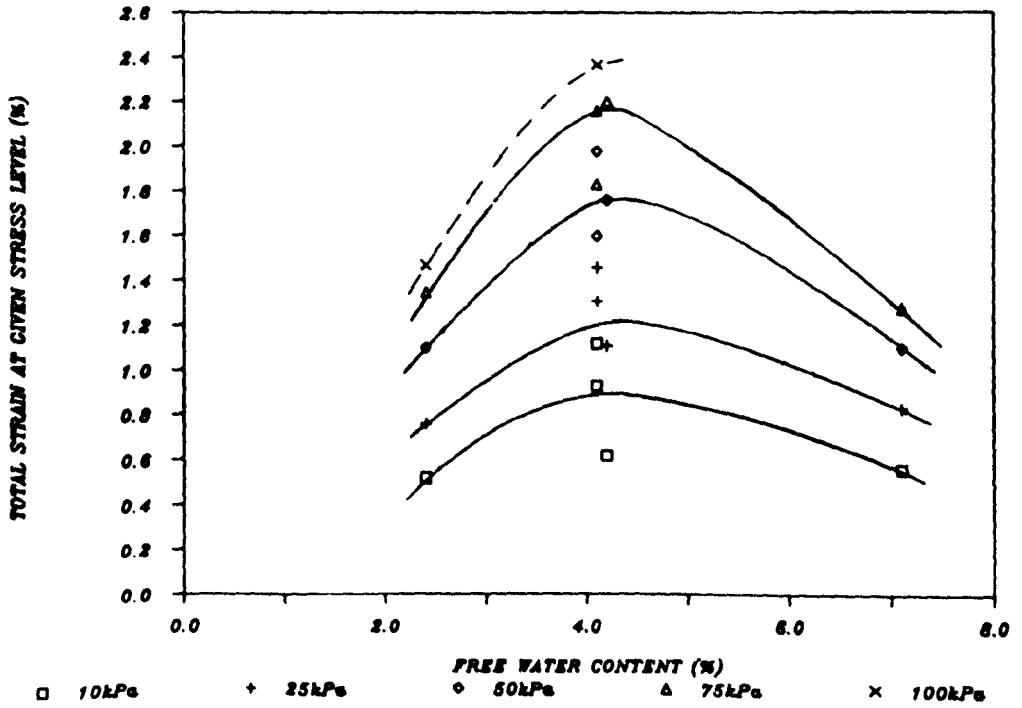

Figure 7.15 – Effect of Free Water Content on Compressibility of Fine Grading from Series A Tests

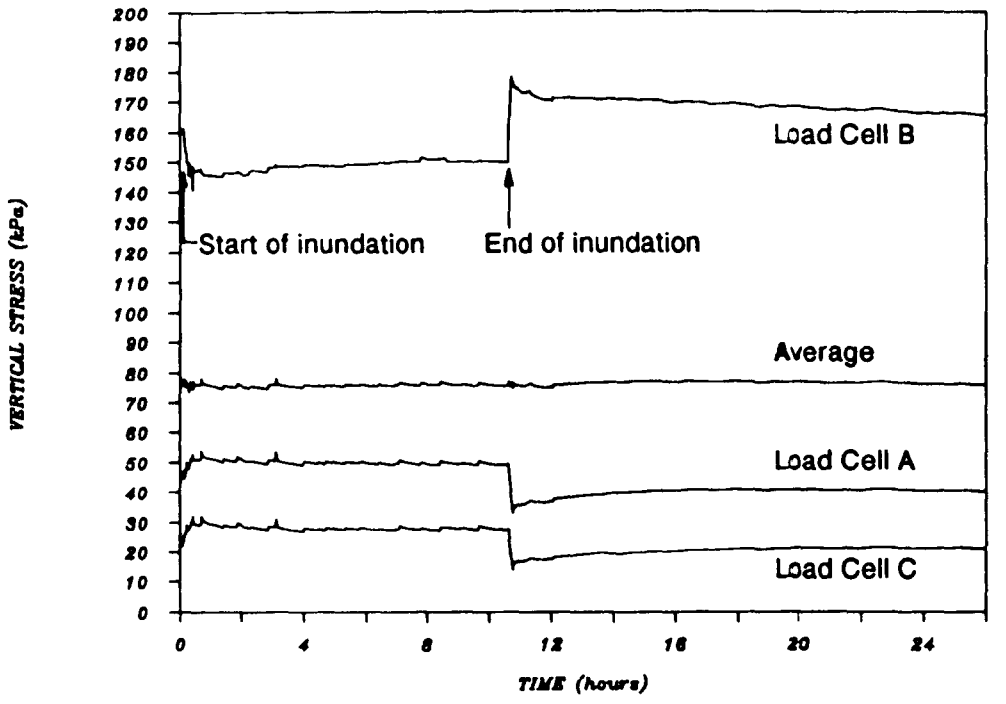

(a) Variation of Load Cell Measurements

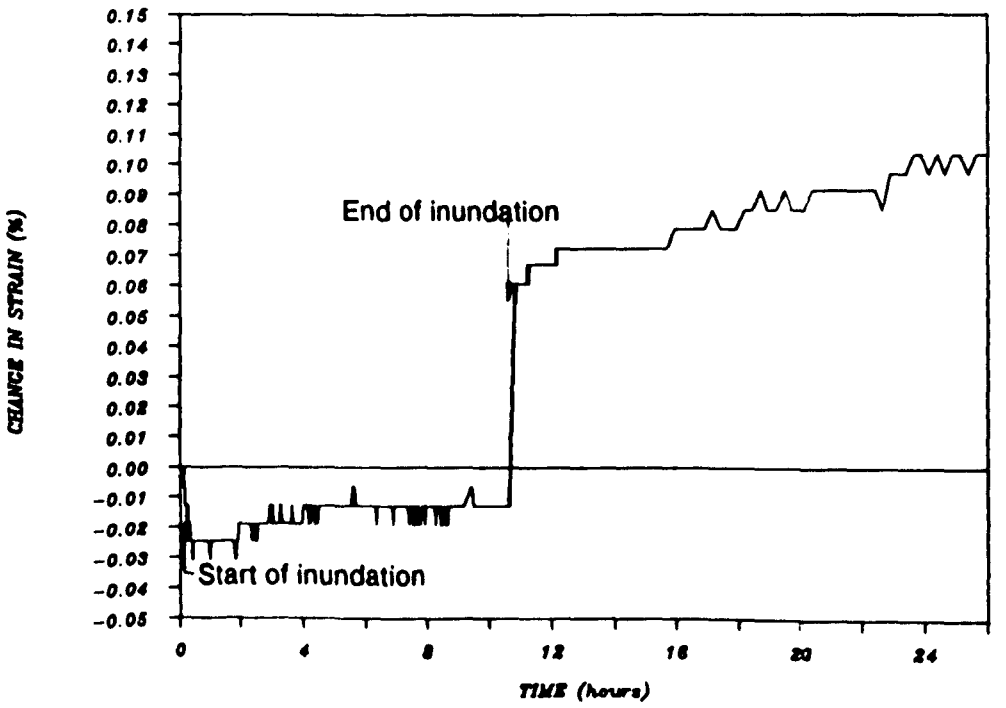

(b) Strain Development During Stage

Figure 7.16 – Typical Variation of Stress Strain and Top Pore Water Pressure During an Inundation Stage (Test B2) (continued overleaf)

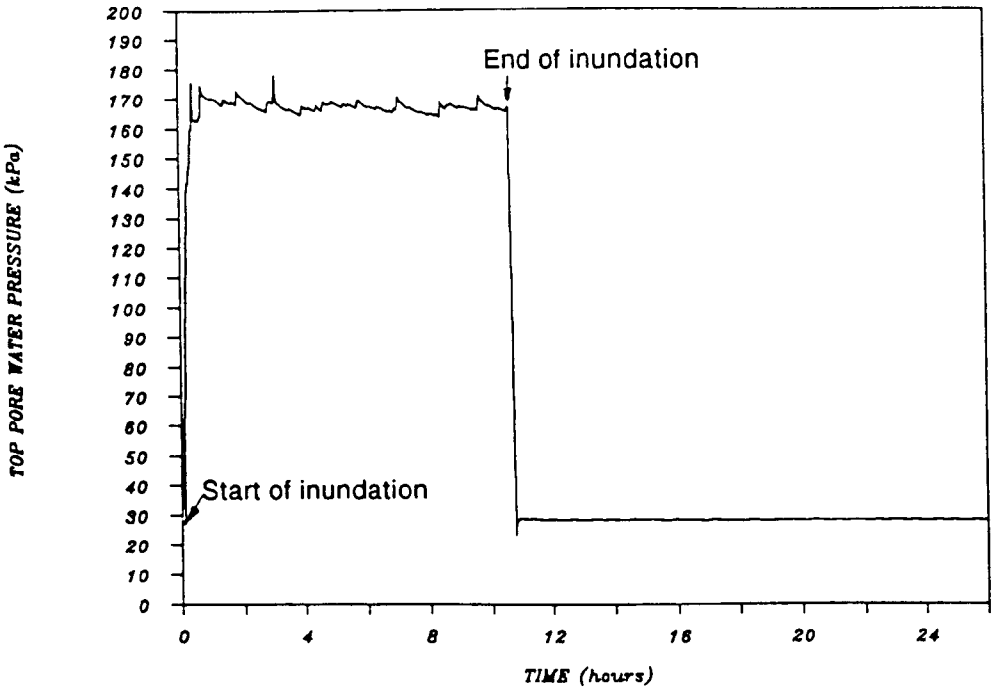

(c) Strain Development During Stage

Figure 7.16 – Typical Variation of Stress Strain and Top Pore Water Pressure During an Inundation Stage (Test B2)

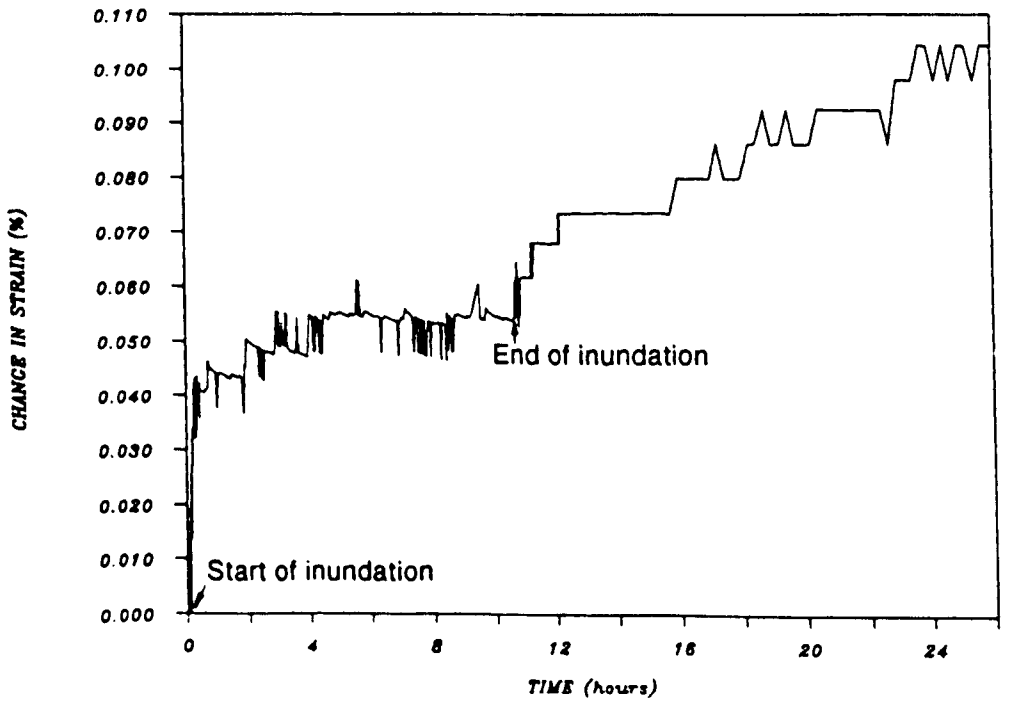

Figure 7.17 – Variation of Strain During Inundation Stage of Test B2 After Correction for Ceramic Deflection Due to Inundation Pressure

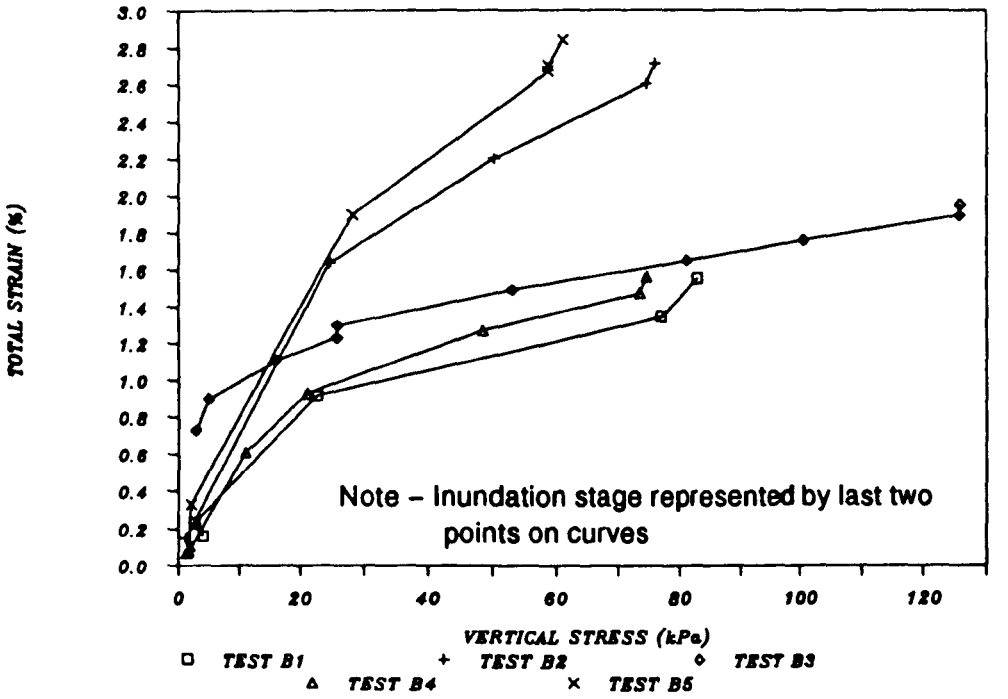

(a) Tests B1 to B5

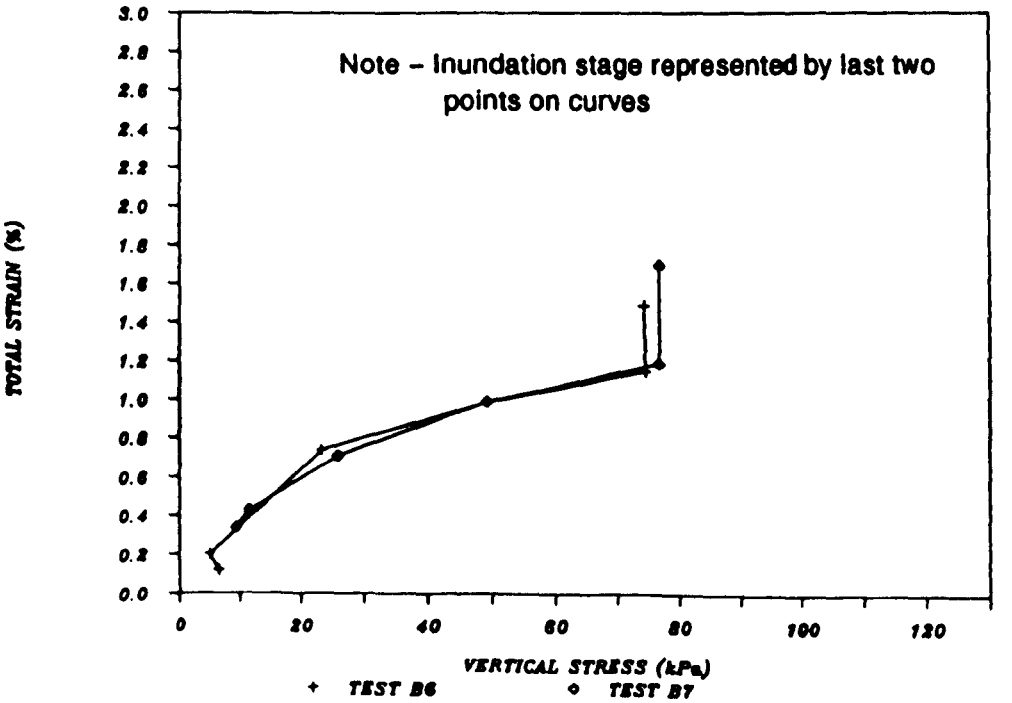

(b) Tests B6 and B7

Figure 7.18 – Effect of Inundation Stage on Strain–Stress Curve for Tests

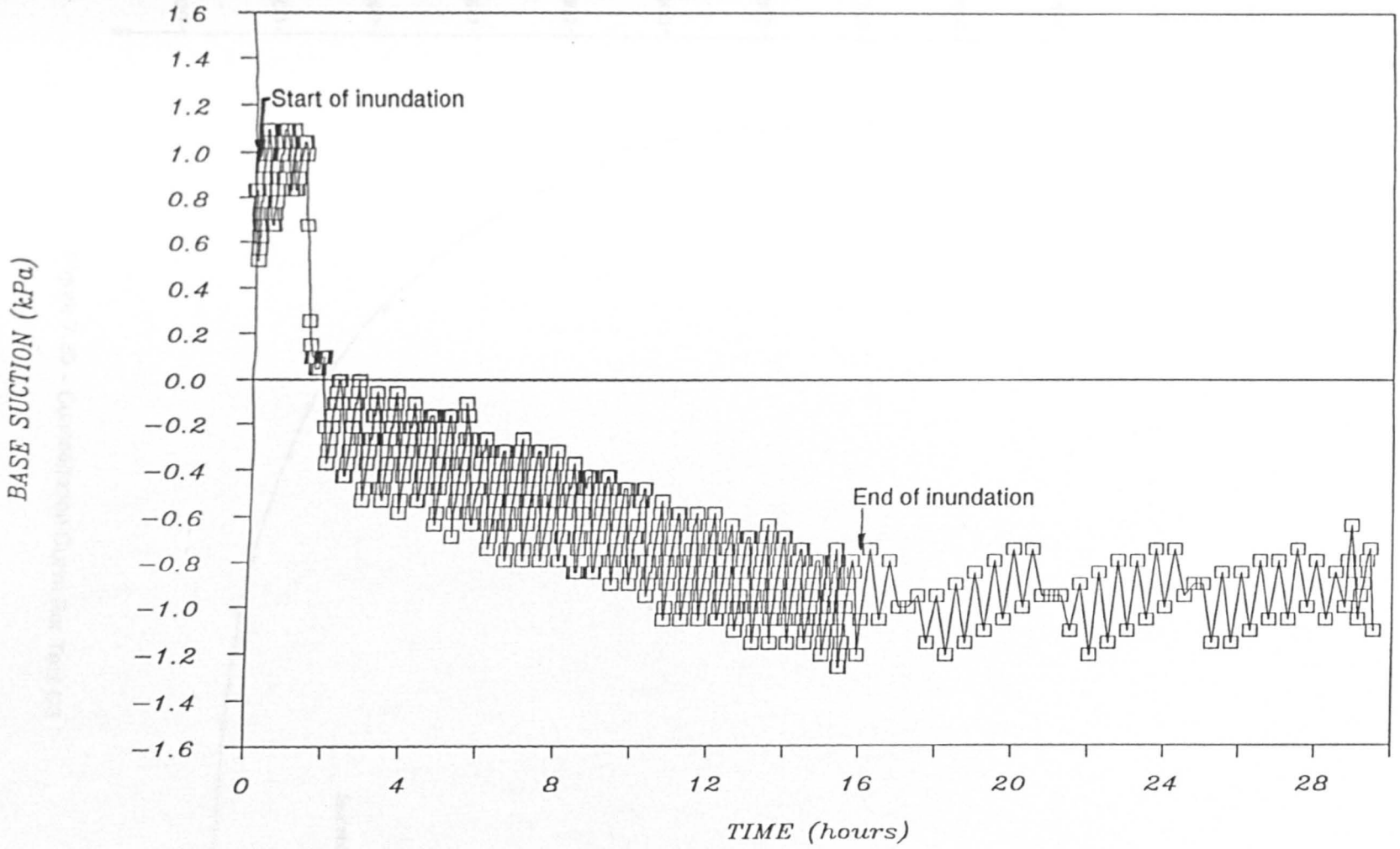

Figure 7.19 – Typical Variation of Base Suction During an Inundation Stage (Test B5)

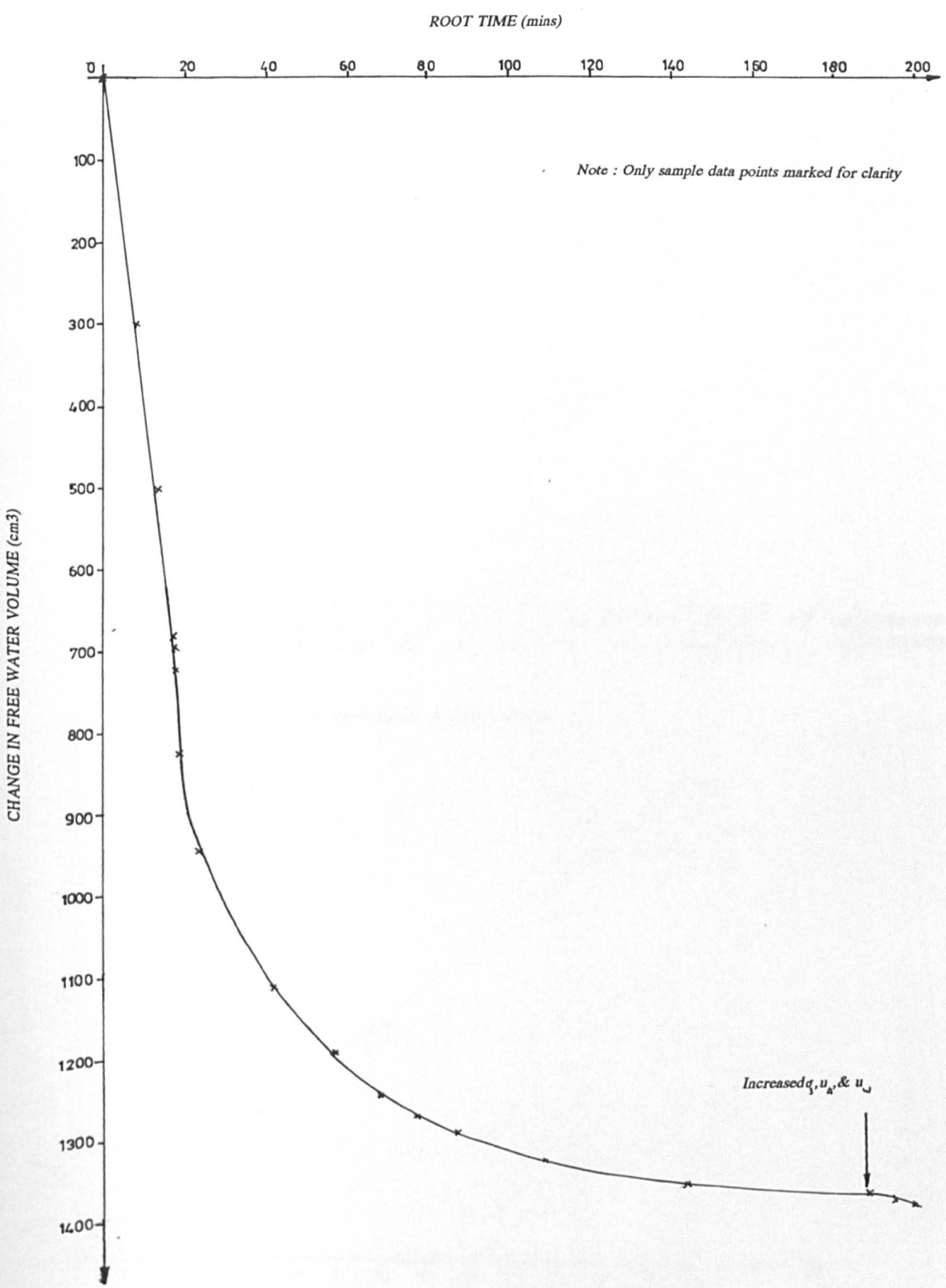

Figure 7.20 – Consolidation Curve For Test C3

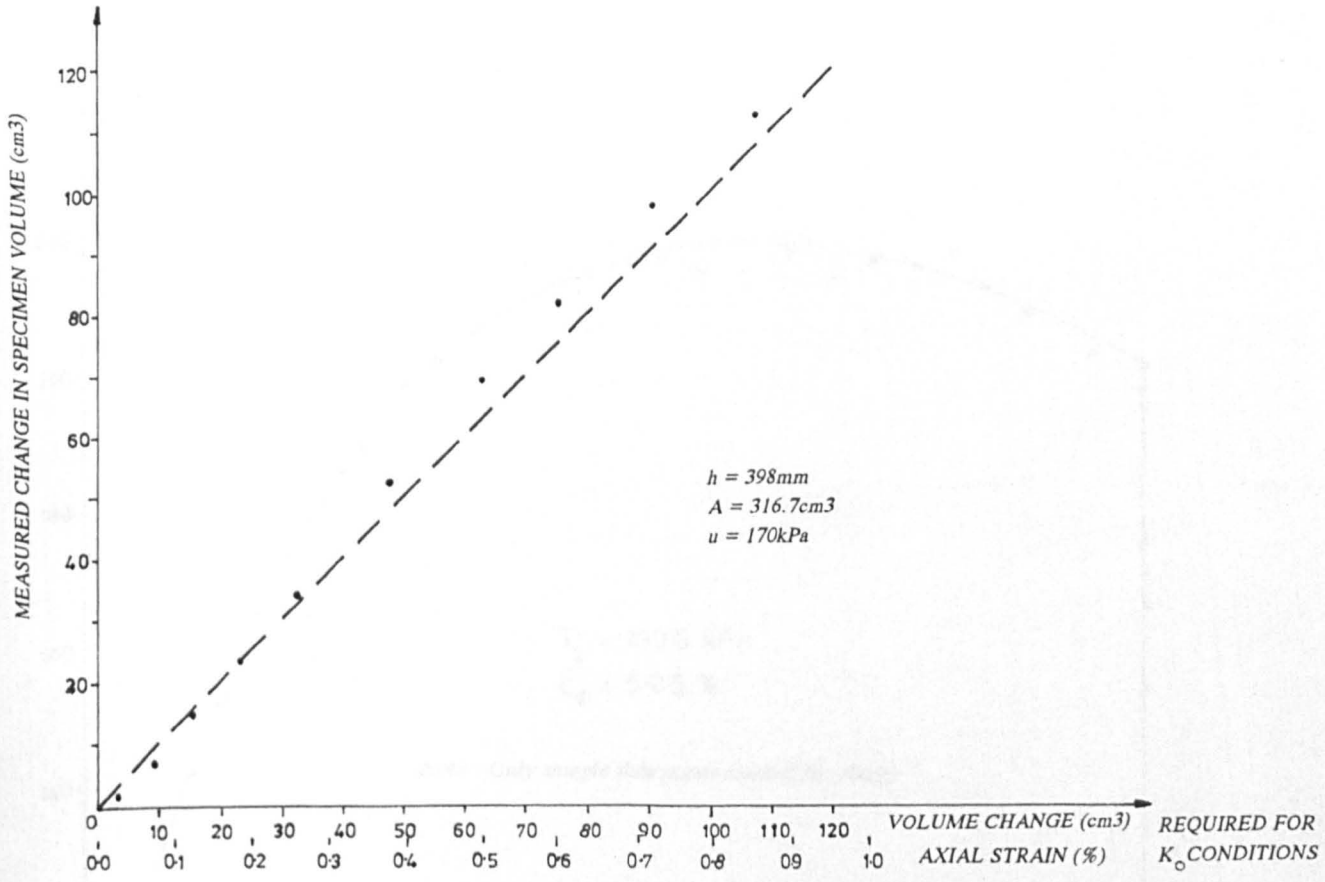

(a) Verification of K_o Conditions

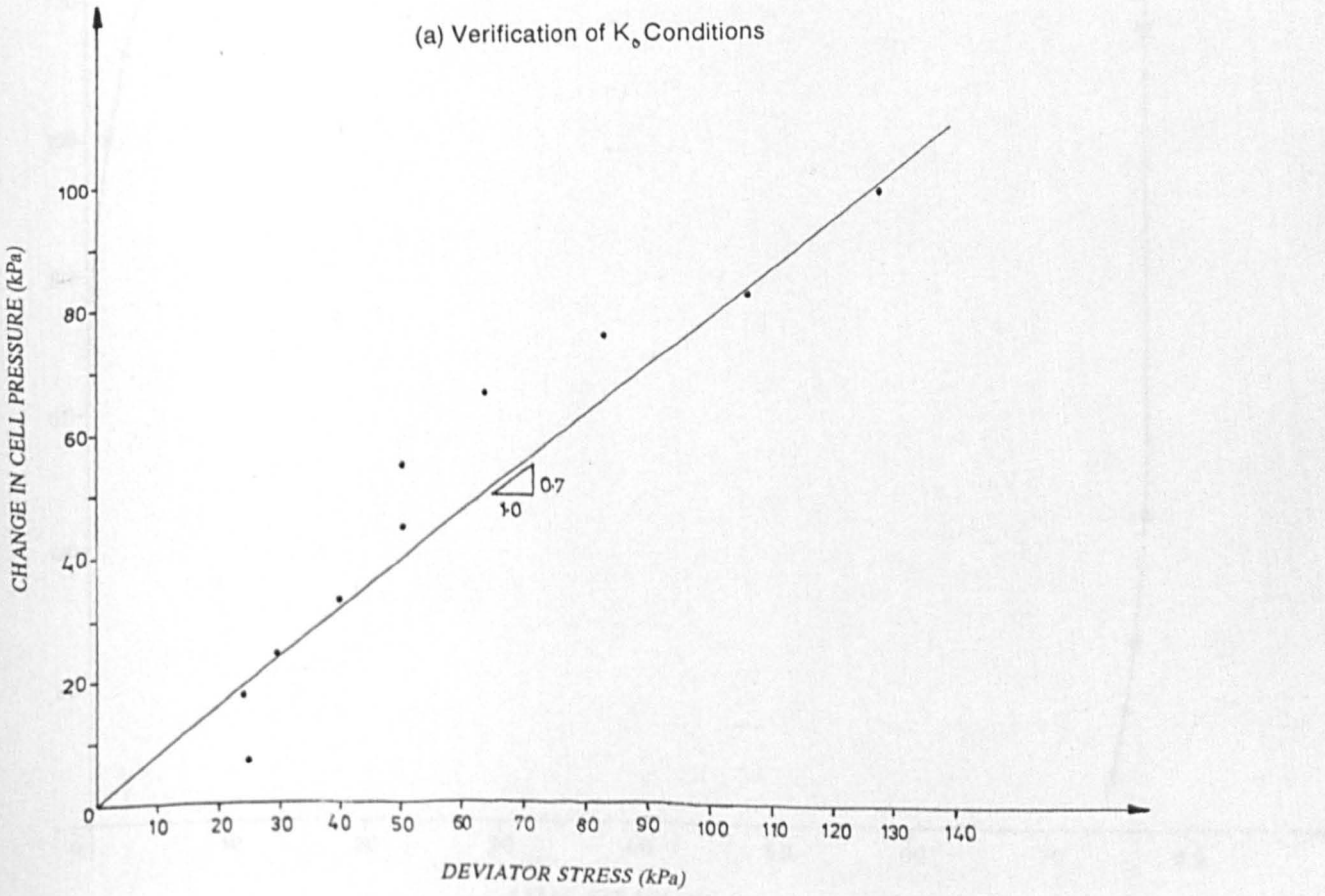

(b) Calculation of K_o

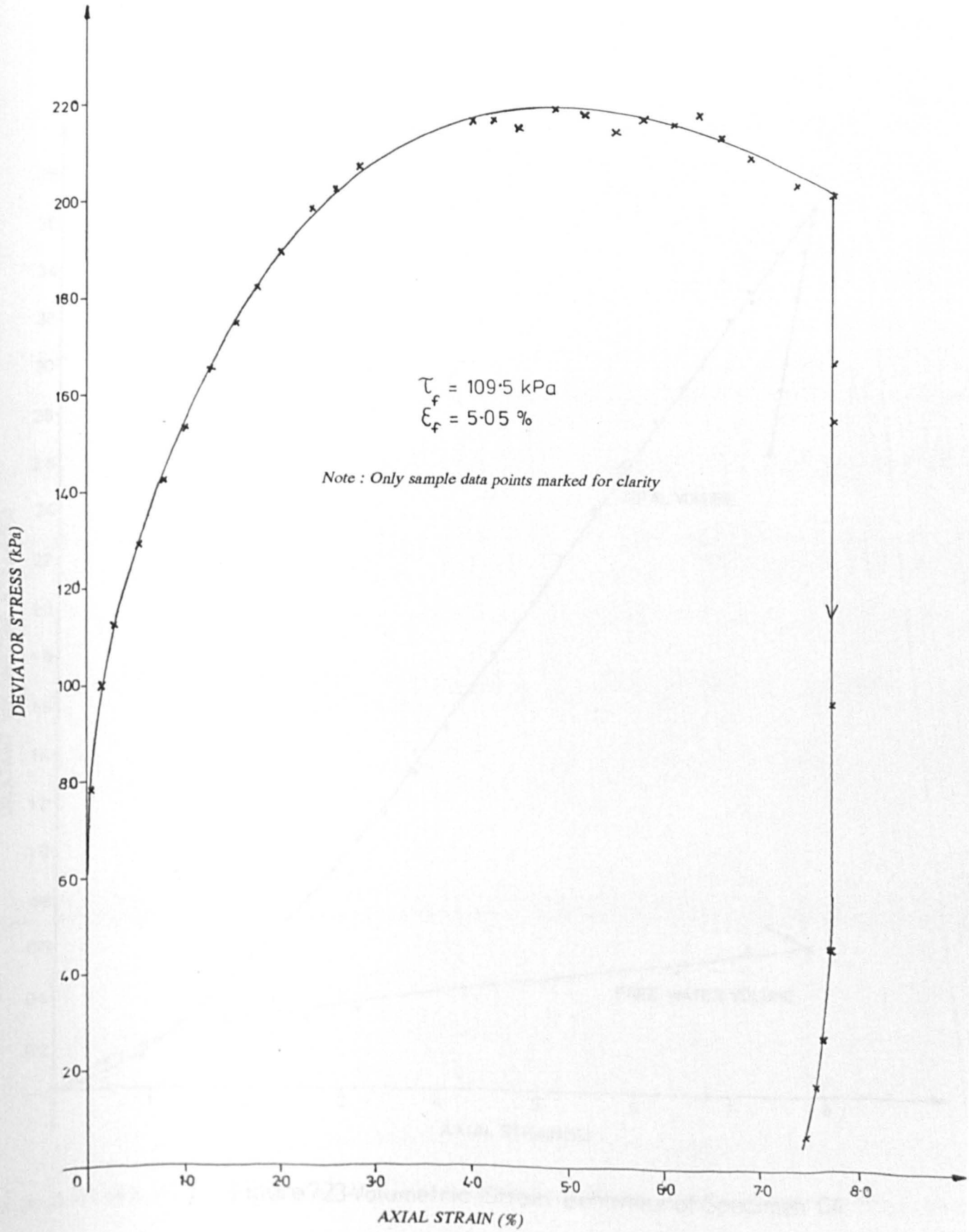

Figure 7.22 – Shear Stress–Strain Curve for Specimen C4

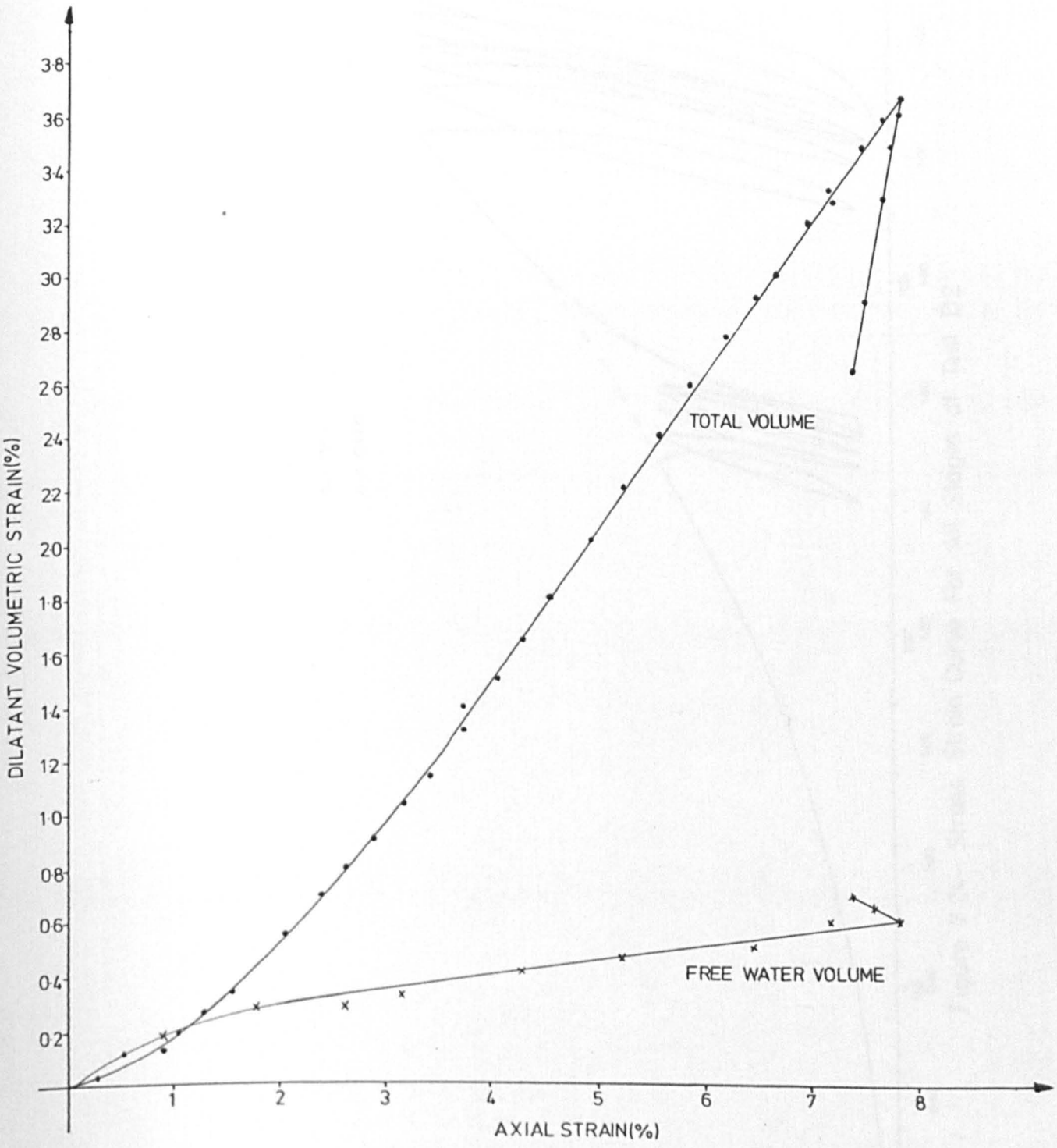

Figure 7·23-Volumetric Strain Behaviour of Specimen C4

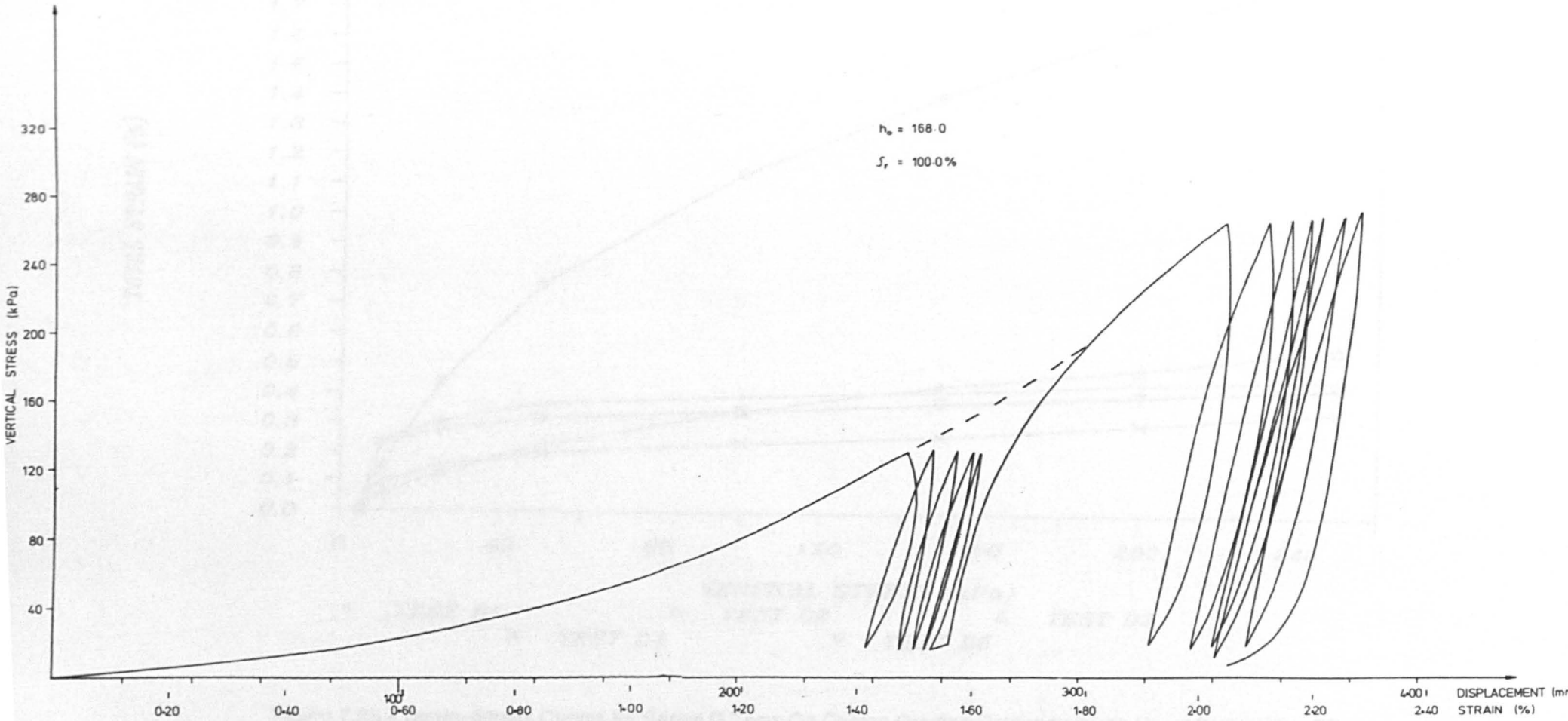

Figure 7·24- Stress Strain Curve For All Stages of Test D2

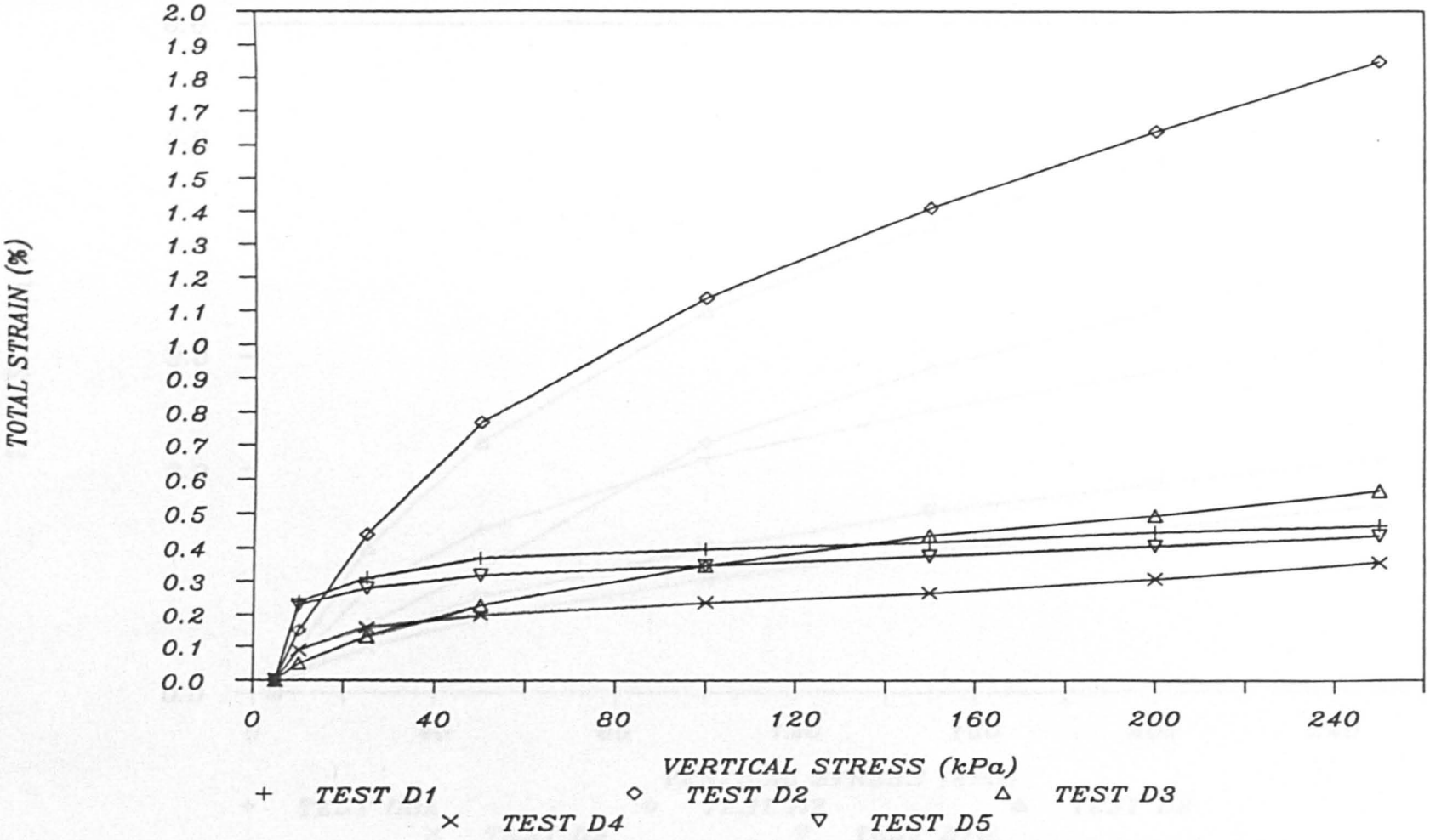

Figure 7.25 – Strain–Stress Curves for Series D Tests On Coarse Grading Compacted with Usual Compactive Effort

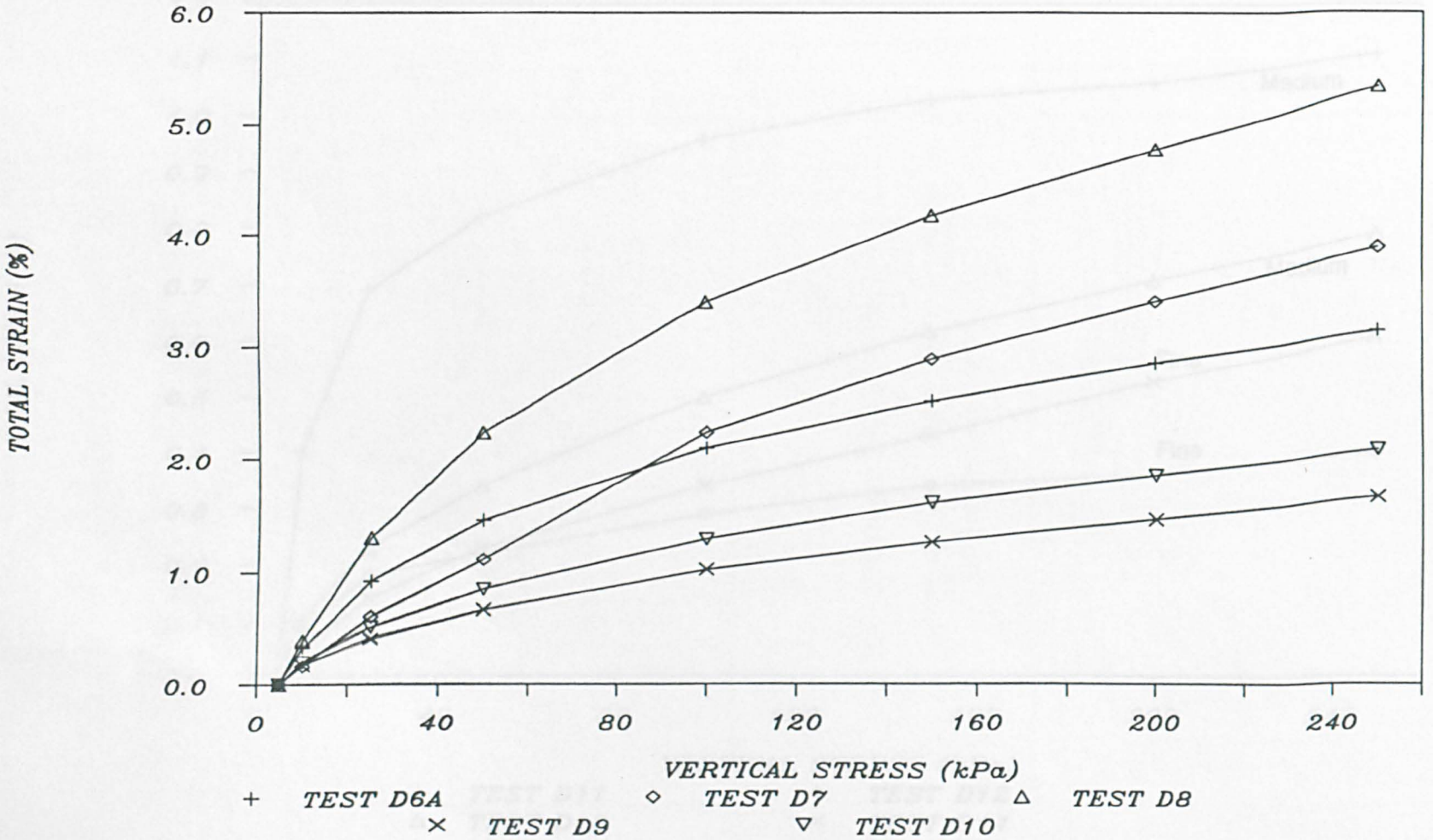

Figure 7.26 – Strain–Stress Curves for Series D Tests On Coarse Grading Compacted with Low Compactive Effort

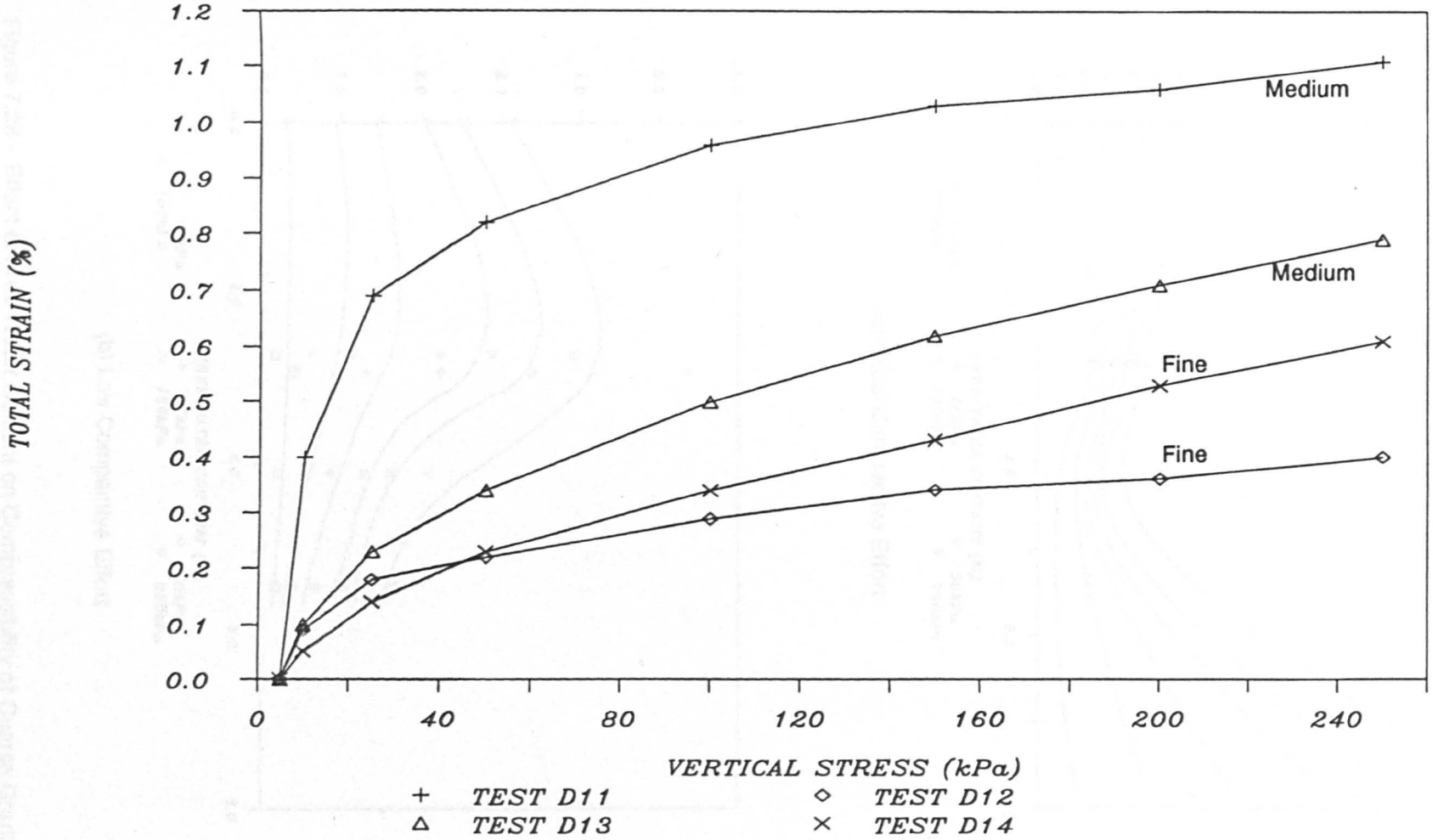

Figure 7.27 – Strain–Stress Curves for Series D Tests On Fine and Medium Gradings

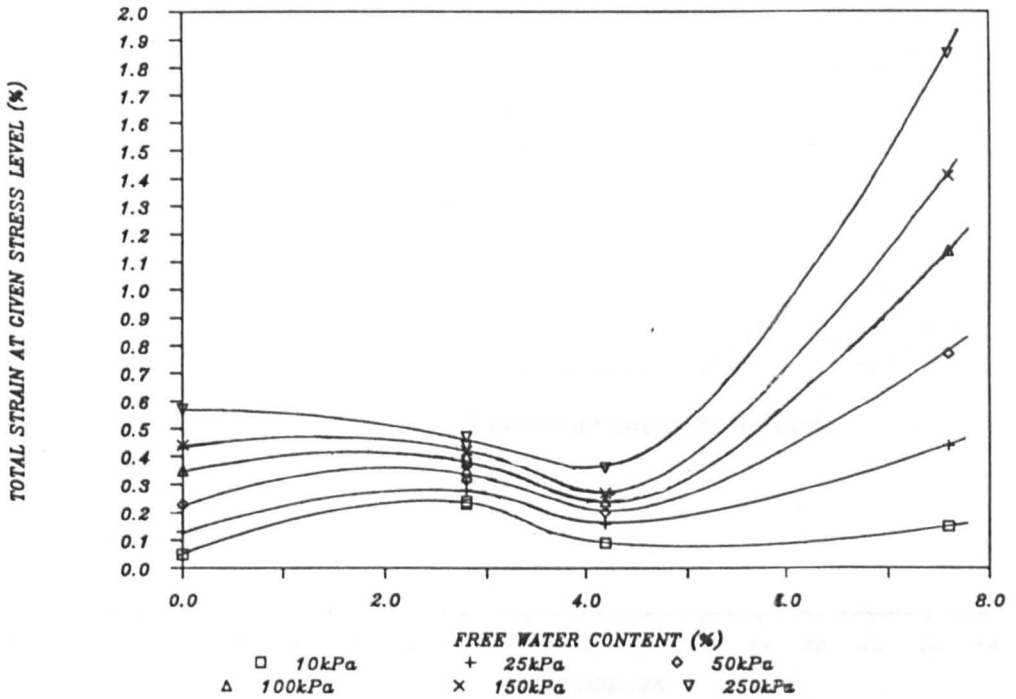

(a) Usual Compactive Effort

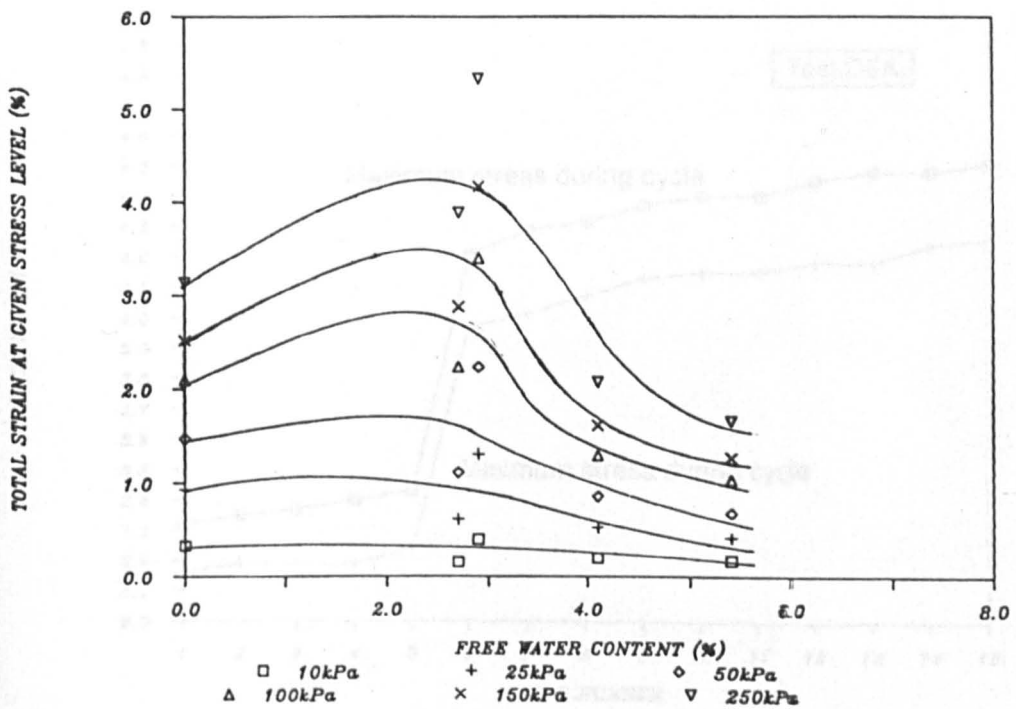

(b) Low Compactive Effort

Figure 7.28 – Effect of Free Water Content on Compressibility of Coarse Grading from Series D Tests

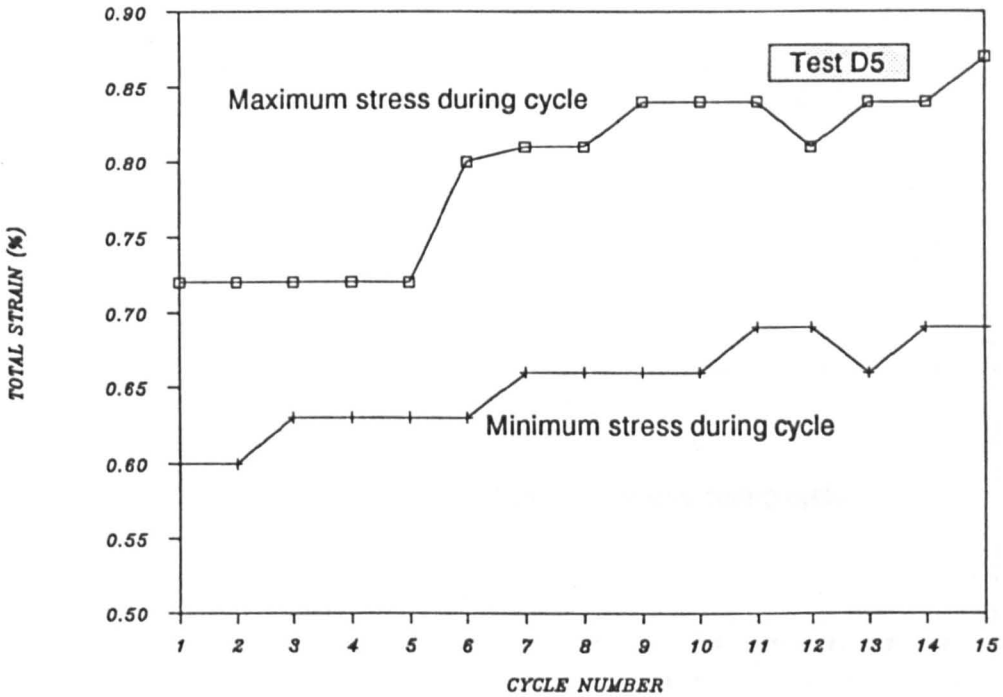

(a) Coarse Grading Compacted With Usual Effort

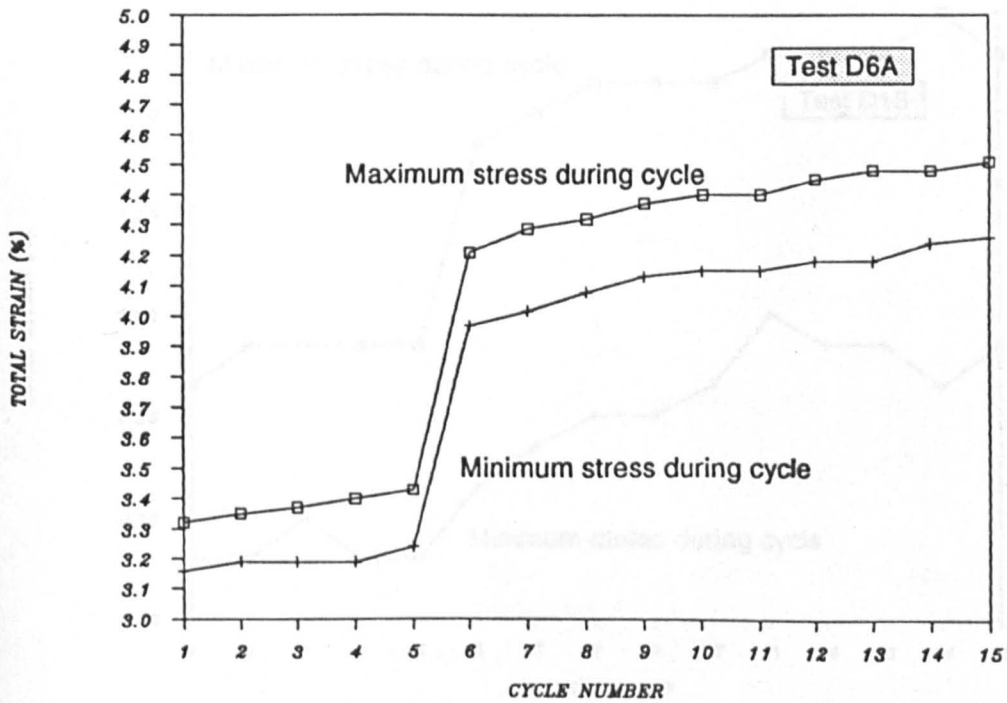

(b) Coarse Grading Compacted With Low Effort

Figure 7.29 – Effect of Grading and Compactive Effort on Strain Accumulation During Repeated Loading Stages of Series D Tests (continued overleaf)

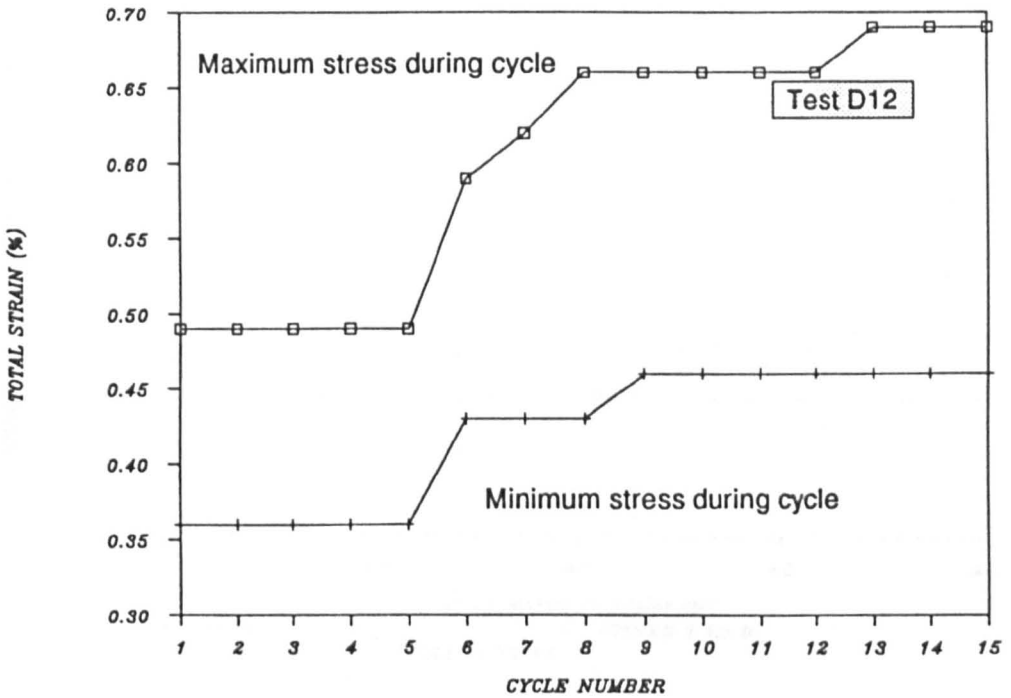

(c) Medium Grading Compacted With Usual Effort

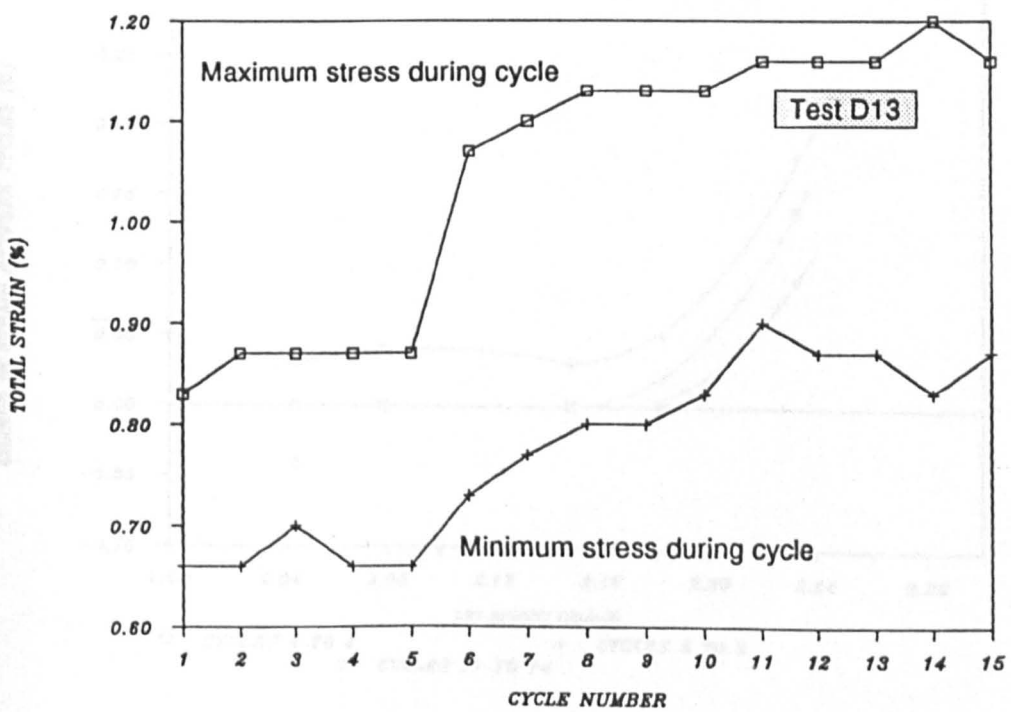

(d) Fine Grading Compacted With Usual Effort

Figure 7.29 – Effect of Grading and Compactive Effort on Strain Accumulation During Repeated Loading Stages of Series D Tests

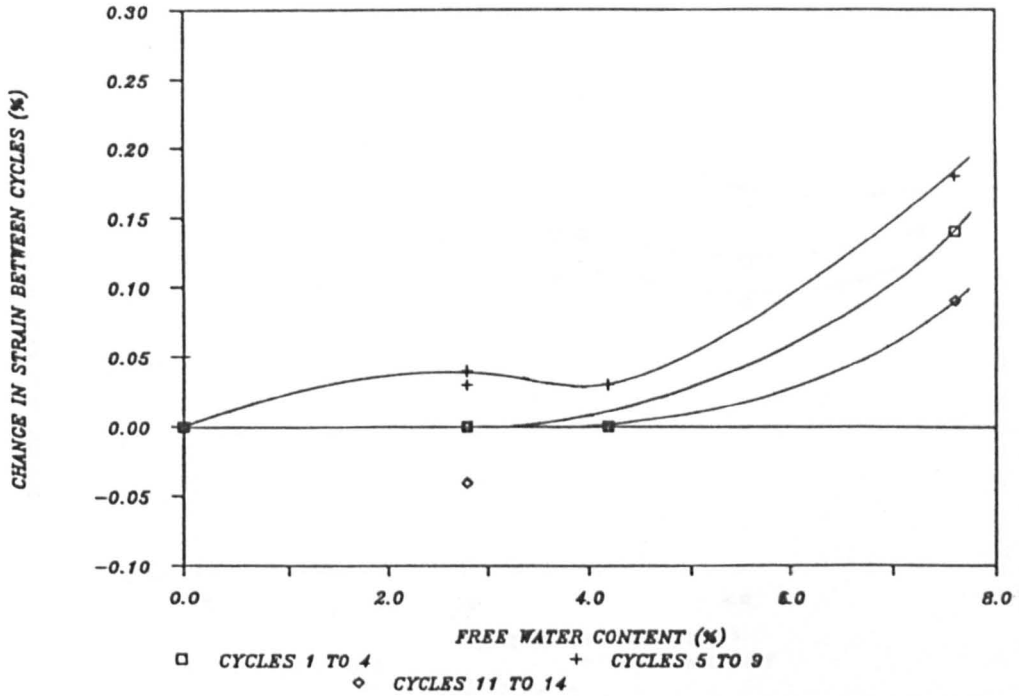

(a) Variation with Free Water Content

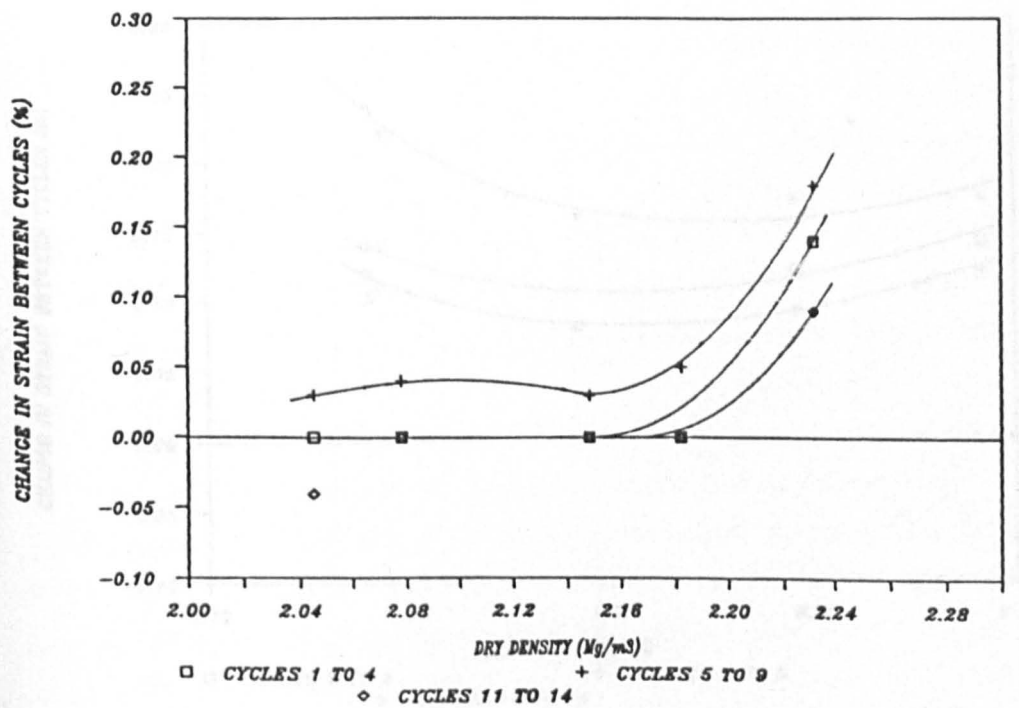

(b) Variation with Dry Density

Figure 7.30 – Effect of Free Water Content and Dry Density on Peak Strain Accumulation During Repeated Loading Stages of Series D Tests on Coarse Grading Compacted With Usual Compactive Effort

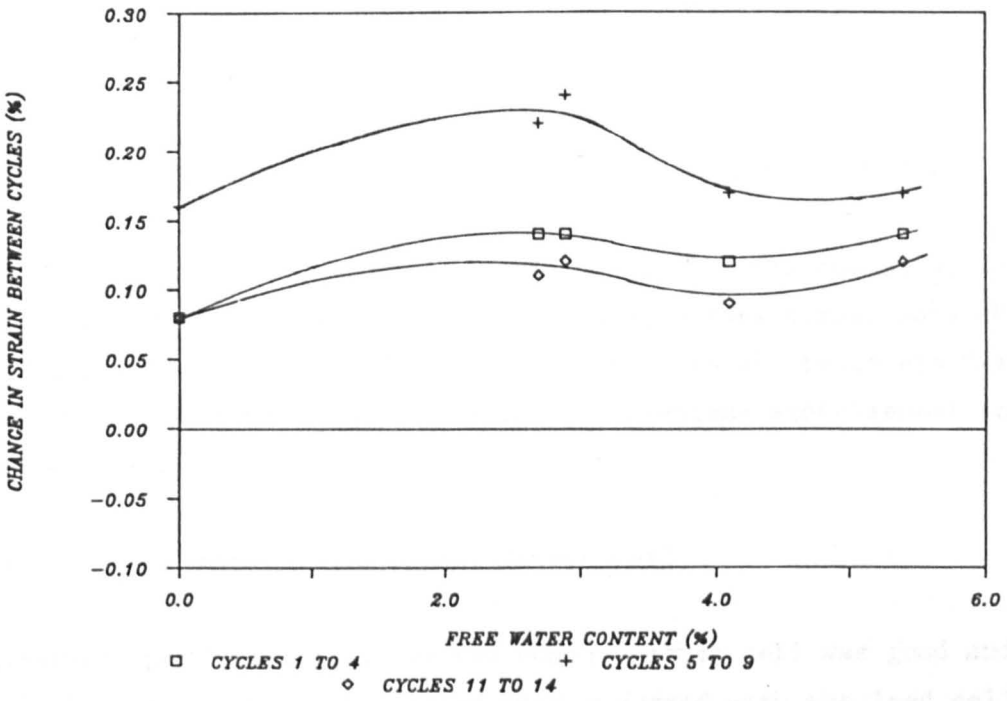

(a) Variation with Free Water Content

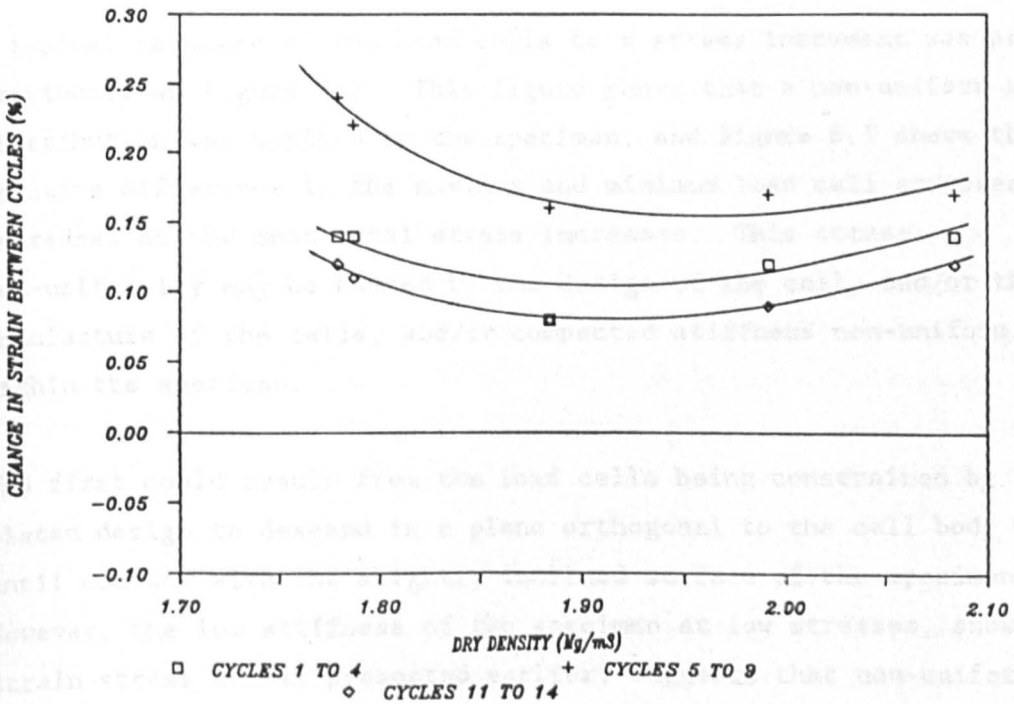

(b) Variation with Dry Density

Figure 7.31 – Effect of Free Water Content and Dry Density on Peak Strain Accumulation During Repeated Loading Stages of Series D Tests on Coarse Grading Compacted With Low Compactive Effort

CHAPTER 8

DISCUSSION OF RESULTS AND COMPARISON WITH OTHER WORK

This chapter commences with a discussion of the performance of the new consolidation cell used for Series A and B, before comparisons and conclusions regarding the behaviour observed in all tests are drawn. Where relevant comparisons are made with previous experimental and theoretical work.

8.1 Performance of New Consolidation Cell

In-service performance of the new consolidation cell was good and deviations from that anticipated only occurred with the load cells. The two deviations are discussed below.

8.1.1 Load Cell Response Characteristics

A typical response of the load cells to a stress increment was presented previously as Figure 7.1. This figure shows that a non-uniform stress distribution was applied to the specimen, and Figure 8.1 shows that the relative difference in the maximum and minimum load cell stresses decreases as the mean total stress increases. This stress non-uniformity may be caused by the design of the cell, and/or the manufacture of the cells, and/or compacted stiffness non-uniformity within the specimen.

The first could result from the load cells being constrained by the top platen design to descend in a plane orthogonal to the cell body wall until contact with the slightly inclined surface of the specimen. However, the low stiffness of the specimen at low stresses, shown by the strain-stress curves presented earlier, suggests that non-uniform compression and particle re-orientation across the specimen should quickly reduce any initial eccentricity. Figure 8.2 plots the ratio of

the peak difference in measured load cell stress to the ambient mean stress against the initial specimen tilt measured after compaction of the specimen. If the design is at fault one would expect the stress variation to increase with tilt. This is clearly not the case.

The possibility of a manufacturing induced feature centres on dimensional variations in the load cell bodies and/or recesses in the top platens predisposing a particular load cell to contact with the soil first. Examination of the frequency at which each load cell recorded the maximum or minimum load revealed an apparently random variation, and physical measurement of the load cell bodies and recesses showed no significant variations. Taken together, these observations suggest that the manufacturing was not at fault, although random variations in the orientation of the cells to the soil, and random insertion of the load cells into the recesses, could partially mask any such pre-disposition.

Hence, the third and most likely explanation is stiffness non-uniformity present within the particulate mass despite the attempt to apply a uniform compactive effort across the whole surface area of the soil. Random variations in particle arrangements would be expected to cause small stiffness variations and previous research by Brady and Kirk (1990) has implied such non-uniformity. In their work, variations in deflections of more than 20% of the mean deflection were measured at circumferential quarter points on a specimen subjected to a point load via a top platen free to tilt within limits imposed by the apparatus dimensions. Larger variations in stresses may have been necessary to cause these measured changes, but variations of up to 100% would be needed to give similar results to those found in the current work.

Based on the above, it is considered that at least part, and probably the majority, of the observed differences in load cell output are due to stiffness non-uniformity. The remainder must be attributed to the apparatus and test procedures although the causes are unclear.

8.1.2 Load Cell Stability

Comparison of the zero outputs from each load cell were made at the start and finish of each test, in order to verify that the bending stress imposed on the load cells by the non-uniform stress distribution was not having an undue effect. These comparisons showed that a small but significant zero-drift (typically less than 0.5 kPa) sometimes occurred. Such variations were inconsistent between tests and could not be related to atmospheric changes or any other variable. In view of this inconsistency, it was not possible to ascertain when the drifts occurred, and it was decided to use the mean zero output for each test for all stress calculations. Therefore, although the calibrated accuracy of the load cells in pure axial compression is typically 0.1 kPa, it is considered that the average stresses recorded in service should be taken to be accurate to 0.5 kPa only. The calibration factors are considered to be unaffected by the non-uniformity in stress distribution.

8.2 Water Volume Changes Due to Total Stress Changes

Test Series A employed water drained conditions in order to investigate the magnitude of water volumetric strains induced in coarse unsaturated soils due to an applied total stress change. Figure 8.3 shows a typical graph of water volume change against time for one stage of a test, with a load increment applied at time zero. It is apparent that very small volume changes are involved, and that the direction of flow is apparently inconsistent with what would be expected to occur as a result of consolidation. Comparison of the results with the measured variation of the base pore water pressure presented as Figure 8.3(b) shows that the curves are synchronised, implying that small changes in base pore water pressure lead to correspondingly small changes in volume. Subsequent calculations assuming the compressibility of water with 10% air (at 100 kPa) mixed in is 0.001 m^2/kN (Fredlund, 1976) and using the approximately known volume of the base chamber of the consolidation cell, showed that these observed changes were about 2 orders of

magnitude greater than expected based on the small fluctuations in water pressure. This suggests the soil is sensitive to small changes in suction, and that unless large water volume changes result from soil fabric changes then the small fluctuations in regulated pressure will mask these changes.

In addition to the above effect, it was noted that apparent water volume changes of less than 1 cm^3 occurred at a rate of between 0.01 and 0.05 cm^3/hr during many tests, and that these changes were always out of the cell even if the total applied stress decreased during that stage. A reasonable degree of correlation was found between these measurements and those of the diffused air flushed out of the consolidation cell periodically, and the rates of movement were of the same order of magnitude as those for air diffusion recorded by Fredlund (1973). It thus appears that air diffusion also masked any "real" water volume changes.

As a result of the above two factors, the possibility of small leakages, and the absence of any large (>3 cm^3) volume changes during any test it was concluded that water volume changes as a result of total stress changes were not a phenomenon of any great significance in this soil provided the soil was initially at equilibrium. Hence results for Series A and B should be very similar. Further it was reluctantly accepted that the current apparatus could not be used for reliable measurement of small volume changes (<3 cm^3) despite the nominal accuracy of the volume change units unless stringent tests were performed to quantify diffusion and leakages.

8.3 Suction Determinations

8.3.1 Repeatability of Data

Figures 7.6 and 7.7 summarised the suction measurements made during series A and B. The graphs showed a large degree of scatter for the coarse grading, but gave good repeatability for the fine grading.

This difference in repeatability is attributed to increasingly random variations in the soil fabric formed at the ends of the different specimens as the coarseness of the soil increases. By the nature of the measurement system, the equilibrium suction is that which results uniformly at each particle-ceramic contact following redistribution of water via the saturated ceramic. Figure 8.4(a) shows conceptually that the initial compaction induced suctions between the ceramic and particles 1 and 2 respectively would be different. The pore pressure behind the ceramic would have to be different at each point of contact for this state to be maintained and hence water flows between the particles and ceramic until an equilibrium measured pore water pressure, u_{wms} is achieved and the suctions at particles 1 and 2 are the same (Figure 8.4b). A preponderence of coarse particles in contact with the ceramic would effectively reduce the equilibrium suction as the effect of any small flow of water to/from them would affect the resultant suction less than if the same small flow affected a smaller particle. In a well graded soil the number of significantly different particle size distributions at the ceramic interface is greater than for a more uniform grading.

The importance of the scatter in the measured suctions must not be overstated though. As shown in Figure 8.4b the local redistribution of water at the ends of the specimens enforced by the measurement system is unlikely to affect the internal suction equilibrium state unless the suctions are continuous through the particles themselves. This is unlikely as the free availability of water would destroy any particle absorption suction. Given the localised nature of the internal suctions then, and the increased probability of particular structural arrangements of grains repeating as the soil volume increases, it may be deduced that a scatter of suction measurements at any particular location (in this case the ends) would not represent the scatter of the average suction condition for the whole specimen. The true reflection of field conditions in the laboratory thus requires an adequate soil volume to be tested, a point which is covered in section 8.4.

8.3.2 Comparison Between Suction Measurements for Coarse and Fine Gradings

Having thus considered the scatter of the data, the similarity of the suctions measured in the coarse and fine gradings merits discussion. From the work by Croney and Coleman reproduced in summary previously as Figure 2.3, the suctions were expected to increase as the water content decreased, and to increase as the coarseness of the soil decreased for any given water content and density. The former is discernible despite the data scatter, but the latter has not been conclusively found. The similarity may be caused by the congregation of fines at particle contacts (see Figure 8.5) with the suctions between these finer particles (which are common to the fine and coarse gradings) dominating the measured equilibrium suctions (be they due to a continuous or lenticular water phase). Alternatively, an equilibrium distribution of initially lenticular water between the numerous contacts resulting in more water around the finer particles than the coarser particles could explain the data.

In order to investigate the latter, use will be made of equation 8.1, which was derived by Haines (1927) for a lenticular water distribution (see Figure 2.4) between two identically sized spherical particles of radius r.

$$u_A - u_w = T \left(\frac{1}{r_1} - \frac{1}{r_2} \right) \quad \text{..... equation 8.1}$$

where T = surface tension force per unit length of the contractile skin
= 74×10^{-5} N/m

r_1, r_2 = radii of the contractile skin in each of its two principal directions

and u_A = zero

From geometry, $r_1 = r_2^2/2\ (r-r_2)$, and hence equation 8-1 reduces to:

$$u_A - u_w = \frac{T\ (2r-3r_2)}{r_2^2} \qquad \text{..... equation 8.2}$$

Table 8.1 presents the suctions calculated using the above equation for particles ranging in size from 0.2 mm to 20 mm, with r/r_2 ratios of 2 and 5. As may be seen, a water distribution resulting in lower r/r_2 values for the finer particles (ie proportionately more water at the fine particle contacts) could explain the similarity in suctions for the fine and coarse gradings. Within a low degree of saturation particulate mass, the lenticular water distribution pattern will be a random one initiated by the degree of mixing and compaction applied, and there exists no reliable method to estimate the relative influence of the coarse and fine particles at present. At the measurement points however, a continuous water phase is enforced and the initially random lenticular water distributions would redistribute to increase the proportion of water at high suction points of contact, which would be more likely to involve fine particles. Hence the conditions required for similar measured suctions in the fine and coarse gradings would be approached at least, to an extent dependent upon the range and frequency of particle sizes in contact with the ceramic, and the initial water content.

The prediction of the range of sizes of particles in contact with the ceramic, and their relative frequencies, could be attempted using a statistical approach similar to that advocated by Marsal (1973). However, the standard deviations of any predicted distribution would be expected to be relatively large, and the accuracy of such an attempt could not be assessed within the limits of the current work. In the absence of a reliable analytical technique but based in part upon the work of Marsal (1973), it is considered that, for the coarse grading, few particles of diameter greater than about 20 mm would be in contact with the ceramic, but that the frequency of contacts would then rapidly increase as the particle size decreases to some peak, before the frequency would decrease once again but at a slower rate as the particle

size decreases further still and these finest particles "stick" on the surface of the coarser particles . The frequency peak may correspond to a particle size in the range 0.5 mm to 5 mm, given the flattening of the grading curve. For the fine grading, a flatter frequency distribution would be expected with a peak corresponding to a particle size of less than 0.5 mm probably. Figure 8.6 idealises this largely intuitive picture, which it must be stressed is not based upon experimental data.

The effect of the initial water content on the suctions needs to be considered within this intuitive framework. Based on Tables 6.2 and 6.3, Table 8.2 compares the initial compacted state of the fine and coarse gradings for the given water contents. As may be seen, the coarse grading achieves lower void ratios and air void ratios, but higher degrees of saturation. The latter is of primary importance, and it states that proportionately more water is present in the total void spaces of the coarse grading.

For the "average" r/r_2 ratio to decrease between the coarse and fine gradings, the degree of saturation should decrease at a slower rate than the decrease in the "average" particle size. This "average" particle size should reflect the range and frequency of particle contacts, which intuitively may fall from maybe 2 mm (coarse grading) to 0.5 mm (fine grading). In contrast, the degree of saturation only increased by between 100% and 150% from the fine to coarse gradings suggesting that, if anything, the "average" r/r_2 ratio increased from the coarse to fine gradings. The tendency for a small redistribution of water via the ceramic would mitigate this increase as previously noted, but not sufficiently for the similarity in suction measurements between the fine and coarse gradings to be due wholly to the equilibrium water distribution pattern. The coarser particles must have a significant influence, in order to account for some of this suction scatter, but the similarity is likely to be caused predominantly by the congregation of fines at the ceramic face.

8.3.3 Vertical Suction-Water Content Profile

The suction-water content curves for the top and base of the specimens shown in Figures 7.6 and 7.7 are not separated by a constant suction value equal to $-h\gamma_w$ (where h = vertical separation) as is often assumed in highway design based on simple capillary theory. Rather, the difference is considerably greater, implying the water phase is not continuous through the specimens, or the simple capillary theory is erroneous, or the suctions measured incorporate also an element of the aggregate suction characteristics due to its incomplete saturation. Fredlund and Rahardjo (1987) present matrix suction values for a glacial till at three depths up to 0.76 m below surface (see Figure 8.7) which shows a similar non-linear variation of suction, which suggests the capillary theory is incorrect as the other explanations would not hold true for this predominantly clay soil. Consequently it is considered that care should be taken in applying the simple capillary theory until further research has been conducted.

8.4 Comparison of Compressibility Results from Series A, B and D

8.4.1 Repeatability of Data

Similar forms of strain-stress curves were obtained for all tests, and inspection of figures 7.14, 7.15 and 7.28 allows the repeatability of the data to be quickly assessed by examining the data for deviations from the average.

Considering the series A and B tests on the coarse grading first (Figure 7.14) tests B6 and B7 at a free water content of 1.1% show excellent agreement, and good agreement exists between tests A7 and A8 (4.9% and 5.2% free water content). The agreement between A2 and B3 (3.9% and 4.1%) is less good at low stresses, but improves as the applied stress increases. The only clear exceptions to the good repeatability otherwise obtained is test B5 (free water content 2.3%), which exhibits very low stiffness at low stresses. The cause of this discrepancy is unclear, specimen B5 not being unusual in any other manner.

The series D tests on the coarse grading (Figure 7.28) showed excellent repeatability when subject to the "standard" compactive effort (tests D1 and D5), and reasonably good repeatability when lightly compacted (tests D7 and D8) despite the large strains involved and the greater relative influences of the soil fabric on the stiffness of such lightly compacted specimens.

The results for the fine grading in Figure 7.15 show excellent repeatability when similar specimens are compared (tests A5 and A10, free water content 4.1%). Further, as shown by comparison of these two tests with the slightly under-compacted test A1 (free water content 4.2%; void ratio 0.48 compared to 0.42 and 0.41 for A5 and A10), small changes in compactive effort do not result in highly significant changes in compressibility of this grading.

From the above comments, it is considered good repeatability was achieved within each piece of apparatus and for each grading. This repeatability supports the assertion made earlier that series A and B tests should be comparable as negligible water drainage occurred during series A tests (section 8.2), and that the scatter of measured suctions would not significantly affect the compressibility as the measured and "average" internal suction conditions would have different standard deviations (section 8.3.1). Further the judgement to use a slightly smaller than usual height to maximum particle size ratio for the new consolidation cell is justified.

8.4.2 Effect of Compaction Water Content and Dry Density on Compressibility of the Coarse Grading for Constant Compactive Effort

Having established the repeatability of the data, the measured variation of compressibility may be confidently discussed. Figure 7.14 for the series A and B tests shows a peak in compressibility at a free water content of about 3.0%, with approximately symmetric decreases either side to the limiting free water contents used of 1.1% and 5.2%. In contrast, the initial dry density of the specimens increased

approximately linearly from 1.93 Mg/m^3 to 2.20 Mg/m^3 over the same free water content range, implying that compressibility is a function of both the compaction water content and dry density. The compressibility contours shown do not close up significantly, indicating low stiffness at very low stresses and an approximately constant and larger stiffness at stresses above about 25 kPa.

The results for series D tests at the same compactive effort (Figure 7.28a) show a similar trend at equivalent stresses, but with a peak at a free water content of about 2%, a minimum at about 3.5%, and a second much larger increase in the compressibility at water contents above this value to a free water content of 7.6%. The low peak at a water content of 2% disappears progressively as the stress level increases, and the compressibility contours show only marginal closing up as the stress level increases beyond a stress of about 25 kPa.

The similar behaviour noted in both pieces of apparatus is attributed to the suction stresses within the soil mass, and possibly an increased intergranular friction coefficient at very low water contents. Starting at a free water content of about 1%, the high localised suctions at particle contacts with a congregation of fines, together with some possibly dry surface contact points increasing the average friction coefficient between the particles, are believed to counteract the low dry density of the mass sufficiently for the soil to have a low compressibility. As the compaction water content increases, the localised suction stresses decrease the internal stability of the mass at a greater rate than the increasing dry density tends to increase this stability. Hence the compressibility increases. As the water content increases further still beyond a critical value of between 2% and 3%, which approximately corresponds to the distinct flattening of the suction-water content relation shown in Figures 7.6 a and 7.7, the increasing dry density increasingly dominates and the compressibility decreases once more.

However, at a free water content of about 4% to 5%, the compressibility once more increases, but this time quite rapidly, despite the water content being about 1.5% to 2.5% below optimum. It is believed this increased compressibility is a function of the formation of a near saturated layer at the base of the material, and the inducement of small reductions in effective stress in the layer. The excess pore pressures would be dissipated internally and upwards due to the low permeability of the base ceramics. Evidence for the progressive formation of this saturated layer was presented previously as Figure 7.11, which plotted the variations of water content between the top and bottom of the specimen, and showed an increased gradient above a free water content of about 4%.

The above explanation would apply in particular at low vertical stresses. As the stress level increases though, the influences of the suctions would be expected to decrease progressively, whilst the influence of the near saturated layer would not be greatly affected. This behaviour pattern has been shown by the series D tests at stresses in excess of 100 kPa, and supports the physical mechanisms suggested.

8.4.3 Effect of Compactive Effort on Compressibility of the Coarse Grading

The results of the series D tests employing a low compactive effort were presented in terms of compressibility in Figure 7.28 b . With the exception of the reducing influence of suction stresses at higher stress levels the same behavioural trends noted and explained above for the higher compactive effort have been found. Although the range of water contents used precluded the large increase in compressibility beyond a free water content of 5.4% from being proven the similarity in trends does appear to include a minimum at a free water content of about 5%. The absence of the reducing influence of the suctions may be attributed to the higher suctions likely to be present within these specimens due to the lower degrees of saturation. Additionally, the lower number of interparticle contacts will serve to reduce the influence of any increased coefficient of friction at low water contents.

The variation of compactive effort may also be used to identify the relative influences of the dry density and free water content individually. Considering the series A and B tests, comparison of tests B2 and B4 with tests A6 and B1, which all have similar dry densities but different water contents, it is apparent that the compressibilities of the former (free water contents of 4.6% and 4.1%) are greater than the latter (2.0% and 1.6%) due to the lower suctions. Similarly, specimen B3 (free water content 4.1%) was less compressible than specimen B4 (4.1%) due to its higher dry density. Similar observations could be made from the series D tests.

8.4.4 Effect of Grading on Compressibility

Comparison of the series A and B test results for the coarse and fine gradings (Figures 7.14 and 7.15) shows that the compressibility trends of both are similar, with peak axial strains of about 1.5% and 1.7% respectively at a stress of 50 kPa. This similarity exists despite the higher dry density, relative density and broader grading of the coarse grading, all of which would be expected to decrease the compressibility of a dry material. It is suggested that the higher suction stresses developed internally within the fine grading may explain the results by virtue of their stiffening influence.

Similarly, evidence for the influence of the suctions on the fine and medium gradings comes from series D tests D6A (coarse grading, dry) and D11 (medium grading, dry) and D11 (medium grading, free water content 2.8%), and tests D8 (coarse grading, free water content 2.9%) and D14 (fine gradings, free water water content 4.3%), which were compacted to dry densities of about 1.86 Mg/m^3 and 1.77 Mg/m^3, respectively. The compressibility of the coarse grading was greatest in each case. Further, the higher water content specimen of each pair of tests on the fine and medium gradings, exhibited a higher compressibility despite the higher dry density.

8.4.5 Comparison of Stress and Strain Controlled Compression Tests

The similarity of the compressibility variations between the stress controlled (series A and B) and strain controlled (series D) compression tests has been noted above in section 8.4.3. The correspondence of the two types of test in terms of the magnitude of strains at any given stress level may be verified if the "immediate" and time dependent strain components of the series A and B tests can be separated. This has been attempted using the incremental stress-strain curves for each stage of every test, as typified by Figure 7.3. The incremental immediate strain component has been taken to be equal to the strain corresponding to the marked change in gradient of the graph, as the stress increment was usually applied within 2 minutes. In some cases, the change in gradient was less clear as the stress increment was applied over a period of up to 5 minutes, and the immediate strain was estimated by fitting two straight lines through the data as shown in Figure 8.8

Figures 8.9 and 8.10 present the immediate strain-stress curves, Table 8.3 summarises the immediate compressibility data, and Figure 8.11 represents the compressibility data graphically. Examination of the curves shows that repeatable compressibility results were obtained within the same limits noted above for the total strain-stress curves. Comparison of the series D data with the "immediate" compressibility data obtained from series A and B (Figure 8.11 shows that although the "immediate" strains from series A and B have been significantly reduced compared with the total strains at any given stress level, they are still approximately twice as large as the strains recorded during the strain controlled tests of series D. This is attributed to the time scale associated with the "immediate" strains, which was between 2 and 5 minutes. For example, points 1 to 6 on Figure 8.8 (Figure 7.3 reproduced and annotated) chart an apparently approximate linear rate of strain development due to what is clearly a non-linear rate of stress application when it is appreciated that each of these data points was taken at 10 second intervals. The "immediate" strain component equals

0.08% (1.60% to 1.68%) when estimated in accordance with the method noted above, but this component includes an element of time dependent movement as shown by the strain between points 3 and 4,and 5 and 6.

A better method of estimating the "immediate" component would have been to take the initial gradient of the incremental stress-strain curve and extrapolate it to the intended final stress level, if constant stress increments had been applied at a very similar rate. This not being the case generally, it may be approximiately applied to Figure 8.8 though. If so applied the "immediate" strain is reduced by about 30%, and data collection at a rate in excess of every 10 seconds would probably reduce this value further still. Hence the initial apparent discrepancy between the two types of test is explainable and the data as a whole presents a consistent picture.

8.4.6 Magnitude of Immediate and Time Dependent Strain Components

The above discussion centred essentially on the separation of the "instantaneous" strains that occur as soon as a stress increment is instantly applied, from the "immediate" strains that occur over the several minutes when the stress increment is being applied. From the current data, the latter is made up of about 50% of the "instantaneous" strains that would have occurred if the full increment were applied instantly, and 50% of short-term time dependent strains. When analysing a physical problem, it is necessary to know the time scale over which the material will be stressed, and hence which compressibility relation to apply. Usually, only two components are identified, they being the immediate and time dependent components, but the time scale over which the "immediate" component is determined is often vague. For example, Brady and Kirk (1990) state that insignificant time dependent strains were recorded in their tests on limestone aggregate when compacted dry of optimum, this component apparently being taken to start "a few minutes" after the load increment was applied.

The data obtained from this work has been investigated over three timsescales:

(i) instant strains, determined from the strain controlled tests

(ii) immediate strains measured as detailed above, over a timescale of 2 to 5 minutes from stress application

(iii) time dependent strains that occur after the first 2 to 5 minutes elapsed

The relation between timescales (i) and (ii) has been dealt with above for the coarse grading, and insufficient data has been obtained for a similar comparison for the fine and medium gradings. The relation between timescales (ii) and (iii) is discussed below for the coarse and fine grading on the basis of the measured ratio of the incremental immediate strain to the total incremental strain for each stage of the series A and B tests.

Figure 8.12 plots this ratio against the total stress at the end of each stage. A large degree of scatter in the data is obvious, but nevertheless clear and similar trends in the data exist for each grading. At low stresses, between 70% and 100% of the incremental strain will be generated immediately, but this percentage gradually decreases to between about 30% and 80%, as the applied stress increases to 100 kPa. This relationship, which clearly identifies a time dependent component when the material is tested dry of optimum, is contrary to the findings of Brady and Kirk (1990) noted above. However, if "immediate" were taken to include the first 30 minutes following stress application and insignificant time dependent strains equates to less than 10% of the total strain, then a similar conclusion could be drawn from this data. This order of straining is not considered insignificant by the author though.

8.5 Comparison of Compressibility Results with those of Brady and Kirk (1990)

Subsequent to the completion of the test programme reported in this thesis, Brady and Kirk (1990) reported the results of incremental loading tests on a limestone aggregate equivalent to the coarse grading of the current research. No suction measurements were attempted in their relatively simple work. The effects of water content and compactive effort were investigated, and to a lesser extent grading influences.

Brady and Kirk used a 500 mm diameter floating ring oedometer, and compacted the specimens into the cell in five equal layers. Three different compactive efforts were used, and the compaction curves (not presented by Brady and Kirk) are presented as Figures 8.13 to 8.15. Their research did not attempt to define the optimum water content and maximum dry density from the actual tests, as revealed by the poor definition of the curves. Rather, optimum total water content was determined to be 4.0% from Test 14 of BS1377:1975, with a maximum dry density of 2.41 Mg/m^3. This contrasts with the optimum water content of about 6% to 9% from Figures 8.13 to 8.15, and 7.2% for the coarse grading used in the current research. Comparing the compaction curves with Figure 3.11 shows Brady and Kirk's medium effort is approximately the same as the 'standard' effort used in the current work.

Brady and Kirk refer to the term compressibility in the title of their report, but present their conclusions with reference not to this parameter, but to its inverse, stiffness, as quantified using the constrained modulus. As shown by graphs 8.16 to 8.18, an attempt was made to relate the measured stiffness to the dry density of the specimens, but the apparent correlation was only achieved by plotting the stiffness on a logarithmic scale. Had the data been presented in terms of compressibility using a graph of the form of Figure 7.28, a very wide scatter of strains at any given stress level and dry density would have been apparent. For example, for the stress range 25 kPa to

100 kPa and a dry density of 2.27 Mg/m^3, the change in strain between these stresses for specimens 17 and 23 may be calculated to be 0.29% and 0.56% respectively. In the light of the preceding discussions in section 8.4, this particular scatter of results becomes more understandable when it is noted specimens 17 and 23 had total water contents of 1.1% and 6.1% and were compacted with the same effort.

In order to compare the two sets of data the author's data has been reanalysed to obtain the constrained moduli for various stress ranges, as shown in Table 8.4. This data has been added to Figure 8.16 and Figures 8.19 to 8.22 plot the moduli for different stress increments derived from the various series for the coarse and fine gradings against total water content. Figure 8.23 to 8.26 plot the same data against the dry density. The Brady and Kirk data has also been re-analysed to plot the moduli against total water content and dry density for each of the three compactive efforts used (see Figures 8.27 to 8.32). Total water content has been used as the absorption characteristics of the limestone used by Brady and Kirk are not known.

Examination of the corresponding curves for both sets of data shows that the few water contents used by Brady and Kirk prevents definitive conclusions from being drawn, as the large data gaps in the curves allows alternative "best-fits" to be drawn (eg Figure 8.27). Additionally, the poor definition of the compaction curves may possibly reflect poor compaction control as well, with its resultant effect on the moduli. Despite this, similar relationships between constrained modulus, and water content and dry density, are discernible for both sets of corresponding data and plotting the series A data on Figure 8.16 shows that similar order of moduli were obtained. Further, the large scatter in data reported by Brady and Kirk has been considerably reduced by separating the different compactive efforts out, which reflects the different form of curve obtained for each of the 3 different compactive efforts. The curve form varies also with the range of stress level considered at the higher compactive efforts.

The observations above are believed to be the result of the combined influence of water content, dry density, and compactive effort on the soil suctions, the influence of dry density alone on the total strain potential of a soil, and the influence of the stress level and increment on the modulus. These various influences may be expressed graphically as shown in Figure 8.33 which plots in three dimensions the total strain at any given stress level against total water content and dry density.

The vertical axis was chosen to be strain in order to identify the influence of stress level more clearly, and because the constrained modulus may be easily calculated from the graph. The reduction of $\Delta\varepsilon_1$ to $\Delta\varepsilon_4$ with increasing stress level results from the reduction in total strain potential, and the reduction of the ratio of the "average" suction stress in the soil to the applied stress. At high stresses, $\Delta\varepsilon_2$ and $\Delta\varepsilon_4$ will reduce to near zero, and may reverse in sign if any influence of decreasing interparticle friction exceeds the relative stiffening influences of the suctions. $\Delta\varepsilon_1$ and $\Delta\varepsilon_3$ will also reduce to near zero, and a more or less unique relation between total strain and dry density will exist. However, the relationship would be less unique for the constrained modulus, as it relies upon the change in strain between two specified stresses.

The above explanation of the scatter in relationship between constrained modulus and dry density contrasts with that offered by Brady and Kirk. They recognised the influence of water content, but attributed it instead to the generation of high pore water pressures during compaction, which in turn could have caused a layer of fine material to migrate towards the top of the layer. During loading, the coarser particles were then conjectured to penetrate into the looser fines-rich layer at the top of the underlying layer. Whilst not rejecting this mecahnism as being responsible for a small part of the observed influence of water content at high water contents, it is considered that the comparable results from the research herein, which employed a single compaction layer only, largely invalidates their suggestion. Further, they only report evidence of such a fines-rich layer in sections of the

wettest specimens. This suggests that the large increase in compressibility as the water content passes optimum could be partially due to this mechanism, but at lower water contents when less water is available to actually generate positive pore water pressures the mechanism is not valid and suctions must be involved.

8.6 Inundation Test Results

8.6.1 Relationship Between Inundation Strains and Soil Suctions

The preceding discussions suggested that the soil suctions are a significant influence on the behaviour of coarse grained soils. It is suggested also that the destruction of suction during inundation is a major parameter affecting the "inundation strains" that occur at a constant vertical (see Figure 7.17) stress. The other possible factors identified in section 2.2, namely reduction of interparticle friction, washing of fines and aggregate softening, are considered to be relatively unimportant for the following reasons:

(i) friction loss: due to the absorption characteristics of the limestone, only specimens with a very low water content and hence relatively dry contact points between particles would be likely to compress further after wetting.

(ii) washing of fines: as described in section 2.2, only the loss of the fines around particle contacts would be expected to cause straining, and this would be due to the loss of the suction induced component of the interparticle forces. Evidence for the presence of such fines has been discussed already in section 8.3.2.

(iii) aggregate softening and loss of stiffness: a medium to long term mechanism such as this would be unable to explain the short term movements during the tests.

The possibility of a relationship between the inundation induced strains and the measured suction has been investigated, and Figure 8.34 shows the resultant graph. The reasonable correlation for the top and bottom of the specimens supports the hypothesis, and the form of the curves is consistent with the hypothesis that a maximum inundation strain exists. The ambient stress level appears to have a negligible effect within the limits of the current work.

The relationship between the relatively immediate straining and destruction of suctions implies also that the suctions are between different particles, and not in the particle interstices, as assumed earlier.

8.6.2 Relationship Between Inundation Strains and Other Parameters

Previous workers have attempted to relate the inundation strains to the void ratio (Egretti and Singh, 1988), the air void ratio (Charles, 1984) or the degree of saturation (Pigeon, 1969), all of which are more readily determined than the soil suctions. Figures 8.35 (a), (b) and (c) plot the current data against each of these parameters. As may be seen, the void ratio is least sensitive which is as expected given its indirect relationship to the soil suction via the compactive effort and compaction water content, but good correlations exist for the air void ratio and degree of saturation. These parameters may thus be inferred to be directly related to the soil suctions, as is confirmed by Figures 8.36 (a) and (b). It is considered the good correlation could have been expected as each of these paramaters reflects the three parameters identified in section 8.5 above, namely water content, dry density and compactive effort.

From the above, it is suggested that practical relationships between inundation strains and either the air void ratio or the degree of saturation may be developed. Recent work by Thompson, Holden and Yilmaz (1990) towards this aim is presented as Figure 8.37, with the authors data annotated upon it. The current data is similar to that for rock

fragments reported by Charles (1984), but the laboratory data appears to be several orders of magnitude smaller than observed field measurements. Insufficient information is available at present to explain this anomaly, but the affects of side friction and field density/water content variations may be the dominant causes.

8.6.3 Combined Effect of Total Stress Changes and Inundation

Figure 8.38 summarises the changes in dry density and water content for the specimens due to both monotonic loading and inundation. This graph shows that for any given initial dry density, an approximately unique final state will be reached irrespective of the stress path followed. This implies that the discontinuity of the state surface shown in Figure 2.5 leads to a second unique state surface in the saturated e - (σ - u_A) plane for soils which have been completely inundated (see Figure 8.39). For this particular soil, this state surface appears to be horizontal over the stress range tested (50 to 125 kPa) as the ambient stress during inundation did not noticeably affect the observed strain. It would normally be expected for the curve to be concave upwards over a large stress range, with the highest final voids ratio at the lowest total stress. For different soils and/or different initial fabric (dry density), a different final fabric would result.

Similar results for a mudstone have previously been communicated to the author by Tanaka (1988) during discussions, but further information is not available at present.

8.7 Repeated Load Behaviour

Although not a primary aim of the research, information on the first unloading characteristics were obtained from the series A and B tests, and information on repeated loading was obtained from the series D tests.

The first unloading curves for each of the series A and B tests exhibited very similar gradients within each series, as shown by Figure 8.40 for the series A data. When the constrained moduli between each stress decrement are plotted against the ambient stress before the next decrement, as shown by Figures 8.41 (a) and (b) for series A and B respectively, the curves fall in a fairly narrow linear band whose gradient is slightly greater for the unsaturated specimens (series A) than the near saturated specimens (series B after inundation). This implies the unsaturated specimens are slightly stiffer for any given stress level, an observation which is attributed to the suction, although a graded influence within the unsaturated specimens was not clear. The tests on the fine grading showed a similar trend, but were stiffer than the series A tests on the coarse grading. From 100 kPa to 25 kPa, the coarse grading strain decreased by about 0.13%, and the fine grading decreased by about 0.10%.

The repeated load data from series D showed similar behaviour during the first and subsequent load cycles for each of the gradings tested, but with different moduli. The previously presented Figures 7.29 to 7.31 summarise the repeated strain data. As may be seen from Figure 7.29, each of the 4 groups of tests (coarse grading with heavy and light compaction, and medium and fine gradings) exhibited a different typical response. The heavily compacted coarse graded specimens showed only small increases of strain with cycling dependent upon the compaction water content and density as shown in Figure 7.30. This figure plots the difference in strain after 1 and 4 cycles, at a peak stress of 125 kPa against the free water content (7.30a) and dry density (7.30b). The form of the curve in Figure 7.30a is very similar to that found for compressibility and is attributed to the same reason, that is the interaction between suctions and dry density. Previous workers (eg Hicks, 1970) found also that the susceptibility to strain accumulation increases as the degree of saturation increases. Figure 7.30b confirms that a higher density does not necessarily mean better performance of the material under load.

Figure 7.31 presents similar curves for the less highly compacted coarse graded specimens. Strain accumulation continued to occur with cycling for all tests, without reducing greatly in rate. No clear trends with water content or dry density are discernible for this compacted state, although it is possible that the susceptibility to strain accumulation increases as the density decreases. If this is correct, it suggests the dry density has an overriding influence if low compaction is applied despite the suctions. This concurs with previous expectations prior to the testing, but is contrary to the suction influence on monotonic behaviour noted earlier. Further work is needed on this aspect before conclusions may be drawn.

The two tests on the medium grading showed a similar behaviour to the heavily compacted coarse graded specimens, that is little or no strain accumulation with load cycling, and the fine grading exhibited some increase but at a noticeably decreasing rate. No conclusions may be drawn regarding the influence of water content or dry density, but it is noted that both gradings were compacted with the same effort as the heavily compacted coarse specimen.

The effect of increasing the strain rate had no apparent influence on behaviour. This concurs with more comprehensive resilient testing reported by Boyce (1976), who found frequency had no influence in the range 0.1 Hz to 20 Hz.

8.8 Effect of Stress Level on Compressibility Behaviour

The preceding discussions have focussed upon the observed behaviour at the mainly low stresses applied during the current research. As the stress level increases, the suction effects would be expected to progressively decrease in importance. The rate of decrease of the suction influence with stress level would be dependent upon the "average" suction, and hence upon the grading and the compactive effort.

Such a decrease was observed in the series D test results for the coarse grading compacted with the usual effort, as remarked upon in section 8.4.2. Above a vertical stress of about 100 kPa, the peak in the compressibility curve shown in Figure 7.28a disappears. This corresponds to a critical vertical stress to measured top suction ratio of between 3.3 and 10 for a free water content of between 1% and 4%.

In contrast, use of a lower compactive effort and hence lower dry densities showed that the probable higher suctions for a given free water content did not affect the measured compressibility at low stresses (Figure 7.28b). However, above a stress of about 100 kPa a peak in the compressibility relation is noticeable. This is interpreted as meaning sufficient densification had occurred for the number of contact points within the soil mass at which soil suctions were present to reach a critical level, such that the local stabilising influence of the suctions was greater than the local shear stresses induced in the soil mass by the applied stresses. It is believed that had the tests been continued to yet higher stresses (>250 kPa) the peak in the curve would have again disappeared as a critical vertical stress to suction ratio was passed. Such a critical ratio is believed to exist, but more comprehensive testing is require to investigate its existence, and the combined effects of compactive effort and stress level. A probabilistic theoretical approach may allow this ratio to be predicted for a given stress field if the suction relationships (ie to water content, stress level and compactive effort) are known.

8.9 Triaxial Test Results

8.9.1 Consolidation Characteristics

The consolidation characteristics were largely as expected but with two exceptions as noted below. Firstly, the dry specimen took 27 hours to consolidate whereas a very rapid period was expected. No satisfactory explanation for this can be offered at present, and it must be assumed the data represents slow reorientation of particles in the dry state under the applied stresses.

The second exception to the expectations concerns specimen C3, (suction 15 kPa), which showed an unusually small total volumetric strain compared with the other tests. Specimens C1 (saturated) and C2 (dry) show a similar strain of 0.72% and 0.88% respectively, whilst C4 (suction 4 kPa) recorded a larger strain of 1.21% due to the large volume of water displaced during the consolidation stage. Further examination of the data for C3 showed that the water volumetric strain was as expected, but only a small cell volume change was recorded. It is unclear whether this result represents real behaviour due to unknown causes or, more likely, a slight leak in the double membrane had developed leading to gradual leak of air into the cell over the 28 day consolidation period. Such a leak would be unlikely to be noticed, and would have the effect of reducing the measured cell volume change as the air replaced true specimen volume change. However, in view of the uncertainty the calculation of the subsequent specimen parameters was made on the basis of the recorded volume changes.

8.9.2 K_o Determinations

Only limited success was met with this stage of the triaxial tests, as noted in section 7.3.3. A reliable K_o value of 0.41 and a tentative value of 0.39 were obtained. These compare favourably with the likely results of between 0.43 and 0.30 for a normally consolidated saturated soil with an effective angle of friction between 35° and 40°, calculated using the Jaky (1948) equation. It should be emphasised however that the current data defines K_o in terms of total stresses, as no single "effective stress" applies to an unsaturated soil.

No conclusion may be drawn with respect to the influence of soil suction, but it is noted that the higher value of a 0.41 was obtained from a test on a dry specimen, and the lower (0.39) from a saturated specimen.

8.9.3 Results of Shear Tests

Before considering the results of the shear tests, it is prudent to consider the stress changes that have been applied to the specimens up to the start of this stage, and the effects of these changes on the specimen. During specimen preparation, a stress of $(\sigma - u_A)$ or $(\sigma - u_W)$ of up to 15 kPa was applied, and this was not exceeded until commencement of isotropic consolidation when this pressure was increased to about 30 kPa. During the attempted K_o stages, σ_1 and σ_3 were increased as required with the air and water phases both drained against a constant back pressure equal to those at the end of consolidation. The water phase was undrained and air phase drained during the anisotropic removal of the deviator stress at constant cell pressure and then the reduction of the cell pressure to its consolidation value. Shearing commenced at this point with a constant cell pressure and the air and water phases drained.

The complex stress paths followed by the specimens, which were summarised in Tables 7.3 to 7.6 together with the impact on the main specimen parameters, require that the shear results be treated with caution, and direct comparison between the tests may not be strictly valid. In particular, the early shear behaviour is likely to be significantly affected by the oversonsolidating stress history. However, the ultimate strength of the specimen should be largely unaffected as the large shear strain required to reach this state will destroy to a very large extent any soil fabric changes induced in the soil by its stress history. The failure data were presented in Table 7.7.

As may be seen, specimens C2 to C4 were tested with a cell pressure of about 200 kPa at the mid height of the specimen. It was decided to test at this moderate rather than low stress level in view of the change in cell pressure over the height of the specimen of 4 kPa, which is a variation of 1% above or below the mid height pressure. This percentage would have increased to an unacceptably high 4% for a cell pressure of 50 kPa. Further, a moderate stress level was used to bring the cell

pressures for these three tests nearer to that necessarily used during test C1 following saturation, and to thereby to give a greater degree of confidence in comparing the results of all four tests.

Previous workers (eg Fredlund et al, 1978) had found that the shear behaviour could be modelled using the stress space shown in Figure 2.8 and expressed mathematically as equation 8.3, although evidence is accumulating for a curvilinear plane at low stress levels.

$$\tau' = c' + (\sigma - u_A) \tan \phi' + (u_A - u_W) \tan \phi^b \quad \text{.... equation 8.3}$$

Attempts were made to plot the limited data obtained in this stress space, and to calculate the values of ϕ' and ϕ^b using the method suggested by Fredlund et al, but a more meaningful two dimensional plot with the suctions annotated is presented in Figure 8.42. The analytical method required the saturated shear strength criteria to be known first, and given that only one saturated test was performed, it was assumed that the data for test C1 (saturated) lay on or close to the saturated line, and the saturated parameters were hence defined to be in the range $c' = 0$kPa to 15 kPa, $\phi' = 37^o$ to 49^o. This contrasts with parameters $c' = 0$, $\phi' = 53^o$ reported by Pappin (1979) on crushed limestone of a similar grading. Despite this wide range of possible values, it is clear from Figure 8.42 that shear strength rapidly increases with decreasing water content (increasing suction). Table 8.4 presents the results of one analytical calculation for $c' = 13.8$ kPa, $\phi' = 43.5^o$, and Figure 8.43 uses the graphical method for calculating the suction influence. Several other similar analyses were made for different strength criteria and the values for ϕ^b were found to lie in the range 70^o to 80^o.

The apparently very large influence of suction on behaviour, such that they are apparently more influential than the total stress $(\sigma - u_A)$, cannot purely be attributed to the suctions themselves. Rather, it is considered that interparticle friction must play a role to some extent. Regardless of the causes though, the importance of the high value for ϕ^b should not be overemphasised, as given that tests C2 and C3 gave similar

results we are in a position to quantify the maximum influence of the suction component. If this maximum coincides with a suction of 10 kPa say, then progressing from the saturated to dry conditions would only give an increase in shear strength of about 40 kPa. At moderate to high stresses, say 200 kPa to 1000 kPa, this equates to about a 25% to 5% increase in strength, respectively. At low stresses, the influence may be very significant if this data obtained at moderate stresses is applicable, but further work is required in this area.

Axial strains at failure were similar for all tests despite the different stress histories, but total volumetric strains to failure varied, being roughly double for the unsaturated soils compared to the saturated soil. The water volumetric strains showed a wide scatter, varying between 0.91% increase in volume and a 3.7% decrease for specimen C3. However, the latter is considered to be suspect in view of the previous discussion about the possibility of a leak affecting volumetric calculations.

Leaving the free water volumetric strain for Test C3 (suction 15kPa) out of the considerations initially the larger free water volumetric strain is observed in the saturated test, as would be expected due to the greater efficiency of an incompressible pore fluid at transmitting dilatancy induced reduced pressures in the specimen to the pressure controlled ends of the specimens. Despite the compressible fluid in the unsaturated soil though, the three dimensional expansion of the soil during shear induced sufficiently large suctions within the specimen for significant water to be drawn in. This contrasts with the negligible free water volume changes measured during series A in which radial movements were prevented.

The larger total volumetric strains in tests C2 (dry), C4 (suction 4 kPa) compared to C1 (saturated) may also be attributed to the compressible pore fluid, but the strain during test C2 was not as large as might have been expected. This may be explained by the lower axial strain at failure, and the larger radial stiffness of the soil compared to the saturated soil due to increased interparticle friction.

8.9.4 Theoretical Compressibility Equation for Two Phase Pore Fluid

Reference has been made in the preceding paragraphs to the influence of the compressible pore fluid on volumetric strain during shear. Numerous theoretical treatments to predict pore water pressure changes due to an applied stress increment have been proposed, and perhaps one of the simplest and most practical equations was suggested by Fredlund (1976).

$$\beta_M = S_r \beta_w + B_{AW} \left(\frac{1 - S_r}{u_A}\right) + B_{AW} \frac{S_r h}{u_A} \quad \text{..... equation 7.1}$$

where β_M = compressibility (= change in volume/change in pressure) of the air-water mixture

β_w = compressibility of pure water = 4.8×10^{-7} m^2/kN

S_r = degree of saturation

u_A = absolute air pressure

B_{AW} = du_A/du_w

h = Henry's coefficient of solubility

Assuming insufficient time was allowed for significant quantities of air to enter solution, and assuming B_{AW} equals unity as suggested by Fredlund for a mixture in which the air is occluded, equation 7.1 reduces to:

$$\beta_M = S_r B_w + \left(\frac{1-S_r}{u_A}\right) \quad \text{..... equation 7.2}$$

The saturation stage of test C1 provided an opportunity to verify this equation. Saturation of the specimen was achieved by raising the cell pressure to compress the pore air. The saturation process involved a succession of two stage pressure increments until the pore pressure parameter B equalled or exceeded 0.95. Stage 1 of each increment involved increasing the cell pressure and measuring the water and air undrained pore water pressure response, such that B could be calculated. If B were less than 0.95, stage 2 entailed raising the pore

water pressure to within 10 kPa of the cell pressure, before the succeeding stage 1 was performed.

The saturation stage data for volumetric changes, degree of saturation and pore pressure parameter B are presented in Figure 8.44, and Table 8.5 summarises the calculations for change in volume, both measured and as predicted using equation 7.2, throughout the saturation stages. It should be noted that actual change in void volume was taken to equal the change in cell volume, after correction for cell swell, during each stage 2 (ie the volumetric rebound of the specimen was considered negligible, as justified in section 7.3.1). Assuming then that all this membrane penetration had occurred during the undrained stage 1, and knowing the total cell volume change, the nominal specimen volume change during stage 1 due to the change in effective stress may be calculated (= cell volume change - membrane penetration), this being equal to the change in void volume. The changes in air volume may also be calculated using the measured changes in water volume, which were zero during stage 1 and greater than zero during stage 2.

Figure 8.45 compares the measured and predicted volume changes during the first saturation stages, and during each stage as a whole. As may be seen, below about 86% free degree of saturation the theoretical predictions do not match the experimental results. This is attributed to the onset of continuous air voids within the specimen, as opposed to the occluded air voids implied in the assumption that B_{AW} equals unity. Between 86% and 94% saturation, good agreement is obtained despite the simplifcations made in the interpretation of the test data, but beyond 94% the curves diverge increasingly again. It is suggested that this divergence is a limit of the test data interpretation, rather than a failure of the theory, as the assumption of zero volumetric rebound may be expected to become less true as saturation is approached and the reducing air volume becomes less able to accommodate the reduction in cell pressure, thereby requiring a greater proportional effort by the soil structure.

8.10 Practical Implications of the Research

It was noted in chapter 1 that the major drive behind this research was the need to establish a performance specification for reinstatements. Data needs to be acquired for the full spectrum of likely reinstatement materials and under a wide variety of stress density and moisture conditions before a comprehensive specification may be written. This research does suggest the following relevant facts though:

(a) unavoidable time dependent strains will occur within heavily compacted materials due to internal creep mechanisms and related loading. Long-term tests are required to estimate reliably the magnitude of this component, but values of 0.2% to 0.5% strain may not be unreasonable for lower bounds from the limited repeated load tests conducted. For a 2 m deep trench, this equates to between 4 mm and 10 mm settlement. Compaction considerably dry of optimum may reduce the magnitude of these movements.

(b) Strains of up to 0.5% will occur within heavily compacted materials due to complete saturation from rainfall ingress, or groundwater rise (unlikely in a free draining highway structure). Compaction at or just below optimum (as determined from a test on the full grading curve) will reduce this component, which equates to 10 mm in a 2 m deep trench.

(c) A higher dry density will result in improved performance for any given compaction water content.

From the above, compaction at a low water content and with a high effort followed by controlled inundation and topping up to eliminate any immediate settlement may minimize the time dependent strain element. This is provided the trench will allow the inundation water to drain freely away and a low water content/high suction equilibrium condition to be achieved. Current practice involving compaction at or near optimum with a specified effort followed by a decrease in the

equilibrium water content due to free drainage will result in greater time dependent strain. Further, variations in the water content will result in significant differential performance of the trench if the same compactive effort were used.

Table 8.1 Effect of Particle Size on Magnitude of Suction for Water in a Lenticular State

Particle Radius, a (mm)	r_b (mm)	Calculated Suction (kPa)
0.1	0.050	14.8
	0.020	259.0
1.0	0.50	1.48
	0.20	25.9
10.0	5.00	0.148
	2.00	2.59

Table 8.2 Comparison of Soil Parameters for Coarse and Fine Gradings

Test Number	Free Water Content (%)	Void Ratio, e		Degree of Saturation Sr		Air Void Ratio,	
		Fine	Coarse	Fine	Coarse	Fine	Coarse
A1	4.2	0.48		23.0		24.9	
A5	4.1	0.42		25.8		21.8	
A10	4.1	0.41		26.1		21.5	
B3	4.1		0.21		51.9		8.8
A3	2.4	0.49		12.9		28.6	
A6	2.0		0.33		16.1		20.8
B5	2.3		0.30		20.2		18.6

Table 8.3 Immediate Strain Components of Series A and B Tests During Loading

Grading	Test Number	Immediate Strain (%) at Various Stress (kPa) Levels 10	25	50	75	100
Coarse	A2	0.42	0.75	0.99	1.12	-
	A6	0.70	0.85	0.89	0.93	0.97
	A7	0.26	0.44	0.75	-	-
	A8	0.37	0.64	0.73	0.79	0.82
	A9	0.81	0.94	1.09	1.19	1.24
Coarse	B1	0.44	0.84	0.99	1.15	-
	B2	0.63	1.47	1.89	2.12*	-
	B3	0.83	0.94	1.01+	1.06+	1.10+
	B4	0.44	0.70	0.87	0.97*	-
	B5	0.54	1.30	1.82	-	-
	B6	0.28	0.63	0.76	0.83*	0.87**
	B7	0.32	0.54	0.73	0.77	0.81**
Fine	A1	0.15	0.49	0.85	0.95	-
	A3	0.41	0.52	0.73	0.83	0.93
	A4	0.33	0.47	0.63	0.72	-
	A5	1.07	1.33	1.75	1.86	1.95
	A10	0.78	1.02	1.23	1.32*	-

+ Strain components corrected for 0.07% inundation straining at 25 kPa

* Estimated by slight extrapolation of strain-stress curve

** Estimated from reload curve allowing for inundation and unloading - loading hysteresis

Table 8.4 Calculation of Shear Strength Parameters Using Method by Fredlund et al (1978)

Test Number	$1/2\ (\sigma_1+\sigma_3-2u_A)$	$1/2(\sigma_1+\sigma_3-2u_W)$	$1/2(\sigma_1-\sigma_3)$	(u_A-u_W)	$1/2\ (\sigma_1-\sigma_3)$	$\Delta\tau_d$	$\Delta\tau_d \cos\Psi'$
1	(134.0)	134.0	100.5	0	102.1	-1.6	-1.3
2	288.9	(288.9)	254.0	-	208.6	45.4	37.4
3	281.5	294.7	249.5	13.2	212.5	37.0	30.5
4	140.5	143.8	109.5	3.3	108.8	0.7	0.6

Notes: (1) All stresses are at failure and measured in kPa

(2) Saturated shear strength = $c' + \sigma' \tan \phi' = d' + [1/2(\sigma_1+\sigma_3-2u_W)]\tan\Psi'$, where $d' = 10$ kPa, $\Psi' = 34.5°$

Table 8.5 Calculation of Theoretical Air-Water Mixture Volume Changes During Saturation Stage of Test C1

Saturation Stage	Sr (%)	Absolute u_w (kPa)	$\beta_M \times 10^{-3}$ (m^2/kN)	Average β_M	Final u_w	Δu_w	Initial V_v	Predicted ΔV_v	Measured ΔV_v
Free-formed I	80.4	85	2.306		-16				
						20		105	31
				1.874		33	2796	173	74
After stage I	83.0	118	1.441		17				
						9		31	38
				1.221		20	2796	68	74
After stage II	86.2	138	1.000		37				
						18		41	43
				0.821		29	2778	66	66
After stage III	89.3	167	0.641		66				
						28		39	40
				0.511		41	2757	58	59
After stage IV	92.1	208	0.380		107				
						43		35	37
				0.297		50	2735	41	48
After stage V	94.5	258	0.214		157				
						43		20	26
				0.172		50	2717	23	34
After stage VI	96.0	308	0.130		207				
						45		13	18
				0.107		50	2710	14	23

/Continued

Table 8.5 Calculation of Theoretical Air-Water Mixture Volume Changes During Saturation Stage of Test C1 (Continued)

Saturation Stage	S_r (%)	Absolute u_w (kPa)	$\beta_M \times 10^{-3}$ (m^2/kN)	Average β_M	Final u_w	Δu_w	Initial V_v	Predicted ΔV_v	Measured ΔV_v
After stage VII	97.0	358	0.084		257				
						48		9	17
				0.068		50	2705	9	20
After stage VIII	97.9	408	0.052		307				
						30		4	4
				0.046		30	2703	4	7
After stage IX	98.3	438	0.039		337				
						30		3	12
				0.034		30	2697	3	14
After stage X	98.7	468			367				
			0.028				2701		

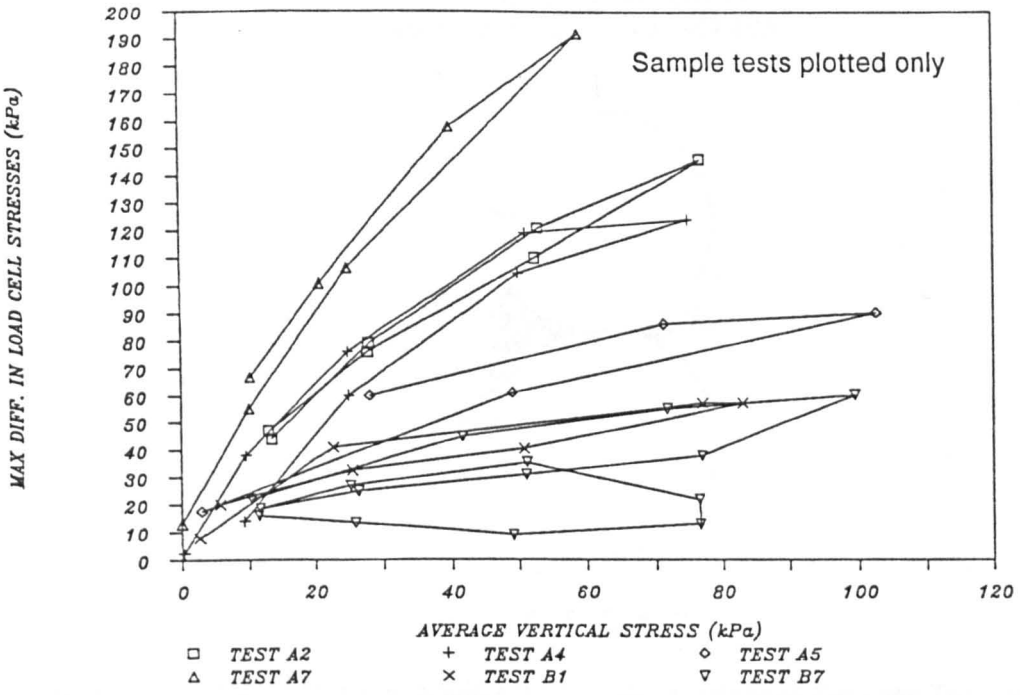

Figure 8.1 – Effect of Stress Level on Range of Measured Load Cell Stresses

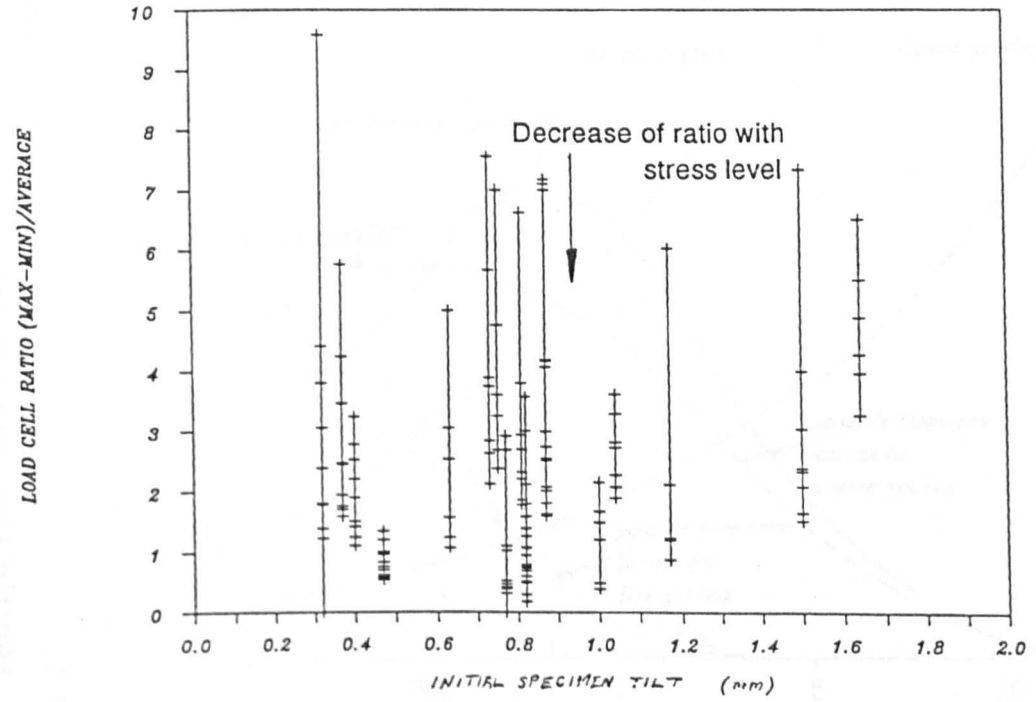

Figure 8.2 – Effect of Specimen Tilt on Range of Measured Load Cell Stresses

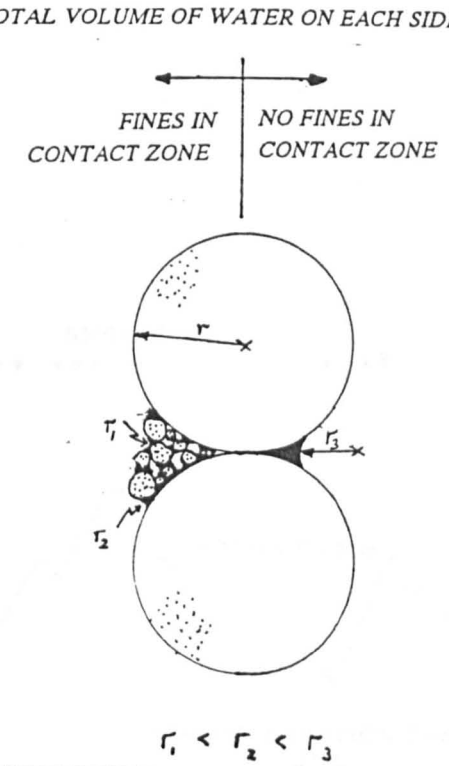

Figure 8.5 – Effect of Fines on Equilibrium Suction Established Between Two Large Particles

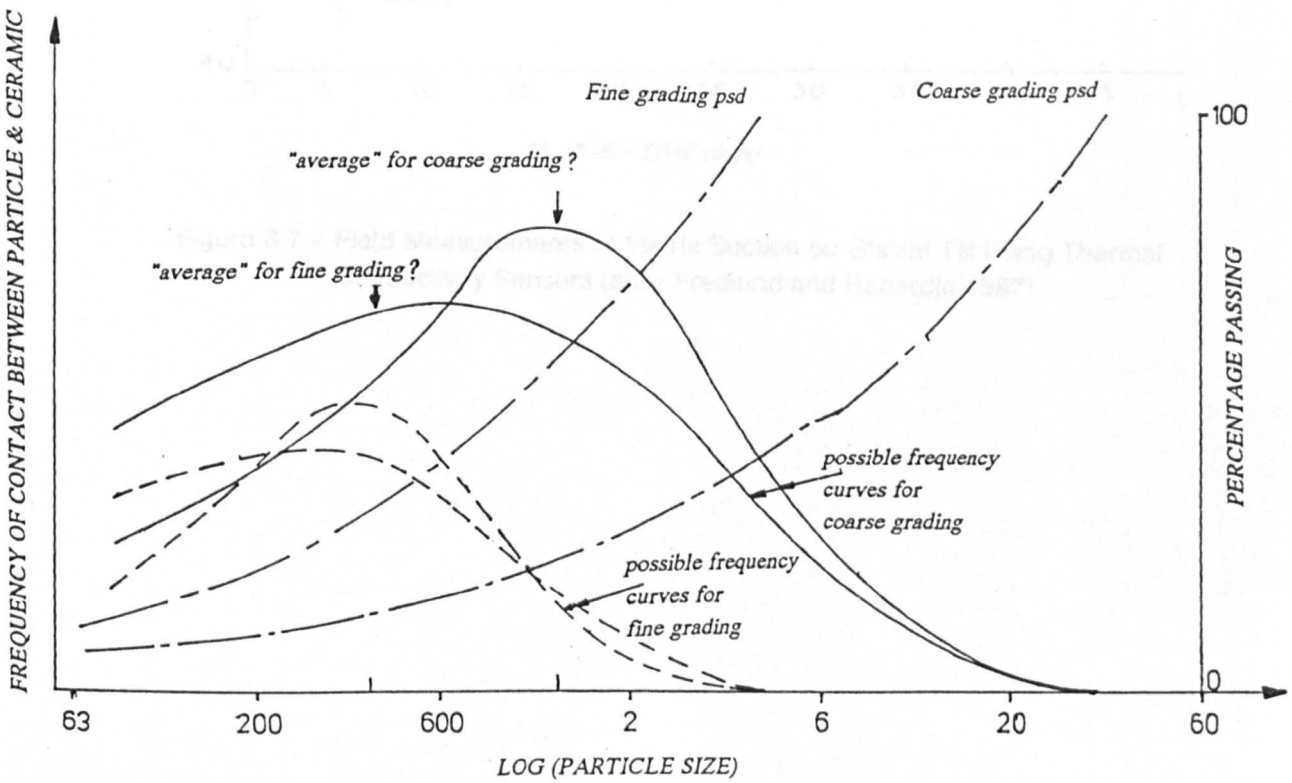

Figure 8.6 – Possible Frequency Distribution for Particle–Ceramic Contacts

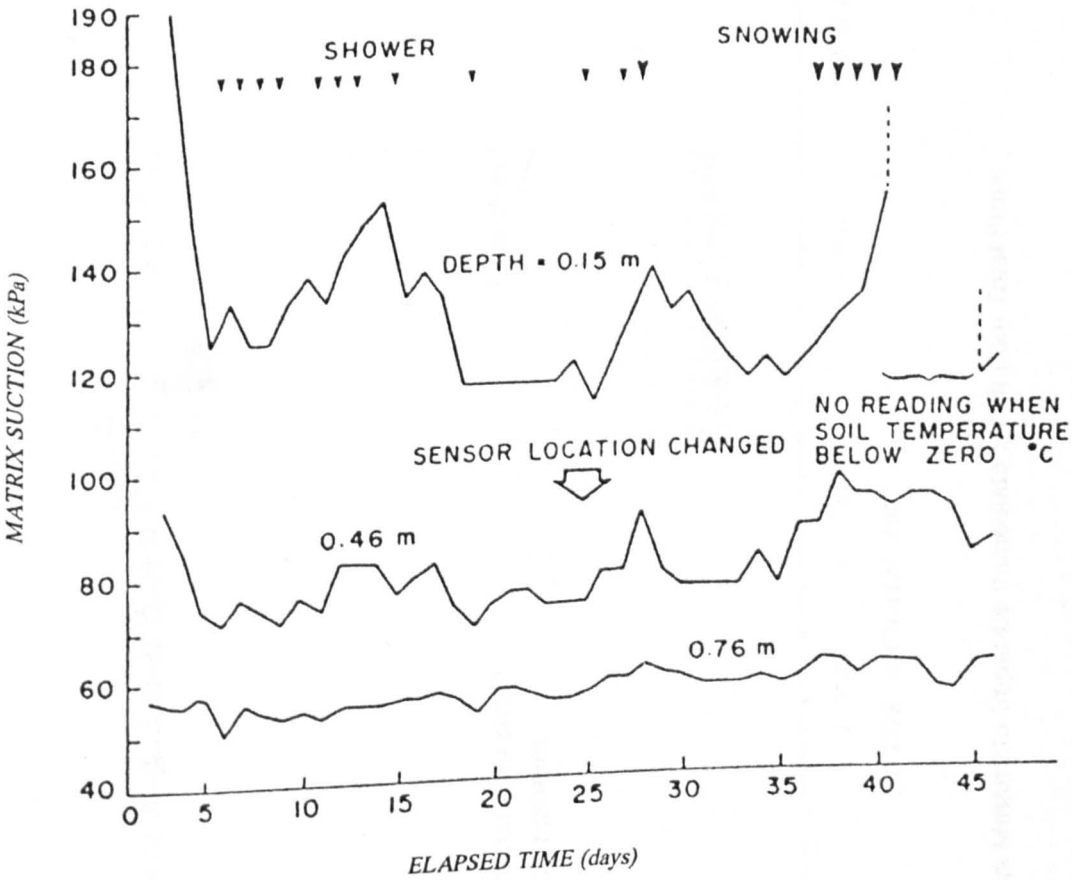

Figure 8.7 – Field Measurements of Matrix Suction on Glacial Till Using Thermal Conductivity Sensors (after Fredlund and Rahardjo,1987)

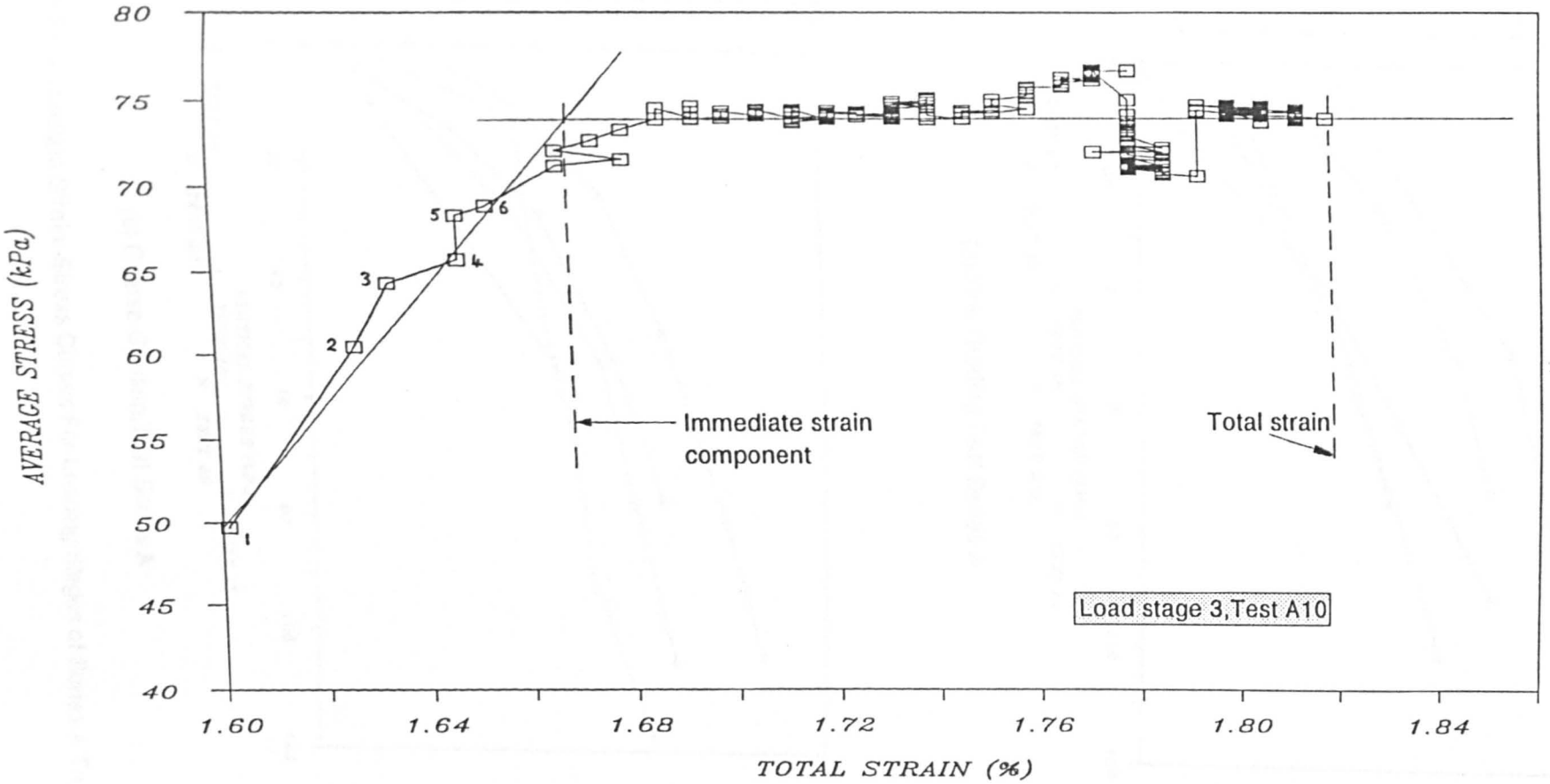

Figure 8.8 – Graphical Method to Separate Immediate Strain from Total Strain

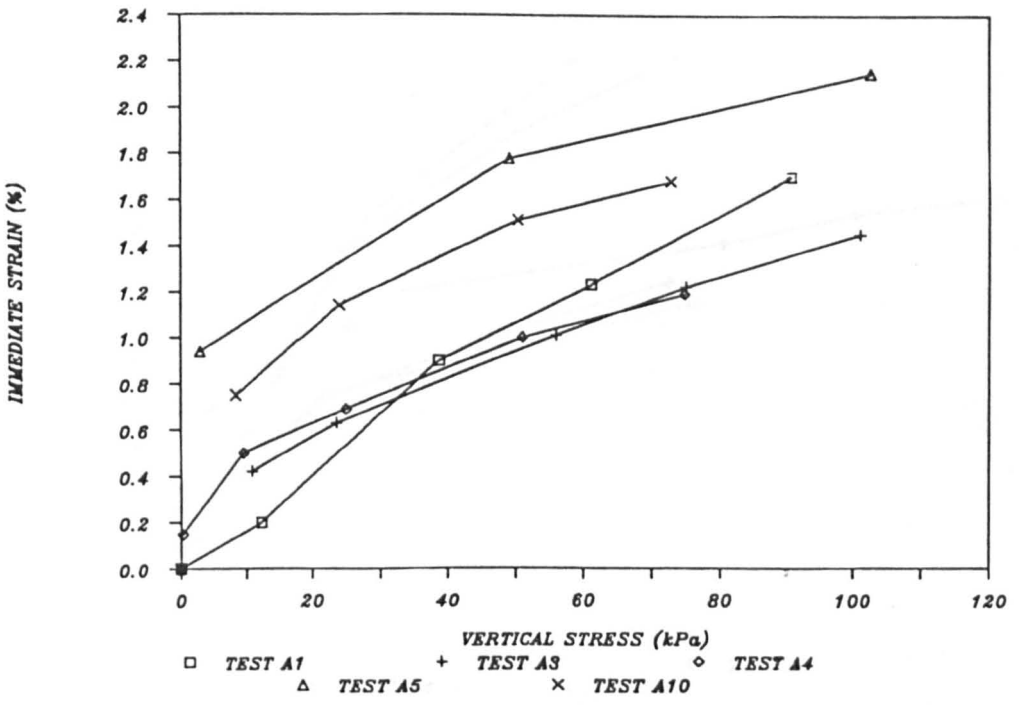

(a) Fine Grading,Test Series A

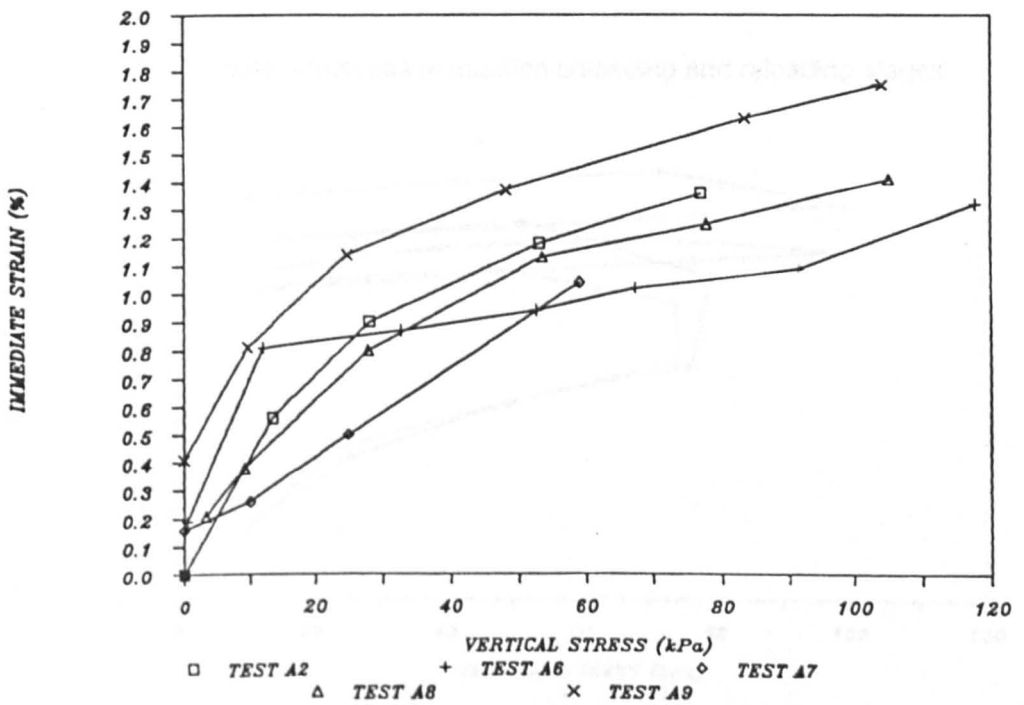

(b) Coarse Grading,Test Series A

Figure 8.9 – Immediate Strain–Stress Curves For Loading Stages of Series A Tests

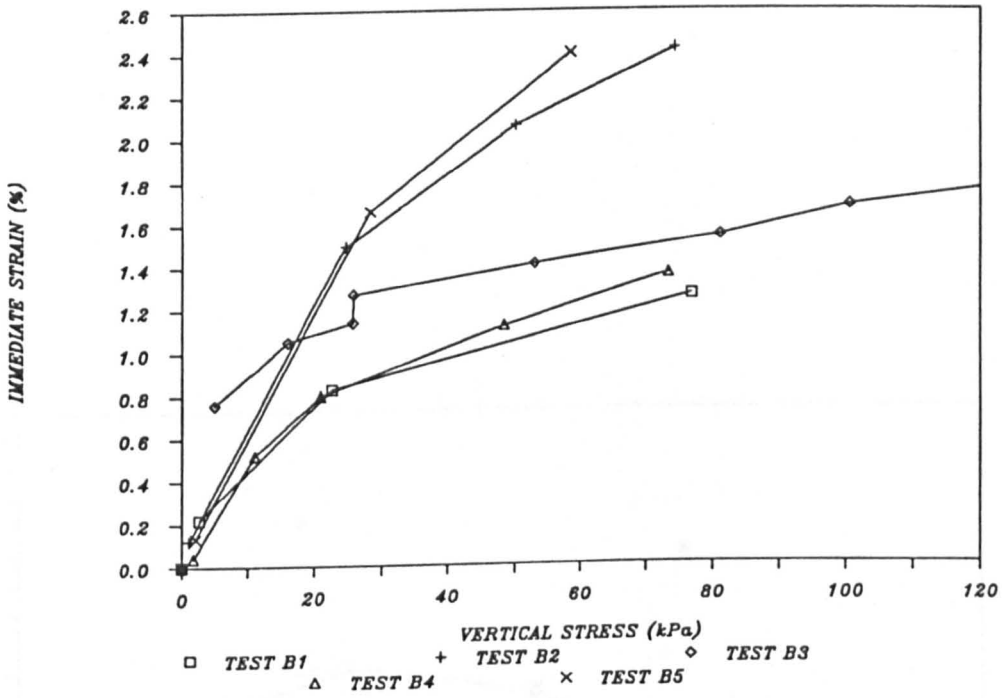

(a) Coarse Grading,Tests B1 to B5

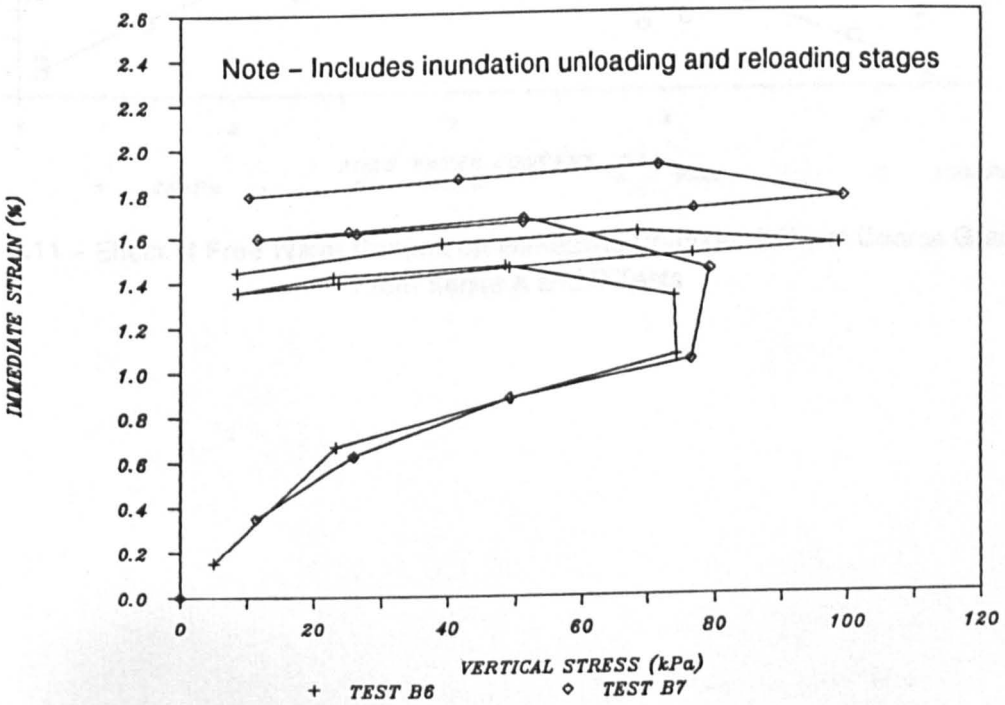

(b) Coarse Grading,Tests B6 and B7

Figure 8.10 – Immediate Strain–Stress Curves For Loading Stages of Series B Tests

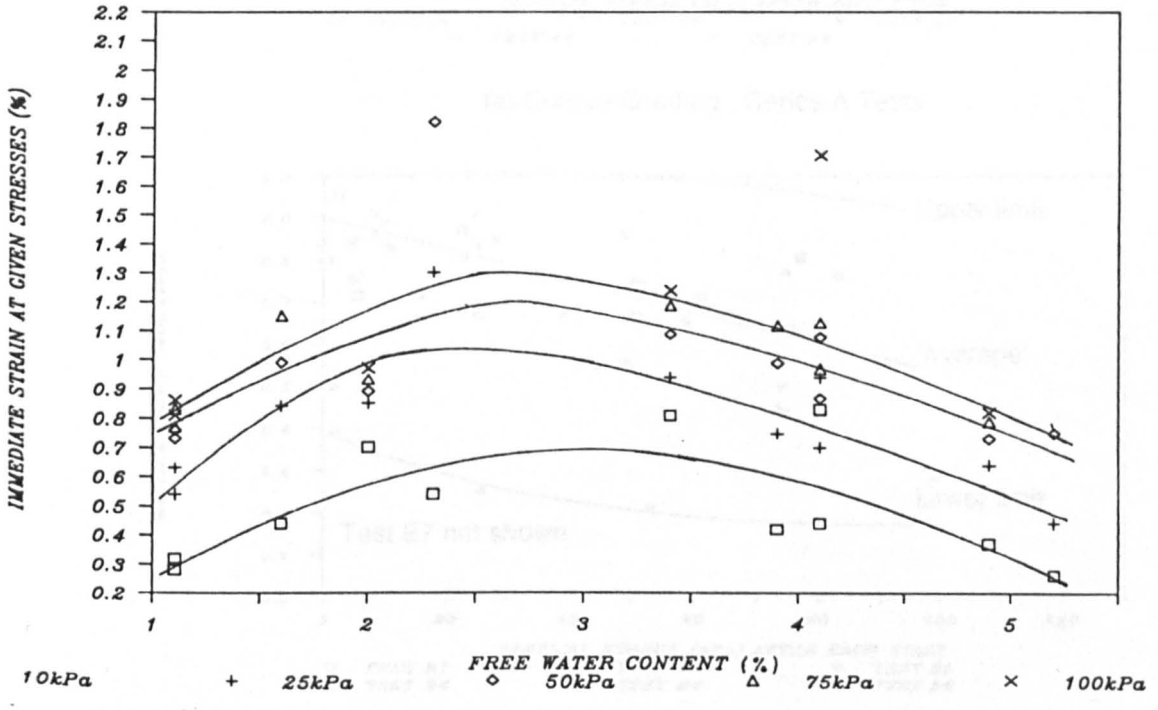

Figure 8.11 – Effect of Free Water Content on Immediate Compressibility of Coarse Grading From Series A and B Tests

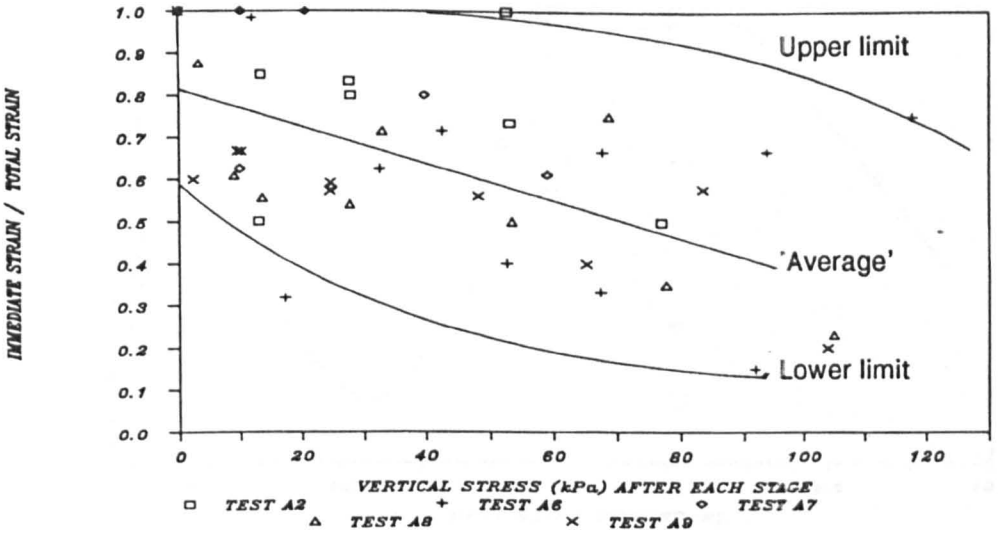

(a) Coarse Grading , Series A Tests

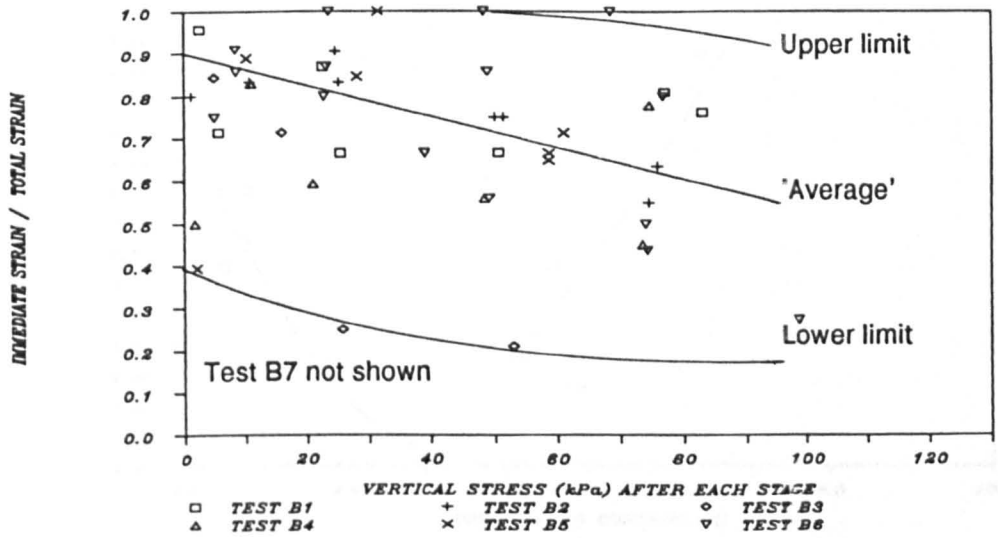

(b) Coarse Grading , Series B Tests

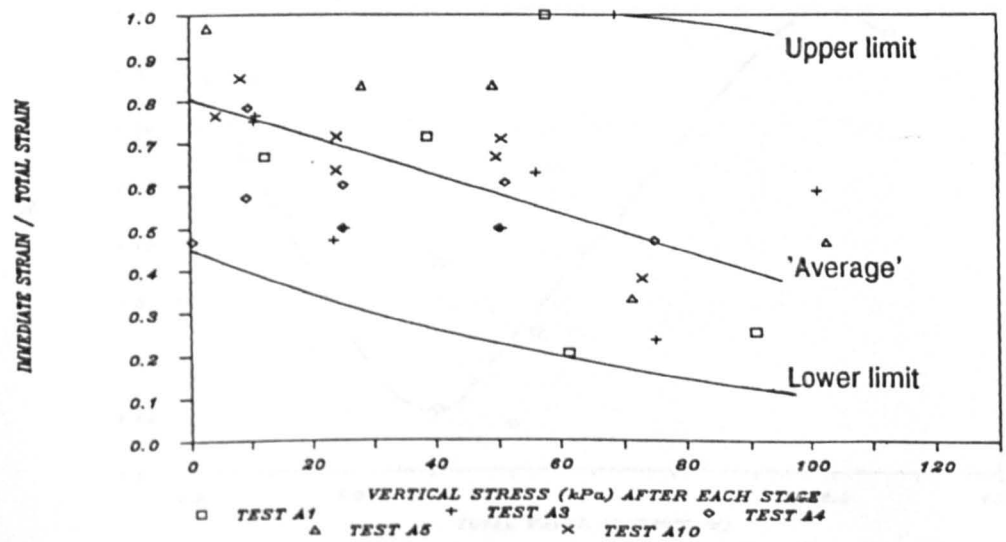

(c) Fine Grading , Series A Tests

Figure 8.12 – Relationship Between Immediate Strain Component and Stress Level

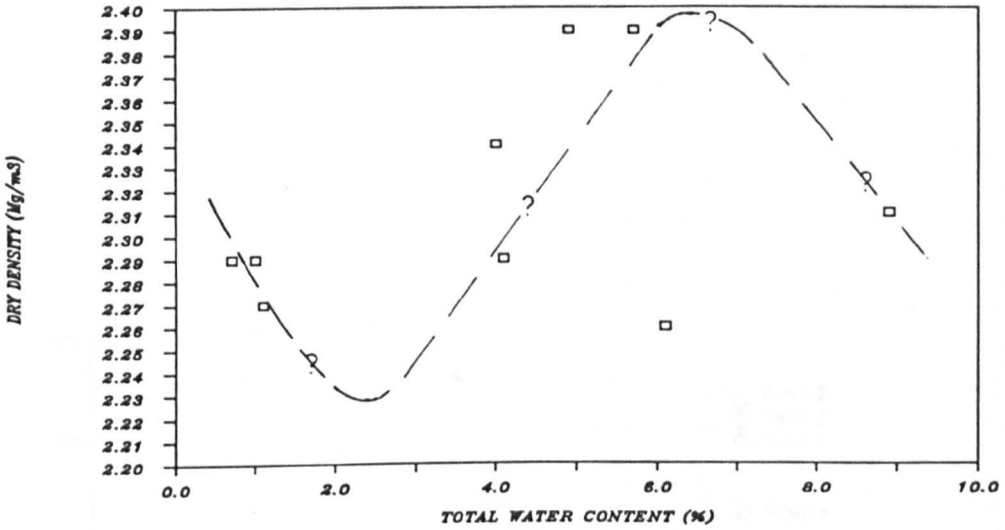

Figure 8.13 – TRRL Compaction Data For High Compactive Effort

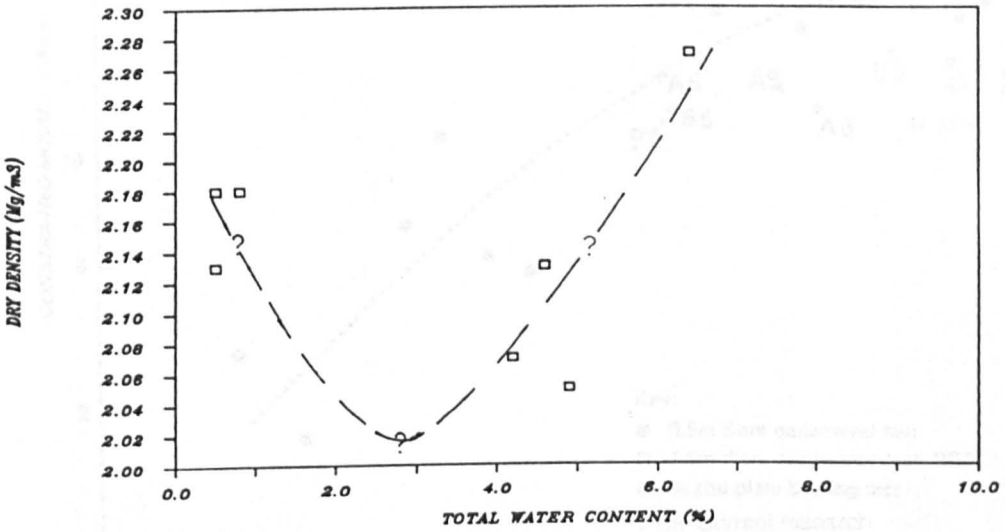

Figure 8.14 – TRRL Compaction Data For Medium Compactive Effort

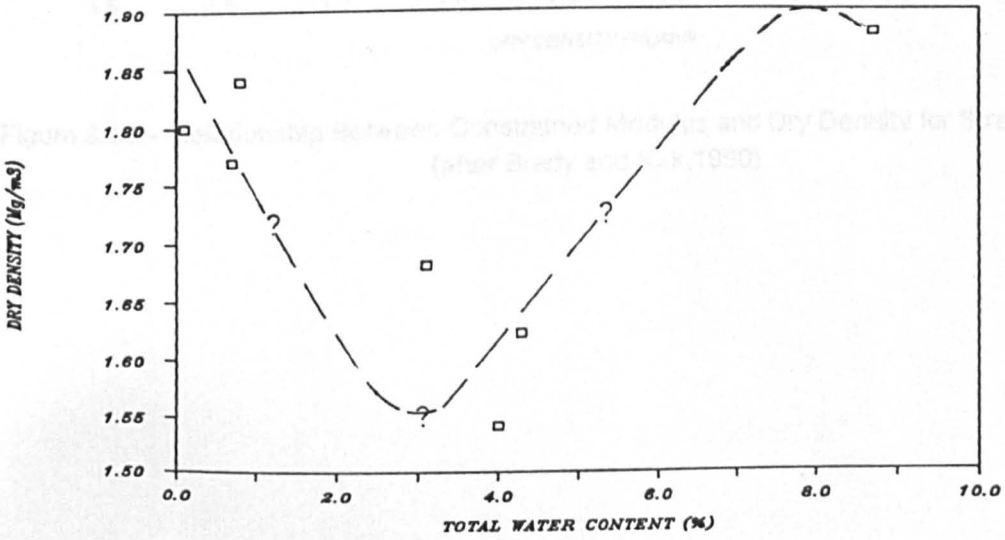

Figure 8.15 – TRRL Compaction Data For Low Compactive Effort

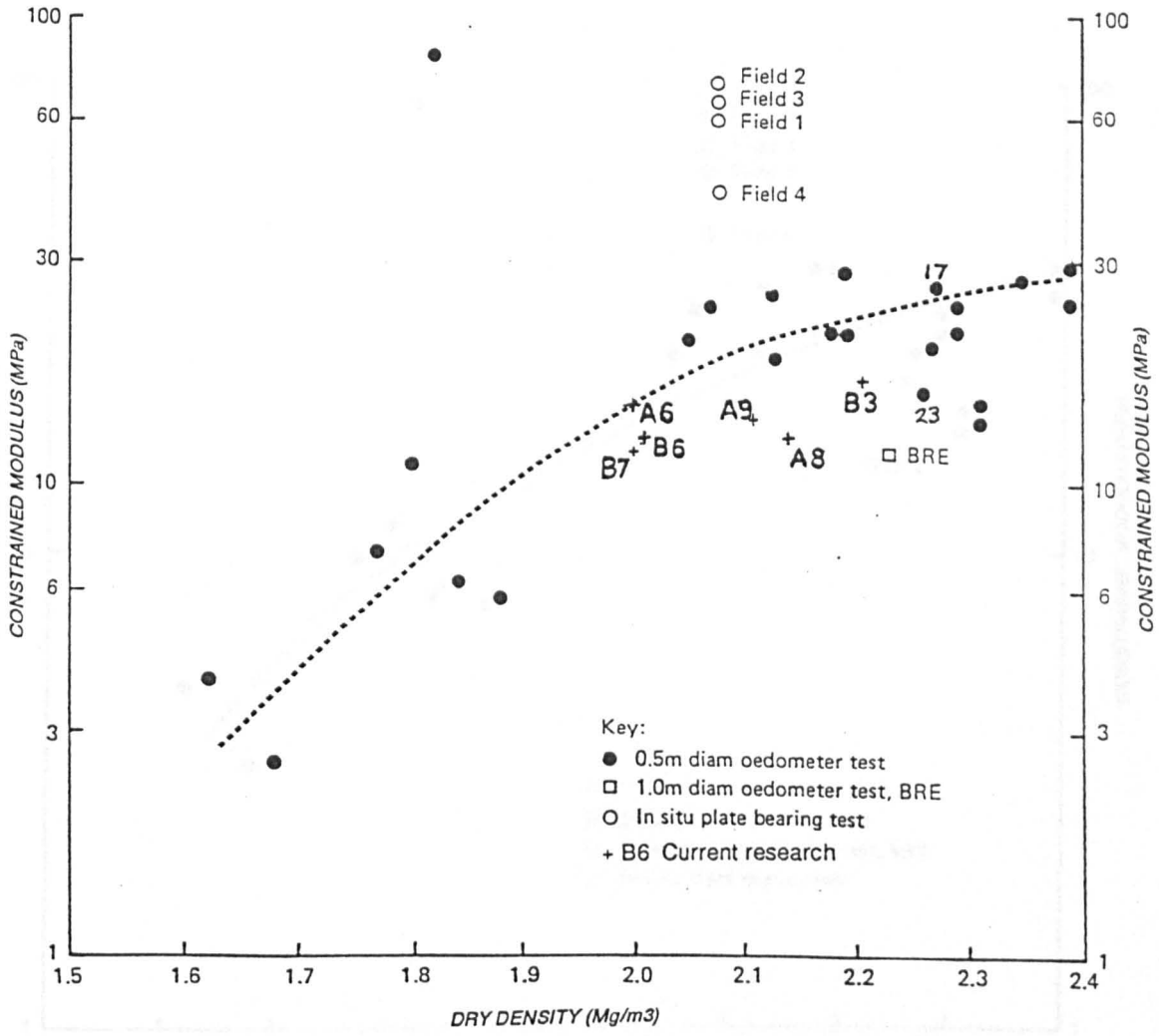

Figure 8.16 – Relationship Between Constrained Modulus and Dry Density for Stress Range 25–100kPa (after Brady and Kirk,1990)

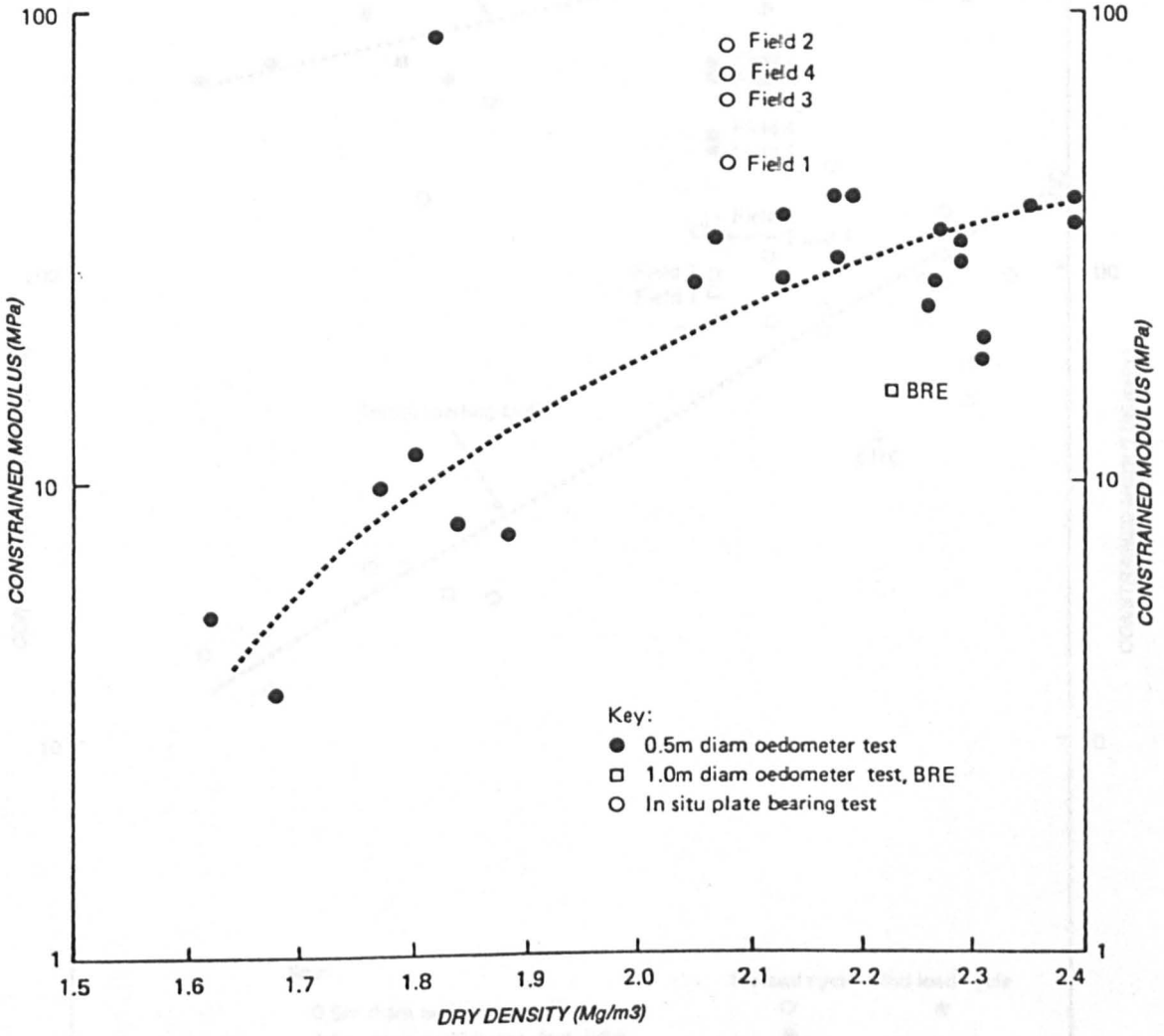

Figure 8.17 – Relationship Between Constrained Modulus and Dry Density for Stress Range 25–250kPa (after Brady and Kirk,1990)

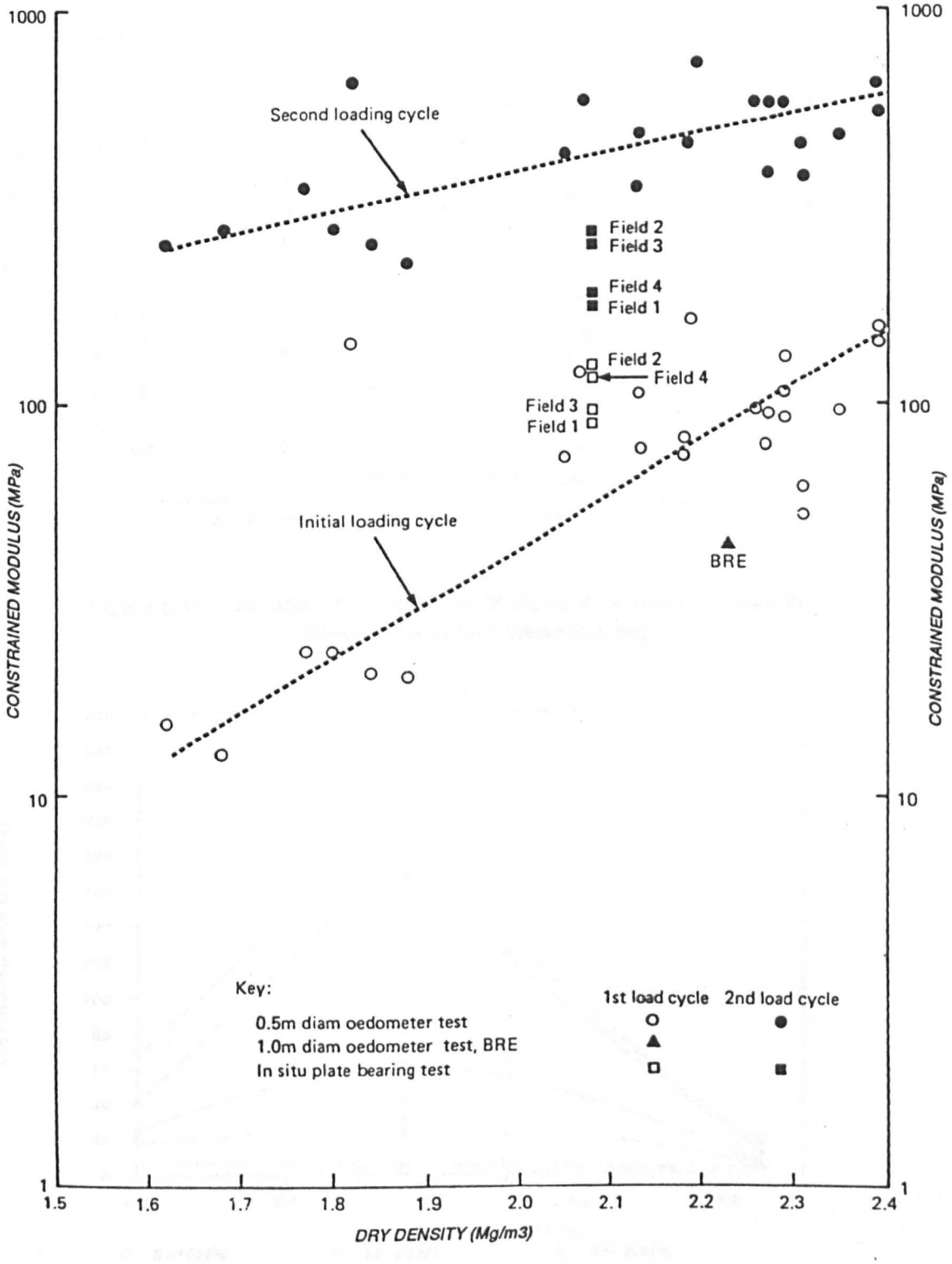

Figure 8.18 – Relationship Between Constrained Modulus and Dry Density for Stress Range 205–820kPa (after Brady and Kirk,1990)

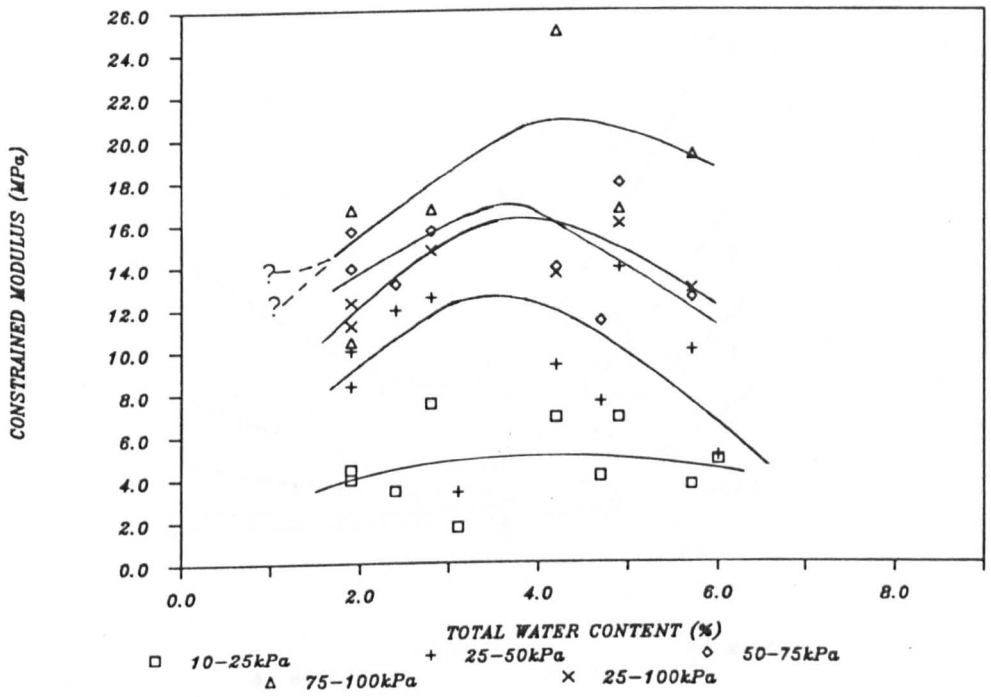

Figure 8.19 – Variation of Constrained Modulus With Water Content For Series A Tests on Coarse Grading

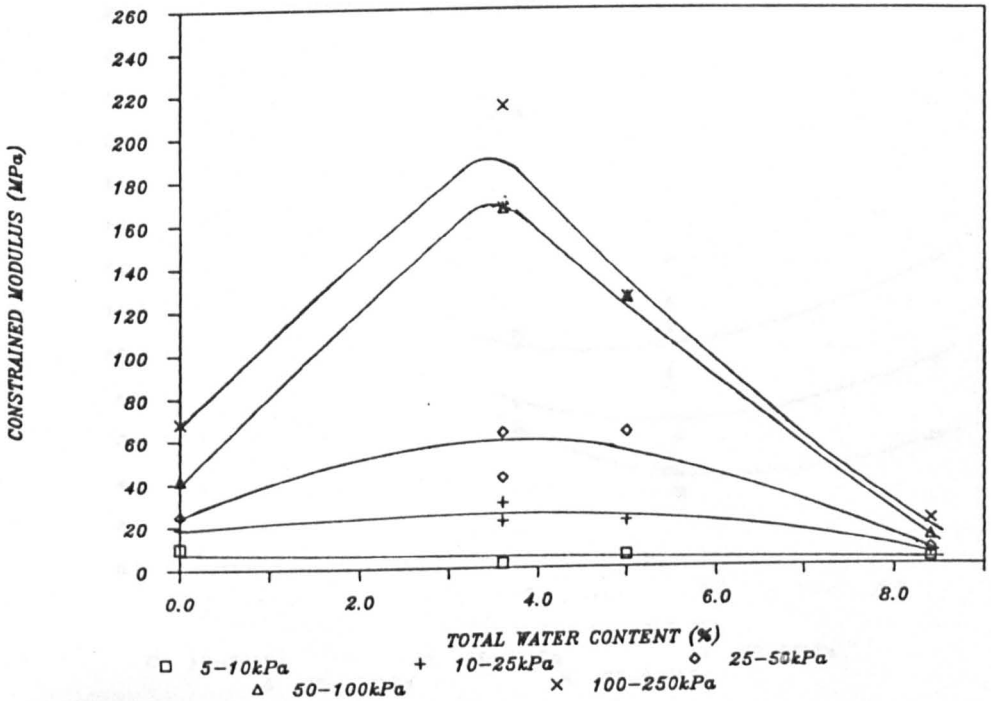

Figure 8.20 – Variation of Constrained Modulus With Water Content For Series D Tests on Coarse Grading Compacted With Usual Effort

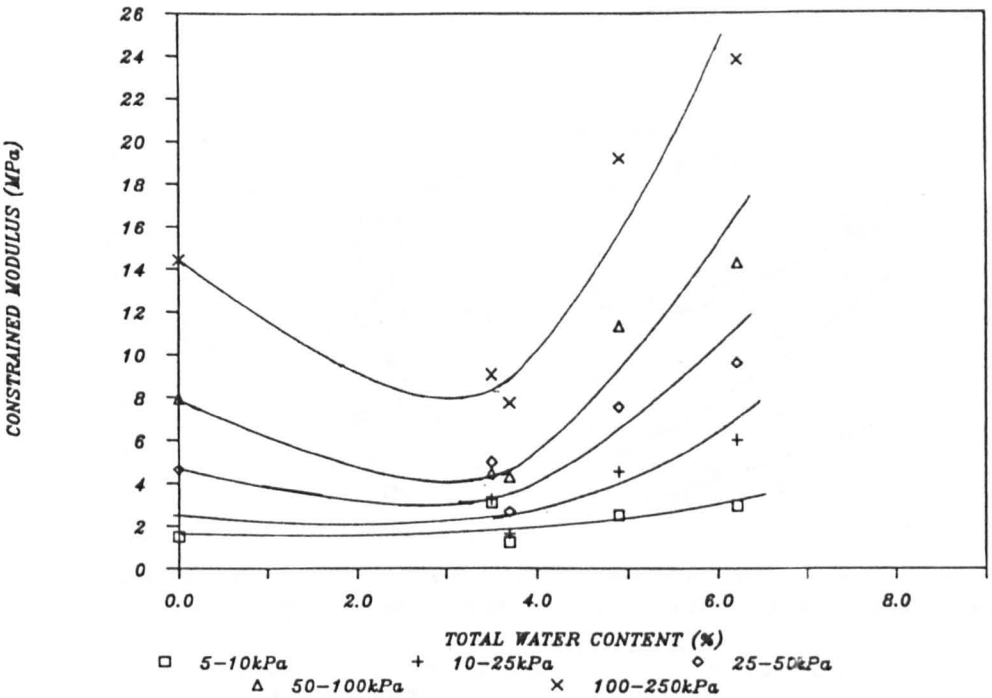

Figure 8.21 – Variation of Constrained Modulus With Water Content For Series D Tests on Coarse Grading Compacted With Low Effort

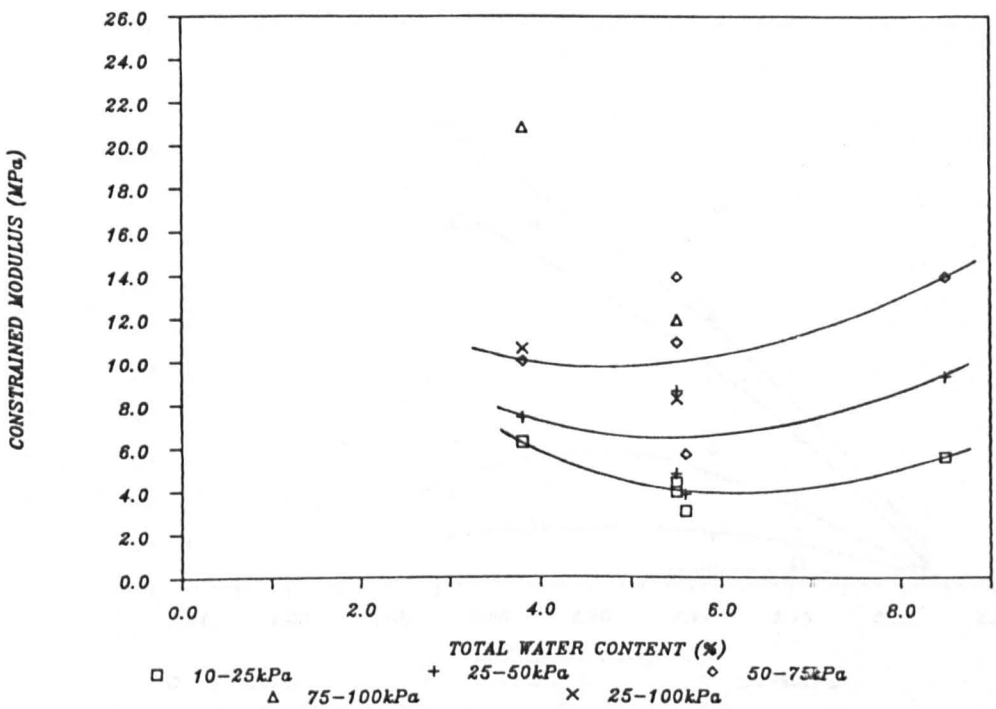

Figure 8.22 – Variation of Constrained Modulus With Water Content For Series A Tests on Fine Grading

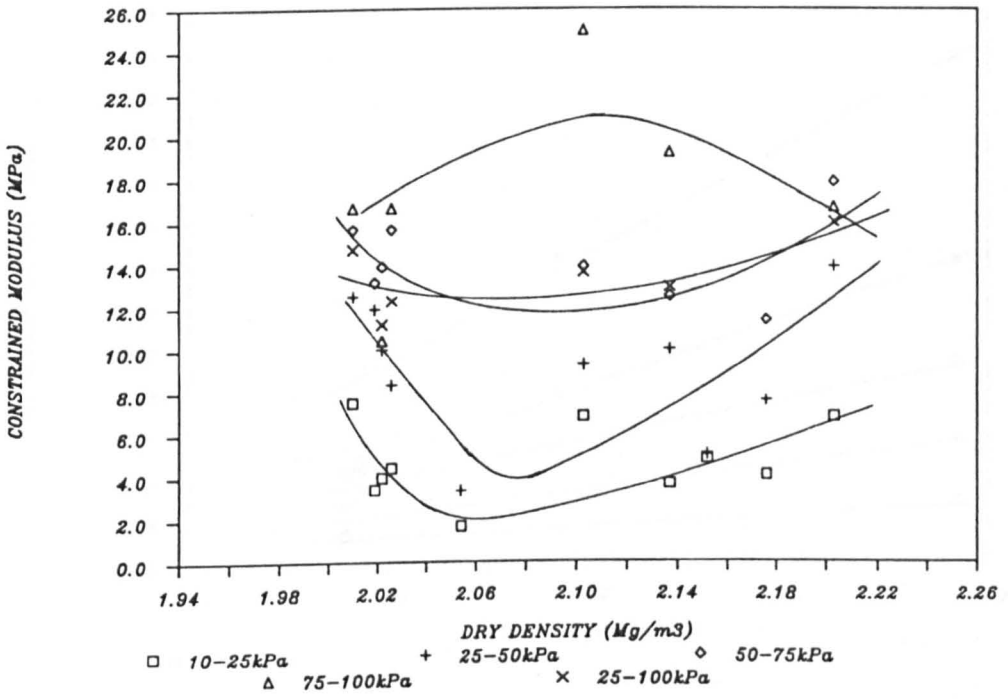

Figure 8.23 – Variation of Constrained Modulus With Dry Density For Series A Tests on Coarse Grading

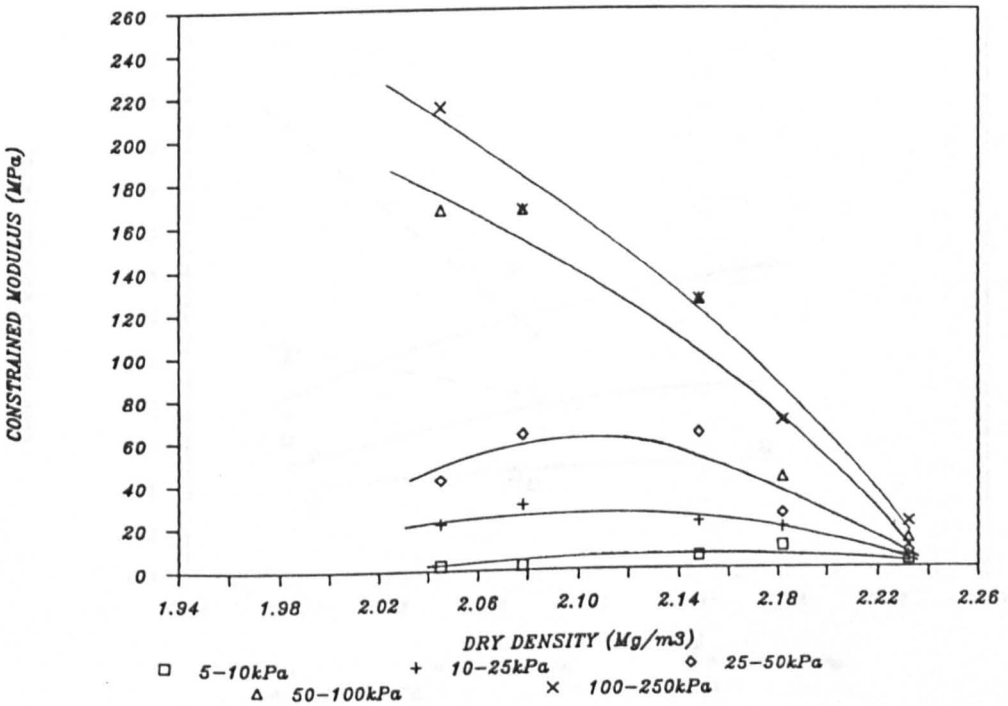

Figure 8.24 – Variation of Constrained Modulus With Dry Density For Series D Tests on Coarse Grading Compacted With Usual Effort

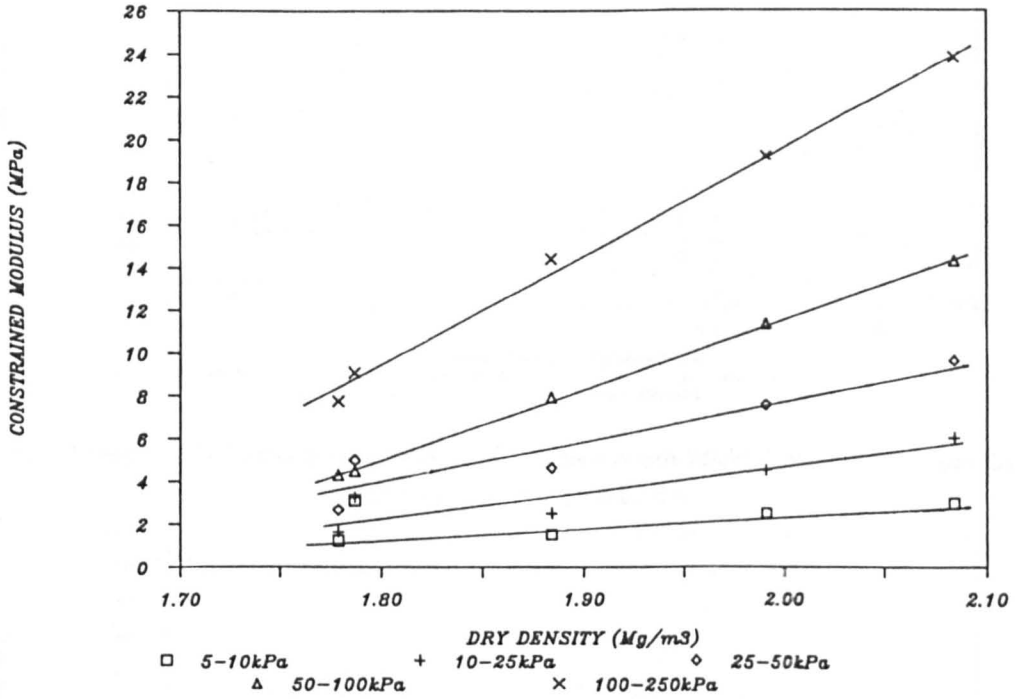

Figure 8.25 – Variation of Constrained Modulus With Dry Density For Series D Tests on Coarse Grading Compacted With Low Effort

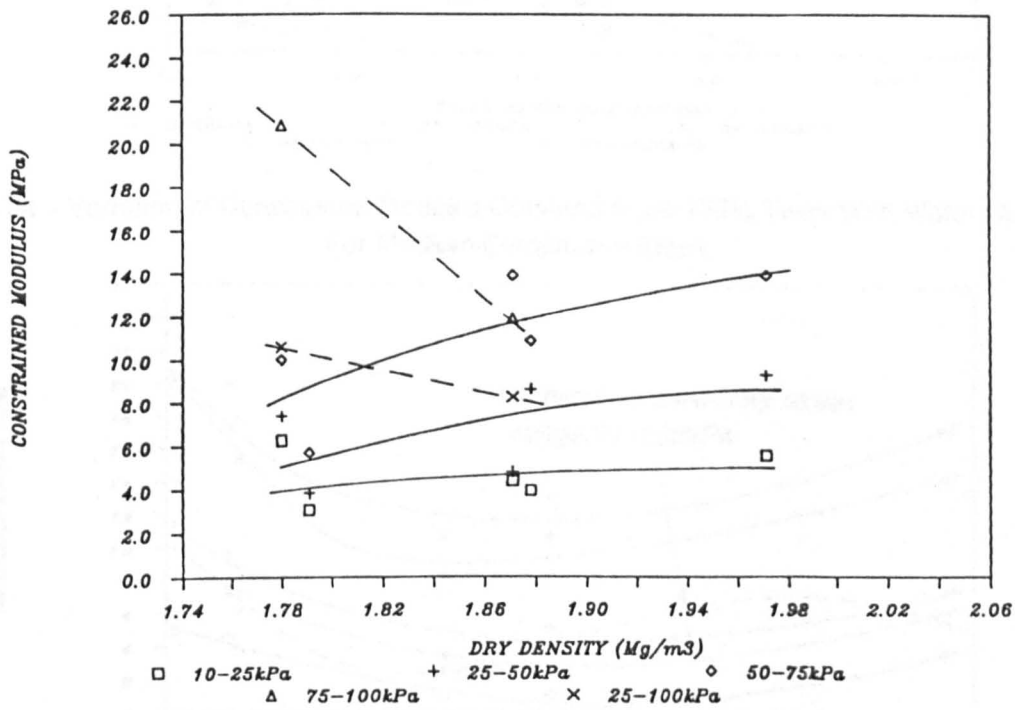

Figure 8.26 – Variation of Constrained Modulus With Dry Density For Series A Tests on Fine Grading

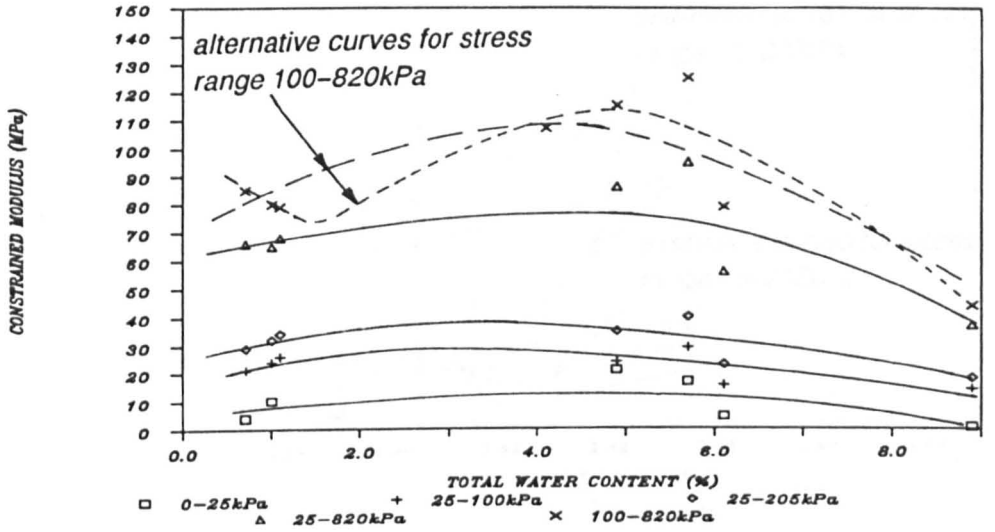

Figure 8.27 – Variation of Constrained Modulus Obtained From TRRL Tests With Water Content For High Compactive Effort

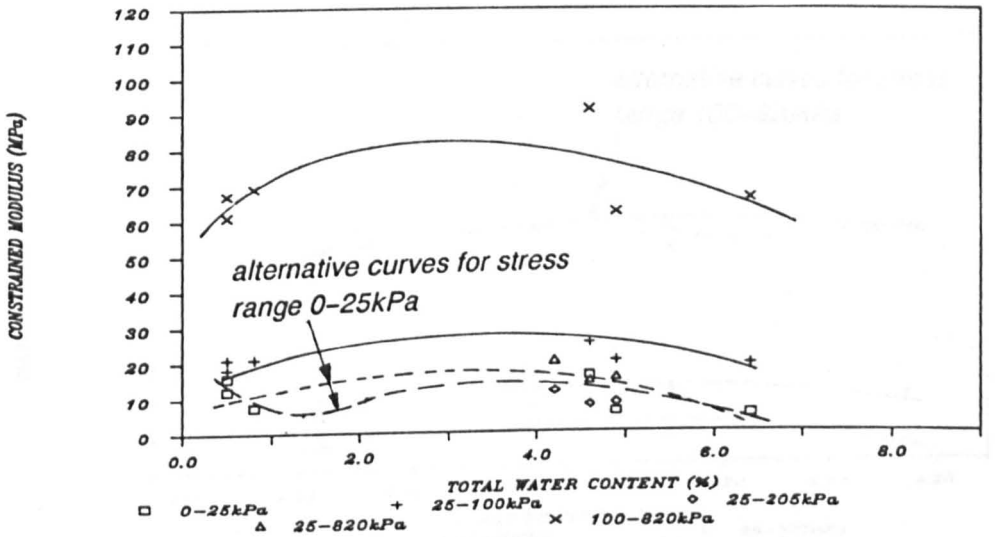

Figure 8.28 – Variation of Constrained Modulus Obtained From TRRL Tests With Water Content For Medium Compactive Effort

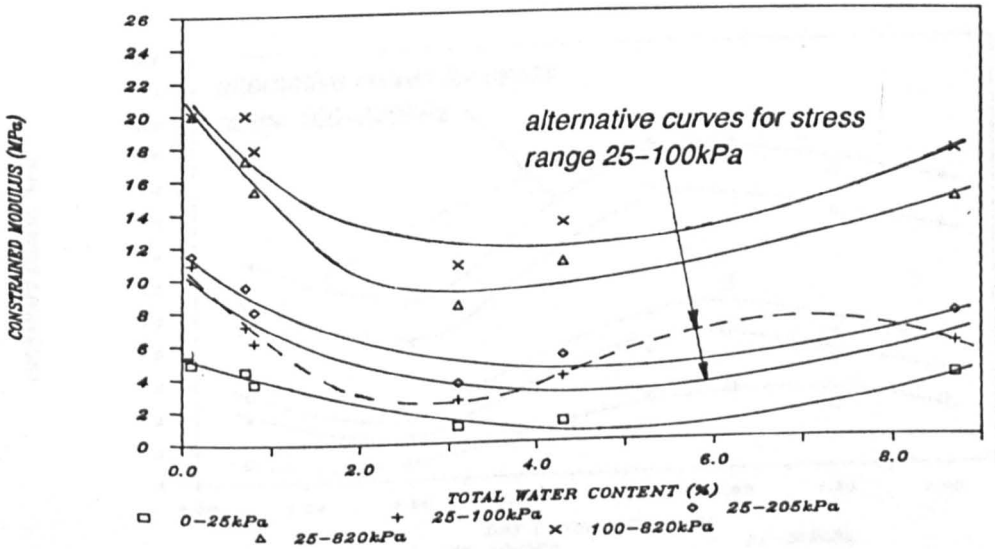

Figure 8.29 – Variation of Constrained Modulus Obtained From TRRL Tests With Water Content For Low Compactive Effort

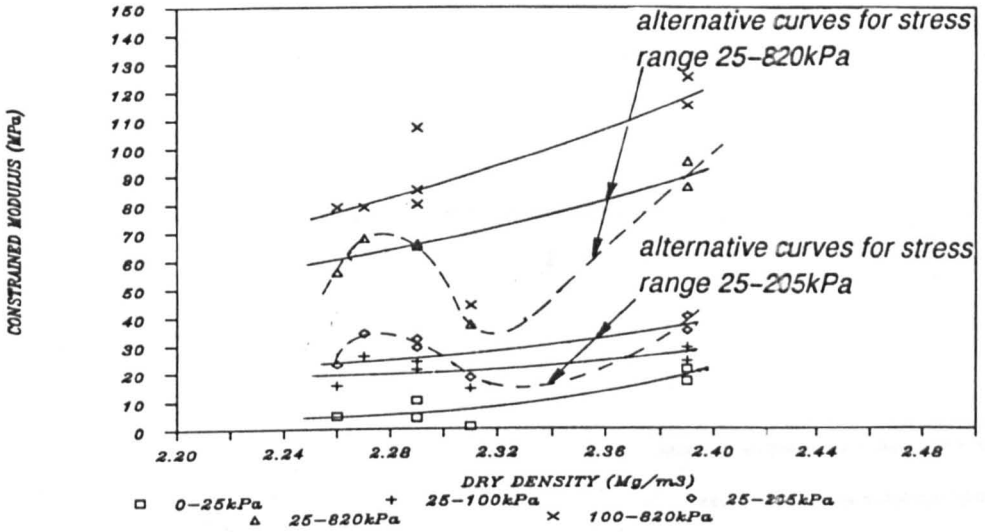

Figure 8.30 – Variation of Constrained Modulus Obtained From TRRL Tests With Dry Density For High Compactive Effort

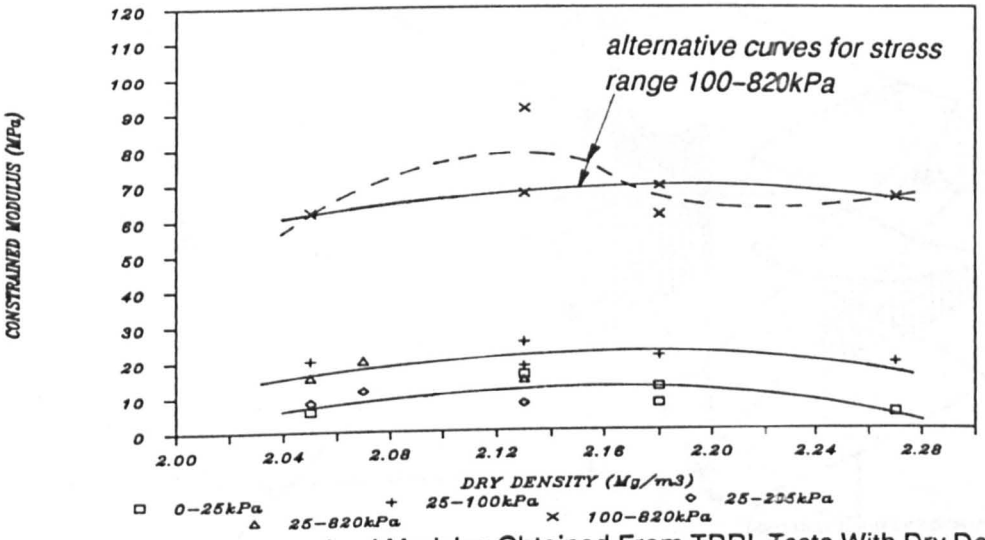

Figure 8.31 – Variation of Constrained Modulus Obtained From TRRL Tests With Dry Density For Medium Compactive Effort

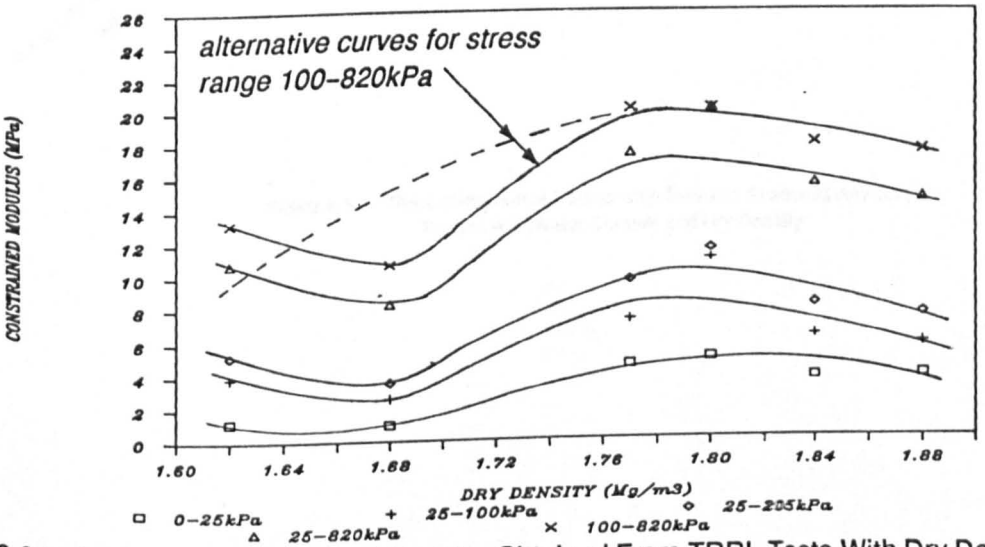

Figure 8.32 – Variation of Constrained Modulus Obtained From TRRL Tests With Dry Density For Low Compactive Effort

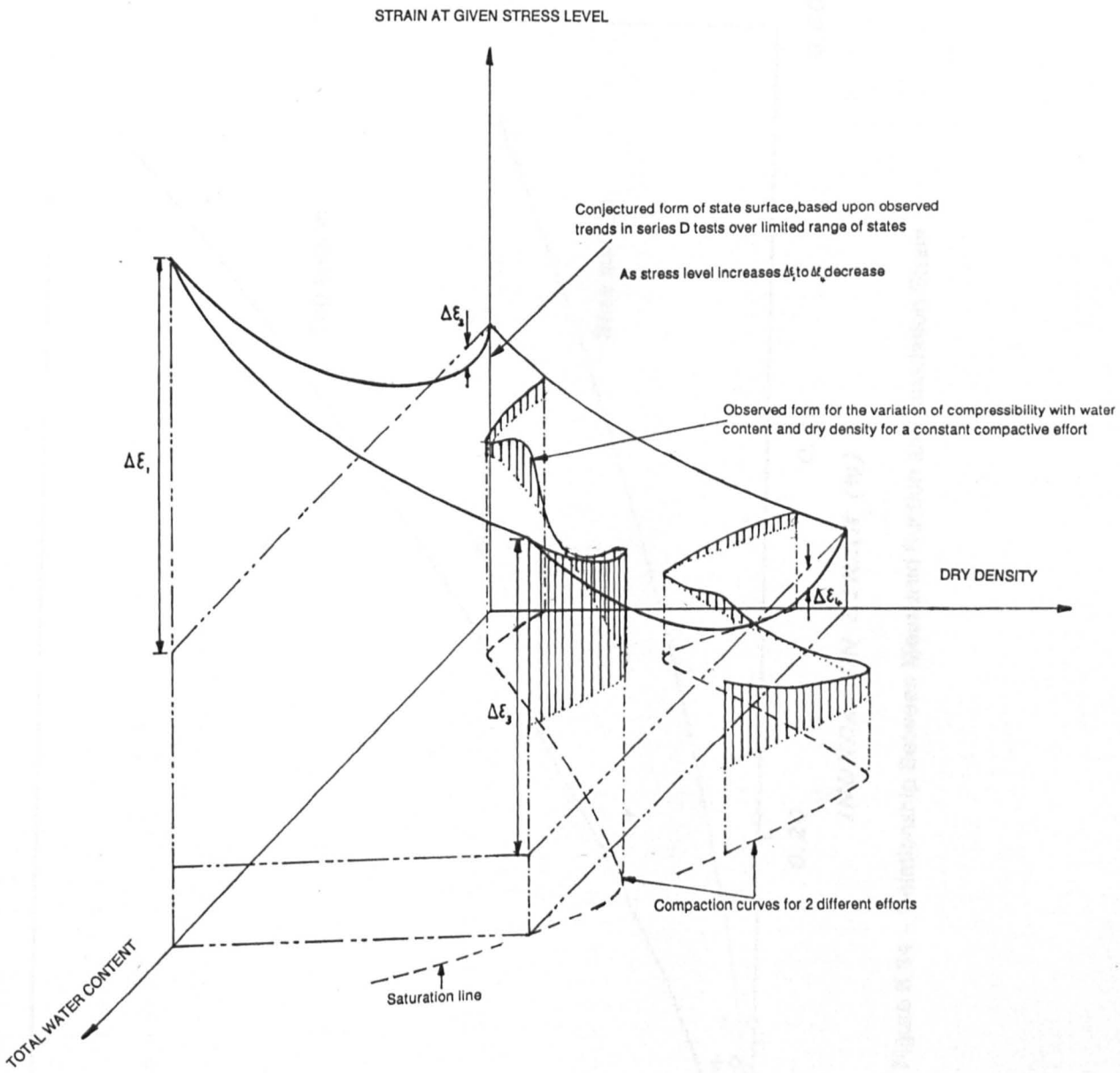

Figure 8.33 – Three Dimensional Relationship Between Strains At Any Given Stress Level,Water Content and Dry Density

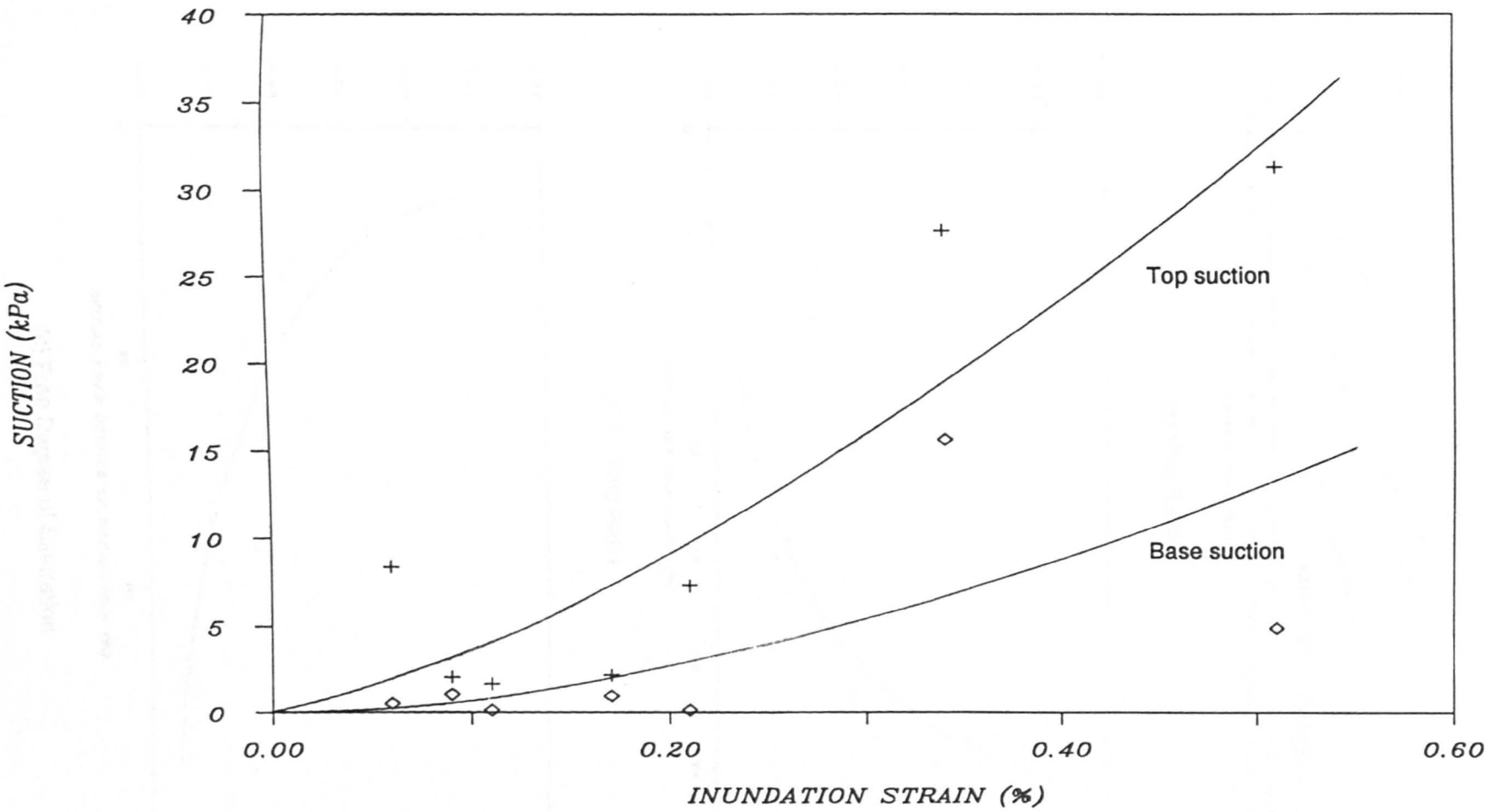

Figure 8.34 – Relationship Between Measured Suction and Inundation Strain

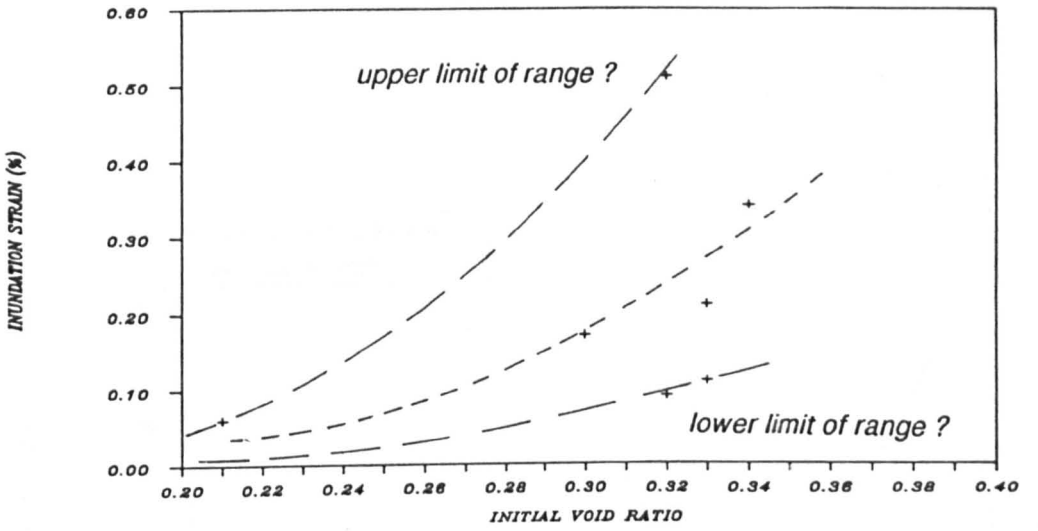

(a) Void Ratio

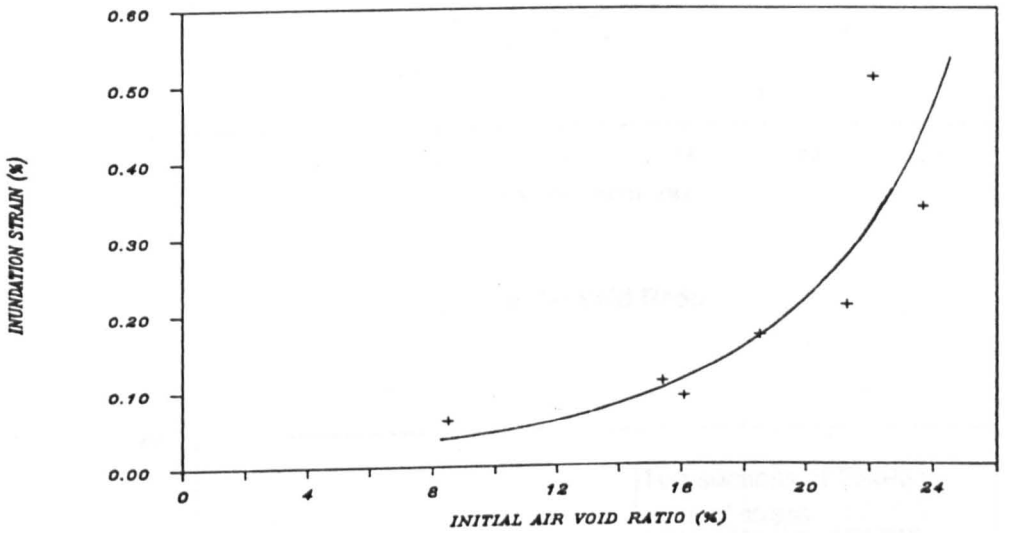

(b) Air Void Ratio

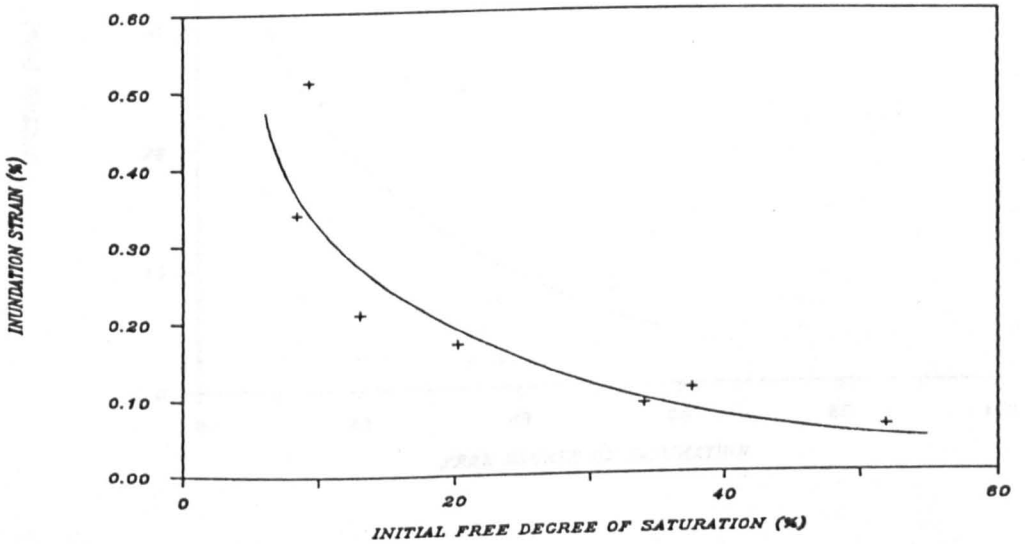

(c) Free Degree of Saturation

Figure 8.35 – Relationships Between Inundation Strain and Soil Parameters Void Ratio,Air Void Ratio and Free Degree of Saturation

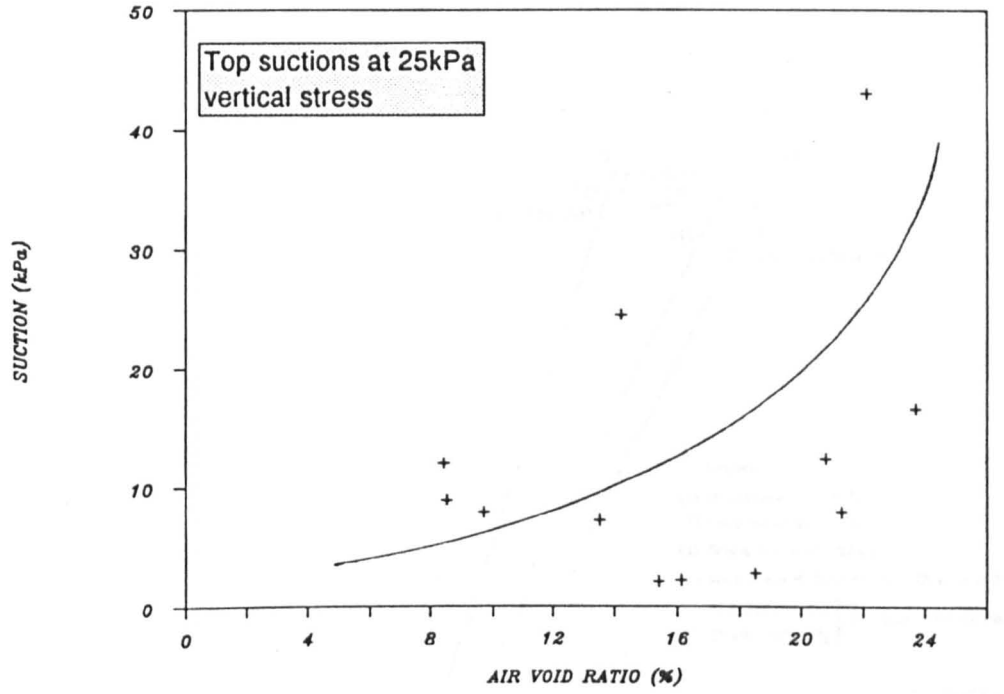

(a) Air Void Ratio

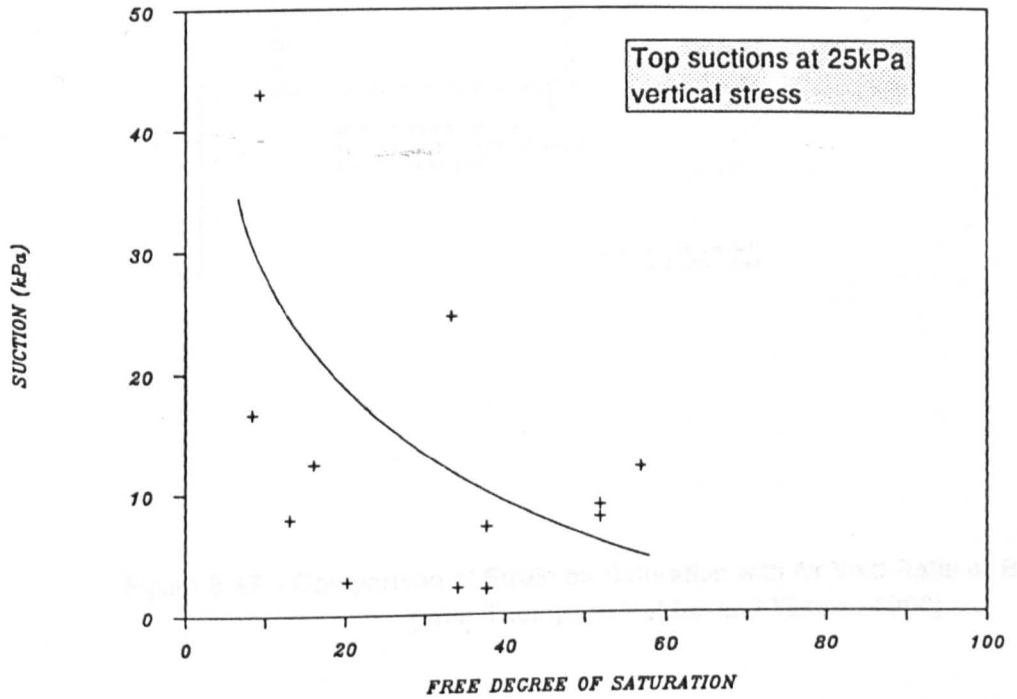

(b) Free Degree of Saturation

Figure 8.36 – Relationship Between Suction,and Air Void Ratio and Free Degree of Saturation

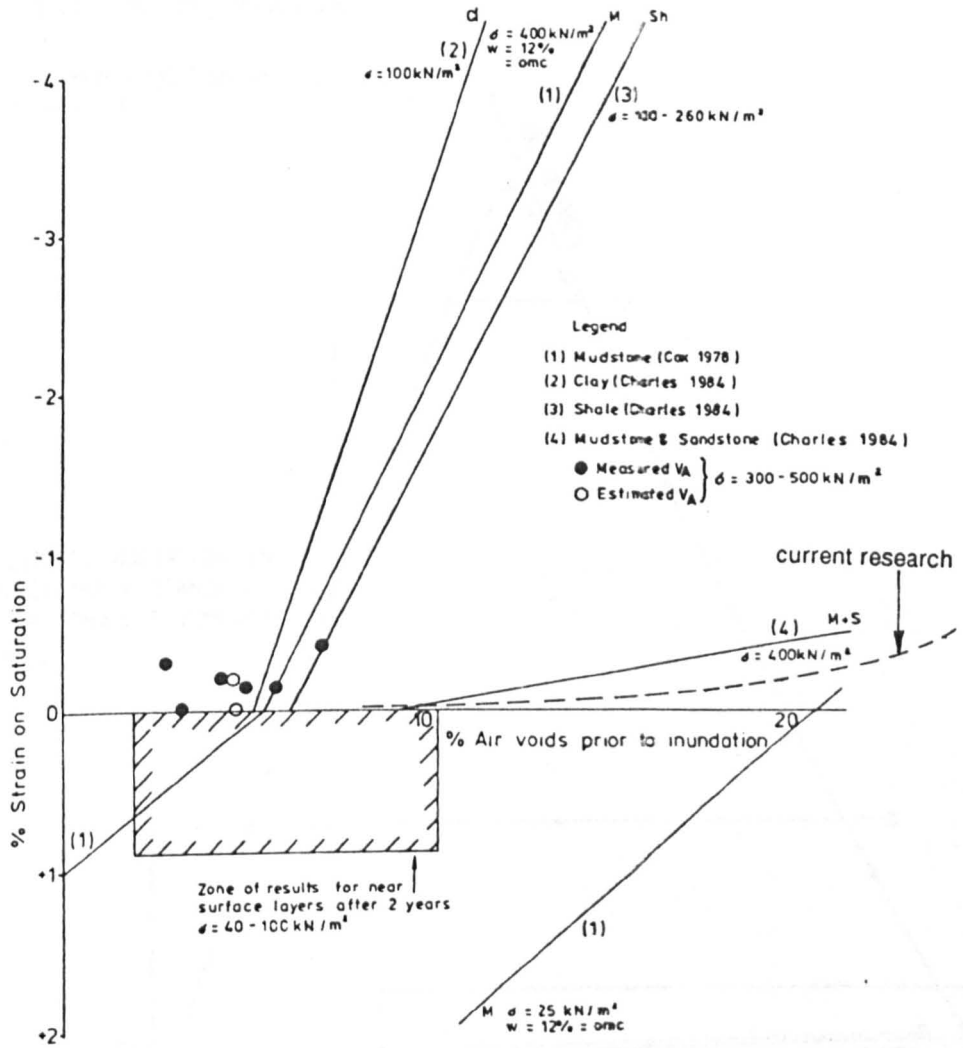

Figure 8.37 – Comparison of Strain on Saturation with Air Void Ratio of Backfill (after Thompson,Holden and Yilmaz , 1990)

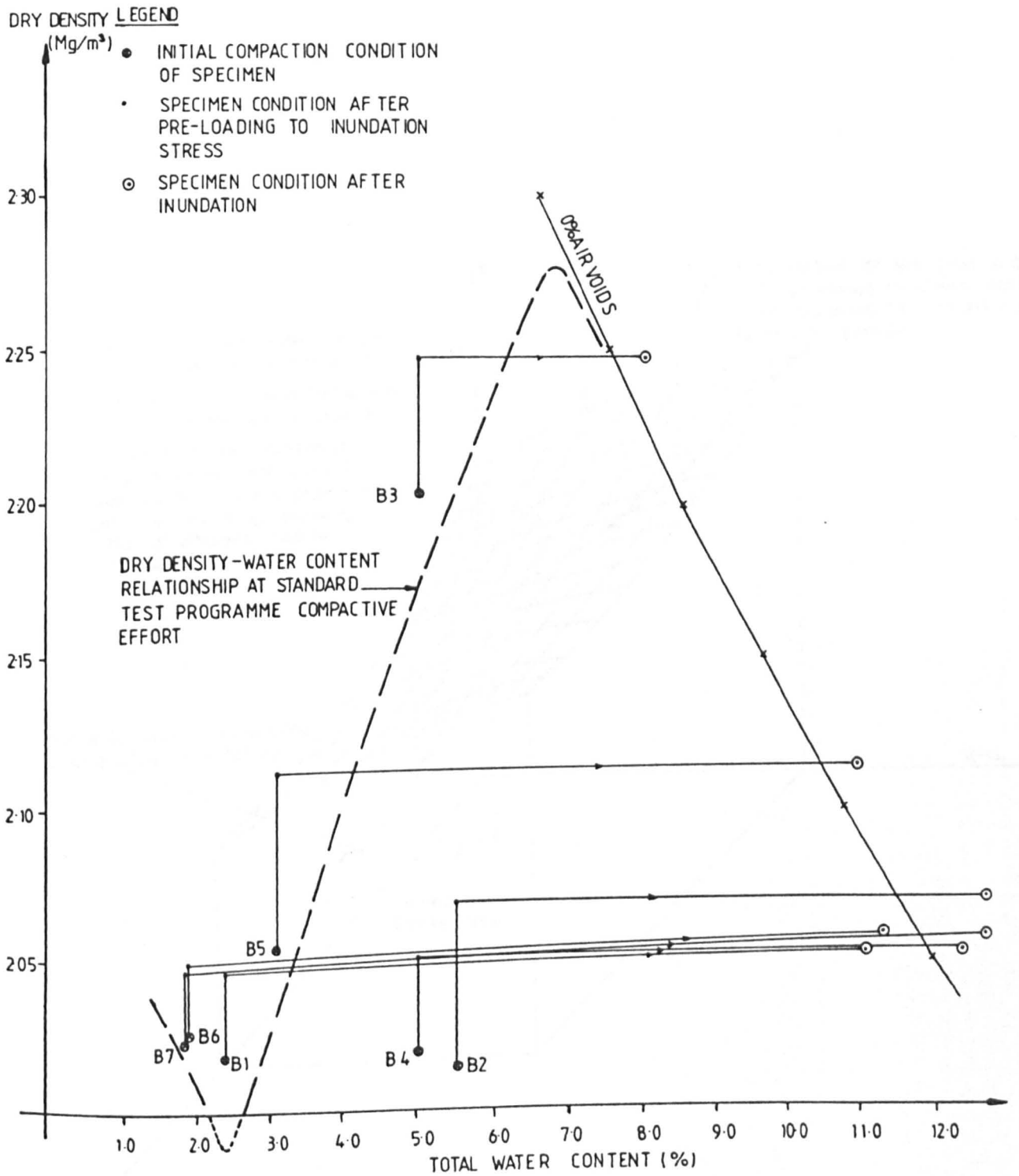

Figure 8.38 – Combined Effect of Total Stress Changes and Inundation on the Dry Density–Water Content Relationship for the Coarse Grading

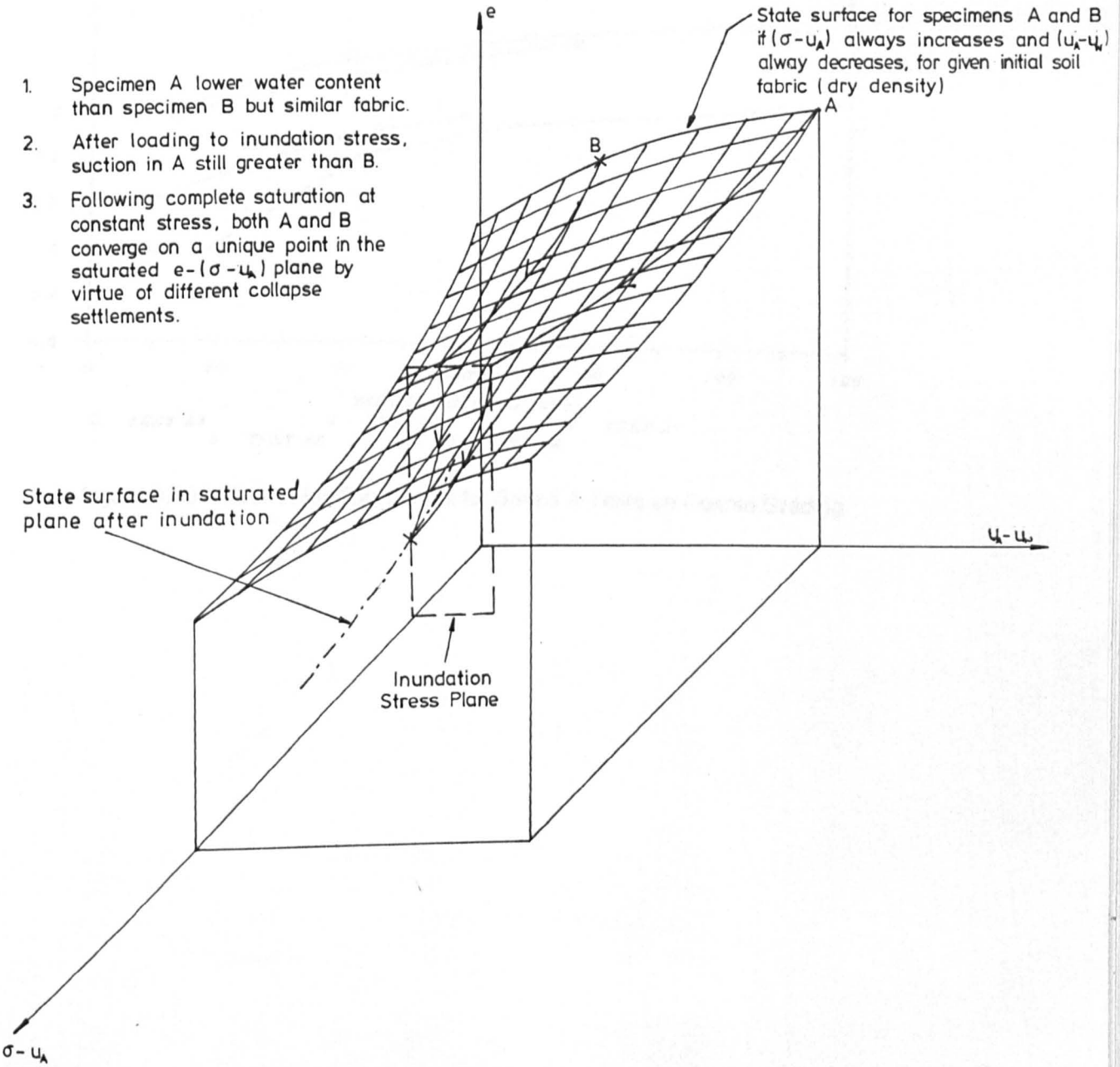

Figure 8.39 - Loading and inundation stress paths for two different specimens showing uniqueness of final saturated state.

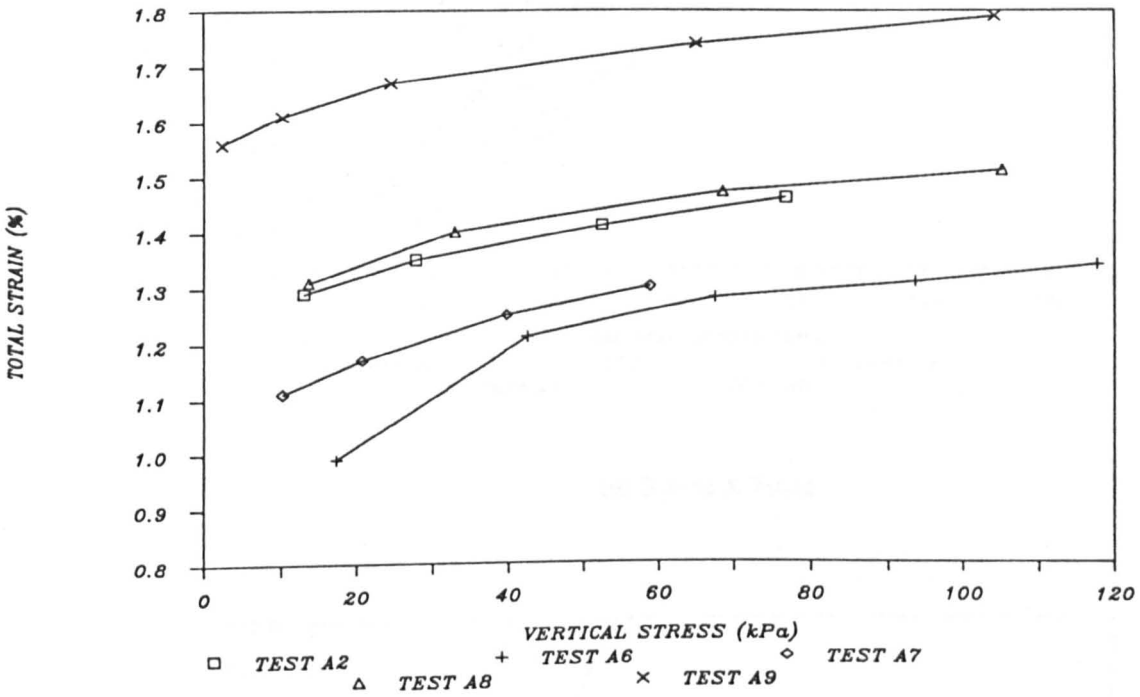

Figure 8.40 – First Unloading Curves for Series A Tests on Coarse Grading

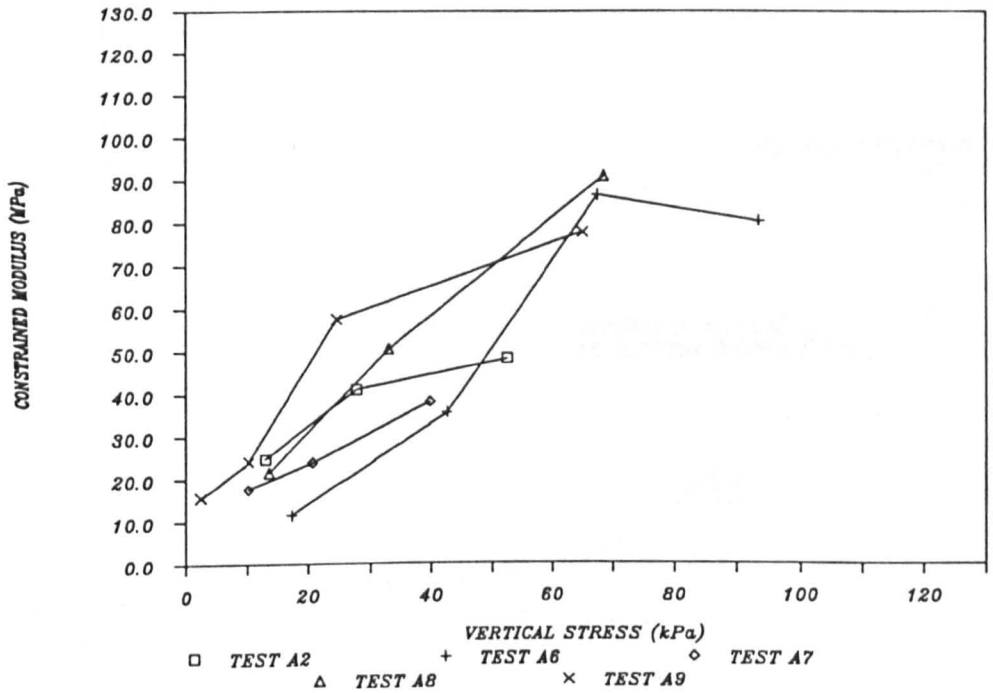

(a) Series A Tests

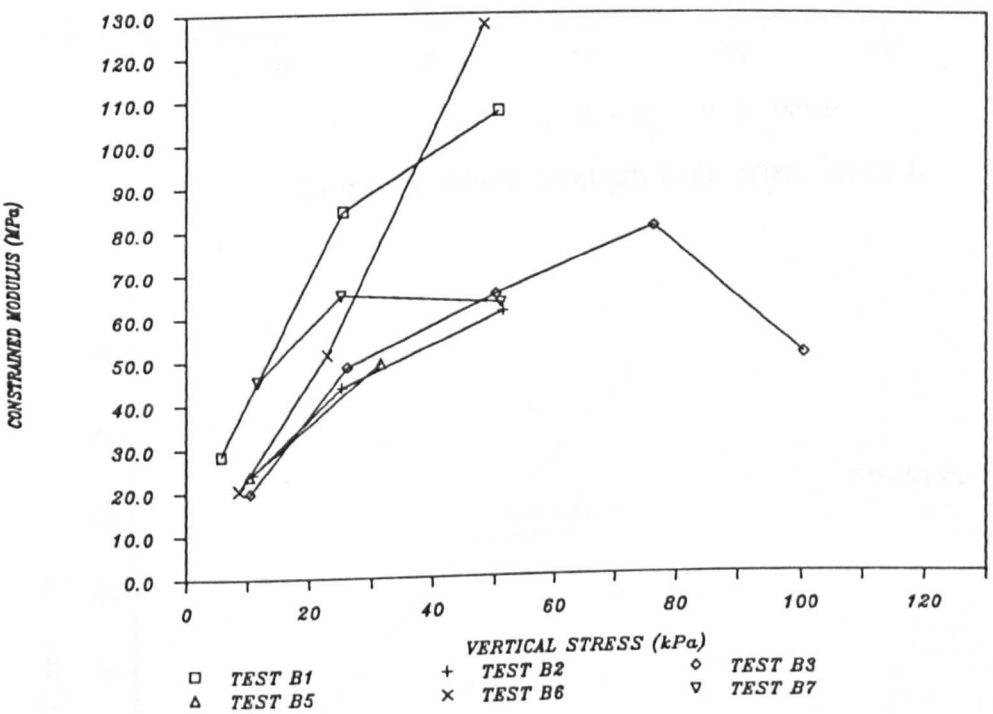

(b) Series B Tests

Figure 8.41 – Effect of Stress Level On Unloading Constrained Modulus For Coarse Grading

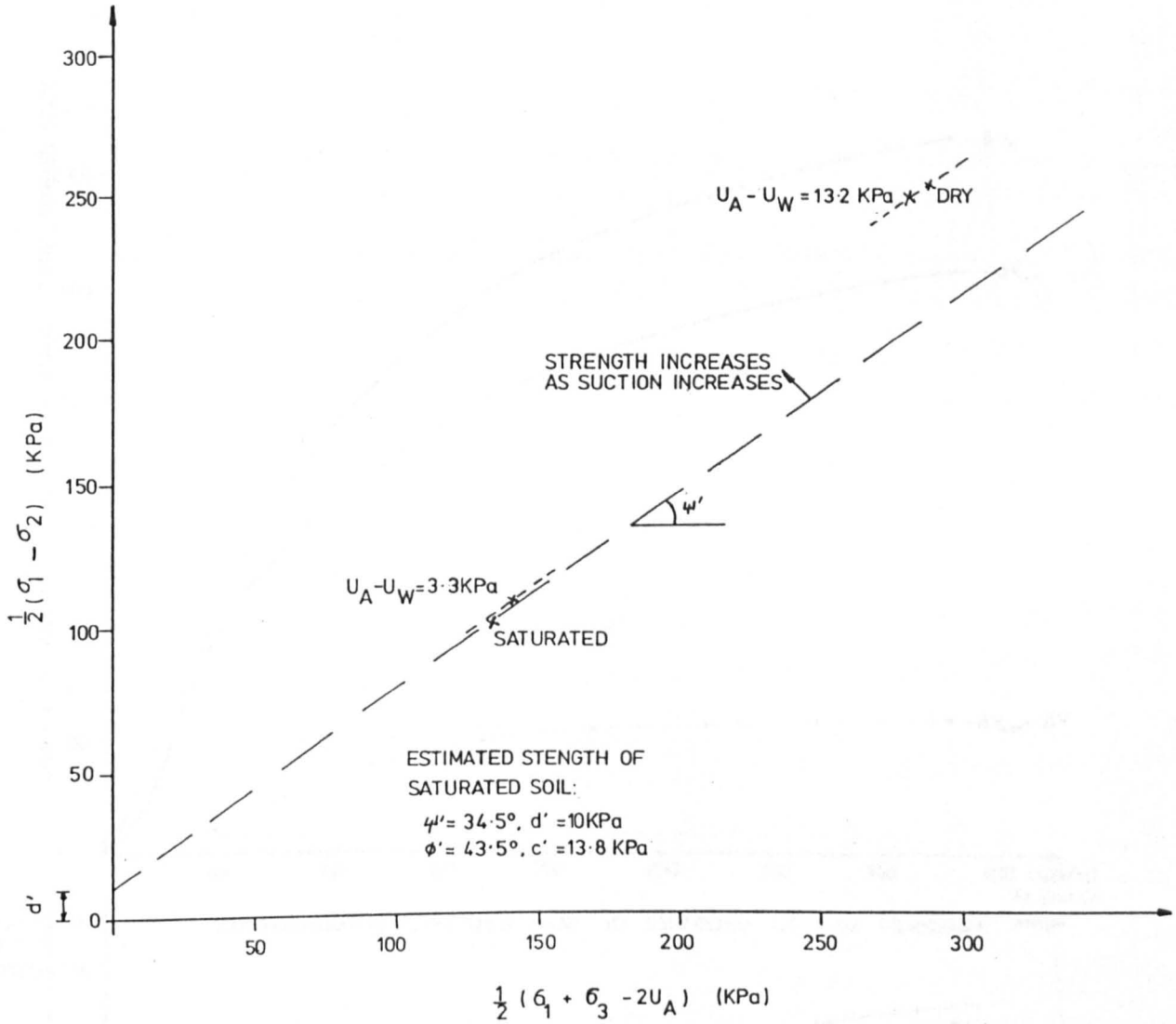

Figure 8·42 - Shear Strength Data From Series C

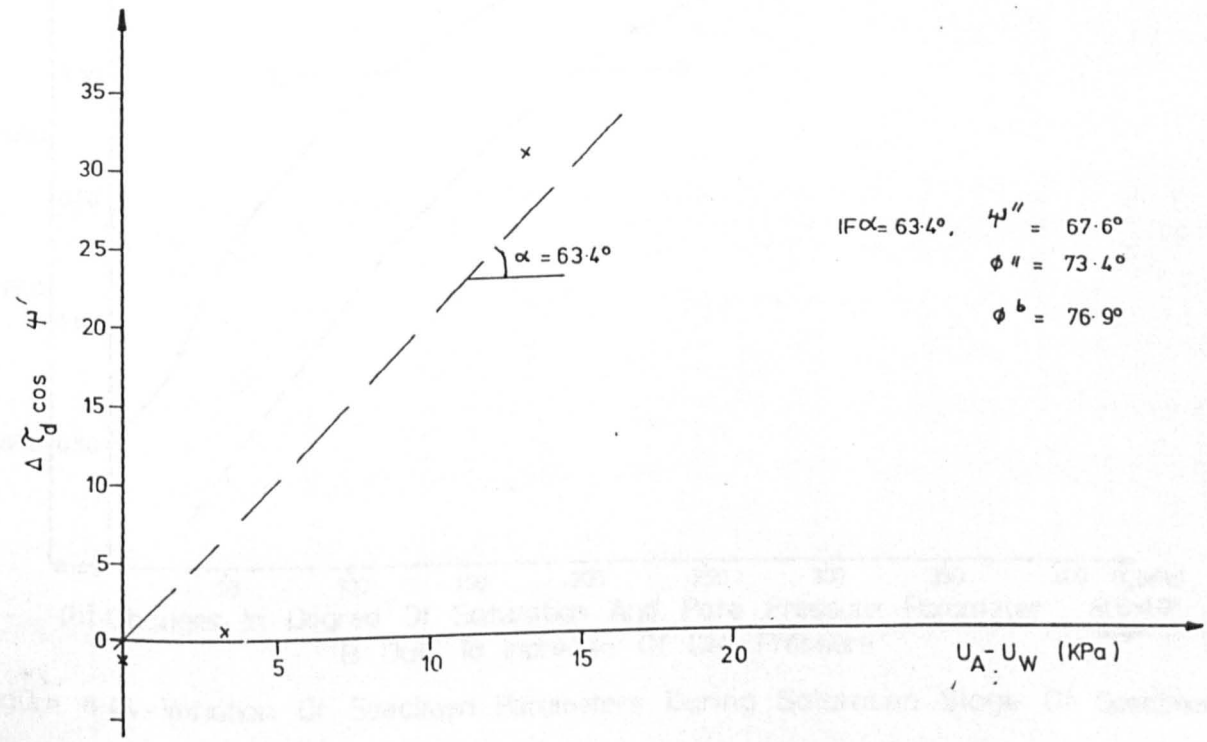

Figure 8·43 - Change in Shear Strength From Saturated Plane

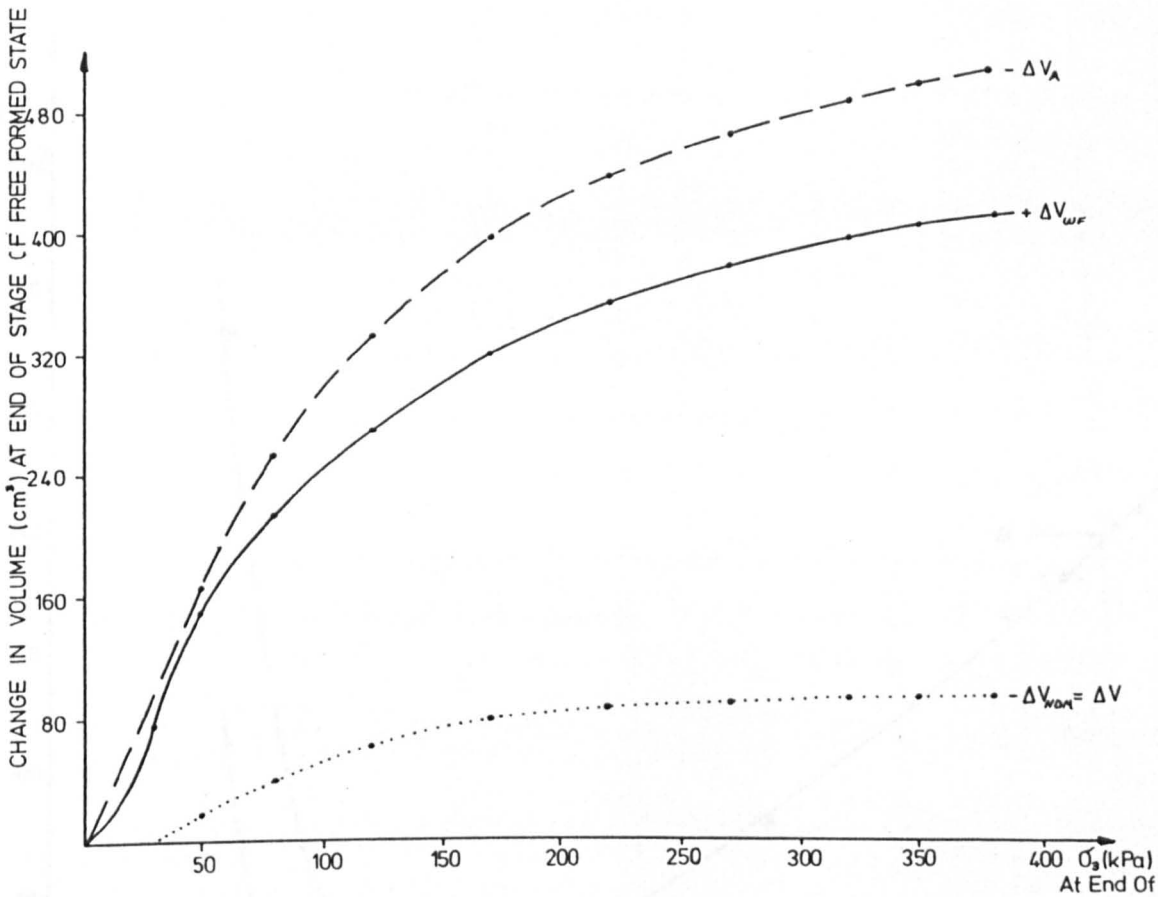

(a) Volumetric Changes Due To Increase Of Cell Pressure

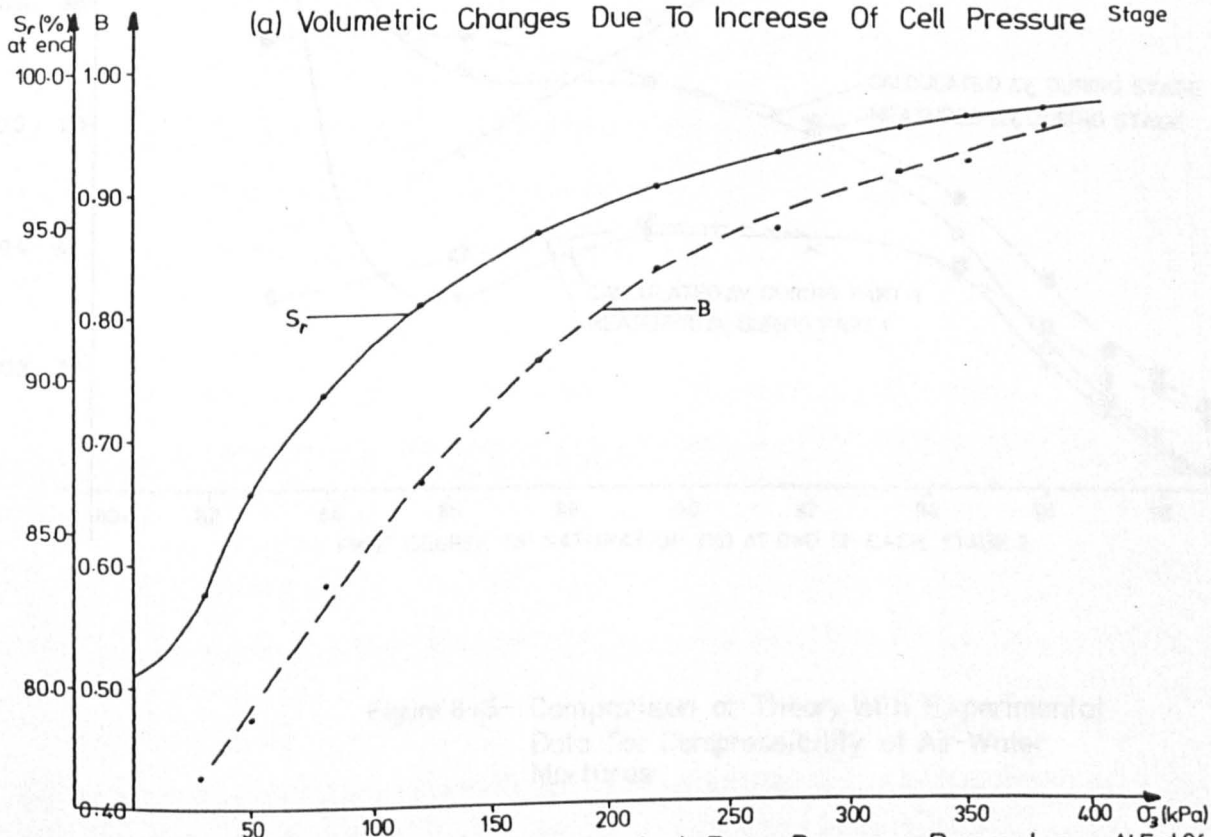

(b) Changes In Degree Of Saturation And Pore Pressure Parameter B Due To Increase Of Cell Pressure

Figure 8·44 - Variation Of Specimen Parameters During Saturation Stage Of Specimen C1

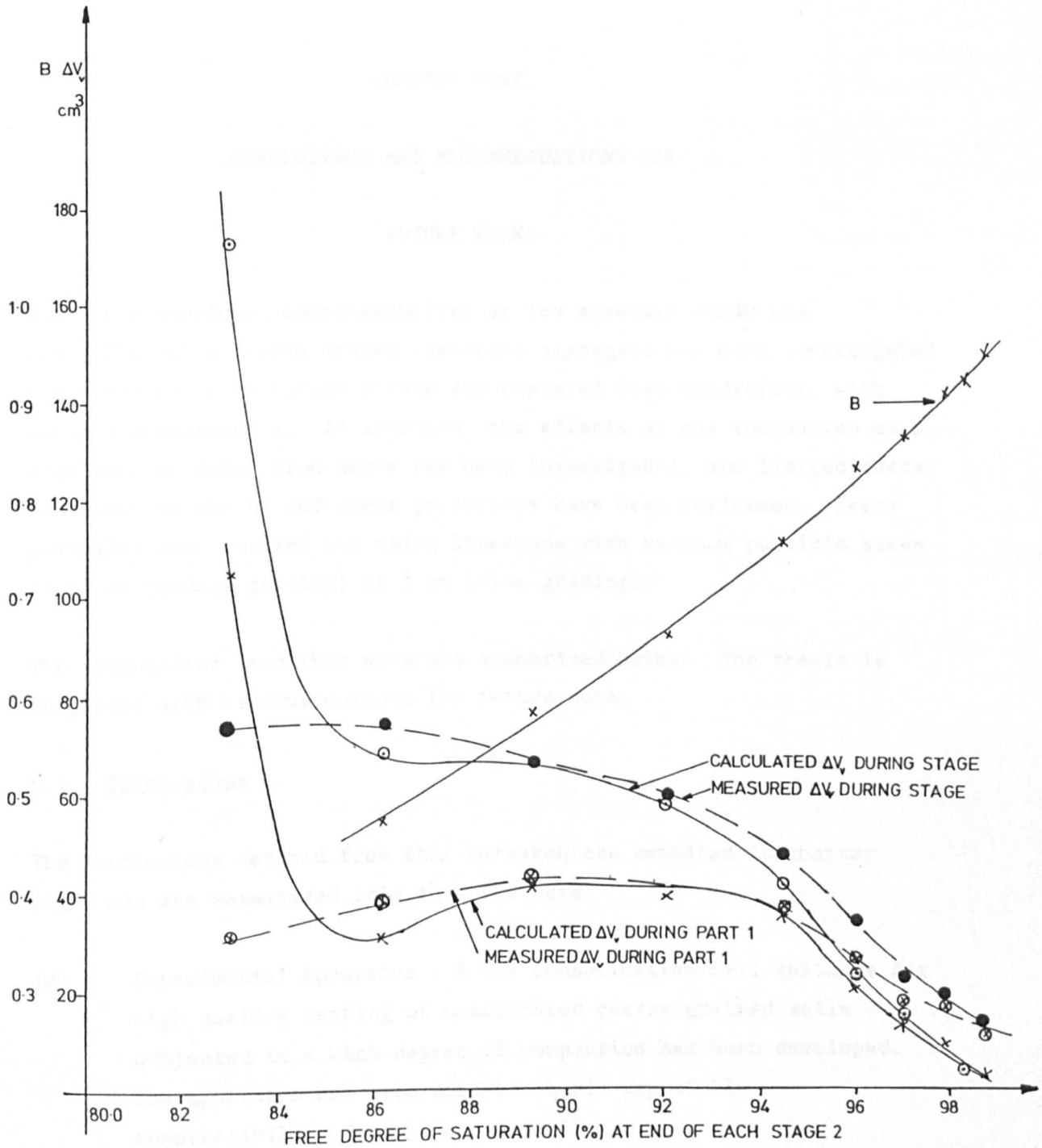

Figure 8·45- Comparison of Theory With Experimental Data For Compressibility of Air-Water Mixtures

CHAPTER NINE

CONCLUSIONS AND RECOMMENDATIONS FOR FUTURE WORK

The one dimensional compressibility at low stresses (<100 kPa typically) of a coarse graded limestone aggregate has been investigated under monotonic, constant strain and repeated load conditions, with suction measurements. In addition, the effects of the inundation at a slow rate of water from above has been investigated, and limited tests to determine the Ko and shear properties have been performed. Tests have also been carried out using limestone with maximum particle sizes of 20 mm (medium grading) or 5 mm (fine grading).

The conclusions from this work are summarised below. The thesis is completed with recommendations for future work.

9.1 Conclusions

The conclusions derived from this research are embodied in chapter eight and are summarised only in brief here:

(a) Experimental Apparatus : A new consolidation cell suitable for high quality testing of unsaturated coarse grained soils subjected to a high degree of compaction has been developed. The apparatus has been used to obtain repeatable compressibility data.

(b) Suctions : Measurable suctions have been demonstrated to exist within even the coarse grained material whose maximum particle size was 37.5 mm and whose silt and clay fraction was 7%. The suctions increased with decreasing water content, and were of similar order of magnitude in both the fine (5 mm maximum particle size, silt and clay fractions 12%) and the coarse

grading. The similarity is attributable to the congregation of fine particles around the contacts between larger particles. Measurement of the "average" suction condition within the soil mass does not reflect the range of suctions that will exist locally within the mass at low degrees of saturation when the water phase is discontinuous.

(c) Compressibility under Monotonic Load Conditions : Analysis of the current and previous research by others shows that the compressibility is a function of the dry density and water content of the compacted mass, particularly at low stresses. For a given compactive effort, compressibility increases to a low peak before decreasing once again as the water content increases from a dry condition to near but below optimum. As optimum is approached and passed, the compressibility rapidly increases. Over the same water content range, dry density tends to increase continually except for a trough at very low water contents and the peak at optimum.

The influence of water content is primarily attributed to the suction stresses within the soil mass, and the compressibility variations may be explained by reference to the measured suction- water content and dry density-water content relations. The increased coefficients of friction between particles at very low contents may be influential to some degree, as may segregation of fines during compaction at very high water contents.

The suction influence decreases as the applied stress increases, although values of constrained modulus from low to high stresses still reflect this factor. A three dimensional plot of compressibility, expressed as strain at any given stress level, against dry density and water content is proposed in order to model correctly the influences identified without introducing the complexity of stress level dependence associated with use of the constrained modulus.

(d) Compressibility under Strain Controlled Conditions : Similar compressibility trends were observed from the monotonic and stain controlled tests, but strains measured during the former were significantly smaller than those during the latter. The difference in stress application period between the tests accounts for all of the apparent discrepancy. "Long-term" strains continued to be developed after several hours during the monotonic tests, and the "immediate" strain component was highly dependent in magnitude upon the time period over which it is measured. Close definition of this period must be made whenever immediate strains are considered.

Defining "immediate" to be the first 2 to 5 minutes after loading, the ratio of the immediate to time dependent components was shown to be related to the total stress. The ratio decreased from 0.7 to 1.0 at very low stresses, to 0.3 to 0.8 at a stress of 100 kPa.

(e) Inundation Effects : Small strains were observed to follow rapidly after onset of inundation at a constant total stress level. These strains were shown to be closely related to the suctions within the soil before inundation, and could also be related to the degree of saturation and air voids ratio which reflect the suction condition of the soil. The immediacy of the strains reflects the dominant suction influence, rather than the longer term mechanism of particle softening.

(f) Repeated Load Effects : The strains developed during the first 4 load cycles of the heavily compacted coarse grained material were shown to vary with the water content in a similar manner to compressibility, that is to be a function of water content and dry density. Use of a lower compactive effort indicated an overriding influence of dry density. Patterns of strain accumulation were different for each effort and for

the other 2 gradings. The heavily compacted specimens showed little strain accumulation after the first cycle, whereas a near linear strain accumulation with load cycle was observed with the lower effort. The medium grading behaved in a similar manner to the heavily compacted coarse grained material, and the fine grained material behaved in a manner intermediate between the two extremes. Strain rate had no apparent influence on behaviour within the range 0.1 mm/minute to 2 mm/minute used in the test programme.

(g) K_o Determinations : The tests produced a reliable value of 0.41 for K_o and a tentative value of 0.39.

(h) Shear Strength : The data revealed an apparently large suction influence in terms of the Mohr-Coulomb type failure parameters for unsaturated soils, with $c' = 13.8$ kPa, $\phi' = 43.5^\circ$ and $\phi^b = 70^\circ$ to 80°. Some of this apparent suction influence on ϕ^b was attributed to interparticle friction coefficients, but its significance was shown to be less dramatic by consideration of the likely maximum suction within the soil that affected shear behaviour.

9.2 Recommendations for Future Work

The establishment of a performance or even end product specification requires a large number of different materials, conditions and stress regimes to be investigated. Some suggestions for future work to achieve this aim, and others of a more fundamental nature, are noted below:

(a) further investigation of the compressibility-dry density-water content relationship under monotonic loading conditions should be completed over a wide range of water contents and compactive efforts, in order to verify and define a three dimensional relationship for the limestone;

(b) the relationship postulated in (a) should be investigated for a wide range of gradings and aggregate types;

(c) the existence of a similar relationship for repeated load conditions should be investigated, for a variety of compactive efforts;

(d) the effect of non-Ko conditions on compressibility should be assessed from triaxial tests;

(e) the factors affecting measured soil suctions in coarse grained materials should be defined, such as maximum particle size, grading, silt/clay contents, particle angularity and particle petrography. The formulation of a theoretical model to predict the measured suctions should be attempted. A statistical approach based upon observed particle distributions is likely to be the most successful technique;

(f) the validity of the capillary theory for coarse grained soils at low degrees of saturation should be investigated using experimental techniques, and its applicability or otherwise to highway design assessed;

(g) the effect of grading, compaction, water content and dry density on inundation strains should be investigated;

(h) the effects of changes in interparticle coefficients of friction and crushing on performance should be investigated;

(i) the apparent large influence of suction (and/or interparticle friction) on shear behaviour at low stresses should be verified.

REFERENCES

Aitchison, G D (1956). "The circumstances of unsaturation in soils with particular reference to the Australian environment", Proc 2nd Australia - New Zealand Conf on SMFE, Christchurch, N Z: 173-191

Aitchison, G D (1965). Contribution to conference technical session 2, Proc 6th ICSMFE, Montreal, 3: 318-321

Aitchison, G D and I B Donald (1956). "Effective stresses in unsaturated soils", Proc 2nd Australia - New Zealand Conf on SMFE, Christchurch, N Z: 192-199

Aitchison, G D and J A Woodburn (1969). "Soil suction in foundation design", Proc 7th ICSMFE, Mexico, 2:1-8

Alonso, E E, A Gens and D W Hight (1987). "General report, Session 5: Special Problem Soils", Proc 9th ECSMFE, Dublin, 3: 1087-1146

Alonso, E E, A Gens and A Josa (1990). "A constitutive model for partially saturated soils", Geotechnique, 40: 405-430

Aschenbrenner, B C (1956). "A new method of expressing particle sphericity", J. Sed. Petrology, 26: 15 - 31

Barden, L, A O Madedor and G R Sides (1969). "Volume change characteristics of unsaturated clay", JSMFD, ASCE, 95 (SM1): 33-52

Barden, L and G R Sides (1970). "Engineering behaviour and structure of compacted clay", JSMFD, ASCE, 96 (SM4): 1171-1200

Bishop, A W (1960). "The principle of effective stress", NGI Pub 32: 1-5. Reprinted from Teknisk Ukeblad, 106 (No 39), 1959

Bishop, A W and G E Blight (1963). "Some aspects of effective stress in saturated and partly saturated soil", Geotechnique, 13: 177-197

Bishop, A W and I B Donald (1961). "The experimental study of partly saturated soil in the triaxial apparatus", Proc 5th ICSMFE, Paris, 1: 13-21

Blight, G E (1965). "Effective stress evaluation for unsaturated soils", JSMFD, ASCE, 93 (SM2): 125-148

Bocking, K A and D G Fredlund (1980). "Limitations of the axis translation technique", Proc 4th Int Conf on Expansive Soils, Colorado, USA: 117-135

Bolt, G H and R D Miller (1958). "Calculation of total and component potentials of water in soil", Trans American Geophys Union, 39: 917-928

Bond, W J and N Collis-George (1981). "Ponded infiltrations into simple soil systems: 1. The saturation and transition zone in the moisture content profiles.", Soil Science, 131: 202-209

Boyce, J R (1976). "The behaviour of a granular material under repeated loading", PhD thesis, Univ of Nottingham

Brady, K C and G Kirk (1990). "The compressibility of a crushed limestone backfill", TRRL Research Report 251

Brandon, T L, M Duncan and W S Gardner (1990). "Hydrocompression settlement of deep fills", J Geotech Eng, ASCE, 116 (GT10): 1536-1548

Brauns, J and H Leussink (1967). Discussion on Marsal (1967), JSMFD, ASCE, 93 (SM6): 383-388

BS1377: 1975 and 1990. "Methods of Test for Soils for Civil Engineering Purposes"

BS812: 1975. "Testing Aggregates"

Burland, J B (1964), Discussion of Bishop and Blight (1963), Geotechnique, 14: 65-68

Burland, J B (1965). "Some aspects of the mechanical behaviour of partly saturated soils". From "Moisute equilibria and moisture changes in soils beneath covered areas - a symposium in print", Butterworths, Australia: 270-278

Campbell, J D (1973). "Pore pressures and volume changes in unsaturated soils", Doctoral thesis, Univ of Illinois, Urbana-Chamaign

Charles, J A (1984). "Some geotechnical problems assocated with the use of coal mining wastes as fill materials", Symp on the Reclamation Treatment and Utilisation of Coal Mining Wastes, Durham

Charles J A, D B Hughes and D Burford (1984). "The effect of a rise of water table on the settlement of backfill at Horsley restored opencast coal mining site, 1973 - 1983", Proc 3rd Int Conf on Ground Movements and Structures, Cardiff

Clements, R P (1984). "Post construction deformation of rockfill dams", J Geotech Eng, ASCE, 110 (GT7): 821-840

Coleman, J D (1962). "Stress/strain relations for partly saturated soil", Geotechnique, 12: 348-350

Collis, L and R A Fox (1985). "Aggregates: sand, gravel and crushed rock aggregate for construction purposes", Geol Soc, Eng Geol SP1

Croney, D and J D Coleman (1948). "Soil thermodynamics applied to the movement of moisture in road foundations", Proc 7th Int Conf for Applied Mechanics, 3: 163-177

Croney, D, J D Coleman and W P M Black (1958). "Movement and distribution of water in soil in relation to highway design and performance". From "Water and its Conduction in Soils", Highway Res Board Sp Rep No 40

Croney, D and J D Coleman (1960). "Pore pressure and suction in soil", Int Soc of SMFE, Proc Conf on Pore Pressure and Suction in Soils, London. Butterworths, 1961: 31-37

Dhir R K, D M Ramsay and N Balfour (1971). "A study of the aggregate impact and crushing value tests", J Inst Highway Eng, 18: 17-27

Dusseault, M B (1979). "Undrained volume and stress change behaviour of unsaturated very dense sands", Can Geotech J, 16: 627-640

Egretti, I and R N Singh (1988). "A laboratory investigation into the effects of air void and water saturation on the collapse settlement of opencast mine backfill", Mining Science and Technology, 7: 87-97

El-Ehwany, M and S L Houston (1990). "Settlement and moisture movement in collapsible soils", J Geotech Eng, ASCE, 116 (GT10): 1521-1535

El-Sohby, M A (1964). "The behaviour of particulate materials under stress", PhD thesis, Univ of Manchester

Escario, V and J F T Juca (1989). "Strength and deformation of partly saturated soils", Proc 12th ICSMFE, Rio de Janeiro, 1: 43-46

Escario, V and J Saez (1986). "The strength of partly saturated soils", Geotechnique, 36: 453-456

Evans, M D (1987). "Undrained cyclic triaxial testing of gravels - the effect of membrane compliance", PhD thesis, Univ of California, Berkeley

Fisher, R A (1926). "On the capillary forces in an ideal soil", J Agr Sci, 16: 492-505

Fredlund, D G (1973). "Volume change behaviour of unsaturated soils", PhD thesis, Univ of Alberta, Canada

Fredlund, D G (1975). "A diffused air volume indicator for unsaturated soils", Can Geotech J, 12: 533-539

Fredlund, D G (1976). "Density and compressibility characteristics of air-water mixtures", Can Geotech J, 13: 386-396

Fredlund, D G (1979). "Appropriate concepts and technology for unsaturated soils", Can Geotech J, 16: 121-139

Fredlund, D G (1982). "Consolidation of unsaturated porous media", Proc of the NATO Advanced Study Institute on Mechanics of Fluids in Porous Media, Newark, Delaware, USA. In "Fundamentals of Transport Phenomenon in Porous Media", Martinus Nijhoff Publishers, Dordrecht, Netherlands, 1984: 525-578

Fredlund, D G and J U Hasan (1979). "One dimensional consolidation theory: unsaturated soils", Can Geotech J, 16: 521-531

Fredlund, D G and N R Morgenstern (1976). "Constitutive relations for volume change in unsaturated soils", Can Geotech J, 13: 261-276

Fredlund, D G and N R Morgenstern (1977). "Stress state variables for unsaturated soils", J of Geotech Eng Div, ASCE, 103 (GT5): 447-466

Fredlund, D G, N R Morgenstern and R A Widger (1978). "The shear strength of unsaturated soils", Can Geotech J, 15: 313-321

Fredlund, D G, H Rahardjo and J K M Gan (1987). "Non-linearity of strength envelope for unsaturated soils", Proc 6th Ind Conf Expansive Soils, New Delhi, 49-54

Frydman, S, J G Zeitlen and I Aplan (1973). "The membrane effect in triaxial testing of granular soils", J of Testing and Evaluation, 1: 37-41

Gibbs, H J and C T Coffey (1969). "Techniques for pore pressure measurements and shear testing of soil", Proc 7th ICSMFE, Mexico, 1: 151-157

Graton, L C and H J Frazer (1935). "Systematic packing of spheres with particular relation to porosity and permeability", J Geol, 43: 785-909

Haines, W B (1925). "A note on the cohesion developed by capillary forces in an ideal soil", J Agr Sci, 15 : 529-535

Head, K H (1980). "Manual of soil laboratory testing, volume 1 - soil classification and compaction tests", Pentech Press, London

Head, K H (1982). "Manual of soil laboratory testing, volume 2 - permeability, shear strength and compressibility tests", Pentech Press, London

Hicks, R G (1970). "Factors influencing the resilient response of granular materials", PhD Thesis, Univ of California

Hilf, J W (1956). "An investigation of pore water pressures in compacted cohesive sols", US Bureau of Rec, Tech Memo 654

Horne, M R (1985). "Review of the public utilities street works act 1950", Review panel report to the Department of Transport

Houston, S L, W N Houston and D J Spadola (1988). "Prediction of field collapse of soils due to wetting", J Geotech Eng ASCE, 114 (GT1): 40-58

Inman, D L (1952). "Measures for describing size of sediments", J Sedimentary Petrology, 22: 125-145

Jaky, J (1948). "Pressure in silos", Proc 2nd ICSMFE, Rotterdam, 1: 103-107

Jennings, J E (1960). "A Revised effective stress law for use in the prediction of the behaviour of unsaturated soils", Int Soc of SMFE, Proc Conf on Pore Pressure and Suction in Soils, London. Butterworths, 1961: 26-30

Jennings, J B and J B Burland (1962). "Limitations to the use of effective stresses in partly saturated soils", Geotechnique, 12: 125-144

Jones, C W (1954). "The permeability and settlement of laboratory specimens of sand and sand-gravel mixtures", Symp on Permeability of Soils, ASTM STP 163

Jones, R H and K G Hurt (1978). "An osmotic method for determining rock and aggregate suction characteristics with applications to frost heave studies", QJEG, 11: 245-252

Karube, D (1988). "New concept of effective stress in unsaturated soil and its proving test". In "Advanced Triaxial Testing of Soil and Rock", ASTM STP 977

Kiekbusch, M and B Schuppenner (1977). "Membrane penetration and its effect on pore pressures", J Geotech Eng Div, ASCE, 103 (GT11): 1267-1279

Kjaernsli, B and A Sandes (1963). "Compressibility of some coarse grained materials", Proc ECSMFE, Wiesbaden, 1: 245-251

Kolbuzewski, J J (1948). "Research on packing and density of sands", PhD thesis, Univ of London

Koning, H L (1963). "Some observations on the modulus of compressibility of water", Proc ECSMFE, Wiesbaden, 1: 33-36

Krahn, J and D G Fredlund (1972). "On total, matrix and osmotic suction", Soil Science, 114 (No 5): 339-348

Lees, G (1963). "A new method for determining the angularity of particles", Sedimentology, 3: 2-21

Lees, G (1964). "The measurment of particle shape and its influence in engineering materials", J of the British Granite and Whinstone Fed, 4: 1-22

Leigh, W P J and K R Rainbow (1979). "Observations of the settlement of restored backfill of opencast mine sites", Proc Symp Eng Behaviour of Industrial and Urban Fill, Univ of Birmingham, E99-E128

Lloret, A and E E Alonso (1980). "Consolidations of unsaturated soils including swelling and collapse behaviour", Geotechnique, 30: 449-477

Lloret, A and E E Alonso (1985). "State surfaces for partially saturated soils", Proc 11th ICSMFE, San Francisco, 2: 557-562

Marsal, R J (1963). "Contact forces in soils and rockfill materials", Proc 2nd Pan-Am. CSMFE, 2: 67-96

Marsal, R J (1965). Contribution to panel discussion, division 2, Proc 6th ICSMFE, 3: 310-316

Marsal, R J (1967). "Large scale testing of rockfill materials", JSMFD, ASCE, 93 (SM2): 27-43

Marsal, R J (1973). "Mechanical properties of rockfill". From "Embankment Dam Engineering - Casagrande Volume", 1973, John Wiley and Sons, New York

Maswoswe, J (1985). "Stress paths for compacted soil during collapse due to wetting", PhD thesis, Univ of London

Matyas, E L and H S Radhakrishna (1968). "Volume change characteristics of partially saturated soils", Geotechnique, 18: 432-448

McVay, M and Y Taesiri (1985). "Cyclic behaviour of pavement base materials", J Geotech Eng, ASCE, 111 (GT1): 1-7

MIT (1963). "Engineering behaviour of partially saturated soils", MIT Phase Report No 1, Soil Stabilisation

Nataatmadja A and A K Parkin (1988). "A large cell for repeated load triaxial testing of base course materials", 14th ARRB Conf, 7: 85-93

Newland, P L and B H Allely (1950). "Volume changes during undrained triaxial tests on saturated dilatant granular materials", Geotechnique, 9: 174-182

Olson, R E and L J Langfelder (1965). "Pore water pressures in unsaturated soils", JSMFD, ASCE, 91 (SM4): 127-150

Owen, R C (1985) "Performance of unbound aggregates in trench reinstatement", Symp Unbound Aggregates in Roads, Univ of Nottingham

Pappin, J W (1979). "Characteristics of a granular material for pavement analysis", PhD thesis, Univ of Nottingham

Pellegrino, A (1965). "Geotechnical properties of coarse grained soils", Proc 6th ICSMFE, Montreal, 1: 87-91

Penman, A D M (1971). "Rockfill", BRE CP15/71

Penman, A D M and J A Charles (1975). "The quality and suitability of rockfill used in dam construction", BRE CP87/75

Pigeon, Y (1969). "The compressibility of rockfill", PhD thesis, Imperial College of Science and Technology, London

Ramana, K V and V S Raju (1982). "Membrane penetration in triaxial tests", J of Geotech Eng Div, ASCE, 108 (GT2): 305-310

Raudkivi, A J and N V U'u (1976). "Soil moisture movement by temperature gradient", J of Geotech Eng Div, ASCE, 102 (GT2): 1225-1244

Roberts, C M (1958). "The Quoich rockfill dam", Trans 6th ICOLD, 3: 101-121

Scholsser K H and L Walter (1986). "Computer simulation of randomly packed spheres - a tool for investigating polydisperse materials", Particle Characterisation, 3: 129-135

Schuurman, I E (1966). "The compressibility of an air/water mixture and a theoretical relation between the air and water pressures", Geotechnique, 16: 269-281

Selley R C (1976). "An introduction to sedimentology", Academic Press, London

Skempton, A W (1960). "Effective stress in soils, concrete and rocks", Int Soc of SMFE, Proc Conf on Pore Pressure and Suction in Soils, London. Butterworths, 1961: 4-16

Sowers, G F, R C Williams and T S Wallace (1965). "Compressibility of broken rock and the settlement of rockfills", Proc 6th ICSMFE, Montreal, 2: 561-565

Tanaka, Y (1988). Private Communication

Tekinsoy, M A and T Haktanir (1990). "One dimensional consolidation of unsaturated fine grained soils", J Geotech Eng, ASCE, 116 (GT5): 838-850

Terzaghi, K (1960). Discussion of Steele and Cooke (1960), Trans ASCE, 125: 139-148

Thom, N H and S F Brown (1988). "Effect of grading and density on the mechanical properties of a crushed dolomitic limestone", 14th ARRB Conf, 7: 94-100

Thompson, J, J M W Holden and M Yilmaz (1990). "Compaction of opencast backfill beneath highways and associated developments", Symp on the Reclamation Treatment and Utilisation of Coal Mining Wastes, Rotterdam: 293-312

Toll, D G (1990). "A framework for unsaturated soil behaviour", Geotechnique, 40: 31-44

Vaid, Y P and D Negussey (1984). "A critical assessment of membrane penetration in the triaxial test", Geotech Testing J, ASTM, 7: 70-76

Verruijt, A (1982). "The theory of consolidation", Proc of the NATO Advanced Study Institute on Mechanics of Fluids in Porous Media, Newark, Delaware, USA. In "Fundamentals of Transport Phenomenon in Porous Media", Martinus Nijhoff Publishers, Dordrecht, Netherlands, 1984: 349-368

Wadell, H (1932). "Volume, shape and roundness of rock particles", J Geology, 40: 443-451

Wheeler, S J (1988). "A conceptual model for soils containing large gas bubbles", Geotechnique, 38: 389-397

Wheeler, S J (1991). "An alternative framework for unsaturated soil behaviour", Geotechnique, 41: 257-261

APPENDIX A

DETAILED TEST PROCEDURES

The following procedures are detailed within this Appendix:

A1 - Batching of Samples
A2 - Test Series A : Drained Incremental Loading Compression
A3 - Test Series B : Inundation under Constant Vertical Stress
A4 - Test Series C : Drained Constant Strain Rate K_0 Compression and Shear
A5 - Test Series D : Undrained Constant Strain Rate Compression

Details of the apparatus used are given in Chapter 4.

A1 - Batching of Samples

A1.1 Using Table A1, determine the optimum batch quantities for each aggregate size to produce the maximum number of main test specimens for the minimum number of particle size distribution tests specimens, for the grading required. Different total batch masses may be used provided the aggregate mix ratio remains constant and provision is made for particle size distribution tests to be made on two sub-samples.

A1.2 Using at least two 35 kg bags of the first aggregate size range required for the test grading, empty the bags onto a clean dry concrete floor and thoroughly mix using a spade. The aggregate should be air dry before proceeding.

A1.3 Riffle or quarter the aggregate mass down to that mass required for sample batching, as given in Table A1. All masses should be weighed to the nearest 100 g. Add the correct mass to a clean dry concrete batcher of 180 kg capacity.

A1.4 Repeat A1.2 and A1.3 for each raw aggregate size range required to prepare the chosen test grading.

A1.5 Mix the aggregate in the concrete mixer for one minute per every 10 kg of total batch mass.

A1.6 Empty the mixed material onto the clean dry concrete floor.

A1.7 Quarter the material successively to form sub-samples of sufficient size for the tests intended, plus two additional sub-sampled for grading analyses.

A1.8 Double bag each sub-sample, and record the date, operator, grading, specimen number, batch number, and designated use of sub-sample.

A1.9 Conduct wet sieve analyses on two of the batch sub-samples to verify the correct grading has been formed before the remaining sub-samples are used in the main test work.

A2 - Test Series A : Drained Incremental Loading Compression

A2.1 Preliminary Preparation (more than 24 hours in advance of start of test)

A2.1.1 Check the following compaction equipment is available and ready for use:

- compaction base, hydraulic ram and compressor (see Plate A1)

- 7 compaction base bolts for attaching cell body to compaction base and 3 compaction base plugs for use during sliding of cell body across compaction base
- electric Kango hammer, power transformer and compaction plate (see Plate A1)
- compaction guide and 4 bolts to maintain Kango vertical during compaction (see Plate A1)
- thin rigid measuring plate of diameter 200 mm to 240 mm and constant thickness
- clock with second hand
- grease
- plasticine
- 300 mm vernier calipers accurate to 0.01 mm
- large water content trays
- chalk

A2.1.2 De-air the ceramics and check the ceramic response times as detailed in Section 5.2.2 after every three tests at least. Immerse ceramics in water when ceramics are sufficiently de-aired.

A2.1.3 Assemble the top platen as shown in Figure 4.2 and Plates A2 and A3 and place the platen such that the face of the top ceramic face is in water. Connect the load cells to the power source and leave for at least 24 hours before commencement of step A2.2.

A2.1.4 Select previously batched test sample (see appendix A1) and oven dry in a dry tray of known mass for a minimum of 12 hours, or 24 hours if water had access to the bag during storage.

A2.1.5 As detailed in Section 5.2.1, check the plumbing system for the test is de-aired, and that all transducers are operational. Leave transducers under power for a minimum of 24 hours before the test.

A2.1.6 Fill the de-aired water header tank with de-aired water, and leave under vacuum.

A2.1.7 Lock the compaction plate shaft in a lathe and if necessary skim the plate surface until it is perpendicular to the shaft at all points.

A2.1.8 Place the compaction guide over the compaction plate shaft, and adjust the guide bolts until the shaft just slides through the guide under gravity, and no play exists between the shaft and guide. Lock the guide bolts in position.

A2.2 Specimen Preparation

A2.2.1 Remove the aggregate to be tested from the oven and leave to cool to room temperature.

A2.2.2 Weigh the aggregate to the nearest gramme, and calculate the volume of water to be added to this mass to prepare a specimen of the desired water content (ie free water plus absorbed water).

A2.2.3 Add the required amount of water to the soil and mix carefully and thoroughly by hand. Leave the mixed soil for two hours, covered with a plastic sheet to reduce evaporation, and prepare the compaction equipment.

A2.3 Preparation of Compaction Equipment

A2.3.1 Lightly grease the compaction base surface and rubber gasket, the gasket on the base of the cell body, and the inner surface of the cell body.

A2.3.2 Set the guides on the compaction base using the adjusting screws such that the cell body is able to slide freely but not deviating from a straight line along the plate to the end guide. The body should not require more than a light push to keep it moving, and should terminate at the end guard with the bolt holes of the cell body and the cell base co-axial. Note the orientation of the cell on the compaction base for which the guides are set.

A2.3.3 Place the cell base on the floor and completely fill the base platen spiral with water, ensuring no air bubbles are visible. Remove the base ceramic from its water filled container and place onto the cell base. Cover the ceramic with damp absorbent paper.

A2.3.4 With the cell base and ceramic placed loosely in the semi-circle of the compaction base, level the compaction base by adjusting the four base legs until the compaction base and ceramic form a near planar surface with the compaction base plane less than 0.5mm above the ceramic. When set, constrain the ceramic and cell base in place with the end guide, and double check the setting. Release the ceramic and base, and make final adjustments as necessary to ensure the correct setting.

A2.3.5 Without disturbing the base, draw chalk rings around the compaction base legs to define their location, and fix their adjustment using the lock nuts. Note the orientation of the assembled cell base and ceramic and move the ceramic away from any source of vibration.

A2.3.6 Form smooth plugs of plasticine in the three cell base and ceramic bolt holes that will lie nearest to the compaction base (holes X, Y, Z in Figure A1).

A2.3.7 Insert the ram head into the hydraulic ram and bolt the cell body (gasket downwards) onto the compaction base in its correct orientation using the seven bolts A to G shown in Figure A1.

A1.3.8 Measure and note the internal depth of the cell at six equidistant positions around the cell circumference using the vernier and measuring to the nearest 0.01 mm.

A2.4 • Specimen Compaction and Initial Cell Assembly

A2.4.1 Remove the plastic sheeting from the prepared specimen and weigh the mixed soil to the nearest gramme.

A2.4.2 Hand mix the specimen again, then carefully add material to the cell until a pre-compacted height of about 130mm is achieved. Ensure the material is placed such that the apparent distribution of particles is even, and take two water content samples (to BS1377: 1975, Clause 1.5.3) after about a third and two thirds of the material have been added. Use the material left in the mixing tray having third water content test. Note all wet and dry masses.

A2.4.3 Place the compaction plate and guide on the cell, letting the plate rest lightly on the soil surface. Bolt the compaction guide onto the Rowe Cell body.

A2.4.4 Lower the Kango unit over the compaction plate shaft and lock in place.

A2.4.5 Compact the specimen for 10 seconds, applying 350N to 400N force to the Kango (see section 4.1.2.1).

A2.4.6 Unbolt the guide from the cell, and slowly rotate the Kango to break any suction before pulling the Kango and guide out of the cell. Negligible material should be left on the compaction plate.

A2.4.7 Lightly place a measuring plate of known thickness onto the compacted surface, and measure the depths to the plate at six equidistant positions around the cell circumference using the vernier. Note depths. If the observed specimen tilt exceeds 1.5mm over the diameter, reject the specimen.

A2.4.8 Remove the measuring plate and cover the cell with a damp cloth to minimise evaporation. Note time.

A2.4.9 Re-locate the compaction base legs in their pre-compaction positions, as indicated by the chalk rings.

A2.4.10 Remove from the cell body the three bolts nearest the semi-circle and replace from underneath with the metal plugs. Ensure the plugs, stamped A, B or C, are placed in the corresponding holes (see Figure A1).

A2.4.11 Remove the remaining four bolts from the cell, thereby releasing it from the compaction base.

A2.4.12 Place the cell base with the ceramic in the semi-circle in its correct orientation, and lock in with the end guide. Check the relative levels of the compaction base and base ceramic for deviations from that set in step A2.3.5. Fine tune the alignment if necessary.

A2.4.13 Push the cell and compacted soil slowly across the base and onto the ceramic using the hydraulic ram (see Plate A4). The ram extension will be required to complete the traverse, and the cell body must be lightly held to prevent rotation. As the cell body starts to encroach upon the base ceramic, remove the absorbent paper from the base ceramic and remove any excess water left on the ceramic by the paper using some dry absorbent paper.

A2.4.14 Stop the traverse when the end guide is reached, and, if necessary, rotate the cell slightly to align the bolt holes.

A2.4.15 Release the end guide and slide the compaction base away from the test cell. Remove the plasticine plugs from the cell base.

A2.4.16 Insert all eight bolts to finger tightness, then tighten opposite bolts in turn, applying only light force. Note time.

A2.5 Platen Insertion and Connection to Test System

A2.5.1 Transfer the partially assembled cell to the hydraulic press area.

A2.5.2 Temporarily disconnect power to the load cells and transfer the assembled top platen from the temperature controlled laboratory to the hydraulic press area.

A2.5.3 Place the top platen on the top of the cell such that all internal plumbing and electrical connections between the cell top and the platen will not interfere with and/or prevent final assembly.

A2.5.4 Place a metal plate of length greater than the external cell diameter but width less than the cell internal diameter, on the top platen (see Plate A5) and ensure the load cell cables are coiled beneath it.

A2.5.5 Place the assembly beneath the press and push the platen slowly and evenly into the cell. Cease pressing when the metal plate contacts the cell body flange at all points.

A2.5.6 Remove the cell from the press and transfer to the temperature controlled laboratory.

A2.5.7 Place a lightly greased thin gasket on top of the cell body. The gasket should be greased on both sides.

A2.5.8 Thread the load cell cables through the cell top and seal fittings, and connect to power. Note time.

A2.5.9 Fill the base pore pressure transducer chamber with de-aired water and connect to the cell base.

A2.5.10 Connect the central piston to the top platen, then lower the cell top over it.

A2.5.11 Connect the internal plumbing lines for air pressure and flushing, whilst supporting the cell top and preventing excessive axial forces being applied to the central piston.

A2.5.12 Bolt cell top to the cell body.

A2.5.13 Connect the external plumbing lines to the cell for air pressure, cell pressure, and flushing (see Figure 4.1b).

A2.5.14 Position the LDVT over the central piston with its armature almost fully compressed (see Plate A6).

A2.5.15 Remove the vacuum from the header tank and open the supply valve (see Figure A2). With water flowing, connect the pipe to the cell pressure bladder cell through the base water vent, then open it.

A2.5.16 Open the cell pressure valve at the cell top and the pressure chamber vent. Water should now flow and slowly fill the cell pressure chamber.

A2.5.17 When water starts to flow out of the cell pressure chamber vent, gently rock the cell with the vent open to remove any trapped air. Close all the valves opened in steps A2.5.15 to A2.5.17 except for the air vent at the top of the header tank.

A2.5.18 Apply 10 kPa pressure to the flushing system with the flushing and drain lines open at the top and bottom of the cell and thereby flush de-aired water through the platens. Continue the flow for several minutes to remove any trapped air then close the drainage valves on the cell.

A2.5.19 Isolate the air volume indicators from the rest of the plumbing system using the AVI bypass and isolation valves. Apply 10 kPa back pressure to the top and bottom of the de-aired volume change units (see section 5.2.1) and, when water starts to flow slowly out of the unconnected pipes from the volume change units and any air that was visible in the pipes is removed, open the drainage valves on the cell. With water flowing slowly from both pipes and both valves, connect the volume change units to the test cell to form a closed de-aired measurement system.

A2.5.20 Adjust the flushing pressure and back pressures such that water flows into or out of the volume change units until the units are set near either end of their travel.

A2.5.21 Close all drainage and flushing valves at the cell, leaving the pore pressure transducers connected to the platens but isolated from the rest of the system.

A2.5.22 Remove the pressure from the flushing and drainage systems.

A2.6 Initialising the Test System

A2.6.1 Initiate the logging system (See section 4.1.3.3 and Appendix C) with a scan rate of 30 seconds. Use gain 1 for the LVDT and use the default calibration factors and offsets.

A2.6.2 Apply a cell pressure of 25 kPa to the top platen using the low pressure regulator.

A2.6.3 Apply 2.5 kPa increments of cell pressure approximately every 30 seconds until the "break loose pressure" is reached, as recorded by the onset of continuous movement of the LVDT armature. Note this pressure, which is typically about 50 kPa.

A2.6.4 Reduce the cell pressure in decrements of 2.5 kPa until movement stops (typically at about 40 kPa). Note this pressure.

A2.6.5 Calculate the estimated LVDT output at which contact will occur between the specimen and the descending top platen, from a knowledge of the initial specimen clearance from the cell top, the height of the assembled top platen, the LVDT calibration factor, and the initial LVDT reading (see Section 6.1.1.3).

A2.6.6 Increase the cell pressure as described in step A2.6.3 until movement restarts, then reduce the applied cell pressure to about 2.5 kPa above that pressure when movement first stopped. Allow the platen to slowly slide towards contact with the soil.

A2.6.7 Constantly compare the estimated LVDT output at first contact with that recorded by the logging system, and when contact is imminent, reduce the cell pressure such that the rate of platen descent is less than 0.1mm every 30 seconds.

A2.6.8 When contact occurs, the load cell outputs will change and LVDT movement will cease. Quickly reduce the cell pressure to about 25 kPa to avoid an excessive load surge being applied to the specimen by a local reduction in friction.

A2.6.9 Increase the cell pressure until the load cells, which will be recording an applied specimen stress somewhere near maximum contact stress due to side friction limiting upwards movement of the platen, start to show a small increase in net applied stress. Hold this first loading stress and note the cell pressure.

A2.6.10 Apply an air pressure of 5 kPa to the specimen using the low pressure regulator thereby reducing the net applied stress to the soil and decreasing the applied specimen (or load cell) stresses.

A2.6.11 Increase the cell pressure by about 5 kPa to re-apply an applied specimen stress equal to the first loading stress.

A2.6.12 Repeat steps A2.6.10 and A2.6.11 until the intended axis-translation pressure (air pressure) is achieved. Usually an air pressure of 100 kPa was used.

A2.6.13 Re-set the position of the LDVT in its clamp until its output is at the top of its maximum accuracy range of output, as determined from the calibrations.

A2.6.14 Stop the data acquisition program and restart immediately as a new file. Input the calibration constants for on screen engineering units output (see Appendix C) and use a scan rate of 900 seconds.

A2.6.15 Leave the specimen for 24 hours or until sensibly constant pore pressures top and bottom are recorded, whichever is the longer. Check the stability of the regulating pressures and voltage supplied periodically. Close the file when this equalisation stage is completed.

A2.7 Initialising Base Drained Conditions

A2.7.1 Initiate a new file with the same calibration constants as used during the equalisation stage. Use an initial scan rate of 1 minute.

A2.7.2 Close the base drainage valve between the pressure transducer and the cell and open the valve between the transducer and drainage system.

A2.7.3 Note the reading of the air volume indicator at atmospheric pressure, with the indicator connected to the main drainage line and the bypass valve closed.

A2.7.4 Apply a back pressure to the drainage line equal to the equilibrium base pore pressure, as recorded by the base pressure transducer.

A2.7.5 Record the new reading of the base air volume indicator.

A2.7.6 Open the base drain between the pore pressure transducer and the cell, thereby allowing drainage at the original equilibrium suction.

A2.7.7 Leave the cell for a minimum of 1 hour to check for leaks - no volume change should occur within the specimen.

A2.8 Application of First Loading Increment (usually 10 kPa)

A2.8.1 Increase the scan rate to 10 seconds.

A2.8.2 Close the cell pressure valve at the top of the cell.

A2.8.3 Increment the cell pressure by 10 kPa and open the cell pressure valve immediately after a noted scan number.

A2.8.4 Observe the increase of average load cell stress for 30 seconds and, if the applied vertical increment of 10 kPa has not been fully transferred within that time, apply a smaller cell pressure movement and observe the change in average applied stress. Repeat every 30 seconds until the applied stress is reached, usually within 2 minutes. Continual checks for load surges due to sudden loss of side friction should be made, and the cell pressure rapidly reduced if necessary. If a large surge occurs such that the average stress applied to the soil exceeds 12 kPa a further cell pressure increment should be applied to achieve a revised target applied stress equal to the surge value.

A2.8.5 When the required average applied stress is recorded by the load cells, leave the apparatus for 5 minutes except for finely adjusting the cell pressure to maintain the applied stress as the side friction decreases. Reduce the scan rate to 30 seconds at the end of this period.

A2.8.6 Continue fine adjustments to the cell pressure as the test proceeds and alter the scan rates approximately as follows:

after a further 10 minutes, reduce the scan rate to every minute
after a further 30 minutes, reduce the scan rate to every 5 minutes
after a further 60 minutes, reduce the scan rate to every 15 minutes
after 24 hours, reduce the scan rate to every 30 minutes

A2.8.9 When the pore pressures and axial strain have sensibly stabilized stop this stage of the test.

A2.9 Application of Subsequent Increments/Decrements

A2.9.1 Application of a load increment follows the procedure detailed in step A2.8 but the cell pressure changes used (step A2.8) should be varied in accordance with the required changes in the average vertical stress. The subsequent increments usually used were 10 kPa to 25 kPa, 25 kPa to 50 kPa, 50 kPa to 75 kPa, and 75 kPa to 100 kPa.

A2.9.2. Application of a load decrement is similar to application of a load increment but load decrement surges were not a problem. Load decrements usually used were 100 kPa to 50 kPa, 50 kPa to 25 kPa, and 25 kPa to 5 kPa.

A2.10 Final Unloading and Dismantling of the Test

A2.10.1 Initiate the last data file and set a scan rate of 10 seconds.

A2.10.2 Close the cell pressure line and reduce the cell pressure to zero. Open the pressure valve immediately after a noted scan number.

A2.10.3 Allow the top platen to be pushed upwards by the air pressure in the cell, and displace cell chamber water. Open the base water vent of the cell pressure bladder cell to accommodate this displacement. Close the vent when the platen travel limit is reached and stop the data logging program.

A2.10.4 Reduce the back pressure to the drainage line to zero. Close the air volume indicator isolation valves, thereby preventing air entering the rest of the plumbing.

A2.10.5 Disconnect the top and bottom drainage lines, open the drain valves to atmospheric pressure, and reduce the cell air pressure to zero.

A2.10.6 Disconnect the load cells from the power source, and disconnect all connections from the top of the cell.

A2.10.7 Unbolt and raise the top of the cell. Disconnect pipes from the top of the cell and remove it. Remove the central piston and flange gasket.

A2.10.8 Remove the water contained in the top platen recess using absorbent paper, then disconnect the air and flushing connections from the top platen.

A2.10.9 Place three spacers on top of the top platen to prevent the screw jack-top platen connection from squashing the load cell cables, then bolt the screw jack to the top platen and to the cell body.

A2.10.10 Operate the screw jack and raise the top platen until it is free of the consolidation cell (see Plate A7). Unbolt and remove the jack.

A2.10.11 Remove the top platen from the cell, invert it, and rest upon two wooden blocks as shown in Plate A3 such that the weight of the top platen does not rest upon the load cell cables.

A2.10.12 Check the top ceramic for surface damage or cracks, remove the locking ring from the top platen and check the underside of the ceramic. Place the ceramic in water immediately to prevent any evaporation and consequent air entry into the ceramic. Note any observations on cracking.

A2.10.13 Examine the O ring seals of the top platen and check for evidence of water seepage past them. Note any observations.

A2.10.14 Remove the specimen in three approximately equal layers and determine the water content of each layer.

A2.10.15 Unbolt the cell body from the base and check the base ceramics for cracking in a manner similar to that given in step A2.10.12. Immerse base ceramic in water.

A2.11 Operation of the Flushing System

Periodically throughout a test, it is necessary to determine the volume of diffused air that has passed through the top and base ceramics. Typically, this should be done at the end of equalisation, and after every 2 loading stages thereafter. The flushing procedure to be used is as follows:

A2.11.1 Reduce the scan rate to 30 seconds.

A2.11.2 With the flushing inlet to the cell closed set a flushing pressure equal to the back pressure plus 10 kPa.

A2.11.3 Note the air volume indicator readings at the current back pressure.

A2.11.4 After the 30 second scan rate has been commenced, open the top flushing inlet and top drain, thereby flushing water and diffused air toward the air volume indicator. Reduce the flushing differential to 5 kPa as the bubbles approach the air volume indicator and start to become trapped.

A2.11.5 Continue flow until the volume change unit nears the end of its travel, and close the flushed line. Note the new air volume indicator reading and the back pressure.

A2.11.6 Reverse the flow direction into the volume change unit using the reversing valve, and re-open the flushing line.

A2.11.7 Repeat steps A2.11.5 and A2.11.6 until no more air is displaced. After the last reverse, increase the flushing differential to 20 kPa. Repeat one more reverse sequence or until no more air is displaced.

A2.11.8 Note the final top air volume indicator reading at the set back pressure, then close the top drain valve beyond the transducer and flushing inlet valve.

A2.11.9 Repeat steps A2.11.4 to A2.11.8 for the base platen.

A2.11.10 Continue the test stage in progress, making gradual decreases in scan rate to that existing before the flushing procedure, such that the pore pressure response curves are recorded.

A3 - Test Series B : Inundation under Constant Vertical Stress

A3.1 Preliminary Preparation to Application of First Loading Increment.

As for test series A, but use an air pressure of 50 kPa and omit stage A2.7.

A3.2 Application of Subsequent Increments and Flushing.

As for tests series A, tests 7 to 10, using the same increments but terminating at either a maximum applied vertical stress of 50 kPa or 75 kPa nominally.

A3.3 Inundation under Load.

A3.3.1 Initiate the next data file with a scan rate of 10 seconds and with the transducer output in engineering units. Take base readings for a minimum of 2 minutes.

A3.3.2 With the back pressure line to the top pressure transducer open, but the transducer isolated from the cell, set a back pressure of 50 kPa as read by the transducer.

A3.3.3 Note the initial volume change unit output and the flow direction set for when inundation starts.

A3.3.4 After a noted scan, and at a noted time, open the top drain line and commence inundation.

A3.3.5 Due to inertia in the system, the inundation pressure will cause a small deflection of the ceramic and an increase in the applied stress. Reduce the cell pressure slightly to compensate for this effect and maintain a constant applied stress.

A3.3.6 Increase the inundation pressure and decrease the cell pressure in small increments, always keeping the total applied stress within 1 kPa of its nominal value. Continue this until the inundation flow rate is between 0.5 cm^3 per minute and 1.5 cm^3 per minute, or the induced ceramic deflection, recorded as a swelling of the specimen, reaches a maximum allowable 0.2 mm.

A3.3.7 Reduce the scan rate to 1 minute.

A3.3.8 Calculate the volume of air voids present in the specimen at the start of the inundation stage, and thereby calculate the approximate inundation volume required to obtain full saturation, from the initial specimen parameters, total axial strain of the specimen, and free water volume change since equalisation.

A3.3.9 When the volume change unit approaches its limit of travel, reverse the flow valves. Note the time, scan number and volume change unit output when reversal occurred. Adjust the inundation pressure regulator to compensate for the addition or loss of the volume change unit piston mass.

A3.3.10 Calculate the total volume inundated up to reversal from the noted change in output of the volume change unit since the last reversal, the volume change unit calibration factor for the flow direction just completed, and inundation total prior to commencement of the cycle just completed. Re-calculate the total volume of inundation required for saturation as detailed in step A3.3.8.

A3.3.11 Continue inundation, reversing valves and adjusting pressures as required, until full saturation is achieved.

A3.3.12 Close the inundation line leaving the top transducer still connected to the cell. Note the time, scan, and volume change unit output, and calculate the final inundated volume.

A3.3.13 As the residual inundation pressure reduces in response to further flow, continually check and increase the cell pressure to maintain a constant applied vertical stress.

A3.3.14 When stable top pore pressure conditions are reached, reduce the scan rate to 5 minutes.

A3.3.15 Leave the specimen overnight at the constant vertical stress during inundation, then close the data file.

A3.4 Load Decrements and Dismantling of the Tests

As detailed in stage A2.10 for test series A, except the final water content of the test specimen is determined on the basis of a single water content test using the whole test specimen rather than in three separate layers.

A4 - Test Series C : Drained Constant Strain Rate K_o Compression and Shear

A4.1 Preliminary Preparation (more than 24 hours in advance of the start of the test)

A4.1.1 Fill the drainage annulus of the triaxial base pedestal with de-aired water then cover with the high entry ceramic which should have been sealed into its locking ring already. Bolt the locking ring and ceramic down onto the base pedestal.

A4.1.2 De-air the high air entry ceramic and check its response time (see Section 5.2.2). When the ceramic is sufficiently de-aired, place a layer of saturated absorbent paper on the surface of the ceramic and encapsulate the base pedestal, absorbent paper, and ceramic, with a cling film wrapping held in place with an elastic band.

A4.1.3 Place the previously batched specimen (see Appendix A1) in an oven at 105°c and leave for 12 hours, or 24 hours if water had access to the sample during storage. The minimum dry mass required is 35 kg.

A4.1.4 De-air the system plumbing (see Section 4.2) in a manner similar to steps A2.5.15 to A2.5.19.

A4.1.5 Connect all transducers to the power supply.

A4.2 Preparation of Equipment Immediately before Preparation

A4.2.1 Remove the sample from the oven and leave to cool to room temperature.

A4.2.2 Check the following apparatus is available and ready for use:

- three piece split former, assembled with internal joints sealed with sellotape
- plasticine
- four '0' rings and two triaxial rubber membranes for sealing specimen
- filter paper
- wooden tamping rod
- de-aired water supply
- vacuum foot pump connected to water manometer and water collector bottle (see Figure A2)
- thin wire more than 0.7 m in length, and metre rule
- fork-lift truck and lifting tackle

A4.2.3 Weigh the sample when cool and note.

A4.3 Specimen Preparation : Part 1 - All Specimens

A4.3.1 Remove the cling film wrapping from the base pedestal ceramic, but leaving the damp absorbent paper covering the ceramic.

A4.3.2 Stretch the membranes, one at a time, over the base pedestal and ceramic.

A4.3.3 Place a double '0' ring seal on the membrane in the conventional arrangement, using the assembled split former as a guide.

A4.3.4 Lower the split former over the pedestal, taking care not to snag the membranes. Push the former down until it is about 5mm or less from the base of the triaxial cell. Seal this small gap with a bead of plasticine.

A4.3.5 Attach the vacuum foot pump to the former and stretch the outer membrane over it. Apply and maintain light suction, smooth the outer membrane to the inner surface of the former and stretch the inner membrane into position.

A4.3.6 Secure the membranes in position with an '0' ring.

A4.3.7 Remove the saturated paper from the ceramic, and replace with a damp filter paper of diameter slightly smaller than the pedestal.

A4.3.8 Place dry soil up to just over the quarter height of the former, in an apparently even particle size distribution. Compact the specimen with 35 evenly distributed blows of the wooden tamping rod.

A4.3.9 Repeat step A4.3.8 for the second to fourth layers, but reapply the vacuum on the membranes after the second layer. The final layer should be about 10 mm below the top of the former before compaction, and 20 mm after. Fine material should be added to the top to present a smooth surface to the top platen.

A4.3.10 Remove and reapply the vacuum again, and add some extra material if small slumping occurs. Lightly tamp in place with a few light blows of the tamper. The final level should be slightly above the mating groove for the top platen (see Plate A8).

A4.3.11 Weigh the unused material and thereby calculate the dry mass of the specimen.

A4.4 Specimen Preparation : Part 2A - Damp and Saturated Specimens Only

A4.4.1 Slowly pour a known volume of de-aired water into the top of the specimen until the former is apparently saturated. Leave for 5 minutes, then top up with more water of noted volume. Cover with cling film and leave for at least 1 hour.

A4.4.2 Remove the cling film and top up once more to the top level of the specimen. Only a little extra water should be required.

A4.4.3 Firmly press the top platen into the top of the former, roll the membranes over it, and seal them in a manner similar to that of the base pedestal.

A4.4.4 Connect the vacuum pump via the manometer and collector bottle to the top platen only (see Figure A2 and Plate A9).

A4.4.5 Apply a maximum suction of 15 kPa to the specimen to suck from the soil. This suction will need to be reapplied every minute approximately to maintain the flow. Measure the total volume that is removed under this vacuum.

A4.4.6 With a suction of 15 kPa applied, close valve A (see Figure A2) and observe the water column between the specimen and the valve. Continuous movement implies the membranes have punctured, and the test must be aborted.

A4.5 Specimen Preparation : Part 2B - Dry Specimens Only

A4.5.1 Press the top platen into position, as in step A4.4.3.

A4.5.2 Connect the vacuum pump and the manometer to the top platen air line, as shown in Figure A2.

A4.5.3 Apply a suction of 15 kPa, hold for 30 seconds, and close valve A.

A4.6 Specimen Preparation : Part 3 - All Soils

A4.6.1 Remove the plasticine seal from the base pedestal.

A4.6.2 Release the screw locks on the split former. Insert a screwdriver into one of the split former joints, and carefully prise apart. Dismantle and remove the former.

A4.6.3 Using the thin wire, measure the circumference of the now free-standing specimen at five equidistant levels over the whole specimen height.

A4.6.4 Using the metre rule, measure the specimen height at six locations equidistant around the specimen circumference.

A4.7 Cell Assembly

A4.7.1 Grease the triaxial cell loading ram and secure at the top of its travel using the clamp.

A4.7.2 Using a fork lift and tackle, lift the cell top over the specimen and seal the chamber. Lower the loading ram into light contact with the specimen. Fill the cell with water.

A4.7.3 Using the fork lift, raise the entire cell and position on the strain controlled triaxial compression machine. Secure in place with rope temporarily.

A4.7.4 Attach the cross beam, level it, and secure the triaxial cell. Remove the rope.

A4.7.5 Taking care not to release the vacuum in the specimen, connect all plumbing and transducers to the cell, bleeding the lines by flushing through with water to ensure no air is trapped.

A4.7.6 Apply a cell pressure of 30 kPa (or 80 kPa for dry specimens) at the specimen mid height.

A4.7.7 Apply a pore water back pressure of 20 kPa to the base pedestal (or a pore air pressure of 70 kPa or 20 kPa to the top platen for dry and unsaturated specimens respectively), thereby releasing the vacuum (see Plate A10).

A4.8 Initial Specimen Saturation (for Saturated Specimens Only)

A4.8.1 Initiate the computer logging system. Check all transducer allocations and start the saturation stage of the software.

A4.8.2 Apply a cell pressure increment of 30 kPa after preventing water drainage from the base. Monitor the pore water pressure response and calculate the B value. Compare the computer calculated value with that calculated by hand from the digital voltmeter output.

A4.8.3 Increment the pore water back pressure by 30 kPa, then return the specimen to a water undrained condition.

A4.8.4 Repeat Steps A4.8.2 and A4.8.3 until B is greater than or equal to 0.95, applying a change in cell pressure of 50 kPa, or as calculated using the equation below, whichever is the lesser. This will ensure a maximum difference between total and pore water pressure of 30 kPa. Return this differential to 10 kPa after calculating B each time. The equation used to determine the maximum increase in cell pressure is given below:

$$\Delta\sigma_3 = \frac{30 + u - \sigma_3}{1-B}$$

where $\Delta\sigma_3$ - change in cell pressure, u = current pore water pressure, and all pressures are in kPa.

A4.8.5 Terminate the saturation stage of the software.

A4.9 Consolidation Stage (for saturated specimens only)

A4.9.1 Start the consolidation stage of the software.

A4.9.2 Increment the cell pressure to the current pore water back pressure plus 30 kPa, and apply to the specimen when the data acquisition unit is activated by the computer.

A4.9.3 Computer readings are taken automatically on a root time basis, but take manual readings of the voltmeters on a root time basis for a back-up.

A4.9.4 Continue consolidation until volumetric straining has sensibly ceased. Stop this stage of the software.

A4.10 Consolidation Stage (for dry specimens only)

A4.10.1 Initiate the computer logging system as in step A4.8.1. Omit the saturation stage of the software.

A4.10.2 Start the consolidation stage of the software.

A4.10.3 Increment the cell pressure to 100 kPa, and apply to the specimen when the data acquisition unit is activated by the computer.

A4.10.4 Perform steps A4.9.3 and A4.9.4, then stop the consolidation stage of the software.

A4.11 Consolidation Stage (for Unsaturated Specimens Only)

A4.11.1 Increment the cell pressure and pore air pressure, respectively, by 10 kPa, until the cell pressure reaches 80 kPA and the air pressure reaches 70 kPa.

A4.11.2 Perform steps A4.10.1 to A4.10.4.

A4.12 Ko Stage

A4.12.1 Start the shear stage of the software, specifying a scan rate of 1 minute.

A4.12.2 When data acquisition begins, start loading the specimen axially at a strain rate of 0.1 mm per minute.

A4.12.3 Using the corrections detailed in Chapter 6, adjust the cell pressure to maintain Ko conditions, until the deviator stress exceeds 100 kPa. Take manual readings frequently throughout this stage.

A4.12.4 Stop the triaxial loading platen and the software.

A4.13 Stages Intermediate Between Ko Stage and Shear Stage

A4.13.1 Start a "new" test with the software, and begin a shear stage again. Use a scan rate of 5 seconds.

A4.13.2 When data acquisition begins, start unloading the specimen by reversing the triaxial machine platen direction at 0.1 mm per minute. The specimen should be air and water undrained during the unloading.

A4.13.3 When the deviator stress is less than 5 kPa, stop the software and the triaxial machine.

A4.13.4 Start a "new" test again as in step A4.13.1.

A4.13.5 When data acquisition begins, start reducing the cell pressure with the specimen air and water undrained at about 10 kPa per minute, until the original consolidation cell pressure is reached.

A4.13.6 Open the drainage line to the specimen and allow the membrane to be pushed out as the pore air pressure is raised back to original pore pressure.

A4.13.7 Stop the software.

A4.14 Shear Stage and Dismantling

A4.14.1 Start a "new" test, as in step A4.13.1, but specify a scan rate of 1 minute.

A4.14.2 When data acquisition begins, start loading the specimen to failure at a strain rate of 0.1 mm per minute and at a constant cell pressure. Take periodic manual readings as a back-up to the computer readings.

A4.14.3 Continue the test until axial straining of the specimen has exceeded the strain at peak stress by about 1%. Reverse the triaxial platen direction and unload the specimen to zero deviator stress.

A4.14.4 Stop the software and reduce the cell pressure to atmospheric pressure.

A4.14.5 Drain and strip the cell.

A4.14.6 Dismantle the specimen in four layers, and determine the water content of each layer.

A4.14.6 Cover the base ceramic with saturated paper and cling film, as detailed in stage A4.1.1.

A5 - Test Series D : Undrained Constant Strain Rate Compression

A5.1 Preliminary Preparation (more than 24 hours in advance of start of test).

A5.1.1 Place a previously batched sample (see Appendix A1) in the oven at 105°C and leave for a minimum of 12 hours, or 24 hours if water had access to the sample during storage. The minimum dry mass required for the main test specimen and two water content tests was 30 kg for the coarse and medium grading, or 25 kg for the fine grading.

A5.1.2 Slide the compaction guide over the compaction plate shaft, and adjust the guide bolts such that the shaft just slides through under gravity and no play exists between the shaft and guide.

A5.1.3 Connect all transducers to power supply.

A5.2 Specimen Preparation

See Appendix A2.2.

A5.3 Specimen Compaction and Cell Assembly

A5.3.1 Ensure the compaction cell is clean and dry, and measure the internal height of the cell at four equidistant locations on the cell circumference. Place the cell on a sound concrete floor.

A5.3.2 Two hours after mixing the sample, uncover the prepared sample and weigh.

A5.3.3 Add the material and compact using compaction method (a) or (b) below, ensuring an apparently even particle size distribution results and two water content samples are taken from the mix material during addition of the aggregate to the cell.

(a) Heavy compaction : add material to form an uncompacted layer 200 mm deep. Place the compaction plate in the cell, lower the guide over the compaction shaft, and bolt the guide to the cell (see Plate A11). Connect the plate to the Kango vibrating hammer and compact for 35 seconds applying a vertical force of 300 N to 400 N. Unbolt the guide, twist the compaction plate slowly and remove the compaction plate.

(b) Light compaction : place the material in a layer 100 mm deep, and tamp evenly with 35 light blows of the compaction rod. Add a second 100 mm deep layer and tamp as before (Plate A12).

A5.3.4 Lower a 300 mm diameter plate of known thickness gently onto the soil surface and measure the depth to this plate at 4 equidistant locations around the cell circumference. The depth should be measured using a steel rule to an accuracy of 0.5 mm.

A5.3.5 Transfer the compaction cell to the platen of the strain controlled load frame, with the load cell and loading plate already attached to this load frame. The platen should be set at the bottom of its travel before the cell is placed on it.

A5.3.6 Lower the load frame cross beam until the load plate just touches the soil as evidenced by a change in output from the load cell.

A5.3.7 Adjust the cross beam until a spirit level indicates it is horizontal, but ensuring that the adjustment process does not increase the contact stress between the specimen and loading plate. Clamp the cross beam in position.

A5.3.8 Clamp the LVDT to the cross beam, and rest its armature on the flat horizontal surface of the compaction cell rim. The LVDT armature should be nearly fully extended.

A5.3.9 Check the LVDT and load cell leads to the computerised data acquisition system, and check the computer channel allocations.

A5.3.10 Check the LDVT operation by inserting slip gauges between the armature and the cell, and comparing the computer output with the known dimensions of the slip gauges.

A5.4 Initial load increment

A5.4.1 Initialise the computer logging system with a scan rate of 5 seconds and a maximum number of scans of 500. Input the initial specimen parameters.

A5.4.2 After at least 30 seconds, start stressing the specimen by raising the triaxial machine platen at a rate of 0.5 mm per minute.

A5.4.3 Stop the platen when the load cell records an average vertical stress on the specimen of 125 kPa. Stop the logging program and retrieve the data.

A5.5 Subsequent load cycling

A5.5.1 Initialise the computer as in step A5.4.1, but using a scan rate of 2 seconds.

A5.5.2 Unload the specimen at a rate of 0.5 mm per minute to a specimen stress of approximately 10 kPa, then apply at least a further 2 complete load cycles between 10 kPa and 125 kPa at the strain rate of 0.5 mm per minute.

A5.5.3 Stop logging program and retrieve the data.

A5.5.4 Initialise a third test stage, with a scan rate of 3 seconds.

A5.5.5 Apply 3 to 5 complete load cycles between 10 kPa and 250 kPa, at a strain rate of 0.5 mm per minute.

A5.5.6 Stop the logging program and retrieve the data.

A5.5.7 Initialise a fourth test stage with a scan rate of 2 seconds.

A5.5.8 Apply 3 to 5 complete load cycles between 10 kPa and 250 kPa, at a strain rate of 2.5 mm per minute.

A5.5.9 Stop the logging program and retrieve the data.

A5.6 Dismantling of the Test.

A5.6.1 Lower the triaxial machine platen to its limit, then raise the cross beam such that the loading plate is about 10 mm clear of the compaction cell.

A5.6.2 Remove the cell from the triaxial machine, but leave the transducers connected to the power supply ready for the next test.

A5.6.3 Remove the specimen in three approximately equal layers and determine the water content of each.

A5.6.4 If required, combine the three water content specimens after drying and use this material to perform a grading analysis on the test material.

Table A1 Recommended Batching Quantities

GRADING	AGGREGATE BATCHING RATIO* (F:M:C:VC)	MASS OF EACH SIZE RANGE REQUIRED (kg) F	M	C	VC	TOTAL BATCH MASS (kg)	MIXING TIME (MINS)
FINE	1:0:0:0	85	--	--	--	85	8.5
MEDIUM	2:1:0:0	60	30	--	--	90	9.0
COARSE	2:1:1:1	60	30	30	30	150	15.0

* AGGREGATE SIZE RANGES SUPPLIED WERE: F - less than 5 mm
M - 5 mm to 10 mm
C - 10 mm to 20 mm
VC - 20 mm to 40 mm

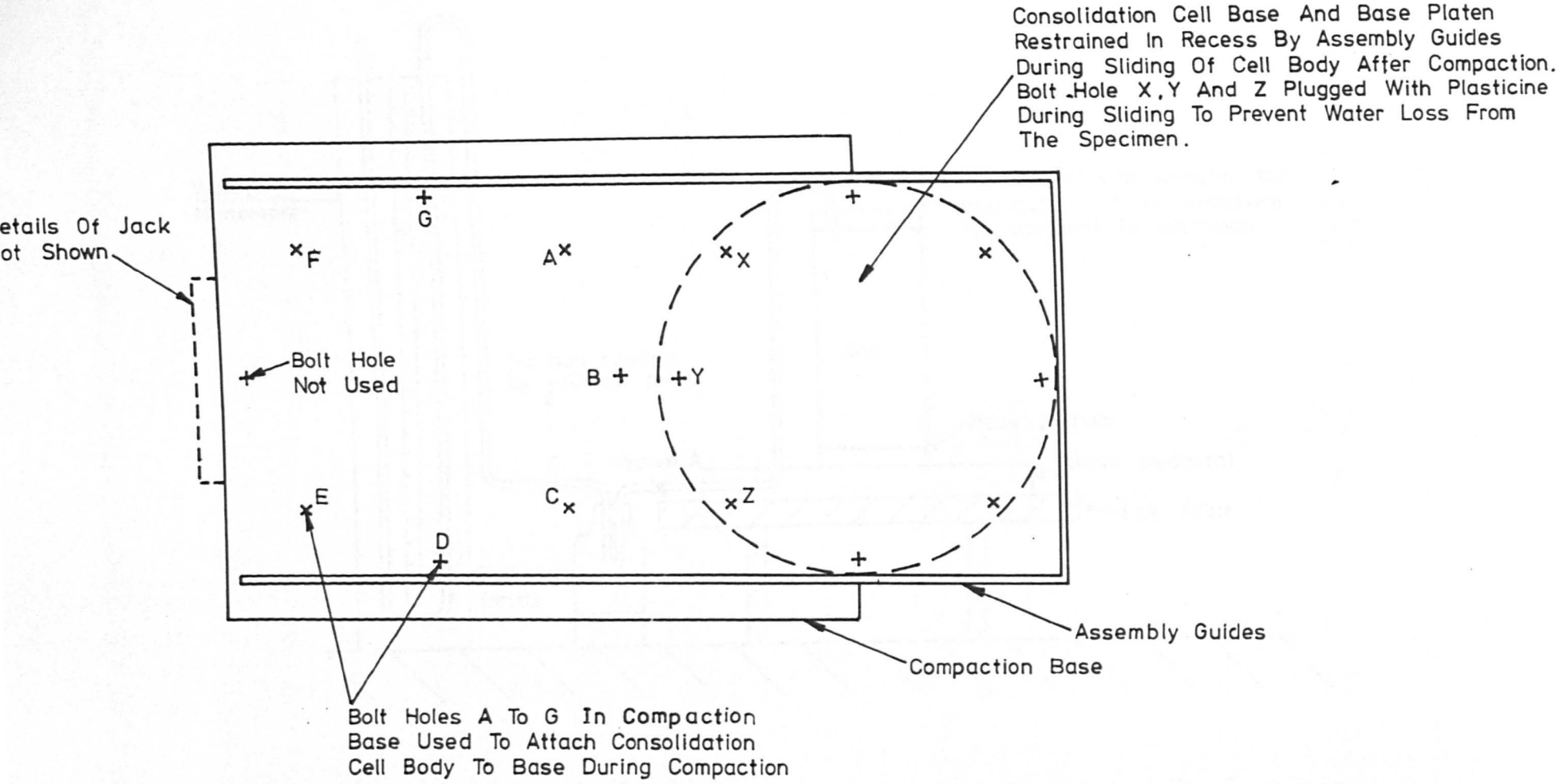

Figure A1 - Bolt Holes In Compaction Base and Consolidation Cell Base

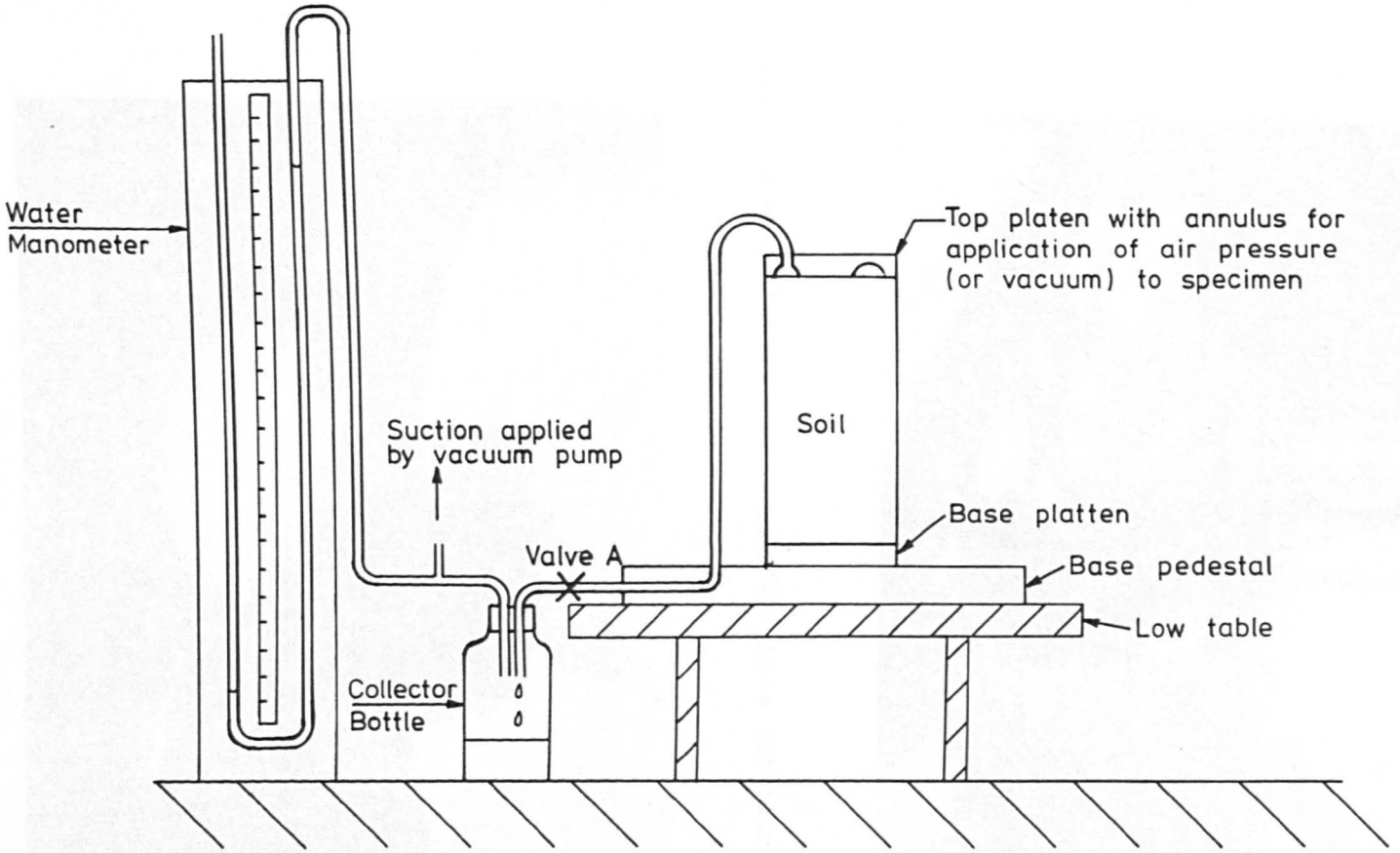

Figure A2 – Suction Pump And Manometer Connection To Specimen Before K_o And Shear Tests

Plate A1 Kango hammer and compaction guide for test series A and B

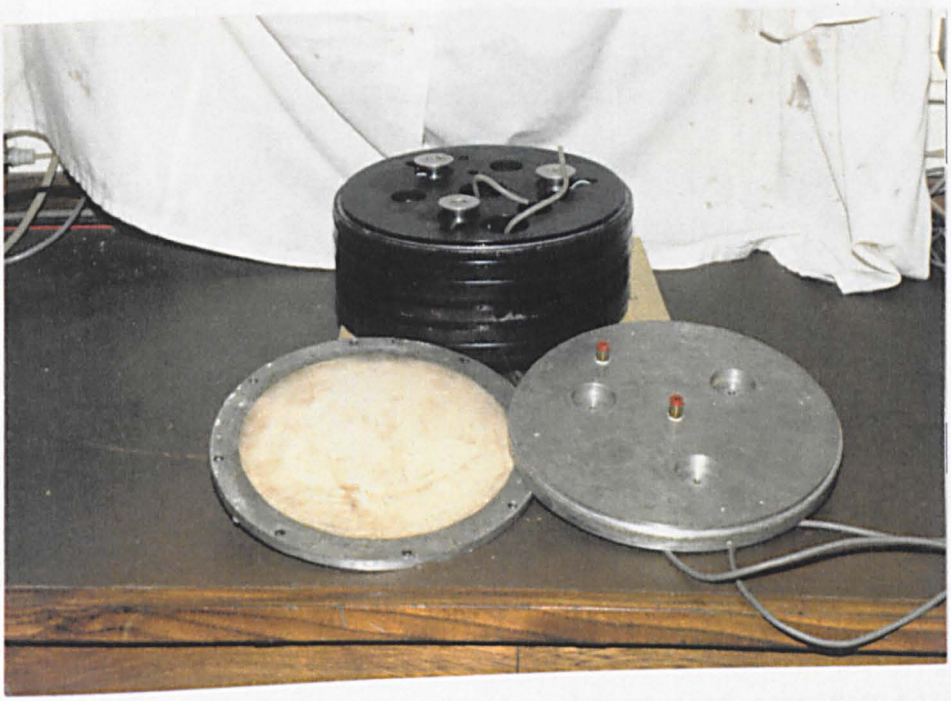

Plate A2 Component parts of top platen for consolidation cell

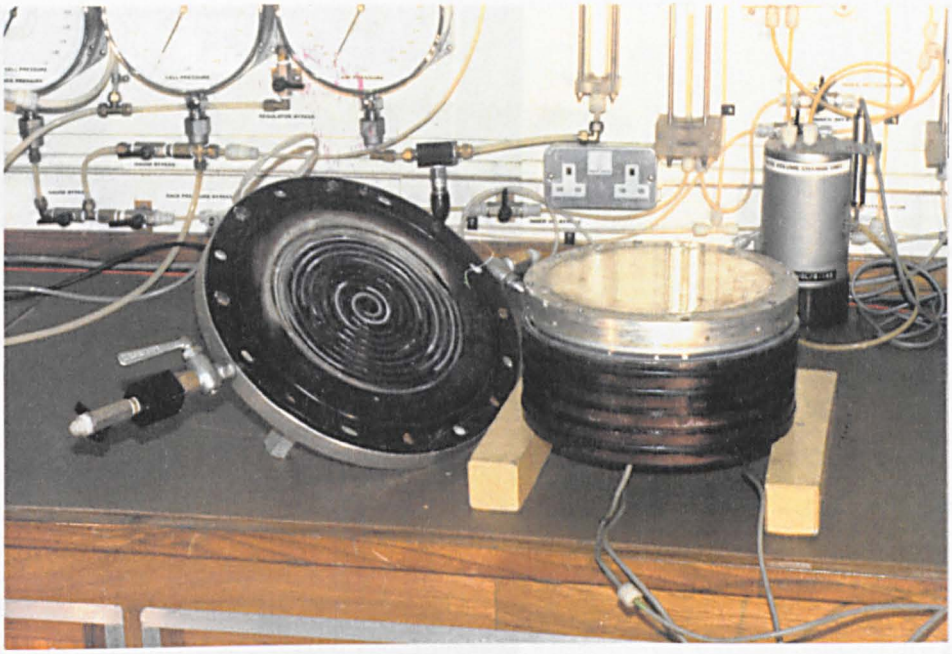

Plate A3 Assembled top platen

Plate A4 Sliding of consolidation cell and compacted specimen across compaction base using the hydraulic ram

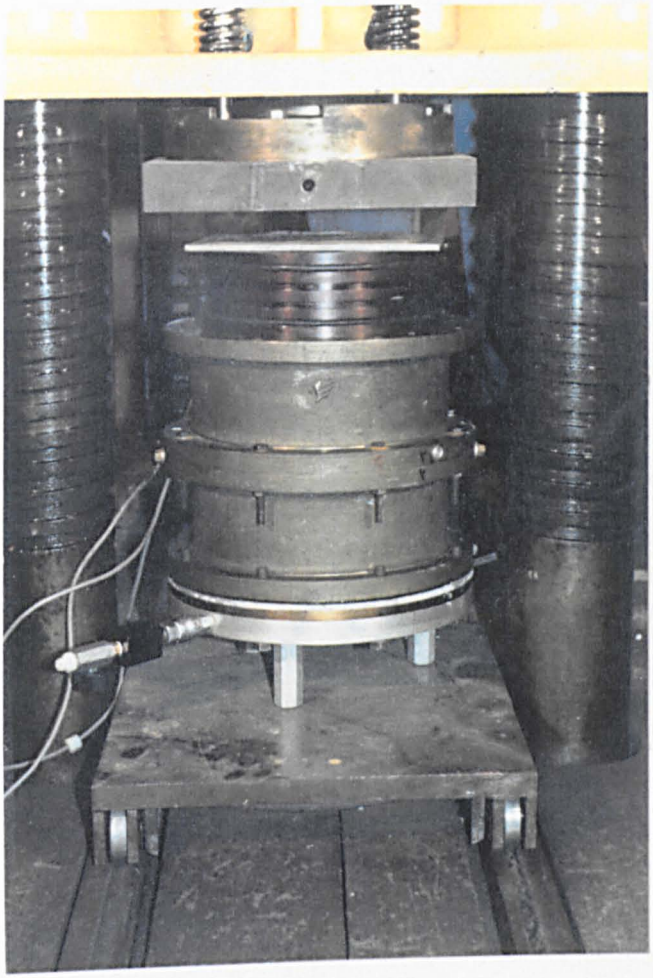

Plate A5 Insertion of top platen into consolidation cell using the hydraulic press

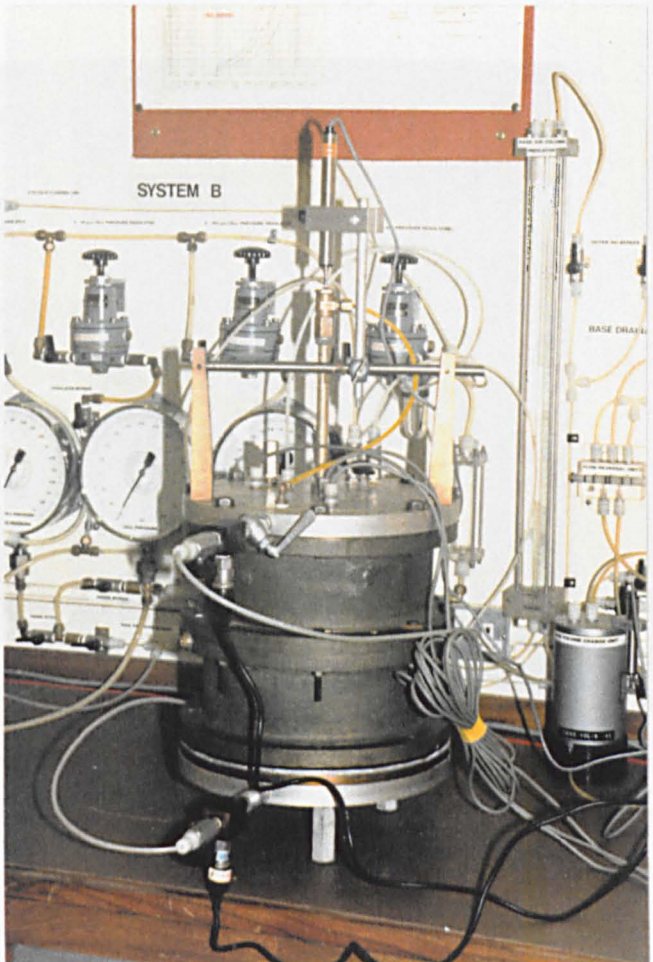

Plate A6 Fully assembled consolidation cell

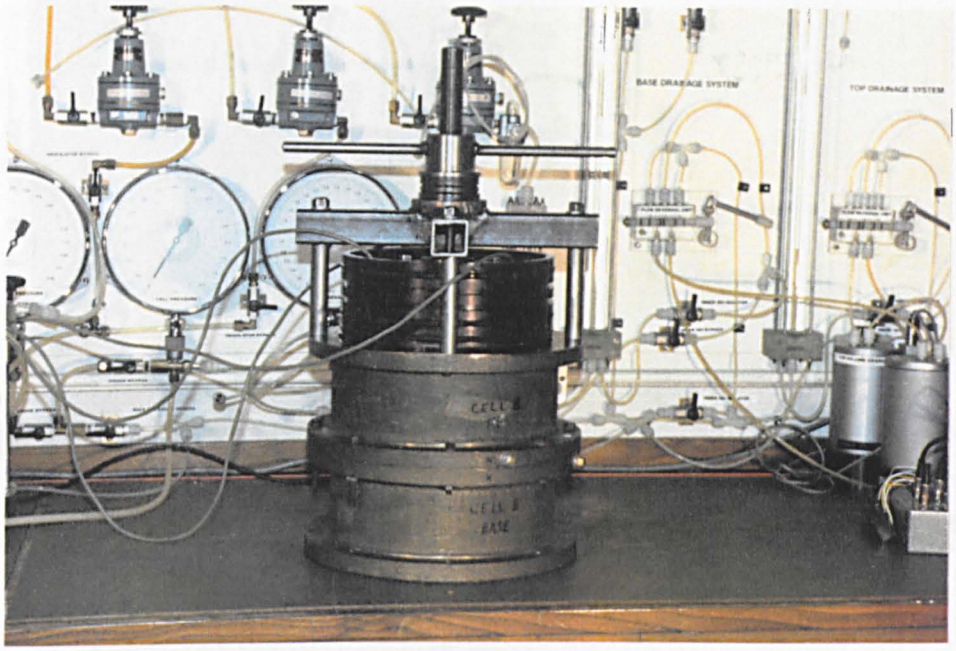

Plate A7 Removal of top platen following completion of test using the screw jack

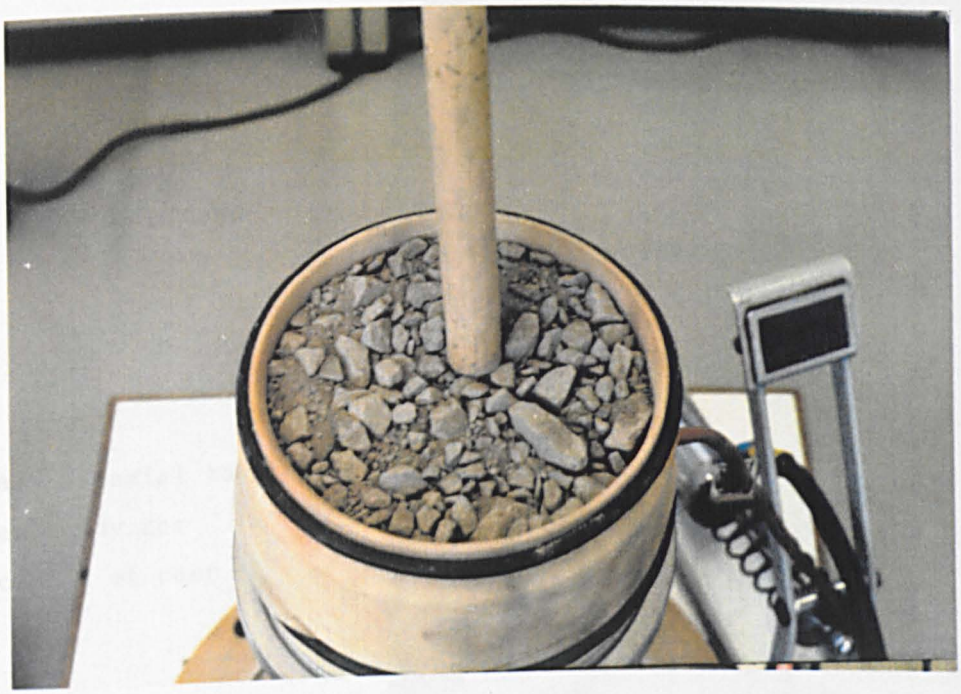

Plate A8 Compaction of triaxial test specimen

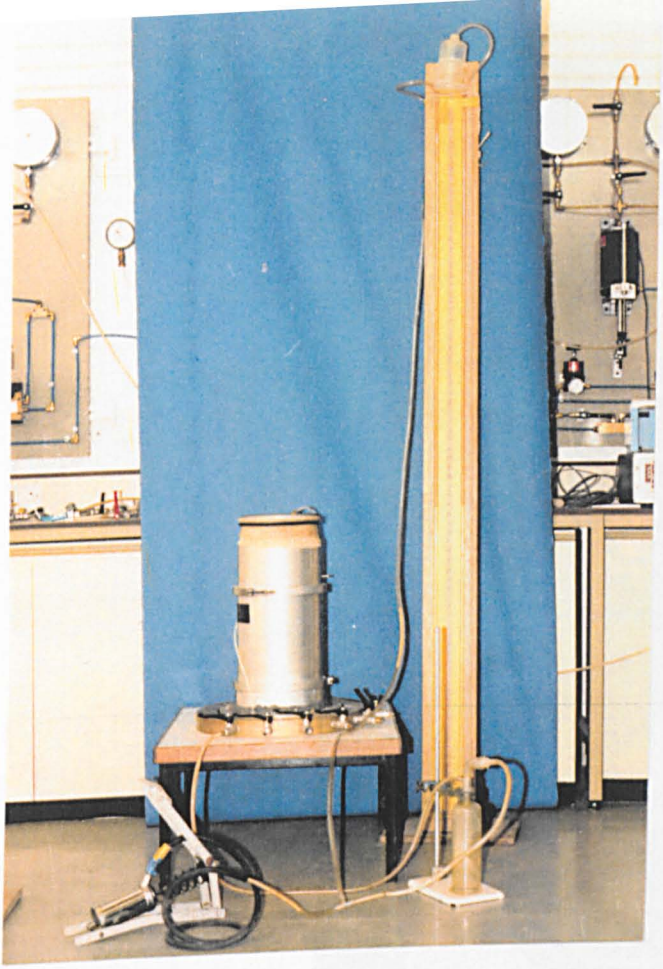

Plate A9 Vacuum pump and manometer used for preparation of triaxial test specimen

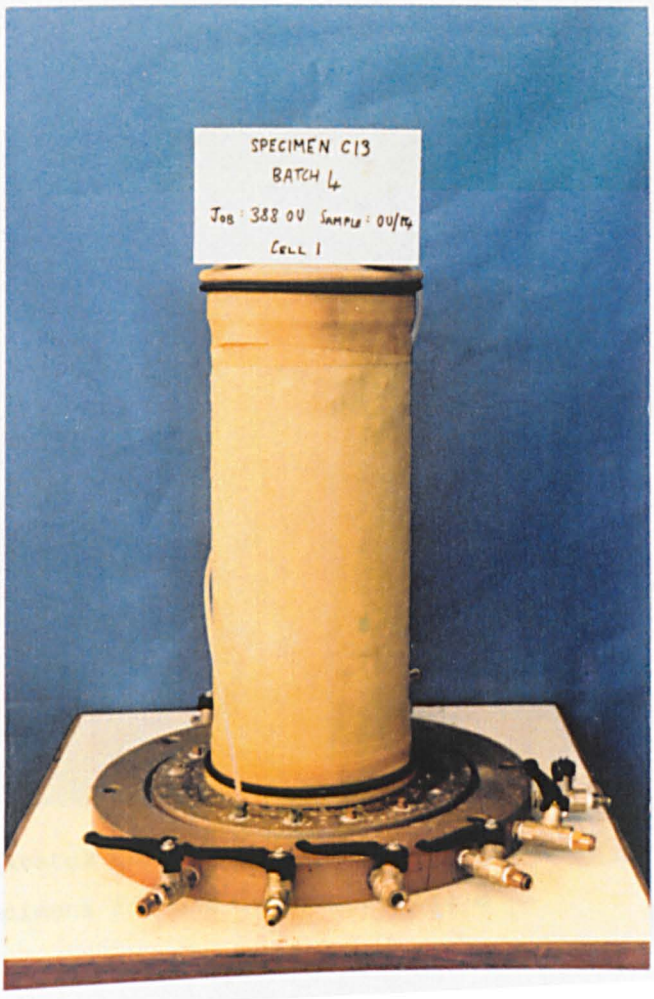

Plate A10 Triaxial test specimen ready for commencement of test

Plate A11 Compaction apparatus used to apply a high compactive effort to test specimens for use in test series D

Plate A12 Compaction apparatus used to apply a low compactive effort to test specimens for use in test series D

APPENDIX B

NAMES AND ADDRESSES OF SPECIALIST EQUIPMENT SUPPLIERS

Item(s) supplied	Name of supplier	Address
A. Volume Change Equipment		
(i) Imperial College Volume Change Units	Shape Instruments Ltd	Transducer Works Toutley Road Wokingham Berkshire RG11 5SS
(ii) GDS Units, Model 8085	Geotechnical Digital Systems Ltd	26 Midway Walton-on-Thames Surrey KT12 3HZ
B. Displacement transducers		
(i) Novatech LSC HS550 (50mm stroke)	Novatech Measurements Ltd	83 Castleham Road St Leonards-on-Sea East Sussex TN38 9NT
(ii) Sangamo, submersible	Sangamo Transducers	North Bersted Bognor Regis West Sussex PO22 9BS
(iii) RDP Type D5/2000A	RDP Electronics Ltd	Grove Street Heath Town Wolverhampton Staffordshire WV10 OPY
(iv) Penny and Giles Rectilinear Potentiometer Type HLP190SA1/ 100mm/4kohm	Penny and Giles Potentiometers Ltd	Somerford Division Christchurch Dorset BH23 3RS

Item(s) supplied	Name of supplier	Address
C. Equipment for manufacture and calibration of 2.5 kN load cells:		
(i) General equipment	Welwyn Strain Measurement	Armstrong Road Basingstoke Hampshire RG24 0QA
(ii) Kyowa strain gauges	Graham and White Instruments	135 Hatfield Road St Albans Hertfordshire AL1 4LZ
(iii) Dead weight testers	Budenburg Grange Co Ltd	Box No 5 Altrincham Cheshire WA14 4ER
D. Commercial load cells		
(i) Model WF17109 10 kN capacity	Whykham Farrance Engineering Ltd	Weston Road Trading Estate Slough Berkshire SL1 4HW
(ii) Sensotec Model 41 (20 kN and 110 kN capacities)	RDP Electronics Ltd	see earlier
E. Pressure transducers		
(i) Bell and Howell Model 4-366-0001-01Mohm	Bell and Howell Ltd	Lennox Road Basingstoke Hampshire RG22 4AW
(ii) Druck PDCR 10	Druck Ltd	Fir Tree lane Groby Leicestershire LE6 OFH

Item(s) supplied	Name of supplier	Address
F. Pressure regulation system		
(i) Bourdon gauges	Budenburg Gauge Co Ltd	see earlier
(ii) Nullmatic Pressure Regulators, Models 40-100 and 40-30HF	Moore Products Co (UK) Ltd	5 Queensbrook Bolton Lancashire 8L1 4AY
G. High air entry value ceramics	Soil Moisture Equipment Corporation	PO Box 30025 Santa Barbara California USA
H. Isuzu thermo-hygro-barograph model 3-1135	Isuzu Seisakusho Co Ltd or	3-8-19 Nishi-Ochiai Shinjuku-ku Tokyo
	J S Holdings (UK Supplier)	56 Spring Drive Stevenage Hertfordshire SG2 8AZ
I. Data acquisition system (University):		
(i) Analogue input unit Model 13683	MC Computers	Strawberry Hill House Newbury Berkshire
(ii) IEEE Interface	Acorn Computers Ltd	Yulbourn Road Cherry Hinton Cambridge CB1 4JN
J. Data acquisition system (British Gas):		
(i) DEC PDP 11/44 mini computer	Digital Equipment Corporation	Wimgrove House Basing View Basingstoke Hampshire
(ii) ADU 700 Datalogger	Mowlem Microsystems Ltd	Eastman Way Hemel Hempstead Hertfordshire HP2 7HB

Item(s) supplied	Name of supplier	Address
(iii) RDP Signal amplifier Rack Model 2031 Amplification Cards 2011 and 2027	RDP Electronics Ltd	see earlier
(iv) Protech Signal Amplifier Rack purpose made by Protech Amplification Cards M17 and M65	Protech Instruments Ltd	241 Selbourne Road Luton LU4 8NP

APPENDIX C

MANUFACTURE OF LOAD CELLS

This Appendix details the stages and procedures leading to manufacture of the load cells used in Test Series A and B. It does not A list of equipment used and their suppliers is included at the end of the Appendix.

C1 - Machining of Load Cell Bodies and Mounting Inserts

C1.1 Cut an approximately 100 mm length of 50 mm diameter Aluminium (metallurgical specification 2014T6) bar, for the basic load cell body.

C1.2 Drill a 12.5 mm diameter central hole and mount the cell on a spindle in a high tolerance Meccanica Cortini H80 lathe with ACC-RITE III digital read out (accurate to 0.001 mm on diameter and 0.01 mm on length), or similar

C1.3 Machine the bar to the dimensions shown in Figure B1, with a smooth surface finish (see plate B2).

C1.4 Cut two 10 mm long pieces from a 12 mm diameter Aluminium (no special specification) bar, for the mounting inserts.

C1.5 Machine the pieces to the dimensions shown in Figure C1. Check the inserts fit smoothly into the load cell.

C1.6 Tap a 4 mm screw thread through the centre of each insert.

C2 - Initial Preparation of Load Cell Bodies Prior to Strain - Gauging

C2.1 Lightly scribe orthogonal axes onto an end face of the cell.

C2.2 Degrease the central section of the cell using Chlorothene SM and soft paper. Rub in one direction only along the axis of the cell.

C2.3 Mount cell body onto spindle of high tolerance lathe, taking care not to touch the degreased area.

C2.4 Rotate lathe at approximately 500 revolutions/minute, and apply M-Prep Conditioner A liberally to 400 grit silicon carbide paper. Hold the rough surface of this paper against the rotating cell body and slowly traverse up and down the central section three of four times. Repeatedly add Conditioner A to keep metal surface wet.

C2.5 With cell body still rotating, apply gauze sponge to dry the surface.

C2.6 Stop lathe and carefully remove cell body without touching the cleaned area. Place on a surface plate.

C2.7 Insert a sharpened 4B pencil into a scribe block, and set pencil point at the approximate level of the long axis of the body.

C2.8 Using a small angle, position one of the orthogonal end axes vertically. Bring the scribe block and pencil into near contact with the end face, and finely adjust the pencil point until it coincides with the horizontal axis on the end face. Check the level by lightly running the point along the scribe line (see Figure C2).

C2.9 Run the pencil point lightly along either side of the cell body to burnish two of the alignment marks.

C2.10 Repeat steps C2.8 and C2.9 with the other end axis vertical, to finish with four orthogonal alignment marks.

C2.11 Stand the load cell on one end face, and adjust the pencil in the scribe line such that its point is 35mm above the surface plate, ie at the mid-height of the load cell. Lightly burnish a circumferential line around the centre of the cell body holding the cell in place with light finger pressure on the cell flange.

C3 - Application of Axial Pair of Strain Gauges

C3.1 Transfer load cell body to the constant temperature body and leave for at least 15 minutes whilst the rest of the equipment is prepared, to allow temperature equalisation.

C3.2 Apply Conditioner A to a clean cotton tip and scrub longitudinally an area sufficient for one strain gauge set on one of the four centre-hair axes of the central portion. Continue scrubbing, replacing soiled tips every few strokes, until a clean tip is not discoloured.

C3.3 Remove residue of Conditioner A by wiping dry, in one direction only, with a clean dry tip. Never allow any solution to dry on the surface, as this will leave a contaminating film and reduce the chance of a good bond.

C3.4 Apply a liberal amount of M-Prep Neutraliser 5 to a cotton tip, and scrub the cleaned area. Take care not to allow excess liquid to run across the rest of the cell. Dry surface with a single slow wipe in one direction with another clean tip.

C3.5 Remove a Strain Gauge (Type FLA-6-350-23) from its acetate envelope using tweezers and place gauge side up on gauge box.

C3.6 Lay load cell body lengthwise onto the bench, with the prepared area uppermost.

C3.7 Lightly place a 2cm to 3cm length of Mylar tape over the gauge face, and carefully pick up the tape with gauge attached, by its ends. If the tape sticks to the envelope, slowly lift away at a shallow angle to break the contact.

C3.8 Without allowing the tape to contact the cell, carefully align the burnished axes and strain gauge markers (see Figure C3). When correct, aligned, lightly roll the tape ends onto the cell body, from the gauge outwards.

C3.9 Check the alignment again - if necessary, further fine adjustment may be made by raising one end of the tape at a time and rotating it slightly before re-laying. If several attempts fail, repeat steps B3.2 to B3.8 with a new gauge.

C3.10 Repeat steps B3.2 to B3.9 with the diametrically opposite axial strain gauge.

C3.11 With both axial gauges aligned and held with tape, slowly peel back at a shallow angle one end of the tape for each gauge, such that both the gauge backings are exposed and accessible (see Figure C4). The Mylar tape will naturally curl up as illustrated.

C3.12 Apply a thin coat of M-Bond 610 (previously prepared to the manufacturers instructions) to both gauge backings, and the Aluminium surface onto which the gauges will lie. Brush in one direction only, and ensure sufficient adhesive is on the brush for complete coverage in one stroke. Do not allow the brush to touch the tape mastic.

C3.13 Leave adhesive to air dry by solvent evaporation for between 35 and 45 minutes. The optimum drying time was found to be 40 minutes for the laboratory conditions of 20°c and a relative humidity of between 50% and 60% (see Figure 5.1).

C4 - Curing of Strain Gauges

C4.1 When air dry, relay gauges carefully by rolling from the tacked end of the tape with light thumb pressure. Do not repeatedly roll in opposite directions or apply heavy pressure.

C4.2 With both gauges and tapes attached to the metal, transfer the body to the pressure pot (see Figure C5), check the 'O' ring seal, and bolt on the top of the pot.

C4.3 Connect the pot to a Budenburg dead weight tester (Model 240) and apply Nitrogen at 220 kPa gauge pressure.

C4.4 Close valve on pot, wait 10 seconds and reopen. If the 'O' ring seal is working, no pressure will have been lost and the tester will register no effect. If the seal is suspect replace quickly and repeat test. When satisfied, re-apply nitrogen at the same pressure and close valve.

C4.5 Disconnect pot and place in room temperature Baby Belling electric oven. Set thermostat to 325°F (162°c) and close door. The oven will reach the set temperature in about 20 minutes, ie at a sufficiently slow rate to preclude the formation of bubbles and uneven glue - lines below the gauges.

C4.6 Leave pot at 325°F for two hours, then turn oven off. Leave the door closed whilst the oven cools.

C4.7 When cool remove the pot and release the pressure. If pressure in the pot is lost due to failure of the 'O' rings reject the gauge assembly and re-start load cell manufacture.

C4.8 Remove load cell from pot. Slowly peel back the tapes at a large angle to coarse check the bond achieved.

C5 - Application of Circumferential Strain Gauges

C5.1 Repeat gauge application similar to that described above, taking care not to damage the first pair of gauges, especially by careless use of fluids and/or laying tape over the first gauges and leadwires.

C5.2 Repeat curing of the new gauges exactly as before.

C6 - Post Curing of Strain Gauge Adhesive

C6.1 Place load cell alone in room temperature Baby Belling oven. Raise temperature to just under 400°F (205°c).

C6.2 Maintain this temperature for 2 hours, then turn oven off. Leave oven closed during cooling.

C6.3 Remove load cell when oven is cool, and check gauges. The backing will have changed colour from green to dark brown if the correct temperature has been used. If temperatures in excess of 400°f have been used, the backings will be black and poorer performance of the cell may result.

C6.4 With a resistance meter, check each bonded gauge has a resistance of 350 ohms. If this condition is not complied with, the cell should be rejected.

C7 - Application of Terminals and Wiring

C7.1 Select four copper faced terminals of three leaved clover format (see Figure C5), and cover each with Mylar tape.

C7.2 Position terminals to allow wiring as shown in Figure B6, and secure in place with the tape. Peel back one end of the tape for each terminal, to expose the terminal backings.

C7.3 For each terminal in turn, apply a thin coating of CN adhesive to the terminal and aluminium, then roll terminal back into position. Apply light thumb pressure to secure the adhesive in seconds. Peel back tape to check bond, and proceed to next terminal. When all terminals are attached, commence wiring.

C7.4 Cut about a 1.5m length of double pair screened cable from its reel, and expose approximately 4 cm of each wire at both ends of the cable.

C7.5 Tin ends of each wire, all four terminals, and the strain gauge leadwires.

C7.6 Solder leadwires and cable wires to terminals, according to the wiring diagram shown in Figure C6.

C7.7 With a resistance meter, check the circuit resistances between terminals complies with that noted in Figure C6. Differences imply a circuit fault, due to earthing or poor soldering, and must be corrected.

C8 - Protective Coating of Load Cell

C8.1 Apply a thin coating of RTV Primer No 1 to gauges, terminals, wires and cable near to cell. Leave to air dry for 15 minutes.

C8.2 Apply RTV 3140 silicone sealant to the primed areas, ensuring complete coverage.

C8.3 Immediately after applying RTV 3140, clamp the cell in a pot shaker, wrap wires carefully around the clamp, and start rotating the shaker. The rotating action was found to form a more even distribution of sealant than hand rotation, given the sealant fluidity and set time.

C8.4 After 30 minutes, stop the shaker and remove excess sealant with thin paper towels, then continue shaking again for a further 2 hours until the sealant is set.

C8.5 Leave the sealed cell for a further 24 hours at 20°C for complete cure of the waterproofing sealant.

C9 - Assembly of Mounting Inserts

C9.1 Thread insert onto 4mm bolt, and apply thin coating of Loctite Engineering Adhesive 290 to circumference of insert.

C9.2 Slip insert into load cell, such that the outer face of the insert is recessed approximately 2mm from the end face.

C9.3 Repeat steps C9.1 and C9.2 for the other insert, and lay load cell horizontally on bench.

C9.4 Leave Loctite to cure at 20°c for 24 hours but removing any excess Loctite after 15 minutes before it sets.

C9.5 Check inserts are firmly held and that end faces are still smooth and unblemished.

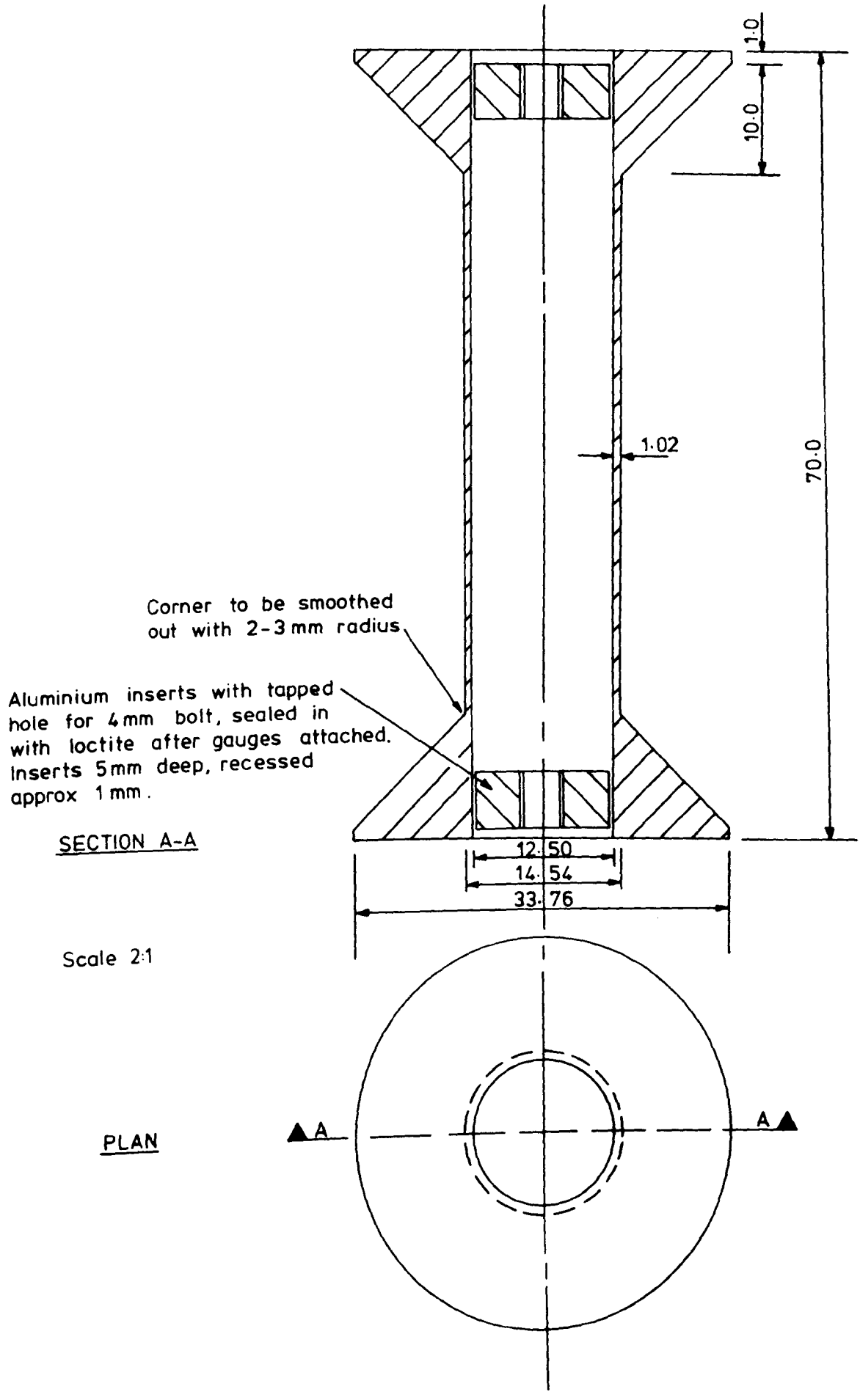

Figure C1 – 2·5kN Load Cell

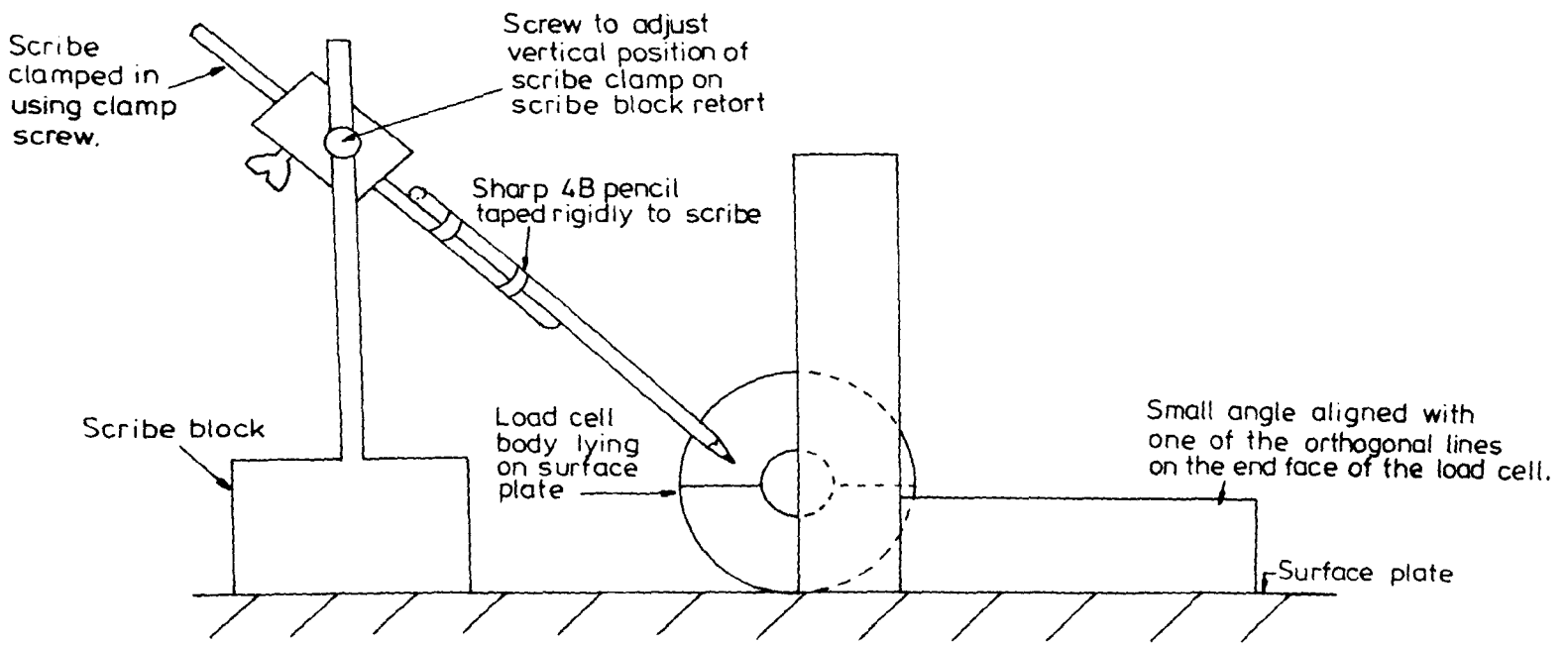

Figure C2-General Arrangement To Set Pencil Level Ready For Burnishing Axes On Load Cell Body

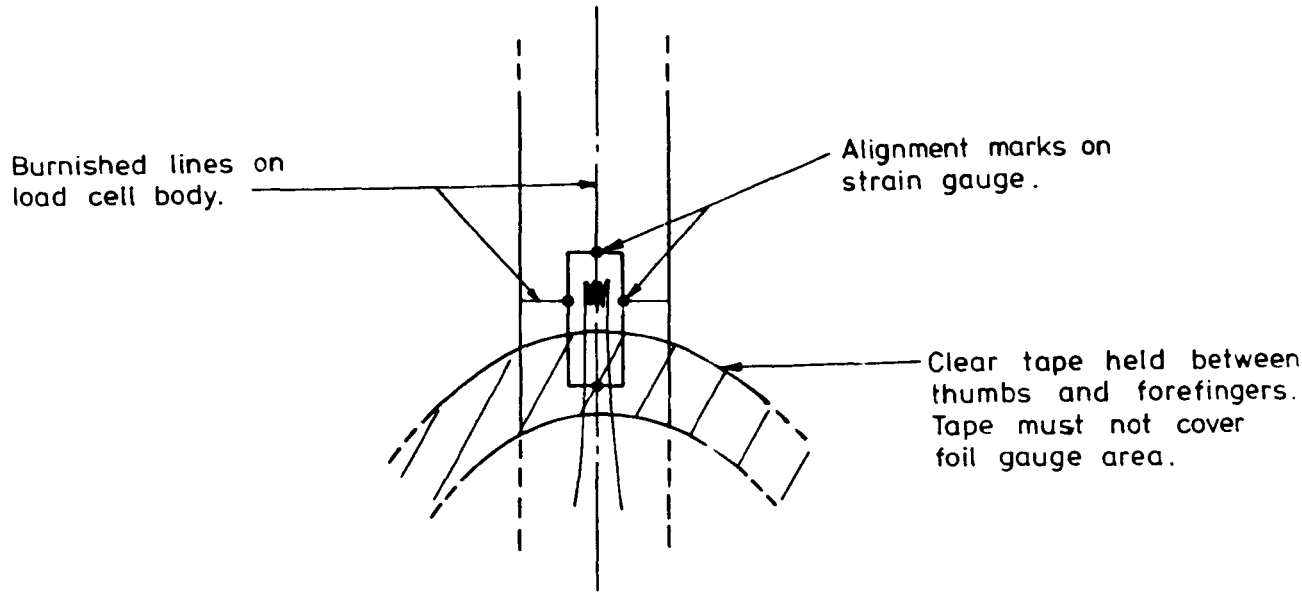

Figure C3 - Picking Up And Positioning A Strain Gauge

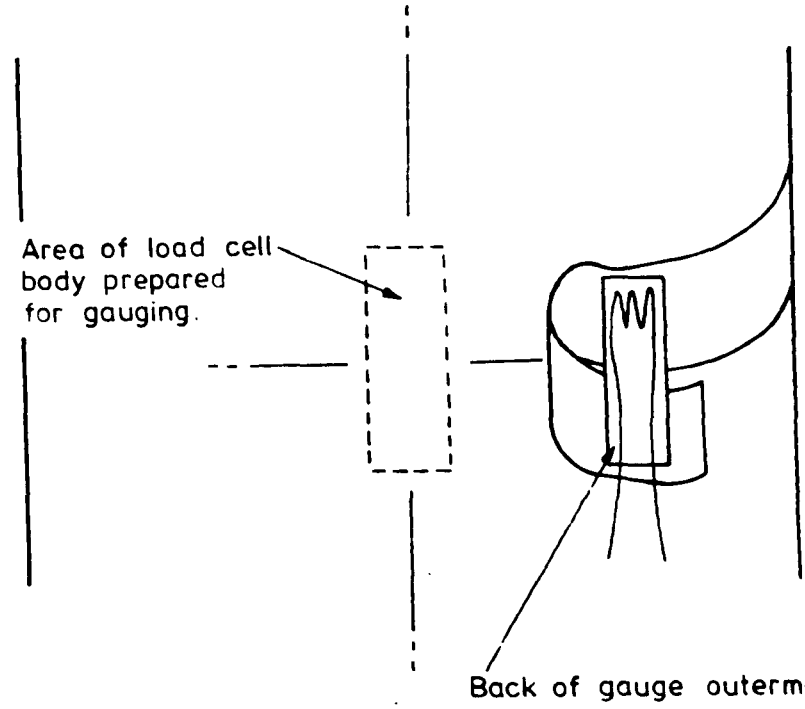

Figure C4 - Position Of Strain Gauges Prior to Applying Adhesive

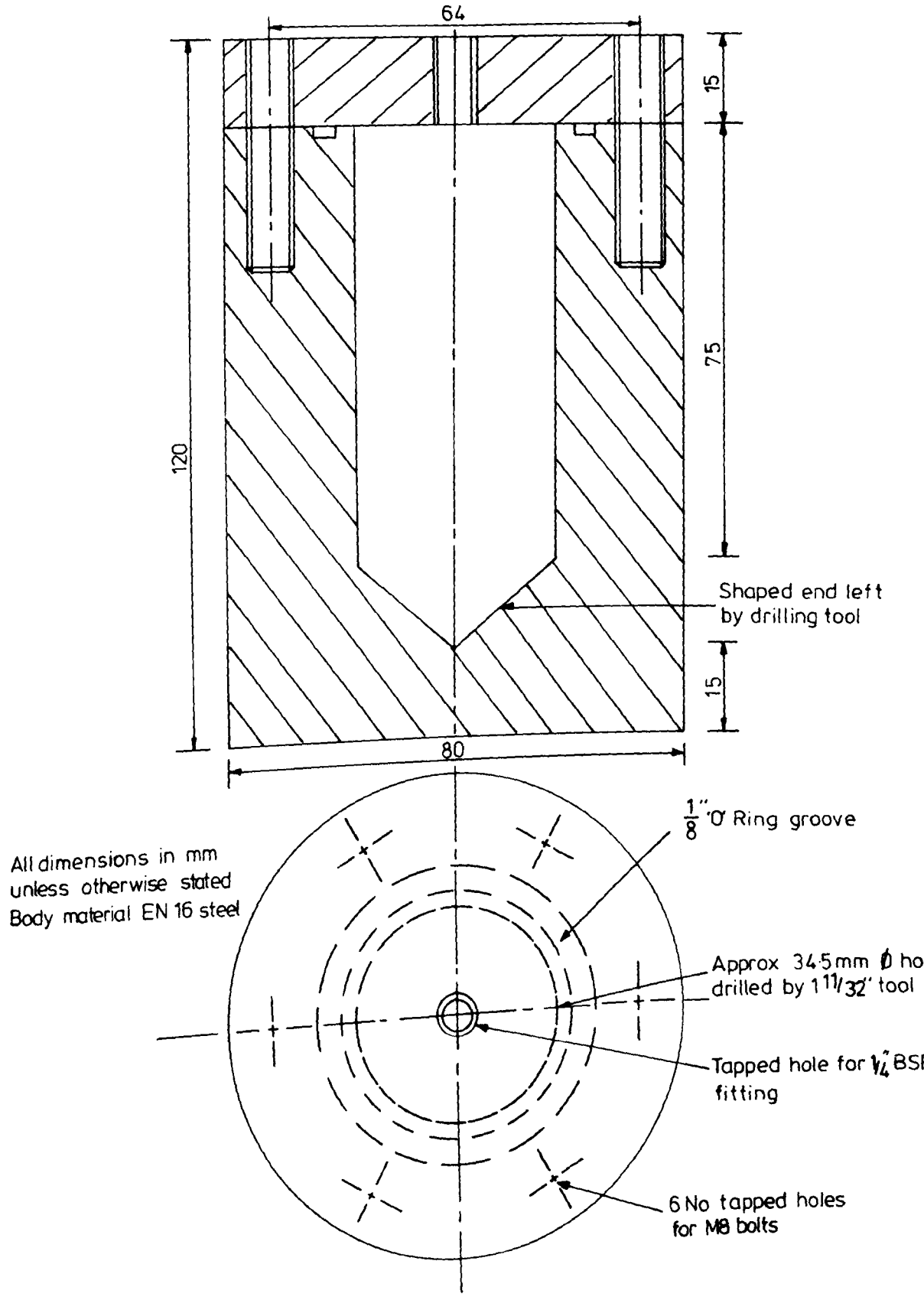

Figure C5-Pressure Chamber for Curing of Strain Gauge Adhesive

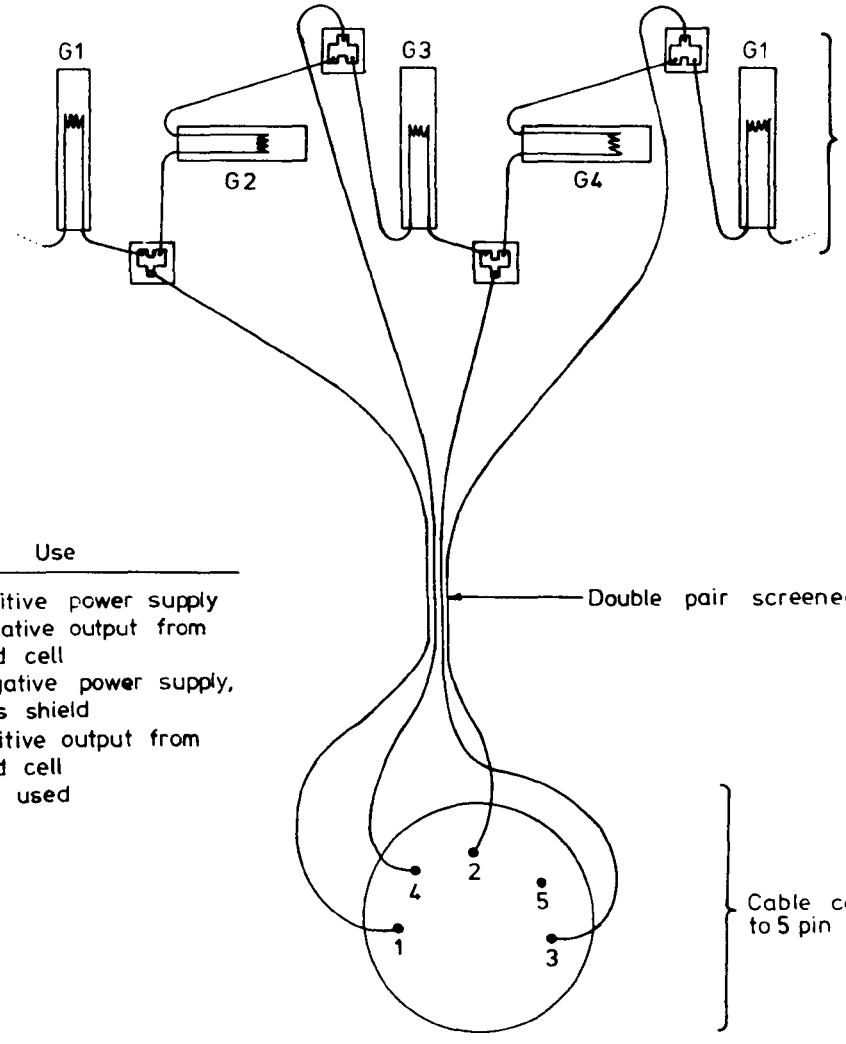

Dim Plug Details

Point	Use
1	Positive power supply
2	Negative output from load cell
3	Negative power supply, plus shield
4	Positive output from load cell
5	Not used

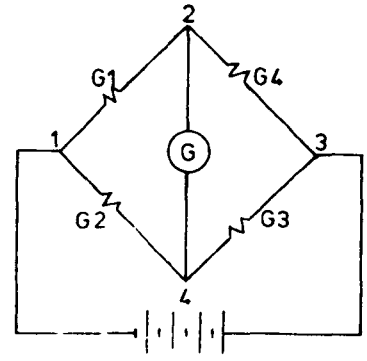

$R_{1-2} = R_{2-3} = R_{3-4} = R_{4-1} = 466.7$ ohm

$R_{1-3} = R_{2-4} = 350$ ohm

Figure C6-Wiring of Load Cell Strain Gauges Into Full Wheatstone Bridge

APPENDIX D

DATA ACQUISITION

A programme listing for the data acquisition software LOG3 written by the author is presented in this appendix. The software was used with a BBC B computer, disc drive, Acorn IEEE interface, MC Computers analogue input unit, and parallel printer.

```
>L.
   10CLOSE£0:MODE7:*TV255,1
   20VDU23,1,0;0;0;0;:*IEEE
   30ONERRORCLS:REPORT:X=GET:PROCmenu
   40DIMC$(16),U$(16),CF(2,16),G%(16),VCU(2,7),GC%(4),GD%(4),AIU$(1,1),K(16),FL$
(2,2),D$(2),S$(2),LC(3,2),AP(1,10),F$(2,2),AVG(2),SZ(2),C(2)
   50PROCinit
   60PROCmenu
   70CLOSE£0
   80*DISC
   90END
  100DEFPROCinit
  110AIU$(0,0)="6":AIU$(0,1)="7":OP$="1":STAT=0:AT1=0:BT1=0:NC%=1:AT=0:BT=0:X$="
0":R$="0":Q%=0:PR=0:PK%=1:PC%=0:PE%=0:PL%=0:AT0=0:BT0=0:SA%=0:SB%=0:AIU=0:A1%=0:
A2%=15:B1%=0:B2%=15
  120FORI%=0TO10:AP(0,I%)=0:AP(1,I%)=0:NEXTI%
  130FORI%=0TO15:CF(0,I%)=1:CF(1,I%)=0:U$(I%)="mV      ":NEXTI%
  140FORX%=1TO2:D$(X%)=STRING$(120," "):S$=STRING$(40," "):NEXTX%
  150FORX%=1TO2:D$(X%)="NONE INPUT":S$(X%)="NONE INPUT":F$(X%,1)="NONE USED ":F$
(X%,2)="NODRIVE":FL$(X%,1)="T":FL$(X%,2)="T":SZ(X%)=0:LC(1,X%)=0:LC(2,X%)=0:LC(3
,X%)=0:C(X%)=0:AVG(X%)=-999:FORI%=1TO7:VCU(X%,I%)=0:NEXTI%:NEXTX%
  160C$(0)="CHAN. 0":C$(1)="CHAN. 1":C$(2)="CHAN. 2":C$(3)="CHAN. 3":C$(4)="CHAN
. 4":C$(5)="CHAN. 5":C$(6)="CHAN. 6":C$(7)="CHAN. 7"
  170C$(8)="CHAN. 8":C$(9)="CHAN. 9":C$(10)="CHAN.10":C$(11)="CHAN.11":C$(12)="C
HAN.12":C$(13)="CHAN.13":C$(14)="CHAN.14":C$(15)="CHAN.15"
  180GC%(0)=OPENIN(AIU$(0,0)):GD%(0)=OPENIN(AIU$(0,1))
  190cmd%=OPENIN("COMMAND"):data%=OPENIN("DATA")
  200PRINT£cmd%,"BBC DEVICE NO",8:PRINT£cmd%,"CLEAR":PRINT£cmd%,"REMOTE ENABLE":
PRINT£cmd%,"END OF STRING",CHR$(13):PRINT£cmd%,"TIMEOUT ON"
  210PROCreadgains:CLS:PRINTTAB(10,5)"DUAL CELL,16 CHANNEL":PRINTTAB(10,6)"=====
==============":PRINTTAB(14,8)"DATA LOGGER":PRINTTAB(14,9)"==========="
  220INPUTTAB(0,18)"In which cell (A or B) will the first   test be set up,or 'Q
' to quit ";CL$:IFCL$<>"A"ANDCL$<>"B"ANDCL$<>"Q"THENPRINTTAB(0,18)SPC(80):GOTO22
0
  230IFCL$="Q"THEN70
  240ENDPROC
  250DEFPROCmenu
  260CLS:PRINT"MAIN MENU":PRINT"========="
  270PRINT"1.........INPUT CHANNEL & TEST INFO"
  280PRINT"2.............DATA RECORDING OPTIONS"
  290PRINT"3.............DISPLAY DISC DIRECTORY"
  300PRINT"4..........CURRENT CHAN/TEST STATUS"
  310PRINT"5.........................START TEST"
  320PRINT"6.............................END"
  330IFNC%=2PRINTTAB(0,20)"Logging of old test is temporarily      halted - use
option 5 to continue       logging & start new test"
  340REPEAT:X$=GET$:UNTILX$>="1"ANDX$<="6"
  350IFX$="1"THENPROCinfo:PROCmenu
  360IFX$="2"THENPROCrecorddata:PROCmenu
  370IFX$="3"THENPROCcat:PROCmenu
  380IFX$="4"THENPROCchanstat:PROCmenu
  390IFX$="5"THENPROCtest:PROCmenu
  400ENDPROC
  410DEFPROCtest
  420CLS:PRINT"OPTION 5 - START TEST":PRINT:STAT=1
  430IFNC%=2THEN540
  440INPUT"Number of first channel to be read ";A1%:B1%=A1%:INPUT"Number of last
 channel to be read ";A2%:B2%=A2%:IFA2%<A1%ORA1%<0ORA2%>15THEN420
  450PRINT:PRINT"Scan interval must exceed ";(B2%-A1%)*0.5;" secs":INPUT"Require
d interval (secs) ";AT:AT=AT*100:BT=AT:PRINT
  460IFAT=0THEN450ELSEINPUT"Correct? Y for yes " A$:IFA$<>"Y"THEN420
  470IFCL$="A"THENX%=1ELSEX%=2
  480IFLC(1,X%)=0THEN500
  490IFLC(1,X%)>A2%ORLC(1,X%)<A1%ORLC(2,X%)>A2%ORLC(2,X%)<A1%ORLC(3,X%)>A2%ORLC(
3,X%)<A1%PRINT"CHANNELS NOMINATED DO NOT INCLUDE LC's":X=GET:GOTO420
  500IFVCU(X%,5)=0THEN520
  510IFVCU(X%,6)>A2%ORVCU(X%,7)>A2%ORVCU(X%,6)<A1%ORVCU(X%,7)<A1%PRINT"CHANNELS
NOMINATED DO NOT INCLUDE VCU's":X=GET:GOTO420
  520IFPR=1THENPROCprint
  530TIME=0:GOTO570
  540IFPR=1THENPROCprint
  550IFCL$="A"THENBT1=TIME:BT0=BT1
```

```
  580IFCL$="B"THENAT1=TIME:AT0=AT1
  570VDU23,1,0;0;0;0;
  580PROClabel:AIU=0:IM%=0
  590FORI%=A1%TOB2%
  600C$="@C"+STR$(I%-IM%)+"I"
  610PROCcommand:PROCgetdata
  620X=INSTR(A$,"I")-1:CH%=VAL(MID$(A$,3,X)):V=VAL(MID$(A$,X+2)):@%=03
  630IFOP$="1"THENK(I%)=V*CF(0,I%)+CF(1,I%)ELSEK(I%)=(V+CF(1,I%))*CF(0,I%)
  640IF(NC%=2ANDCL$="A"ANDI%>=A1%ANDI%<=A2%)ORNC%=1THENPRINTTAB(0,I%-A1%+7)I%,TA
B(5,I%-A1%+7)C$(I%):@%=&20309:PRINTTAB(12,I%-A1%+7)V,TAB(22,I%-A1%+7)K(I%),TAB(3
2,I%-A1%+7)U$(I%):@%=10:GOTO660
  650IFCL$="B"ANDI%>=B1%ANDI%<=B2%THENPRINTTAB(0,I%-B1%+7)I%,TAB(5,I%-B1%+7)C$(I
%):@%=&20309:PRINTTAB(12,I%-B1%+7)V,TAB(22,I%-B1%+7)K(I%),TAB(32,I%-B1%+7)U$(I%)
:@%=10
  660NEXTI%:K$=INKEY$(10)
  670IFK$="O"PROCrunops
  680IFX$="E"THENX$="NONE":GOTO860
  690IFX$="S"THENX$="NONE":GOTO940
  700IFK$="O"PROClabel
  710IF(TIME>=AT1)OR(TIME>=BT1)THEN720ELSE590
  720IFNC%=1ANDCL$="A"THENPC%=1:T=(TIME-AT0)/100
  730IFNC%=1ANDCL$="B"THENPC%=2:T=(TIME-BT0)/100
  740IFNC%=2AND(AT1<BT1)THENPC%=1:T=(TIME-AT0)/100
  750IFNC%=2AND(AT1>=BT1)THENPC%=2:T=(TIME-BT0)/100
  760IFPR=1PROCprint
  770IFPC%=1THEN780ELSE810
  780AT1=AT1+AT:SA%=SA%+1:IFCL$="A"PRINTTAB(26,3)"SCAN NO. ";SA%-1
  790IFSZ(1)<>0THENR$="A":PROCdatadisc
  800GOTO830
  810BT1=BT1+BT:SB%=SB%+1:IFCL$="B"PRINTTAB(26,3)"SCAN NO. ";SB%-1
  820IFSZ(2)<>0THENR$="B":PROCdatadisc
  830IFNC%=1ANDCL$="A"THENBT1=AT1:SB%=SA%
  840IFNC%=1ANDCL$="B"THENAT1=BT1:SA%=SB%
  850GOTO590
  860IFCL$="A"ANDSZ(1)<>0THENR$="A":PROCwindup
  870IFCL$="B"ANDSZ(2)<>0THENR$="B":PROCwindup
  880IFCL$="A"THENA1%=B1%ELSEB2%=A2%
  890IFPR=1THENPE%=1:PROCprint
  900IFNC%=1THEN930ELSENC%=1
  910IFCL$="A"THENCL$="B":AT=BT:AT1=BT1:SA%=SB%:A2%=B2%:SZ(1)=0:D$(1)="NONE INPU
T":S$(1)="NONE INPUT":F$(1,1)="NONE USED":F$(1,2)="NODRIVE":VCU(1,5)=0:AVG(1)=-9
99:C(1)=C(2):FORI%=0TO10:AP(0,I%)=0:NEXTI%:GOTO700
  920IFCL$="B"THENCL$="A":BT=AT:BT1=AT1:SB%=SA%:B1%=A1%:SZ(2)=0:D$(2)="NONE INPU
T":S$(2)="NONE INPUT":F$(2,1)="NONE USED":F$(2,2)="NODRIVE":VCU(2,5)=0:AVG(2)=-9
99:C(2)=C(1):FORI%=0TO10:AP(1,I%)=0:NEXTI%:GOTO700
  930CLS:PRINT"LOGGING COMPLETED - ALL VARIABLES RE-SETTO DEFAULT VALUES":X=GET:
PROCinit
  940ENDPROC
  950DEFPROCreadgains
  960AIU=0:IM%=0:FORI%=0TO15
  970C$="@C"+STR$(I%-IM%)+"?":PROCcommand:PROCgetdata
  980X=INSTR(A$,"?")-1:V$=MID$(A$,X+2):G%(I%)=VAL(MID$(V$,2,2)):NEXTI%:ENDPROC
  990DEFPROCsetgains
 1000AIU=0:IM%=0:CLS:PRINT"CHAN  GAIN"
 1010FORI%=0TO15:@%=&00004:PRINTI%;:@%=&00006:PRINTG%(I%):NEXTI%:PRINT:@%=10
 1020INPUT"CHANNEL TO CHANGE OR Q TO QUIT "G$
 1030IFG$="Q"THEN1080
 1040IF(ASC(G$)>=48ANDASC(G$)<=57)AND(VAL(G$)>=0ANDVAL(G$)<=15)THENI%=VAL(G$)ELS
E1000
 1050IF(NC%=2ANDCL$="A"ANDI%<=A2%)OR(NC%=2ANDCL$="B"ANDI%>=B1%)PRINT"TEST CURREN
TLY RUNNING IN THIS CELL - NOAMMENDMENTS ALLOWED":X=GET:GOTO1000
 1060INPUTTAB(0,19)"NEW GAIN = "G$:IFVAL(G$)<0ORVAL(G$)>11OR(VAL(G$)-INT(VAL(G$)
))>0THENPRINTTAB(0,19)SPC(40):GOTO1060
 1070C$="@C"+STR$(I%-IM%)+"G"+G$
 1080PROCcommand:PROCgetdata:PROCreadgains:GOTO1000
 1090ENDPROC
 1100DEFPROCcommand
 1110PRINT&omd%,"LISTEN",GC%(AIU),"EXECUTE":PRINT&data%,C$:PRINT&omd%,"UNLISTEN"
:ENDPROC
```

```
1120DEFPROCgetdata
1130PRINT&cmd%,"TALK",GD%(AIU):INPUT&data%,A$:PRINT&cmd%,"UNTALK":ENDPROC
1140DEFPROCdatadisc
1150*DISC
1160IFR$="B"THEN1200
1170OSCLI(F$(1,2))
1180PRINT&AX%,T
1190FORI%=A1%TOA2%:PRINT&AX%,K(I%):NEXTI%:GOTO1230
1200OSCLI(F$(2,2))
1210PRINT&BX%,T
1220FORI%=B1%TOB2%:PRINT&BX%,K(I%):NEXTI%
1230*IEEE
1240ENDPROC
1250DEFPROCcat
1260CLS:PRINT"OPTION 3 - DISC DIRECTORY":PRINT
1270*DISC
1280INPUT"DISC DRIVE NO. ";D$:D$="*DRIVE "+D$:OSCLI(D$):*CAT
1290*IEEE
1300X=GET:ENDPROC
1310DEFPROCwindup
1320CLS:*DISC
1330IFR$="A"THENOSCLI(F$(1,2)):A0=PTR&AX%:X%=1
1340IFR$="B"THENOSCLI(F$(2,2)):A0=PTR&BX%:X%=2
1350PRINT"TEST COMPLETED - CLOSE FILE ROUTINE":PRINT:INPUT"ENTER DURATION OF TE
ST (TIME AND/OR DATE";S$(X%):INPUT"ENTER REMARKS/TEST DESCRIPTION";D$(X%)
1360IFX%=2THEN1400
1370PTR&AX%=0:PRINT&AX%,SA%:PTR&AX%=A0
1380FORI%=A1%TOA2%:PRINT&AX%,C$(I%),CF(0,I%),CF(1,I%),U$(I%),G%(I%):NEXTI%
1390PRINT&AX%,OP$,S$(1),D$(1):FORI%=0TO10:PRINT&AX%,AP(0,I%):NEXTI%:CLOSE&AX%:S
Z(1)=0:GOTO1430
1400PTR&BX%=0:PRINT&BX%,SB%:PTR&BX%=A0
1410FORI%=B1%TOB2%:PRINT&BX%,C$(I%),CF(0,I%),CF(1,I%),U$(I%),G%(I%):NEXTI%
1420PRINT&BX%,OP$,S$(2),D$(2):FORI%=0TO10:PRINT&BX%,AP(1,I%):NEXTI%:CLOSE&BX%:S
Z(2)=0
1430*IEEE
1440ENDPROC
1450DEFPROCinfo
1460CLS:@%=10:PRINT"OPTION 1 - INPUT CHANNEL & TEST INFO":PRINT
1470PRINT"MENU":PRINT"===="
1480PRINT"1.....NAME CHANNELS"
1490PRINT"2.....SET CONVERSION FACTORS & OFFSETS"
1500PRINT"3.....ADD TEST INFO"
1510PRINT"4.....ADD UNITS"
1520PRINT"5.....READ & SET GAINS"
1530PRINT"6.....ADD VOLUME CHANGE UNIT INFO"
1540PRINT"7....ADD LOAD CELL & AIR PRESSURE INFO"
1550PRINT"8.....RETURN TO MAIN MENU"
1560REPEAT:X$=GET$:UNTILX$>="1"ANDX$<="8"
1570IFX$="1"PROCname
1580IFX$="2"PROCfacs
1590IFX$="3"PROCtestinfo
1600IFX$="4"PROCunit
1610IFX$="5"PROCsetgains
1620IFX$="6"PROCvolstart
1630IFX$="7"PROClostart
1640IFX$<>"8"THEN1460ELSEENDPROC
1650DEFPROCname
1660CLS:PRINT"NAME CHANNELS - MAX OF 7 CHARACTERS/NAME"
1670PRINT"CHAN  NAME"
1680FORI%=0TO15:@%=&00004:PRINTI%;:@%=&00007:PRINTTAB(6)C$(I%):NEXTI%
1690PRINT:INPUT"CHANNEL TO CHANGE OR Q TO QUIT "A$
1700IFA$="Q"THEN1740
1710IF(ASC(A$)<48ORASC(A$)>57)OR(VAL(A$)<0ORVAL(A$)>15)THEN1660
1720INPUTTAB(0,21)"NEW NAME "C$(INT(VAL(A$))):IFLEN(C$(INT(VAL(A$))))>7PRINT"TO
O LONG":GOTO1720
1730GOTO1660
1740CLS:ENDPROC
```

```
 1750DEFPROCfacs
 1760CLS:PRINT:PRINT"SET CONVERSION FACTORS AND OFFSETS":PRINT
 1770IFNC%<>2GOTO1800
 1780PRINT"FACTOR OPTION ";OP$;" HAS ALREADY BEEN SELECTED FOR CELL ";CL$;" & TH
IS MAY NOT BE ALTERED.":PRINT:IFOP$="1"PRINT"OPTION 1.....(OUTPUT*CON.FACTOR)+OF
FSET"ELSEPRINT"OPTION 2.....(OUTPUT+OFFSET)*CON.FACTOR"
 1790X=GET:GOTO1820
 1800PRINT"AN OPTION EXISTS FOR APPLYING THE FACTORS :":PRINT"  1.........(OUTPU
T*CON.FACTOR)+OFFSET":PRINT"  2.........(OUTPUT+OFFSET)*CON.FACTOR"
 1810REPEAT:OP$=GET$:UNTILOP$="1"OROP$="2"
 1820CLS:PRINT"CHAN CON.FACTOR"
 1830FORI%=0TO15:@%=&00004:PRINTI%;:@%=&2030B:PRINTCF(0,I%):NEXTI%
 1840PRINT:INPUT"CHANNEL TO CHANGE OR Q TO QUIT "A$
 1850IFA$="Q"THEN1910
 1860IF(ASC(A$)<48ORASC(A$)>57)OR(VAL(A$)<0ORVAL(A$)>15)THEN1820
 1870IF(NC%=2ANDCL$="A"ANDVAL(A$)<=A2%)OR(NC%=2ANDCL$="B"ANDVAL(A$)>=B1%)PRINT"T
EST CURRENTLY RUNNING IN THIS CELL - NOAMMENDMENTS ALLOWED":X=GET:GOTO1820
 1880IFVAL(A$)=0THEN1900
 1890IFVAL(A$)=VCU(1,8)ORVAL(A$)=VCU(1,7)ORVAL(A$)=VCU(2,8)ORVAL(A$)=VCU(2,7)THE
NINPUT"FACTOR FOR THIS CHANNEL SET BY VCU      OPTION - SURE YOU WANT TO CHANGE
? Y FOR YES "B$:IFB$<>"Y"THEN1820
 1900INPUTTAB(0,19)"NEW VALUE "CF(0,VAL(A$)):GOTO1820
 1910CLS:PRINT"CHAN      OFFSET"
 1920FORI%=0TO15:@%=&00004:PRINTI%;:@%=&2030B:PRINTCF(1,I%):NEXTI%
 1930PRINT:INPUT"CHANNEL TO CHANGE OR Q TO QUIT "A$
 1940IFA$="Q"THEN1980
 1950IF(ASC(A$)<48ORASC(A$)>57)OR(VAL(A$)<0ORVAL(A$)>15)THEN1910
 1960IF(NC%=2ANDCL$="A"ANDVAL(A$)<=A2%)OR(NC%=2ANDCL$="B"ANDVAL(A$)>=B1%)PRINT"T
EST CURRENTLY RUNNING IN THIS CELL - NOAMMENDMENTS ALLOWED":X=GET:GOTO1910
 1970INPUTTAB(0,19)"NEW VALUE "CF(1,VAL(A$)):GOTO1910
 1980@%=10:ENDPROC
 1990DEFPROCtestinfo
 2000CLS:IFNC%=2ANDCL$="A"PRINT"TEST CURRENTLY RUNNING IN CELL A & THE  TEST INF
O MAY NOT BE ALTERED":PRINT:GOTO2040
 2010IFNC%=1ANDCL$<>"A"GOTO2040
 2020PRINT"CELL A":INPUT"ENTER TEST DESCRIPTION TO BE SHOWN ON SCREEN DURING TES
T :  "D$(1):IFLEN(D$(1))>120PRINT"TOO LONG":GOTO2020
 2030PRINT:INPUT"START OF TEST :  "S$(1):IFLEN(S$(1))>40PRINT"TOO LONG":GOTO2030
 2040IFNC%=2ANDCL$="B"PRINT"TEST CURRENTLY RUNNING IN CELL B & THE  TEST INFO MA
Y NOT BE ALTERED":GOTO2080
 2050IFNC%=1ANDCL$<>"B"GOTO2080
 2060PRINT"CELL B":INPUT"ENTER TEST DESCRIPTION TO BE SHOWN ON SCREEN DURING TES
T :  "D$(2):IFLEN(D$(2))>120PRINT"TOO LONG":GOTO2060
 2070PRINT:INPUT"START OF TEST :  "S$(2):IFLEN(S$(2))>40PRINT"TOO LONG":GOTO2070
 2080CLS:ENDPROC
 2090DEFPROCunit
 2100CLS:PRINT"ADD UNITS FOR NAMED CHANNELS - MAX OF 8 CHARACTERS/UNIT":PRINT
 2110PRINT"CHAN  NAME"
 2120FORI%=0TO15:@%=&00004:PRINTI%;:@%=&00008:PRINTTAB(6);U$(I%):NEXTI%
 2130PRINT:INPUT"CHANNEL TO CHANGE OR Q TO QUIT "A$
 2140IFA$="Q"THEN2190
 2150IF(ASC(A$)<48ORASC(A$)>57)OR(VAL(A$)<0ORVAL(A$)>15)THEN2100
 2160IF(NC%=2ANDCL$="A"ANDVAL(A$)<=A2%)OR(NC%=2ANDCL$="B"ANDVAL(A$)>=B1%)PRINT"T
EST CURRENTLY RUNNING IN THIS CELL - NOAMMENDMENTS ALLOWED"
 2170INPUTTAB(0,22)"NEW UNITS "U$(VAL(A$)):IFLEN(U$(VAL(A$)))>8PRINT"TOO LONG":G
OTO2170
 2180GOTO2100
 2190CLS:ENDPROC
 2200DEFPROClostart
 2210CLS:FORX%=1TO2
 2220IFX%=1PRINT"CURRENT STATUS OF CELL A:":Y%=A1%:J%=A2%
 2230IFX%=2PRINT"CURRENT STATUS OF CELL B:":Y%=B1%:J%=B2%
 2240IF(X%=1ANDNC%=1ANDCL$="B")OR(X%=2ANDNC%=1ANDCL$="A")PRINT"CELL IDLE":X=GET:
GOTO2370
 2250IF(X%=1ANDNC%=2ANDCL$="A")OR(X%=2ANDNC%=2ANDCL$="B")PRINT"TEST RUNNING IN T
HIS CELL ALREADY - NO  AMMENDMENTS ALLOWED":X=GET:GOTO2370
 2260IFAVG(X%)=-999PRINT"OPTION OFF":GOTO2280
 2270PRINT"OPTION ON":PRINT"LOAD CELL CHANNELS = ";LC(1,X%);",";LC(2,X%);",";LC(
3,X%):PRINT"AIR PRESSURE IN SPECIMEN (kPa) = ";AP((X%-1),0):PRINT
 2280INPUT"CHANGE STATUS ? Y/N "A$:IFA$<>"Y"ANDA$<>"N"THEN2280
 2290IFA$="N"THEN2370
```

```
 2300IFAVG(X%)=0THENAVG(X%)=-999:GOTO2370
 2310AVG(X%)=0:CLS:PRINTTAB(0,20)"Note - load cells may not occupy chan.0":INPUT
TAB(0,0)"ENTER LOAD CELL CHANNELS - 1st "LC(1,X%):IFLC(1,X%)<Y%ORLC(1,X%)>J%ORLC
(1,X%)=0PRINTTAB(0,0)SPC(40):GOTO2310
 2320INPUTTAB(27,1)"2nd "LC(2,X%):IFLC(2,X%)<Y%ORLC(2,X%)>J%ORLC(2,X%)=0PRINTTAB
(0,1)SPC(40):GOTO2320
 2330INPUTTAB(27,2)"3rd "LC(3,X%):IFLC(3,X%)<Y%ORLC(3,X%)>J%ORLC(3,X%)=0PRINTTAB
(0,2)SPC(40):GOTO2330
 2340PRINTTAB(0,22)"Note - air pressure must exceed zero"
 2350INPUTTAB(0,3)"AIR PRESSURE IN SPECIMEN (kPa) "AP((X%-1),0):IFAP((X%-1),0)<=
0PRINTTAB(0,3)SPC(40):GOTO2350
 2360INPUT"OK? N FOR NO "A$:IFA$="N"GOTO2310
 2370CLS:NEXTX%
 2380CLS:ENDPROC
 2390DEFPROCvoustart
 2400CLS:FORX%=1TO2
 2410IFX%=1PRINT"CELL A:":Y%=A1%:J%=A2%
 2420IFX%=2PRINT"CELL B:":Y%=B1%:J%=B2%
 2430IF(X%=1ANDNC%=1ANDCL$="B")OR(X%=2ANDNC%=1ANDCL$="A")PRINT"CELL IDLE":X=GET:
GOTO2660
 2440IF(X%=1ANDNC%=2ANDCL$="A")OR(X%=2ANDNC%=2ANDCL$="B")PRINT"TEST RUNNING IN T
HIS CELL ALREADY - NO  AMMENDMENTS ALLOWED":X=GET:GOTO2660
 2450IFVCU(X%,5)=0PRINT"OPTION OFF":GOTO2500
 2460PRINTTAB(27)"FLOW":PRINT"CHAN NAME       CON_FAC     INTO":PRINT"----------
--------------------"
 2470FORI%=1TOVCU(X%,5)
 2480@%=00004:PRINTVCU(X%,I%+5);:@%=&00007:PRINTTAB(5)C$(VCU(X%,I%+5));:@%=&2030
A:PRINTCF(0,VCU(X%,I%+5));:IFFL$(X%,I%)="T"PRINTTAB(27)"TOP"ELSEPRINTTAB(27)"BAS
E":PRINT
 2490NEXTI%:PRINT
 2500INPUT"CHANGE STATUS ? Y/N "A$:IFA$<>"Y"ANDA$<>"N"THEN2500
 2510IFA$="N"THEN2660
 2520IFVCU(X%,5)>0THENVCU(X%,5)=0:GOTO2660
 2530VCU(X%,7)=0:PRINT"TO USE THIS OPTION REQUIRES THE  FOLLOWING INFO"
 2540INPUT"ENTER NO. OF UNITS - MAX OF 2 "VCU(X%,5):IFVCU(X%,5)<>2ANDVCU(X%,5)<>
1THEN2540
 2550FORI%=1TOVCU(X%,5)
 2560CLS:PRINTTAB(0,20)"Note - VCU may not occupy channel 0"
 2570PRINTTAB(0,0)"UNIT ";I%:PRINT"------":PRINT:INPUT"VCU CHANNEL
       = "VCU(X%,I%+5):IFVCU(X%,I%+5)<Y%ORVCU(X%,I%+5)>J%ORVCU(X%,I%+5)=0PRINTT
AB(0,3)SPC(40):GOTO2570
 2580PRINTTAB(0,22)"Note - cal. factor +ve if vcu o/p       increases as volume
expelled from soil"
 2590INPUTTAB(0,4)"CAL. FACTOR FOR FLOW INTO TOP    = "VCU(X%,I%):IFVCU(X%,I%)=0
PRINTTAB(0,4)SPC(40):GOTO2580
 2600INPUTTAB(0,5)"CAL. FACTOR FOR FLOW INTO BASE   = "VCU(X%,I%+2):IFVCU(X%,I%+
2)=0PRINTTAB(0,5)SPC(40):GOTO2600
 2610IF(VCU(X%,I%)>0ANDVCU(X%,I%+2)>0)OR(VCU(X%,I%)<0ANDVCU(X%,I%+2)<0)PRINTTAB(
0,6)"FACTORS MUST BE OF OPPOSITE SIGNS !":PRINTTAB(0,4)SPC(120):GOTO2590
 2620INPUTTAB(0,6)"INITIAL FLOW TO TOP OR BASE (T/B)= "FL$(X%,I%):IFFL$(X%,I%)<>
"T"ANDFL$(X%,I%)<>"B"PRINTTAB(0,6)SPC(40):GOTO2620
 2630IFFL$(X%,I%)="T"THENCF(0,(VCU(X%,I%+5)))=VCU(X%,I%)ELSECF(0,(VCU(X%,I%+5)))
=VCU(X%,I%+2)
 2640PRINT:PRINT"THE INITIAL CON.FACTOR IS NOW SET.THE   OFFSET MUST STILL BE SE
T USING OPTION 2":X=GET
 2650NEXTI%
 2660CLS:NEXTX%
 2670CLS:ENDPROC
 2680DEFPROCrecorddata
 2690FORX%=1TO2
 2700CLS:PRINT"OPTION 2 - DATA RECORDING OPTIONS":PRINT
 2710IFX%=1PRINT"CELL A:"ELSEPRINT"CELL B:"
 2720IF(NC%=2ANDCL$="A"ANDX%=1)OR(NC%=2ANDCL$="B"ANDX%=2)PRINT"OPTIONS FOR THIS
CELL ALREADY SET & MAY NOT BE CHANGED":X=GET:GOTO3060
 2730IF(NC%=1ANDCL$="B"ANDX%=1)OR(NC%=1ANDCL$="A"ANDX%=2)PRINT"CELL IDLE":X=GET:
GOTO3060
 2740PRINT"MENU":PRINT"===="
 2750PRINT"Data to disc during test - on    type 1"
 2760PRINT"                         - off   type 2"
 2770PRINT"Data to printer          - on    type 3"
 2780PRINT"                         - off   type 4"
 2790PRINT"End of options for this cell     type 5":X$=GET$
```

```
 2800IFX$="1"THEN2870
 2810IFX$="2"THENSZ(X%)=0:GOTO2700
 2820IFNC%=2AND(X$="3"ORX$="4")PRINTTAB(0,12)"THE PRINTER OPTION HAS ALREADY BEE
N SET BY THE FIRST TEST & MAY NOT BE CHANGED":X=GET:GOTO2700
 2830IFX$="3"THEN3030
 2840IFX$="4"THENPR=0:GOTO2700
 2850IFX$="5"THEN3060
 2860CLS:GOTO2700
 2870IF(NC%=1ANDCL$="A")OR(NC%=2ANDCL$="B")THENJ%=A2%-A1%ELSEJ%=B2%-B1%
 2880CLS:PRINT"RESERVATION OF SPACE FOR TEST DATA :":PRINT:INPUT"  NO. OF CHANNE
LS TO BE USED ";CN%:INPUT"  APPROX. NO. OF SCANS EXPECTED ";AN%:IF(CN%>(J%+1))OR
AN%<1THEN2880
 2890INPUT"  ENTER FILENAME FOR DATA ";F$(X%,1):IFLEN(F$(X%,1))>10PRINT"TOO LONG
":GOTO2890
 2900PRINT:PRINT"DISC DRIVE NO. FOR ";F$(X%,1);:INPUTJ%:IFJ%<0ORJ%>3THEN2870ELSE
F$(X%,2)="*DRIVE "+STR$(J%)
 2910PRINT"INSERT DISC AND HIT RETURN TO CONTINUE":X=GET:*DISC
 2920OSCLI(F$(X%,2)):SZ(X%)=((CN%+1)*AN%*6)+734:EF$=STR$~SZ(X%):FS$="SAVE"+CHR$3
4+F$(X%,1)+CHR$34+" 00000 "+EF$:OSCLI(FS$)
 2930PRINT"RESERVED DISC SPACE FOR ";F$(X%,1);" = ";SZ(X%);" BYTES"
 2940IFX%=2THEN2980
 2950AX%=OPENUP(F$(X%,1))
 2960PRINT&AX%,AN%,CN%
 2970GOTO3000
 2980BX%=OPENUP(F$(X%,1))
 2990PRINT&BX%,AN%,CN%
 3000PRINT"LEAVE DISC IN DRIVE FOR REST OF TEST ":X=GET
 3010*IEEE
 3020CLS:GOTO2700
 3030CLS:PRINT:PRINT"DATA PRINTOUT DURING TEST":PRINT"THE OUTPUT FROM THE CHANNE
LS WILL BE    PRINTED OUT DURING THE TEST,AFTER THE   RAW OUTPUT IN mV HAS BEEN
INTERPRETED   USING THE CONVERSION FACTORS & OFFSETS."
 3040PRINT"VALUES FOR THESE CALIBRATION CONSTANTS  WILL BE O/P AT THE START OF T
HE TEST.":PRINT:PRINT"CHECK SUFFICIENT PAPER IS AVAILABLE!"
 3050PR=1:X=GET:CLS:GOTO2700
 3060CLS:NEXTX%
 3070ENDPROC
 3080DEFPROClabel
 3090CLS:PRINTTAB(8,0)"DATA OUTPUT FROM CELL ";CL$:PRINTTAB(8,1)"==============
========"
 3100IFCL$="A"THENX%=1:S%=SA%
 3110IFCL$="B"THENX%=2:S%=SB%
 3120PRINTTAB(0,3)"DATA FILE=";F$(X%,1):IFS%=0PRINTTAB(26,3)"SCAN NO. 0"ELSEPRIN
TTAB(26,3)"SCAN NO. ";S%-1
 3130PRINT:PRINT"CHAN NAME    O/P(mV)  ENG'G O/P UNITS":PRINT"----------------
------------------"
 3140PRINTTAB(6,24)"O = DISPLAY RUNNING OPTIONS";
 3150@%=10:ENDPROC
 3160DEFPROCrunops
 3170CLS:PRINT"RUNNING OPTIONS DURING LOGGING:":PRINT"-----------------------
----"
 3180PRINTTAB(0,3)"CELL ";CL$;" - C=DISPLAY TEST & CHANNEL INFO"
 3190PRINTTAB(9,5)"A=DISPLAY AVG STRESSES":PRINTTAB(9,7)"R=CHANGE SCANNING RATE"
:PRINTTAB(9,9)"V=REVERSE FLOW DIR'N INTO VCU":PRINTTAB(9,11)"E=END CURRENT TEST"
 3200IFCL$="A"PRINTTAB(0,14)"CELL B - S=START NEW TEST"ELSEPRINTTAB(0,14)"CELL A
 - S=START NEW TEST"
 3210PRINTTAB(9,16)"D=DISPLAY CURRENT O/P & ACCESS":PRINTTAB(11,17)"RUNNING OPTI
ONS":PRINTTAB(0,20)"RETURN TO SKIP":X$=GET$
 3220IFX$="V"PROCrevvcu
 3230IFX$="C"PROCchanstat
 3240IFX$="R"PROCaltertime
 3250IFX$="A"PROCavglo
 3260IFX$="D"ANDNC%=2PROCchangecell
 3270IFX$="S"ANDNC%=2THENX$="0"
 3280IFX$="S"ANDNC%=1PROCnewtest
 3290@%=10:ENDPROC
```

```
 3300DEFPROCprint
 3310*FX5,1
 3320*FX8
 3330*FX3,10
 3340IFPK%=0ANDPE%=0ANDPL%=0THEN3540
 3350IFPK%=1PRINTSPC(20)"***DATA OUTPUT FROM AIU LOGGING PROGRAM***":PRINT
 3360IFPE%=0THEN3380ELSEPRINT"END OF TEST IN CELL ";CL$:PRINT"----------------
----------------------------------------------------"
 3370IFNC%=1THEN3620ELSEPRINT:PRINT"ONLY SINGLE TEST CONTINUING"
 3380IFPL%=1PRINT:PRINT"-----------------------------------------------------
--------------":PRINT"NEW TEST STARTED !":PRINT"CHANNEL ALOCATIONS ARE : CELL A
 = ";A1%;" TO ";A2%:PRINTSPC(25)"CELL B = ";B1%;" TO ";B2%:PL%=0
 3390IF(NC%=1ANDCL$="B")OR(PE%=1ANDCL$="A")THEN3420
 3400PRINT"CELL A:":PRINT"TEST STARTED      : ";S$(1):PRINT"SCAN INTERVAL     : ";
AT/100;" SECS"
 3410PRINT"DATA FILE         : ";F$(1,1):PRINT"DISC DRIVE        : ";F$(1,2):PRINT
"TEST DESCRIPTION : ";D$(1):PRINT:IFNC%=1ORPE%=1THEN3440
 3420PRINT"CELL B:":PRINT"TEST STARTED      : ";S$(2):PRINT"SCAN INTERVAL     : ";
BT/100;" SECS"
 3430PRINT"DATA FILE         : ";F$(2,1):PRINT"DISC DRIVE        : ";F$(2,2):PRINT
"TEST DESCRIPTION : ";D$(2):PRINT
 3440PRINT"CHAN  TRANSDUCER       CON.FACTOR          OFFSET              GAIN"
 3450FORI%=A1%TOB2%
 3460@%=03:PRINTI%;:@%=10:PRINTTAB(6)C$(I%);:@%=&20410:PRINTTAB(18)CF(0,I%),CF(1
,I%),G%(I%)
 3470NEXTI%
 3480@%=10:PRINT:IFPK%=1PRINT"TEST DATA":PRINT"==========":PK%=0:GOTO3500
 3490PRINT"TEST DATA CONT'D":PRINT"================"
 3500PRINT:FORI%=A1%TOB2%
 3510IFI%=B2%OR(I%-A1%)=7THENPRINT"    CHAN ";I%:GOTO3530
 3520PRINT"    CHAN ";I%,;
 3530NEXTI%:PE%=0:GOTO3620
 3540IFPC%=1PRINT"CELL A ELAPSED TIME = ";T;" SECS"ELSEPRINT"CELL B ELAPSED TIME
 = ";T;" SECS"
 3550FORI%=A1%TOB2%
 3560@%=&02030A
 3570IF((PC%=1ANDI%>A2%)OR(PC%=2ANDI%<B1%))AND(I%=B2%OR(I%-A1%)=7)THENPRINT"    "
:GOTO3610
 3580IF((PC%=1ANDI%>A2%)OR(PC%=2ANDI%<B1%))THENPRINT"    ",;:GOTO3610
 3590IFI%=B2%OR(I%-A1%)=7PRINTK(I%):GOTO3610
 3600PRINTK(I%),;
 3610NEXTI%
 3620@%=10
 3630*FX3,0
 3640ENDPROC
 3650DEFPROCaltertime
 3660IFCL$="A"THENT=AT ELSET=BT
 3670CLS:PRINT"CURRENT TIME INTERVAL = ";T/100;" SECS":PRINT"MINIMUM TIME INTERV
AL = ";(B2%-A1%)*0.5;" SECS":PRINT
 3680PRINT"NEW TIME INTERVAL FROM AFTER":INPUT"NEXT SCAN (SECS) = ";T:IFCL$="A"T
HENAT=T*100ELSEBT=T*100
 3690IFT=0THEN3670
 3700ENDPROC
 3710DEFPROCavglc
 3720CLS:IF(CL$="A"ANDAVG(1)=-888)OR(CL$="B"ANDAVG(2)=-888)THEN3860
 3730IFCL$="A"THENX%=1:T0=AT0
 3740IFCL$="B"THENX%=2:T0=BT0
 3750AVG=(K(LC(1,X%))+K(LC(2,X%))+K(LC(3,X%)))/3
 3760CLS:@%=10:PRINTTAB(6,0)"LOAD CELL DATA ANALYSIS":PRINTTAB(6,1)"==========
==========":PRINT
 3770PRINT"LOAD  ENG'G O/P  DEV OF O/P FROM AVG":PRINT"CELL    (kPa)      (kPa)
      (%)":PRINT"-----------------------------------"
 3780FORJ%=1TO3:@%=&00004:PRINTLC(J%,X%);:@%=&20308:PRINTK(J%);:@%=&20308:PRINTA
VG-K(J%);:@%=&2030A:PRINT(AVG-K(J%))*100/AVG:NEXTJ%
 3790PRINTTAB(0,12)"AVG. PRESSURE TRANSMITTED":PRINTTAB(0,13)"BY LOAD CELLS
       =";:@%=&20308:PRINTAVG,TAB(36,13)"kPa"
 3800PRINTTAB(0,14)"AIR PRESSURE IN SPECIMEN  =";:@%=&20308:PRINT(AP((X%-1),C(X%
))),TAB(36,14)"kPa"
 3810PRINTTAB(0,15)"NORMAL STRESS ON SPECIMEN =";:@%=&20308:PRINT(AVG-AP((X%-1),
C(X%))),TAB(36,15)"kPa"
```

```
 3820PRINTTAB(0,20);"-----------------------------------":PRINTTAB(0,21)"C=CHAN
GE AIR        R=RETURN TO MAIN":PRINTTAB(0,22)"  PRESSURE SHOWN      DISPLAY":X$
=GET$
 3830IFX$="C"THENC(X%)=C(X%)+2
 3840IFX$="C"INPUT"NEW PRESSURE ";AP((X%-1),C(X%)):AP((X%-1),(C(X%)-1))=(TIME-T0
)/100:IFAP((X%-1),C(X%))<=0PRINTTAB(0,23)SPC(40):GOTO3840
 3850IFX$="R"GOTO3860ELSEGOTO3750
 3860@%=10:ENDPROC
 3870DEFPROCrevvou
 3880IFCL$="A"THENX%=1ELSEX%=2
 3890CLS:IFVCU(X%,5)=0GOTO4050ELSEPRINTTAB(9,0)"REVERSAL OF VCU's":PRINTTAB(9,1)
"================":PRINT
 3900PRINTTAB(34)"FLOW":PRINT"CHAN NAME      CON_FAC    OFFSET   INTO":PRINT"----
---------------------------------"
 3910FORI%=1TOVCU(X%,5)
 3920@%=00004:PRINTVCU(X%,I%+5);:@%=&00007:PRINTTAB(5)C$(VCU(X%,I%+5));:@%=&2030
A:PRINTCF(0,VCU(X%,I%+5));:@%=&2030A:PRINTCF(1,VCU(X%,I%+5));:IFFL$(X%,I%)="T"PR
INTTAB(34)"TOP"ELSEPRINTTAB(34)"BASE"
 3930NEXTI%
 3940PRINTTAB(0,11)"RTN TO SKIP OR R TO REVERSE":A$=GET$:IFA$="R"THEN3950ELSE405
0
 3950INPUTTAB(0,11)"CHANNEL OF VCU TO REVERSE  "RC:IF(RC<>VCU(X%,6)ANDRC<>VCU(X%
,7))ORRC=0PRINTTAB(0,11)SPC(40):GOTO3950
 3960PRINT"HIT ANY KEY IMMEDIATELY FLOW REVERSED":X=GET
 3970C$="$C"+STR$(RC)+"I":PROCcommand:PROCgetdata
 3980X=INSTR(A$,"I")-1:K(RC)=VAL(MID$(A$,X+2))
 3990IFRC=VCU(X%,6)THENJ%=1ELSEJ%=2
 4000IFFL$(X%,J%)="B"THEN4030
 4010FL$(X%,J%)="B":IFOP$="2"THENCF(1,RC)=(K(RC)+CF(1,RC))*CF(0,RC)/VCU(X%,J%+2)
-K(RC)ELSECF(1,RC)=K(RC)*(VCU(X%,J%+2)-VCU(X%,J%))+CF(1,RC)
 4020CF(0,RC)=VCU(X%,J%+2):GOTO3890
 4030FL$(X%,J%)="T":IFOP$="2"THENCF(1,RC)=(K(RC)+CF(1,RC))*CF(0,RC)/VCU(X%,J%)-K
(RC)ELSECF(1,RC)=K(RC)*(VCU(X%,J%)-VCU(X%,J%+2))+CF(1,RC)
 4040CF(0,RC)=VCU(X%,J%):GOTO3890
 4050@%=10:ENDPROC
 4060DEFPROCchanstat
 4070CLS:IFSTAT=1THEN4080ELSEPRINT"OPTION 4 - CURRENT CHANNEL/TEST STATUS":PRINT
 4080IFNC%=2PRINT"CHANNELALLOCATIONS ARE:":PRINT" CELL A = ";A1%;" TO ";A2%:PRIN
T" CELL B = ";B1%;" TO ";B2%
 4090IFNC%=1ANDCL$="A"PRINT"CHANNELS FOR CELL A = ";A1%;" TO ";A2%
 4100IFNC%=1ANDCL$="B"PRINT"CHANNELS FOR CELL B = ";B1%;" TO ";B2%
 4110X=GET:CLS:PRINT"CHAN NAME    UNITS":PRINT"-----------------":FORI%=0TO15:@
%=&00004:PRINTI%;:@%=&00007:PRINTTAB(5)C$(I%);:@%=&00008:PRINTTAB(13)U$(I%):NEXT
I%
 4120X=GET:CLS:PRINT:PRINT"CHANNEL    CON_FAC   OFFSETS":PRINT"----------------
-----------"
 4130FORI%=0TO15:@%=&00007:PRINTI%;:@%=&2030A:PRINTCF(0,I%);:@%=&2030A:PRINTCF(1
,I%):NEXTI%:PRINT:PRINT
 4140IFOP$="1"THENPRINT"FACTOR OPTION 1 SELECTED                i.e (O/P*CON.FACT
OR)+OFFSET"ELSEPRINT"FACTOR OPTION 2 SELECTED               i.e (O/P+OFFSET)*CON
.FACTOR"
 4150X=GET:CLS:PRINT"CHAN  GAIN":PRINT"----------"
 4160FORI%=0TO15:@%=&00004:PRINTI%;:@%=&00006:PRINTG%(I%):NEXTI%:X=GET
 4170CLS:FORX%=1TO2
 4180IFX%=1PRINT"CELL A:":T=AT:IFNC%=1ANDCL$="B"PRINT"CELL IDLE":GOTO4210
 4190IFX%=2PRINT"CELL B:":T=BT:IFNC%=1ANDCL$="A"PRINT"CELL IDLE":GOTO4210
 4200PRINT"TEST STARTED      : ";S$(X%):PRINT"DATA FILE         : ";F$(X%,1):PRINT
"DISC DRIVE        : ";F$(X%,2):PRINT"SCAN INTERVAL     : ";T/100;" SECS":PRINT"TE
ST DESCRIPTION : ";D$(X%)
 4210PRINT:NEXTX%:X=GET
 4220CLS:PRINT:PRINT"DOUBLE LOGGING          - ";:IFNC%=2PRINT"ON"ELSEPRINT"OFF"
 4230FORX%=1TO2
 4240IFX%=1PRINT:PRINT"CELL A:":IFNC%=1ANDCL$="B"PRINT"CELL IDLE":GOTO4310
 4250IFX%=2PRINT"CELL B:":IFNC%=1ANDCL$="A"PRINT"CELL IDLE":GOTO4310
 4260PRINT"DATA TO DISC           - ";:IFSZ(X%)=0PRINT"OFF"ELSEPRINT"ON"
 4270PRINT"DATA TO PRINTER        - ";:IFPR=0PRINT"OFF"ELSEPRINT"ON"
 4280PRINT"VCU REVERSAL           - ";:IFVCU(X%,5)=0PRINT"OFF"ELSEPRINT"ON"
 4290PRINT"LOAD CELL ANALYSIS     - ";:IFAVG(X%)=-999PRINT"OFF"ELSEPRINT"ON"
 4300PRINT"DATA ANALYSIS FACTORS - OPTION ";OP$
 4310PRINT:NEXTX%:X=GET:ENDPROC
```

```
 4320DEFPROCnewtest
 4330CLS:INPUT"THE OPTION TO START A NEW TEST HAS BEEN SELECTED.ARE YOU SURE (Y/
N) ";A$:IFA$<>"Y"ANDA$<>"N"THEN4330
 4340IFA$="N"THENX$="0":GOTO4470
 4350PRINT:PRINT"THE OPTION TO SIMULTANEOUSLY LOG 2 CELLSHAS BEEN SELECTED.AS A
RESULT THE DATA  MONITORING OF THE EXISTING TEST HAS BEENTEMPORARILY HALTED."
 4360PRINT:PRINT"THE PRINTED OUTPUT OPTION CAN NOT BE    CHANGED FROM THAT SET F
OR THE EXISTING  TEST.IF THE PRINTER IS ON,OUTPUT WILL BEEXTENDED TO INCLUDE THE
 NEW CHANNELS.":X=GET:CLS
 4370PRINT"FOR THE SIMULTANEOUS LOGGING OF 2 CELLS THE CHANNELS USED MUST BE CON
TINUOUS,   WITH CHANNELS FOR CELL A PRECEDING THOSEFOR CELL B":PRINT
 4380PRINT"CHANNELS CURRENTLY IN USE ARE:":IFCL$="A"PRINT"   START CHAN = ";A1%:
PRINT"   END CHAN   = ";A2%
 4390IFCL$="B"PRINT"   START CHAN = ";B1%:PRINT"   END CHAN   = ";B2%
 4400PRINT:PRINT"INFO FOR NEW TEST:"
 4410INPUTTAB(0,10)"   START CHAN = "Y%:INPUTTAB(0,11)"   END CHAN   = "J%:IFY%<
0ORY%>15ORJ%<0ORJ%>15ORY%>J%THEN4410
 4420PRINTTAB(0,13)"SCAN INTERVAL FOR NEW TEST MUST BE      GREATER THAN ";(B2%-
A1%)*0.5;:INPUT" SECS   : "T:IFT=0PRINTTAB(0,13)SPC(80):GOTO4420
 4430IFCL$="A"THENB1%=Y%:B2%=J%:BT=T*100:SB%=0:C(2)=0
 4440IFCL$="B"THENA1%=Y%:A2%=J%:AT=T*100:SA%=0:C(1)=0
 4450IFB2%<A2%ORB1%<A1%THENCLS:GOTO4370
 4460STAT=0:PL%=1:NC%=2
 4470CLS:ENDPROC
 4480DEFPROCchangecell
 4490IFCL$="A"THENCL$="B"ELSECL$="A"
 4500ENDPROC
```

APPENDIX E

EXPERIMENTAL INVESTIGATIONS INTO THE PROPERTIES OF THE HIGH AIR ENTRY VALUE CERAMICS

Experimental investigations were made into the properties of the high air entry value ceramics used in the main test programme in order to aid the design of the top and base platens for the new consolidation cell. The following tests were carried out on 3 bar ceramics:

(a) determination of the modulus of rupture of the ceramic using a three-point loading test

(b) determination of the elastic properties from load - deflection measurements with circular plates of various diameters

(c) determination of the effect of bending strain on the air entry value of the ceramic

E1 - Determination of the Modulus of Rupture

A total of 13 specimens of the dimensions noted in Table E1 were set up as shown in Figure E1 then loaded to failure in a 2 kN range Amsler force control loading machine (accurate to ± 1N) at a rate of loading between 0.01 N/mm^2 and 0.1 N/mm^2. The results of the work are summarised in Table E1 and the failed specimens are shown in Plate E1. In Table E1, the modulus of rupture (or the maximum stress in the section at failure) was calculated using equation E1, which was derived from small strain bending theory by assuming a linear strain distribution within the specimens at failure.

$$M_R = \frac{3Fl}{2bd^2} \qquad \text{..... equation E1}$$

where M_r - modulus of rupture
F - failure load
l - span of specimen
b - width of specimen
d - depth of specimen

Within the limits of the experimental work, neither the strain rate nor the specimen dimensions appeared to have a significant effect on the results, and the average modulus of rupture measured was 35.4 N/mm^2, with a standard deviation of 2.3 N/mm^2. This value was used to calculate the factor of safety against failure of the ceramic in bending when supported on a smooth metal plate with 4 mm wide recesses machined into its surface. Assuming values of b = 1 cm, d = 0.635 cm, an applied uniformly distributed load of 200 kPa and a two span continuous beam analogy, the maximum stress acting on the beam may be calculated to be 5.95 N/mm^2, giving a factor of safety of 5.9.

E2 - Determination of the Elastic Properties

The elastic properties were measured using the apparatus shown in Figures E2 and E3, end Plate E2. The equipment consisted of 6.3 mm thick de-aired ceramic plates of either 25 mm or 30 mm diameter sealed using RTV732 sealant into a perspex body, which was itself resting on the base pedestal of a triaxial cell. Pressurised air in the triaxial cell was used to apply a uniformly distributed load to the upper surface of the ceramic, with the underside maintained with water at a constant 20 kPa back pressure. Pressures were measured using Bourdon gauges, and deflections were measured at the centre of the plate with the 10 mm range Sangamo submersible LVDT referred to in Table 5.7.

The zero reading of the LVDT was taken with the cell pressure and back pressure each at 20 kPa. Thereafter the cell pressure was increased in 40 kPa increments to a maximum of 320 kPa and the equilibrium deflection of the ceramic recorded after 30 minutes. Before each load increment was applied, the drainage basin beneath the ceramic was flushed using a small pressure differential and the volume of any air that had passed through the ceramic was measured.

The results of the four tests performed are shown in Figure E4 as a graph of net applied pressure against ceramic deflection. From plate bending theory, the central deflection of a simply supported circular plate subjected to a uniformly distributed load across its space is given by equation E2:

$$\delta = \frac{3wr^4 (m-1)(5m+1)}{16Em^2 t^3} \quad \text{... equation E2}$$

where δ - plate deflection

w - uniformly distributed load expressed as force per unit area

r - radius of plate

t - thickness of plate

m - inverse of poissons ratio for the ceramic

E - Youngs Modulus of elasticity for the ceramic

The values of δ/wr^4 derived from Figure E2 are presented in Table E2. The results clearly show that test L1 gives an anomalously low value of δ/wr^4, suggesting that the plate is either stiffer than the others tested or an element of fixity was induced around the edge support by use of a slightly oversized ceramic. Ignoring this test, the average value of δ/wr^4 calculated was 1.20×10^{-6}/Nm, implying E values of between 2877 N/mm^2 if $\nu = 0.1$, and 2325N/mm^2 if $\nu = 0.3$. Due to the relatively simple nature of the tests and the range of results obtained, it was concluded that E approximately equals 2500 $N/mm^2 \pm 500$ N/mm^2.

E3 - Determination of the Effect of Bending Strains on the Air Entry Value

The series of tests reported in the previous section were designed to allow both the elastic properties to be determined and the effects of bending strain on the air entry value to be assessed. The measurement of the volume of air that had accumulated beneath the ceramic during each loading stage was intended to identify the critical pressure at which bending induced micro-cracking of the ceramic allowed air to pass freely through. The short duration of the loading stages was intended to prevent air accumulation due to slow diffusion from being mistaken for micro-cracking.

Air flow was recorded at a net applied pressure of 250 kPa through ceramic L1, which as shown in Figure E5 corresponds to a bending strain (expressed as plate deflection divided by free span) of 4.9 microstrain. Air flow was not recorded in the other tests, although small bubbles of air were noticed to be gradually forming across the whole area of ceramic L2 at a net pressure of 280 kPa. The lack of a distinct line of air bubbles and the proximity of the applied pressure to the nominal air entry value of 300 kPa suggests that the air entry value of this particular ceramic was about 280 kPa. In contrast, the air entry value of ceramic M2 must be greater than 320 kPa, and that of ceramic M1 in excess of 240 kPa.

Based on the foregoing, it was assessed that the risk of ceramic micro-cracking by flexure across the 4 mm wide drainage prove was negligible even if a large point load was applied by a soil particle at mid span.

Table E1 Results of Modulus of Rupture Tests

Specimen No	Section Sizes b x d x l (mm^3)	Section Area (mm^2)	Span (mm)	Failure Rate Aimed For (N/mm^2 Sec)	(N/Sec)	Failure Time (Secs)	Failure Load (N)	Failure Rate Achieved (N/mm^2 Sec)	(N/Sec)	Modulus of Rupture (N/mm^2)
1	6.26 x 6.35 x 24.51	39.75	19.0	0.05	1.99	-	>200	-	-	>22
2	5.98 x 6.28 x 24.58	37.55	19.0	0.05	1.88	160	304	1.90	0.051	36.7
3	6.34 x 6.30 x 24.71	39.94	19.0	0.05	2.00	175	340	1.94	0.049	38.5
4	6.17 x 6.30 x 24.38	38.87	19.0	0.05	1.94	152	298	1.96	0.050	34.7
5	6.22 x 6.26 x 24.38	38.94	19.0	0.05	1.95	164	316	1.93	0.049	36.9
6	6.52 x 6.29 x 24.27	41.01	19.0	0.05	2.05	151	300	1.99	0.048	33.1
7	6.44 x 6.30 x 24.63	40.57	19.0	0.05	2.03	152	304	2.00	0.049	33.9
8	6.23 x 6.32 x 24.64	39.37	19.0	0.10	3.94	81	330	4.07	0.103	37.9
9	5.78 x 6.24 x 24.40	36.07	19.0	0.10	3.61	85	292	3.44	0.095	35.0
10	6.43 x 6.25 x 24.21	40.19	19.0	0.01	0.40	867	344	0.40	0.010	37.0
A	12.48 x 6.27 x 25.59	78.25	19.0	0.05	3.91	143	572	4.00	0.051	33.2
B	12.17 x 6.30 x 25.47	76.67	19.0	0.05	3.83	139	532	3.83	0.050	31.4
C	6.47 x 6.38 x 48.27	41.28	38.0	0.05	2.06	78	156	2.00	0.048	33.8
D	6.78 x 6.38 x 48.69	43.26	38.0	0.05	2.16	90	186	2.07	0.048	38.4

Table E2 Results of Ceramic Deflection Tests

Specimen Number	Average value of δ/wr^4 ($x10^{-6}$/Nm)
L1	0.66
L2	1.15
M1	1.42
M2	1.02
Average	1.20*

* excludes results from specimen L1

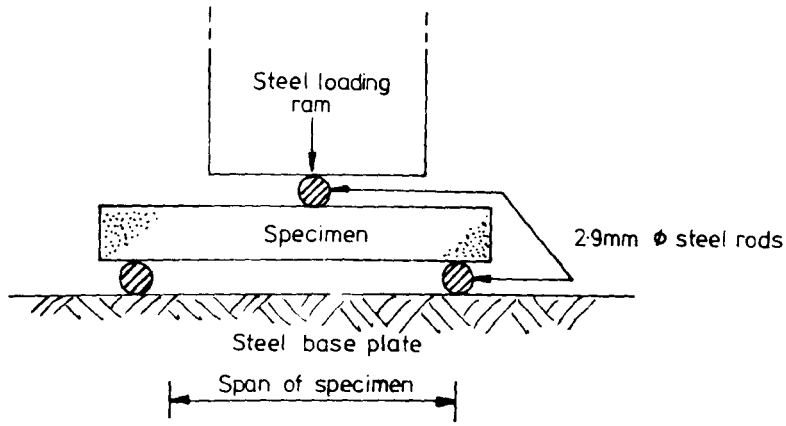

Figure E1 - Apparatus For The Determination of The Modulus of Rupture

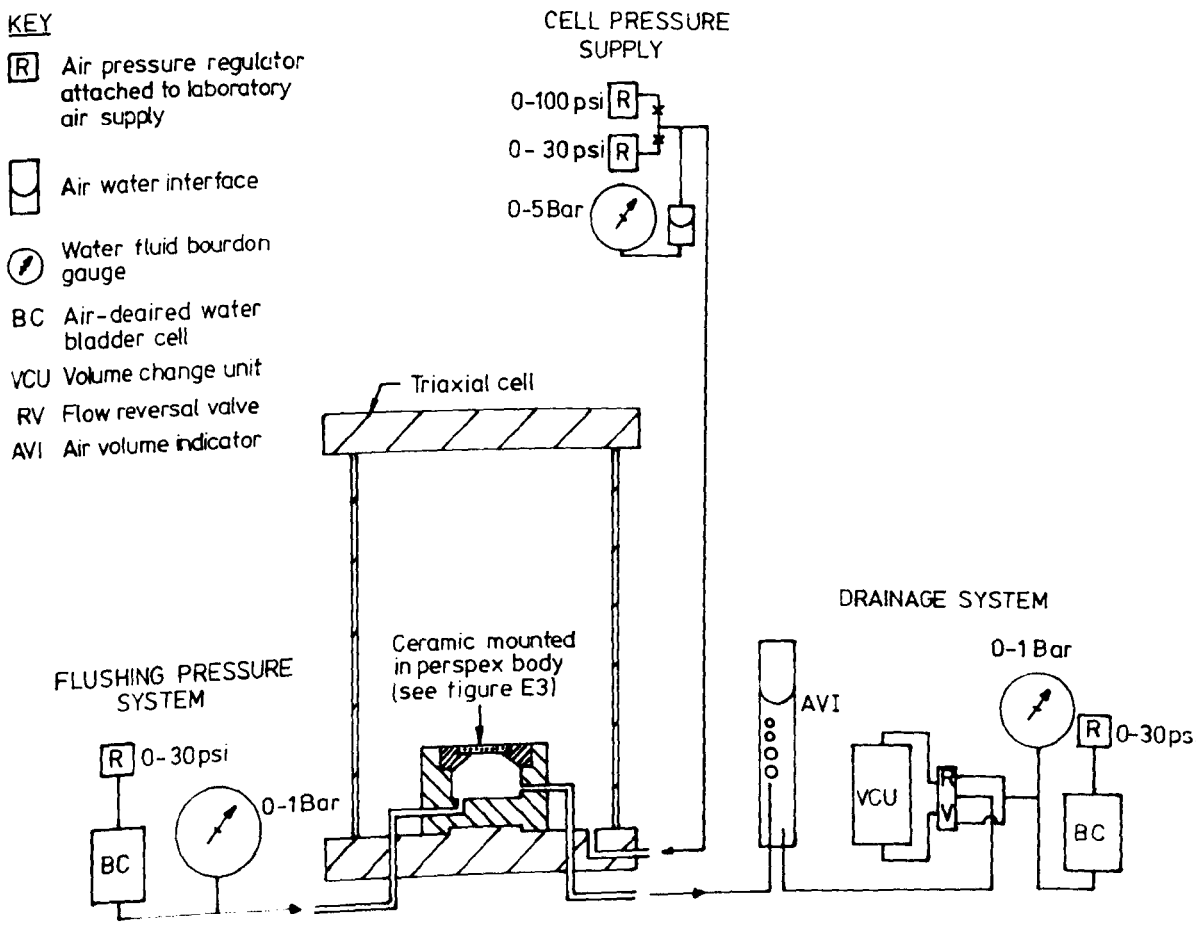

Figure E2 - General Arrangement of Apparatus Used to Determine The Elastic Properties of The Ceramics

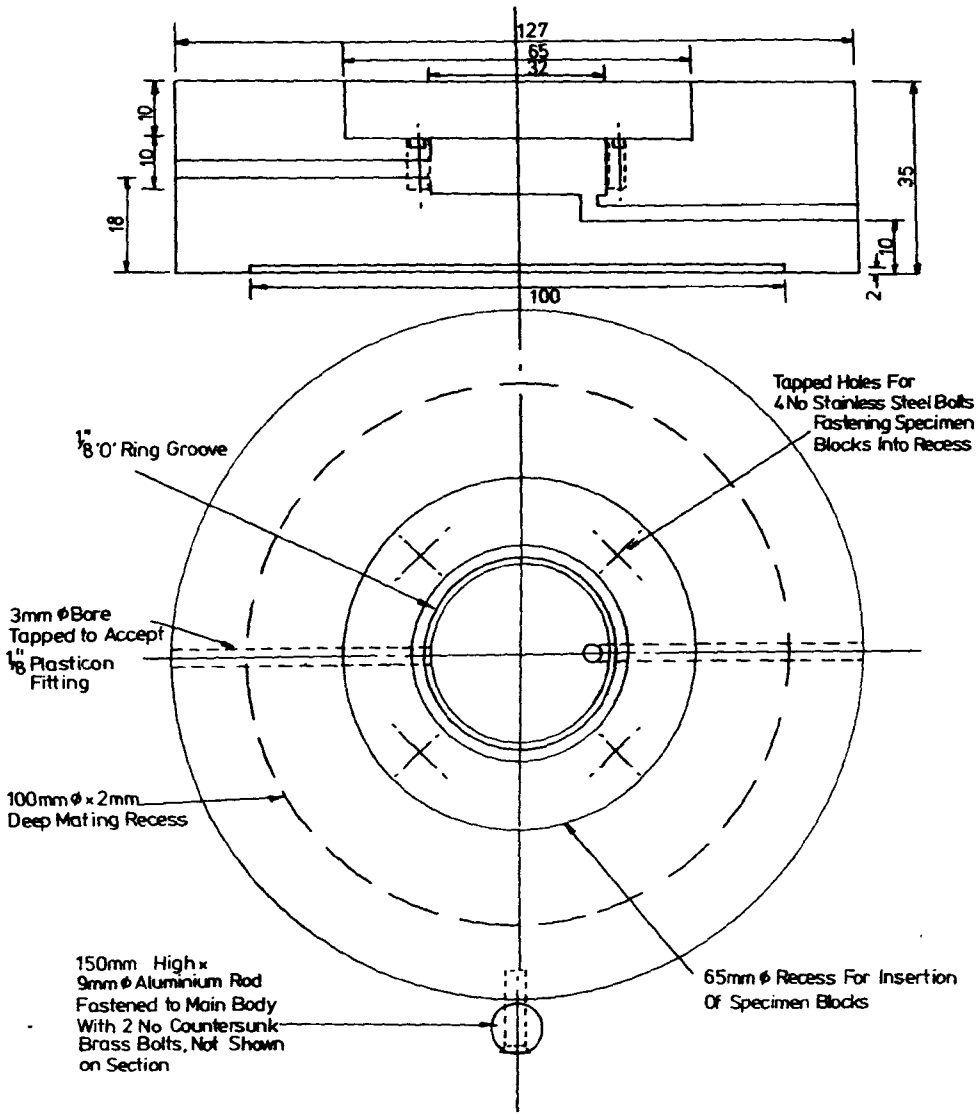

(a) Plan And Section Of Mounting Block

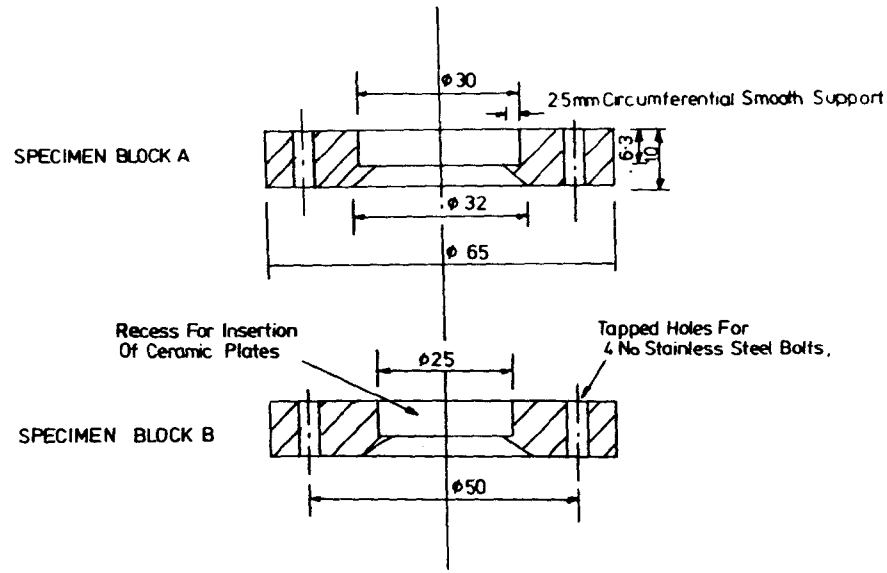

(b) Sections of Ceramic Holders

Figure E3 - Details of Perspex Mounting Block And Ceramic Holders

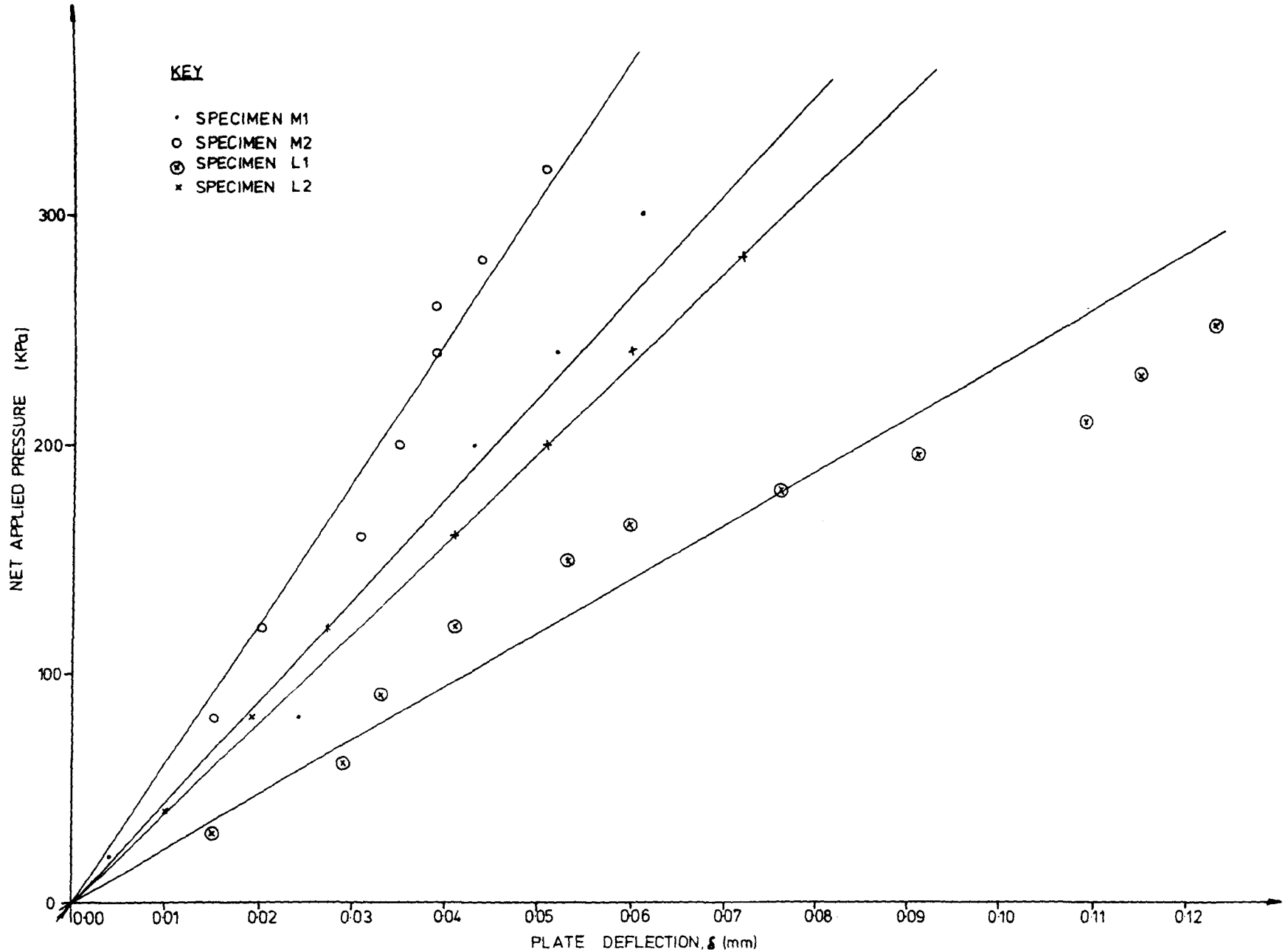

Figure E4- Results of Ceramic Deflection Tests

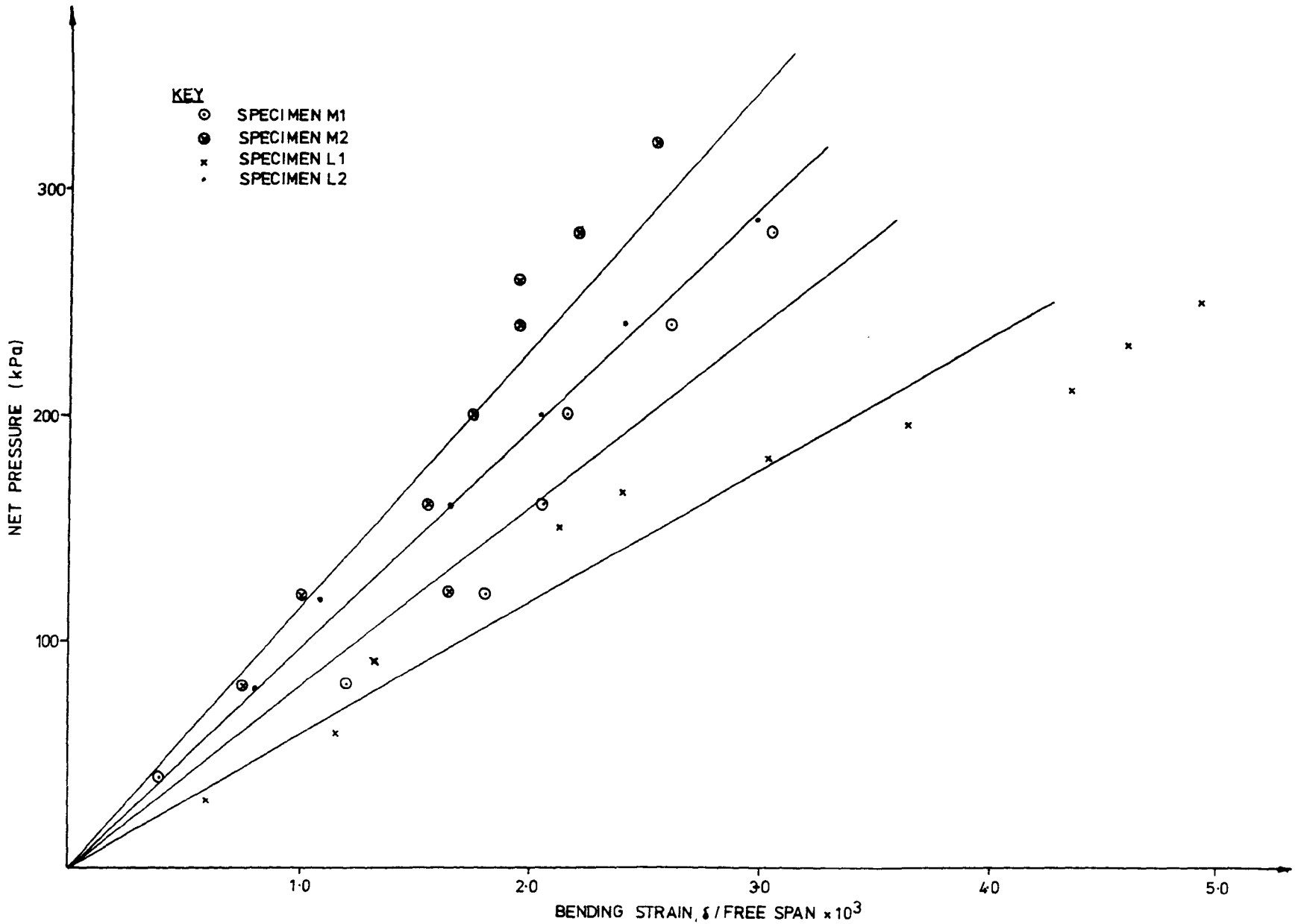

Figure E5 - Bending Strains Developed During Ceramic Deflection Tests

MODES OF FAILURE OF CERAMIC IN 3 POINT STRENGTH TESTS

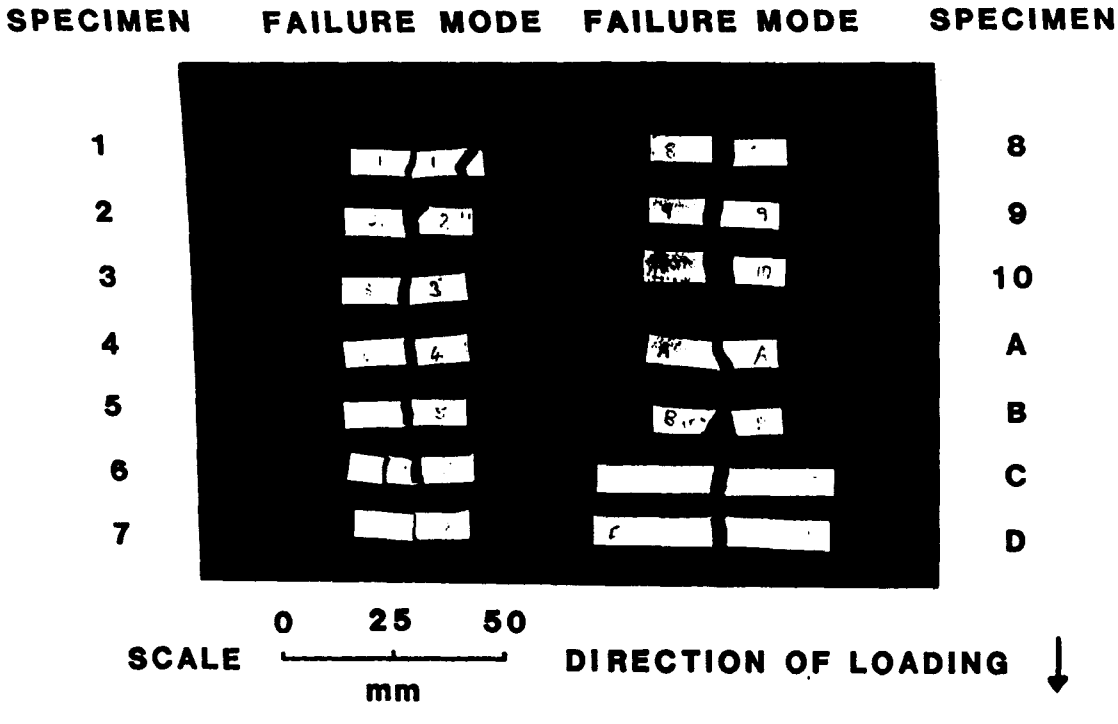

Plate E1 - Specimens Used in Modulus of Rupture Tests

Plate E2 - Perspex Mounting Block and Inserts Used in Ceramic Deflection Tests

C10 - Equipment Used During the Manufacture of the Load Cells

No	Item	Details of item	Specialist Supplier*
1	High tolerance lathe	Mechanica Cortini H80, with ACC-RITE III digital read out	non specialist
2	Local cell body material	50 mm diameter bar of extruded Aluminium of specification 2014T6	non specialist
3	Degreasing agent	Chlorothene NV	WSM+
4	Acidic cleaning agent	M-Prep Conditioner A	WSM
5	Cleaning agent neutraliser	M-Prep Neutraliser 5	WSM
6	Surface finishing for Aluminium	400 grit silicon carbide paper	WSM
7	Strain gauges	FLA-6-350-23	GWI+
8	Strain gauge mounting tape	Mylar JG Tape	WSM
9	Strain gauge adhesive	M-Bond 610	WSM
10	Electrical terminals	CTF-60D	WSM
11	Protective coating	RTV Primer No 1	WSM
12	Protective coating	RTV 3140 Silicone Sealant	WSM
13	Glue for mounting inserts	Locite Engineering Adhesive 290	non specialist
14	Electrical cable	2 pair, screened	non specialist
15	Terminal adhesive	CN CC-3A cyanoacrylate	GWI
16	Dead Weight tester	Budenburg Model 240	BGC+

* Full names and addresses of the spcialist suppliers are presented in Appendix B.

+ Key to abbreviations used in table:

WSM - Welwyn Strain Measurement
GWI - Graham and White Instruments
BGC - Budenburg Gauge Company Limited